

**THE CHEMICAL ANALYSIS AND
BIOLOGICAL EFFECTS OF GINGER**
(Zingiber officinale)

**A joint PhD based at Kingston University and St George's University
of London**

THERESA A. HAGUE

*A thesis submitted in partial fulfilment of the requirements of Kingston
University for the degree of Doctor of Philosophy*

Abstract

Introduction. Ginger, a traditional Chinese herbal medicine, is used to treat digestive disorders in particular to alleviate symptoms of nausea and/or vomiting.

Aims. Major aims were to measure the concentration of [6]-gingerol (6G), and elements in fresh ginger rhizome juice (GJ) by HPLC and ICP-AES and investigate their effects on gastrointestinal functions

Methods. Short circuit current (I_{SC}) effects of 6G and the dietary phytochemicals quercetin and kaempferol (100 μ M) were measured in a Caco-2 cell monolayer. *In vitro* isometric recording was used to investigate GJ (50 μ L, 200 μ L), 6G [1.59×10^{-5} M- 1×10^{-4} M], a selected combination of elements (K [4.6×10^{-2} M], Mg [7.4×10^{-3} M], Mn [8.3×10^{-4} M], Na [1.1×10^{-3} M], Ca [5.1×10^{-4} M]), and a “faux” ginger juice on contractile activity of proximal and distal stomach and duodenum segments from *Suncus murinus*. The effect of 6G (1×10^{-2} M- 1×10^{-4} M, po.) and a ginger capsule suspension on motion-induced emesis was investigated *in vivo* in *Suncus*.

Results. The concentration of 6G in GJ was 239.43 ± 7.92 mg/L. 6G had no effect on I_{SC} , however quercetin and kaempferol caused a significant increase on I_{SC} and the ATP – induced chloride ion secretion. GJ (50 μ L and 200 μ L) caused a dose-related biphasic effect resulting in an overall increase in tension on both regions of the stomach at 25 minutes and an inhibitory effect on duodenal contractions. “Faux” GJ (200 μ L) only partially accounted for the effects of GJ. 6G and a ginger capsule suspension had no anti-emetic activity *in vivo*.

Conclusions. Quercetin and kaempferol may be able to augment the signalling in the intestinal epithelia resulting in an increase in fluid secretion which could facilitate stool

passage. "Faux" GJ did not fully account for the motility effects of GJ, indicating that there were other bioactive constituents present in GJ (e.g. [6]-shogaol). GJ was most effective on the duodenum, suggesting this as a target for an enteric coated ginger capsule for gastrointestinal disorders.

Acknowledgements

I have to give my unequivocal thanks to my supervisors, Prof. Declan P. Naughton and Prof. Paul L. Andrews. Thank you for your patience, support and advice through the duration of this PhD.

Prof. Ke Nie thanks for helping me with the initial investigation into ginger juice and GI motility – we will get that paper out soon, I promise!

Dr. Mark Carew thanks for letting me work in your little lab with the Caco-2 cells. Good luck with your research!

Thank you to the technicians for all your expertise in NMR, HPLC, cell culture, *in vitro* and *in vivo* work based at Kingston University, St George's University of London and the Chinese University of Hong Kong.

Nathalie – sorry for leaving you on your own at St. George's, but thanks for helping to set things up at SGUL and HK.

Mags and Tam, thanks for all the times in the lab when we helped each other out and gave each other advice. Tam you are a lifesaver – thanks for the use of your laptop – I hope I haven't broken it!

Delphine, thanks for being so understanding this year, I won't forget the night that we were trying to be good with, "just the one bottle of wine".

Teri – my old flatmate. How I miss those nights we spent knitting in bed rather than sitting down reading papers – perhaps not the best time spent but hey, I finally got there and you will too.

Polls – I miss you!

Jen and Alex, thanks for making me smile during the many times I wanted to cry!

Mr Booth – thank you for being amazingly supportive, except for the times you repeatedly asked, "How many pages now?!" Well it's finally done, woo! Keep up the HARD work!

Fox, my darling, with both our dilemmas over the past two years, we have managed to be there for each other. Thank you, you're one in a million!

To Emily, thanks for those hour long conversations from NZ that you paid to let me talk your ear off – I truly love you and miss you!

Katrina, thank you so much for everything and for all the drafts you proof read time and time again (good night-time reading eh?).

Thank you to all my friends and family who have given me support during this PhD.
I love you!

Table of contents

Abstract.....	iii
Acknowledgements	v
Table of contents	vi
List of Figures.....	xi
List of Equations.....	xvii
List of Tables	xviii
Abbreviations.....	xix
CHAPTER ONE	1
1.1 Natural products and health.....	2
1.2 Ginger as a plant extract.....	3
1.3 Selected elements found in ginger	5
1.3.1 Copper.....	5
1.3.2 Zinc.....	6
1.3.3 Silicon.....	6
1.3.4 Potassium	7
1.4 Organic compounds found in plants and their biological effects	7
1.4.1 Gingerols, shogaols and paradols.....	8
1.4.2 Quercetin and Kaempferol.....	11
1.4.3 Cu(II)-curcumin complexes.....	14
1.5 Catalytic anti-oxidants	15
1.6 Anti-tumour and anti-inflammatory effects of ginger	17
1.7 Ginger and the gastrointestinal tract	23
1.8 Pathways leading to vomiting.....	26
1.9 The effect of ginger on motion sickness, pregnancy sickness, and postoperative and chemotherapy-induced nausea and vomiting in humans.....	32
1.10 The effect of ginger against emesis induced in animals.....	37

1.11	Objectives.....	41
CHAPTER TWO.....		43
2.1	Introduction	44
2.2	Materials and methods	46
2.2.1	<i>Materials, chemicals and reagents.....</i>	46
2.2.2	<i>Preparation of ginger and stock solutions.....</i>	48
2.2.3	<i>Methods to extract the ginger rhizome constituents</i>	49
2.2.4	<i>Modification of an analytical high performance liquid chromatography (HPLC) method for the detection of [6]-gingerol and vitamin E.....</i>	52
2.2.5	<i>Assessment of element concentrations by ICP-AES</i>	55
2.2.6	<i>Thin layer chromatography on ginger samples.....</i>	56
2.2.7	<i>Nuclear magnetic resonance spectroscopy</i>	57
2.2.8	<i>Complexation studies of Cu(II) ions by [6]-gingerol.....</i>	57
2.2.9	<i>Scanning electron microscopy on the [6]-gingerol Cu(II) complex.....</i>	59
2.3	Results	60
2.3.1	<i>Extraction of the ginger constituents</i>	60
2.3.2	<i>Liquid chromatography</i>	62
2.3.3	<i>The element concentrations in ginger juice assessed via ICP-AES analysis</i>	72
2.3.4	<i>The element concentrations in infusions of ginger and lemon via ICP-AES analysis</i>	73
2.3.5	<i>Thin layer chromatography (TLC) on ginger extracts</i>	74
2.3.6	<i>Stability studies using spectroscopy</i>	76
2.3.7	<i>Metal complexation studies</i>	80
2.3.8	<i>Scanning electron microscopy</i>	81
2.4	Discussion.....	83
2.4.1	<i>Element content of "crude" extracts</i>	83
2.4.2	<i>Stability of the ginger juice extract.....</i>	84
2.4.3	<i>Liquid chromatography analyses of the ginger rhizome extracts.....</i>	86
2.4.4	<i>Studies of [6]-gingerol binding to Cu(II) ions</i>	90
2.4.5	<i>Conclusion.....</i>	90
CHAPTER THREE		93
3.1	Introduction	94
3.1.1	<i>Aims.....</i>	98
3.2	Materials and methods	99

3.2.1	<i>Materials, chemicals and reagents</i>	99
3.2.2	<i>Investigation into SOD activity using the NBT assay</i>	101
3.2.3	<i>Thin Layer Chromatography and anti-oxidant activity</i>	103
3.2.4	<i>Cell culture procedures</i>	103
3.2.5	<i>Quantification of IL-8 and CINC-1 levels</i>	104
3.2.6	<i>Ussing Chamber Experiments</i>	105
3.2.7	<i>Statistics</i>	106
3.3	Results	107
3.3.1	<i>The NBT assay results with [6]-gingerol and Cu(II) ions solution</i>	107
3.3.2	<i>The DPPH/TLC assay results</i>	111
3.3.3	<i>The growth curves of NRK-52E and Caco-2 cells</i>	111
3.3.5	<i>The CINC-1 levels of the NRK-52E cells</i>	113
3.3.6	<i>The IL-8 levels of the Caco-2 cells</i>	114
3.3.7	<i>Ussing Chamber studies using [6]-gingerol, quercetin and kaempferol</i>	116
3.4	Discussion	121
3.4.1	<i>The potential anti-oxidant activity of [6]-gingerol</i>	121
3.4.2	<i>The investigation into the CINC-1 levels in rat kidney cells</i>	123
3.4.3	<i>The investigation into the IL-8 levels in human colon cancer cells</i>	123
3.4.4	<i>The investigation into the effect of [6]-gingerol, quercetin and kaempferol on I_{SC} in Caco-2 cell monolayers</i>	125
3.4.5	<i>Conclusions and further work</i>	126
CHAPTER FOUR	129
4.1	Introduction	130
4.1.1	<i>Aims</i>	132
4.2	Materials and methods	133
4.2.1	<i>Materials and Instrumentation</i>	133
4.2.2	<i>Animals</i>	134
4.2.3	<i>Euthanasia of <i>Suncus murinus</i></i>	134
4.2.4	<i>Tissue bath protocol</i>	135
4.2.5	<i>Test substances</i>	137
4.2.6	<i>Analysis</i>	138
4.2.7	<i>Statistics</i>	139
4.3	Results	141
4.3.1	<i>Basal Activity</i>	141

4.3.2	<i>The effect of increasing volumes of ginger juice on the upper GI tract</i>	154
4.3.3	<i>The effect of a single “low” volume of ginger juice and its constituents on the upper GI tract</i> ...	159
4.3.4	<i>A “low” volume (50 µL) of ginger juice followed by a “low” volume of ginger juice (50 µL) on the upper GI tract</i>	168
4.3.5	<i>The effect of a “high” volume (200 µL) of ginger juice on the upper GI tract</i>	177
4.3.6	<i>The effect of a “low” volume (50 µL) of ginger juice followed by a “high” volume of ginger juice (200 µL) on the upper GI tract</i>	189
4.3.7	<i>The effect of the element solution on the proximal and distal stomach, and the duodenum</i>	199
4.3.8	<i>The effect of [6]-gingerol at the concentration in ginger juice on the upper GI tract</i>	204
4.3.9	<i>The effect of [6]-gingerol at $1 \times 10^{-4} M$ on the upper GI tract</i>	210
4.3.10	<i>The effect of the “faux” ginger juice on the upper GI tract</i>	216
4.4	Discussion	224
4.4.1	<i>Basal Motility</i>	224
4.4.2	<i>Volume related ginger juice effects</i>	226
4.4.3	<i>Were the elements in the ginger juice responsible for the effect of ginger juice?</i>	234
4.4.4	<i>Was [6]-gingerol at the concentration of ginger juice responsible for the effect of ginger juice?</i> 236	
4.4.5	<i>Did the “faux” ginger juice successfully mimic the effect of ginger juice?</i>	237
4.4.6	<i>The potential pharmacology of the responses</i>	240
4.4.7	<i>Conclusions and further work</i>	242
CHAPTER FIVE		245
5.1	Introduction	246
5.1.1	<i>Aim</i>	247
5.2	Materials and methods	248
5.2.1	<i>Materials</i>	248
5.2.2	<i>Animals</i>	248
5.2.3	<i>Pre-screening</i>	249
5.2.4	<i>Experimental Protocol</i>	250
5.2.5	<i>Experimental groups</i>	250
5.2.6	<i>Statistics</i>	251
5.3	Results	252
5.3.1	<i>Pre-screening</i>	252
5.3.2	<i>The effect of the vehicle on the latency and number of emetic episodes</i>	254
5.3.3	<i>The effect of [6]-gingerol and the ginger capsule suspension on the latency and number of emetic episodes</i>	257

5.4	Discussion	260
5.4.1	<i>The effect of the vehicle on the latency and number of emetic episodes.....</i>	<i>260</i>
5.4.2	<i>The effect of [6]-gingerol and the ginger capsule suspension on the latency and number of emetic episodes during motion</i>	<i>261</i>
5.4.3	<i>Conclusions and further work.....</i>	<i>264</i>
CHAPTER SIX	267
6.1	General conclusion	268
Bibliography	273
APPENDICES	1A
Appendix 1	2A
Appendix 2	37A
Appendix 3	52A
Appendix 4	53A

List of Figures

Figure 1. A photograph of a ginger rhizome (<i>Zingiber officinale</i>)	4
Figure 2. The chemical structure of (A) [6]-gingerol, (B) [6]-shogaol and (C) [6]-paradol	8
Figure 3. The chemical structure of (A) quercetin dihydrate and (B) kaempferol	12
Figure 4. The chemical structure of curcumin and the proposed structure of Cu(II)-curcumin (Barik, <i>et al.</i> , 2005).	15
Figure 5. The structure of the 5HT _{3A} receptor adapted from Hu and Lovinger (2005)	23
Figure 6. The structure of the non selective ion channel, TRPV1, adapted from Gunthorpe, <i>et al.</i> (2002).....	24
Figure 7. The chemical structures of (A) capsaicin and (B) resiniferatoxin	25
Figure 8. The motor outputs from the brain-stem nuclei after the pathways have been activated.	31
Figure 9. Flow diagrams to show the different methods of ginger extraction.	51
Figure 10. The percentage yield of the ginger extracts as residue.	61
Figure 11. A typical HPLC trace of VE at 250 mg/L from the HPLC system.	62
Figure 12. Calibration curve for VE. N = 2 replicates at each concentration.	63
Figure 13. HPLC trace of ginger juice from Sainsbury's collected at 48 hours.	64
Figure 14. HPLC traces depicting; (A) 6G standard at 500 mg/L; (B) 6G standard spiked with VE both at 125 mg/L; and (C) a ginger juice sample spiked with VE at 250 mg/L.	66
Figure 15. Calibration curve for 6G.	67
Figure 16. HPLC trace of methanolic ginger capsule extract at 1 mg/mL.	70
Figure 17. Bar charts displaying the (a) "high" (5 - 300.0 mg/L) (b) "medium" (0.2 - 2.5 mg/L), and (c) "low" (0 - 0.125 mg/L) concentration ranges for elements in ginger juice detected by ICP-AES.	72
Figure 18. Two bar charts displaying the concentration of elements in lemon and ginger infusion, (A) had highest concentration of elements (mg/L) whereas (B) displayed the lower concentration of elements in mg/L.	73
Figure 19. Examples of the TLC plate with the vanillin sulfuric acid reagent with the mobile phase either as (A) hexane : diethyl ether highlighting the [6]-gingerol spot ($R_f \sim 0.2$) and (B) toluene : ethyl acetate highlighting the zingiberene spot ($R_f \sim 0.9$).	74
Figure 20. ¹ H NMR spectrum of ginger juice	76
Figure 21. "Aliphatic" region of the ¹ H NMR spectrums at: (b) ~1 hour 45 minutes; (d) 12 hours; and (e) 25 hours after pressing.	78
Figure 22. "Aromatic" region of the ¹ H NMR spectrums at: (b) ~1 hour 45 minutes; (d) 12 hours; and (e) 25 hours after pressing.	79
Figure 23. The spectrum of Cu(II) ions and 6G over a range of 11 concentrations.....	80
Figure 24. The golden brown precipitate of a 1:1 Cu(II) ions and 6G solution.	81
Figure 25. S.E.M. picture of Cu(II)6G precipitate at (A) 2µM and (B) 200nm	82
Figure 26. The decrease in [6]-gingerol concentration in ginger juice 48 hours after pressing the ginger.	85
Figure 27. A diagram depicting the NBT assay – adapted from Fisher, 2004. XO = Xanthine oxidase.....	102
Figure 28. A basic diagram of the Caco-2 cells mounted in the Ussing chamber, identifying the basolateral and apical membrane.	105
Figure 29. A graph to show the NBT assay at different concentrations of Cu(II) ions and [6]-gingerol at a 1.5:1 ratio.....	108

Figure 30. A graph to show the % inhibition of NBT reduction to formazan by solutions of Cu(II) ions and [6]-gingerol at a 1.5:1 ratio.	109
Figure 31. A graph to show the % inhibition of NBT reduction to formazan by varying ratios of Cu(II) ions to [6]-gingerol in solution.	110
Figure 32. Examples of the TLC plate with the DPPH reagent spray with the mobile phase either as (A) hexane : diethyl ether highlighting the [6]-gingerol spot ($R_f \sim 0.2$) or (B) toluene : ethyl acetate highlighting the vitamin E spot ($R_f \sim 0.6$).	111
Figure 33. Growth curves of (A) Caco-2 and (B) NRK-52E cells over a week.	112
Figure 34. The levels of CINC-1 after the NRK-52E cells were incubated with either (A) Mn(II)-EHPG (50 μM) or (B) [6]-gingerol (25 μM) or vitamin E (25 μM) for 12 hours followed by 24 hours of incubation with rat TNF- α (10 ng/mL).	113
Figure 35. The levels of IL-8 after the Caco-2 cells were incubated with either (A) [6]-gingerol (0.25, 2.5 and 25 μM) or (B) vitamin E (0.25, 2.5 and 25 μM) or (C) Mn(II)-EHPG (0.25, 2.5 and 25 μM) for 3 hours followed by 24 hours of incubation with TNF- α (100 ng/mL).	115
Figure 36. Three graphs displaying the effect of different test substances applied to the apical side of the monolayers on the I_{sc} over a 10 minute period: (A) [6]-gingerol (100 μM); (B) Quercetin (100 μM); and (C) Kaempferol (100 μM).	117
Figure 37. Three traces displaying the effect of different test substances applied to the basolateral side of the monolayers on the I_{sc} over a 6 minute period: (A) [6]-gingerol (100 μM); (B) Quercetin (100 μM); and (C) Kaempferol (100 μM).	118
Figure 38. Two traces from the Ussing chamber displaying the effect of apically applied ATP (10 μM) when the membrane was pre-treated with (A) vehicle (EtOH 0.5%) or (B) quercetin (100 μM).	119
Figure 39. The effect of 100 μM of either [6]-gingerol, quercetin and kaempferol on the ATP response on (A) the peak response and (B) the time it took to peak response.	120
Figure 40. A diagrammatical representation of the <i>Suncus murinus</i> stomach specifying where the segments of were taken.	135
Figure 41. A diagram depicting 5 contractions indicating the tone and contraction amplitude.	138
Figure 42. (A) A 15 minute trace of the proximal stomach baseline activity with an expanded 60 second section. (B) A 15 minute trace of the baseline activity of the distal stomach with an expanded 60 second section (C) A 15 minute trace of the baseline activity of the duodenum with an expanded 60 second section.	145
Figure 43. (A, B, C) Bar charts displaying the mean resting tone, contraction amplitude and frequency in the proximal stomach over 15 minutes. (D, E, F) Bar charts displaying the mean resting tone, contraction amplitude and frequency in the distal stomach over 15 minutes. (G, H, I) Bar charts displaying the mean resting tone, contraction amplitude and frequency in the duodenum over 15 minutes.	146
Figure 44. Histograms displaying the frequency distribution for the tone of the (A) proximal stomach (C) distal stomach and (E) duodenum and frequency distribution for the contraction amplitude of the (B) proximal stomach (D) distal stomach and (F) duodenum.	147
Figure 45. Histograms displaying the frequency distribution for the frequency of contraction of the (A) distal stomach and (B) duodenum.	148
Figure 46. Scatter graphs displaying the resting tone plotted against the matching contraction amplitude for the: (A) proximal stomach, (B) distal stomach and (C) duodenum.	149

Figure 47. Scatter graphs displaying the resting contraction amplitude plotted against the matching frequency of contractions for the: (A) distal stomach, and (B) duodenum.	150
Figure 48. (A,C,E,F) Graphs displaying the tone of the proximal and distal stomach and the duodenum and the contraction amplitude of the duodenum. (B,D) Box and whisker plots displaying the contraction amplitude of the proximal and distal stomach strips. The results for (B,D) are expressed as median with the upper and lower quartile ranges. (G,H,I) Histograms of the frequency of contraction from the: proximal and distal stomach strips and the duodenum segments after receiving 200 μ L Krebs' solution.	152
Figure 49. (A,C,E,F) Graphs displaying the tone of the proximal and distal stomach and the duodenum and the contraction amplitude of the duodenum. (B,D) Box and whisker plots displaying the contraction amplitude of the proximal and distal stomach strips. The results for (B,D) are expressed as median with the upper and lower quartile ranges. (G,H,I) Histograms of the frequency of contraction from the: proximal and distal stomach strips and the duodenum segments after receiving the [6]-gingerol vehicle.	153
Figure 50. The effects of increasing volumes of ginger juice on the proximal stomach strips on (A) tone displayed by a line graph and (B) contraction amplitude displayed by box and whisker.	156
Figure 51. The effects of increasing volumes of ginger juice on the distal stomach strips on (A) tone displayed by a line graph.	157
Figure 52. The effects of increasing volumes of ginger juice on the duodenum on (A) tone displayed by a line graph, (B) contraction amplitude displayed by a graph and (C) area under the curve displayed by a bar graph.	158
Figure 53. Two 30 minute traces from proximal stomach before and after a "low" volume (50 μ L) of ginger juice was added showing the two different responses to ginger juice.	160
Figure 54. Line graphs displaying; (A) the tone of all the proximal stomach before and after addition of 50 μ L of ginger juice: (B) the tone of both population X and Y of the proximal stomach before and after the addition of 50 μ L of ginger juice. Box and whisker plot (C) is the contraction amplitude of the proximal stomach after a 50 μ L volume of ginger juice was applied to the tissue bath. (D) Histogram displaying the frequency of contractions pre and post application of 50 μ L of ginger juice.	161
Figure 55. Two 30 minute traces from the distal stomach 5 minutes before and 25 minutes after 50 μ L of ginger juice was applied to the tissue baths.	162
Figure 56. Line graphs displaying: (A) the tone of all the distal stomach before and after addition of 50 μ L of ginger juice: (B) the tone of both population X and Y of the distal stomach before and after the addition of 50 μ L of ginger juice. Box and whisker plot (C) is the contraction amplitude of the distal stomach after a 50 μ L volume of ginger juice was applied to the tissue bath. (D) Histogram displaying the frequency of contractions pre and post application of 50 μ L of ginger juice.	164
Figure 57. Two 30 minute traces from the duodenum before and after a "low" volume (50 μ L) of ginger juice was added with the two different responses to ginger juice.	165
Figure 58. (A) Line graph displaying the duodenal tone of population Y and the Krebs' control before and after addition of 50 μ L of ginger juice, (B) a graph displaying the duodenal contraction amplitude of population Y after the addition of 50 μ L ginger juice, (C) a histogram displaying the frequency of contractions of the population Y duodenum after a 50 μ L volume of ginger juice was applied to the tissue bath.	166
Figure 59. Two traces from proximal stomach before and after two "low" volumes (50 μ L) of ginger juice were added showing the two different responses to ginger juice.	168

Figure 60. Line graphs displaying: (A) the tone of all the proximal stomach before and after the addition of two volumes of 50 μ L ginger juice (B) the tone of the proximal stomach before and after the addition of both volumes of 50 μ L ginger juice with population X and Y (C) box and whisker plots the contraction amplitude of all the proximal stomach before and after the addition of two volumes of 50 μ L ginger juice (D) histogram of the frequency of contractions from the proximal stomach after receiving two volumes of 50 μ L ginger juice.	170
Figure 61. 60 minute original traces from two different distal stomach preparations before and after two volumes of 50 μ L ginger juice were applied to the tissue baths.	171
Figure 62. Line graphs displaying: (A) the tone of all the distal stomach before and after the addition of two volumes of 50 μ L ginger juice (B) the tone of the distal stomach before and after the addition of both volumes of 50 μ L ginger juice with population X and Y (C) box and whisker plots the contraction amplitude of all the distal stomach before and after the addition of two volumes of 50 μ L ginger juice (D) histogram of the frequency of contractions from the distal stomach after receiving two volumes of 50 μ L ginger juice.	173
Figure 63. Two 60 minute traces from duodenum before and after two 50 μ L volumes of ginger juice were added with the two different responses to ginger juice.	174
Figure 64. (A) Line graph displaying the duodenal tone of population Y before and after addition of two 50 μ L of ginger juice, (B) a graph displaying the duodenal contraction amplitude of population Y after the addition of two 50 μ L ginger juice, (C) a histogram displaying the frequency of contractions of the population Y duodenum after a 50 μ L volume of ginger juice was applied to the tissue bath.	176
Figure 65. Two 30 minute traces from proximal stomach before and after a "high" volume (200 μ L) of ginger juice was added with the two different responses to ginger juice.	177
Figure 66. Line graphs displaying: (A) the tone of all the proximal stomach before and after addition of 200 μ L of ginger juice: (B) a close up of the tone of all the proximal stomach strips before and after addition of 200 μ L of ginger juice: and (C) the tone of both population X and Y of the proximal stomach before and after the addition of 200 μ L of ginger juice.	179
Figure 67. (A) A box and whisker plot for the contraction amplitude of the proximal stomach after a 200 μ L volume of ginger juice was applied to the tissue bath. (B) A histogram displaying the frequency of contractions pre and post application of 200 μ L of ginger juice.	180
Figure 68. Two 30 minute traces from the distal stomach 5 minutes before and 25 minutes after 200 μ L of ginger juice were applied to the tissue baths.	181
Figure 69. Line graphs displaying: (A) the tone of all the distal stomach before and after addition of 200 μ L of ginger juice: (B) the tone of both population X and Y of the distal stomach before and after the addition of 200 μ L of ginger juice. (C) A box and whisker plot for the contraction amplitude of the distal stomach after a 200 μ L volume of ginger juice was applied to the tissue bath. (D) A histogram displaying the frequency of contractions pre and post application of 200 μ L of ginger juice.	183
Figure 70. A 30 minute trace from a duodenum before and after a "high" volume (200 μ L) of ginger juice was added with the response to ginger juice.	184
Figure 71. Line graphs displaying: (A) the tone of all the duodenum segments before and after addition of 200 μ L of ginger juice and the Krebs' control: and (B) a close up of the tone of all the duodenum segments before and after addition of 200 μ L of ginger juice and the Krebs' control.	187

Figure 72. (A) A graph for the contraction amplitude of the duodenal segments after a 200 μL volume of ginger juice was applied to the tissue bath. **(B)** A close up of the tone of all the duodenum segments before and after addition of 200 μL of ginger juice **(C)** A histogram displaying the frequency of contractions of the duodenal segments pre and post application of 200 μL of ginger juice.188

Figure 73. Two traces from proximal stomach before and after two volumes of ginger juice, a “low” volume (50 μL) followed by a “high” volume (200 μL), was added with the two different responses to ginger juice.190

Figure 74. Line graphs displaying: **(A)** the tone of all the proximal stomach before and after the addition of 50 μL and 200 μL ginger juice **(B)** the tone of the proximal stomach before and after the addition of 50 μL and 200 μL ginger juice with population X and Y **(C)** box and whisker plots the contraction amplitude of all the proximal stomach before and after the addition of 50 μL and 200 μL **(D)** histogram of the frequency of contractions from the proximal stomach after receiving 50 μL and 200 μL of ginger juice.192

Figure 75. Two traces from distal stomach before and after two volumes of ginger juice, a “low” volume (50 μL) followed by a “high” volume (200 μL), were added showing the two different responses to ginger juice. ...193

Figure 76. Graphs displaying: **(A)** the tone of all the distal stomach before and after the addition of 50 μL and 200 μL ginger juice **(B)** the tone of the distal stomach before and after the addition of 50 μL and 200 μL of ginger juice with population X and Y **(C)** box and whisker plots of the contraction amplitude of all the distal stomach before and after the addition of 50 μL and 200 μL **(D)** a histogram of the frequency of contractions from the distal stomach after receiving 50 μL and 200 μL of ginger juice.195

Figure 77. A trace recorded from the duodenum before and after two volumes of ginger juice was added, a “low” volume (50 μL) followed by a “high” volume (200 μL).196

Figure 78. (A) A graph displaying the duodenal tone of population Y before and after addition of two different volumes of ginger juice, **(B)** a graph displaying the duodenal contraction amplitude of population Y after addition of two different volumes of ginger juice, **(C)** a histogram displaying the frequency of contractions of the population Y duodenum after addition of two different volumes of ginger juice.198

Figure 79. (A) A line graph displaying the tone of all the proximal stomach before and after addition the element solution or the Krebs’ control. **(B)** A box and whisker plot of the contraction amplitude of the proximal stomach after the element solution. **(C)** A histogram displaying the frequency of contractions pre and post application of the element solution.....201

Figure 80. (A) A line graph displaying the tone of the distal stomach before and after addition the element solution or the Krebs’ control. **(B)** A box and whisker plot of the contraction amplitude of the distal stomach after the element solution. **(C)** A histogram displaying the frequency of contractions pre and post application of the element solution on the distal stomach.202

Figure 81. (A) Line graph displaying the duodenal tone after the element solution against the Krebs’ control, **(B)** a graph displaying the duodenal contraction amplitude after the addition of the element solution, **(C)** a histogram displaying the frequency of contractions of the duodenum after the element solution added to the tissue bath.203

Figure 82. (A) Line graph displaying the proximal stomach tone after the addition of [6]-gingerol ($1.59 \times 10^{-5}\text{M}$) and the vehicle, **(B)** a box and whisker plot displaying the proximal stomach contraction amplitude after the addition of [6]-gingerol ($1.59 \times 10^{-5}\text{M}$), **(C)** a histogram displaying the frequency of contractions of the proximal stomach after the addition of [6]-gingerol ($1.59 \times 10^{-5}\text{M}$).....206

Figure 83. (A) A line graph displaying the tone of the distal stomach before and after addition of [6]-gingerol (1.59x10 ⁻⁵ M) and the [6]-gingerol vehicle. (B) A box and whisker plot of the contraction amplitude of the distal stomach after the addition of [6]-gingerol (1.59x10 ⁻⁵ M). (C) A histogram displaying the frequency of contractions pre and post application of [6]-gingerol.....	207
Figure 84. (A) Line graph displaying the duodenal tone after the addition of [6]-gingerol (1.59x10 ⁻⁵ M) and the vehicle, (B) a graph displaying the duodenal contraction amplitude after the addition of [6]-gingerol (1.59x10 ⁻⁵ M), (C) a histogram displaying the frequency of contractions of the duodenum after the addition of [6]-gingerol (1.59x10 ⁻⁵ M) and the vehicle.	208
Figure 85. (A) Line graph displaying the proximal stomach tone after the addition of [6]-gingerol (1x10 ⁻⁴ M) and the Krebs' control, (B) a box and whisker plot displaying the proximal stomach contraction amplitude after the addition of [6]-gingerol.	211
Figure 86. (A) A line graph displaying the tone of the distal stomach before and after addition of [6]-gingerol or [6]-gingerol vehicle. (B) A box and whisker plot of the contraction amplitude of the distal stomach after the addition of [6]-gingerol. (C) A histogram displaying the frequency of contractions pre and post application of [6]-gingerol.	212
Figure 87. (A) Line graph displaying the duodenal tone after the addition of [6]-gingerol (1x10 ⁻⁴ M) and the vehicle, (B) a graph displaying the duodenal contraction amplitude after the addition of [6]-gingerol (1x10 ⁻⁴ M), (C) a histogram displaying the frequency of contractions of the duodenum after the addition of [6]-gingerol (1x10 ⁻⁴ M).	214
Figure 88. (A) Line graph displaying the proximal stomach tone after the addition of the "faux" ginger juice and the Krebs' control, (B) a box and whisker plot displaying the proximal stomach contraction amplitude after the addition of the "faux" ginger juice.	218
Figure 89. (A) A line graph displaying the tone of the distal stomach before and after addition of "faux" ginger juice and the vehicle. (B) A box and whisker plot of the contraction amplitude of the distal stomach after the addition of "faux" ginger juice. (C) A histogram displaying the frequency of contractions pre and post application of "faux" ginger juice.	219
Figure 90. Line graphs (A) displaying the duodenal tone after the addition of "faux" ginger juice and the vehicle, (B) displaying a close up of the duodenal tone after the addition "faux" ginger juice.	220
Figure 91. Graphs (A) displaying the duodenal contraction amplitude after the addition of "faux" ginger juice, (B) displaying a close up of the duodenal contraction amplitude after the addition "faux" ginger juice. (C) A histogram displaying the frequency of contractions of the duodenum after the addition of "faux" ginger juice.	221
Figure 92. The effect of the test substances on the percentage of the original tone at 5 and 25 minutes on the (A) proximal stomach and (B) distal stomach.	235
Figure 93. The effect of the test substances on the percentage of the original duodenal parameters at 5 and 25 minutes (A) tone (B) contraction amplitude and (C) frequency of contractions per minute.	235
Figure 94. <i>Suncus murinus</i> on the reciprocal shaker.	249
Figure 95. Horizontal scatter plots depicting the latency and the emetic episodes during 10 minutes exposure to motion on (A) female and (B) male <i>S. murinus</i>	253
Figure 96. (A) A horizontal scatter plot of the latency of emetic episodes after motion; and (B) a bar graph of the number of emetic episodes in the separated groups a week prior to the addition of the treatments.	254

Figure 97. (A) A box and whisker plot displaying the effect of the vehicle, administered via an intragastric tube 1 hour prior to motion, on the latency of emetic episodes compared to the previous week when no drug was applied. (B) A bar chart displaying individual *S. murinus* latency of emetic episodes after the vehicle and motion and motion only.255

Figure 98. (A) A box and whisker plot displaying the effect of the vehicle, administered via an intragastric tube 1 hour prior to motion, on the number of emetic episodes compared to the previous week when no drug was applied. (B) A bar chart displaying individual *S. murinus* number of emetic episodes to the vehicle.256

Figure 99. (A) A horizontal scatter plot displaying the latency of the emetic episodes for each of the treatment groups. (B) A box and whisker plot displaying the number of emetic episodes for each of the treatment groups.257

List of Equations

Equation 1. To determine the % *IoF*.107

List of Tables

Table 1. A list of a sample of studies investigating the anti-tumour, anti-inflammatory, and anti-oxidant activities of various ginger extracts and constituents.	20
Table 2. A summary of studies on ginger and motion sickness in humans.	35
Table 3. Reagents and solvents used throughout Chapter 2.....	46
Table 4. A list of instruments used throughout Chapter 2.	47
Table 5. Vitamin E sample preparation details.....	48
Table 6. The HPLC gradient system developed for the identification of VE.....	53
Table 7. The gradient HPLC system developed for the calibration curves and identification of VE and 6G concentrations.....	54
Table 8. 6G and VE sample preparation details.	54
Table 9. The different ratios of Cu(II) ions to 6G.	58
Table 10. VE calibration curve and the R ² value: variations by section.....	63
Table 11. The R ² values for different areas of the 6G calibration curve.....	67
Table 12. 6G concentrations in the unspiked and spiked ginger juice solutions after 0 hours and 48 hours.	68
Table 13. The estimated concentration of 6G in the methanolic ginger extracts.	69
Table 14. Comparison of the integration of peaks found in the ginger capsule and the ginger extract.	70
Table 15. Vanillin sulfuric acid reagent R _f values on the hexane : diethyl ether TLC plates and toluene : ethyl acetate TLC plates.	75
Table 16. ¹ H NMR reference table.....	77
Table 17. The percentage and concentrations of gingerols, shogaol and galanolactone in various extracts of ginger (<i>Zingiber officinale roscoe</i>).	88
Table 18. Reagents and solvents used in Chapter 3.	99
Table 19. A list of instrumentation used throughout Chapter 3.	101
Table 20. The contents in cuvette for each set.	102
Table 21. The% <i>IoF</i> levels for Cu(II) ions:[6]-gingerol at 1.5:0 and 1.5:1 ratios.	109
Table 22. Reagents and solvents used in Chapter 4.	133
Table 23. A list of instruments used throughout Chapter 4.	134
Table 24. A summary of the effects of the test substances on the proximal stomach; tone, contraction amplitude and frequency of contractions.	231
Table 25. A summary of the effects of the test substances on the distal stomach; tone, contraction amplitude and frequency of contractions.	232
Table 26. A summary of the effects of the test substances on the duodenum; tone, contraction amplitude and frequency of contractions.	233
Table 27. Reagents used in Chapter 5.	248
Table 28. A list of instruments used throughout Chapter 5.	248
Table 29. The mean latency of emetic episodes and the number of emetic episodes.	253
Table 30. The latency and number of emetic episodes in each of the treatment groups and the pre-screened animals.	258

Abbreviations

5-HT	5-Hydroxytryptamine / Serotonin
5-HT₃ RA	5-HT ₃ Receptor-Antagonist
6G	[6]-Gingerol
ANOVA	Analysis of Variance
AT_n	Averaging Time for Non-Carcinogens
ATP	Adenosine Triphosphate
AUC	Area Under Curve
Caco-2	Human Colonic Carcinoma Cells
CCK	Cholecystokinin
CINC-1	Cytokine-Induced Neutrophil Chemoattractant-1
CINV	Chemotherapy-Induced Nausea and Vomiting
CMC	Carboxymethylcellulose
CNS	Central Nervous System
COX-2	Cyclooxygenase-2
CuCl₂	Cupric Chloride
Cu(II) ions	Cupric ions
CuZnSOD	Copper-Zinc Superoxide Dismutase
DHFR	Dihydrofolate Reductase
DMEM	Dulbecco's modified Eagle's medium
DMSO	Dimethyl Sulfoxide
DPPH	2,2-Diphenyl-1-Picrylhydrazyl
DRC	Dose Response Curve
DS	Distal Stomach
DUO	Duodenum
EC	Enterochromaffin

EC-SOD	Extracellular Superoxide Dismutase
EGCG	Epigallocatechin Gallate
EGG	Electrogastrogram
EGTA	Ethylene Glycol-O,O'- bis(β-aminoethyl ether)-N,N,N',N'-Tetraacetic acid
EHPG	Ethylenebis(Hydroxyl Phenyl Glycine)
EU	European Union
FT-NMR	Fourier Transformed – Nuclear Magnetic Resonance
GC-MS	Gas Chromatography – Mass Spectrometry
GI	Gastrointestinal
H₂O₂	Hydrogen Peroxide
HPLC	High Performance Liquid Chromatography
GC-MS	Gas Chromatography – Mass Spectrometry
GJ	Ginger Juice
ICP-AES	Inductively Coupled Plasma – Atomic Emission Spectrometry
ICP-MS	Inductively Coupled Plasma – Mass Spectrometry
IL-6	Interleukin-6
IL-8	Interleukin-8
iNOS	Inducible Nitric Oxide Synthase
IoF	Inhibition of Formation of Formazan
i.p.	Intraperitoneal
i.v.	Intravenous
I_{sc}	Short Circuit Current
LoD	Limit of Detection

LPS	Lipopolysaccharide
MeOH	Methanol
MHRA	Medicines and Healthcare Products Regulatory Agency
MnSOD	Manganese Superoxide Dismutase
MORI	Market and Opinion Research International
MW	Molecular Weight
NBT	Nitroblue Tetrazolium Dichloride
NK₁	Neurokinin ₁
NO[•]	Nitric Oxide
NOAEL	No-Observed-Adverse-Effect Level
NF-κB	Nuclear Factor kappa B
NMR	Nuclear Magnetic Resonance
NRK-52E	Rat Kidney Cells
NTS	Nucleus Tractus Solitarius
O₂^{••}	Superoxide
[•]OH	Hydroxyl Radical
ONOO⁻	Peroxynitrite
PGE₂	Prostaglandin E ₂
PKC-α	Protein Kinase C – α
p.o.	Per Os (Oral intake)
PONV	Post-Operative Nausea and Vomiting
PS	Proximal Stomach
RCT	Randomised Controlled Trial
R_f	Retention Factor
ROS	Reactive Oxygen Species
RONS	Reactive Oxygen and Nitrogen Species
RTX	Resiniferatoxin
s.c.	Subcutaneously

SEM	Standard Error of the Mean
SOD	Superoxide Dismutase
STAT-1	Signal Transducer and Activity of Transcription-1
TBA	Thiobarbituric Acid
TEAC	Trolox Equivalent Anti-oxidant Capacity
THQ	Target Hazard Quotient
TLC	Thin Layer Chromatography
TNF-α	Tumour Necrosis Factor – α
TPA	12-O-Tetradecanoylphorbol-13-Acetate
TRAIL	Tumour necrosis factor-Related Apoptosis-Inducing Ligand
TRVP1	Transient Receptor Potential Vanilloid
UL	Upper Intake Level
UVB	Ultraviolet B
UTP	Uridine Triphosphate
VE	Vitamin E / α -Tocopherol
WHO	World Health Organisation
WWII	World War II

CHAPTER ONE

INTRODUCTION

1.1 Natural products and health

Some of the best conventional medicines come from nature including aspirin (salicin in willow plants), malaria treatments (quinine from Cinchona bark; artemesin from *Artemisia annua*), treatments for heart conditions (digitalis from *Digitalis purpurea*), leukaemia treatments (vincristine from *Catharanthus roseus*) and morphine (from *Papaver somniferum*) (Royal Botanic Gardens, 2009; Thomas, 2006). The pharmaceutical industry harnesses the beneficial properties from plants leading to drug discovery which are finally used as treatments in conventional medicine (Balunas and Kinghorn, 2005).

A qualitative study conducted by the Medicines and Healthcare products Regulatory Agency (MHRA) and Ipsos MORI (Market and Opinion Research International) reported that the public perception of herbal medicines included words such as “safe”, “natural” and “pure” (MHRA and Ipsos MORI, 2008). One group of participants of a survey reported that the result of taking herbal medicines treated the “whole body” rather than medicines prescribed from the doctors which treated the “symptoms” (MHRA and Ipsos MORI, 2008). There are risks attached to taking herbal medicines as well as benefits. For example taking St John’s wort has been shown to help treat depression. However, it can interact with other prescribed medicines (U.S. National Library of Medicine and National Institutes of Health, 2009). Surprisingly, 36% of those surveyed by the MHRA did not attach risk to taking herbal medicines (MHRA and Ipsos MORI, 2008).

A natural product is a substance produced from natural sources. A plant extract is a substance derived solely from plants. Herbal medicines are comprised of plant extracts and are used to treat symptoms of illness and promote health (Encyclopædia Britannica, 2009; Peters, 2008).

The combination of phytochemicals within herbal remedies may aid the bioactivity of a plant extract. In a review by Houghton, *et al.*, (2007), it has been discussed that the original plant extract may have higher bioactivity when compared to fractions of the extract or vice versa. The former could be due to synergy, where one component could be suppressing a side effect of another. When the original extract is fractioned, the labile compounds may no longer be protected, could become oxidised and no longer bioactive. By contrast, the isolated compounds may not have the same pronounced effect when combined with the original extract (Houghton, *et al.*, 2007).

1.2 Ginger as a plant extract

Ginger root (*Zingiber officinale* Roscoe) is a spice traditionally used in cooking and is renowned for its odour and pungent properties (Evans, 2002; Kim, *et al.*, 2005; Tjendraputra, *et al.*, 2001; Wohlmuth, *et al.*, 2005). The rhizome of ginger is the main area used for medicinal purposes; see Figure 1 (Fleming, 1998). It is either cultivated or grows in the wild in India, West Africa and the Caribbean as well as Southeast Asia.

It has been used as a medicinal aid for at least a century and is used in many cultures including China (Grzanna, *et al.*, 2005; Tapsell, *et al.*, 2006; Young, *et al.*, 2005). The length of time that ginger has been used as Chinese herbal medicine is hard to assess, however ginger is well established within Chinese herbal medicine. Ginger is often taken in either crystallised or biscuit form and recommended to individuals experiencing motion-induced nausea and vomiting (Collins, 2006; Wong, 2009).



Figure 1. A photograph of a ginger rhizome (*Zingiber officinale*).

Fresh rhizomes of ginger were analysed by Jolad *et al.*, (2004) and they detected and identified 63 compounds: with the most abundant being [6]-gingerol. [6]-Gingerol is thought to be one of the main bioactive compounds within ginger. The levels of inorganic elements in ginger have not been widely researched, although soil quality has been shown to affect the elemental uptake of the ginger rhizome (Govender, *et al.*, 2009).

Elements and organic compounds can have either synergistic, antagonistic or no effects on the body. Other plant extracts, for example pomegranate rind extracts, together with cupric sulphate or vitamin C combinations have been shown to work synergistically as an anti-microbial on clinical isolates of *Pseudomonas aeruginosa* (Gould, *et al.*, 2009). Turmeric (*Curcuma longa*) belongs to the same family as ginger, *Zingiberaceae*, and contains the phytochemical curcumin (Norajit, *et al.*, 2007). Curcumin has been shown to mimic enzyme activity when combined with cupric ions (Cu(II) ions) (discussed in detail later) (Barik, *et al.*, 2007). Cu(II) ions can also interact with free radicals and perpetuate the effect of free radicals in the body (Halliwell and Gutteridge, 2001). Therefore there are several areas to focus on; the toxic effect of elements; the proposed beneficial effects of organic compounds and the combined effects of the

elements and organic compounds *in vitro*. Elements and natural products can have both beneficial and toxic effect on the body.

1.3 Selected elements found in ginger

Discussed here are 5 of 30 elements detected which could cause both beneficial and toxic effects when ingested. It is important to measure the levels of these various elements to identify if there are any elements (including heavy metals) which could potentially be toxic over long term exposure. The next section includes illustrative effects of selected elements which have been found in ginger in Chapter 2.

1.3.1 Copper

Copper is an integral part of the superoxide dismutase (SOD) enzyme, and the effects of copper on the body can be both harmful and beneficial (Cherny, *et al.*, 2001; Fisher and Naughton, 2005a). An accumulation of copper in the body is due to Wilson's disease. It is characterised by Kayser-Fleischer rings (a blue ring) around the iris. If not treated early enough it can have detrimental effects on the body including: acute liver failure or neurological problems (Merle, *et al.*, 2007).

The concentration of copper (copper sulfate form) in drinking water was investigated with the acute no-observed-adverse-effect level (NOAEL) of nausea in an international human population (Araya, *et al.*, 2001). The effects were screened for 24 hours with the most common effect being nausea within the first 15 minutes of ingestion. The acute NOAEL was determined to be 4-6 mg/L of copper in drinking water and this is higher than the World Health Organisation (WHO) and European Union (EU) drinking water standards for copper which is 2 mg/L (Araya, *et al.*, 2001; Lenntech, 1998).

1.3.2 Zinc

Zinc has been shown to be both beneficial and detrimental to the body. It is contained within specific reactive oxygen species (ROS) enzymes and stabilises SOD (Halliwell and Gutteridge, 2001). It has been shown to act as a secondary messenger in cell signalling (Yamasaki, *et al.*, 2007). An efflux of zinc is released from within the cell (primarily the endoplasmic reticulum) when mimicking the immune activation of mast cells by stimulating a membrane bound surface receptor, together with an influx of extracellular calcium. This efflux of zinc modulates the high affinity immunoglobulin E receptor (Fcε receptor I) which can, when activated, induce gene expression of interleukin-6 (IL-6) and tumour necrosis factor-α (TNF-α) in mast cells (Yamasaki, *et al.*, 2007). Zinc may also have a role in prostate cancer. Although prostate cancer cells are impermeable to zinc(II) ions, the extracellular zinc(II) ions and zinc-citrate have been shown to advance tumour growth of the prostate. Treatment with chelators for zinc could be beneficial here in reducing the cancer cell growth (Dubi, *et al.*, 2008). Therefore increased zinc (in either supplements or food) in the diet during prostate cancer might be harmful depending upon whether it was absorbed into the circulatory system via the gut.

1.3.3 Silicon

Kolesnikov and Gins, (2001) showed that silicon was detectable in the leaves of 21 medicinal plants in three forms: organic; soluble mineral; and polymeric. In 21 day old female Sprague-Dawley rats with silicon depleted diets there was an increase in longitudinal bone growth, whilst there was a decrease in silicon levels in the tibia (Jugdaohsingh, *et al.*, 2008).

1.3.4 Potassium

Potassium is an essential element for the body's function. When there is depleted potassium in the body, due to taking diuretics for the treatment of high blood pressure for instance or vomiting and diarrhoea, it is called hypokalaemia (National Institute of Health, 2009). Hyperkalaemia is the reverse where there is too much potassium in the blood, caused by severe infection or reduced renal function, e.g. people on dialysis for kidney failure. Both hypokalaemia and hyperkalaemia can cause cardiac arrhythmias (National Institute of Health, 2009). A low level diet of potassium has been linked with an increased risk of stroke, in a prospective study of a representative sample of the US general population; although this low level of potassium could be due to a confounding factor (Bazzano, *et al.*, 2001).

1.4 Organic compounds found in plants and their biological effects

It is essential to know what is in the natural product and how it can interact with biological processes, to identify the active compounds and see if there are any negative effects on the biological system and/or potential interactions with therapeutic medicines. Although a natural product can be known for its beneficial effects due to specific phytochemicals, other compounds can cause detrimental effects. To recommend a natural product for its anti-oxidant/anti-inflammatory activities, a comprehensive view of all the compounds (organic and inorganic) within the natural product is necessary. For example red wine contains resveratrol which has been shown to be very beneficial to the body however there are elements in the wine which might cause harm if ingested regularly over a long period of time (Hague, *et al.*, 2008). Often metal ions have been

shown to bind to the phytochemicals within the natural products and act as an anti-oxidant enzyme mimetic *in vitro* (Barik, *et al.*, 2005). The organic compounds are also thought to have dual effects depending on the concentration both pro- and anti-oxidant. The following are selected examples of relevant organic compounds in natural products.

1.4.1 Gingerols, shogaols and paradols

Gingerols are one of the main constituents of ginger and provide the pungent components in fresh ginger root, whilst the pungency of dried ginger is due to shogaols (Ali, *et al.*, 2008; Wohlmuth, *et al.*, 2005). The odour is mainly due to the volatile oil within ginger which includes monoterpenoids and sesquiterpenoids (Evans, 2002). [6]-Gingerol consists of an aromatic ring, alkyl side chain with a hydroxy and carbonyl group along carbon -3, -5 of the side chain. [6]-Shogaol is a dehydrated form of [6]-gingerol, where the hydroxyl group is replaced with a double bond (Figure 2A,B).

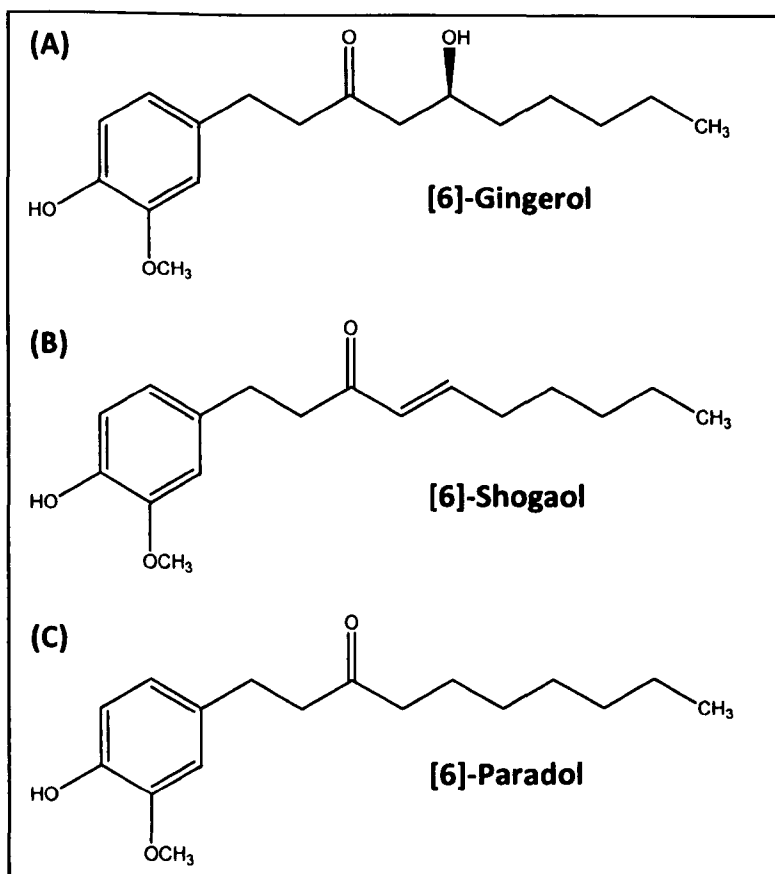


Figure 2. The chemical structure of (A) [6]-gingerol, (B) [6]-shogaol and (C) [6]-paradol.

[6]-Gingerol can be dehydrated to [6]-shogaol and hydrated back to [6]-gingerol in both simulated intestinal fluids and aqueous solutions (Bhattarai, *et al.*, 2007). The inter-conversion between the two compounds mainly depends on the pH in aqueous solutions and pH 4 was found to be the optimum environment for [6]-gingerol to be the most stable (Bhattarai, *et al.*, 2007). This has implications for biological experiments using [6]-gingerol. Because [6]-gingerol could be converted to [6]-shogaol, when the effects of [6]-gingerol are studied the effects of [6]-shogaol should also be considered.

Increased free radical production is involved in chronic inflammatory diseases and neurological disorders. [6]-Gingerol caused an inhibition of nitric oxide (NO[•]) production which was dose dependent and effectively protected against peroxynitrite mediated damage (Ippoushi, *et al.*, 2003). There was also a reduction in inducible nitric oxide synthase (iNOS) protein levels in lipopolysaccharide (LPS) stimulated mouse macrophages due to [6]-gingerol at 2.5 and 25 μM. An increase in NO[•] is due to pro-inflammatory cytokines and other stimuli (e.g. bacteria). If there is a reduction of iNOS production due to a compound it would be regarded as having anti-inflammatory effects. [6]-Gingerol (30 μM), [6]-shogaol and [8]-paradol had inhibitory effects on cyclooxygenase-2 (COX-2) enzyme activity at either 1, 10 and 100 μM (paradols are 5-deoxygingerols) (Kim, *et al.*, 2007; Pan, *et al.*, 2008; Tjendraputra, *et al.*, 2001). Thus the inflammatory mediators downstream of COX-2 will be augmented e.g. prostaglandins and leukotrienes potentially reducing the inflammatory reaction.

The inhibitory effects depended on the structure of the compound: a 14 carbon side chain had the optimal inhibitory activity on the COX-2 enzyme, a hydroxy group on C5 of the side chain contributed to the inhibitory activity and there was strong inhibitory COX-2 activity when there were hydroxyl groups on the C3 or C4 of the aromatic ring

(Tjendraputra, *et al.*, 2001). C57BL/6 mice injected with B16F10 melanoma cells were exposed to [6]-gingerol every other day given via intraperitoneal (i.p.) injection at 100 µg and 5 mg/kg for 3 weeks. [6]-Gingerol significantly reduced the number of colonies of tumour cells in their lungs and surprisingly the vehicle dimethyl sulfoxide (DMSO) increased the number of colonies (Kim, *et al.*, 2005a). [6]-Gingerol is known to have analgesic activities when injected i.p. at 25-50 mg/kg (Young, *et al.*, 2005). Like gingerols, paradols have been shown to have anti-tumour effects (see Table 1 for further information) (Chung, *et al.*, 2001).

[6]-Gingerol, [8]-gingerol, [10]-gingerol and [6]-shogaol were given per os (orally p.o.) to human volunteers between 100 mg and 2 g doses and blood samples were measured at 15 minutes to 72 hours. The compounds were detected from 30 minutes to 60 hours. There were glucuronide conjugates of each of the compounds given however, there were no free compounds detected, and the half-lives in the plasma were less than 2 hours (Zick, *et al.*, 2008). As there were no free compounds detected in the plasma, it suggests that future work on these compounds investigating the inflammatory effect within the body (post absorption) should be focussed on the glucuronide conjugates of [6]-gingerol, rather than of [6]-gingerol alone.

[6]-Gingerol was rapidly cleared from the plasma in rats given intravenous [6]-gingerol (3 mg/kg). The half-life was 7.23 minutes and was removed through renal excretion and partly due to the liver (Ding, *et al.*, 1991; Naora, *et al.*, 1992). Orally administered ginger does take longer to clear the body, as there is interaction with intestinal epithelia and potential metabolism from the bacteria within the gut. [6]-Gingerol (50 mg/kg) was orally administered to male Sprague-Dawley rats and the bile and urine were collected at 12 hourly intervals during the 60 hours post administration

and analysed. The major metabolite was (S)-[6]-gingerol-4'-O- β -glucuronide, whilst there were 6 minor metabolites found in an ethyl acetate extract of urine which had undergone enzymatic hydrolysis, possible by gut flora. Of the [6]-gingerol detected at 60 hours, 48.44% was in the bile and 16.01% was in the urine (Nakazawa and Ohsawa, 2002). In the first 12 hour urine collection period approximately 70% of the [6]-gingerol was detected, indicating that [6]-gingerol is cleared relatively quickly from the body although the plasma concentrations were not monitored here (Nakazawa and Ohsawa, 2002).

In a study by Jiang, *et al.*, (2008), a 240 mg/kg extract of ginger containing 53% [6]-gingerol was administered p.o. to Sprague-Dawley rats. At 10 minutes post dosing the [6]-gingerol concentration in the plasma was 4.23 $\mu\text{g/mL}$. The levels of [6]-gingerol in the tissues were well distributed, with the highest concentrations in most of the tissues at 30 minutes post dosing. The total body clearance of [6]-gingerol was 40.8 hours. [6]-Gingerol was measured by homogenising the tissue, extracting the compound with methanol and injecting the solution onto the high performance liquid chromatography for concentration determination. The tissues with the highest concentration of [6]-gingerol were within the gastrointestinal tract. At 5 minutes, the stomach tissue had ~500 $\mu\text{g/g}$ of [6]-gingerol, whilst at 30 minutes both the intestine and the stomach tissues had ~300 $\mu\text{g/g}$ of [6]-gingerol. It was also detected in the brain at 30 minutes, with a concentration of ~2.3 $\mu\text{g/g}$ (Jiang, *et al.*, 2008). As it was detected within the brain Jiang, *et al.*, (2008) have shown that [6]-gingerol can cross the blood brain barrier, therefore [6]-gingerol may have a direct effect on the nervous system.

1.4.2 Quercetin and Kaempferol

Quercetin is a flavonol and is found in purple grapes (*Vitis vinifera*) (largely the skin and seeds) from which red wine is made, onions and the cocoa element of chocolate

(Lamuela-Raventós, *et al.*, 2001; Slimestad, *et al.*, 2007). Kaempferol is similar in structure to quercetin, see Figure 3 (Ciolino, *et al.*, 1999).

These flavonols have been shown to bind with both Fe(III) and Cu(II) ions; when quercetin was bound to Fe(III) ions the complex was an effective superoxide dismutase enzyme mimetic (Moridani, *et al.*, 2003). Both of these flavonols are found in low levels in the urine of unsupplemented volunteers, indicating absorption of these compounds from the diet. When the urine was subjected to β -glucuronidase there was an increase in the concentration of kaempferol and quercetin which was detected by gas chromatography – mass spectrometry (GC-MS). Therefore much of the absorbed flavonols in a general diet are converted to glucuronides before excretion through urine (Watson and Oliveira, 1999). A synthesised water soluble version of quercetin (QC12) was used in a human healthy volunteer trial. This trial demonstrated that QC12 was not orally bioavailable but when given intravenously there was ~20-25% bioavailability (Mulholland, *et al.*, 2001).

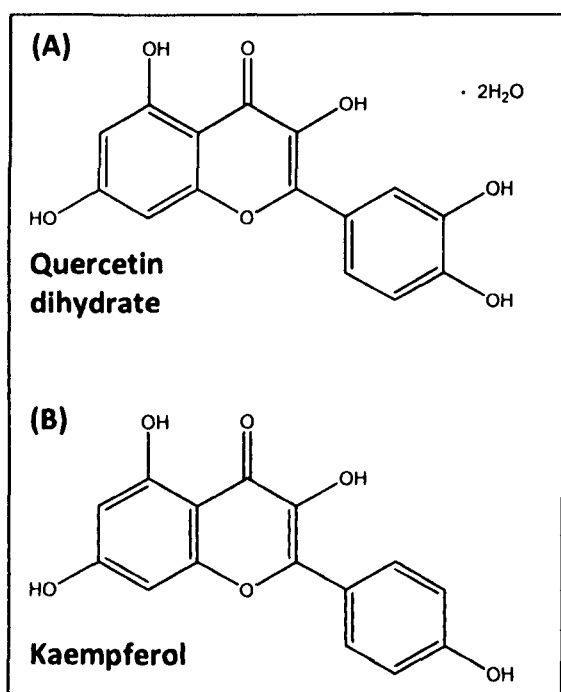


Figure 3. The chemical structure of (A) quercetin dihydrate and (B) kaempferol.

Ion channel secretion has been shown to be modulated by quercetin and kaempferol in rat and mouse colon using Ussing chambers (Cermak, *et al.*, 1998; Cermak,

et al., 2001; Lee, *et al.*, 2005). Quercetin has been reported to induce chloride secretion in rat colon dependent on Ca^{2+} -calmodulin (Cermak, *et al.*, 1998; Cermak, *et al.*, 2000). Chloride ion secretion enables the lumen to be lubricated through osmosis, which aids faecal matter transport in the gastrointestinal tract (Yang, *et al.*, 2008).

Quercetin and kaempferol have been shown to inhibit the activation of transcription factors for iNOS which include: nuclear factor kappa B (NF- κ B); and the signal transducer and activator of transcription-1 (STAT-1). Kaempferol was more effective than quercetin in reducing LPS (100 ng/mL)-induced iNOS protein expression in a 24 hour time period on J774 cells, whereas quercetin was more effective in reducing STAT-1 levels in the same cells (Hämäläinen, *et al.*, 2007). Other compounds were tested for the same properties (isorhamnetin, naringenin, pelargonidin and daidzen), but not all of these compounds inhibited STAT-1 activation compared to kaempferol or quercetin. Therefore there is much dependence on the structure of the flavonol compound and the anti-inflammatory effects it exerts *in vitro*. At high doses it should be noted that quercetin and kaempferol have been shown to be pro-oxidant (Laughton, *et al.*, 1989; Martínez-Flórez, *et al.*, 2002; Sahu and Washington, 1992; Sahu and Gray, 1994).

Quercetin and kaempferol have been shown to affect the transepithelial potential in rat and mouse colon (Cermak, *et al.*, 1998; Cermak, *et al.*, 2001; Lee, *et al.*, 2005). In the colon there is an uptake of water and Na^+ , this causes a charge imbalance between the apical and basolateral membranes. This charge imbalance or potential difference can be measured via the Ussing chamber. In an open circuit colonic epithelium has a voltage of -5 mV, this is due to Na^+ going into the cell on the apical side and 3Na^+ is being pumped out on the basolateral side, whilst K^+ is being pumped out of the cell on the apical side. In a short circuit the voltage can be clamped to 0 mV by applying a current, with periodic

current jumps to ensure the membrane is intact, this current is the net result of all the charges moving. As quercetin was applied there was an increase in the transepithelial potential indicating that the cations are moving to the basolateral membrane. In Chapter 3 the effect of quercetin, kaempferol and [6]-gingerol on a human colonic cancerous cell line was investigated. This was to identify if there was an effect in a human cell line rather than in rat or mouse colon.

1.4.3 Cu(II)-curcumin complexes

Chronic inflammatory conditions have been associated with forming cancers e.g. inflammatory bowel disease-associated colorectal cancer (MacArthur, *et al.*, 2004). Curcumin has been shown to interrupt NF- κ B signalling and may be valuable for the treatment of cancer (Lin and Lin, 2008; Singh and Aggarwal, 1995). Cupric ions have been found to be chelated by curcumin in both a 1:1 complex and a 1:2 (Cu(II):curcumin) complex (Barik, *et al.*, 2007). The Cu(II) ions binds to the two oxygen atoms on the aliphatic side chain of curcumin, see Figure 4. Both complexes were found to exhibit SOD mimicry using the nitroblue tetrazolium dichloride (NBT) assay. The 1:1 complex had a higher SOD activity when compared to the 1:2 complex, 0.17 μ M and \sim 2 μ M, respectively (Barik, *et al.*, 2007). To synthesise the complex the Cu(II) ions were heated to 60°C in dry ethanol for 3 hours under a nitrogen atmosphere with the slow addition of curcumin (Barik, *et al.*, 2007; Barik, *et al.*, 2005). The complex was found to be soluble in lipids, membranes and DMSO whilst it was relatively insoluble in organic solvents (Barik, *et al.*, 2005). Therefore this complex is unlikely to form within the body.

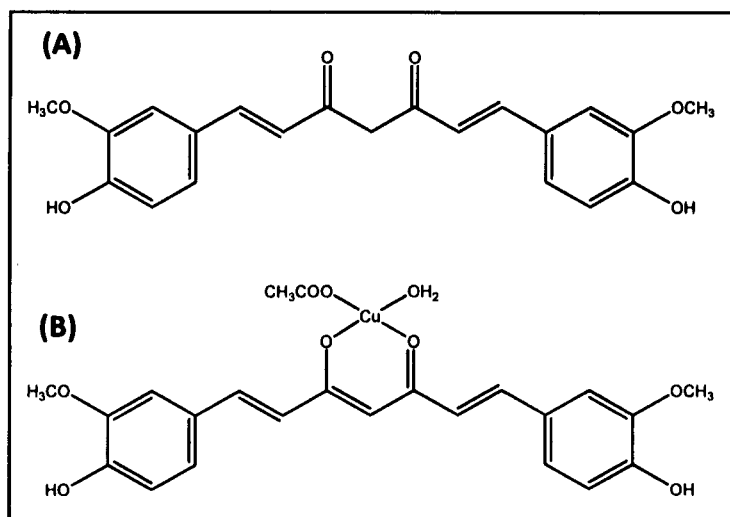


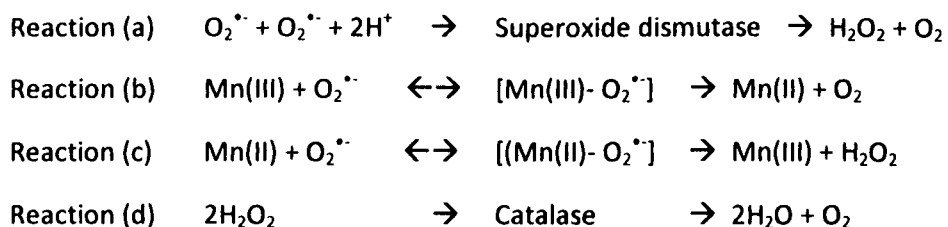
Figure 4. The chemical structure of curcumin and the proposed structure of Cu(II)-curcumin (Barik, *et al.*, 2005).

There have been suggestions that the Cu(II) ions chelating ability of curcumin would be beneficial in Alzheimer's disease, as it could potentially chelate Cu(II) ions (implicated in Alzheimer's disease) and then act as a SOD mimic (Shen, *et al.*, 2005). Although this complex is soluble in lipid environments it is unlikely that the curcumin would bind to Cu(II) ions and form a complex in the body, given the conditions which the complex requires to form being the previously mentioned high temperature and organic solvents. Because [6]-gingerol has carbonyl and hydroxy groups along the alkyl side chain (Figure 2A), there is a possibility that Cu(II) ions could also bind here and have SOD mimicry.

1.5 Catalytic anti-oxidants

Both natural and synthetic anti-oxidants appear to be beneficial to the body although some consumers prefer natural anti-oxidants (Pokorný, 2007). It is necessary for both the organic and inorganic compounds, to be quantified to ensure that there is no hazard to the consumer. It is likely that the safety limits of natural anti-oxidants are similar to synthetic anti-oxidants (Pokorný, 2007).

Redox active metal ions (e.g. Cu(II) and Fe(III) ions) can perpetuate inflammation through reaction with reactive oxygen and nitrogen species (RONS) such as superoxide, $O_2^{\cdot -}$; hydroxyl radical, $\cdot OH$; nitric oxide, NO^{\cdot} ; peroxynitrite $ONOO^-$ and hydrogen peroxide H_2O_2 (Fisher and Naughton, 2003a; Fisher and Naughton, 2003b). Poor metal ion control has been implicated in several neurodegenerative diseases, often increasing redox metal ion concentrations within the cerebrospinal fluid which perpetuates inflammation (Levine, 1997; Strausak, *et al.*, 2001). Mn(II), Cu(II), Zn(II) ions are found in the key anti-oxidant enzymes SOD and Fe(III) ions are found in catalase. SOD dismutates superoxide to hydrogen peroxide and oxygen as shown in reaction (a). There are three different types of SOD *in vivo*; copper-zinc SOD (CuZnSOD) present intracellularly; extracellular CuZnSOD (EC-SOD) found in extracellular fluid and manganese SOD (MnSOD), located within the mitochondria (Halliwell and Gutteridge, 2001). The Mn(II) ions interacts directly with the superoxide radicals, depicted below in reaction (b) and (c) (Halliwell and Gutteridge, 2001). Catalase suppresses H_2O_2 to produce water and oxygen (reaction (d)). Catalase, found in high levels in erythrocytes and in the liver, has four subunits which each contain a ferric haem group. The haem group dissociates from H_2O_2 , which in turn protects the cell (Halliwell and Gutteridge, 2001).



A study by Keane, *et al.*, (2004) suggests that SOD activity levels increase after exposure to SOD mimetics *in vivo* in the nematode *Caenorhabditis elegans*, although this did not increase the lifespan. Natural and synthetic compounds have been shown to

chelate Cu(II) and/or Fe(III) ions *in vitro* and act as SOD and catalase mimetics (Barik, *et al.*, 2007; Fisher and Naughton, 2003a; Fisher, *et al.*, 2004; Fisher and Naughton, 2005b; Moridani, *et al.*, 2003). If these compounds could chelate the excess Cu(II) and Fe(III) ions in inflammatory disorders *in vivo*, that would be a very positive therapeutic approach (Hague, *et al.*, 2006; 2007). Synthetic compounds such as ethylene glycol-O,O'- bis(β -aminoethyl ether)-N,N',N'-tetraacetic acid (EGTA) and ethylenebis (hydroxyl phenyl glycine) (EHPG) bound to Cu(II) and Mn(II) ions (30-100 μ M) were found to reduce paraquat-induced renal cytotoxicity in NRK-52E cells which further indicates that synthetic compounds are effective at scavenging free radicals *in vitro* and are not cytotoxic (Samai, *et al.*, 2008).

In a transgenic mouse model of Alzheimer's disease, the metal chelator, clioquinol, was found to be very effective in reducing the accumulation of β -amyloid which forms plaques (Cherny, *et al.*, 2001). So not only do chelators have anti-inflammatory effects they also used to treat Alzheimer's disease (Hegde, *et al.*, 2009).

1.6 Anti-tumour and anti-inflammatory effects of ginger

The main methods in which ginger extracts and constituents were studied for anti-inflammatory effects include inhibiting: reactive oxygen species; proinflammatory cytokines (e.g. TNF- α); and inhibiting the up-expression of iNOS and COX-2 leading to a reduction in the iNOS and COX-2 enzymes (Ippoushi, *et al.*, 2003; Lee, *et al.*, 2009; Pan, *et al.*, 2008; Tripathi, *et al.*, 2008). These anti-inflammatory effects involve the protein kinase C – α (PKC- α) pathways and the NF- κ B pathways (Lee, *et al.*, 2009). PKC- α , NF- κ B and TNF- α have key roles in inflammation. PKC- α is activated by stress within or around the cell and when activated it is moved from the cytosol to the membrane (Lee, *et al.*,

2009). This then initiates a signalling cascade of proinflammatory cytokine expression. The expression of the COX-2 enzyme is modulated by PKC- α , PKC- α has been shown to activate NF- κ B as has TNF- α (Gao, *et al.*, 2001; Giroux and Descoteaux, 2000). TNF- α can also activate mitogen-activated protein kinase pathways and initiate the cell death sequence. The transcription of iNOS is regulated by several factors including NF- κ B activation (Xie, *et al.*, 1994).

Ginger and several ginger constituents have been reported to exhibit anti-hypertensive effects, and are reported to exhibit anti-emetic, anti-spasmodic, anti-angiogenic, anti-microbial, anti-cancer and anti-inflammatory properties (Chrubasik, *et al.*, 2005; Fleming, 1998; Kim, *et al.*, 2005a; Park, *et al.*, 2006). The anti-hypertensive effects were possibly due to the blockade of voltage-dependent calcium channels (Ghayur and Gilani, 2005a; Ghayur and Gilani, 2006). A study by Surh, *et al.*, in 1998, indicates that the gingerol has anti-tumour properties. When rats were given ginger prior to colon cancer induced with 1,2-dimethylhydrazine, there was no reduction in tumours, although there was a significant decrease in cholesterol levels (Dias, *et al.*, 2006). Several reports have demonstrated that extracts and metabolites of ginger constituents were capable of inhibiting and modulating the pathways of inflammation, see Table 1 for a summary of effects (Aktan, *et al.*, 2006; Ippoushi, *et al.*, 2003; Lantz, *et al.*, 2007; Tjendraputra, *et al.*, 2001).

Acute renal failure in patients with cancer can occur due to chemotherapy treatment with cisplatin. [6]-Gingerol (12.5, 25 and 50 mg/kg) has been shown to dose dependently inhibit cisplatin-induced acute renal failure in rats and reduce the increase of SOD and catalase enzymatic activities due to cisplatin. [6]-Gingerol decreases SOD and catalase levels back to “normal” levels after exposure to cisplatin (Kuhad, *et al.*, 2006).

Cisplatin is also a cause of chemotherapy-induced nausea and vomiting and ginger extracts have been investigated for their anti-nausea and anti-emetic effects, see section 1.8 and 1.9 for further information (Hickok, *et al.*, 2007).

Table 1. A list of a sample of studies investigating the anti-tumour, anti-inflammatory, and anti-oxidant activities of various ginger extracts and constituents.

Compounds	Active concentration	Application	Biological system	Inflammatory stimuli	Result	Reference
[6]-gingerol	2.5 and 25 μ M 0.1, 1, 10 and 100 μ M	In wells	J774.1 murine macrophages	LPS (10 μ g/mL) Peroxynitrite (750 μ M)	Inhibition of iNOS enzyme induction by LPS Inhibited peroxynitrite mediated DNA damage	(Ippoushi, et al., 2003)
[6]-gingerol	100 μ g, 5 mg/kg	i.p. injection	C57BL/6 Mice	B16F10 melanoma cells	Reduced colonies of lung tumour cells	(Kim, et al., 2005a)
[6]-gingerol		Topical	Mice	TPA	Pre-treatment of [6]-gingerol suppressed I κ -B α degradation and p65 translocation reducing NF- κ B transcription activity. By blocking the p38 MAP kinase-NF- κ B signalling pathway COX-2 expression was inhibited	(Kim, et al., 2005b)
[6]-gingerol	30 μ M	Topical	Mice	UVB irradiation (5 kJ/m ²)	Inhibition of COX-2 mRNA and protein induction Inhibition of NF- κ B translocation	(Kim, et al., 2007)
[6]-shogaol and [6]-gingerol	25 μ M each	In wells	3T3-L1 adipocytes	TNF- α	[6]-Shogaol was a PPAP γ agonist and increased PPAP γ transcription activity, [6]-gingerol did not. [6]-gingerol inhibited TNF- α mediated JNK activation	(Isa, et al., 2008)
[6]-gingerol	10 μ M	In wells	MDA-MB-231 human breast cancer cells	N/A	Inhibited metastasis of the breast cancer cells	(Lee, et al., 2008b)
[6]-gingerol	6 and 10 μ M	In wells	Murine macrophages	LPS (100 ng/mL)	Inhibition of LPS induced up-expression of iNOS	(Pan, et al., 2008)
[6]-gingerol	100-4 μ M	In wells	Rat YYT colon cancer cells	N/A	Direct inhibition of colon cancer cell growth	(Brown, et al., 2009)
[10]-gingerol	10-100 mM	In wells	Human colorectal cancer SW480 cells	N/A	[10]-Gingerol caused cell death concentration-dependently – thought to be linked to intracellular calcium levels	(Chen, et al., 2009)
[6]-gingerol	20, 40 and 80 μ M	In wells	RAW 264.7 mouse macrophages	LPS	Dose dependently inhibited ROS and iNOS through suppression of PKC- α and NF- κ B pathways	(Lee, et al., 2009)

[6]-shogaol	6.2 mg/kg on 0.2 mL peanut oil	Orally	Sprague-Dawley rats	Complete Freund's adjuvant which induced monoarthritis	[6]-Shogaol reduced the inflammatory response and protected the femoral cartilage from damage	(Levy, <i>et al.</i> , 2006)
[6]-shogaol		In wells	Mahlavu cells Human hepatoma cells	N/A	Induced cell death by an increase in ROS and decrease of BSH leading to DNA fragmentation	(Chen, <i>et al.</i> , 2007)
[6]-shogaol	6 and 10 μ M	In wells	RAW 264.7 murine macrophages	LPS (100 ng/mL)	Inhibition of LPS induced up-expression of COX-2 and iNOS	(Pan, <i>et al.</i> , 2008)
[3]-, [6]- and [10]-paradol	10 μ M	Topical	Female ICR Mice	TPA	Reduced percentage number of mice with tumours and reduced H ₂ O ₂ production after application of TPA and paradols	(Chung, <i>et al.</i> , 2001)
[6]-paradol	1,10,100 μ M	In wells	Human airway epithelial A549 cells	Arachidonic acid (30 μ M)	Dose dependent inhibition of COX-2 enzyme	(Tjendraputra, <i>et al.</i> , 2001)
Ginger extract	10 μ g/mL	In wells	Human synoviocytes	TNF- α	The extract suppressed chemokine expression	(Phan, <i>et al.</i> , 2005)
Ethanollic dried ginger extract	50-800 mg/kg	i.p. injection	Rats	Injections of 0.5 mL/kg of fresh egg albumin to induce hind paw oedema	Dose related significant decrease in albumin-induced acute inflammation of the rat hind paw by measuring the linear diameter of the rat raw post injection	(Ojewole, 2006)
Aqueous ginger extract	45-720 mg/kg	i.p. injection	Mouse model of inflammation	Ovalbumin injections	Reduced airway inflammation and suppression of Th2-mediated immune responses	(Ahui, <i>et al.</i> , 2008)
Ethanollic ginger extract	100 mg/kg	Oral	Male Wistar Rats	8 week diet of choline deficient food with 0.1% ethionine to induce liver cancer	There was a significant decrease in NF- κ B and TNF- α immunohistochemical staining of tissue samples.	(Habib, <i>et al.</i> , 2008)
Alcoholic ginger extract	1 μ L/mL	In wells	Murine peritoneal macrophages	LPS	Inhibited IL-2, IL- β , TNF- α , RANTES, and MCP-1 production. The extract indirectly inhibited T-cell activation	(Tripathi, <i>et al.</i> , 2008)
Hydroalcoholic extract of ginger	50 - 200 mg/kg/day	i.p. injection	Rat	Collagen induced arthritis	Reduced disease incidence, joint temperature, swelling, cartilage destruction, and serum levels of IL-1 β , IL-2, IL-6 and TNF- α . The highest dose was superior to 2mg/kg/day of indomethacin	(Fouda and Berika, 2009)

DCM extract of dried ginger and gingerol fraction	26 mg gingerols /kg/day	i.p injection	Female Lewis Rats	Streptococcal cell wall-induced arthritis	Both extracts reduced swelling, destruction of articular cartilage and the granulomatous inflammatory response although the DCM extract was more efficacious	(Funk, <i>et al.</i> , 2009)
Hexane ginger extract	1 and 10 µg/mL	In wells	BV2 microglial cells	LPS	Inhibited NO* production and proinflammatory cytokines via the NF-κB pathway	(Jung, <i>et al.</i> , 2009)

COX-2= cyclooxygenase-2; IL = interleukin; iNOS = inducible nitric oxide synthase; LPS = lipopolysaccharide; TPA = 12-O-tetradecanoylphorbol-13-acetate; UVB = ultraviolet B

1.7 Ginger and the gastrointestinal tract

[6]-Gingerol has been shown to induce apoptosis in human colonic carcinoma cells (Caco-2) and other human colorectal cancer cells (Lee, *et al.*, 2008a). In a 2006 report by Abdel-Aziz, *et al.*, the binding effects of gingerols and shogaol on the 5-HT_{3A} and 5-HT_{3AB} receptors in N1E 115 cells were investigated. [¹⁴C] Guanidinium influx mediated by 5-HT_{3A} and 5-HT_{3AB} receptors decreased after addition of gingerols or shogaol. Therefore the compounds were potentially antagonists of the 5-HT_{3A} and 5-HT_{3AB} receptors, as there was a decrease in [¹⁴C] guanidinium in the N1E 115 cells. Gingerols or shogaol did not undergo any competitive binding with other potent 5-HT antagonists therefore gingerols and shogaol may be binding to another area of the 5-HT_{3A} and 5-HT_{3AB} receptors rather than the serotonin binding site.

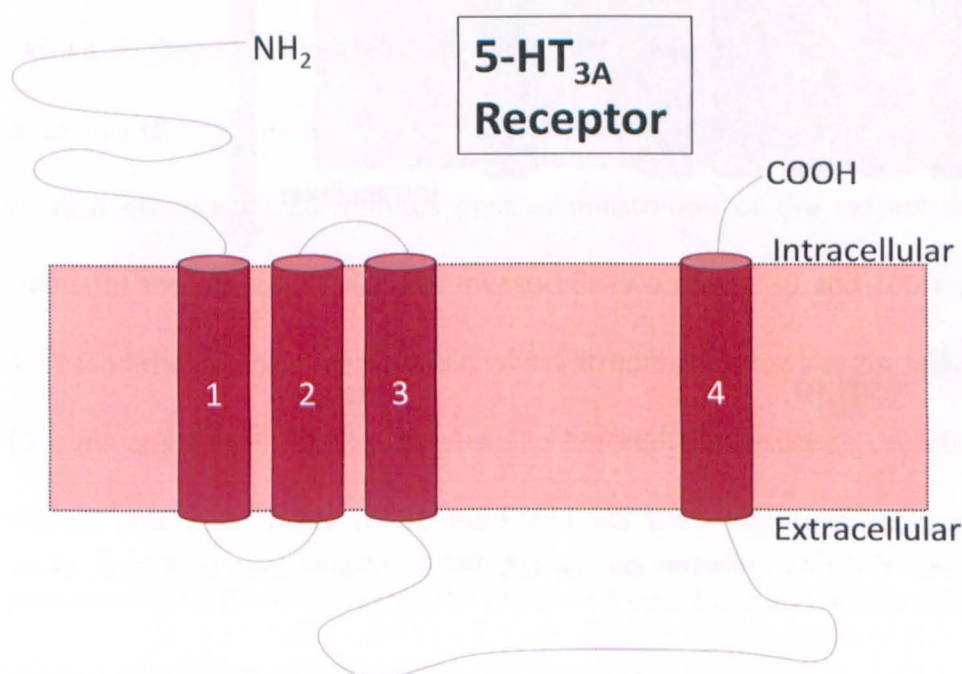


Figure 5. The structure of the 5HT_{3A} receptor adapted from Hu and Lovinger (2005).

There remains uncertainty as to whether [6]-gingerol and the other gingerols and shogaols actually act as 5-HT₃ antagonists, as they do not appear to fully mimic the effects seen from a selective 5-HT₃ antagonist, although the binding of the gingerols and shogaol

to the 5-HT_{3A} and 5-HT_{3AB} receptors is likely (Abdel-Aziz, *et al.*, 2006). The 5-HT_{3A} receptor is comprised of ligand gated ion channels with 4 transmembrane proteins see Figure 5 (Hu and Lovinger, 2005).

A study by Someya, *et al.*, in 2003, suggests [6]-gingerol acts on the vanilloid receptor (TRPV1) on the neurone, the same receptor capsaicin acts on. TRPV1 has six transmembrane domains, a pore loop and 3 ankyrin repeats adjacent to the N terminal, see (Gunthorpe, *et al.*, 2002). TRPV1 is a non selective cation channel, including Ca²⁺ and Na⁺ (Gunthorpe, *et al.*, 2002).

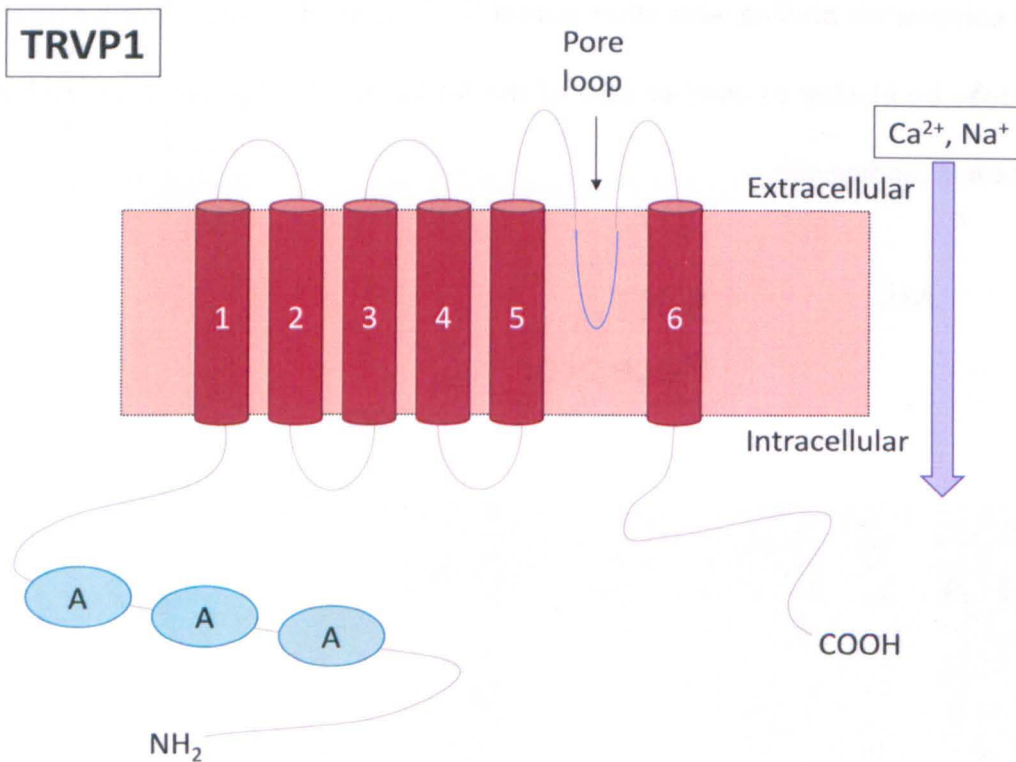


Figure 6. The structure of the non selective ion channel, TRPV1, adapted from Gunthorpe, *et al.* (2002). A = ankyrin.

Cells which have TRPV1 are nociceptors, "pain sensory cells", which are stimulated by capsaicin, resiniferatoxin (RTX) and by heat. Resiniferatoxin, a potent analogue of capsaicin, was first extracted from *Euphorbia resinifera*. Capsaicin and RTX have a similar vanilloid region, which gingerols also contain (structures in Figure 7). Hence, gingerols

may work by the same action as capsaicin and RTX as they are weak TRPV1 agonists (Dedov, *et al.*, 2002).

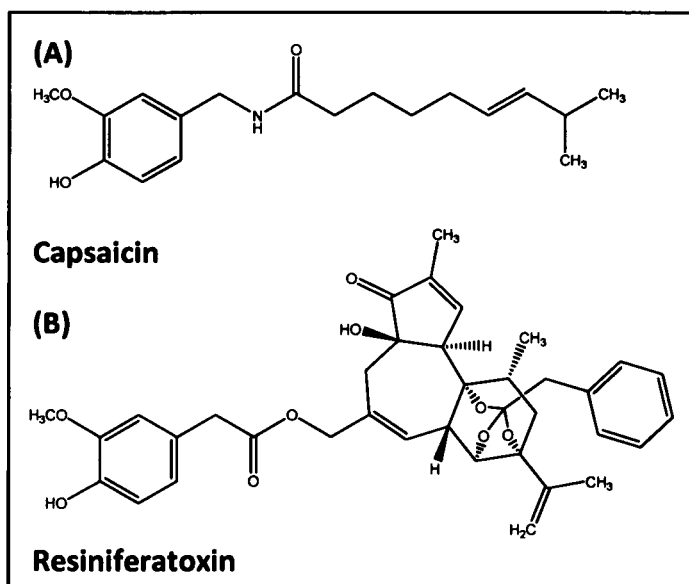


Figure 7. The chemical structures of (A) capsaicin and (B) resiniferatoxin.

Ghayur and Gilani, (2005b) investigated the effect of a 70% aqueous methanolic extract of ginger on the gastrointestinal tract. The extract was administered p.o. to mice prior to a charcoal meal, the upper gastrointestinal tract was excised from the mice after cervical dislocation, 30 minutes post administration of the extract and the length of transit of the charcoal meal was measured. Two doses, 30 and 100 mg/kg, significantly increased the charcoal meal transit, whilst atropine blocked this dose dependent increase (Ghayur and Gilani, 2005b). As atropine blocked the response the effect of the ginger extract was most likely to be mediated via the muscarinic receptors in the upper gastrointestinal tract. Therefore the effect of ginger juice on the two areas of the stomach studied here may be due to muscarinic receptors.

Through the blockade of voltage-dependent calcium channels, an aqueous extract of ginger exhibited both relaxant and stimulant properties on rat, rabbit and guinea pig ileum and rat stomach fundus and rabbit jejunum (Ghayur and Gilani, 2006). There were

differences in responses dependent upon both the regions of the gut tested and the species. The effects of ginger on the rat and rabbit ileum segments were possibly mediated through muscarinic receptors as the stimulatory response was blocked by atropine, unlike the guinea pig ileum (Ghayur and Gilani, 2006). The same group have also identified that the ginger extract may be an agonist for post synaptic muscarinic M3 receptors together with a possible inhibitory action on pre-synaptic muscarinic autoreceptors (Ghayur, *et al.*, 2007b). There are several reports investigating the anti-emetic effect of ginger, so before the effect of ginger can be understood, the following section examines the pathways leading to vomiting and/or nausea.

1.8 Pathways leading to vomiting

Vomiting is emptying of the stomach contents through the mouth by force. The root cause of vomiting can vary from ingestion and absorption of drugs or toxic substances, to pathology within the body (gastrointestinal (GI) or non-GI related), to motion, and finally stimulation of the central nervous system (CNS) (Sanger and Andrews, 2006). Ingested toxic substances/materials within the lumen of the gut can in part stimulate vagal afferents terminating near the mucosa. Once the vagal afferents have been stimulated they activate the nucleus tractus solitarius (NTS) in the dorsal brain stem, and input to the area postrema. Enterochromaffin (EC) cells and other enteroendocrine cells which are found in the mucosa contain cellular mediators including cholecystokinin (CCK), substance P and 5-HT which are released when EC cells detect the toxic (and other) substances (Gershon, 1999; Grundy, 2006). Approximately 90% of 5-HT within the body is stored in the EC cells and when animal models of emesis are exposed to 5-HT, it induces emesis (Torii, *et al.*, 1991).

Suncus murinus, otherwise known as house musk shrews, are used as an animal model of both motion- and chemotherapy- induced emesis. When *Suncus murinus* were exposed to 5-HT (i.p., i.v.), it rapidly induced emesis (Torii, *et al.*, 1991). Therefore, there has been a large focus on 5-HT release and the interaction with the 5-HT₃ receptors on the abdominal vagal afferent terminals which when activated can lead to emesis (Sanger and Andrews, 2006). The receptive fields of the vagal afferents near the luminal surface of the gut are believed to be stimulated by the cellular mediators 5-HT, substance P and CCK.

Toxic exogenous substances absorbed by the body and endogenous substances circulating the body are able to cross the permeable regions of the blood brain barrier. The area postrema in the brain (within the medulla oblongata) is a circumventricular organ, meaning it has an incomplete blood brain barrier: therefore, the absorbed and endogenous substances are able to interact here (Sanger and Andrews, 2006). The outputs from the area postrema to the dorsal brain stem lead to vomiting as shown in Figure 8.

The most accepted explanation as to why people develop motion-induced nausea and vomiting is due to a “toxin detector”. It is hypothesised that in addition to the vestibular functions of maintenance of balance and spatial orientation there is a “toxin detector” within the vestibular system (Golding, 2006). The brain evolved to distinguish any abnormality of expected visual / vestibular patterns to be associated with a CNS malfunction. The body, in defence, instigates vomiting to expel the “toxin” which may be causing the abnormality in visual / vestibular patterns. The ‘toxin’ theory is currently the favoured cause of vestibular stimulation and in evolutionary terms this is the most rational explanation (Golding, 2006).

Nausea is usually a precursor to emesis, in most of the instances above however, the end point is not always emesis. The Oxford English Dictionary describes nausea as “a feeling of sickness, with loathing of food and inclination to vomit” (Simpson and Weiner, 1989). The research and drugs available to treat nausea and vomiting tend to focus more on vomiting than nausea. There is likely to be a common pathway for nausea and vomiting because the anti-emetic drugs are effective against nausea to some degree. It is suggested that another pathway/receptor needs to be identified before nausea can be fully treated (Sanger and Andrews, 2006).

During the twentieth century there was an increased interest in the study of nausea and vomiting, for two main reasons: firstly World War II (WWII) (Tyler and Bard, 1949) and secondly the discovery of the anti-cancer drug cisplatin. In WWII, the increase in the use of planes and boats in military activity, led to an increase in both airsickness and seasickness which would have prevented servicemen from performing their duties appropriately. Between 1940 and 1944, over 100 papers documented motion sickness. They attempted to identify a) the pathways of nausea and vomiting, b) the treatments for this ailment, and c) the susceptible individuals before being given certain duties (i.e. air gunners) (Tyler and Bard, 1949). There are standard anti-emetic drugs to treat motion sickness including: cinnarizine – a histamine H₁ receptor antagonist; metoclopramide – a dopamine D₂ receptor antagonist; and scopolamine – a non-selective muscarinic receptor antagonist (Henry, 2007). These drugs have some side effects including drowsiness and it would be advantageous if natural remedies could be as effective as these drugs without side effects.

The cytotoxic drug cisplatin is very effective as an anti-cancer drug, however, the side effects include acute and delayed nausea and vomiting. Acute phase nausea and

vomiting occurs in the first 24 hours of exposure to chemotherapy, whilst delayed phase nausea and vomiting occurs 3-5 days post chemotherapy. These side effects could not be successfully treated by the most widely used standard anti-emetic metoclopramide at low doses, however at high doses metoclopramide was an effective anti-emetic (Henry, 2007). Although, metoclopramide was effective at high doses in treating vomiting induced by chemotherapy it was not as effective treating nausea (Sanger and Andrews, 2006). As it did not treat nausea, further research was warranted to identify other receptors and drugs which were effective against chemotherapy-induced nausea and vomiting (CINV). One hypothesis suggested for cisplatin-induced vomiting, is that cisplatin stimulates free radical generation within the EC cells. Cisplatin, administered through i.p. injection, has been found to increase thiobarbituric acid (TBA) in the brain, small intestine and liver within 60 minutes in *S. murinus* (Torii, *et al.*, 1993). An increase in TBA indicates an increase in lipid peroxidation. Exposure of *S. murinus* to pyrogallol, a free radical generator, resulted in emesis: a further indication that free radicals are involved in emesis (Torii, *et al.*, 1994). It is hypothesised that the free radicals weaken and rupture the membrane of the vesicles containing 5-HT, thereby causing the release of 5-HT adjacent to the vagal afferent terminals. The 5-HT acts on the 5-HT₃ receptors on the vagal afferent terminals, after which it is believed that the vagus nerve becomes sensitised to the other cellular mediators released. The vagal afferents are stimulated by these mediators and signal to the NTS in the brain stem.

The anti-emetic 5-HT₃ receptor-antagonist (5-HT₃ RA) drugs, bemesetron, granisetron, ondansetron and tropisetron, otherwise known as primary 'setrons' were effective against treating acute CINV, but not delayed phase nausea and vomiting (Jordan, *et al.*, 2007). A newer 5-HT₃ RA, palonosetron, was shown to be efficacious in treating

delayed phase nausea and vomiting, unlike other 5-HT₃ RA such as dolasetron and ondansetron (Eisenberg, *et al.*, 2003; Gralla, *et al.*, 2003). Any 5-HT₃ receptor antagonists are recommended to be taken with dexamethasone, a steroid, in the prevention of CINV as it is beneficial against delayed phase nausea and vomiting (Jordan, *et al.*, 2007). The neurokinin₁ (NK₁) receptor antagonist, aprepitant, is a broad spectrum anti-emetic drug and has been found to be effective against the delayed phase CINV (Navari, 2004; Tremont-Lukats, *et al.*, 2004). These drugs are usually prescribed together to treat both acute and delayed phase CINV. Although, these drugs are effective in treating CINV, there remain other mild and transient side effects to anti-emetics including: headaches, constipation, diarrhoea, dizziness, sedation and anorexia (Jordan, *et al.*, 2007). This is not meant to be a complete list only an indication of the side effects presented. The efficacy of these anti-emetic drugs do need improvement and this is where natural remedies, such as ginger, could provide a useful complement to these treatments. Although the efficacy of ginger when used for nausea is debatable because there are different conclusions drawn in each study, a detailed review suggested that the clinical data are inadequate to obtain firm conclusions (Ernst and Pittler, 2000). However, a meta-analysis investigating the efficacy of using ginger for reducing postoperative nausea and vomiting found 1 g or more of ginger to be more effective than a placebo but not as effective as active medication such as palonosetron (Chaiyakunapruk, *et al.*, 2006).

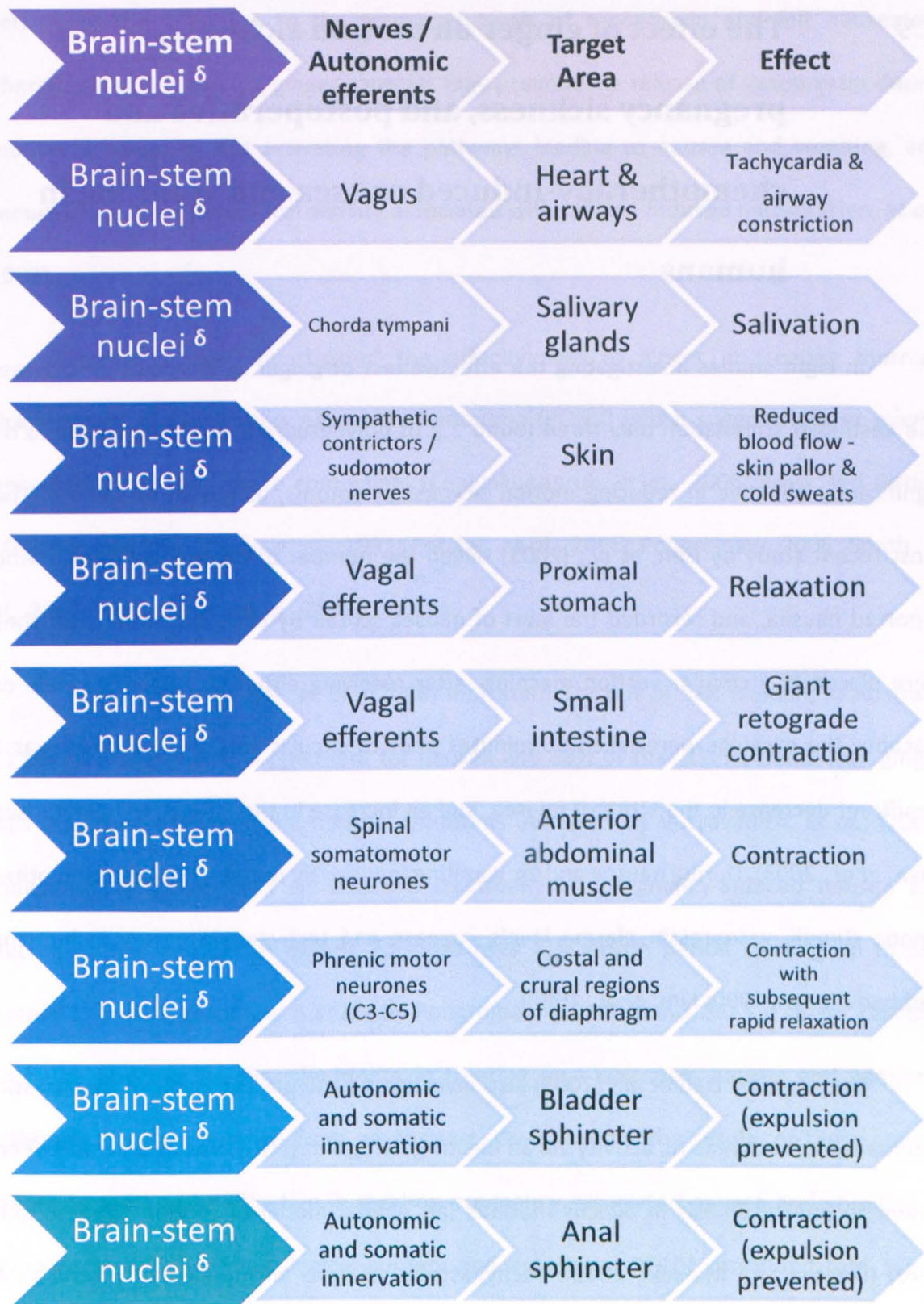


Figure 8. The motor outputs from the brain-stem nuclei after the pathways have been activated. δ = Brain-stem nuclei: Nucleus Tractus Solitarius (NTS); Bötzingner Complex; and Parvicellular Reticular Formation (PRF) (Interpreted from papers by Sanger and Andrews, 2006 and Yates, *et al.*, 1998).

1.9 The effect of ginger on motion sickness, pregnancy sickness, and postoperative and chemotherapy-induced nausea and vomiting in humans

In eight studies investigating the effectiveness of ginger against motion sickness and vestibular stimulation only three found 1 g of powdered/encapsulated ginger to be significantly effective in reducing motion sickness symptoms, as shown in Table 2. The most recent study by Lien, *et al.*, (2003) tallied the number of healthy volunteers who reported nausea, and recorded the level of nausea scored by each individual after they were placed in a circularvection machine, after receiving either the ginger capsule or placebo. The capsules were taken 30 minutes prior to circularvection, and there was a significant decrease in the score of nausea, and an increase in the latency to mild nausea (Lien, *et al.*, 2003). During nausea and/or vomiting induced by motion, cisplatin, and other emetic stimuli, vasopressin plasma levels increase and tachygastria occurs in humans (Cubbedu, *et al.*, 1990; Kim, *et al.*, 1997).

The study by Lien *et al.*, (2003) also investigated the plasma levels of vasopressin and measured tachygastric activity via an electrogastragram (EGG). Vasopressin has been shown to induce emesis in *Suncus murinus* (an animal model of motion sickness and CINV) (Ikegaya and Matsuki, 2002). Tachygastric activity is an increase of gastric slow wave frequency (peristalsis within the stomach). The levels of vasopressin were lower and the tachygastria was decreased significantly after circularvection in the ginger group compared to the placebo group. However, when vasopressin was infused, the ginger capsule did not have the same effect. The participants still experienced an increase in

activity of the EGG due to the increased levels of vasopressin and felt nauseated. Therefore the 1 g and 2 g ginger capsules may prevent the release of vasopressin during motion sickness, by not activating the pathways leading to nausea and vomiting, and reducing the gastric electrical activity associated with motion-induced nausea (Lien, *et al.*, 2003).

Several studies investigated the effectiveness of ginger in treating morning sickness and post-operative nausea and vomiting (PONV) which suggests ginger maybe beneficial in treating these complaints (Chaiyakunapruk, *et al.*, 2006; Ernst and Pittler, 2000; Fischer-Rasmussen, *et al.*, 1991; Forster, *et al.*, 2006; Pongrojapaw, 2006; Smith, *et al.*, 2004; Vutyavanich, *et al.*, 2001).

Research by Forster, *et al.*, (2006) indicated that out of 588 women, in Australia 11.6% took ginger as a supplement for nausea and 83% of that 11.6% found that ginger was effective in treating the nausea symptoms. A report by Vutyavanich, *et al.*, (2001) indicates 1 g ginger was an effective treatment for pregnancy-induced nausea and decreased the number of emetic episodes over a 5 month period starting up to and before 17 weeks gestation. A study by Pongrojapaw (2006) found 2x0.5 g ginger capsules to be as effective as dimenhydrinate in treating post operative nausea and vomiting, although this data is taken from an abstract. Overall, from the results of these studies ginger appears to be effective in treating pregnancy associated nausea and vomiting. A meta-analysis into gynaecological surgery and associated PONV concluded that 1 g of ginger can significantly reduce 24 hour PONV (Chaiyakunapruk, *et al.*, 2006). For pregnancy associated nausea and vomiting the UK government only recommends women to eat little and often to help treat the symptoms. (Directgov, 2009)

In 1999, Micklefield, *et al.*, investigated the effect of ginger on gastroduodenal motility in fasting and fed states of 12 volunteers. Gastroduodenal motility was enhanced by 2x 100 mg ginger rhizome extract capsules in both the fasting and postprandial states. Previously, Stewart, *et al.*, (1991) reported that ginger did not affect gastric emptying rates of a liquid, although the study by Micklefield, *et al.*, using a standardised meal suggests otherwise. A recent study in 2008, by Wu, *et al.*, (2008) found 1200 mg ginger root capsules to be effective on gastric emptying by stimulating antral contractions after a nutrient liquid meal.

The ginger root tablets in the Wu, *et al.*, (2008) report were from Nature's Way Products Inc., the same source as the Lien, *et al.*, (2003) study, which found ginger to be effective against motion sickness. A current phase II/III clinical trial for chemotherapy-induced nausea is underway, where the patients are being treated with ginger together with 5-HT₃ receptor antagonists. It is anticipated that the ginger should improve control of both acute and delayed nausea, and anticipatory nausea (Hickok, *et al.*, 2007).

Table 2. A summary of studies on ginger and motion sickness in humans.

Trial type	Participants	Fasting?	Drugs	Time taken relative to stimuli	Type of stimuli	End Point	Result	Reference
Randomised trial	18 Female 18 Male Age 18-20 Susceptible to motion sickness	Not stated	Powdered ginger (0.94 g) Powdered chickweed (0.94 g) Dimenhydrinate (0.1 g)	20-25 minutes prior to exposure	Revolving chair with magnitude estimations of gastrointestinal sensations	6 minutes in the chair, a three-fold increase in magnitude estimations, request to stop, or vomiting	The ginger group had significantly lower magnitude estimations for gastrointestinal sensations	(Mowrey & Clayson, 1982)
Double-blind comparative trial	16 Male Age 20-44	Not stated	1 g powdered ginger root, 0.0006 g scopolamine hydrobromine, 0.015 g cinnarizine all in gelatine capsules	2 hours prior to exposure	Cross coupled (Coriolis) stimulation of the semi-circular canals, through head movements and acceleration of the horizontal turntable the participants were seated on	A seven point scale rating system was used to rate motion sickness, movement stopped when the participant reached 7	The ginger group was not distinguishable from the placebo on time on the turntable	(Stott, <i>et al.</i> , 1984)
Double-blind randomised cross over trial	8 participants Age 16-56	Not stated	1 g powdered ginger root, 1 g lactose (placebo)	1 hour prior to exposure	Irrigation of the vestibular system and nystagmus was recorded	Nausea	Ginger root did not significantly affect the vestibular system as there was no change in nystagmus compared to the placebo	(Grøntved & Hentzer, 1986)
Double-blind randomised trial	80 healthy naval cadets 79 completed their scorecards correctly Age 16-19	Not stated	Powdered ginger (1 g) Lactose (1 g)	During heavy seas Monitored for 4 hours	Heavy seas on a full-rigged ship with scorecards for seasickness symptoms: nausea; vertigo; vomiting and cold sweating	Nausea and/or vomiting	After 4 hours ginger was significantly effective in decreasing the vomiting and cold sweats scores but only a tendency to decrease nausea when compared to the placebo	(Grøntved, <i>et al.</i> , 1988)

Double-blind randomised trial	8 participants per group Age 18-35	Not stated	1 g fresh minced ginger, 0.5 g and 1 g of powdered ginger root, or placebo and 7 other anti-emetic drugs	2 hours prior to exposure	Contraves Goerz rotating chair monitoring the number of head movements	16 points on the Graybiel scale of motion sickness	Powdered ginger and fresh ginger was not effective in treating NASA motion sickness tests.	(Wood, <i>et al.</i> , 1988)
Double-blind RCT	20 Female 18 Male Age 22-34 Screened prior to selection	Not stated	1 g powdered ginger root (<i>rhizome zingerberis</i> , Zintona®, Pharmaton SA), 0.1 g dimenhydrinate, placebo (lactose) all in gelatin shells	90 minutes prior to exposure	Clockwise and anti-clockwise rotatory chair exposure. Post rotatory nystagmus was measured for 1 minute	3 minutes in the rotatory chair	Ginger root did not reduce the nystagmus response to rotary stimuli, unlike the anti-emetic dimenhydrinate.	(Holtman, <i>et al.</i> , 1989)
RCT	16 Male Age 18-40	Yes - for 12 hours	0.5 g or 1 g ground ginger (McCormick and Co., Hunt Valley, Md.) into capsules 0.0006 g scopolamine HBr or lactose 1 g freshly chopped ginger in a capsule	1 hour prior to exposure for ginger capsules and placebo 30 minutes for Scopolamine HBr	Rotating chair with scoring on the Graybiel scale of motion sickness monitoring the number of head movements	Rotational velocity reaches 35 rpm, 16 points on the Graybiel scale	Fresh and dried ginger was not effective in treating motion sickness. Scopolamine was significantly more effective in treating motion sickness.	(Stewart, <i>et al.</i> , 1991)
Double-blind crossover RCT	10 Female 8 Male – only 13 underwent circular vection Age 18-40 History of motion sickness	Fasted overnight, followed by a meal 30 minutes prior to exposure	1 g or 2 g Ginger capsules (Nature's Way, Springfield, UT) Placebo (Starch)	1 hour prior to exposure	Circular vection Scoring of symptoms of nausea, EGG recordings and plasma vasopressin levels	Nausea	Ginger was statistically significant in reducing nausea and tachygastric activity. The plasma levels of vasopressin were lower in the ginger group	(Lien, <i>et al.</i> , 2003)

RCT = Randomised controlled trial; EGG = Electrogastragram

1.10 The effect of ginger against emesis induced in animals

Akita, *et al.*, (1998) studied the effects of [6]-, [8]-, [10]-gingerol and [6]-, [8]-, [10]-shogaol on chicks in which emesis was induced by copper sulfate solutions administered i.p. It was reported a dose of 50 mg/kg p.o. [10]-shogaol and [6]-gingerol were found to be more effective in inhibiting the number of retches with 69.0% and 58.0% inhibition, respectively (Akita, *et al.*, 1998). In 2002, other diarylheptanoids were investigated in chicks by Yang, *et al.*, only one other extract from *Alpinia katsumadai* was as efficacious as [10]-shogaol. This extract, (3*R*, 5*S*)-*trans*-3,5-dihydroxy-1,7-diphenyl-1-heptene, inhibited the number of retches by 70.8% (Yang, *et al.*, 2002).

Copper sulfate pentahydrate administered p.o. induced vomiting in leopard and ranid frogs and [6]-, [8]- and [10]-shogaols and gingerols were used in an attempt to increase the latency of emesis. The frogs were fed 3 hours prior to the experiments. [10]-shogaol, at 20 mg/kg, was most effective in prolonging the latency of emesis by 146.8%, out of the shogaols and gingerols tested, however methyleugenol delayed the latency by 166.9% (Kawai, *et al.*, 1993). A chloroform extract of *Z. officinale* tested on the frogs prolonged the latency of emesis by 157.4%, though the dose was 1000 mg/kg - a relatively large dose. It is unknown whether by delaying the latency the number of retches was reduced in total. Also, the occurrence and the levels of nausea cannot be determined in frogs or chicks. Although these are avian and amphibian studies, they provide further indications that ginger constituents have the potential to be anti-emetic in humans.

Acetone extracts of ginger were efficacious against cisplatin-induced emesis in dogs, although the 5-HT₃ receptor antagonist granisetron was found to have a higher efficacy. All the dogs vomited when exposed to cisplatin, with each of the treatments. The mean number of emetic episodes decreased at the 100 and 200 mg/kg p.o. doses of the acetone ginger extracts (Sharma, *et al.*, 1997). Granisetron caused a decrease in the mean number of emetic episodes and an increase in the latency to 151.5% of the original latency. The vanilloid aspect of gingerol could be causing the pro-emetic effects, as capsaicin and RTX are both pro-emetic at high doses acting on the TRPV1 receptor (Rudd and Wai, 2001).

Qian, *et al.*, (2009) investigated the anti-emetic effects of gingerol on cisplatin-induced emesis in minks. Gingerol (7.5 mg/kg p.o.) was an effective anti-emetic in minks and was shown to dose dependently down-regulate the expression of 5-HT, dopamine and substance P in the area postrema and ileum. Ondansetron, an effective 5-HT₃ receptor antagonist, did not affect 5-HT release from the minks' ileum, or affect the release of dopamine from the area postrema and ileum of the minks, or affect expression of substance P in the minks' ileum and area postrema (Qian, *et al.*, 2009). There were no significant differences between ondansetron (2mg/kg i.p.) and gingerol (200 mg/kg p.o.) in the number of emetic episodes induced by cisplatin (7.5 mg/kg i.p.) in minks. However, 50 mg/kg (p.o.) of gingerol significantly increased the latency of onset of cisplatin-induced emesis (Qian, *et al.*, 2009). Whereas Yamahara, *et al.*, reported doses of 25 and 50 mg/kg administered p.o. to be effective against cyclophosphamide-induced emesis in *S. murinus* (Yamahara, *et al.*, 1989).

Rats do not have an emetic reflex. When rats are exposed to stimuli they display pica instead (Liu, *et al.*, 2005; Vera, *et al.*, 2006). Pica is the intake of material that has no

nutritional value (Liu, *et al.*, 2005). It is believed that pica occurs when the animal has ingested toxins and is unable to expel these toxins and so ingests non-nutritional material to 'soak-up' these toxins (Liu, *et al.*, 2005). Pica has been used as a model for nausea, however, some animals with the emetic reflex still exhibit pica (chimpanzee, humans), and other animals without the emetic reflex do not (C57 mice) (Liu, *et al.*, 2005). Therefore caution should be taken when analysing the results from a pica model: despite a compound reducing pica it may not necessarily reduce nausea and/or emesis.

Pica is measured by kaolin intake. Kaolin is a non nutritional mineral and a type of clay. Pica does not occur as frequently in rats when they are treated with anti-emetics suggesting that pica works along the same pathways as nausea and vomiting (Takeda, *et al.*, 1993). As well as vomiting, gastroparesis (a delay in gastric emptying) is a side effect of chemotherapeutic drugs which include cisplatin and cyclophosphamide (Hecht, *et al.*, 1997). When exposed to cisplatin rats increased their ingestion of kaolin. Cisplatin also caused a delay in gastric emptying in rats, as well as a release of 5-HT from the enterochromaffin cells, like humans (Sharma and Gupta, 1998).

Thirty minutes prior to administration of cisplatin (10 mg/kg i.p.), acetone and 50% ethanolic extracts as well as ginger juice were administered p.o. to rats. The rats only had access to water 2-24 hours before the experiment. The 50% ethanolic ginger extract did not significantly reduce the gastric emptying delay caused by cisplatin in rats at 100 and 200 mg/kg, although it was significant at 500 mg/kg. The acetone ginger extract (200 and 500 mg/kg) and the pressed ginger juice (2 and 4 mL/kg) were more effective at reducing the gastric emptying delay induced by cisplatin, compared to the ethanolic extract (Sharma and Gupta, 1998). Ginger juice, at 4 mL/kg, almost completely reversed

the effect of cisplatin-induced gastric emptying, and was superior to the treatment of ondansetron (3 mg/kg).

It is interesting that Sharma and Gupta used the natural juice extract as well as the alcoholic extracts of ginger, as many studies focus only on the use of alcoholic extracts. This study indicates that ginger prevents the effect of cisplatin-induced gastroparesis. By the same group, an acetone extract of ginger has also been shown to reverse the same effects caused by pyrogallol, a free radical generator (Gupta and Sharma, 2001).

Anti-oxidant herbs have been used in an attempt to reduce cisplatin-induced pica in rats. This could support the hypothesis that free radicals are involved in cisplatin-induced pica / nausea and vomiting (Mehendale, *et al.*, 2004; Sanger and Andrews, 2006). An extract from *Scutellaria baicalensis* (3 mg/kg i.p.) did significantly reduce the kaolin intake in rats after cisplatin treatment. This suggests there is a role for herbal extracts with anti-oxidant activity in treating CINV.

In conclusion there is partial evidence for the ginger rhizome to be efficacious in humans and animal models for motion sickness, cancer chemotherapy-induced emesis and inflammatory based diseases. There are no *in vivo* studies with ginger in animal models of motion-induced nausea and vomiting in *S. murinus* (an emetic species), nor are there *in vitro* studies on the gastrointestinal tract in *S. murinus* only rodents and lagomorphs. There is only one abstract indicating [6]-gingerol has an effect on short circuit current, indirectly measuring transepithelial ion transport, in rat colonic epithelium (O'Leary, *et al.*, 2004a), further work would be beneficial investigating the effect of [6]-gingerol, quercetin and kaempferol in other colonic monolayers. The ginger juice used in the study by Sharma, *et al.*, (1997) was not chemically analysed. Further chemical analysis of this ginger juice to identify what constituents are bioactive is warranted.

1.11 Objectives

The overarching aim of this study is to investigate key aspects identifying both the detrimental and beneficial effects of ginger extracts on the human condition.

Chapter 2

- To measure the concentration of [6]-gingerol in fresh ginger juice by using analytical HPLC.
- To measure the concentration of metal ions in fresh ginger juice by using ICP-AES.
- To determine the metal binding characteristics of cupric ions to [6]-gingerol using UV-visible absorption spectrometry.
- To use NMR to establish the stability of fresh ginger juice.

Chapter 3

- To investigate the effect of [6]-gingerol, quercetin and kaempferol on the ion channels of Caco-2 cell monolayers using Ussing chambers.
- To investigate the anti-inflammatory effect of [6]-gingerol, a ginger extract and synthetic compounds on NRK-52E and Caco-2 cells.
- To determine the SOD activity of [6]-gingerol when bound to redox active metal atoms by using the NBT assay.

Chapter 4

- To identify the effect of fresh ginger juice, [6]-gingerol, the five elements at highest concentrations in ginger and a “faux” ginger juice on *Suncus murinus* upper gastrointestinal tract motility *in vitro*.

Chapter 5

- To identify the potential anti-emetic effect of oral doses of 3 different concentrations of [6]-gingerol and one dose of a ginger capsule proven to be effective in humans on motion-induced emesis in *Suncus murinus*.

CHAPTER TWO

**EXTRACTION OF GINGER and
ANALYSES OF “CRUDE”
EXTRACTS**

2.1 Introduction

The methods used to analyse ginger rhizome extracts in a number of studies include: thin layer chromatography (TLC); high performance liquid chromatography (HPLC); hydrodistillation; soxhlet extraction; GC-MS; solid-phase microextraction supercritical extraction; electrospray ionization-mass spectrometry and nuclear magnetic resonance (NMR) spectroscopy (Balachandran, *et al.*, 2006; Catchpole, *et al.*, 2003; Jiang, *et al.*, 2005; Rai *et al.*, 2006; Saha, *et al.*, 2003; Schwertner and Rios, 2007; Wagner and Bladt, 2001; Yu, *et al.*, 2007).

The soil quality and elemental uptake of the ginger rhizome were measured by Govender, *et al.*, (2009) who identified a synergistic relationship between the uptake of chromium and manganese and an antagonistic relationship between iron and chromium. The peeled ginger rhizome contained the most manganese and magnesium, and none of the elements identified were found to pose toxicity issues (Govender, *et al.*, 2009).

The levels of certain elements in foodstuffs and beverages could potentially be toxic over a long time period of exposure. There were 2680 food alerts in the UK between January and November 2007, 8% of which were due to metal contamination, which were due to lapses in quality control measures or errors in processing (Laboratory of the Government Chemist, 2007).

Cu(II) ions are able to bind to curcumin on the two oxygen atoms on the aliphatic side chain. This complex was formed under strict conditions with dry ethanol at 60°C for 3 hours in a nitrogen atmosphere (Barik, *et al.*, 2005). It may be possible for Cu(II) ions to bind to the oxygen and hydroxyl group on [6]-gingerol and form a similar complex, if so it may have anti-oxidant activities like the Cu-curcumin complex.

2.1.1 Aims

The aims of this chapter are:

- To quantify the levels of [6]-gingerol in ginger juice and ginger infusions by using HPLC.
- To quantify the levels of elements in ginger juice, ginger and lemon infusions by inductively coupled plasma-atomic emission spectroscopy (ICP-AES).
- To examine ginger juice decomposition by nuclear magnetic resonance (NMR) spectroscopy up to 25 hours from pressing.
- To assess the binding capability of Cu(II) ions to [6]-gingerol by UV-spectroscopy.

2.2 Materials and methods

2.2.1 Materials, chemicals and reagents

The sources of chemicals including grade and batch details are given in Table 3, whilst the instrumentation list used is in Table 4.

Table 3. Reagents and solvents used throughout Chapter 2.

Chemical	Grade	Source	Catalogue Number	Batch
α – Tocopherol from vegetable oil	Type IV	Sigma Aldrich	T1539	
Copper (II) chloride	99%	Sigma Aldrich	203149	
Manganese (II) Sulfate	Cell culture tested	Sigma Aldrich	M1144	084K06431
Zinc Oxide	Meets USP testing specifications	Sigma Aldrich	Z0385	114K0576
[6]-gingerol	98%	Wako Chemical GmbH	074-05061	WKM0536
Dimethyl Sulfoxide (DMSO)	99.5%	Sigma Aldrich	D5879	015K0151
Ginger root capsule		Nature's Way		530519
Vanillin	98%	Sigma Aldrich	94750	
Sulfuric acid	95%	Sigma Aldrich	84716	

Table 4. A list of instruments used throughout Chapter 2.

Instrument	Make	Model	Serial Number	Additional Information
Scales	AandD Instruments	HR-120-EC	13700790	Max 120 g Min 10 mg
Centrifuge	Megafuge 1.0	Heraeus Sepatech		Max Speed 2800min ⁻¹ Max Load 360 g
Fourier transformed NMR	Jeol USA Inc	Eclipse+ 400		Auto-tune 5 mm broad band probe
ICP-AES	Jobin Yvon	Ultima 2C		Running at 40.68 MHz and 1 KW plasma power
RP-C18 HPLC Column	Phenomenex	Sphereclone 5 μ ODS (2)	349981	
Analytical Cartridge System	Phenomenex	SecurityGuard TM		
HPLC Pumps	Varian	Pro-star	04736 and 04737	
UV/visible lamp and detector	Varian	Pro-star	210	
Quadrupole ICP-MS	Agilent Technologies	7500c	JP14100755	Cross flow nebuliser

Batches of ginger root were purchased from local outlets as detailed below. The ginger was refrigerated prior to use, and stored for no longer than 7 days. [6]-Gingerol standards (20 mg, 98%) were obtained from Biomol International and Wako, GmbH. De-ionised water was prepared in house. For HPLC studies high purity grade water was prepared in house by distillation.

2.2.2 Preparation of ginger and stock solutions

Vitamin E: Serial methanolic dilutions of vitamin E (VE) (α -tocopherol) were prepared as detailed in Table 5 to give final volumes of 10 mLs. These stock solutions were refrigerated and protected from light by foil covers, and were used within one month of preparation. HPLC analyses of samples stored for longer than one month indicated decomposition occurred under these conditions, possibly owing to the presence of oxygen or trace transition metal ions.

Table 5. Vitamin E sample preparation details.

Label	mg/L	Concentration (mM)
VA	520.00	1.207
VB	260.00	0.604
VC	130.00	0.302
VD	65.00	0.151
VE1	32.50	0.075
VF	16.25	0.038
VG	8.13	0.019
VH	4.06	0.009

[6]-Gingerol: The samples were acquired from Wako GMBH in oil form in 20 mg aliquots supplied by the manufacturer in photoprotective packaging and were stored frozen at -20°C . Methanolic and DMSO stock solutions of 2 mg/mL were prepared and stored refrigerated and with foil protection.

Ginger: The ginger samples were obtained from seven different locations, from two local shops (LS1 and LS2), Sainsbury's (S), Waitrose (W), a market stall (MS), Somerfield (Som), and Tesco (T). Ginger samples were purchased as a large root, apart from Somerfield and Tesco, where the ginger was already broken into pieces and pre-packaged. After purchase, the largest extending branch of the root was used for analysis, except for Somerfield and Tesco, where the largest piece of ginger was used for analyses.

Ginger Capsules: The contents of the ginger capsules were emptied, weighed to 1 g, and added to 10 mLs of methanol (MeOH). The solution was sonicated for 1 hour (to enhance the dissolving of the capsule), preceding overnight evaporation of the MeOH. The solutions were prepared in MeOH at 1 mg/mL for analyses by HPLC.

Ginger and Lemon Infusions: Three lemons were obtained from Sainsbury's. The lemons were sliced in half with a single slice taken from each and weighed (including the peel and pips). A slice of peeled ginger was taken from three separate rhizomes of ginger: each slice was cut into quarters and weighed. 250 mLs of boiling deionised water were added to each piece of lemon or ginger quarters and brewed for 15 minutes, using acid washed glassware, followed by filter sterilisation. The infusions were stored in the fridge for a maximum of 24 hours prior to analyses by ICP-AES and HPLC.

2.2.3 Methods to extract the ginger rhizome constituents

Several approaches were investigated to determine the optimal method to extract the constituents of ginger as indicated in Figure 9. The principle variations in the methods are in the final extraction: Method 1 – solvent free pressing; Method 2 – pressing combined with solvent extraction; Method 3 – solvent extraction; Method 4 – pre-drying and solvent extraction. Method 1 was chosen selected for further studies as there was no exposure to solvents and this would not affect the experiments in Chapter 4. Methods 2 to 4 are all combined with solvents and were analysed to identify which method produced the highest concentration of [6]-gingerol in fresh and dried ginger.

Method 1: The ginger was peeled, weighed, wrapped in foil, placed within two metal plates (also covered in foil), and the juice was extracted via a 2 ton press (Nie, 2005). The ginger juice (GJ) was collected in a 50 mL centrifuge tube prior to

centrifugation at ~450 g for 15 minutes and filtration with grade 1 Whatman filter paper. The white substance remaining was tested with iodine to identify it as starch. The ginger juice was usually kept and stored in the fridge for up to 6 hours.

Method 2: The ginger was pressed as in Method 1, 1 g of the juice was added to 10 mLs of MeOH and sonicated for 1 hour prior to overnight evaporation of the MeOH. After evaporation, the yellow/brown substance was re-dissolved in MeOH to make 1 mg/mL solutions.¹

Method 3: The ginger was peeled and cut into small pieces (~5 mm³ in size). Sliced ginger (1 g) was added to 10mLs of MeOH, sonicated for 1 hour, filtered and left to evaporate overnight to remove the MeOH. After evaporation, the yellow/brown substance was re-dissolved in MeOH to make 1 mg/mL solutions.

Method 4: The ginger was peeled and cut into ~5 mm³ pieces. Sliced ginger (20 g) was covered in foil and dried in a fan oven for 4 hours at 50°C. The dried ginger (1 g) was subjected to extraction by Method 3.

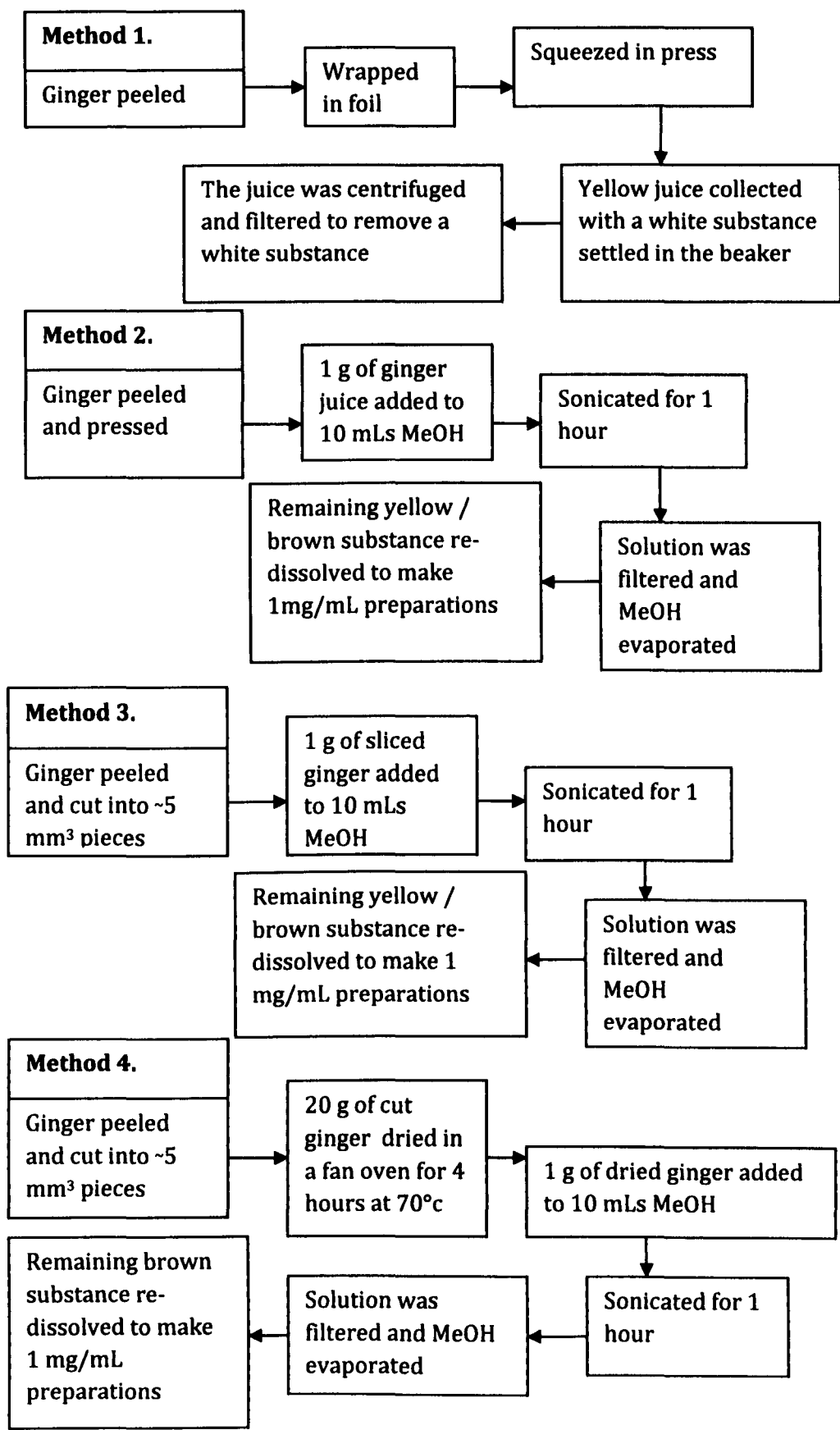


Figure 9. Flow diagrams to show the different methods of ginger extraction.

2.2.4 Modification of an analytical high performance liquid chromatography (HPLC) method for the detection of [6]-gingerol and vitamin E

2.2.4.1 HPLC calibration curve for [6]-gingerol (Method 1)

Stock solutions of [6]-gingerol (6G) were prepared containing 20 mg of 6G in 10 mLs of MeOH, equivalent to 2 g in 1 L (6.79 mM). The following serial dilutions were prepared using HPLC grade MeOH: 1, 2, 4, 10, 16, 32, 64, 100, 160, 320, 640 and 1000 mg/L.

The HPLC instrument was equipped with a RP-C18 column using a MeOH / H₂O eluent, with a ratio of 70:30 respectively. The detector was set at 280 nm for the aromatic moiety. This method was described for the detection of 6G and other compounds in West Indian ginger (Balladin, *et al.*, 1998). 6G eluted at ~4 minutes, however due to pressure build up within the HPLC system, using method 1, the elution time did vary. So a cartridge system was introduced to filter the solution prior to HPLC analysis in Method 2.

2.2.4.2 HPLC assay for Vitamin E (Method 2)

A Phenomenex RP-C18 HPLC SphereClone 5 μ ODS (2) column was purchased for use with an analytical SecurityGuardTM cartridge system attached to a Varian Pro-star pump, with UV/visible detection, capable of detecting dual wavelengths. The Galaxy workstation software for Varian systems version 1.8.508.1 was used to analyse the data.

As the software did not allow temperature control, an internal standard was added to the test solutions, to verify satisfactory column performance. The internal standard selected was VE, owing to structural similarities to 6G, to ensure that the 6G

calibration curve was accurate and to compensate for uncontrollable variables (e.g. temperature).

On application of the VE standard to Method 1, the elution profile was unsatisfactory in the isocratic mode and therefore a gradient method with high methanolic concentrations was developed as shown in Table 6.

Table 6. The HPLC gradient system developed for the identification of VE.

Time (min)	Flow rate (mL/min)	MeOH (%)	H ₂ O (%)
Pre run	1	60	40
3	1	70	30
9	1	100	0
25	1	85	15
28	1	60	40

2.2.4.3 [6]-Gingerol and Vitamin E calibration curves (Method 3)

Method 1, which was developed for separation of 6G could not be feasibly adapted to include VE owing to a poor elution profile. Therefore, Method 2, which allowed detection of VE, was adjusted through modification of the gradient ratios to enable identification of 6G, see Table 7. Again, the mobile phase consisted of MeOH (A): H₂O (B), with the gradient tabulated below. This gradient system was found to give the optimal peaks for both 6G and VE, with the peak for 6G having higher symmetry than originally obtained for Method 1. Peak detection was by UV absorbance at 280 nm corresponding to the aromatic moieties of VE and 6G. The upper pressure limit was set at 2400 psi. Thus, Method 3, which was found to be the optimal method for 6G quantification using VE calibration, was developed.

Table 7. The gradient HPLC system developed for the calibration curves and identification of VE and 6G concentrations.

Time (min)	Flow rate (mL/min)	MeOH (%)	H ₂ O (%)
Pre run	1	55	45
3	1	70	30
9	1	100	0
25	1	90	10
28	1	55	45

The methanolic solutions (V6D) spiked with VE, as shown in Table 8, were injected using HPLC Method 3. At higher concentrations, (> 250 mg/L) the use of VE as internal standard was hampered owing to poor solubility. This restriction affords an upper concentration limit of 250 mg/L of VE for the assay.

Table 8. 6G and VE sample preparation details.

Label	6G	mg/L	Concentration (mM)	VE	mg/L	Concentration (mM)
6A	Y	2000.00	6.794	N	-	-
6B	Y	1000.00	3.397	N	-	-
6C	Y	500.00	1.698	N	-	-
V6D	Y	500.00	1.698	Y	260.00	0.604
V6E	Y	250.00	0.849	Y	260.00	0.604
V6F	Y	125.00	0.425	Y	130.00	0.302
V6G	Y	62.50	0.212	Y	65.00	0.151
V6H	Y	31.25	0.106	Y	32.50	0.075
V6I	Y	15.63	0.053	Y	16.25	0.038
V6J	Y	7.81	0.027	Y	8.13	0.019

Comparative peak analyses were employed to establish column integrity. The peaks of the analyte and standard were routinely monitored to detect changes in the column resulting from solvent impurities or parameter alterations such as temperature fluctuations. If the area under the curve (AUC) values for the VE standards varied by more than twice the standard deviation of the mean, the 6G calibration results were adjusted accordingly by 5-8%, which only occurred on one occasion.

2.2.4.4 Determination of [6]-gingerol concentration in ginger extracts using HPLC

The standard VE (2 mLs of a 520 mg/L solution), was mixed with the filtered GJ (2 mLs). This spiked solution of GJ contained 260 mg/L of VE and half the original concentration of 6G amongst other ginger constituents, and did not affect detection of 6G. The spiked solutions were analysed three times to ensure repeatability, whilst the un-spiked solution was run only once. Injection of spiked and un-spiked GJ resulted in a pressure increase in the column that required insertion of a guard column for protection and stabilization of the pressure. The guard cartridges were changed when the pressure went above 2400 psi. The spiked and un-spiked GJ samples were protected from photo-degradation with foil, and stored on the bench for 48 hours at room temperature. These samples were analysed 48 hours after the original injection into the HPLC system to monitor any degradation which may have occurred. The concentration of 6G in ginger infusion, the ginger capsule and the methanolic extracts (M1, M2 and M4) prepared as described in 2.2.1 and 2.2.2 were also quantified via HPLC Method 3 as it was found to be produced the highest and thinnest peaks for 6G and VE, which indicate high-quality extraction.

2.2.5 Assessment of element concentrations by ICP-AES

The ginger was protected in foil when pressed and the juice was analysed by ICP-AES to detect for 20 elements with limits of detections in mg/L as follows: Al (0.009), Ca (0.020), Cd (0.008), Co (0.005), Cr (0.008), Cu (0.009), Fe (0.010), K (0.020), Li (0.004), Mg (0.020), Mn (0.008), Na (0.020), Ni (0.004), Pb (0.008), Si (0.010), Sr (0.020), Ti (0.008), V (0.005), Zn (0.020) and Zr (0.008). In addition, the elemental profile was required to prepare artificial controls for further *in vitro* studies. The ginger and lemon infusions were

also analysed by ICP-AES and detected the above elements plus P (0.010 mg/L). Prior to use the ICP-AES was calibrated with 50 mg/L standards of Al, Ca, Cd, Co, Cr, Cu, Fe, Mg, Mn, Ni, P, Pb, Si, Sr, Ti, Zn and Zr and 100 mg/L standards of K, Li, Na and V. Results are presented in mg/L with standard errors of the mean (SEM).

After pressing the ginger root, all the samples were centrifuged and filtered to remove the starch and small pieces of ginger so they would not interfere with the readings on the ICP-AES. Aliquots (1 mL) were taken from these filtrates and were made up to 10 mLs with de-ionised water prior to ICP-AES analyses.

ICP-AES analyses were conducted on 10 samples of GJ relating to the *in vitro* work discussed in Chapter 4. ICP-AES was also conducted on the ginger and lemon infusions. T-tests were performed to compare the levels of individual elements within the ginger and lemon infusions.

2.2.6 Thin layer chromatography on ginger samples

TLC was conducted on the methanolic ginger extracts, ginger juice, [6]-gingerol and vitamin E. The extracts and controls were prepared to 1 mg/mL, prior to 20 μ L aliquots of each solution being added to the TLC plates. The first mobile phase consisted of diethyl ether and hexane with a ratio of 40:60, respectively, the second mobile phase was toluene (93) and ethyl acetate (7) (Rai, *et al.*, 2006; Wagner and Bladt, 2001). A photosensitive vanillin sulfuric solution was stored in a brown bottle. It consisted of 6 g of vanillin, in 95 mLs of ethanol, with 3x 0.5 mL additions of concentrated sulfuric acid, which was mixed after each addition to prevent the solution separating. The plates were removed when the solvent front reached ~1 cm from the top of the plate. The vanillin solution was tipped over the plates, individually, and placed on a hotplate at 100°C for 10

minutes. The retention factor (R_f) values were recorded and compared to reference compounds.

2.2.7 Nuclear magnetic resonance spectroscopy

The Fourier transformed – nuclear magnetic resonance (FT-NMR) instrument was used to analyse the potential degradation of ginger juice as there was a loss of bioactivity within 6 hours of squeezing. The ginger juice was squeezed, centrifuged, filtered through celite and cotton wool and pipetted into an NMR tube containing a D_2O insert. To keep the sample pure, instead of spiking the sample with tetramethyl silane (as an internal standard) the presence of the water peak enabled alignment of the chemical shifts detected. The sample was analysed by 1H NMR (1H frequency = 400MHz) spectroscopy on the presaturation setting and was measured three times over a 25 hour period from the original time of pressing the ginger, with spectra taken ~1 hour 45 minutes, 12 hours and 25 hours after pressing. In total three different ginger juice samples were analysed by 1H NMR spectroscopy over a 24 hour period on three different occasions. The data was analysed by the Delta NMR processing software by JEOL USA Inc Version 4.3.6 copyright © 1990-2006 (both on Windows NT and Linux).

2.2.8 Complexation studies of Cu(II) ions by [6]-gingerol

The metal complexation studies were to determine the binding capabilities of Cu(II) ions by [6]-gingerol. Barik, *et al.*, (2005 and 2007) have demonstrated a complex formation between Cu(II)-curcumin, whereby the Cu(II) ions are bound to the keto-enol group with one acetate and one water molecule completing the complex. This complex has been shown to be a superoxide dismutase (SOD) mimic. However, it was noted that the conditions used to prepare this complex were very specific, with the use of dry

ethanol and refluxing under a nitrogen atmosphere (Barik, *et al.*, 2005), or an alternative route in DMSO (Barik, *et al.*, 2007). The 1:1 Cu(II)-curcumin complex was soluble in alkaline water, but insoluble in neutral water. The 1:2 Cu(II)-curcumin complex was insoluble in water over a range of pHs.

2.2.8.1 Job plot of [6]-gingerol and Cu(II) ions

Table 9 displays the ratios of Cu(II) ions and 6G used in the study. The concentration of the cupric chloride (CuCl₂) solution in DMSO was 2 mM, as was the 6G solution. Spectra of the 11 solutions were recorded using the Varian Cary 300 UV/visible spectrophotometer operating between the range of 900 nm-300 nm.

Table 9. The different ratios of Cu(II) ions to 6G.

Cuvette No.	Cu(II) ions (mL)	6G (mL)	Ratio Cu(II) ions	: 6G
0	0	0	-	-
1	0	2	-	-
2	0.2	1.8	1	9
3	0.4	1.6	1	4
4	0.6	1.4	1	2.3
5	0.8	1.2	1	1.5
6	1	1	1	1
7	1.2	0.8	1.5	1
8	1.4	0.6	2.3	1
9	1.6	0.4	4	1
10	1.8	0.2	9	1
11	2	0	-	-

2.2.8.2 Attempts to prepare a complex of Cu(II) ions and [6]-gingerol

Solutions of 6G and CuCl₂ (at 2 mM) were prepared in DMSO or MeOH. They were combined in a 1:1 solution and refluxed under ambient conditions at 70°C ± 5°C for 3 hours. At time 0, 1, 2, and 3 hours the solution was measured by UV/visible spectrometry from 900-300 nm. A golden brown precipitate formed during refluxing. The precipitate was exposed to neutral, acidic and alkaline conditions. The precipitate was added to 10 different solvents and glycerol in attempts to dissolve the precipitate including: toluene;

absolute ethanol; industrial methylated spirit; acetone; ethyl acetate; dichloromethane; methanol; diethyl ether; hexane; and butanol. HPLC was also used to analyse the concentration of 6G before and after refluxing.

2.2.9 Scanning electron microscopy on the [6]-gingerol Cu(II) complex

The scanning electron microscopy (S.E.M.) instrument analysed the solution containing the potential Cu(II)-6G complex. The solution was critical point dried with a Polaron E3000. By using rapid drying varnish a sample of the Cu(II)-6G potential complex was mounted onto flat stubs and sputter coated with gold (Polaron E5075). The dehydrated sample was studied with a JSM-T6310 scanning electron microscope (JEOL) at 80KV. The S.E.M. images were converted from JEOL-ITEX format using Foster Findlay Associates X-Image format conversion software to distortion-corrected bitmaps. The digital images were captured at a resolution of 2 μ m and 200nm.

2.3 Results

2.3.1 Extraction of the ginger constituents

Four methods were explored for the extraction of the ginger constituents: *Method 1*: directly pressing the ginger to obtain the GJ; *Method 2*: pressed ginger combined with solvent extraction; *Method 3*: solvent extraction with freshly sliced ginger; and *Method 4*: pre-drying with solvent extraction. The dehydration method for the sliced ginger samples was explored using a fan- and standard-oven. This investigation revealed the need for a fan-oven for optimum dehydration at relatively low temperatures, which are required to preserve the sample. Thus, within four hours at 50°C, the fan-oven resulted in a reduction of 91.5% of the original sample weight of the ginger root, whereas the standard-oven caused a weight loss of only 16%. It was noticeable in the standard-oven the rate loss was such that it would not achieve 90% weight loss as found for the fan oven. Thus, the fan oven was the most successful way of harvesting the dry ginger samples, whilst the ginger press was the most effective way of acquiring the fresh extract of ginger. However, it is notable that the pressing process and the heating in an oven may result in a loss of the volatile components of the ginger.

Solvent extraction was used on the ginger samples (fresh, dried and juice) to isolate the constituents. However, for solvent extraction the need to remove solvents at a later stage, coupled with potential loss of volatiles, led to the use of the press. The press was the most direct way of obtaining the fresh constituents of ginger. The juice was in its purest form when pressed, which led to this method being chosen. Typically the resulting GJ was centrifuged and filtered for further use unless otherwise stated.

The percentage yield of the oil residue in the fresh ginger sonicated with MeOH was ~2%, whereas the dried ginger provided twice as much [6]-gingerol at ~4% (Figure 10). When these samples were dehydrated, it was notable that the brown residue from the dried ginger and the contents of the ginger capsule displayed similarities in colour, whereas the juice and the methanolic fresh ginger extracts produced a vivid yellow residue. The ginger juice alone produced the highest percentage yield when compared to the other extracts; however this could be due to a higher retention of H₂O within the extract as MeOH was easier to evaporate than H₂O.

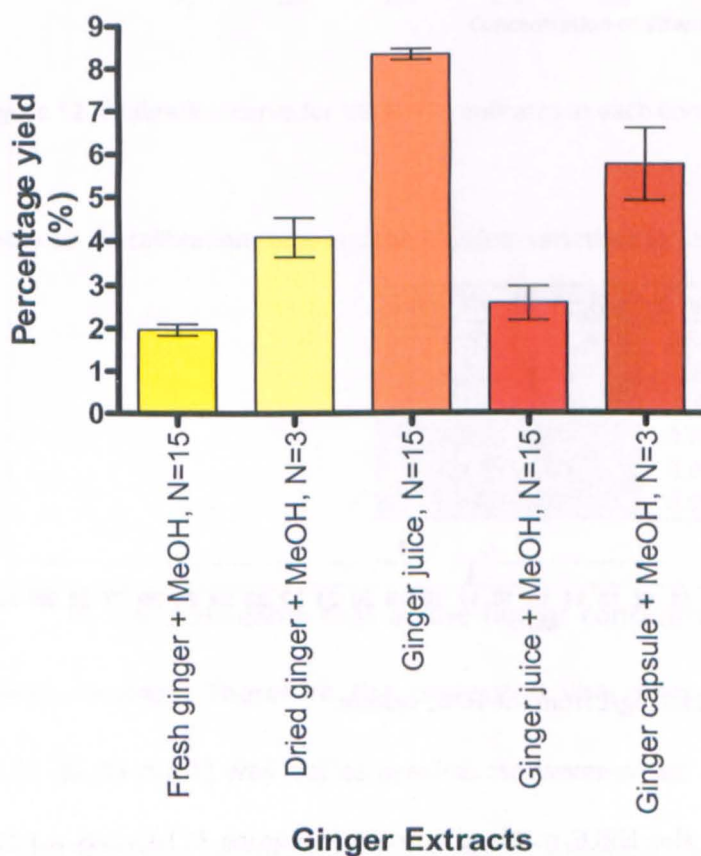


Figure 10. The percentage yield of the ginger extracts as residue. The results are expressed as mean \pm SEM. N = The number of extracts.

2.3.2 Liquid chromatography

2.3.2.1 Development of a calibration curve for vitamin E

The area under the curve values on the HPLC trace after each VE injection were recorded as a function of the concentration of standards to produce a calibration curve. The peaks detected by HPLC were generally automatically integrated. The mean VE retention time was 17.67 ± 0.22 minutes, $N=14$, as shown in Figure 11. There was a minor impurity peak next to the VE peak in this commercial standard which may be a degradation product such as shogaol (Bhattarai, *et al.*, 2001).

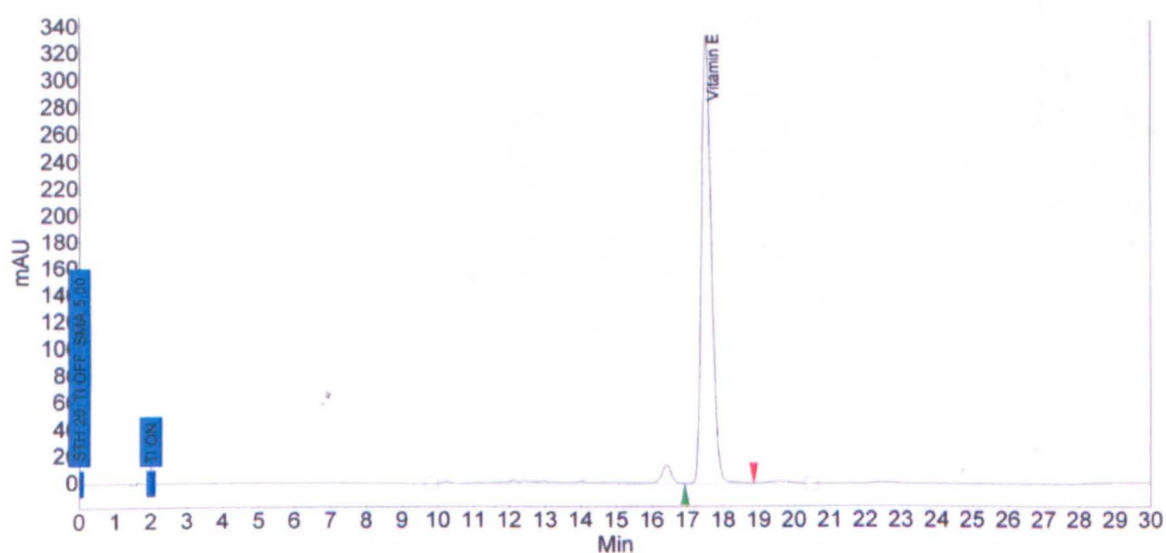


Figure 11. A typical HPLC trace of VE at 250 mg/L from the HPLC system.

The calibration curve from the HPLC method (shown in Figure 11) shows a near unity R^2 value indicating the 'goodness of fit' of the regression line (Table 10). The total R^2 value of 0.9946 represents minimal variance of the data along the regression line. However, variances in the square of the standard deviation are seen along the line of regression. The range of R^2 values is from 0.9837 to 0.998 and it was considered acceptable to use the entire working range, 3.91 – 500 mg/L for analytical purposes.

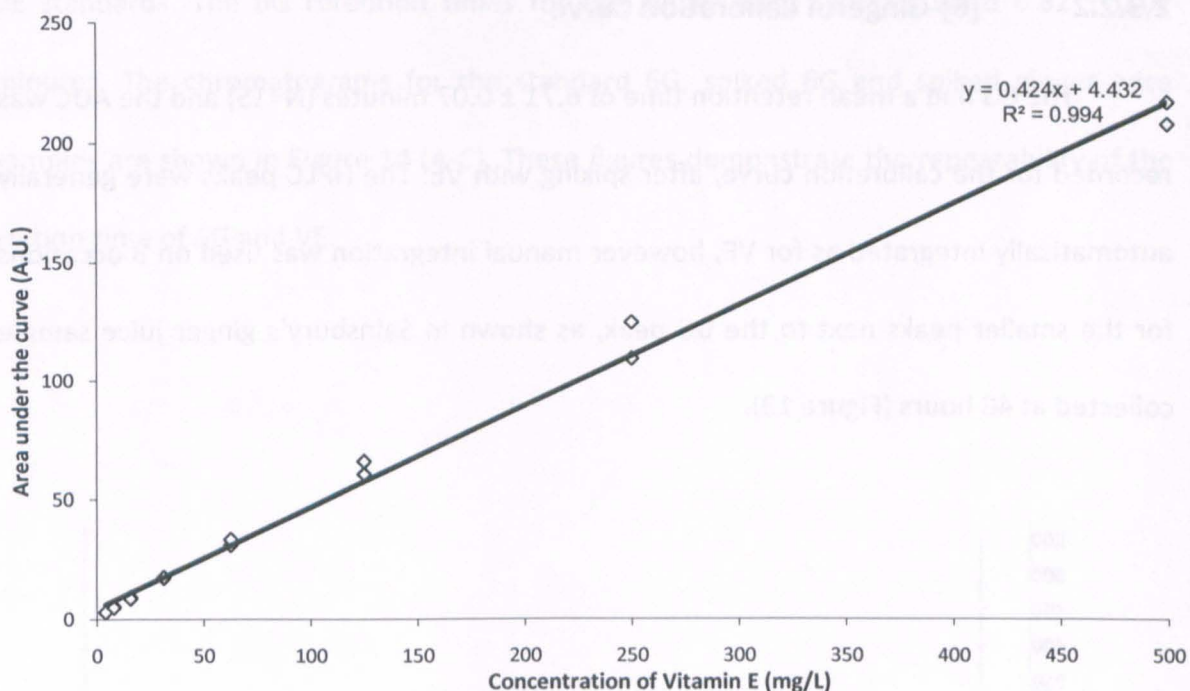


Figure 12. Calibration curve for VE. N = 2 replicates at each concentration.

Table 10. VE calibration curve and the R² value: variations by section.

Concentration (mg/L)	R ² Value
3.91 – 7.81	0.9837
7.81 – 31.25	0.998
31.25 – 125	0.992
31.25 – 250	0.9874
31.25 – 500	0.9939
3.91 – 500	0.9946

It was noticeable that at the higher concentrations (260-520 mg/L) there were fewer readings. Therefore the regression line compared to the lower concentrations (3.91-31.25 mg/L) was not as precise. However when all of the points were included the R² was 0.9946. Therefore, a near unity R² value can be misleading giving a false positive result. Although there were fewer readings at the high concentrations, the majority of solutions analysed did not exceed a concentration of 250 mg/L.

2.3.2.2 [6]-Gingerol Calibration Curve

The 6G had a mean retention time of 6.71 ± 0.07 minutes (N=15) and the AUC was recorded for the calibration curve, after spiking with VE. The HPLC peaks were generally automatically integrated as for VE, however manual integration was used on 3 occasions for the smaller peaks next to the 6G peak, as shown in Sainsbury's ginger juice sample collected at 48 hours (Figure 13).

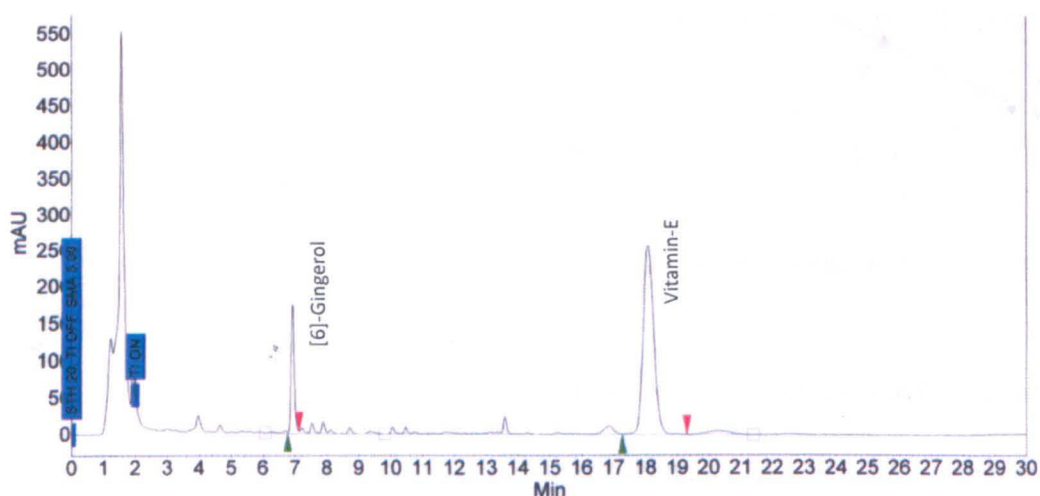


Figure 13. HPLC trace of ginger juice from Sainsbury's collected at 48 hours.

The VE was selected as the internal standard with cross referenced standardisation to the original VE calibration curve. The potential effects of temperature changes on the column necessitated the use of an internal standard to avoid discrepancies. The VE internal standard values were within two standard deviations of the mean for all but one of the 6G spiked standards. In this instance, the spiked standard was lower than two standard deviations at a concentration of 31.25 mg/L for 6G and VE, with the VE result being 5-8% less than the original calibration curve. Thus, the 6G results were adjusted accordingly using percentages. In contrast the 500 mg/L 6G standard solution was not spiked with VE owing to the poor solubility of VE. The average VE retention times for the spiked ginger juice samples were 17.94 ± 0.25 minutes, commensurate with the

VE standards. The 6G retention times for the ginger juice samples were 6.82 ± 0.07 minutes. The chromatograms for the standard 6G, spiked 6G and spiked ginger juice samples are shown in Figure 14 (A-C). These figures demonstrate the repeatability of the elution time of 6G and VE.

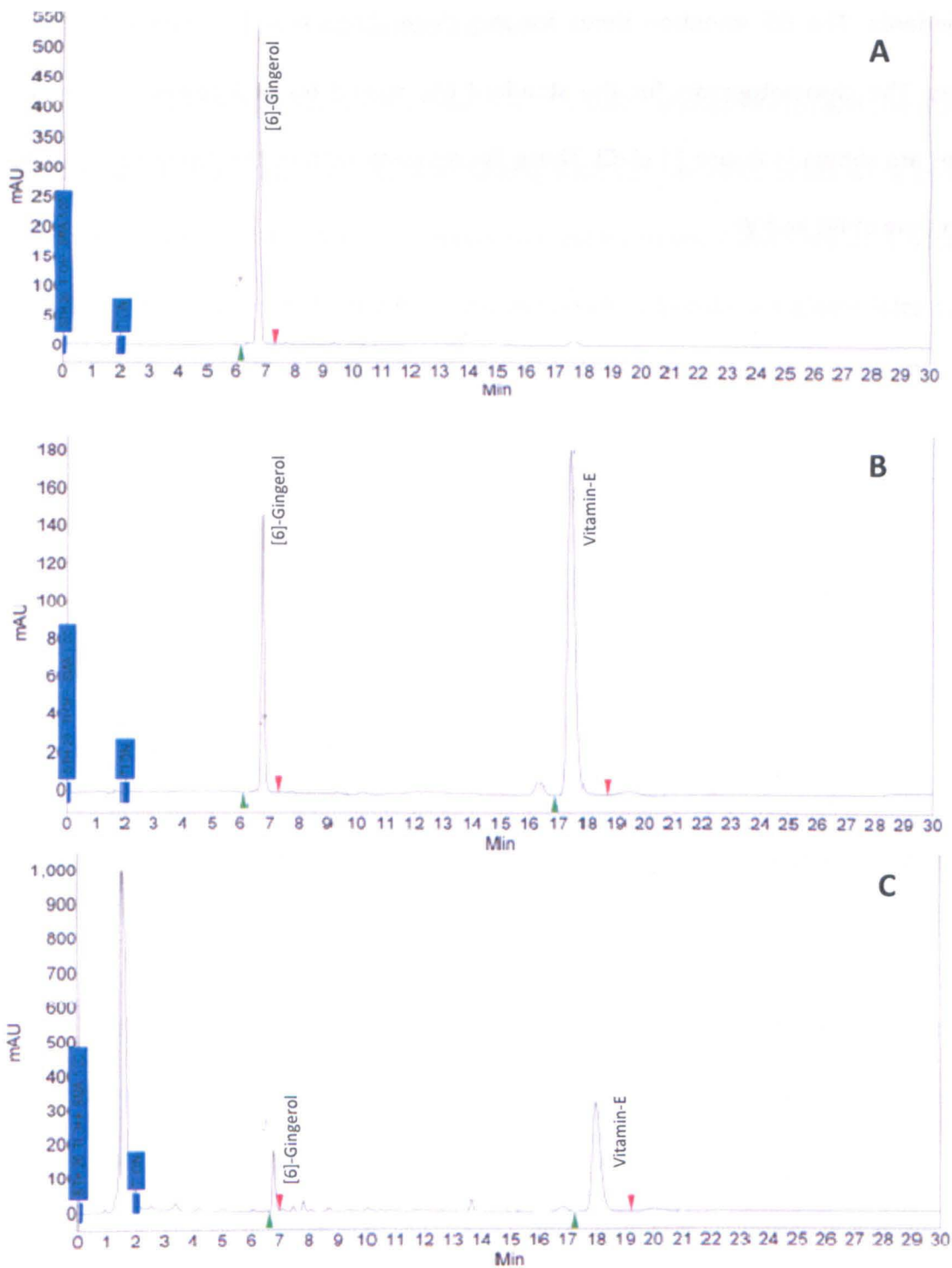


Figure 14. HPLC traces depicting; (A) 6G standard at 500 mg/L; (B) 6G standard spiked with VE both at 125 mg/L; and (C) a ginger juice sample spiked with VE at 250 mg/L.

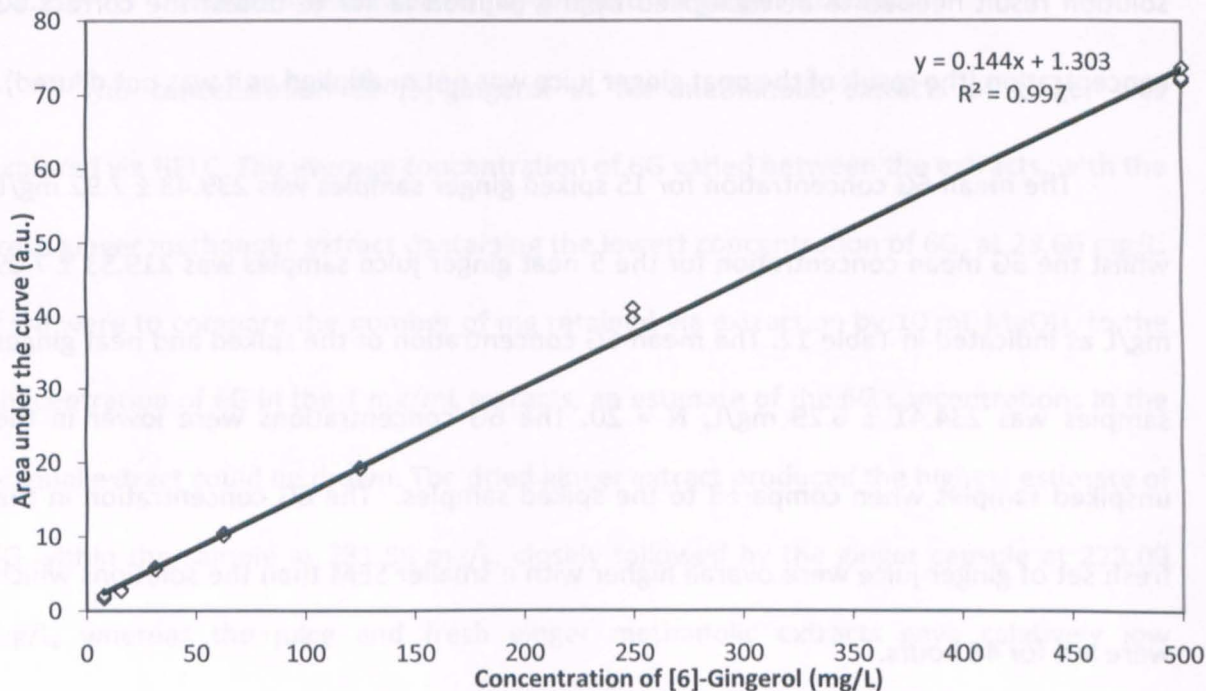


Figure 15. Calibration curve for 6G. N = 2 for each of the concentrations except 500 mg/L where N = 3.

The adjusted calibration curve for the 6G is shown in Figure 15. The R^2 value was 0.997 over the concentration range of 7.81 and 500 mg/L. Again, the areas of the calibration graph were studied in more depth to try to identify the weaker areas i.e. lower R^2 values as shown in Table 11. The analytical working range was between 7.81 – 500 mg/L.

Table 11. The R^2 values for different areas of the 6G calibration curve.

Concentration (mg/L)	R^2 Value
7.81 – 15.63	0.8901
15.63 – 62.5	0.9944
31.25 – 125	0.9994
62.5 – 250	0.9972
125 – 500	0.9952
7.81 – 500	0.9977

The calibration line of best fit followed the equation $y = 0.1447x + 1.3035$, which was used to determine the unknown 6G concentrations in samples of GJ. The spiked

solution result needed to be multiplied by the dilution factor to obtain the correct 6G concentration (the result of the neat ginger juice was not multiplied as it was not diluted).

The mean 6G concentration for 15 spiked ginger samples was 239.43 ± 7.92 mg/L whilst the 6G mean concentration for the 5 neat ginger juice samples was 219.33 ± 7.09 mg/L as indicated in Table 12. The mean 6G concentration of the spiked and neat ginger samples was 234.41 ± 6.29 mg/L, $N = 20$. The 6G concentrations were lower in the unspiked samples when compared to the spiked samples. The 6G concentration in the fresh set of ginger juice were overall higher with a smaller SEM than the solutions which were left for 48 hours.

Table 12. 6G concentrations in the unspiked and spiked ginger juice solutions after 0 hours and 48 hours.

Sample	6G Concentration (mg/L \pm SEM) Time 0 hours	6G Concentration (mg/L \pm SEM) Time 48 hours
Local shop spiked ginger juice (mean)	197.60 \pm 2.11	187.47 \pm 5.13
Local shop unspiked ginger juice	178.97	171.36
Sainsbury's spiked ginger juice (mean)	275.46 \pm 1.66	270.40 \pm 2.01
Sainsbury's unspiked ginger juice	254.99	259.82
Waitrose spiked ginger juice (mean)	224.78 \pm 0.46	204.51 \pm 6.96
Waitrose unspiked ginger juice	215.59	219.05
Market stall spiked ginger juice (mean)	250.59 \pm 3.02	236.76 \pm 3.77
Market stall unspiked ginger juice	223.20	210.76
Tesco spiked ginger juice (mean)	248.74 \pm 2.88	238.15 \pm 4.40
Tesco unspiked ginger juice	223.89	239.78

2.3.2.3 The concentration of [6]-gingerol in ginger extracts

The concentration of [6]-gingerol in the methanolic extracts of ginger was explored via HPLC. The average concentration of 6G varied between the extracts, with the fresh ginger methanolic extract containing the lowest concentration of 6G, at 28.66 mg/L. If we were to compare the number of mg retained via extraction by 10 mL MeOH, to the concentration of 6G in the 1 mg/mL extracts, an estimate of the 6G concentrations in the original extract could be drawn. The dried ginger extract produced the highest estimate of 6G within the sample at 231.56 mg/L, closely followed by the ginger capsule at 223.09 mg/L, whereas the juice and fresh ginger methanolic extracts gave relatively low concentrations of 6G, as shown in Table 13.

Table 13. The estimated concentration of 6G in the methanolic ginger extracts.

Extract	Average mg retained from 10 mL MeOH ginger extracts (\pm SEM) (x)	Average [6G] (mg/L) from 1 mg/mL extracts (\pm SEM)	Estimation of [6G] (mg/L) in original extracts
Fresh ginger + MeOH	20.50 \pm 1.41	26.88 \pm 2.42	55.11
Dried ginger + MeOH	41.27 \pm 4.71	56.11 \pm 14.27	231.56
Ginger juice + MeOH	25.95 \pm 4.01	28.26 \pm 5.38	73.35
Ginger capsule + MeOH	59.20 \pm 9.06	37.68 \pm 4.50	223.09

The HPLC spectrum from the MeOH freshly sliced ginger, and MeOH ginger juice extracts displayed a similar profile to ginger juice on the HPLC spectrum, although the ginger juice concentration is obviously not as high. The methanolic extracts of the ginger capsule and the dried ginger also had a similar profile. In addition to the [6]-gingerol peak, 7 main peaks appeared with a mean retention time of 7.18, 8.72, 9.35, 10.04, 11.20, 11.60 and 13.43 minutes, as shown in Figure 16 and Table 14.

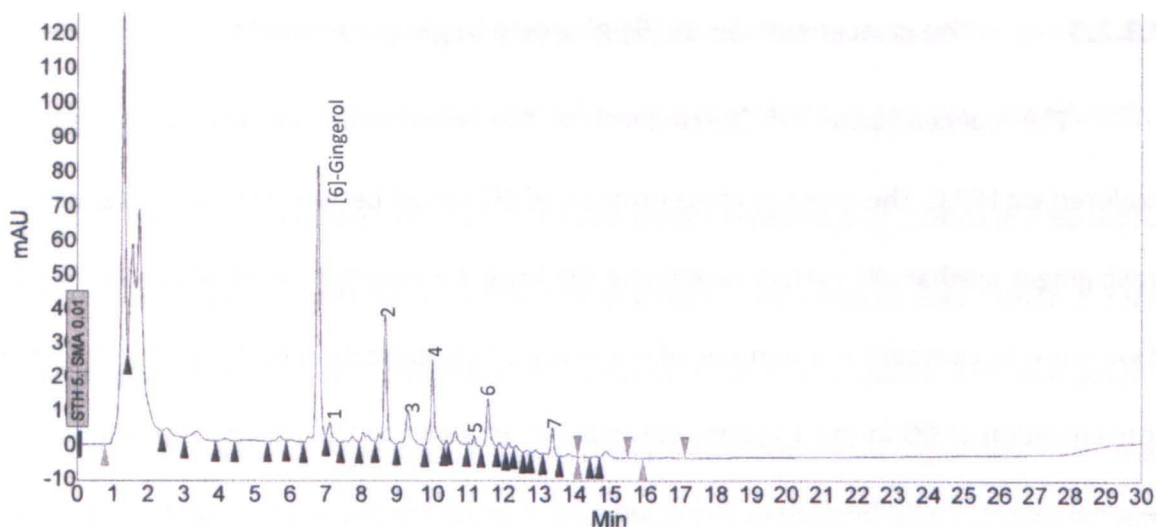


Figure 16. HPLC trace of methanolic ginger capsule extract at 1 mg/mL.

The peaks detected by HPLC for the methanolic dried ginger extract and the methanolic ginger capsule extract were analysed by an unpaired t-test. The only peak, an unknown substance, which was significantly different ($p \leq 0.03$) between the two extracts was at 13.43 minutes with the ginger capsule having a higher area under the curve value than the dried ginger MeOH extract. Analytical HPLC was used rather than GC-MS to identify and quantify [6]-gingerol, with the intention to perform semi-preparatory HPLC to isolate and collect [6]-gingerol to use in further studies, however as the compound was so diluted after semi-preparatory HPLC this was discontinued.

Table 14. Comparison of the integration of peaks found in the ginger capsule and the ginger extract, N = 3 per extract.

Peak Number	Retention time (mins)	Integration of ginger capsule extract peaks on HPLC (mAU)	Integration of dried ginger extract peaks on HPLC (mAU)
1	7.18	0.94 ± 0.24	1.52 ± 0.14
2	8.724	4.26 ± 0.58	3.74 ± 0.93
3	9.354	1.76 ± 0.32	2.26 ± 0.60
4	10.041	3.36 ± 0.57	2.66 ± 0.74
5	11.198	1.48 ± 0.41	0.56 ± 0.23
6	11.601	2.56 ± 0.47	1.38 ± 0.52
7	13.432	$*2.14 \pm 0.43$	$*0.64 \pm 0.15$

The mean concentration of 6G in the ginger infusion was investigated and quantified. The concentration of 6G in the ginger infusion (N=3) was 5.64 ± 1.57 mg/L, (equivalent to $19 \mu\text{M}$), which was relatively low compared to the ginger juice. The HPLC spectrum for ginger infusions did not have as many peaks compared to the 1 mg/mL MeOH ginger extracts. There were only two peaks; an initial peak where the carbohydrates would be expected to have eluted (on the reverse-phase column) (Skoog, *et al.*, 1999) and the 6G peak, which eluted at 6.89 ± 0.03 minutes.

2.3.3 The element concentrations in ginger juice assessed via ICP-AES analysis

The concentrations of 20 metals were measured in the ginger juice obtained by pressing the ginger. The mean pH of the ginger juice was $\text{pH } 5.73 \pm 0.07$. The 6 metals in the highest concentration (above 20 mg/L) in ginger juice are Ca, K, Mg, Mn, Na, and Si, as shown in Figure 17. The presence of a high concentration of silicon arises from the plant taking up silicon from the soil in which the ginger was grown.

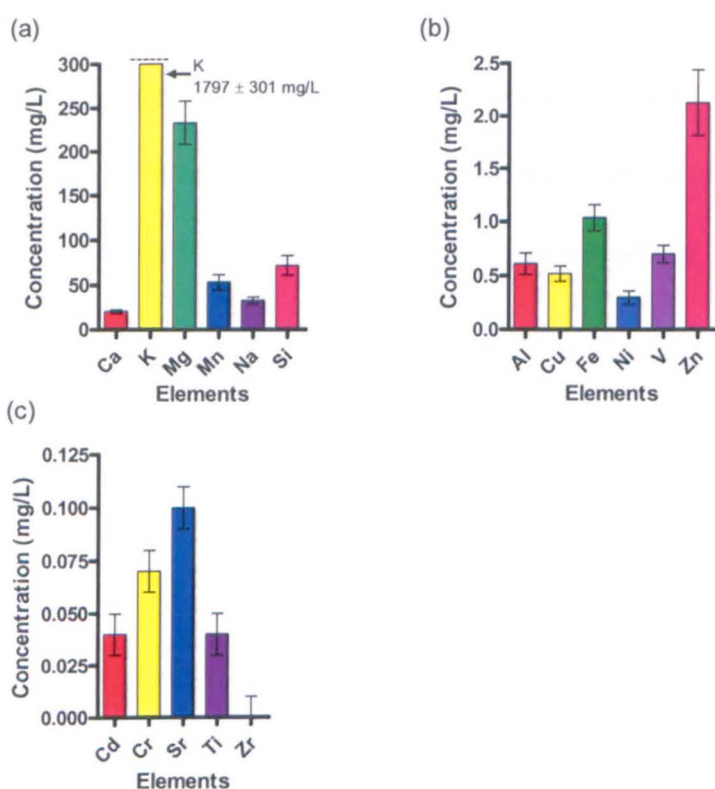


Figure 17. Bar charts displaying the (a) “high” (5 - 300.0 mg/L) (b) “medium” (0.2 - 2.5 mg/L), and (c) “low” (0 - 0.125 mg/L) concentration ranges for elements in ginger juice detected by ICP-AES. The results are expressed as mean \pm SEM. N = 20.

*Note: Co, Li and Pb were not displayed as they were below the limits of detection

2.3.4 The element concentrations in infusions of ginger and lemon via ICP-AES analysis

The mean weight of a slice of lemon was $10.75 \text{ g} \pm 0.68 \text{ g}$, $N = 3$, the ginger quarters weighed $9.10 \text{ g} \pm 0.45 \text{ g}$, $N = 3$. The mean pH of the lemon infusion was 3.36 ± 0.02 , $N = 3$, whilst the mean pH of the ginger infusion was 6.43 ± 0.05 , $N = 3$.

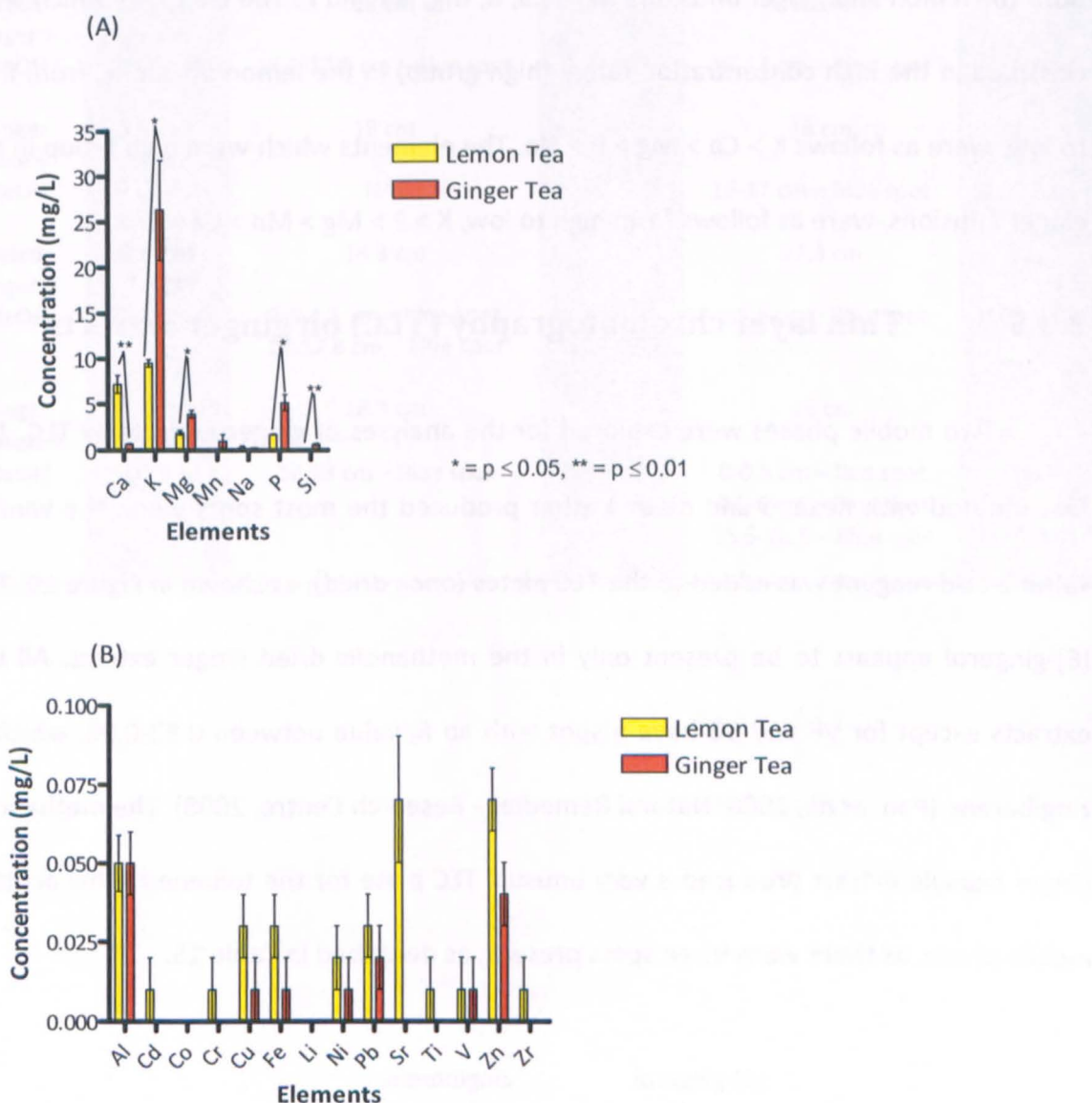


Figure 18. Two bar charts displaying the concentration of elements in lemon and ginger infusion, (A) had highest concentration of elements (mg/L) whereas (B) displayed the lower concentration of elements in mg/L. Results are displayed as mean + SEM. * = $p \leq 0.05$ ** = $p \leq 0.01$.

The elements analysed by the ICP-AES were as follows: Al, Ca, Cd, Co, Cr, Cu, Fe, K, Li, Mg, Mn, Na, Ni, P, Pb, Si, Sr, Ti, V and Zn. A two-tailed unpaired t-test was used to

compare and analyse each individual element from the lemon infusion against each of the elements in the ginger infusion. The elements which were significantly different in each infusion were Ca, Cu, K, Mg, P, and Si, in Figure 18A there was no significant difference in any of the metals in Figure 18B.

The elements which were classified in the high concentration range (≥ 0.2 mg/L) in both the lemon and ginger infusions were Ca, K, Mg, Na and P. The elements which were classified in the high concentration range (high group) in the lemon infusions, from high to low, were as follows $K > Ca > Mg > P > Na$. The elements which were high group in the ginger infusions, were as follows from high to low, $K > P > Mg > Mn > Ca > Si > Na$.

2.3.5 Thin layer chromatography (TLC) on ginger extracts

Two mobile phases were explored for the analyses of ginger extracts by TLC. The first method with hexane and diethyl ether produced the most spots when the vanillin sulfuric acid reagent was added to the TLC plates (once dried), as shown in Figure 19. The [6]-gingerol appears to be present only in the methanolic dried ginger extract. All the extracts except for VE and 6G have a spot with an R_f value between 0.92-0.98, which is zingiberene (Pan, *et al.*, 2008; Natural Remedies - Research Centre, 2008). The methanolic ginger capsule extract produced a very unusual TLC plate for the toluene : ethyl acetate mobile phase, as there were three spots present, as described in Table 15.

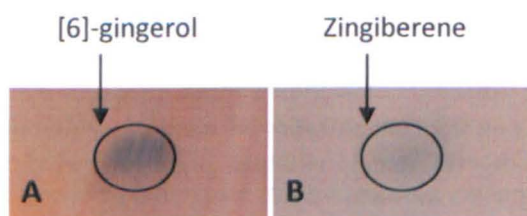


Figure 19. Examples of the TLC plate with the vanillin sulfuric acid reagent with the mobile phase either as (A) hexane : diethyl ether highlighting the [6]-gingerol spot ($R_f \sim 0.2$) and (B) toluene : ethyl acetate highlighting the zingiberene spot ($R_f \sim 0.9$).

Table 15. Vanillin sulfuric acid reagent R_f values on the hexane : diethyl ether TLC plates and toluene : ethyl acetate TLC plates.

Extract		Hexane : diethyl ether TLC plates	R_f value	Toluene : ethyl acetate TLC plates	R_f value
VE	Solvent Front	18.2 cm		18 cm	
	TLC Spot	8-10 cm – Brown spot	0.44-0.55	N/A	
6G	Solvent Front	18.1cm		18.2 cm	
	TLC Spot	2-3.5 cm – Blue spot	0.11-0.19	N/A	
Fresh ginger + MeOH	Solvent Front	18 cm		18 cm	
	TLC Spot	16.5-17.5 cm – Blue spot	0.92-0.97	16-17 cm – Blue spot	0.89-0.94
Ginger juice + MeOH	Solvent Front	18 cm		18 cm	
	TLC Spot	N/A		16-17 cm – Blue spot	0.89-0.94
Dried ginger + MeOH	Solvent Front	18.3 cm		17.3 cm	
	TLC Spot	3.5-4.5 cm – Blue spot 17-17.8 cm – Blue spot	0.19-0.25 0.93-0.97	1-1.5 cm – Blue spot	0.06-0.09
Ginger capsule + MeOH	Solvent Front	18.3 cm		18 cm	
	TLC Spot	17-18 cm – Blue spot	0.93-0.98	0-0.5 cm – Red spot 4.5-6 cm – Blue spot 15.5-16.5 – Blue spot	0-0.3 0.25-0.33 0.86-0.92

2.3.6 Stability studies using spectroscopy

The NMR spectrum of ginger juice was recorded to investigate stability and potential decomposition. The first NMR spectrum was recorded ~2 hours after pressing the ginger and 40+ peaks were obtained. The peaks are broad but several do maintain the tall thin shape required from a standard NMR analysis, as shown by Figure 20. This distortion of the peaks is occasionally due to the masking of the water peak. As the peaks are broad it is hard to measure the data quantitatively. This method is far more qualitative. It is also important to note that the integral was not used as a comparison technique.

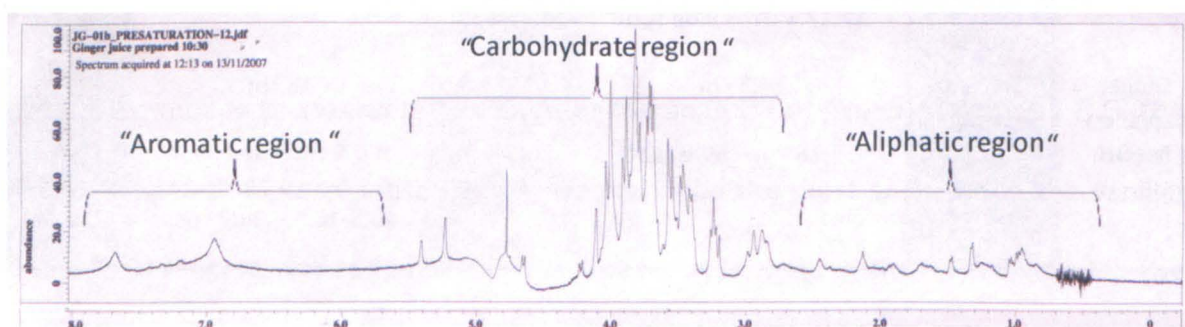


Figure 20. ^1H NMR spectrum of ginger juice.

25 hours after pressing the juice 2 peaks appeared/increased in size at 2.390 and 1.966 in the NMR spectrum. From assessing NMR tables the singlet peaks at 2.390 and 1.966 were succinate and acetate, respectively. This experiment was repeated three times but only once did the ^1H NMR spectrum change.

Table 16. ¹H NMR reference table.

Region	¹ H NMR	Compound	Reference
"Aliphatic"	0.968	Leucine	(Bailey, <i>et al.</i> , 2003) (Cuny, <i>et al.</i> , 2008) (Holmes, <i>et al.</i> , 1997)
	0.990	Valine	(Bailey, <i>et al.</i> , 2003) (Holmes, <i>et al.</i> , 1997)
	1.008	Isoleucine	(Bailey, <i>et al.</i> , 2003) (Holmes, <i>et al.</i> , 1997)
	1.044	Valine	(Bailey, <i>et al.</i> , 2003) (Holmes, <i>et al.</i> , 1997)
	1.333	Lactate	(Bailey, <i>et al.</i> , 2003) (Holmes, <i>et al.</i> , 1997)
	1.346	Lactate	(Bailey, <i>et al.</i> , 2003) (Holmes, <i>et al.</i> , 1997)
	1.499	Alanine	(Bailey, <i>et al.</i> , 2003) (Holmes, <i>et al.</i> , 1997)
	1.966	Acetate	(Bailey, <i>et al.</i> , 2003) (Gavaghan, <i>et al.</i> , 2000) (Holmes, <i>et al.</i> , 1997)
	2.147	Glutamine	(Bailey, <i>et al.</i> , 2003) (Singh, <i>et al.</i> , 2003)
	2.390	Succinate	
	2.464	Undefined	
	2.847	Undefined	
	2.856	Undefined	
	2.899	Trimethylamine	(Gavaghan, <i>et al.</i> , 2000) (Holmes, <i>et al.</i> , 1997)
2.955	Dimethylglycine	(Holmes, <i>et al.</i> , 1997)	
3.480	<i>Trans</i> -aconitic acid	(Holmes, <i>et al.</i> , 1997)	
3.502	Undefined		
3.560	Glycine	(Holmes, <i>et al.</i> , 1997)	
3.589	Undefined		
3.696	Mannitol	(Holmes, <i>et al.</i> , 1997)	
3.716	Undefined		
3.730	Undefined		
3.745	Undefined		
3.798	Undefined		
3.823	Undefined		
3.838	Undefined		
3.900	Free β -Glucose	(Cuny, <i>et al.</i> , 2008)	
3.928	Creatine	(Gavaghan, <i>et al.</i> , 2000) (Holmes, <i>et al.</i> , 1997)	
4.019	Undefined		
4.052	Undefined		
4.650	Free β -Glucose	(Holmes, <i>et al.</i> , 1997)	
4.668	Undefined		
4.782	Water	(Holmes, <i>et al.</i> , 1997)	
4.798	Water	(Holmes, <i>et al.</i> , 1997)	
4.955	Undefined		
5.115	Undefined		
5.250	2-hydroxyglutarate	(Holmes, <i>et al.</i> , 1997)	

"Aromatic"	5.419	Sucrose	(Bailey, <i>et al.</i> , 2003)
	6.956	Undefined	
	7.199	Gingerols	(Catchpole, <i>et al.</i> , 2003)
	7.339	Gingerols	(Catchpole, <i>et al.</i> , 2003)
	7.686	Gingerols	(Catchpole, <i>et al.</i> , 2003)
	7.712	Gingerols	(Catchpole, <i>et al.</i> , 2003)

Table 16 exhibits the peaks from the NMR spectrum of ginger juice. In the aliphatic region there were five amino acids identified: alanine; glutamine; isoleucine; leucine; and valine, and three acids identified: acetate, lactate and succinate. This region has also been enlarged in Figure 21, it highlighted the growth over three times periods of the acetate and succinate peaks. In the carbohydrate region there were a high number of sugars, most of which were undefined due to the formation of the peaks, although free β -glucose and sucrose were identified along with the H_2O peak (Table 16).

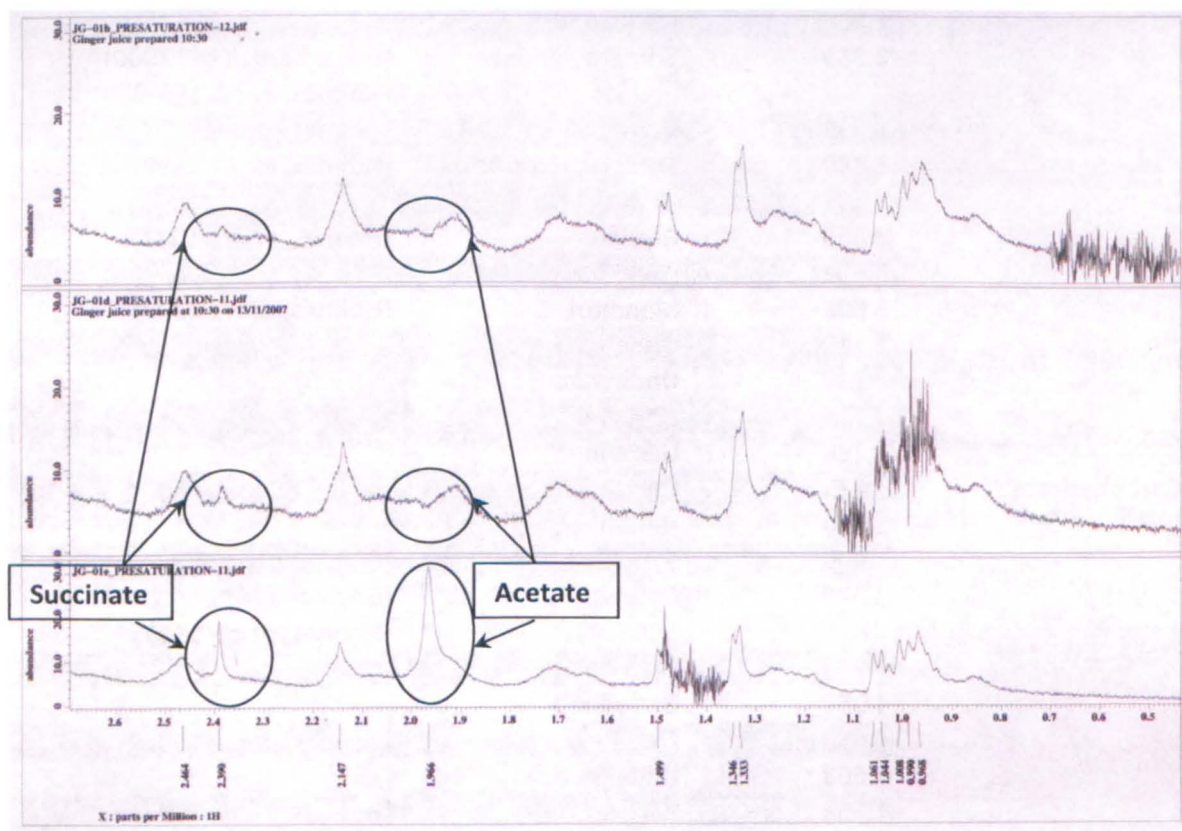


Figure 21. "Aliphatic" region of the 1H NMR spectra at: (b) ~1 hour 45 minutes; (d) 12 hours; and (e) 25 hours after pressing.

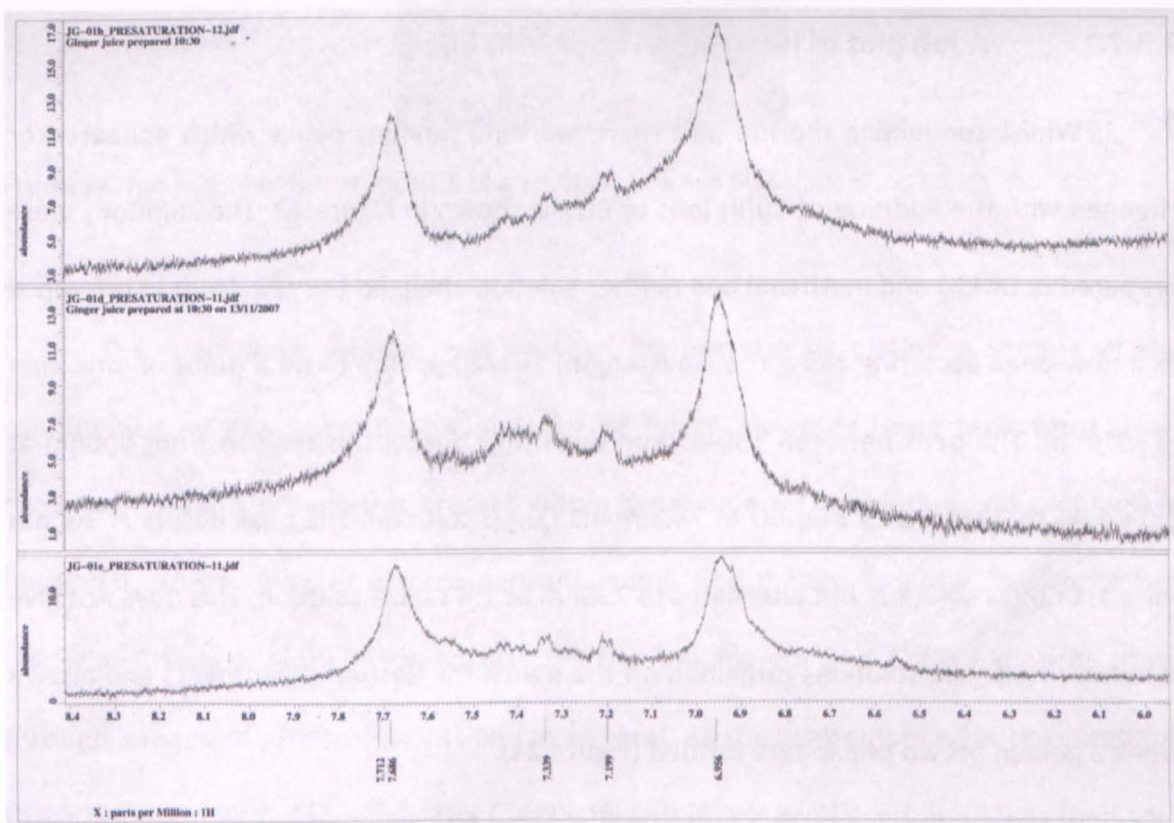


Figure 22. “Aromatic” region of the ^1H NMR spectrums at: (b) ~1 hour 45 minutes; (d) 12 hours; and (e) 25 hours after pressing.

Using the data from the Catchpole, *et al.*, (2003) report the gingerol peaks were identified in the aliphatic region at 7.199, 7.339, 7,686 and 7.712, see Table 16. These peaks are shown over three time periods in Figure 22 and appear to decrease. However it is unreliable to concentrate on the y-axis of abundance as the focus is on where the peaks develop along the ^1H NMR spectrum. There also appears to be a peak developing at 6.55 in after 25 hours Figure 22.

2.3.7 Metal complexation studies

2.3.7.1 A Job plot of [6]-gingerol and Cu(II) ions

Whilst conducting the Job plot there were no obvious peaks which appeared or changed with the addition of Cu(II) ions or 6G, as shown in Figure 23. The solutions were prepared in DMSO and methanol and neither solution changed the spectrum in reference to a new peak occurring along the wavelength. There appears to be a point of inflection at ~410nm. The peak between 750-850nm does shift during the analysis from 800nm at 1:0 Cu:6G to 823nm at 9:1 Cu:6G to 780nm 4:1 Cu:6G solution. The peak occurs at 800nm for a 1:1 Cu:6G solution, but alternates to 790nm at 1:4 Cu:6G solution. This does not give a stable result. The solutions remained on the bench for further experiments and after a week a golden brown precipitate formed (Figure 24).

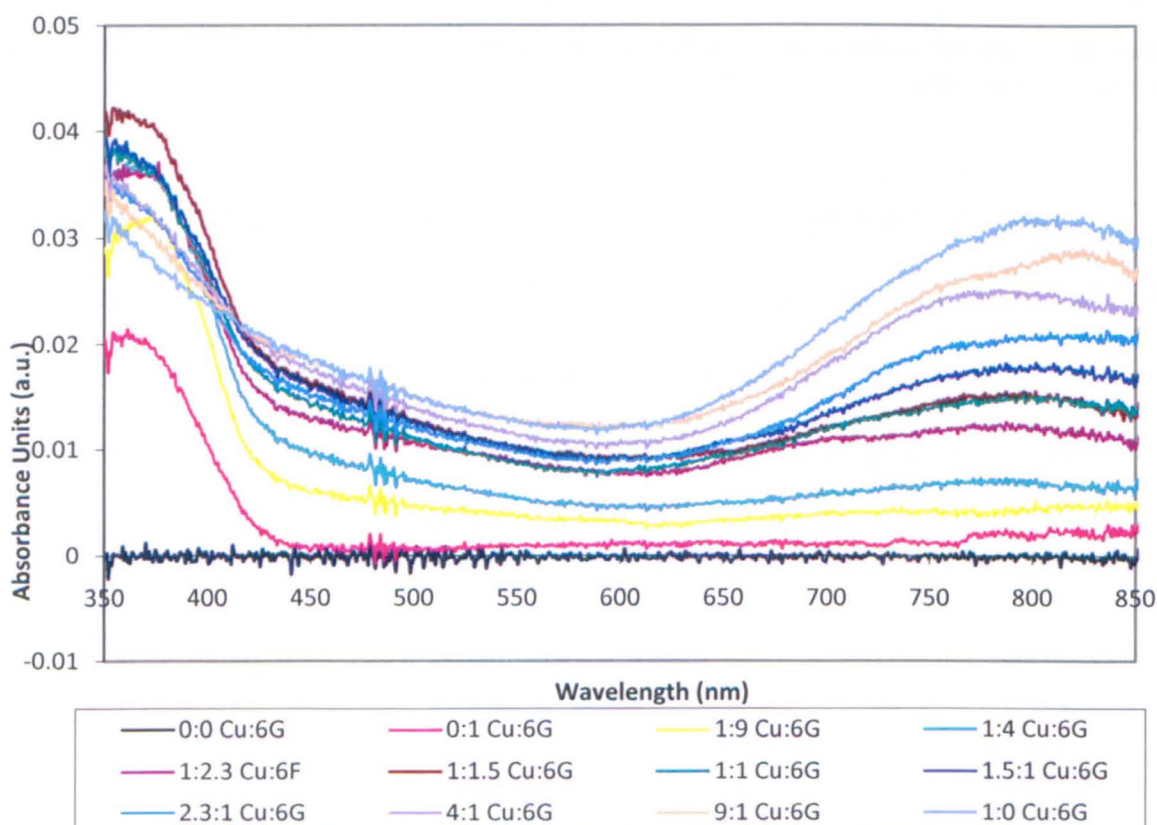


Figure 23. The spectrum of Cu(II) ions and 6G over a range of 11 concentrations.



Figure 24. The golden brown precipitate of a 1:1 Cu(II) ions and 6G solution.

The precipitate solution was checked for bacteria by plating a sample of the solution out on agar then incubating it for 48 hours. However these tests were clear, there were no microorganisms present within the solution. The solution was prepared in methanol, where common microorganisms would find it hard to grow as alcohol kills bacteria. Attempts were made to dissolve the [6]-gingerol and Cu(II) ions precipitate through a range of pHs, in solvents and in glycerol. All these attempts were unsuccessful, the precipitate did not dissolve. The Cu(II) ions and [6]-gingerol precipitate was then sent for scanning electron microscopy to identify the binding but no crystal structure was derived.

2.3.8 Scanning electron microscopy

Figure 25 displays the scanning electron microscopy image of the dehydrated golden brown precipitate containing Cu(II) and 6G, after sputter coating with gold. The pictures indicate that the effects of the binding are not random, but are not crystal like.

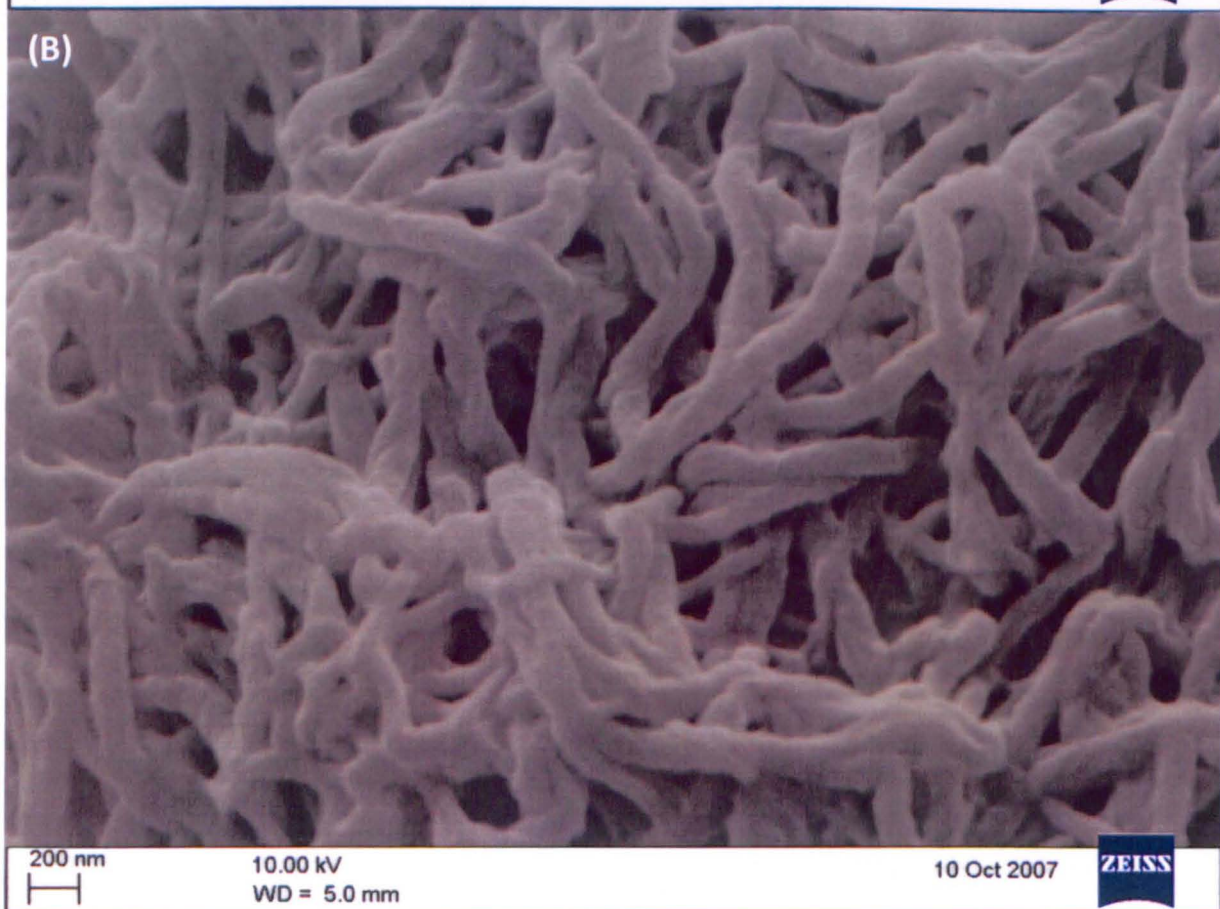
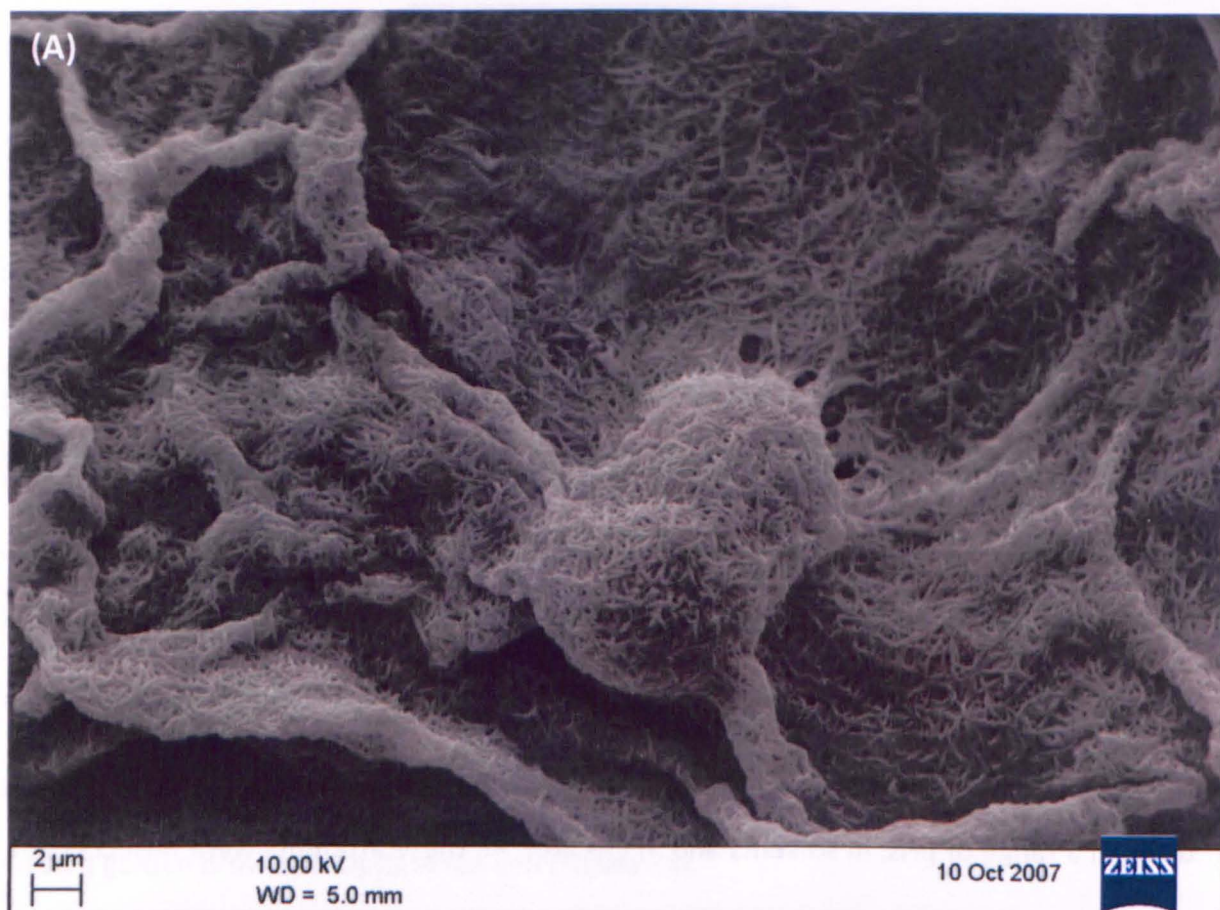


Figure 25. S.E.M. picture of Cu(II)6G precipitate at (A) 2 μM and (B) 200nm

2.4 Discussion

2.4.1 Element content of “crude” extracts

Foodstuffs regularly contain the micronutrient manganese, and manganese is found in some enzymes including mitochondrial superoxide dismutase (Hague, *et al.*, 2008; Prystai, *et al.*, 1999). With the “crude” infusions there was a difference in comparing ginger and lemon infusions. The ginger infusion contained nearly 10 times as much manganese when compared to the lemon infusions but unfortunately the SEM was also very large therefore the t-test result was insignificant. All the commercially available beverages and the “crude” ginger infusion contained manganese.

The lemon and ginger infusions were chosen as these are drinks which are regularly consumed in Western countries and are viewed as “detox” beverages (Wong C., 2007). The lemon infusion was far more acidic (pH 3.36 ± 0.02), when compared to the ginger infusion, (pH 6.43 ± 0.05) due to the citric acid content within the lemon infusion (Penniston, *et al.*, 2008). This acidity may cause the increase in the release of calcium seen in the lemon infusion which is approximately 10 times higher than the ginger infusion. The highest metal found in both the ginger and lemon infusions was potassium, although the concentrations are significantly different, with the ginger infusion containing approximately 3 times more potassium than the lemon infusion. The sodium concentrations were similar in the ginger and lemon infusions between 0.2-0.3 mg/L. The concentration of magnesium in the ginger tea was twice as high as the lemon tea magnesium concentration, whereas the phosphate levels were nearly three times the concentration in ginger tea when compared to lemon tea. The silicon concentration was

far higher in the ginger infusion, and this was thought to be due to the uptake of silicon from the soil (Hou, *et al.*, 2008; Meunier, 2003).

The elements which were found in the highest concentrations in the ginger juice were similar to the highest concentration of elements detected in the ginger infusions but the ginger juice had a higher concentration of these elements due to the dilution of water in the ginger infusions. The elements which were similar included potassium, magnesium, silicon, manganese, sodium and calcium, on average the concentrations of these elements in ginger juice were ~100 fold higher than the ginger infusions. This suggests that the ginger juice was 100 times more concentrated than the ginger infusions, however this hypothesis does not correlate with the [6]-gingerol concentrations as the ginger juice [6]-gingerol concentration (239.4 ± 7.1 mg/L) was only ~40 times more concentrated than the ginger infusions (5.64 ± 1.6 mg/L).

2.4.2 Stability of the ginger juice extract

Stability studies of the ginger juice extract by NMR spectroscopy have indicated that there is the potential for the constituents of the juice to degrade and increase the levels of acetate and succinate, although this only occurred in one out of three instances in a 24 hour period. There were 27 peaks detected in the carbohydrate region of the NMR spectrum, whilst there were only 11 peaks in the aliphatic region (consisting of amino acids and lactic, succinic and acetic acid) and 5 peaks in the aromatic region (mainly consisting of the gingerols). The ginger juice was also heated after 24 hours and the spectrum was measured on the NMR, however there was no change in the spectrum (data not shown).

In other foodstuffs including cloudy apple juice, freshly squeezed orange juice, and paprika and chilli powder some of the enzymes such as peroxidase and polyphenol oxidase, are capable of degrading after heat exposure (Hirsch, *et al.*, 2008; Krapfenbauer, *et al.*, 2006; Schweiggert, *et al.*, 2005). Polyphenol oxidase is responsible for browning which oxidises phenolic compounds, whilst peroxidase is responsible for flavour alterations. Both enzymes can cause a decline in the characteristics including pungency, colour stability and taste. Unpasteurised juices have a very short shelf life as these oxidative enzymes begin to act very soon after the extraction procedure. There is also a loss of ascorbic acid, flavour degradation and microbial growth also contributing to a short shelf life. Polyphenol oxidase or peroxidase could be responsible for the degradation of ginger juice seen in the NMR spectrum (Figure 21).

The [6]-gingerol concentrations decreased in 48 hours from pressing for 5 different spiked ginger juice samples repeated three times. One hour after pressing the [6]-gingerol concentration in the ginger juice sample was 234.41 ± 6.29 mg/L, whilst 48 hours after pressing the [6]-gingerol concentration fell to 225.63 ± 6.85 mg/L in the same sample, a drop of ~4%, as shown in Figure 26.

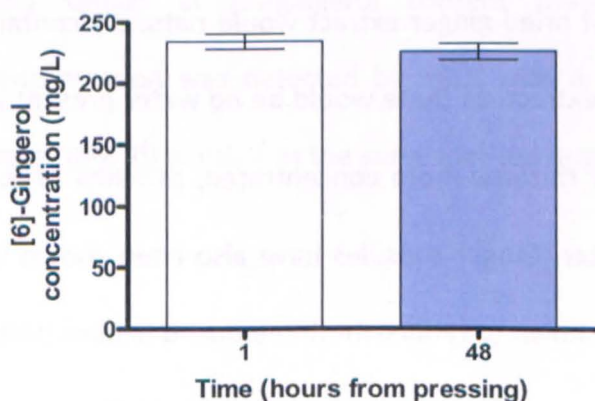


Figure 26. The decrease in [6]-gingerol concentration in ginger juice 48 hours after pressing the ginger. N=15

The [6]-gingerol decrease over a 48 hour period correlates with the NMR spectrum which indicated a degradation of the constituents of ginger juice with the increase in acetate and succinate. It may be that the [6]-gingerol is being enzymatically degraded forming acetate and succinate as by-products or that the [6]-gingerol is converting to [6]-shogaol as reported by (Bhattarai, *et al.*, 2001; Bhattarai, *et al.*, 2007).

2.4.3 Liquid chromatography analyses of the ginger rhizome extracts

Ginger juice had the highest percentage yield at ~8%, whilst the methanolic fresh ginger extract had the lowest percentage yield of ~2%, and the methanolic ginger capsule extract had a percentage yield of 6%. [6]-gingerol was detected by both HPLC and TLC with the vanillin sulphuric acid reagent. The concentration of [6]-gingerol in the methanolic extracts ranged from 26.88 ± 2.42 mg/L to 56.11 ± 14.27 mg/L, with the methanolic dried ginger extract having the highest concentration. There were more peaks detected with an increase in the integration values in the methanolic dried ginger and capsule extract when compared to the methanolic fresh ginger extracts. It is likely that the increase in these peaks is due to the processing and drying carried out to produce the ginger capsule and the dried ginger. 1 g of dried ginger extract would naturally contain more compounds than 1 g of fresh ginger extract, as there would be no water present in the dried extract, making the dried ginger rhizome more concentrated, as >90% of the fresh ginger rhizome was made up of water. Ginger capsules have also been shown to have biological activity, as they have been shown to reduce motion-induced nausea (Lien, *et al.*, 2003). The extract from the ginger capsule had a very similar profile to the extract of the dried ginger juice with the [6]-gingerol peak having the highest value of integration and 7 smaller peaks. The dried ginger extract may have a similar anti-nausea effect to the

ginger capsule extract as it has a similar HPLC profile. Further, if the effects of the ginger capsule are mainly due to [6]-gingerol, ginger juice, which has the highest concentration of [6]-gingerol, may also act similarly to the ginger capsule on the gastrointestinal tract and prevent motion-induced nausea.

In previous research the concentration of [6]-gingerol was ascertained in a number of different ginger extracts including: steam distilled, ground, solar dried ginger rhizomes; non-steam distilled, ground, solar dried ginger rhizomes; air drying; freeze drying; nitrogen drying; carbon dioxide drying and vacuum drying as shown in Table 17.

Steam distilled, ground, solar dried ginger rhizomes gave ~50% more [6]-gingerol content compared to non-steam distilled, ground, solar dried ginger rhizomes (McHale, *et al.*, 1989). Whilst the [6]-gingerol content in separately sourced ginger rhizomes was relatively similar, with the fresh ginger root from Japan having a high percentage, Vietnam also had a higher content compared to other locations (although it appears there is only one sample from Vietnam and the fresh ginger root from Japan) (Yoshikawa, *et al.*, 1993). The concentration of [6]-gingerol varied from ~6-12 mg/g of dried ginger with different methods of drying. Ginger rhizomes dried by nitrogen and carbon dioxide were very similar in [6]-gingerol content (Hawlder, *et al.*, 2006). The [6]-gingerol concentration was detected by HPLC with an isocratic mobile phase of methanol and water (60:40) which was the same method originally used in this study.

Table 17. The percentage and concentrations of gingerols, shogaol and galanolactone in various extracts of ginger (*Zingiber officinale roscoe*).

Ginger extract	Compounds	Relative proportion (%)	Reference	Ginger extract	Compounds	Relative proportion (%)	Reference
TPO	[6]-Gingerol	40.9 ± 5.39	(McHale, <i>et al.</i> , 1989)	LCO ₂ O	[6]-Gingerol	53.97 ± 3.07	(McHale, <i>et al.</i> , 1989)
TPO	[8]-Gingerol	8.85 ± 0.96	(McHale, <i>et al.</i> , 1989)	LCO ₂ O	[8]-Gingerol	13.12 ± 1.90	(McHale, <i>et al.</i> , 1989)
TPO	[10]-Gingerol	10.98 ± 1.01	(McHale, <i>et al.</i> , 1989)	LCO ₂ O	[10]-Gingerol	16.37 ± 0.92	(McHale, <i>et al.</i> , 1989)
TPO	[6]-Shogaol	25.42 ± 3.71	(McHale, <i>et al.</i> , 1989)	LCO ₂ O	[6]-Shogaol	12.82 ± 2.85	(McHale, <i>et al.</i> , 1989)
TPO	[8]-Shogaol	6.57 ± 1.93	(McHale, <i>et al.</i> , 1989)	LCO ₂ O	[8]-Shogaol	3.02 ± 0.91	(McHale, <i>et al.</i> , 1989)
TPO	[10]-Shogaol	7.30 ± 1.28	(McHale, <i>et al.</i> , 1989)	LCO ₂ O	[10]-Shogaol	3.98 ± 0.95	(McHale, <i>et al.</i> , 1989)
Percentage (%)				Percentage (%)			
Chinese Ginger	[6]-Gingerol	0.43 ± 0.04	(Yoshikawa, <i>et al.</i> , 1993)	Taiwanese Ginger	[6]-Gingerol	0.40	(Yoshikawa, <i>et al.</i> , 1993)
Chinese Ginger	[6]-Shogaol	0.11 ± 0.02	(Yoshikawa, <i>et al.</i> , 1993)	Taiwanese Ginger	[6]-Shogaol	0.15	(Yoshikawa, <i>et al.</i> , 1993)
Chinese Ginger	Galanolactone	nd	(Yoshikawa, <i>et al.</i> , 1993)	Taiwanese Ginger	Galanolactone	nd	(Yoshikawa, <i>et al.</i> , 1993)
Japanese Ginger	[6]-Gingerol	0.42 ± 0.02	(Yoshikawa, <i>et al.</i> , 1993)	Vietnamese Ginger	[6]-Gingerol	0.83	(Yoshikawa, <i>et al.</i> , 1993)
Japanese Ginger	[6]-Shogaol	0.06 ± 0.01	(Yoshikawa, <i>et al.</i> , 1993)	Vietnamese Ginger	[6]-Shogaol	0.21	(Yoshikawa, <i>et al.</i> , 1993)
Japanese Ginger	Galanolactone	0.54 ± 0.08	(Yoshikawa, <i>et al.</i> , 1993)	Vietnamese Ginger	Galanolactone	nd	(Yoshikawa, <i>et al.</i> , 1993)
Japanese Fresh Ginger	[6]-Gingerol	1.51	(Yoshikawa, <i>et al.</i> , 1993)				
Japanese Fresh Ginger	[6]-Shogaol	0.01	(Yoshikawa, <i>et al.</i> , 1993)				
Japanese Fresh Ginger Root	Galanolactone	2.43	(Yoshikawa, <i>et al.</i> , 1993)				

		per g (dry weight basis) Content (x 10 ³ g)			per g (dry weight basis) Content (x 10 ³ g)		
NSTDG	[6]-Gingerol	16.34 ± 0.00	(Balladin, <i>et al.</i> , 1996)	STDG	[6]-Gingerol	35.29 ± 0.08	(Balladin, <i>et al.</i> , 1996)
NSTDG	[8]-Gingerol	70.34 ± 0.06	(Balladin, <i>et al.</i> , 1996)	STDG	[8]-Gingerol	nd	(Balladin, <i>et al.</i> , 1996)
NSTDG	[10]-Gingerol	nd	(Balladin, <i>et al.</i> , 1996)	STDG	[10]-Gingerol	nd	(Balladin, <i>et al.</i> , 1996)
NSTDG	[6]-Shogaol	48.90 ± 0.06	(Balladin, <i>et al.</i> , 1996)	STDG	[6]-Shogaol	22.22 ± 0.00	(Balladin, <i>et al.</i> , 1996)
NSTDG	[8]-Shogaol	270.98 ± 0.01	(Balladin, <i>et al.</i> , 1996)	STDG	[8]-Shogaol	428.64 ± 0.10	(Balladin, <i>et al.</i> , 1996)
NSTDG	[10]-Shogaol	54.85 ± 0.05	(Balladin, <i>et al.</i> , 1996)	STDG	[10]-Shogaol	177.88 ± 0.06	(Balladin, <i>et al.</i> , 1996)
		per g (dry weight basis) Content (x 10 ⁴ g)			Percentage (%)		
FMG	[6]-Gingerol	324.44 ± 0.01	(Balladin, <i>et al.</i> , 1996)	TLC Shogaol Fraction	[6]-Shogaol	88.18	(Chen, <i>et al.</i> , 1986)
FMG	[8]-Gingerol	143.72 ± 0.03	(Balladin, <i>et al.</i> , 1996)	TLC Shogaol Fraction	[8]-Shogaol	6.09	(Chen, <i>et al.</i> , 1986)
FMG	[10]-Gingerol	201.33 ± 0.05	(Balladin, <i>et al.</i> , 1996)	TLC Shogaol Fraction	[10]-Shogaol	3.34	(Chen, <i>et al.</i> , 1986)
FMG	[6]-Shogaol	10.59 ± 0.00	(Balladin, <i>et al.</i> , 1996)	TLC Shogaol Fraction	[12]-Shogaol	< 0.10%	(Chen, <i>et al.</i> , 1986)
FMG	[8]-Shogaol	nd	(Balladin, <i>et al.</i> , 1996)				
FMG	[10]-Shogaol	nd	(Balladin, <i>et al.</i> , 1996)				

TPO = Traditionally produced oleoresin; LCO₂O = Liquid carbon dioxide extracted oleoresin;
 NSTDG = Non-steam distilled, ground, solar dried ginger samples (trichloromethane extract);
 nd = Not detected

FMG = Fresh macerated ginger samples (trichloromethane extract)
 STDG = Steam distilled, ground, solar dried ginger samples (trichloromethane extract)

2.4.4 Studies of [6]-gingerol binding to Cu(II) ions

[6]-Gingerol did not bind to Cu(II) ions as expected, the complex precipitated out in a range of solutions and did not redissolve in the solvents tested or at different pH levels or by heating the solution. Obviously something was occurring during the Job plot analysis but possibly the solution was binding and precipitating out and affecting the absorbance. This precipitate was not microbial or fungal. Whilst examining the binding of Cu(II) ions to [6]-gingerol using the UV-spectrophotometer to perform a Job plot there were no new visible peaks. It was expected that the Cu(II) ions would bind to [6]-gingerol like Cu(II) ions bound to curcumin, but unfortunately it did not (Barik, *et al.*, 2005; Barik, *et al.*, 2007). This type of binding was thought to be due to the structure of [6]-gingerol. This precipitate appeared to form a polymer-like structure, not a 1:1 or 1:2 crystalline structure as seen in Figure 25.

2.4.5 Conclusion

Overall the [6]-gingerol concentrations were determined in six different ginger extracts. There is the potential for the constituents of the ginger juice to degrade as shown by NMR spectroscopic and HPLC analyses as there was an increase in acetate and succinate in a 24 hour period and a decrease of 5% of [6]-gingerol concentration in a 48 hour period. Cu(II) ions did bind to [6]-gingerol, however it formed a polymer-like structure which precipitated out and did not redissolve in a range of solvents and lipids or in a range of pH levels. However at very low concentrations no precipitate could be seen. For this reason the Cu(II)-[6]-gingerol solution was tested further for its anti-oxidant activity in Chapter 3.

Further work in this area would involve analysing the ginger and capsule extracts further to identify the extra peaks detected and attempt to quantify the resulting compounds. This could be performed by liquid chromatography – mass spectrometry. Further analysis of the extracts via FT-NMR spectroscopy could also prove useful. There would also be attempts to ascertain the levels of [6]-shogaol in ginger juice. Quercetin is found in a large range of food stuffs. It would be interesting to identify if quercetin was present in the ginger juice or the other ginger extracts as well as the commercially available beverages, as quercetin has been shown to modulate ion channels in Caco-2 cell monolayers in Chapter 3.

CHAPTER THREE

**THE ANTI-OXIDANT CAPACITY
OF [6]-GINGEROL TOGETHER
WITH THE EFFECT OF [6]-
GINGEROL AND OTHER
SUBSTANCES ON CACO-2 CELL
MONOLAYERS**

3.1 Introduction

Curcumin has been shown to interrupt NF- κ B signalling through inhibiting I- κ B kinase, and may be a potential cancer chemotherapeutic agent (Lin and Lin, 2008). As curcumin derives from turmeric a member of the same botanical family as ginger (*Zingiberaceae*) it would be beneficial to investigate if gingerol affects any of the oxidant and inflammatory pathways.

Chohan, *et al.*, (2008) have shown that ginger, after stewing, increased in anti-oxidant activity using the Trolox Equivalent Anti-oxidant Capacity (TEAC) assay. The ginger root alone did not have a high anti-oxidant capacity compared to the other culinary herbs tested. However, other assays have indicated that ground ginger, alcoholic extracts and the essential oil of ginger have high anti-oxidant capacity using different assays (Dang, *et al.*, 2001; Halvorenson, *et al.*, 2006; Stoilova, *et al.*, 2007). The difference in results could be due to both the type of assay and the preparation of the ginger sample (Chohan, *et al.*, 2008). When rats were fed a diet containing 1% of ginger root powder for one month, the levels of SOD and catalase in the liver increased by ~210% and ~165%, respectively (Kota, *et al.*, 2008). This indicates that ginger may protect tissue through increased enzyme activity or that there was an increase in the protective enzymes due to an increase in oxidative status.

EGTA and EHPG have been shown to chelate Mn(II) and Cu(II) ions and act as SOD mimetics (Fisher, *et al.*, 2004). Following this report, these compounds were used on rat kidney cells (NRK-52E cells) to identify if they affected paraquat (1 mM) induced toxicity in such cells (Samai, *et al.*, 2007). The Mn(II)-EHPG complex at 30 and 100 μ M was the most effective at reducing the lactate dehydrogenase enzyme release into the media (an

indicator of cell death) and reducing the cytotoxic effects induced by the herbicide, paraquat, in NRK-52E cells (Samai, *et al.*, 2007).

Rat cytokine-induced neutrophil chemoattractant-1 (CINC-1) is a member of the interleukin-8 family, and at sites of inflammation CINC-1 increases neutrophil infiltration at the site of inflammation (Ohtsuka, *et al.*, 1996; Takaishi, *et al.*, 2000). CINC-1 is produced by rat kidney (NRK-52E) cells and has a role in inflammatory reactions (Takaishi, *et al.*, 2000). In NRK-52E cells over-expression of I κ B α , a natural inhibitor of NF- κ B, leads to an inhibition of CINC-1 production (Takaishi, *et al.*, 2000). TNF- α has been shown to increase CINC-1 levels in rat gastric epithelial cells, and increase CINC levels in rat kidney fibroblasts (Handa, *et al.*, 2004; Nakagawa, *et al.*, 1993). Another plant-derived natural product has been used to identify the anti-inflammatory effects on CINC-1 levels. Reynosin, a compound from *Saussurea lappa* Clarke, a plant used in Korean herbal medicine, is used to treat gastrointestinal disorders and has been shown to inhibit CINC-1 levels in NRK-52E cells when stimulated with lipopolysaccharide (Jung, *et al.*, 1998).

Oxidative stress often leads to inflammation. When there is increased production of ROS, there is an increase in lipid peroxidation of DNA and proteins. It has also been documented that increased ROS activates proinflammatory mediators, these instances have been documented *in vitro* and *in vivo* (Zhao and Robbins, 2009). Therefore if SOD mimetics could reduce oxidative stress, there is the potential for it to reduce inflammation and act as an anti-inflammatory. As Mn(II)-EHPG has been shown to have SOD-mimicry effects and reduce paraquat induced cytotoxicity, there may be a possibility that it could reduce inflammatory mediators induced by TNF- α in NRK-52E cells. Therefore this chapter will attempt to investigate the effect of Mn(II)-EHPG on CINC-1 release in NRK-52E cells after exposure to TNF- α .

Bacterial infections in intestinal epithelial cells can cause an immune response resulting in an increase in cytokines (Tammali, *et al.*, 2007). TNF- α is a mediator involved in Crohn's disease and chronic inflammatory bowel disease. Caco-2 cells incubated with TNF- α (2nM) induced prostaglandin E₂ (PGE₂) production and cyclooxygenase activity (Tammali, *et al.*, 2007).

Interleukin-8 (IL-8) is a primary inflammatory mediator which is produced by cells (including macrophages and epithelial cells) and by chemotaxis, attracts neutrophils to inflamed sites. IL-8 is produced in response to TNF (Matsushima and Oppenheim, 1989; Son, *et al.*, 2008). IL-8 can be overproduced in the intestine and cause a higher infiltration of neutrophils. Intestinal diseases including inflammatory bowel disease and Crohn's disease often display increased infiltration of neutrophils (Mukaida, *et al.*, 1998; Son, *et al.*, 2008). Therefore if the IL-8 production can be halted or reduced at the primary site of release (intestine) it may relieve patients with inflammatory bowel disease of some symptoms.

Cadmium (10 μ M) and TNF- α have been shown to induce IL-8 production in Caco-2 cells (Hyun, *et al.*, 2008). Carnosine (1-50 mM), a dietary dipeptide, has been shown to reduce IL-8 levels in Caco-2 cells in the presence of TNF- α (100 ng/mL) at 14 days post seeding (Son, *et al.*, 2008). In ulcerative colitis, there is an increased apoptosis rate of the mucosal cells in the colon (Seidelin and Nielsen, 2009). The reason for the increased apoptosis has been identified primarily due to the local inflammatory response. Therefore if the following test substances (Mn(II)-EHPG, [6]-gingerol and vitamin E) have anti-oxidant effects they may have anti-inflammatory effects and may be able to reduce the inflammatory response within the colon. It would be interesting to identify if [6]-gingerol,

Mn(II)-EHPG, and vitamin E would affect the IL-8 levels in 14 day old Caco-2 cells after TNF- α was applied.

Caco-2 cells are also used as a model of the epithelium of the gut to study ion channels and absorption of compounds (van de Kerkhof, *et al.*, 2007). Quercetin and other phytochemicals, including [6]-gingerol, have been shown to affect ion channel secretion in rat and mouse colon (Cermak, *et al.*, 1998; Cermak, *et al.*, 2001; Lee, *et al.*, 2005; O'Leary, *et al.*, 2004a). The Caco-2 cells were used as they are a well characterised intestinal cell line for the investigation into ion channels, and ATP was used as a positive control as it is a well known agonist.

Quercetin and kaempferol are frequently ingested in the diet and may have significant effects on the intestine. Quercetin glycoside (quercetin with a sugar moiety attached), is likely to be metabolised to quercetin (aglycone form) in the large intestine by enterobacteria and absorbed by epithelial cells in the large intestine (Murota and Terao, 2003). Therefore it would be interesting to identify if [6]-gingerol, quercetin and kaempferol (phytochemicals) at concentrations present in the gut, affect ion channel secretion in a human colon cancer cell line, rather than in rat or mouse colon.

Overall, the main aims of this chapter are to identify the anti-oxidant effects and anti-inflammatory and secretory effects on the gut of [6]-gingerol and other test substances.

3.1.1 Aims

The aims of this chapter are:

- To quantify the SOD activity of [6]-gingerol when bound to Cu(II) ions by using the NBT assay
- To measure the anti-oxidant activity on ginger extracts on TLC plates
- To undertake a preliminary investigation on the IL-8 levels of Caco-2 cells after exposure to TNF- α pre-treated with vitamin E, [6]-gingerol or Mn(II)-EHPG
- To measure the CINC-1 levels of NRK-52E cells after exposure to rat TNF- α and to investigate the effect of pre-treatment with vitamin E, [6]-gingerol or Mn(II)-EHPG
- To characterise the effect of [6]-gingerol, quercetin and kaempferol on short-circuit current (I_{sc}), (indirectly measuring transepithelial ion transport) in Caco-2 cells.
- To investigate the effects of [6]-gingerol, quercetin and kaempferol on ATP-mediated chloride ion secretion

3.2 Materials and methods

3.2.1 Materials, chemicals and reagents

All chemicals were obtained from various sources including Fisher Scientific UK, Loughborough, Leicester and Sigma-Aldrich Ltd, Poole, Dorset, and details are listed in Table 18, whilst a list of instrumentation used is in Table 19.

Table 18. Reagents and solvents used in Chapter 3.

Chemical	Grade	Source	Catalogue Number
Dulbecco's Modified Eagles Medium (DMEM)		Fisher	VX12491023
Fetal Bovine Serum		Fisher	VX10106151
Phosphate Buffer Solution		Fisher	VX14200067
Trypan Blue		Fisher	VX15250061
L-Glutamine		Fisher	VX25030024
Trypsin		Fisher	VX25300054
Xanthine	≥99%	Sigma Aldrich	X7375
Xanthine Oxidase Grade IV from Bovine Milk	Grade IV	Sigma Aldrich	X4875
2,2-Diphenyl-1-Picrylhydrazyl		Sigma Aldrich	D9132
Super Oxide Dismutase from Bovine Erythrocyte	~98% biuret	Sigma Aldrich	S2515
Hydrogen Peroxide	50 weight% in H ₂ O	Sigma Aldrich	516813
α – Tocopherol from vegetable oil	Type IV	Sigma Aldrich	T1539
Copper(II) chloride	99.9%	Sigma Aldrich	203149
Magnesium sulphate	Cell culture tested	Sigma Aldrich	M2643

Manganese (II) Sulfate	Cell culture tested	Sigma Aldrich	M1144
[6]-gingerol		Wako Chemical GmbH	074-05061
Potassium Chloride	99.5%	BDH AnalaR	101984L
D(+) - Glucose		BDH AnalaR	1011747
Sodium Chloride	99.5%	Sigma Aldrich	S6191
Potassium DiHydrogen Orthophosphate	≥99% ACS Reagent	Sigma Aldrich	P0662
Sodium Bicarbonate	99.5%	Sigma Aldrich	S6297
Calcium Chloride solution	1mol.L ⁻¹	BDH AnalaR	190464K
Dimethyl Sulfoxide	99.5%	Sigma Aldrich	D5879
95% Oxygen 5% Carbon Dioxide		BOC Gases	07355010
<i>cis</i> -Platinum-II diammine dichloride		Sigma-Aldrich	479306
Ginger root capsule		Nature's Way	
Human IL-8 ELISA kit		RandD Systems	D8000C
Rat CINC-1		RandD Systems	RCN100
Snapwell Permeable supports (0.4 μM polyester membrane, 12 mm diameter)	Corning Inc	Costar 3801	

Table 19. A list of instrumentation used throughout Chapter 3.

Instrument	Make	Model	Serial Number	Additional Information
Scales	AandD Instruments	HR-120-EC	13700790	Max 120 g Min 10 mg
Centrifuge	Megafuge 1.0	Heraeus Sepatech		Max Speed 2800min ⁻¹ Max Load 360 g
Class II Cabinet	Labcaire BH	BS5726	BH12 095	
Binocular Light Microscope	Olympus BH2	BHS215398	963577	
2 x CO ₂ Incubators	Life Technologies	ICN Flow	9130-012 / 9130-002	
Voltage-clamp amplifier	World Precision Instruments	DVC-1000		
Analog-digital convertor	Biopac Systems	MP100		

3.2.2 Investigation into SOD activity using the NBT assay

The potential SOD mimicry of [6]-gingerol when bound to metals was determined using the modified NBT assay. The modified NBT assay indirectly monitored the production of superoxide, by converting NBT to formazan. A pink solution containing superoxide and urate formed through the enzymatic interactions between xanthine and xanthine oxidase, which can be measured at 295nm. When NBT was present, the superoxide converts to formazan: a blue colour, which can be measured at 550nm. If there was SOD or a SOD mimic the formation of formazan should decrease, hence there would be a decrease in absorbance at 550nm (Fisher, *et al.*, 2004).

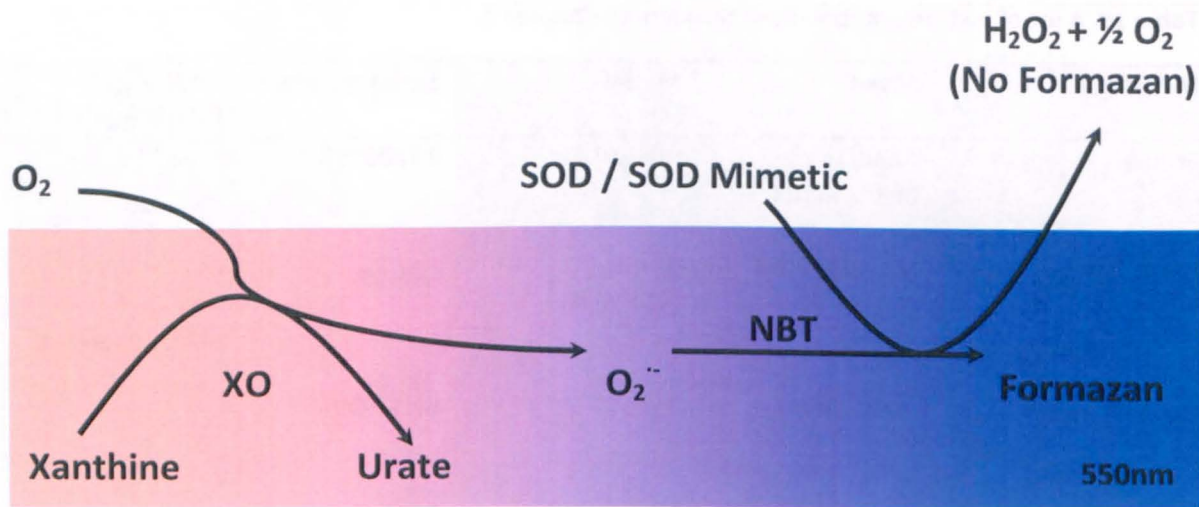


Figure 27. A diagram depicting the NBT assay – adapted from Fisher, 2004. XO = Xanthine oxidase

The test compound together with the NBT assay was equilibrated to 25°C. Following 5 minutes incubation xanthine oxidase was added to the assay and measured spectrophotometrically at 550nm for 3 minutes. The required concentration of xanthine oxidase added to the control was sufficient to change the absorbance at 500nm by was ~0.025 a.u. per minute (control rate required). If there was a decrease in the gradient of the graph it meant a decrease in colour change, inhibiting formazan formation and potentially converting the superoxide to hydrogen peroxide. Therefore, if the compound decreases the formazan formation it could be acting as a SOD mimetic.

Table 20. The contents in cuvette for each set.

NBT solution (mL)	Water (μL)	Tested Compound (μL)	Xanthine Oxidase (μL)
3	30	0	20
3	20	10	20
3	10	20	20
3	0	30	20

A control was needed to show that the test compound was not reacting with NBT. This was done by adding 0.1-1 mM of [6]-gingerol to 100 mM of NBT and following the absorbance of the compound at 550nm at pH 7.8. If [6]-gingerol reacted with the NBT as

seen on the absorbance then the tested compound could not be used within the NBT assay, but [6]-gingerol did not react.

3.2.3 Thin Layer Chromatography and anti-oxidant activity

The TLC plates were identical to the previous Chapter in section 2.2.6 (Rai, *et al.*, 2006; Wagner and Bladt, 2001). TLC was conducted on the methanolic ginger extracts, ginger juice, [6]-gingerol and vitamin E. The extracts and controls were prepared to 1 mg/mL, prior to 20 μ L aliquots of each solution added to the TLC plates. The 2,2-diphenyl-1-picrylhydrazyl (DPPH) spray was prepared by dissolving 8 mg of DPPH to 30 mLs of methanol. The DPPH was sprayed on the TLC plates after they had dried and the areas which did not turn pink were identified as spots with anti-oxidant activity.

3.2.4 Cell culture procedures

Caco-2 cells and NRK-52E cells were cultured at 37°C in humidified air containing 5% CO₂. Caco-2 cells between passage 48 and 60 and NRK-52E cells between passage 32 and 40 were used in the experiments. The media used for the Caco-2 and NRK-52E cells (separate bottles of media were used for each of the different types of cells) was advanced Dulbecco's modified Eagle's medium (DMEM) containing D-glucose, NEAA, sodium pyruvate, without L-glutamine supplemented with 10% fetal bovine serum (20% fetal bovine serum for Caco-2 cells), 1% penicillin-streptomycin and 1% L-glutamine. The culture medium was replaced every 3-4 days.

To determine the growth rate of the Caco-2 and NRK-52E cells were seeded to the multiwell plates (2.6 mLs x6) at 2×10^5 cells.mL and (1 mL x 12) 2×10^5 cells.mL, respectively. The cells were trypsinised daily over a week and aliquots of the trypsinised cells were diluted with a 1 to 1 solution of trypan blue. Trypan blue stains non-viable

(dead) cells. The trypan blue cell solution was injected into the wells of the haemocytometer and the number of viable cells were counted and calculated to determine the number of cells per millilitre each day.

Caco-2 cells which were used for the interleukin-8 studies were seeded to the multiwell plates (2.6 mLs x6) at 2×10^5 cells/mL and experiments were conducted 13-15 days post seeding. Caco-2 Cells which were used for Ussing chamber experiments were seeded at 2×10^5 cells/cm² onto Snapwell permeable supports and experiments were conducted 14-19 days after seeding. NRK-52E cells used for the cytokine-induced neutrophil chemoattractant-1 (CINC-1) studies were seeded onto 12 well plates at 2×10^5 cells/mL and experiments were conducted 24 hours after seeding.

3.2.5 Quantification of IL-8 and CINC-1 levels

Caco-2 cells were treated with media containing [6]-gingerol (25 μ M), Vitamin E (25 μ M), EHPG (25 μ M), Mn(II) sulfate (25 μ M), Mn(II)-EHPG (25 μ M), blank and incubated for 3 hours at day 13-15 post seeding. At 3 hours TNF- α (100 ng/mL) was added to the wells and incubated for a further 24 hours when the supernatant was collected, centrifuged (~350 g) and stored at -80°C for up to a month then tested for the IL-8 levels (Hyun, *et al.*, 2008; Lee, *et al.*, 2008a; Son, *et al.*, 2008). An IL-8 enzyme-linked immunosorbent assay (ELISA) kit was performed to the manufacturer's guidelines.

The NRK-52E cells were treated with media containing [6]-gingerol (25 μ M), Vitamin E (25 μ M), EHPG (50 μ M), Mn(II) ions (50 μ M), Mn(II)-EHPG (50 μ M), blank and incubated for 12 hours, 24 hours after seeding. Rat TNF- α (10 ng/mL) was added to the wells and the cells were incubated for a further 24 hours when the supernatant was collected. The supernatants were centrifuged (~350 g) and stored at -80°C for up to a

month then tested for the CINC-1 levels. A CINC-1 enzyme-linked immunosorbent assay (ELISA) kit was performed to the manufacturer's protocol.

3.2.6 Ussing Chamber Experiments

The permeable supports, containing the 14-19 day old Caco-2 cells, were mounted in Ussing chambers and the current associated with ions (e.g. Na^+ , K^+ , and Cl^-) moving through and between the cells was measured. Krebs-Henseleit buffer consisting of: NaCl 117 mM; NaHCO_3 25 mM; KCl 4.7 mM; MgSO_4 1.2 mM; KH_2PO_4 1.2 mM; glucose 11 mM; and CaCl_2 2.5 mM was prepared and 12 mL was added to each side of the heated water-jacketed buffer reservoirs (37°C) (see Figure 28). The Ussing chamber was bubbled with 95% O_2 /5% CO_2 to prevent the calcium chloride from precipitating out and the pH was maintained at 7.4.

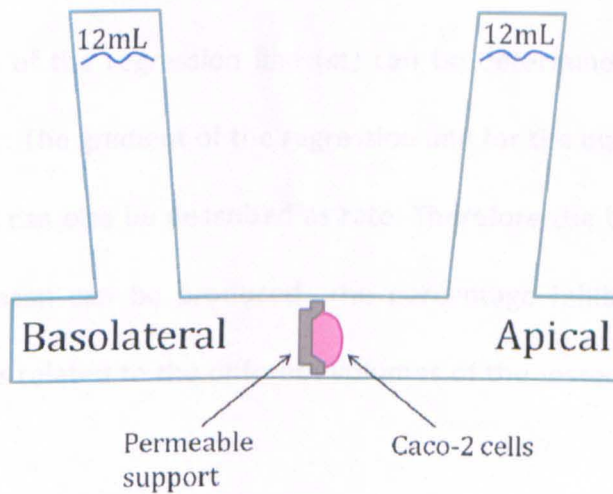


Figure 28. A basic diagram of the Caco-2 cells mounted in the Ussing chamber, identifying the basolateral and apical membrane.

Ag/AgCl electrodes were filled with 2.5% agar in 3M KCl . These current passing and voltage-sensing electrodes were connected to the pre-amplifier and headstage of a voltage clamp amplifier. Short-circuit current (I_{sc}) was converted by an analog-digital converter and the Caco-2 monolayer was voltage-clamped in Ussing chambers to 0 mV.

To calculate transepithelial resistance (Ohm's law) the change in current was used. This was measured by applying small voltage steps (0mV-1mV, 2s duration). I_{sc} ($\mu\text{A}/\text{cm}^2$) was corrected for fluid resistance with a blank Snapwell in the chamber, before experimentation began. The data was displayed either as traces using AcqKnowledge version 3.8.1 or depicted as a graph using GraphPad Prism 4.00 for Windows.

3.2.7 Statistics

Data are expressed as mean \pm SEM. One-way ANOVA was performed using GraphPad Prism version 4.00 for Windows (GraphPad Software, San Diego California USA). $P < 0.05$ was accepted as statistically significant.

3.3 Results

3.3.1 The NBT assay results with [6]-gingerol and Cu(II) ions solution

A range of ratios of the Cu(II) ions (0.1 mM) and [6]-gingerol (0.1 mM) solution was assessed for SOD activity via the NBT assay. A regression line (trend line) and line equation were taken for each of the line graphs for the NBT assay as depicted in Figure 29. Figure 29 displays a reduction in absorbance at 550nm from 1 minute to 3 minutes for each of the concentrations of the Cu(II)-[6]-gingerol solution. The reduction in absorbance at 550nm is related to the reduction in the production of formazan. As formazan forms from $O_2^{\bullet -}$, the $O_2^{\bullet -}$ is being used up within the SOD reaction (a) (page 18) and therefore there is a small amount of SOD activity present for the Cu(II)-[6]-gingerol solution.

The gradient of the regression line (m) can be determined when placed in the format of $y = m x + c$. The gradient of the regression line for the blank was 4.14E-04 (4.14×10^{-4}). The gradient can also be described as rate. Therefore the blank was the greatest rate at which formazan can be produced. The percentage inhibition of formation of formazan (% *IoF*) was related to the different volumes of the tested compounds in Figure 29 by Equation 1.

Equation 1 To determine the % *IoF*.

$$\% IoF = (-241546 \times m) + 100$$

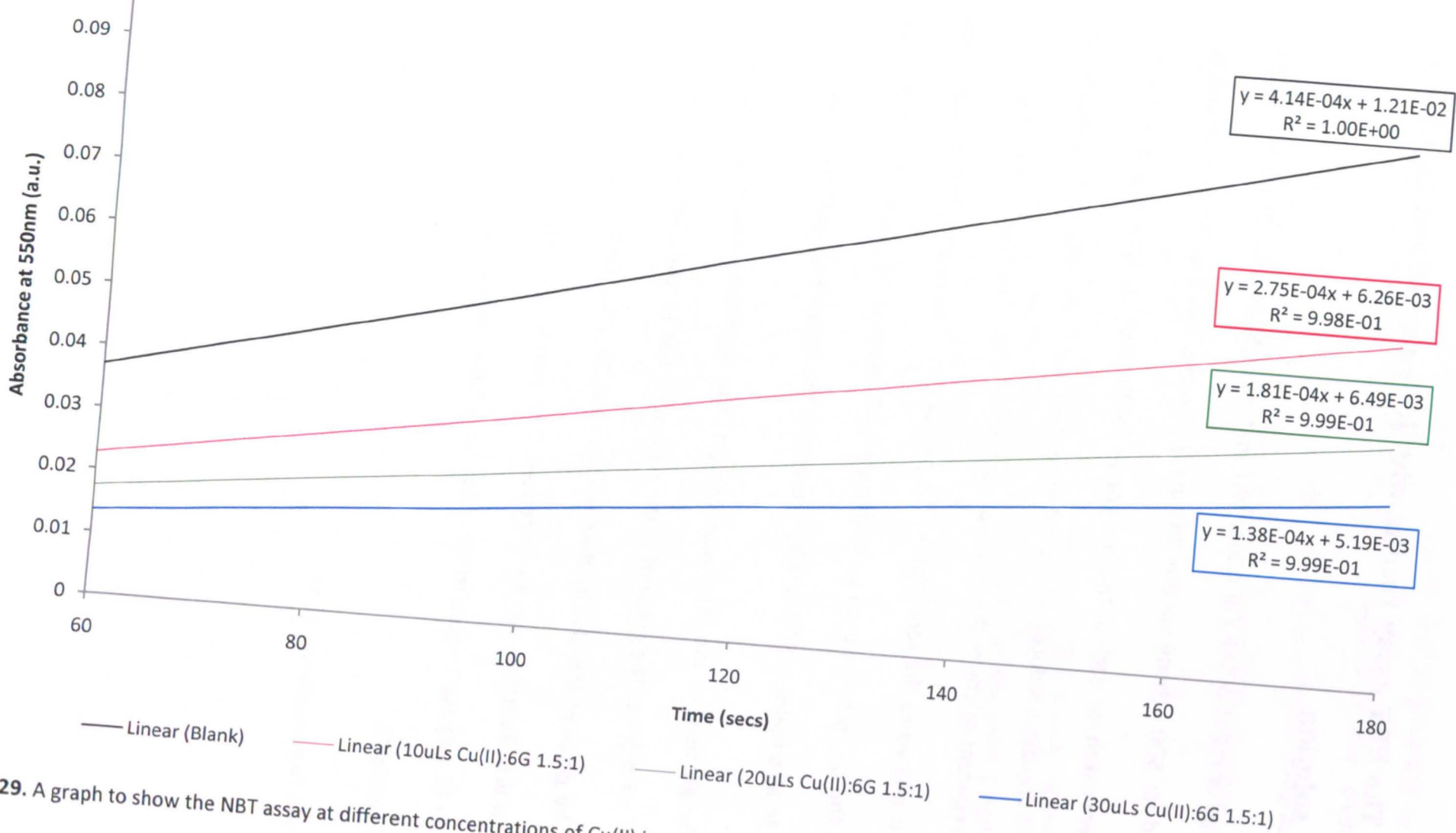


Figure 29. A graph to show the NBT assay at different concentrations of Cu(II) ions and [6]-gingerol at a 1.5:1 ratio.

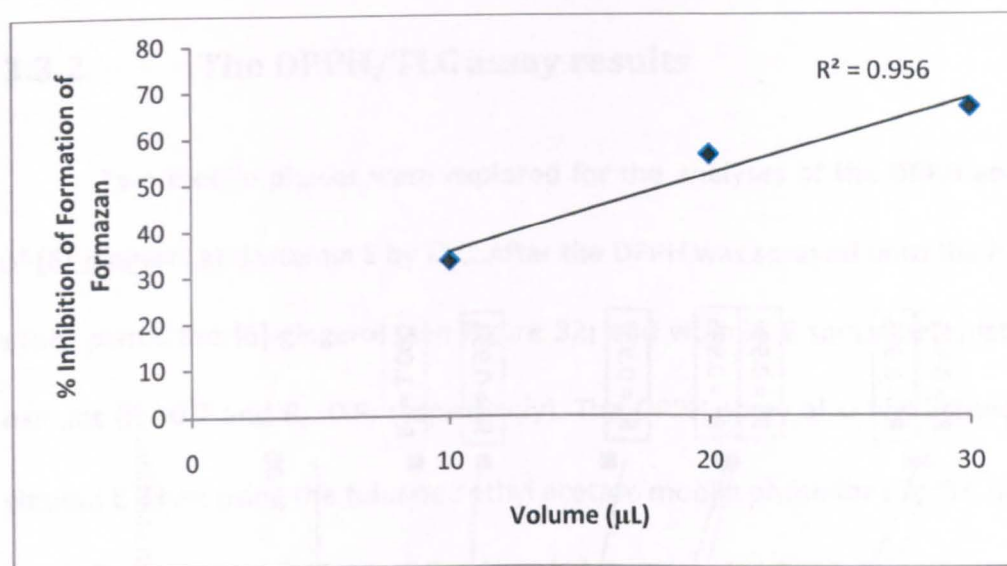


Figure 30. A graph to show the % inhibition of NBT reduction to formazan by solutions of Cu(II) ions and [6]-gingerol at a 1.5:1 ratio.

As previously described in section 2.3.2.1 the R^2 value indicates the 'goodness of fit' of the regression line. The R^2 value of 0.956 represents minimal variance of the data along the regression line. There is a strong relationship between the concentration and the percent inhibition of NBT reduction to formazan. This effect was mainly down to the Cu(II) ions as seen in Table 21.

Table 21. The % *IoF* levels for Cu(II) ions:[6]-gingerol at 1.5:0 and 1.5:1 ratios.

Volume (µL)	% <i>IoF</i> Cu(II) ions:[6]-gingerol solution 1.5:0	% <i>IoF</i> Cu(II) ions:[6]-gingerol solution 1.5:1
10	31.2 ± 8.2%	26.9 ± 3.8%
20	48.5 ± 4.7%	48.9 ± 3.8%
30	58.1 ± 4.2%	64.7 ± 1.5%

Other ratios of Cu(II)-[6]-gingerol solution were tested and the results are displayed in Figure 31. There was no interaction between [6]-gingerol alone and the NBT assay. Bovine erythrocyte superoxide dismutase (1 Unit) was tested to determine the percent inhibition of NBT reduction to formazan, and it was found to inhibit ~85% of formazan production.

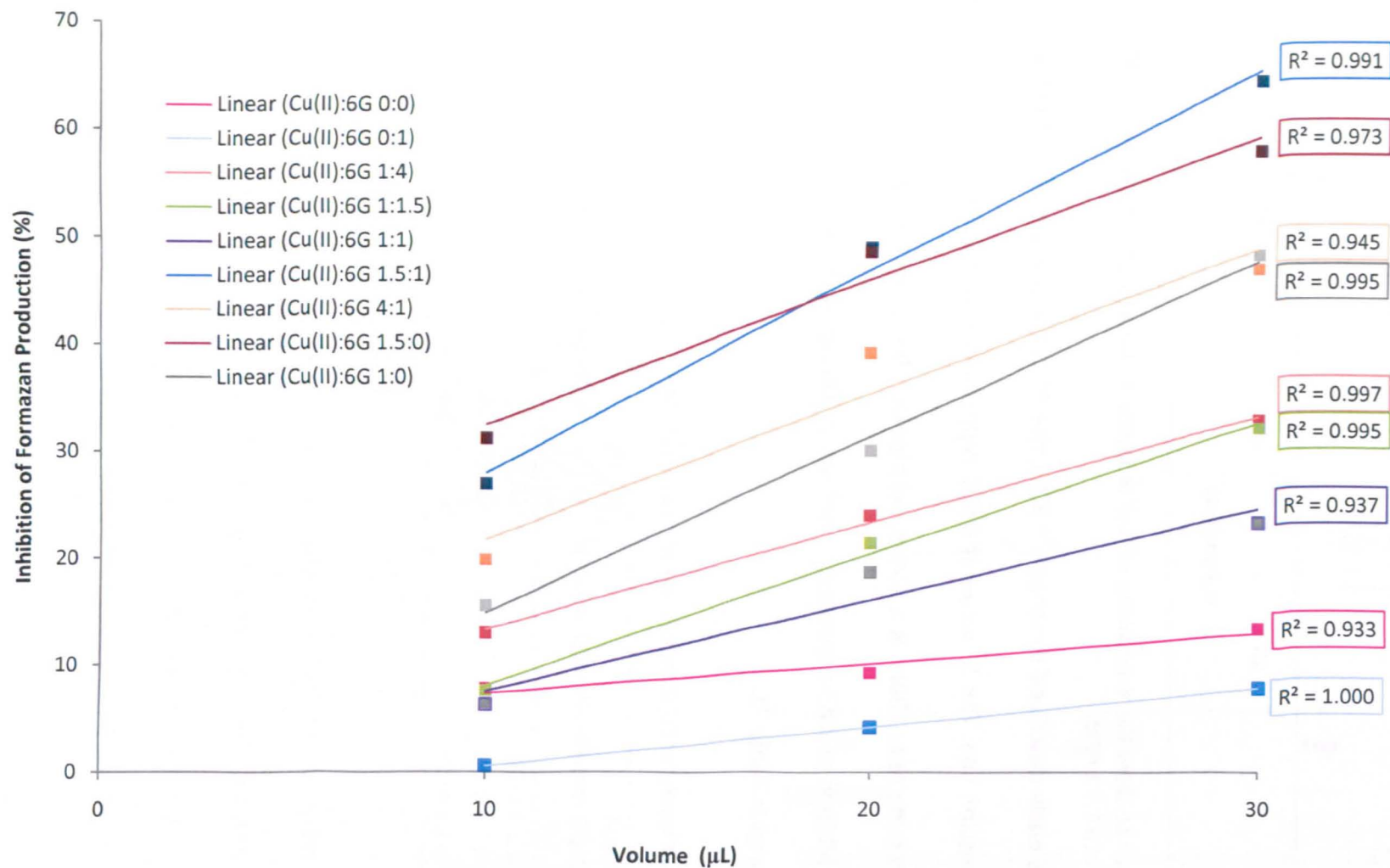


Figure 31. A graph to show the % inhibition of NBT reduction to formazan by varying ratios of Cu(II) ions to [6]-gingerol in solution.

3.3.2 The DPPH/TLC assay results

Two mobile phases were explored for the analyses of the DPPH anti-oxidant activity of [6]-gingerol and vitamin E by TLC. After the DPPH was sprayed onto the hexane and diethyl ether plates the [6]-gingerol (see Figure 32) and vitamin E spots were detected to be anti-oxidant ($R_f \sim 0.2$ and $R_f \sim 0.9$, respectively). The DPPH spray also highlighted [6]-gingerol and vitamin E when using the toluene : ethyl acetate mobile phase for the TLC plates ($R_f \sim 0.04$ and $R_f \sim 0.63$, respectively). None of the 1 mg/mL ginger extracts contained any DPPH free radical scavenging activity.

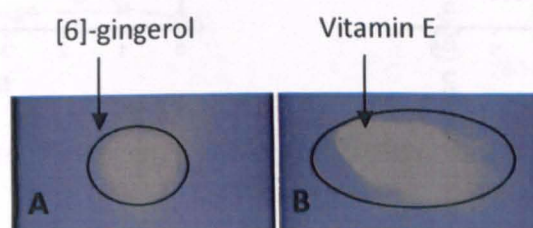


Figure 32. Examples of the TLC plate with the DPPH reagent spray with the mobile phase either as (A) hexane : diethyl ether highlighting the [6]-gingerol spot ($R_f \sim 0.2$) or (B) toluene : ethyl acetate highlighting the vitamin E spot ($R_f \sim 0.6$).

3.3.3 The growth curves of NRK-52E and Caco-2 cells

Growth curves for the NRK-52E cells and Caco-2 cells were calculated over a 7 day period and were repeated every three weeks in duplicate. Day 0 is the first day the cells are seeded. The NRK-52E cells had a very fast rate of growth compared to Caco-2 cells, see Figure 33, as human cells have a slower doubling time. By day 6 there was a 45 fold increase in growth in cells when compared to day 0, the day the cells were seeded. There was a slowing

of the growth between day 5 and day 6 when compared to day 4 and day 5. This was due to the cells colonising most of the surface area of the well.

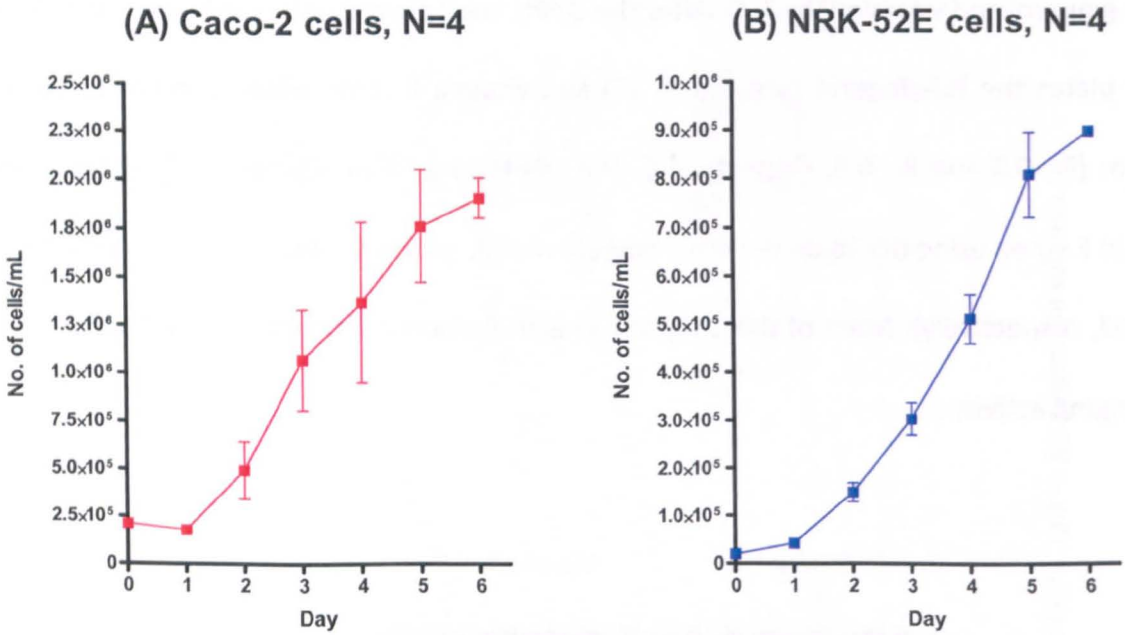


Figure 33. Growth curves of (A) Caco-2 and (B) NRK-52E cells over a week. N = The number of replicates.

The Caco-2 cells had a much slower growth rate compared to the NRK-52E cells (Figure 33). There was a reduction of growth on day 1 in Caco-2 cells, which was due to lack of cell adhesion and cell death. On day 6 there was a ~9 fold increase in the number of Caco-2 cells compared to day 0. The Caco-2 cells and the NRK-52E cells grew exponentially over the 7 day period.

3.3.5 The CINC-1 levels of the NRK-52E cells

The levels of CINC-1 in the media from NRK-52E cells were investigated after the cells were treated with rat TNF- α (10 ng/mL) and pre-treated with either [6]-gingerol (25 μ M), vitamin E (25 μ M) or Mn(II)-EHPG (50 μ M). The Mn(II)-EHPG complex (50 μ M) and the controls did not reduce the levels of CINC-1 in the media from the NRK-52E cells after rat TNF- α was added. There was approximately a 250% increase in CINC-1 levels when rat TNF- α was added to the cells when compared to the vehicle (media) in Figure 34A.

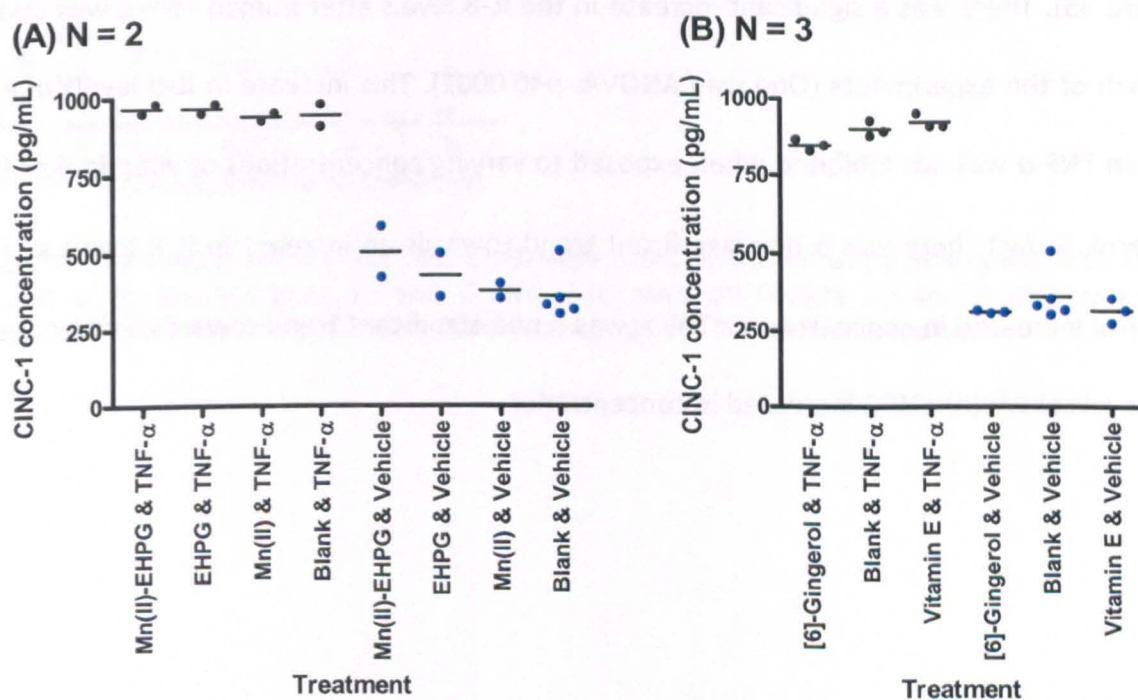


Figure 34. The levels of CINC-1 after the NRK-52E cells were incubated with either (A) Mn(II)-EHPG (50 μ M) or (B) [6]-gingerol (25 μ M) or vitamin E (25 μ M) for 12 hours followed by 24 hours of incubation with rat TNF- α (10 ng/mL). N = The number of replicates, although the blank and TNF- α , and blank and vehicle have an N = 5.

There was a trend for the CINC-1 concentration from the media incubated with [6]-gingerol and rat TNF- α to be less when compared to the blank with rat TNF- α , it was not valid to apply statistics as the N number was so low. Vitamin E and TNF- α has a higher

concentration of CINC-1 when compared to [6]-gingerol. The blank and vehicle appears to have a higher concentration of CINC-1 when compared to the [6]-gingerol and vitamin E, but was not significant.

3.3.6 The IL-8 levels of the Caco-2 cells

The levels of IL-8 in the media from Caco-2 cells were investigated after the cells were treated with human TNF- α (100 ng/mL) and pre-treated with either [6]-gingerol (0.25, 2.5 and 25 μ M), vitamin E (0.25, 2.5 and 25 μ M) or Mn(II)-EHPG (0.25, 2.5 and 25 μ M) or a blank (Figure 35). There was a significant increase in the IL-8 levels after human TNF- α was added to each of the experiments (One way ANOVA, $p < 0.0001$). This increase in IL-8 levels due to human TNF- α was not inhibited when exposed to varying concentrations of vitamin E or [6]-gingerol. In fact there was a non-significant trend towards an increase in IL-8 levels as [6]-gingerol increased in concentration. There was a non-significant trend towards a decrease in IL-8 levels as Mn(II)-EHPG increased in concentration.

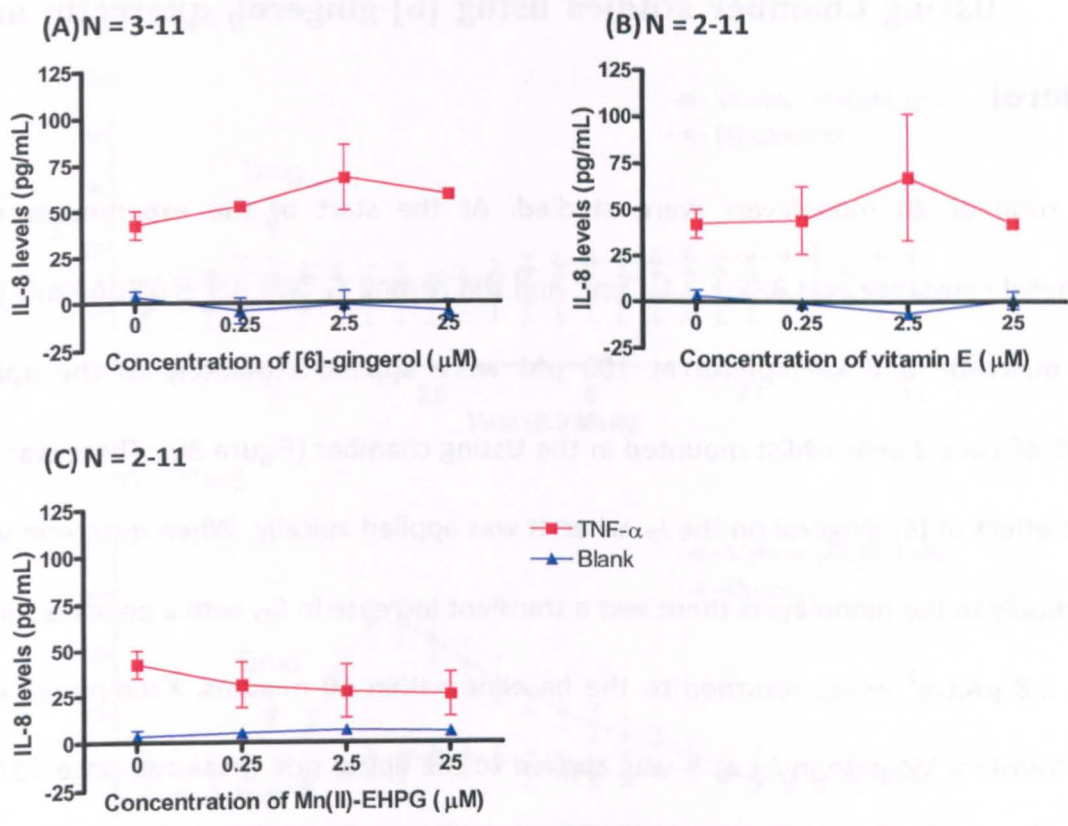


Figure 35. The levels of IL-8 after the Caco-2 cells were incubated with either (A) [6]-gingerol (0.25, 2.5 and 25 μM) or (B) vitamin E (0.25, 2.5 and 25 μM) or (C) Mn(II)-EHPG (0.25, 2.5 and 25 μM) for 3 hours followed by 24 hours of incubation with TNF- α (100 ng/mL). N = The number of replicates.

3.3.7 Ussing Chamber studies using [6]-gingerol, quercetin and kaempferol

A total of 20 monolayers were studied. At the start of the experiments the transepithelial resistance was $325 \pm 3.1 \Omega\text{cm}^2$ and the resting I_{SC} was $4.9 \pm 0.8\mu\text{A}/\text{cm}^2$. [6]-gingerol, quercetin and kaempferol at $100 \mu\text{M}$ were applied separately to the apical membrane of Caco-2 cells whilst mounted in the Ussing chamber (Figure 36). There was no significant effect of [6]-gingerol on the I_{SC} when it was applied apically. When quercetin was applied apically to the monolayers there was a transient increase in I_{SC} , with a peak response of $15.5 \pm 2.8 \mu\text{A}\cdot\text{cm}^2$ which returned to the baseline within 10 minutes. Kaempferol also caused a transient increase in I_{SC} as it was applied to the apical side (peak response $10.9 \pm 1.59 \mu\text{A}\cdot\text{cm}^2$) which returned to the baseline within 10 minutes. Interestingly the vehicle controls of 0.5% ethanol caused an increase in I_{SC} , whilst 0.5% methanol did not. When [6]-gingerol, quercetin and kaempferol were applied basolaterally there was no effect on I_{SC} as shown in Figure 37).

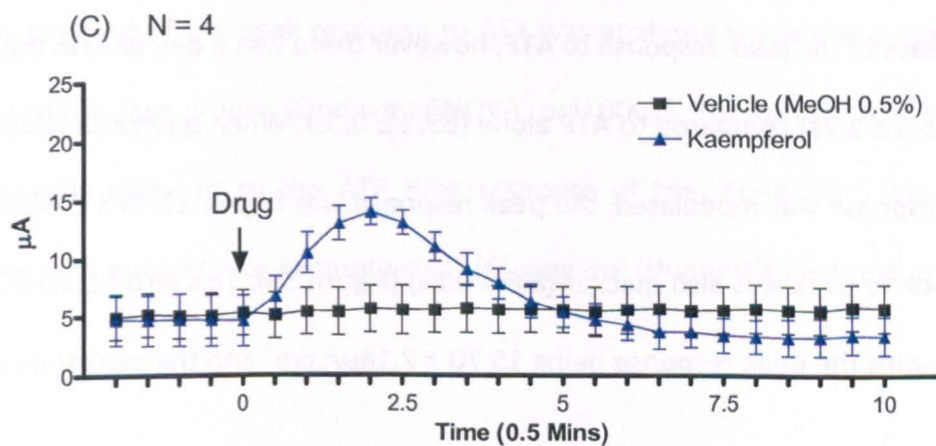
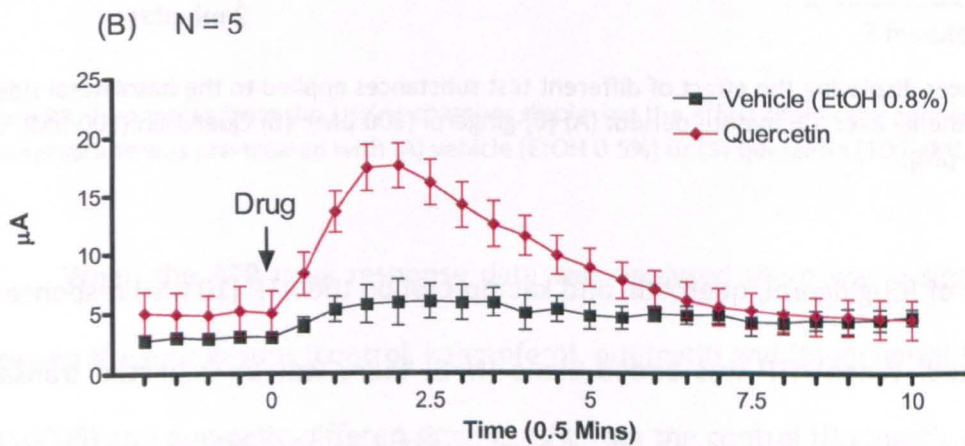
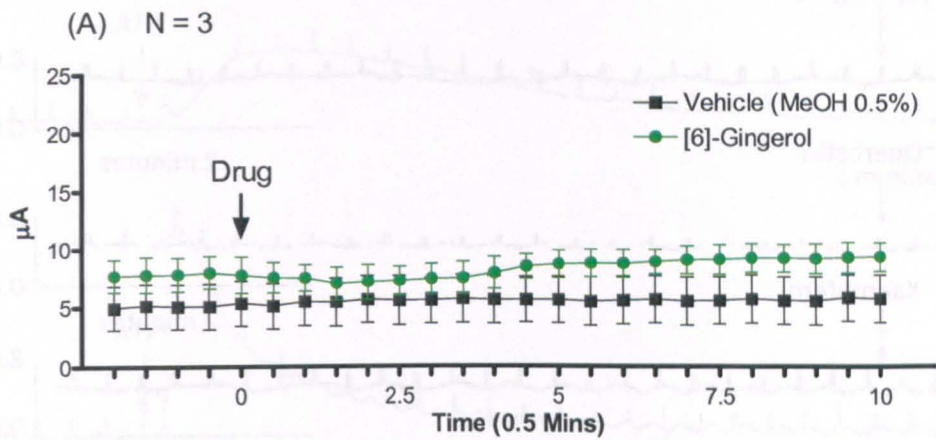


Figure 36. Three graphs displaying the effect of different test substances applied to the apical side of the monolayers on the I_{SC} over a 10 minute period: (A) [6]-gingerol (100 μ M); (B) Quercetin (100 μ M); and (C) Kaempferol (100 μ M). N = The number of replicates.

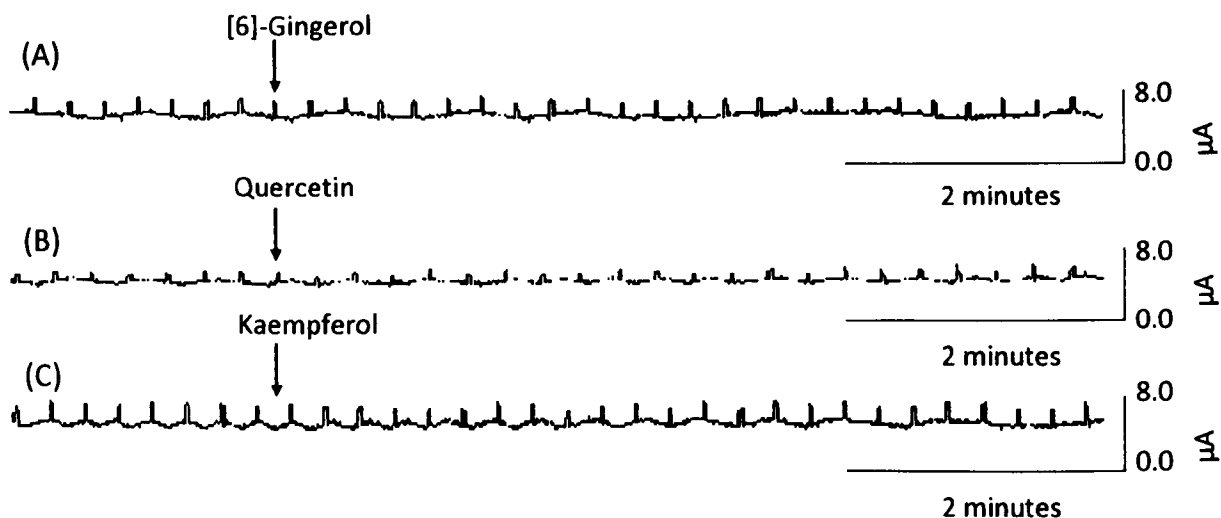


Figure 37. Three traces displaying the effect of different test substances applied to the basolateral side of the monolayers on the I_{SC} over a 6 minute period: (A) [6]-gingerol (100 μM); (B) Quercetin (100 μM); and (C) Kaempferol (100 μM).

The effect of [6]-gingerol, quercetin and kaempferol on the ATP (10 μM) response on I_{SC} was investigated. When ATP was added alone (N=8) there was an expected transient increase in I_{SC} , the peak response was $10.58 \pm 1.01 \mu\text{A} \cdot \text{cm}^2$ (Figure 38A). [6]-gingerol (N=3) did not cause an increase in the peak response to ATP, however there was a decrease in the time it took to peak ($35.3 \pm 1.7\text{s}$) compared to ATP alone ($69.1 \pm 0.3\text{s}$). When quercetin (N=5) was applied the ATP response was modulated, the peak response was higher $17.55 \pm 2.68 \mu\text{A} \cdot \text{cm}^2$ and the time it took to peak was also quicker ($8.6 \pm 0.8\text{s}$) (Figure 39). This also occurred with kaempferol (N=4) with the peak response being $15.70 \pm 2.14 \mu\text{A} \cdot \text{cm}^2$ and the peak time being $8.7 \pm 0.4\text{s}$.

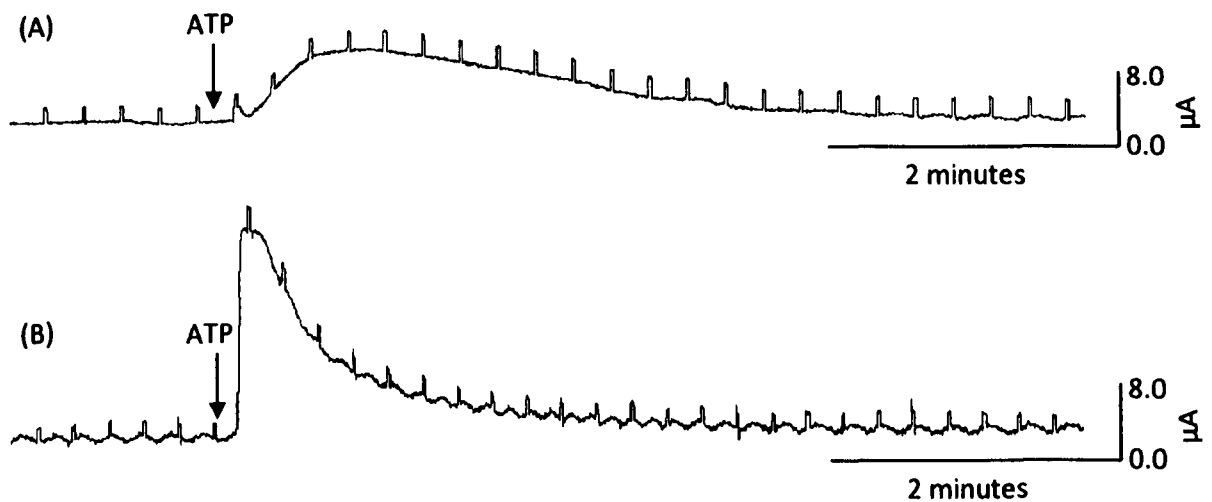


Figure 38. Two traces from the Ussing chamber displaying the effect of apically applied ATP (10 μ M) when the membrane was pre-treated with (A) vehicle (EtOH 0.5%) or (B) quercetin (100 μ M).

When the ATP peak response data was analysed there was a significant difference between the four groups (control, kaempferol, quercetin and [6]-gingerol) (One way ANOVA, $p < 0.0096$) and quercetin differed significantly from the control (Dunnett's post test, $p < 0.05$). When the time of the peak response to ATP was analysed there was a significant difference between the four groups (One way ANOVA, $p < 0.0001$). The control ATP time response was significantly different to the ATP time response of the monolayers which had been pre-treated with quercetin or kaempferol or [6]-gingerol (Dunnett's post test, $p < 0.001$) see Figure 39B.

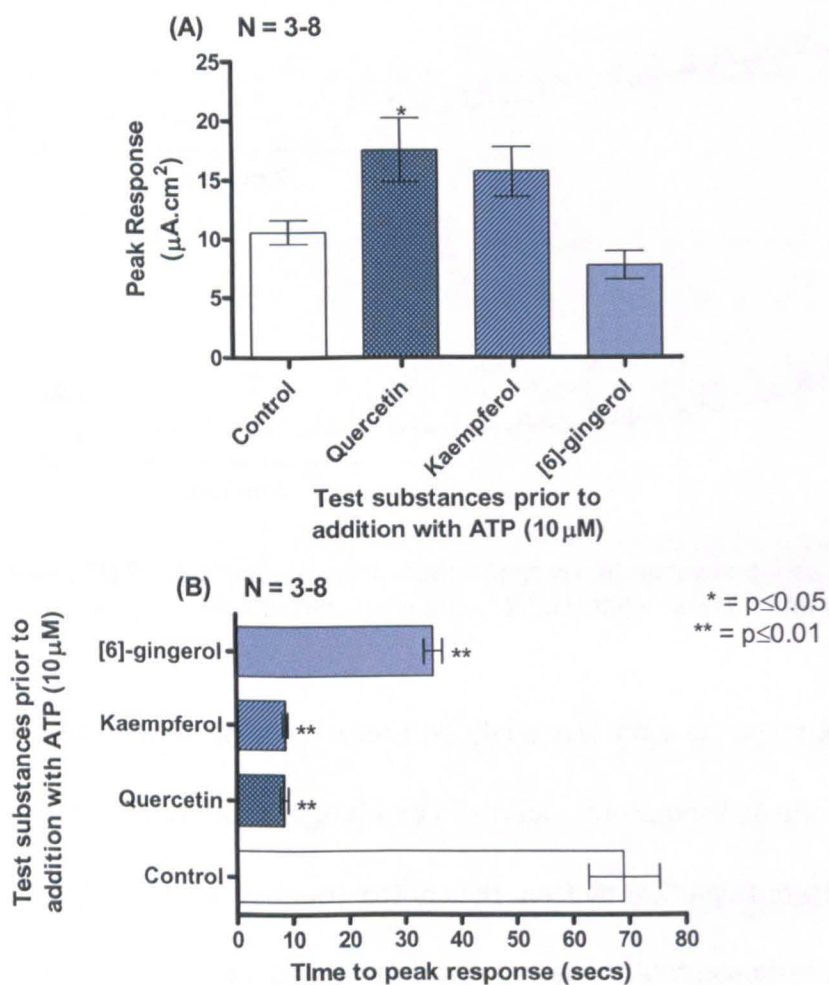


Figure 39. The effect of $100\mu\text{M}$ of either [6]-gingerol, quercetin and kaempferol on the ATP response on (A) the peak response and (B) the time it took to peak response. N = The number of replicates.

* = $p \leq 0.05$, ** = $p \leq 0.01$

[6]-gingerol may have caused a small change in I_{SC} but there were no statistically significant effects on the I_{SC} of the Caco-2 monolayers, although it did increase the response time of the ATP peak. On the whole, the responses of quercetin and kaempferol on the I_{SC} of the Caco-2 monolayer were very similar, as were the effects on the augmentation of the ATP response.

3.4 Discussion

The anti-inflammatory and anti-oxidant effects of [6]-gingerol, vitamin E and Mn(II)-EHPG were investigated in non-cell based assays, NRK-52E cells and Caco-2 cells. [6]-Gingerol, quercetin and kaempferol were also investigated for the effect on transepithelial ion transport in Caco-2 cells, and ATP-mediated chloride secretion.

3.4.1 The potential anti-oxidant activity of [6]-gingerol

The TLC plates with 20 μ Ls of 1 mg/mL methanolic ginger extracts, ginger juice, [6]-gingerol and vitamin E were investigated for their anti-oxidant activity using a DPPH spray. None of the methanol extracts displayed any anti-oxidant activity (yellow spot), whilst [6]-gingerol and vitamin E did. It may be that the extracts were not concentrated enough to generate anti-oxidant activity against the free radical DPPH. CO₂ extracts of ginger have been shown to significantly inhibit DPPH up to 90.1% at 20 μ g/mL (Stoilova, *et al.*, 2007). By contrast, another study indicated that a ginger extract had $6.0 \pm 0.4\%$ anti-oxidant activity of conjugated diene measurement of methyl linoleate after 72 hours (Rababah, *et al.*, 2004). This study showed the variability of the anti-oxidant activity in the type of ginger extract, a possible explanation as to why the ginger extract did not display the DPPH anti-oxidant activity in this instance.

Iberogast® (STW-5) is used as a treatment for gastrointestinal disorders and is a combination of nine medicinal plant ethanolic extracts (Schempp, *et al.*, 2006). The anti-oxidant properties of this herbal extract were found to be higher when each of the plant extracts were included, if one plant was removed the anti-oxidant capacity decreased. This

indicates the need for a combination of plant extracts, and the synergism of the plant extracts, as there were pro-oxidant effects of single components but when combined they were no longer pro-oxidant. Iberogast® has also been shown to affect the rat small intestine by desensitising the afferents (Müller, *et al.*, 2006). These types of combined herbal extracts have been shown to be useful in treating gastrointestinal disorders including non-ulcer dyspepsia as they may affect the oxidant status as well as desensitising the afferents.

When [6]-gingerol was combined with Cu(II) ions in varying ratios the SOD activity was investigated using the NBT assay. There was SOD activity present in the 1.5:1 ratio of Cu(II) ions and [6]-gingerol. However when running the controls for this experiment of Cu(II) ions and [6]-gingerol it appears that the Cu(II) ions are mostly responsible for the effect on formazan formation see Table 21. Therefore the Cu(II)-[6]-gingerol solution was not more effective than the control of Cu(II) ions alone on the percent inhibition of NBT reduction to formazan. This solution was used at low concentrations (0.1 mM), to prevent precipitation and this may have hindered the investigation into SOD activity. The 1:1 Cu(II)-curcumin complex, at 0.17 μ M, was very effective as a SOD mimetic (Barik, *et al.*, 2007).

Unfortunately, this solution of Cu(II)-[6]-gingerol did not behave as expected, that is, like the Cu(II)-curcumin complex. This may be due to the structure of [6]-gingerol. Other complexes have also been shown to have SOD mimicry including Cu(II)-EHPG and Mn(II)-EHPG and to prevent cytotoxic effects of paraquat in rat kidney cells (NRK-52E) (Fisher, *et al.*, 2004; Samai, *et al.*, 2008).

3.4.2 The investigation into the CINC-1 levels in rat kidney cells

The NRK-52E cells grew exponentially. When the cells were treated with TNF- α (10 ng/mL), the CINC-1 levels increased by ~250% CINC-1 levels. However, when [6]-gingerol (25 μ M), vitamin E (25 μ M) and Mn(II)-EHPG (50 μ M) compounds were added to the NRK-52E cells prior to rat TNF- α there was no reduction in the CINC-1 levels. So although Mn(II)-EHPG has been shown to be effective against paraquat-induced renal cytotoxicity in NRK-52E cells, it did not prevent increases in the cytokine CINC-1 levels in rat kidney cells after TNF- α was applied. Therefore the SOD mimetic compounds may only affect the anti-oxidant activity rather than also interrupting inflammatory signalling.

Overall, 10 ng/mL TNF- α increased the CINC-1 levels to ~250% of the original levels, and cisplatin (1 μ g/mL), [6]-gingerol (25 μ M), vitamin E (25 μ M) and Mn(II)-EHPG (50 μ M) had no effect on the inflammatory levels in NRK-52E cells. Mn(II)-EHPG may be effective as an anti-oxidant and prevent the generation of reactive oxygen species by paraquat and prevent cytotoxicity in NRK-52E cells at high concentrations (30-100 μ M), but it does not appear to affect the anti-inflammatory cytokines.

3.4.3 The investigation into the IL-8 levels in human colon cancer cells

Caco-2 cells grew exponentially after day 2 and this is similar to the growth curve of Caco-2 cells by Panagiotou, 2006. The treatment with human TNF- α (100 ng/mL) did increase the IL-8 levels to 42.5 ± 7.5 pg/mL from 3.0 ± 3.2 pg/mL without TNF- α in Caco-2 cells. [6]-gingerol, vitamin E, and Mn(II)-EHPG (0.25, 2.5 and 25 μ M) did not modulate the IL-8 levels of

Caco-2 cells after being treated with human TNF- α (100 ng/mL). These compounds were not effective in altering the IL-8 levels, although this does not mean that they would not alter the activity and/or production of COX-2 or prostaglandins.

[6]-gingerol (12.5-50 $\mu\text{g/mL}$) has been shown to increase apoptosis in human gastric cancer cells with the aid of tumour necrosis factor-related apoptosis-inducing ligand (TRAIL), but not alone. [6]-shogaol (2 $\mu\text{g/mL}$) was capable of apoptosis of the gastric cancer cells alone, and increased apoptosis induced by TRAIL, suggesting that although the compounds are very similar in structure the mechanism of action for apoptosis of these gastric cancer cells is different (Ishiguro, *et al.*, 2007). However, [6]-gingerol (200 μM) alone has been shown to induce cell growth arrest and apoptosis in Caco-2 cells (8%) for 72 hours (Lee, *et al.*, 2008a).

In human monocytic THP-1 cells a ginger extract inhibited the activation of proinflammatory cytokines and inhibited the expression on the genes for TNF- α , IL-1 β , and COX-2 (Grzanna, *et al.*, 2004). Thus the ginger extract may be working on the inflammatory pathways prior to TNF- α expression rather than post TNF- α expression. Lipopolysaccharide-induced PGE₂ production was inhibited by ginger extracts in U937 cells, the most active extracts contained [6]-, [8], and [10]-gingerol (Jolad, *et al.*, 2005; Lantz, *et al.*, 2007).

Human synoviocytes stimulated with TNF- α had reduced mRNA and protein secretion levels of interferon- γ -inducible protein-10 and macrophage chemoattractant protein-1 when exposed to ginger extracts (Talhouk, *et al.*, 2007). In mouse skin, when exposed to [6]-gingerol (25 μM), phorbol 12-myristate 13-acetate-induced COX-2 expression and NF- κB

activation was inhibited (Kim, *et al.*, 2004). All these reports suggest that there are various effects of ginger constituents on the inflammatory and apoptotic processes.

Vitamin E has been used as a positive control for [6]-gingerol; however a study by Habsah, *et al.*, (2000) found that dichloromethane and methanolic extracts of ginger were equivalent to vitamin E or higher for anti-oxidant activity. Vitamin E has been shown to act post-transcriptionally on COX-2 activity in Caco-2 cells when stimulated with interleukin-1 β , but not pre-transcriptionally on the COX-2 mRNA expression (O'Leary, *et al.*, 2004b). Whereas the anti-oxidant, quercetin, has been shown to act pre and post-transcriptionally on COX-2 expression in Caco-2 cells (O'Leary, *et al.*, 2004b).

3.4.4 The investigation into the effect of [6]-gingerol, quercetin and kaempferol on I_{sc} in Caco-2 cell monolayers

The Caco-2 cells were grown on snapwells for 14 days and grew an effective confluent monolayer shown by good resistance. Here [6]-gingerol had no significant effect on I_{sc} in Caco-2 cells, unlike the effect noted by O'Leary, *et al.*, (2004a). They reported that 100 μ M of [6]-gingerol added bilaterally inhibited chloride secretion in rat colonic mucosae, and indicated that [6]-gingerol may close tight junctions in canine tissue under basal conditions. Although there was no effect of [6]-gingerol on the Caco-2 cells, it could be because the monolayer is different to the mucosae from the two species used in the O'Leary, *et al.*, (2004a) study. The responses due to quercetin and kaempferol were likely to represent chloride secretion. When the test substances were applied basolaterally, there was no effect on I_{sc} (Figure 37).

Sánchez de Medina, *et al.*, (1997) used quercetin bilaterally on T84 monolayers and found quercetin was active on both sides, however in the Caco-2 cells here, the apical side was the only side active for quercetin and kaempferol. Quercetin induces chloride secretion in the rat colon and has previously been reported to be dependent on Ca^{2+} -calmodulin, not due to the cyclic AMP (Cermak, *et al.*, 1998; Cermak, *et al.*, 2000). However, further work by Carew, *et al.*, (submitted 2009) studied the effect of quercetin and kaempferol on the ATP response in detail in the Caco-2 cells and rat colonic mucosae and the proposed pathway was cyclic AMP mediated. This pathway has been shown to be concurrent with other research investigating the effect of flavonoids on the secretory response: for example, naringenin in isolated rat colonic mucosae and baicalein in T84 intestinal epithelial cell monolayers (Yang, *et al.*, 2008; Yue, *et al.*, 2004). These flavonoids may be in high concentrations in the colon where the enterobacteria are located in the aglycone form. As these flavonoids increase the response to ATP (up to 8 fold), they may be able to stimulate chloride ion secretion which in turn lubricates the lumen through osmosis. Flavonoids may be able to assist individuals with constipation, but in high concentrations they may also cause diarrhoea (Yang, *et al.*, 2008).

3.4.5 Conclusions and further work

The effect of the Cu(II)-[6]-gingerol solution on the NBT assay was fully accountable by the effect of Cu(II) ions alone. There were no anti-oxidant effects of the methanolic ginger extracts (1 mg/mL) on TLC plates on the DPPH spray. TNF- α did significantly increase the cytokine levels in NRK-52E and Caco-2 cells. There were no effects of [6]-gingerol, vitamin E, Mn(II)-EHPG, on TNF- α - induced increase in cytokines in NRK-52E and Caco-2 cells. [6]-gingerol had no effect on the I_{sc} of the Caco-2 cells, however apical quercetin and kaempferol

did increase the I_{sc} and augmented the ATP response which is likely to be due to chloride secretion. The mechanism of action includes stimulation of adenylyl cyclase. In further work MDL12330A (an adenylyl inhibitor) prevented the I_{sc} increase of quercetin and kaempferol but did not affect the secretory result of ATP.

Further work using the Caco-2 cells would consist of investigating 1) other cytokines including PGE_2 , 2) other compounds present in ginger including [6]-shogaol and 3) applying different inflammatory stimulants e.g. H_2O_2 on the Caco-2 cells. The ion channel work proved successful in observing the effect of quercetin and kaempferol on chloride ion secretion and the ATP response. Further work in this area could include investigating the effect of other compounds (isoliquiritigenin or capsaicin) on the Caco-2 cells and also using colonic mucosae from the mouse or rat.

CHAPTER FOUR

IN VITRO INVESTIGATION OF THE
GASTROINTESTINAL MOTILITY
EFFECTS OF GINGER JUICE AND
ITS SELECTED CONSTITUENTS IN
SUNCUS MURINUS

4.1 Introduction

Borrelli, *et al.*, (2004) demonstrated that when a ginger rhizome acetone extract, standardised to contain 0.8% essential oils (0.01-1000 µg/L) was applied to rat ileum *in vitro* there was a dose dependent inhibitory effect on the electrically stimulated and acetylcholine evoked contractions. Zingerone, a constituent of ginger, was not found to inhibit the contractions of the rat ileum produced by the same stimuli. Guinea-pig ileum studies also showed an inhibition of contraction evoked by acetylcholine or substance P when in the presence of [6], [8] or [10]-gingerol or [6]-shogaol (Abdel-Aziz, *et al.*, 2006). On 5-HT evoked contractions on guinea pig ileum gingerols and shogaol caused a powerful inhibition of contraction, indicating that the gingerols and shogaol may be acting on the 5-HT receptors. It appears that there may be an overlap with the vanilloid receptor and the 5-HT₃ receptor, as [6]-gingerol is thought to be a weak TRPV1 agonist as it mimicked the effects of capsaicin and resiniferatoxin, causing inhibition of contraction (Abdel-Aziz, *et al.*, 2006; Dedov, *et al.*, 2002). It may be that the gingerols and shogaols interact with the 5-HT₃ receptors as an antagonist as well as acting on the vanilloid receptor, as [6]-gingerol has the vanilloid region, like capsaicin. The mechanism of action for [6]-gingerol has not fully been established, therefore it may be a mix of these two receptors or it may even cause an effect on another receptor entirely.

Galanolactone, a diterpenoid, isolated from Japanese ginger was described as being a 5-HT₃ receptor antagonist on guinea pig ileum (Huang, *et al.*, 1991). The effect of a 70%:30% aqueous: methanolic extract of ginger on the gastrointestinal tract was investigated in isolated rat and mouse stomach fundus, rabbit jejunum, rat, mouse and guinea pig ileum,

and guinea pig colon (Ghayur and Gilani, 2005b). The ginger extract (0.003, 0.03, 0.3 and 3 mg/mL) reduced the K^+ -induced contractions (80 mM) of each of the jejunum, ileum and colonic tissues in a dose dependent manner and had a similar effect to the calcium channel blocker, verapamil. However, the extract caused an increase in stomach fundus contractility, which was blocked by atropine. Therefore there is a regionally specific effect of the ginger extract on the gastrointestinal tract, 1) a spasmogenic (contractile) effect on the stomach mediated by cholinergic receptors and 2) a spasmolytic (relaxing) effect on the intestine due to antagonism of the Ca^{2+} channels (Ghayur and Gilani, 2005b).

The ileum of the *Suncus murinus* has been studied for the involvement of 5-HT receptors, and neurokinin(1), 2 and 3 receptors on the contraction of the ileum (Cheng, *et al.*, 2008; Javid and Naylor 1999a). There is little work on the upper gastrointestinal tract of the *S. murinus*, despite the fact that the species is capable of emesis, unlike rats. Javid and Naylor (1999a) took 8x1cm longitudinal segments of intestine originating 1cm distal to the pyloric sphincter named S1-S8 and characterised the 5-HT receptors involved with contraction of the intestine. The 5-HT_{2C} receptor was identified as mediating the contractions throughout the intestine; however the 5-HT₃ receptors also played a role in the central and terminal regions of the intestine (Javid and Naylor, 1999a; Javid and Naylor, 1999b). In human jejuna mucosa, 5-HT has been shown to act through 5-HT₄ receptors and to induce the secretion of chloride ions (Kellum, *et al.*, 1994). Receptor distributions will always differ between species. Interestingly, all of the studies of the effect of ginger on the gastrointestinal tract have been performed on the non-emetic species (rodents and lagomorphs). To date, there have been no *in vitro* studies on the effect of ginger on *S. murinus* gastrointestinal tract.

This chapter investigates the effects of ginger juice on the upper gastrointestinal tract including the proximal and distal stomach and the duodenum from a species capable of vomiting, *S. murinus*. The effects of the separate and combined constituents of ginger juice identified in Chapter 2 being [6]-gingerol and five elements previously detected in high concentrations in ginger juice (potassium chloride; magnesium chloride; manganese sulphate; sodium chloride; and calcium chloride) are also studied on the upper gastrointestinal tract. When these constituents at the concentrations found in ginger juice were combined this solution was named “faux” ginger juice. These constituents were investigated to identify if they may be responsible for the reported effects on the gastrointestinal tract.

4.1.1 Aims

The aims of this chapter are:

- To investigate the effect on the tone, contraction amplitude and frequency of contractions of the proximal and distal stomach and the duodenum by: -
 - a. ginger juice,
 - b. [6]-gingerol,
 - c. an element solution containing five elements previously detected in high concentration in ginger juice and
 - d. “faux” ginger juice.

4.2 Materials and methods

4.2.1 Materials and Instrumentation

The sources of chemicals including grade and batch details are given in Table 22, whilst the instrumentation list used is in Table 23.

Table 22. Reagents and solvents used in Chapter 4.

Chemical	Grade	Source	Catalogue Number	Batch
DiPotassium Hydrogen Orthophosphate Trihydrate	≥98% ACS reagent	Sigma Aldrich	P3786	
Potassium DiHydrogen Orthophosphate	≥99% ACS Reagent	Sigma Aldrich	P0662	
Magnesium sulphate	Cell culture tested	Sigma Aldrich	M2643	025K01541
Magnesium chloride	Cell culture tested	Sigma Aldrich		
Manganese (II) Sulfate	Cell culture tested	Sigma Aldrich	M1144	084K06431
[6]-gingerol		Wako Chemical GmbH	074-05061	WKM0536
Potassium Chloride	99.5%	BDH AnalaR	101984L	K31372738
D(+)-Glucose		BDH AnalaR	1011747	
Sodium DiHydrogen Orthophosphate	99%	Fisons Analytical Reagent	S376053	73153142
Sodium Chloride		Sigma Aldrich	S6191	
Sodium Bicarbonate	99.5%	Sigma Aldrich	S6297	055K0190
Calcium Chloride (Fused mesh granules)	90%	BDH AnalaR	27587	9341140D
Calcium Chloride solution	1mol.L ⁻¹	BDH AnalaR	190464K	OC493153
Dimethyl Sulfoxide	99.5%	Sigma Aldrich	D5879	015K0151

95% Oxygen 5% Carbon Dioxide		BOC Gases	07355010	664016
------------------------------	--	-----------	----------	--------

Table 23. A list of instruments used throughout Chapter 4.

Instrument	Make	Model	Serial Number	Additional Information
2x6 Analog-digital convertor	Biopac Systems	MP100 A-CE	#1 1094236 #2 206A4584	
12x Tension Adjusters	Biopac Systems	HDW100A		
Water heating circulating bath	Techne	FTE-10AEC Tempette®	141988-15	

4.2.2 Animals

Adult male and female *S. murinus* were bred at St George's University of London. The mean weight of males was $49.1 \text{ g} \pm 1.2$ (N = 39) and females was $40.8 \text{ g} \pm 0.6$ (N= 48). The adults were kept two to a cage and given access to food and water *ad libitum*. There was a 12 hour light and dark cycle between the hours of 7am and 7am.

4.2.3 Euthanasia of *Suncus murinus*

All *S. murinus* were killed by a Schedule 1 (Home Office) method (CO₂ asphyxiation followed by cervical dislocation). An incision along the abdomen was made immediately *post mortem* to expose the liver, stomach, intestines and reproductive organs. The stomach and small intestine were excised from the abdomen and immediately placed into chilled Krebs' solution gassed with 95% O₂ and 5% CO₂.

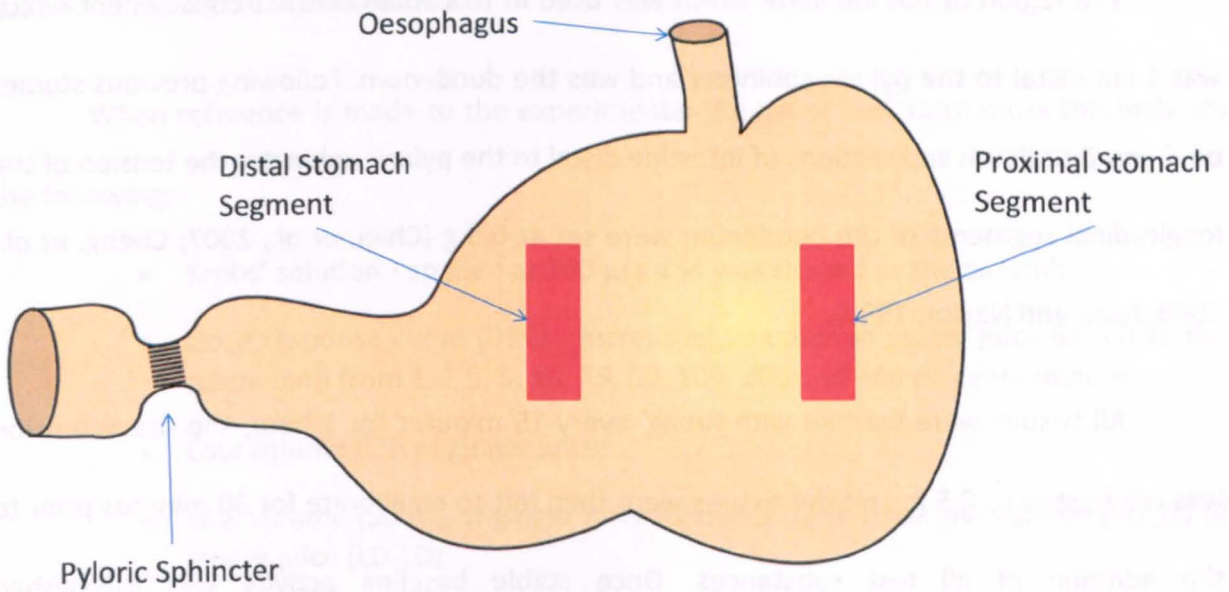


Figure 40. A diagrammatical representation of the *Suncus murinus* stomach specifying where the segments of were taken.

4.2.4 Tissue bath protocol

All excess connective tissue and fat was removed from the excised tissue. Circular strips (4 mm by 8 mm) of proximal and distal stomach were taken from the whole stomach (Figure 40). Using standard tissue bath techniques the circular strips were both attached to a TSD124C force transducer (Biopac MP100, Santa Barbara, CA, USA) and to a fixed metal arm using silk sutures, with a resting tension of 0.5 g. The force transducer had been calibrated by adding a known weight to the transducer prior to each experiment. The proximal and distal stomach strips were inserted into a 10 mL tissue bath filled with warmed Krebs' solution (37°C), warmed through a water jacket on the tissue bath. The tissue bath had an adjoining chamber where the Krebs' solution was constantly gassed with 95% O₂ and 5% CO₂. This gassing maintained the pH and this prevented the Ca²⁺ precipitating out of the solution (Percy, 1996).

The region of the intestine which was used in this study was a 1 cm segment which was 1 cm distal to the pyloric sphincter and was the duodenum. Following previous studies on *S. murinus* ileum and sections of intestine distal to the pyloric sphincter the tension of the longitudinal segments of the duodenum were set at 0.5 g (Chan, *et al.*, 2007; Cheng, *et al.*, 2008; Javid and Naylor, 1999).

All tissues were washed with Krebs' every 15 minutes for 1 hour, the tissue tension was readjusted to 0.5 g, and the tissues were then left to equilibrate for 30 minutes prior to the addition of all test substances. Once stable baseline activity was established experimentation started. The test substances were added to the gas chamber enabling full circulation of the test substance in the Krebs' solution, without direct interference with the tissue. The effects of the test substances on the tissue were measured for 25 minutes, with the exception of the dose response curve where the measurement was measured for 20 minutes from the first volume of 1 μ L. If a second volume was added to the tissue bath, this was added at 30 minutes and the contractile parameters were measured for another 25 minutes.

4.2.5 Test substances

When reference is made to the experimental groups or test substances this includes the following:

- Krebs' solution - applied at 200 μ Ls and was classed as the control;
- Dose response curve (DRC) - increasing volumes of ginger juice added to the tissue bath from 1, 2.5, 5, 10, 25, 50, 100, 200 and 400 μ L every minute;
- Low volume (LD) of ginger juice;
- Low volume (50 μ L) of ginger juice followed by another low volume (50 μ L) of ginger juice (LD-LD);
- "High" volume (HD) of ginger juice - 200 μ L;
- Low volume (50 μ L) of ginger juice followed by a "high" volume (200 μ L) of ginger juice (LD-HD);
- [6]-gingerol at 1.59×10^{-5} M (the concentration of [6]-gingerol in ginger juice – previously identified in Chapter 2 – in the organ bath) 6G[GJ];
- [6]-gingerol at 1×10^{-4} M;
- [6]-gingerol vehicle - Dimethyl sulfoxide (DMSO) and deionised water (the concentration of DMSO in the organ bath was always less than 1% when [6]-gingerol was added to the organ bath);
- Elements - five elements previously detected in high concentrations in ginger juice (potassium chloride; magnesium chloride; manganese sulphate; sodium chloride; and calcium chloride) combined as an equivalent solution and added at 200 μ L
- "Faux ginger juice" - a mimic of the natural ginger juice with the concentration of [6]-gingerol and the five elements equivalent to ginger juice

The reasoning for challenging the tissue with a low and high volume of ginger juice was to identify if there were different physiological effects dependant on volume. For the proximal stomach especially there was a different response dependant on volume, whilst the

response from the duodenum was magnified by the higher volume. This is why the two volumes were applied.

4.2.6 Analysis

The analytical package used to measure the tissue tension and contractile activity was AcqKnowledge 3.8.1 (1992-2004, BIOPAC Systems, Inc. Santa Barbara, CA, USA). The spontaneous contractile activity of the proximal and distal stomach and the duodenum was measured by tone (g), contraction amplitude (g) and frequency of contraction (n).

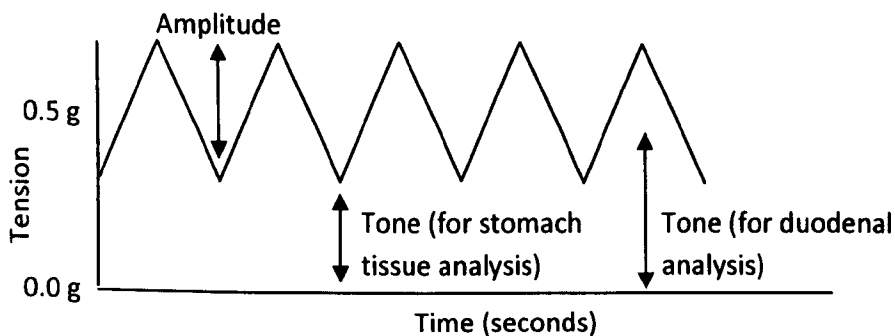


Figure 41. A diagram depicting 5 contractions indicating the tone and contraction amplitude.

The tone of the duodenum was measured from within the centre of the sine wave, from where the contraction originated. This was different to the analysis of the proximal and distal stomach where the contraction was derived from the base of the non-sinusoidal waveform. This meant that the tone was measured from the minimum point of the wave (Figure 41 and Figure 42).

When ginger juice was added to the proximal and distal stomach and duodenum two populations were identified and designated as population X and Y. The baseline area under the curve (AUC) for each of the tissues was averaged for the last five minutes before the

ginger juice was added. Thereafter, at three different time intervals, 1-2, 10-11, 20-21 minutes, the AUC values were compared to the corresponding average baseline AUC. If the AUC had an overall increase (2/3 or 3/3 time points increased) after the ginger juice was applied, the population was classified as population X. The group in which the AUC either decreased or did not change was categorised into population Y.

4.2.7 Statistics

The statistical package used to analyse the measurements of the contractile activity was GraphPad Prism 4.0 (1992-2003, GraphPad Software, Inc). The data is presented as $n =$, mean \pm SEM.

The data was analysed by the Kolmogorov-Smirnov Test, which analyses the distribution of the tissue parameters. A further Skewness test was applied to those parameters which did not have a normal distribution, to identify whether the data was positively or negatively skewed. The skewed data (the contraction amplitudes of the proximal and distal stomach circular strips) were analysed by non-parametric tests throughout this chapter. As non-parametric tests are less stringent than parametric tests, the normally distributed data was analysed by corresponding parametric tests (Motulsky, 1995). The median and interquartile ranges were reported instead of the mean \pm SEM for the non-parametric data.

The tone of the proximal and distal stomach and duodenum (except for the LD-LD and LD-HD tone) were analysed against the corresponding Krebs' control tone and this was analysed by a two-way ANOVA. The tonal LD-LD data and LD-HD data were analysed by

measuring the five minutes prior to adding the separate volumes of ginger juice, i.e. between -5-0 and 25-30 minutes and were analysed by a two-tailed unpaired t-test. The frequency of contractions for the proximal and distal stomach strips and the duodenal segments were also analysed against the 5 minute baseline prior to the addition of the test substances and this analysis was performed using a two-tailed unpaired t-test.

The contraction amplitudes for the proximal and distal stomach were variable with spontaneous contractions and ranging from 0.02-1.06 g and 0.02-1.07 g, respectively. With this information coupled with the skewed data for the contraction amplitude of proximal and distal stomach data these were analysed against the 5 minute baseline prior to addition of the test substances. This analysis was performed with the Mann-Whitney U test for the proximal and distal stomach strips. The duodenum contraction amplitude was also analysed against the 5 minute baseline prior to the addition of test substances and was analysed using a two-tailed unpaired t-test. This was because the contraction amplitude was variable (0.15-1.33 g) and in 3 out of 6 instances the relevant controls for the contraction amplitude were significantly different prior to the addition of test substances so it was better to keep the analysis consistent.

When comparing the baselines of populations X and Y, as defined in section 4.2.6 and 4.3.3, and the area under the curve, the data was analysed by a two-way ANOVA.

4.3 Results

4.3.1 Basal Activity

4.3.1.1 Proximal Stomach

The proximal stomach baseline motor activity is described below in terms of the tone, contraction amplitude, frequency and pattern with example of which is shown in Figure 42A.

4.3.1.1.1 Tone:

The resting tone of the proximal stomach was stable over 15 minutes prior to the addition of test substances with the mean tone for all of the tissues studied being $0.42 \text{ g} \pm 0.01 \text{ g}$ (N=79) (Figure 43A). There was no significant difference in basal tone between the three successive five minute intervals immediately prior to the addition of the test substances or between all of the proximal stomach groups except for the vehicle group.

4.3.1.1.2 Contraction amplitude:

The median resting contraction amplitude of the proximal stomach over 15 minutes was 0.07 g with the lower and upper quartile range between 0.05 g and 0.14 g (N=79). There was no statistically significant difference in the amplitude of basal activity between the three five minute time periods (Figure 43B). Nor was there any statistically significant difference between the baselines of the different experimental groups.

4.3.1.1.3 Frequency of contractions:

The frequency was difficult to quantify for the proximal stomach, and in 25/79 (31.6%) instances it was not possible to quantify frequency, as the contractions were not sufficiently clearly defined. The remaining 54/79 (68.4%) proximal stomachs had visible

contractions and were included in the analysis in Figure 43C. The mean frequency of contractions per minute in the proximal stomach was measured over 15 minutes and showed that there was no significant change in contraction frequency with time. In addition, there was no difference between the experimental groups. The mean frequency of contraction was 2.09 ± 0.28 contractions per minute (N=54).

4.3.1.2 Distal Stomach

The distal stomach baseline motor activity is described below in terms of the tone, contraction amplitude and frequency and pattern and an example is shown in Figure 42B. The basal activity of the distal stomach was stable for 15 minutes prior to the application of the various test substances.

4.3.1.2.1 Tone:

The tone of the distal stomach was stable over a 15 minute period prior to the addition of the test substances. There was no statistically significant difference in basal tone activity between the three successive five minute intervals (Figure 43D). In addition, there was no difference in the basal tone of the distal stomach between the different experimental groups. The mean tone for all of the distal stomachs was $0.48 \text{ g} \pm 0.01 \text{ g}$ (N=87).

4.3.1.2.2 Contraction amplitude:

The median resting contraction amplitude of the distal stomach over 15 minutes was 0.15 g with the lower and upper quartile range between 0.07 g and 0.38 g (N=87). There was no statistically significant difference between the distal stomach amplitude basal activity in

the three five minute groups as shown in Figure 43E. There was also no difference between the basal contraction amplitude in the five different experimental groups.

4.3.1.2.3 Frequency of contractions:

The contractions in the distal stomach were usually very distinct, facilitating quantification of frequency and hence all the data have been included, unlike the proximal stomach. The baseline frequency of contractions 15 minutes before the test substance was added was 8.77 ± 0.27 contractions per minute (N=87). There was no significant difference in the frequency of contractions over time or any difference between the experimental groups.

4.3.1.3 Duodenum

The duodenum basal motor activity is described below in terms of the tone, contraction amplitude and frequency and pattern and an example is shown in Figure 42A. The duodenum had regular basal activity and was analysed over 15 minutes before the application of the test substances.

4.3.1.3.1 Tone:

The mean resting tone over 15 minutes was $0.62 \text{ g} \pm 0.02 \text{ g}$ (N=73) and indicated that there was no difference in basal tone activity between the five minute intervals of the duodenum, nor the resting tone between the different experimental groups. This can be seen in Figure 43G.

4.3.1.3.2 Contraction amplitude:

The mean baseline contraction amplitude over 15 minutes was $0.64 \text{ g} \pm 0.03 \text{ g}$ (N=73). There was no difference between the distal stomach amplitude basal activity in the three five

minute periods as shown in Figure 43H. There was no statistically significant difference between the basal contraction amplitude for the different experimental groups.

4.3.1.3.3 Frequency of contractions:

The frequency of contractions in the duodenum was always very clear, as shown in Figure 42C. The baseline frequency of contractions per minute from the duodenum 15 minutes prior to the addition of test substance was 35.65 ± 0.44 contractions per minute (N=73). There was no significant difference in the frequency of contractions over time or any difference between the experimental groups (Figure 43I).

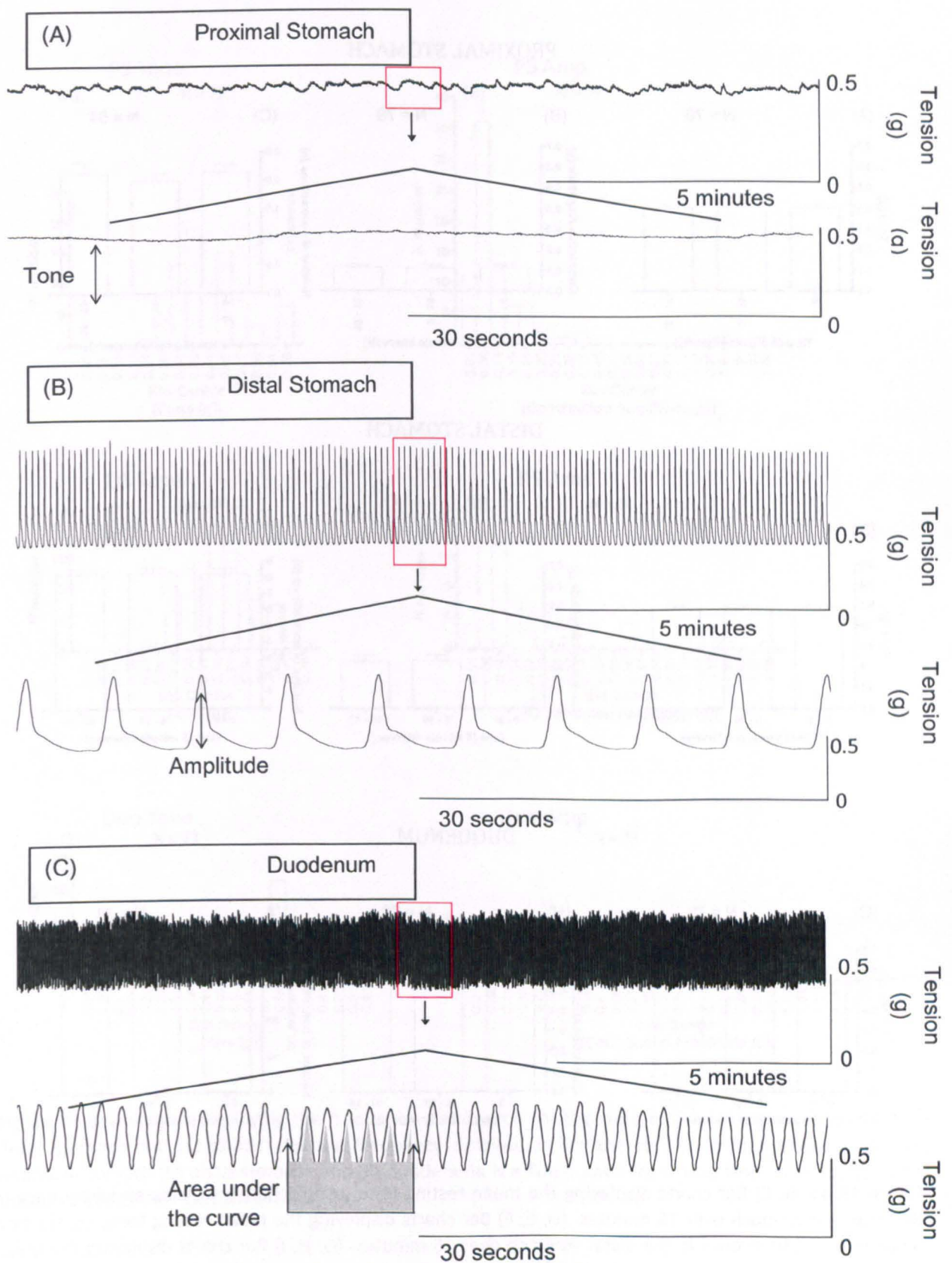
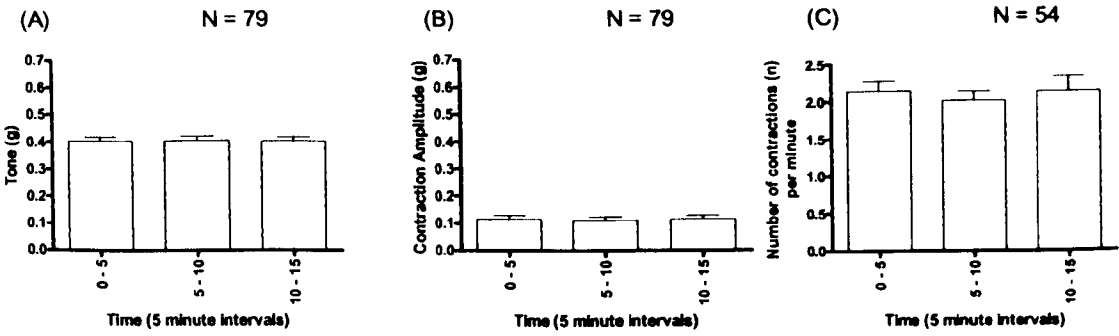
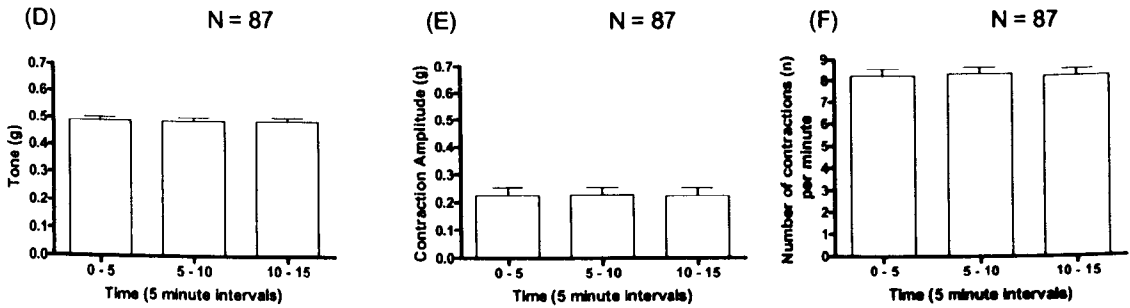


Figure 42. (A) A 15 minute trace of the proximal stomach baseline activity with an expanded 60 second section. (B) A 15 minute trace of the baseline activity of the distal stomach with an expanded 60 second section (C) A 15 minute trace of the baseline activity of the duodenum with an expanded 60 second section.

PROXIMAL STOMACH



DISTAL STOMACH



DUODENUM

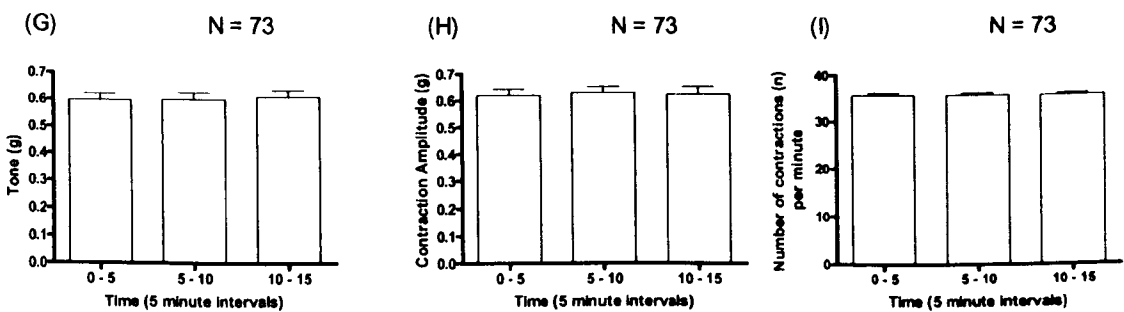


Figure 43. (A, B, C) Bar charts displaying the mean resting tone, contraction amplitude and frequency in the proximal stomach over 15 minutes. (D, E, F) Bar charts displaying the mean resting tone, contraction amplitude and frequency in the distal stomach over 15 minutes. (G, H, I) Bar charts displaying the mean resting tone, contraction amplitude and frequency in the duodenum over 15 minutes. The results are expressed as mean + SEM. N = The number of tissues from each region and is shown above in the respective bar chart.

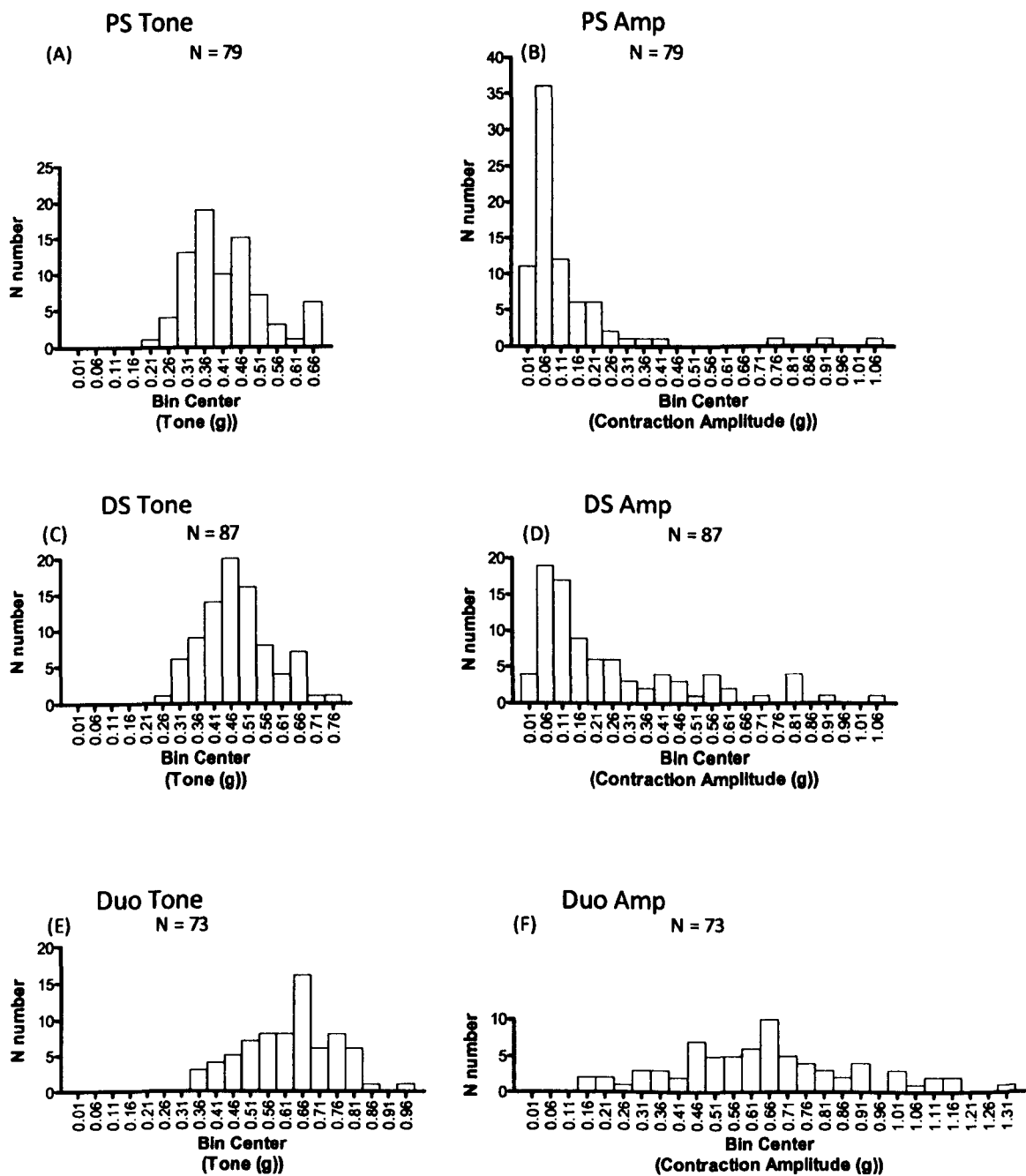


Figure 44. Histograms displaying the frequency distribution for the tone of the (A) proximal stomach (C) distal stomach and (E) duodenum and frequency distribution for the contraction amplitude of the (B) proximal stomach (D) distal stomach and (F) duodenum. N = The number of tissues from each region and is shown above in the respective histogram.

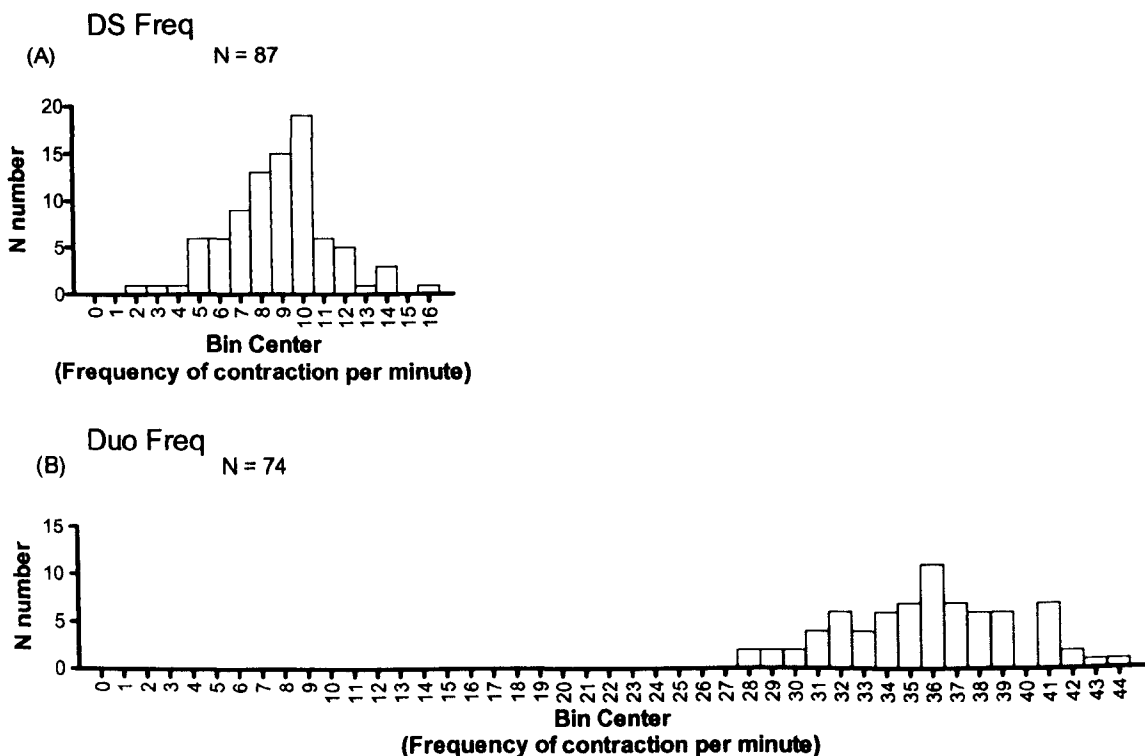


Figure 45. Histograms displaying the frequency distribution for the frequency of contraction of the (A) distal stomach and (B) duodenum. N = The number of tissues from each region and is shown above in the respective histogram.

4.3.1.4 The frequency distribution of tone, contraction amplitude and frequency of contraction for the stomach and the duodenum

The frequency distribution was plotted for the tone and contraction amplitude for the proximal and distal stomach and the duodenum as shown in Figure 44. Figure 44 shows the range of the data and highlights the distribution of tone and contraction amplitude of the the three areas of the upper gastrointestinal tract. The duodenum was normally distributed for tone, contraction amplitude and frequency of contraction. The contraction amplitude was for the duodenum was evenly spread from 0.16g to 1.31g. The proximal and distal stomach were normally distributed for tone and frequency of contraction, however the distribution was

positively skewed for the contraction amplitudes, (Skew value = 3.64) (Skew value = 1.39), respectively. The proximal and distal stomach contraction amplitude ranged from 0.01g to 1.06g with the majority of the proximal and distal stomach contraction amplitudes being within 0.06g to 0.11g. The frequencies of contractions for the duodenum are distinctly higher than the distal stomach as demonstrated in Figure 45.

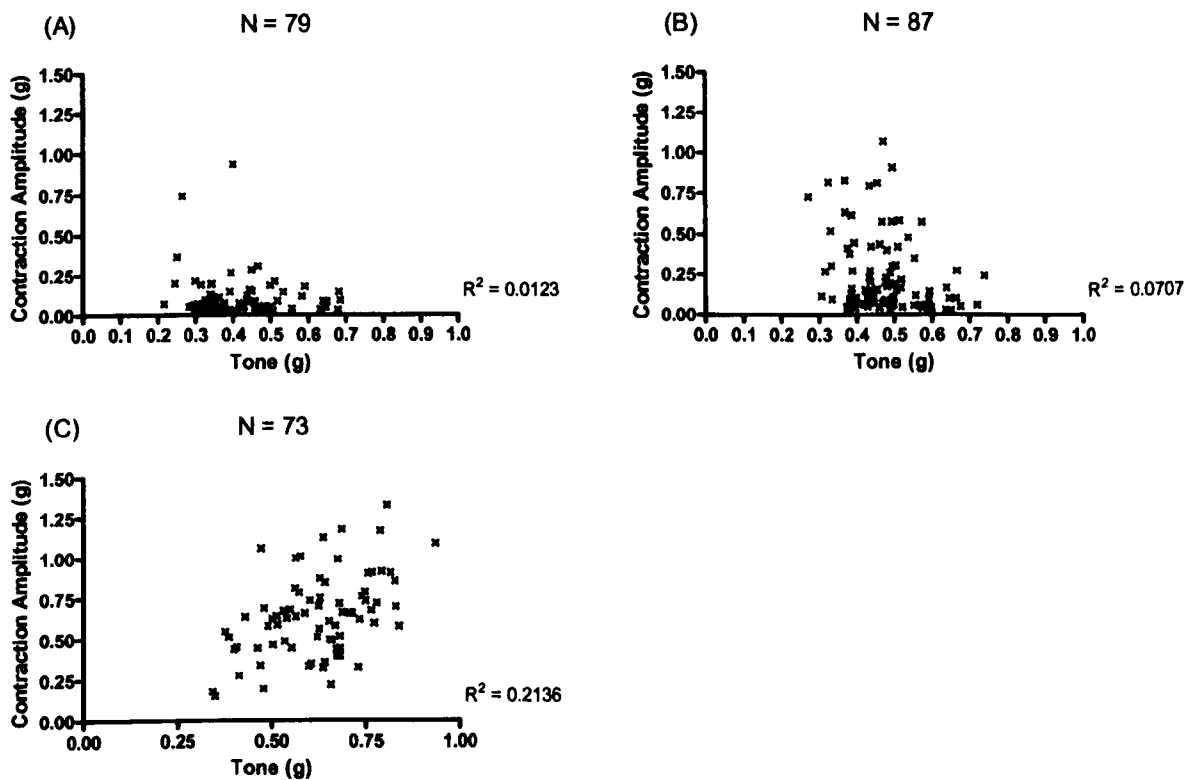


Figure 46. Scatter graphs displaying the resting tone plotted against the matching contraction amplitude for the: (A) proximal stomach, (B) distal stomach and (C) duodenum.

Contraction amplitude was plotted against the equivalent resting tone for both regions of the stomach, and the duodenum (see Figure 46). The R^2 values for each of the areas are very “low”, between 0.0123 and 0.2136. This indicates that the magnitude of the resting tone does not define the contraction amplitude. Although the R^2 is “low”, the

duodenum shows a trend, the higher the tone the higher the contraction amplitude (Figure 46).

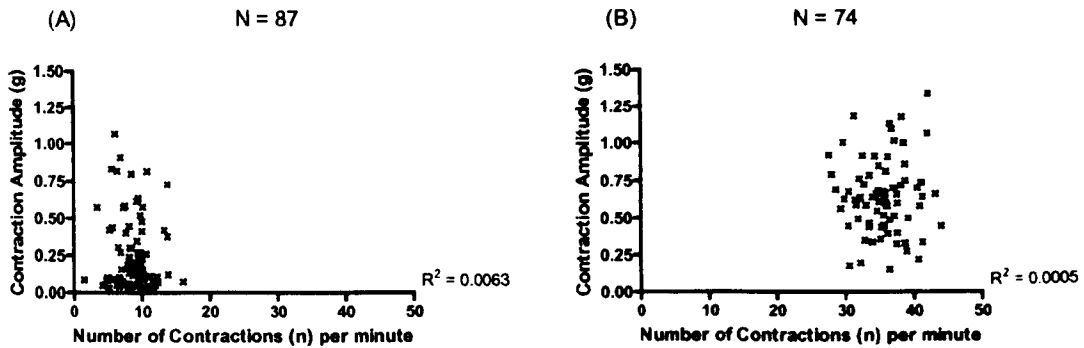


Figure 47. Scatter graphs displaying the resting contraction amplitude plotted against the matching frequency of contractions for the: (A) distal stomach, and (B) duodenum.

The number of contractions per minute was plotted against the corresponding contraction amplitude for the distal stomach and duodenum (Figure 47). The R^2 values were very low, indicating that the magnitude of the contraction amplitude does not define the frequency of contractions per minute.

4.3.1.5 The effect of the addition of Krebs' solution on the proximal and distal stomach and the duodenum

The Krebs' solution control was effectively a time control, as well as illustrating that a large volume injected into the bath did not affect the activity of the gut segments. The baseline was recorded for 15 minutes then 200 μL Krebs' solution was added to the proximal and distal stomach and the duodenum. The volume, 200 μL , was the highest volume used in all studies except the volume response study.

The proximal and distal stomach and duodenum tone, contraction amplitude, and frequency of contractions were not affected by the addition of the Krebs' solution over 25 minutes (see Figure 48). This indicates that when adding 200 μ L of ginger juice to the tissue bath that it is not the force of adding 200 μ L which causes an effect on the tissues.

4.3.1.6 The effect of the [6]-gingerol vehicle on the proximal and distal stomach and the duodenum

The concentration of the [6]-gingerol vehicle (DMSO) was equivalent to the highest concentration of [6]-gingerol (1×10^{-4} M). The [6]-gingerol vehicle significantly increased the tone of the duodenum from 2-3 minutes ($p > 0.0005$) until 24-25 minutes ($p > 0.0001$). The [6]-gingerol vehicle had no effect on the contraction amplitude or frequency of contractions on the duodenum. The [6]-gingerol vehicle had no effect on the tone, contraction amplitude or the frequency of contractions on the proximal or distal stomach, although there was a trend for the contraction amplitude of the proximal stomach to increase, see Figure 49. This indicates that the effects of adding [6]-gingerol and the "faux" ginger juice to the proximal and distal stomach were not due to the vehicle, except in the case of the duodenal tone where there was an increase.

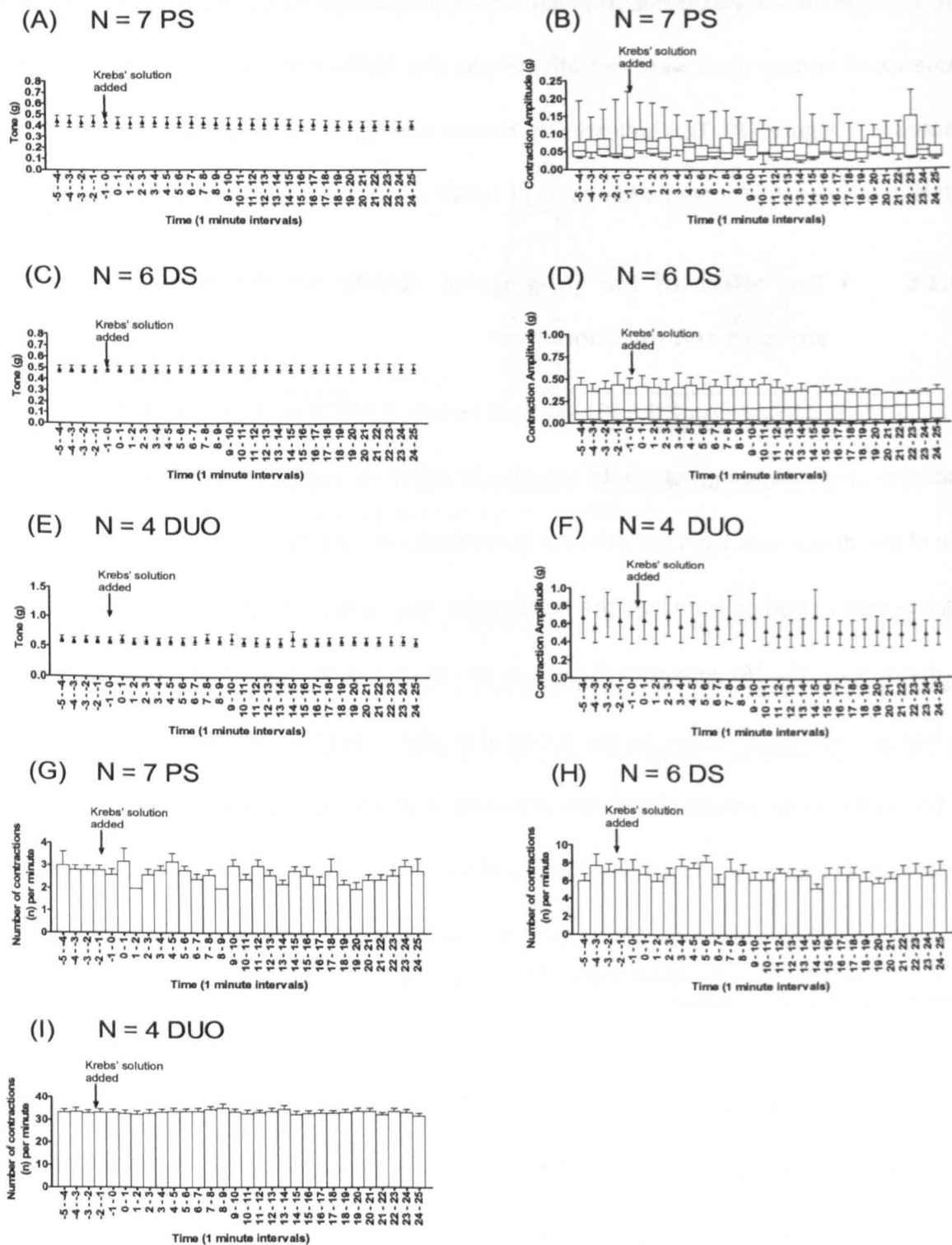


Figure 48. (A,C,E,F) Graphs displaying the tone of the proximal and distal stomach and the duodenum and the contraction amplitude of the duodenum. (B,D) Box and whisker plots displaying the contraction amplitude of the proximal and distal stomach strips. The results for (B,D) are expressed as median with the upper and lower quartile ranges. (G,H,I) Histograms of the frequency of contraction from the: proximal and distal stomach strips and the duodenum segments after receiving 200 μ L Krebs' solution. The results are expressed as mean \pm SEM. N = The number of tissues from each region and is shown above in the respective histogram. PS = Proximal stomach. DS = Distal Stomach. DUO = Duodenum.

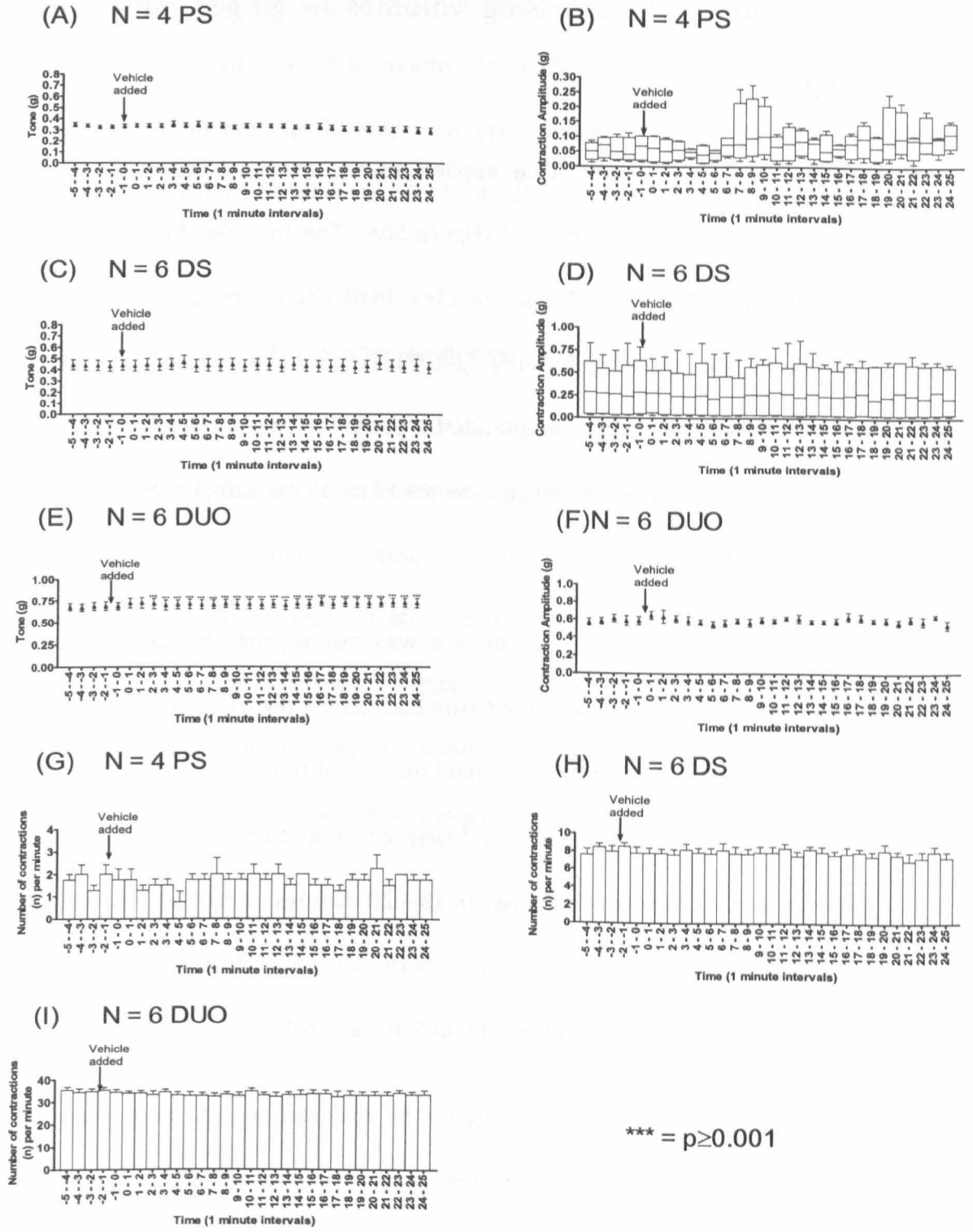


Figure 49. (A,C,E,F) Graphs displaying the tone of the proximal and distal stomach and the duodenum and the contraction amplitude of the duodenum. (B,D) Box and whisker plots displaying the contraction amplitude of the proximal and distal stomach strips. The results for (B,D) are expressed as median with the upper and lower quartile ranges. (G,H,I) Histograms of the frequency of contraction from the: proximal and distal stomach strips and the duodenum segments after receiving the [6]-gingerol vehicle. The results are expressed as mean \pm SEM. N = The number of tissues from each region and is shown above in the respective histogram. PS = Proximal stomach. DS = Distal Stomach. DUO = Duodenum. *** = $p \geq 0.001$

4.3.2 The effect of increasing volumes of ginger juice on the upper GI tract

Increasing volumes of ginger juice applied to the proximal stomach caused a statistically significant difference on tone (g) (Figure 50A). The tone significantly increased from 9-10 minutes ($p < 0.0390$) to 19-20 minutes ($p < 0.0002$). The proximal stomach contraction amplitude increased significantly ($p < 0.0357$) from the addition of 5 μL (2-3 minutes), compared to the contraction amplitude baseline. The total volume of ginger juice after the final 400 μL was 1093.5 μL of ginger juice in a 10 mL tissue bath, i.e. over 10% of the volume of the tissue bath.

The distal stomach contraction amplitude was not significantly affected by the increasing concentration of ginger juice in the tissue bath during the exposure to ginger juice. The ginger juice appeared to have a transient effect on tone of the distal stomach. There was a trend towards a decrease in tone at the lower concentrations and was statistically significant between 5 and 7 minutes and between 18 – 20 minutes ($p < 0.0114$) when the tone significantly increased. This increase did not stabilise after the final volume: the tone appeared to increase until the last measurement, unlike the proximal stomach.

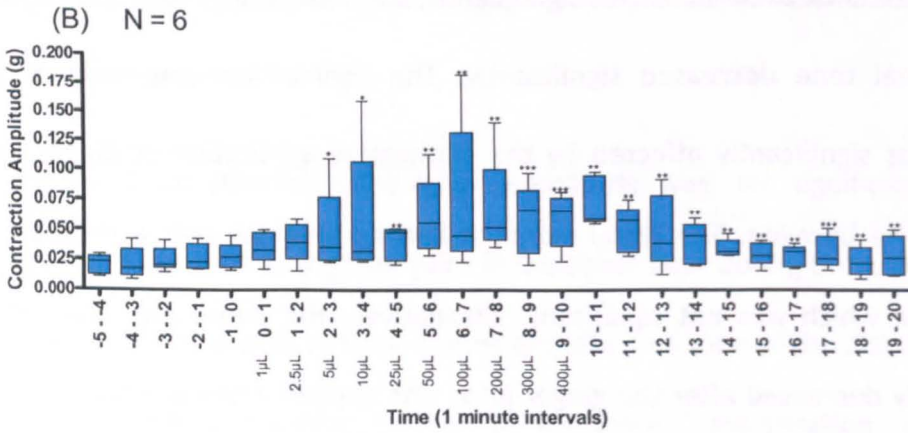
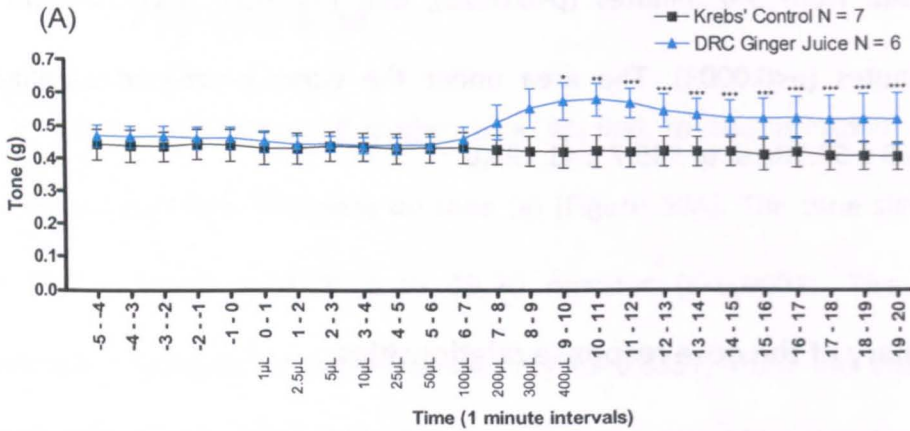
The duodenum was significantly affected by the dose response curve of ginger juice. The ginger juice caused a significant effect on the tone, contraction amplitude and the area under the curve of the duodenum. The tone significantly decreased at 7-8 minutes ($p < 0.0088$), after the 200 μL volume was added (393.5 μL cumulative), and remained decreased until the last reading at 19-20 minutes ($p < 0.0001$). The contraction amplitude decreased down to ~6% of the original baseline from 0.437 ± 0.102 g (-1-0 minutes) to 0.027

± 0.007 g (19-20 minutes) (Figure 52). The contraction amplitude of the duodenum was significantly decreased from 5-6 minutes ($p < 0.0325$), and remained decreased for the duration, 19-20 minutes ($p < 0.0003$). The area under the curve decreased significantly ($p < 0.0003$) from 565.9 ± 52.30 a.u. to 349.7 ± 41.29 a.u.

4.3.2.1 Summary of the dose response relationships

When ginger juice was added, the AUC decreased significantly for the duodenum. The proximal and distal stomach tone increased significantly after the ginger juice was added, whereas the duodenal tone decreased significantly. The contraction amplitude of the proximal stomach was significantly affected by the cumulative application of ginger juice when compared to the baseline. The distal stomach had a trend towards a decrease in contraction amplitude which was not significant, alternatively the duodenum contraction amplitude significantly decreased after the ginger juice was applied when compared to the baseline.

PROXIMAL STOMACH



* = $p \leq 0.05$ ** = $p \leq 0.01$ *** = $p \leq 0.001$

Figure 50. The effects of increasing volumes of ginger juice on the proximal stomach strips on (A) tone displayed by a line graph and (B) contraction amplitude displayed by box and whisker. (A) results are expressed as mean \pm SEM (B) results expressed as median and interquartile ranges. N = The number of tissues from each region and is shown above in the respective graph.

* = $p \leq 0.05$ ** = $p \leq 0.01$ *** = $p \leq 0.001$

DISTAL STOMACH

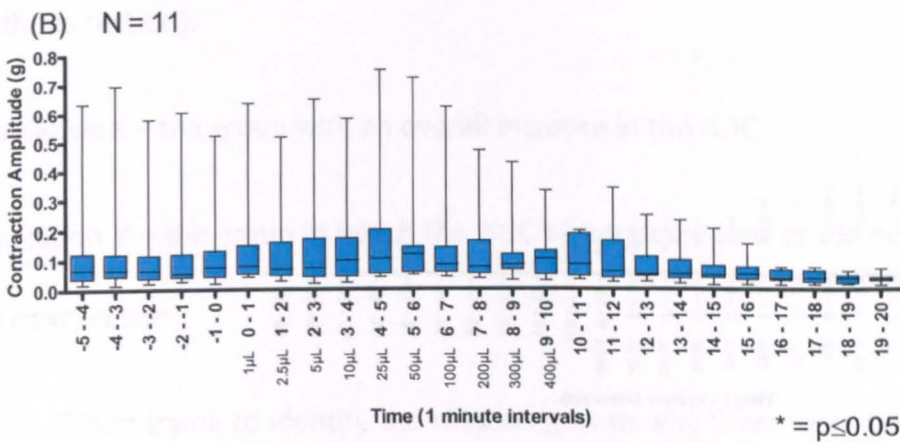
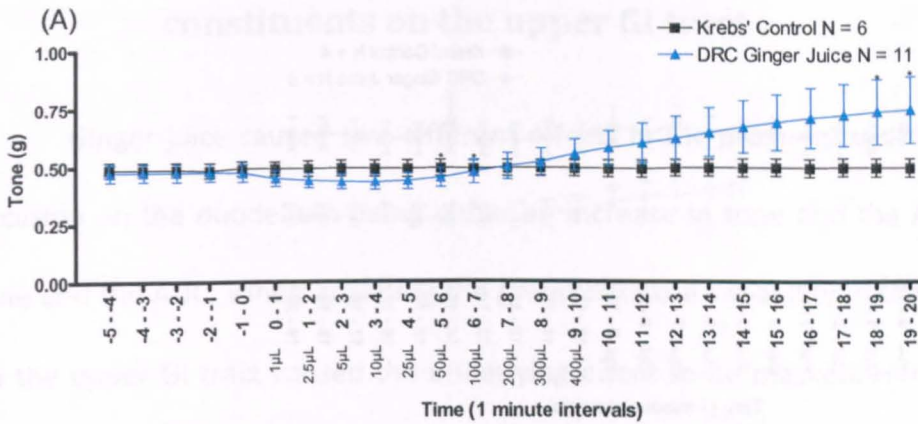
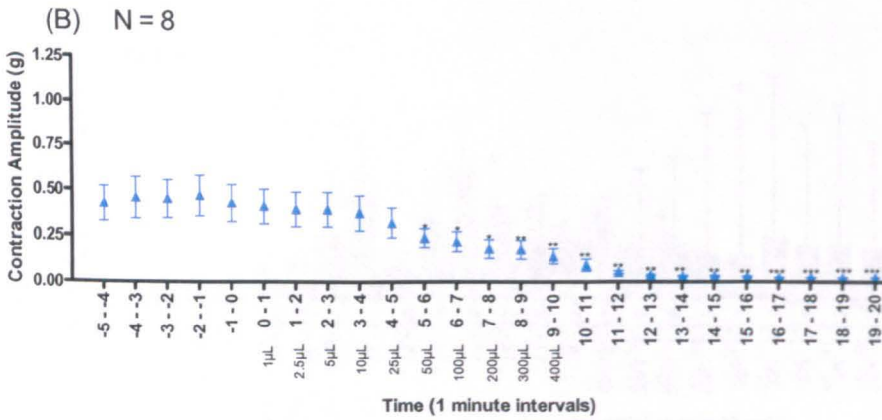
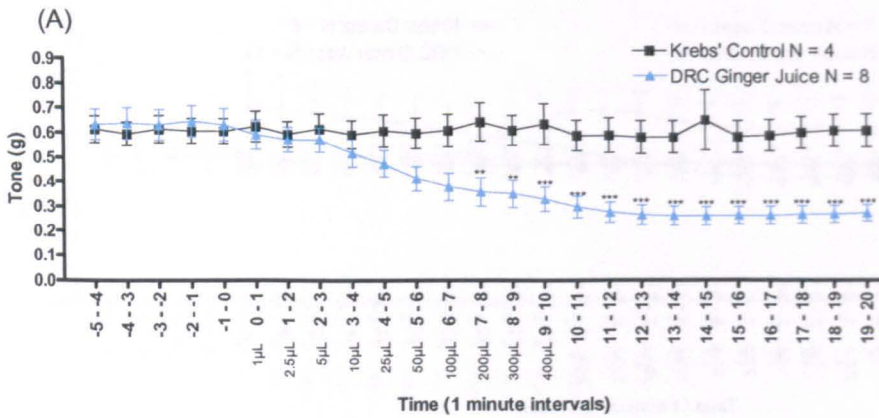


Figure 51. The effects of increasing volumes of ginger juice on the distal stomach strips on (A) tone displayed by a line graph. (A) Results are expressed as mean \pm SEM. (B) Contraction amplitude displayed by box and whisker plots. (B) Results expressed as median and interquartile ranges. N = The number of tissues from each region and is shown above in the respective graph.
 * = $p \leq 0.05$ ** = $p \leq 0.01$ *** = $p \leq 0.001$

DUODENUM



* = $p \leq 0.05$ ** = $p \leq 0.01$ *** = $p \leq 0.001$

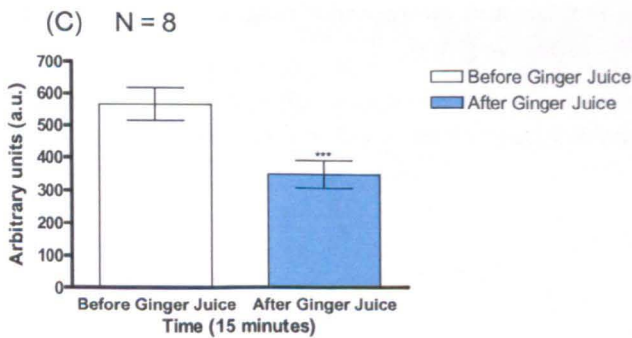


Figure 52. The effects of increasing volumes of ginger juice on the duodenum on (A) tone displayed by a line graph, (B) contraction amplitude displayed by a graph and (C) area under the curve displayed by a bar graph. The results are expressed as mean \pm SEM. N = The number of tissues from each region and is shown above in the respective graph.
 * = $p \leq 0.05$ ** = $p \leq 0.01$ *** = $p \leq 0.001$

4.3.3 The effect of a single “low” volume of ginger juice and its constituents on the upper GI tract

Ginger juice caused two different effects in the proximal and distal stomach and on occasion on the duodenum being either an increase in tone and the AUC, or a decrease in tone and the AUC. When analysing the group data the variability in the effect of ginger juice on the upper GI tract caused the underlying effect to be masked. Hence, the proximal and distal stomach and duodenum results were split into two populations (as described in the methods section):

Population X – the group with an overall increase in the AUC

Population Y – the group in which the AUC either decreased or did not change (examples in the next section).

When trying to identify the reasoning as to why there were two populations, the fed state, time of day of dissection, male and female responses and metal concentration were compared. There was no correlation between population x and y and the above variables. Instead the physiological response may have been due to the quantity of receptors present in the strips of tissue – be it muscarinic or vanilloid.

4.3.3.1 The single “low” volume (50 μ L) of ginger juice on the proximal stomach

4.3.3.1.1 The tone of the proximal stomach after 50 μ L volume of ginger juice

When all results from the proximal stomach were combined, the overall observed effect from adding a 50 μ L volume of ginger juice was a trend for the tone to increase over

time, as seen in Figure 54A. These effects of the “low” volume of ginger juice on tone were statistically significant when the populations were separated and compared with the Krebs’ control. These effects were significant from 10-11 minutes ($p < 0.0333$) until 19-20 minutes ($p < 0.0001$), which can be observed in Figure 54B.

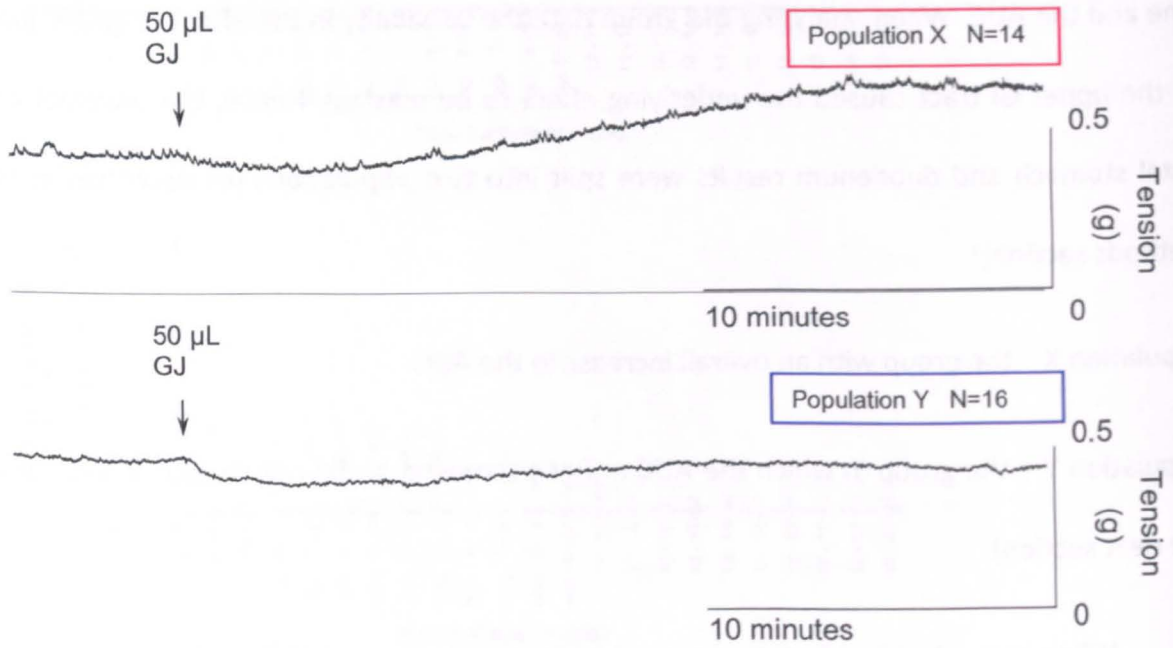


Figure 53. Two 30 minute traces from proximal stomach before and after a “low” volume (50 μL) of ginger juice was added showing the two different responses to ginger juice.

4.3.3.1.2 The contraction amplitude and the frequency of contractions of the proximal stomach after a 50 μL volume of ginger juice

There was an increasing trend in contraction amplitude initially after the ginger juice was applied compared to the baseline. However, there was no statistically significant difference after the ginger juice was applied. There was no significant difference between the two populations when the baselines were analysed against each other. The number of contractions for the proximal stomach per minute after a single “low” volume of ginger juice was analysed and was not significantly different from before addition of ginger juice.

PROXIMAL STOMACH

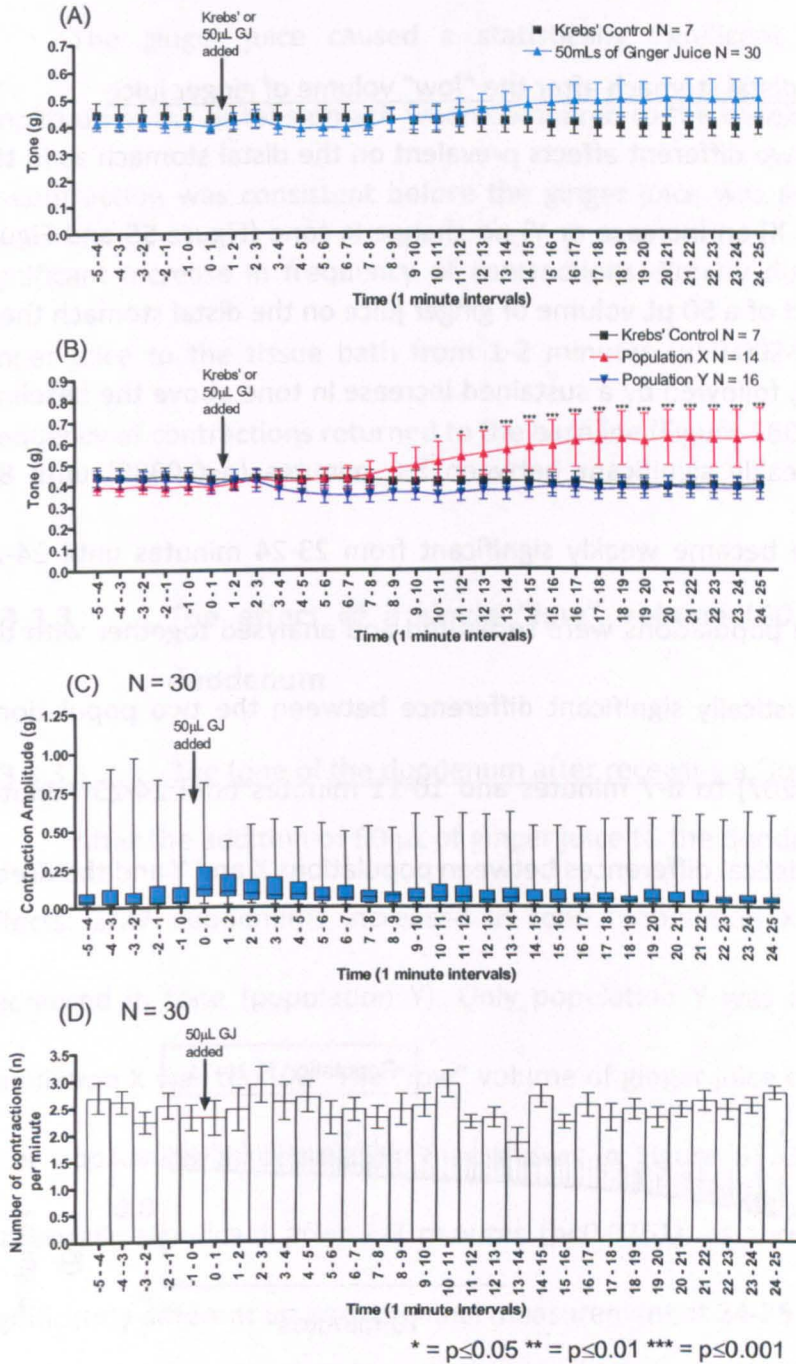


Figure 54. Line graphs displaying; (A) the tone of all the proximal stomach before and after addition of 50 µL of ginger juice: (B) the tone of both population X and Y of the proximal stomach before and after the addition of 50 µL of ginger juice. The results are expressed as mean ± SEM. Box and whisker plot (C) is the contraction amplitude of the proximal stomach after a 50 µL volume of ginger juice was applied to the tissue bath. The results for (C) are expressed as median with the interquartile ranges. (D) Histogram displaying the frequency of contractions pre and post application of 50 µL of ginger juice. N = The number of tissues from each region and is shown above in the respective graphs.

* = $p \leq 0.05$ ** = $p \leq 0.01$ *** = $p \leq 0.001$

4.3.3.2 The effects of a "low" volume (50 μ L) of ginger juice on the distal stomach

4.3.3.2.1 The tone of the distal stomach after the "low" volume of ginger juice

There appeared to be two different effects prevalent on the distal stomach as in the case of the proximal stomach: X) an increase or Y) no change in tone (Figure 55 and Figure 56A,B). For the combined effect of a 50 μ L volume of ginger juice on the distal stomach there was an initial decrease in tone, followed by a sustained increase in tone above the baseline. The decrease in tone was weakly significant between 5-6 minutes ($p < 0.0380$) until 8-9 minutes. The increase in tone became weakly significant from 23-24 minutes until 24-25 minutes ($p < 0.0400$). When the populations were separated and analysed together with the Krebs' control, there was statistically significant difference between the two populations' tone from 2-3 minutes ($p < 0.0207$) to 6-7 minutes and 10-11 minutes until 24-25 minutes ($p < 0.0001$). There were no statistical differences between populations X and Y and the Krebs' control baselines.

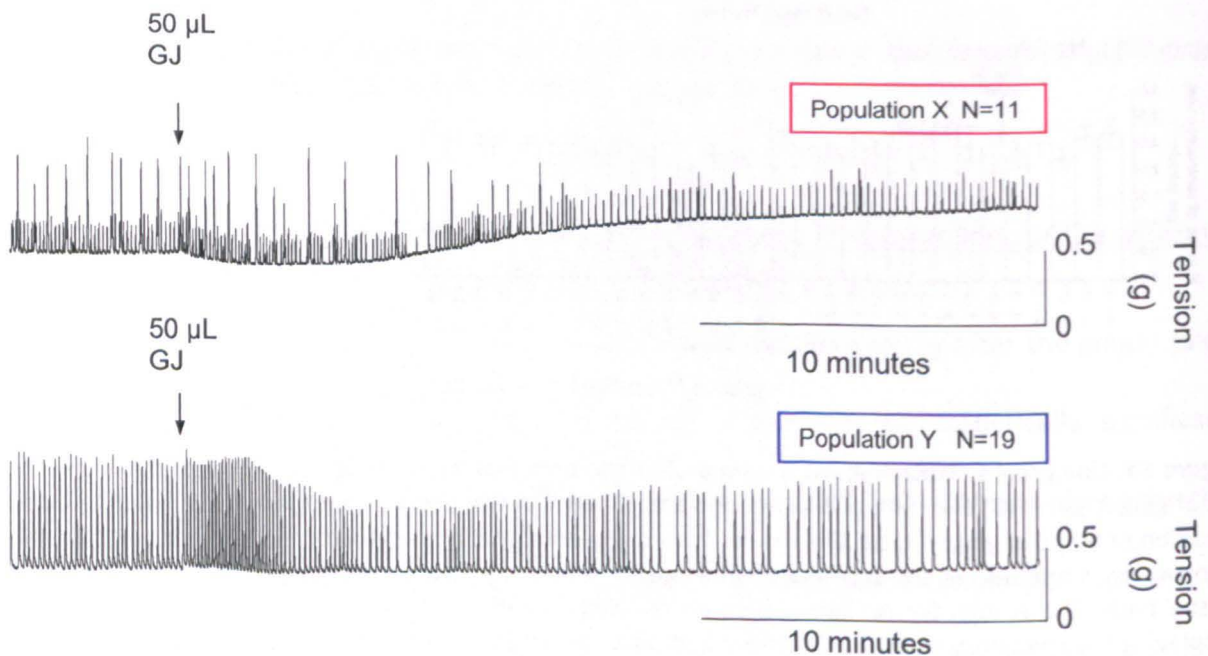


Figure 55. Two 30 minute traces from the distal stomach 5 minutes before and 25 minutes after 50 μ L of ginger juice was applied to the tissue baths.

4.3.3.2.2 The contraction amplitude and the frequency of contractions of the distal stomach after the “low” volume of ginger juice

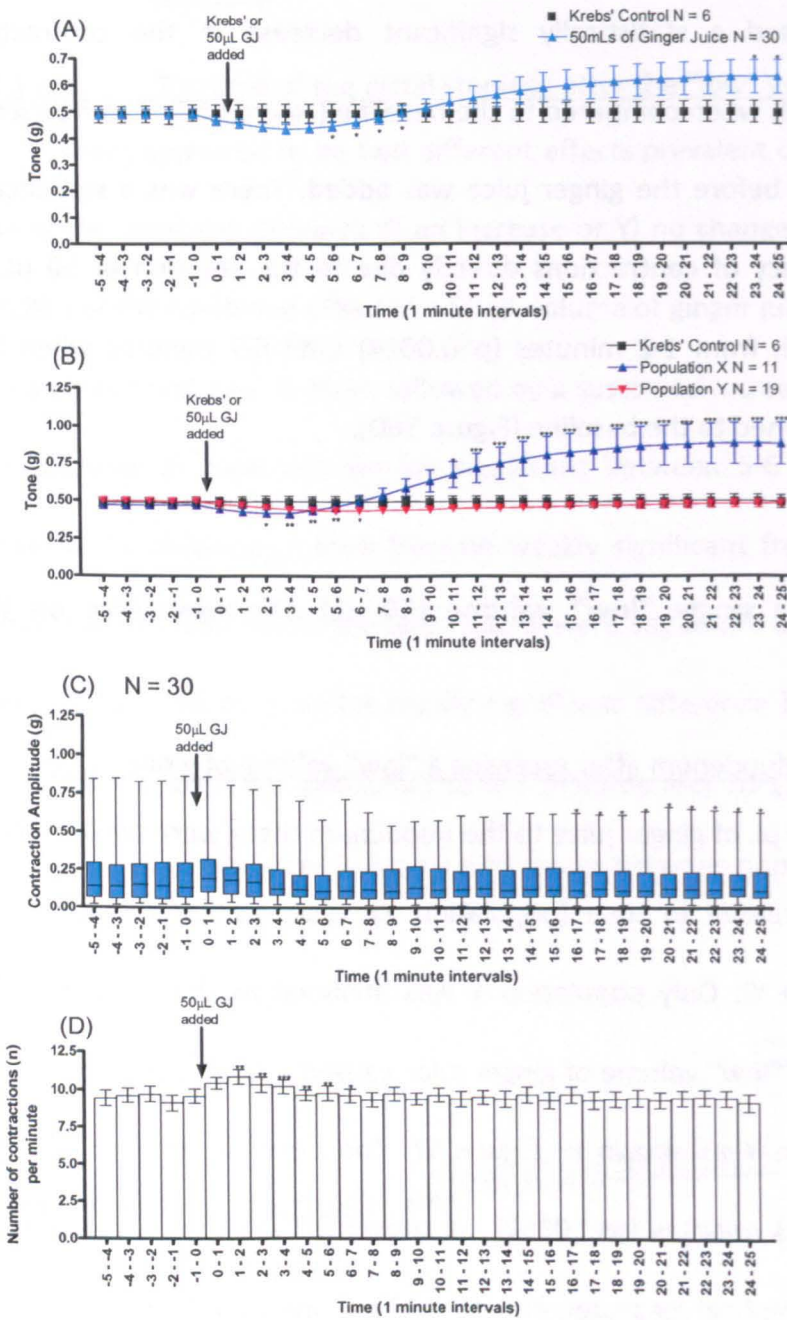
The ginger juice caused a statistically significant decrease in the contraction amplitude of the distal stomach when compared to the baseline (Figure 56C). The frequency of contraction was consistent before the ginger juice was added. There was a statistically significant increase in frequency of contractions directly due to the addition of 50 μ L of ginger juice to the tissue bath from 1-2 minutes ($p>0.0024$) until 6-7 minutes when the frequency of contractions returned to the baseline (Figure 56D).

4.3.3.3 The effect of a single “low” volume (50 μ L) of ginger juice on the duodenum

4.3.3.3.1 The tone of the duodenum after receiving a “low” volume of ginger juice

After the addition of 50 μ L of ginger juice to the duodenum there were two observed effects: 2/27 duodenum increased in tone (population X), whereas 25/27 duodenum decreased in tone (population Y). Only population Y was analysed as the N number for population X was too low. The “low” volume of ginger juice caused a rapid decrease in tone after application in population Y as shown in Figure 57. The decrease in tone became statistically significant after 2-3 minutes ($p<0.0261$), as shown in Figure 58A. It remained significantly different up until the final measurement at 24-25 minutes ($p<0.0001$).

DISTAL STOMACH



* = $p \leq 0.05$ ** = $p \leq 0.01$ *** = $p \leq 0.001$

Figure 56. Line graphs displaying: (A) the tone of all the distal stomach before and after addition of 50 µL of ginger juice: (B) the tone of both population X and Y of the distal stomach before and after the addition of 50 µL of ginger juice. The results are expressed as mean ± SEM. Box and whisker plot (C) is the contraction amplitude of the distal stomach after a 50 µL volume of ginger juice was applied to the tissue bath. The results in (C) are expressed as median with the interquartile ranges. (D) Histogram displaying the frequency of contractions pre and post application of 50 µL of ginger juice. N = The number of tissues from each region and is shown above in the respective graphs.

* = $p \leq 0.05$ ** = $p \leq 0.01$ *** = $p \leq 0.001$

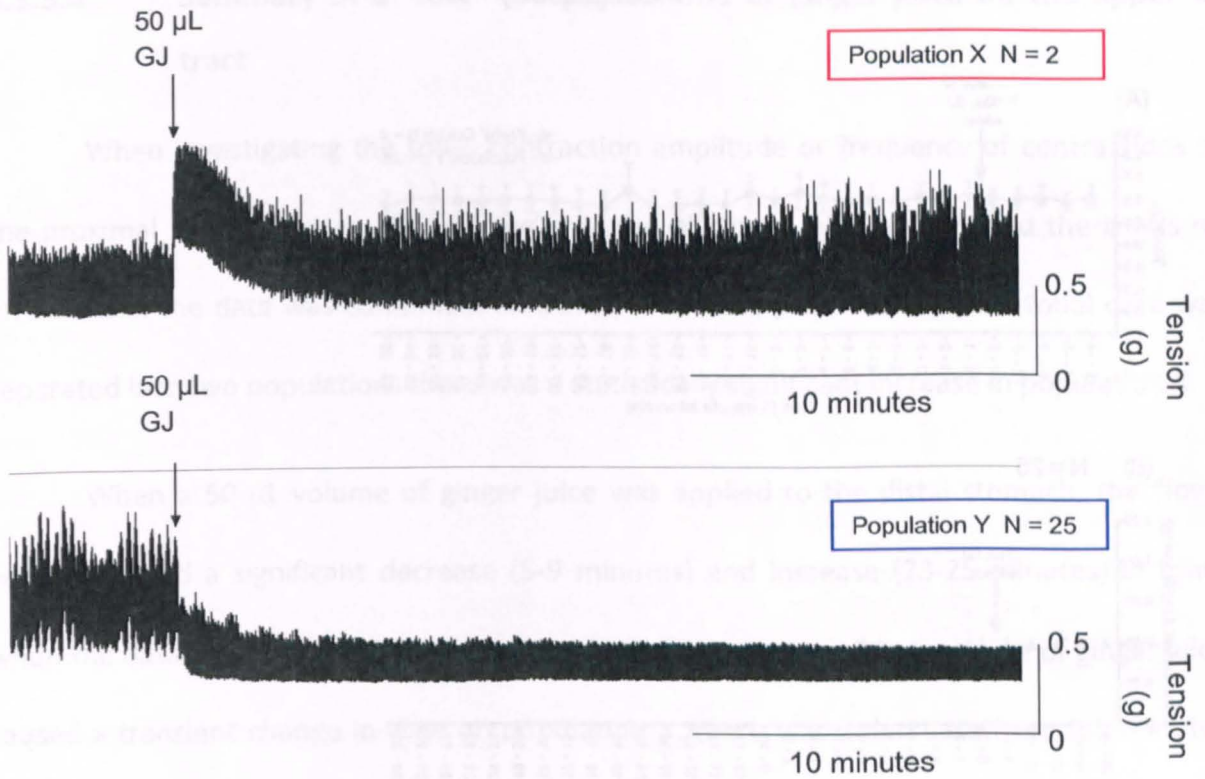
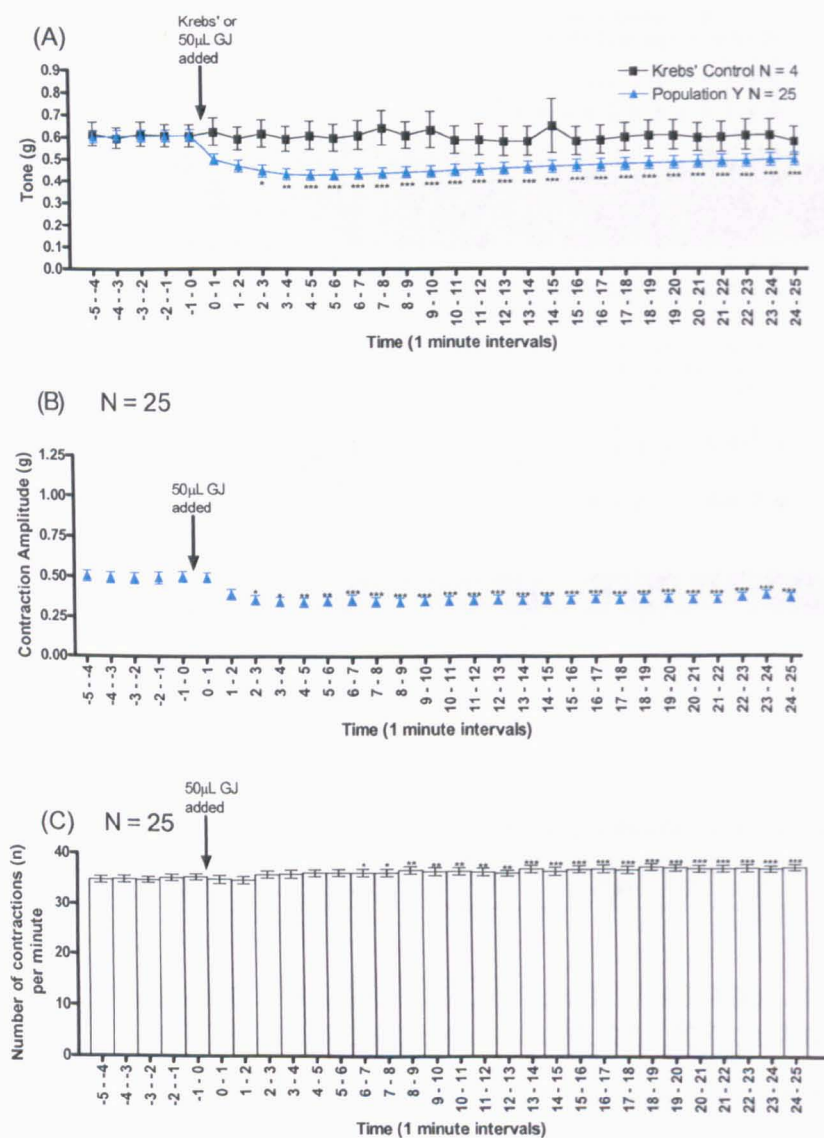


Figure 57. Two 30 minute traces from the duodenum before and after a “low” volume (50 µL) of ginger juice was added with the two different responses to ginger juice.

4.3.3.3.2 The contraction amplitude and the frequency of contractions of the duodenum after the addition of 50 µL of ginger juice (population Y)

After addition of 50 µL of ginger juice to the tissue bath, the contraction amplitude of the duodenum decreased significantly which was similar to the duodenal tone for the entirety of exposure ($p < 0.0001$). The duodenal frequency of contraction significantly increased after the 50 µL of ginger juice was applied to the 10 mL tissue bath compared to the frequency baseline from 6-7 minutes ($p > 0.0277$) until 24-25 minutes ($p < 0.0001$).

DUODENUM



* = $p \leq 0.05$ ** = $p \leq 0.01$ *** = $p \leq 0.001$

Figure 58. (A) Line graph displaying the duodenal tone of population Y and the Krebs' control before and after addition of 50 μL of ginger juice, (B) a graph displaying the duodenal contraction amplitude of population Y after the addition of 50 μL ginger juice, (C) a histogram displaying the frequency of contractions of the population Y duodenum after a 50 μL volume of ginger juice was applied to the tissue bath. The results are expressed as mean \pm SEM. N = The number of tissues from each region and is shown above in the respective graph.

* = $p \leq 0.05$ ** = $p \leq 0.01$ *** = $p \leq 0.001$

4.3.3.4 Summary of a “low” (50 μ L) volume of ginger juice on the upper GI tract

When investigating the tone, contraction amplitude or frequency of contractions of the proximal stomach strips after a “low” volume of ginger juice was applied there was no effect when the data was combined. However, when the proximal stomach tonal data was separated into two populations there was a statistically significant increase in population X.

When a 50 μ L volume of ginger juice was applied to the distal stomach, the “low” volume caused a significant decrease (5-9 minutes) and increase (23-25 minutes) in tone, when the data was combined. When the data was separated the 50 μ L volume of ginger juice caused a transient change in tone on population X, there was a decrease from 2-7 minutes and an increase from 10-25 minutes. The distal stomach contraction amplitude decreased after exposure to ginger juice as did the duodenal contraction amplitude, but not to the same extent as the duodenum. The frequency of contraction of the distal stomach significantly increased from 2-7 minutes after 50 μ L of ginger juice was added, but returned to baseline, whilst the duodenal contraction frequency increased from 6 minutes onwards. For the duodenum, there was a significant decrease in tone for population Y, after 50 μ L of ginger juice was applied, and an increase in frequency of contractions.

4.3.4 A “low” volume (50 μ L) of ginger juice followed by a “low” volume of ginger juice (50 μ L) on the upper GI tract

Two “low” volumes (50 μ L) of ginger juice were applied consecutively with a 25 minute interval between two volumes to the upper GI regions. Two different populations (X+Y) were distinguishable after the first volume of ginger juice was applied. When two volumes of ginger juice were applied (a “low” volume of ginger juice followed by a “low” volume of ginger juice). The population of the second volume was defined by the first volume.

4.3.4.1 A “low” volume (50 μ L) of ginger juice followed by a “low” volume of ginger juice (50 μ L) on the proximal stomach

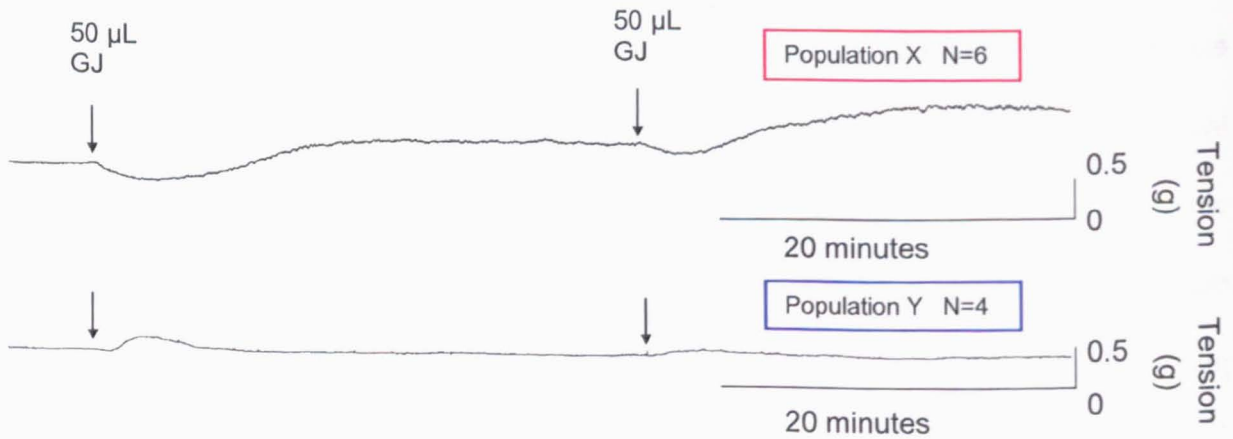


Figure 59. Two traces from proximal stomach before and after two “low” volumes (50 μ L) of ginger juice were added showing the two different responses to ginger juice.

4.3.4.1.1 The tone of the proximal stomach after the two 50 μ L volumes of ginger juice

The tone of the proximal stomach changed significantly after both the first and the second volume of ginger juice. At 14-15 minutes there was a significant increase in tone which continued until 24-25 minutes ($p < 0.0042$) (Figure 60A). The effect of ginger juice after

the second volume replicated the first volume, there was a significant increase in tone from 2-3 minutes after the second volume and this increase persisted for the entire measurement.

There was a statistical difference between the two baselines of populations X and Y ($p > 0.0001$), therefore the effects of ginger juice could not be statistically analysed. Population Y had a higher basal tone mean ($0.58 \text{ g} \pm 0.004 \text{ g}$) compared to population X ($0.44 \text{ g} \pm 0.001 \text{ g}$). There was an increasing trend in population X after both volumes, whilst population Y did not have this trend.

4.3.4.1.2 The contraction amplitude and the frequency of contractions of the proximal stomach after the two 50 μL volumes of ginger juice

After each volume of ginger juice, there was a statistically significant increase in contraction amplitude 2-3 minutes ($p < 0.0357$) after the ginger juice was applied, followed by a decrease of the contraction amplitude. When the populations were combined, there was a significant effect of the ginger juice on the proximal stomach contraction amplitude. The second volume of ginger juice caused a significant effect in contraction amplitude from 2-3 minutes until 18-19 minutes ($p > 0.0404$). The statistical significance on the contraction amplitude was lower after the second volume. When the basal contraction amplitude between the two populations was compared there were statistically significant differences between the two populations ($p < 0.0006$). The effect of the second volume of ginger juice on the contraction amplitude of the proximal stomach was very similar to the effect of the first volume of ginger juice. It was only possible to measure the frequency from two groups because with such a small N number, it was not valid to use statistics.

PROXIMAL STOMACH

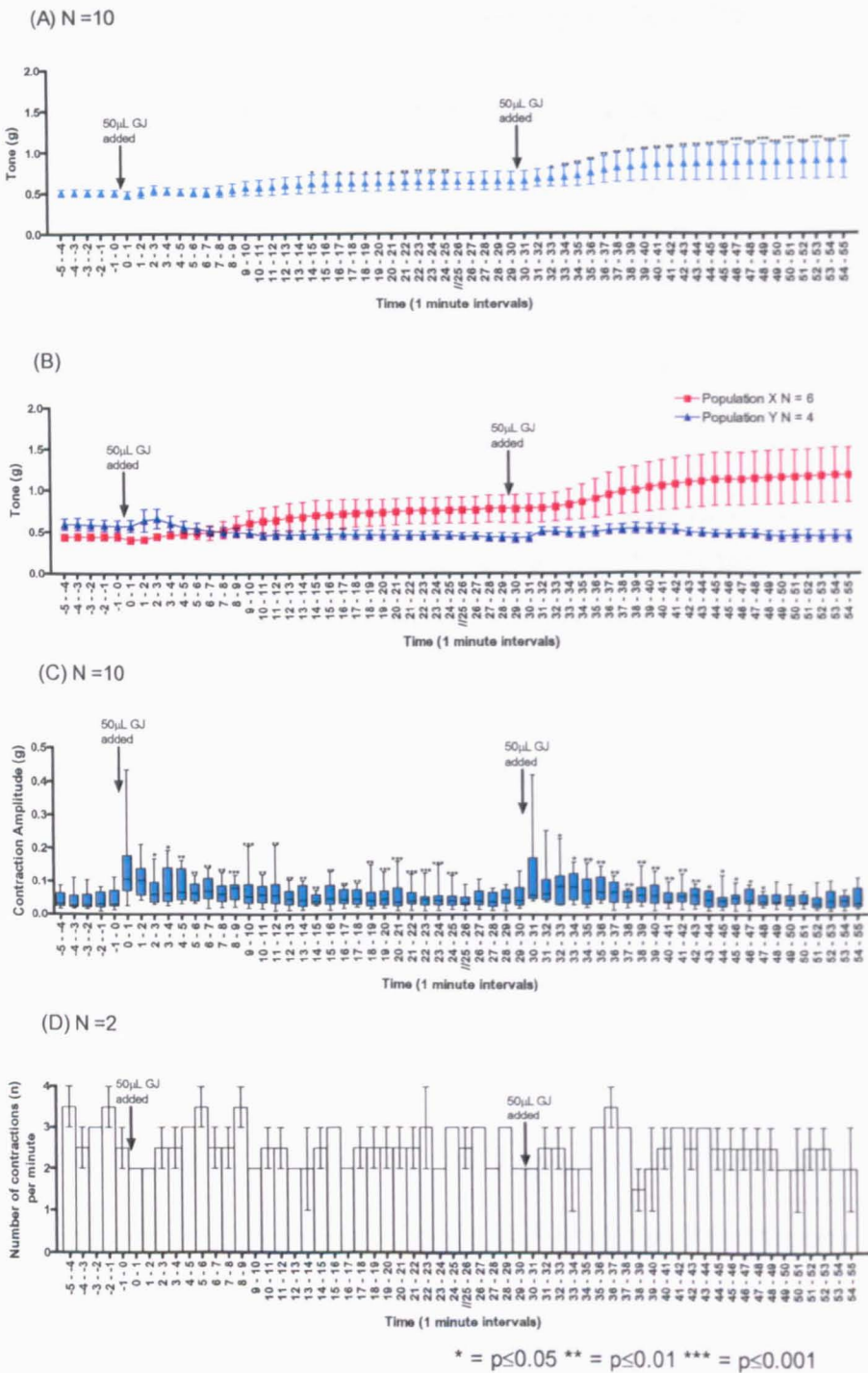


Figure 60. Line graphs displaying: (A) the tone of all the proximal stomach before and after the addition of two volumes of 50 μ L ginger juice (B) the tone of the proximal stomach before and after the addition of both volumes of 50 μ L ginger juice with population X and Y (C) box and whisker plots the contraction amplitude of all the proximal stomach before and after the addition of two volumes of 50 μ L ginger juice (D) histogram of the frequency of contractions from the proximal stomach after receiving two volumes of 50 μ L ginger juice. The results are expressed as mean \pm SEM. The results in (C) are expressed as median with the interquartile ranges. N = The number of tissues from each region and is shown above in the respective graph.

* = $p \leq 0.05$ ** = $p \leq 0.01$ *** = $p \leq 0.001$

4.3.4.2 The effect of two “low” volumes of ginger juice on the distal stomach

A “low” volume followed by a second “low” volume of ginger juice was applied to the distal stomach to identify if there was a difference in the effect of the ginger juice on the three parameters, tone, contraction amplitude and frequency, after the second volume was applied.

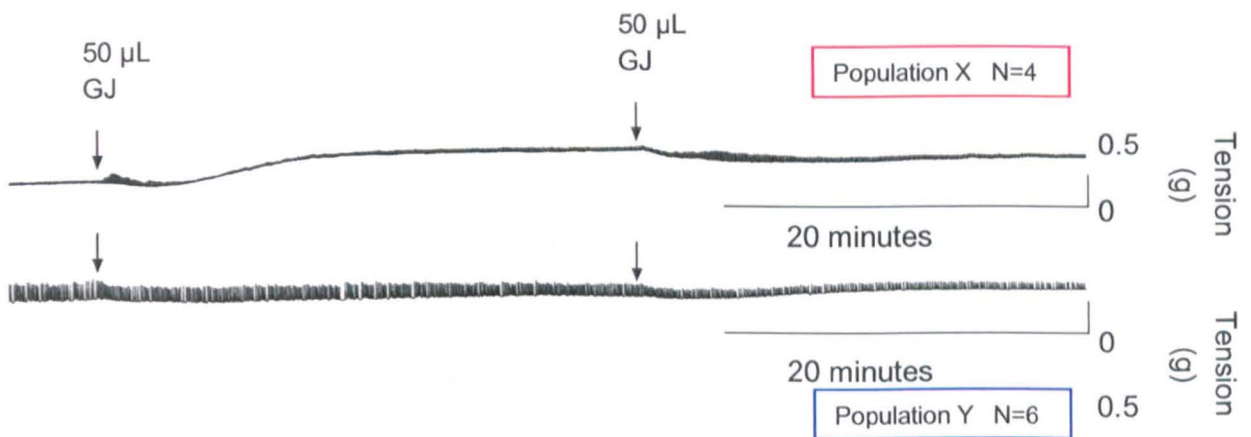


Figure 61. 60 minute original traces from two different distal stomach preparations before and after two volumes of 50 µL ginger juice were applied to the tissue baths.

4.3.4.2.1 The tone of the distal stomach after the two “low” (50 µL) volumes of ginger juice

When the results of the tone of the distal stomach were combined, there were significant effects from the addition of low volumes of ginger juice. There was a significant decrease in tone from 1–9 minutes, after the first volume. There was a significant decrease in tone after the second volume from 1-11 minutes. These results were very similar and it appears that the effect of ginger juice was not diminished by the first volume. Each volume of ginger juice appeared to cause a transient effect which was an initial decrease in tone followed by an increase in tone, (Figure 62A). Again the results were separated into populations X and Y. When the baselines of population X were compared against population Y there was a statistically significant difference between the two population baselines

($p < 0.0001$): population Y had a higher baseline tone at $0.49 \text{ g} \pm 0.001 \text{ g}$, whereas population X had a basal tone of $0.44 \text{ g} \pm 0.000 \text{ g}$. Population Y displayed a very slight non-significant reduction in tone after the two “low” volumes of ginger juice. Population X had a trend towards a non-significant increase in tone, as seen in Figure 62B. After the second $50 \mu\text{L}$ volume of ginger juice on population X, there was a non-significant tendency towards a decrease in tone followed by an increase in tone; in effect the tone increased to twice the original baseline tone after the two volumes were applied.

4.3.4.2.2 The contraction amplitude and the frequency of contractions of the distal stomach strips after the two “low” volumes of $50 \mu\text{L}$ ginger juice were applied

After the first volume of ginger juice, the contraction amplitude increased slightly from 2-4 minutes ($p < 0.0159$) then decreased significantly from 21-25 minutes (Figure 62C). The second $50 \mu\text{L}$ volume of ginger juice decreased the contraction amplitude from 15-16 minutes ($p < 0.0431$) until 24-25 minutes ($p < 0.0089$). By 54-55 minutes, it appears that the contraction amplitude was nearly half the original baseline before the ginger juice was applied. After the first $50 \mu\text{L}$ volume of ginger juice there was an increase in the frequency of contractions from 1-2 minutes ($p < 0.0374$); however, after the second volume there was a decrease in the number of contractions from 17-18 minutes to 24-25 minutes ($p < 0.0126$) (Figure 62D).

DISTAL STOMACH

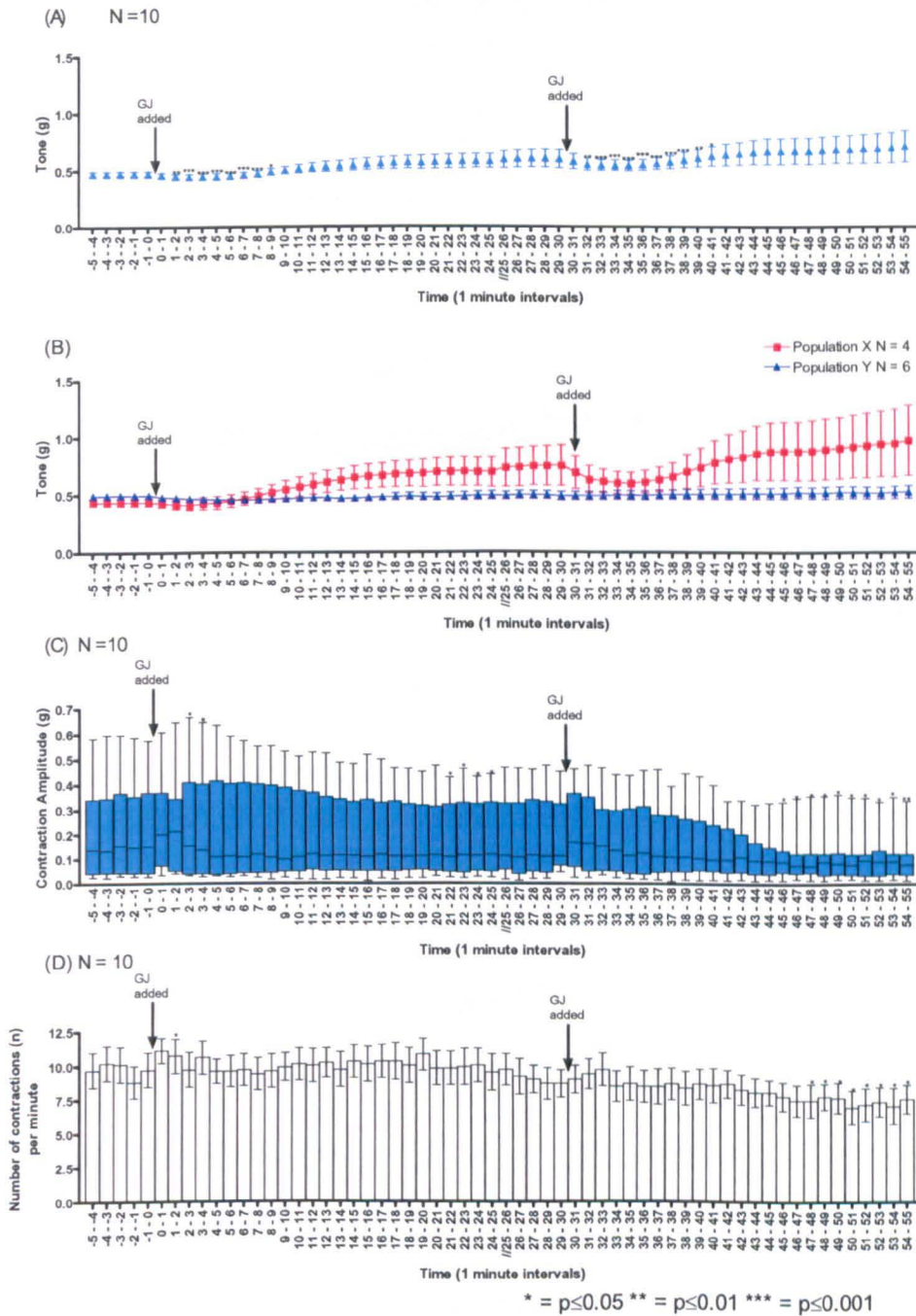


Figure 62. Line graphs displaying: (A) the tone of all the distal stomach before and after the addition of two volumes of 50 μL ginger juice (B) the tone of the distal stomach before and after the addition of both volumes of 50 μL ginger juice with population X and Y (C) box and whisker plots the contraction amplitude of all the distal stomach before and after the addition of two volumes of 50 μL ginger juice (D) histogram of the frequency of contractions from the distal stomach after receiving two volumes of 50 μL ginger juice. The results are expressed as mean \pm SEM. The results in (C) are expressed as median with the interquartile ranges. N = The number of tissues from each region and is shown above in the respective graph.

* = $p \leq 0.05$ ** = $p \leq 0.01$ *** = $p \leq 0.001$

4.3.4.3 The effect of a “low” volume of ginger juice followed by a “low” volume of ginger juice on the duodenum

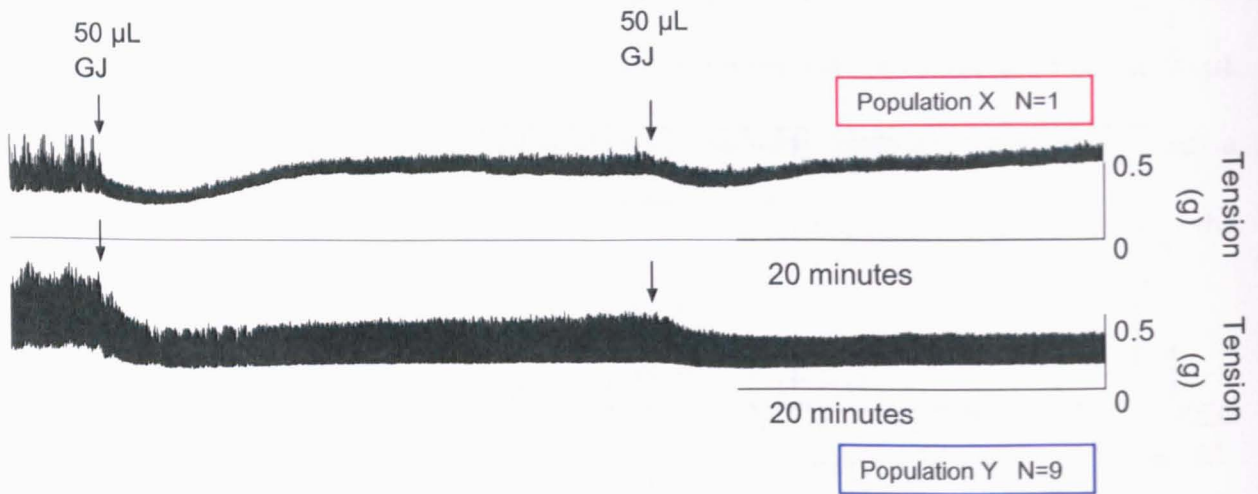


Figure 63. Two 60 minute traces from duodenum before and after two 50 µL volumes of ginger juice were added with the two different responses to ginger juice.

4.3.4.3.1 The tone of the duodenum after exposure to two “low” volumes of 50 µL ginger juice

The effects of the addition of two 50 µL volumes of ginger juice applied to the 10 mL tissue bath containing duodenal tissue were recorded, as shown in Figure 63. It was not valid to analyse the data from population X, as the N number was one. Therefore, all of the analysis here was conducted on population Y. The first 50 µL ginger juice upon the duodenum caused a significant decrease in tone between 1-2 minutes after application ($p < 0.0001$) until 24-45 minutes ($p < 0.0001$). The second volume caused a significant decrease from 1-2 minutes ($p < 0.0052$) until 24-35 minutes after the second application ($p < 0.0004$) (Figure 64A).

4.3.4.3.2 The contraction amplitude and the frequency of contractions of the duodenum after two “low” volumes of 50 µL ginger juice were applied

The contraction amplitude of the duodenum was significantly decreased after the first volume of ginger juice, after 3-4 minutes until 24-25 minutes after both applications of the low volume of ginger juice (Figure 64B). The frequency of contractions did change significantly after the first (increase) and the second volume (decrease) of ginger juice.

4.3.4.4 Summary of two “low” volumes of ginger juice on the upper GI tract

The tone of the proximal stomach was significantly increased after exposure to two “low” volumes of ginger juice. There was no statistically significant effect of the two “low” volumes of 50 µL of ginger juice on frequency of the contractions on the proximal stomach. There was a significant effect of the two volumes of 50 µL of ginger juice on the contraction amplitude after the volumes were applied to the proximal stomach. The combined tonal data for distal stomach strips displayed a transient effect due to the two volumes of 50 µL of ginger juice and there was a significant decrease in tone after both additions followed by a non significant trend towards an increase. The duodenum had a significant decrease in tone and amplitude for population Y, after the first volume and second volume of 50 µL of ginger juice were applied. There were statistically significant decreases in frequency of contraction on the distal stomach and duodenal segments after the second volume. The effect of the second volume was very similar to the first volume in the proximal and distal stomach and the duodenum. Overall the effects of ginger juice on tone, contraction amplitude and frequency of contractions were replicable on the same tissue at the same volume.

DUODENUM

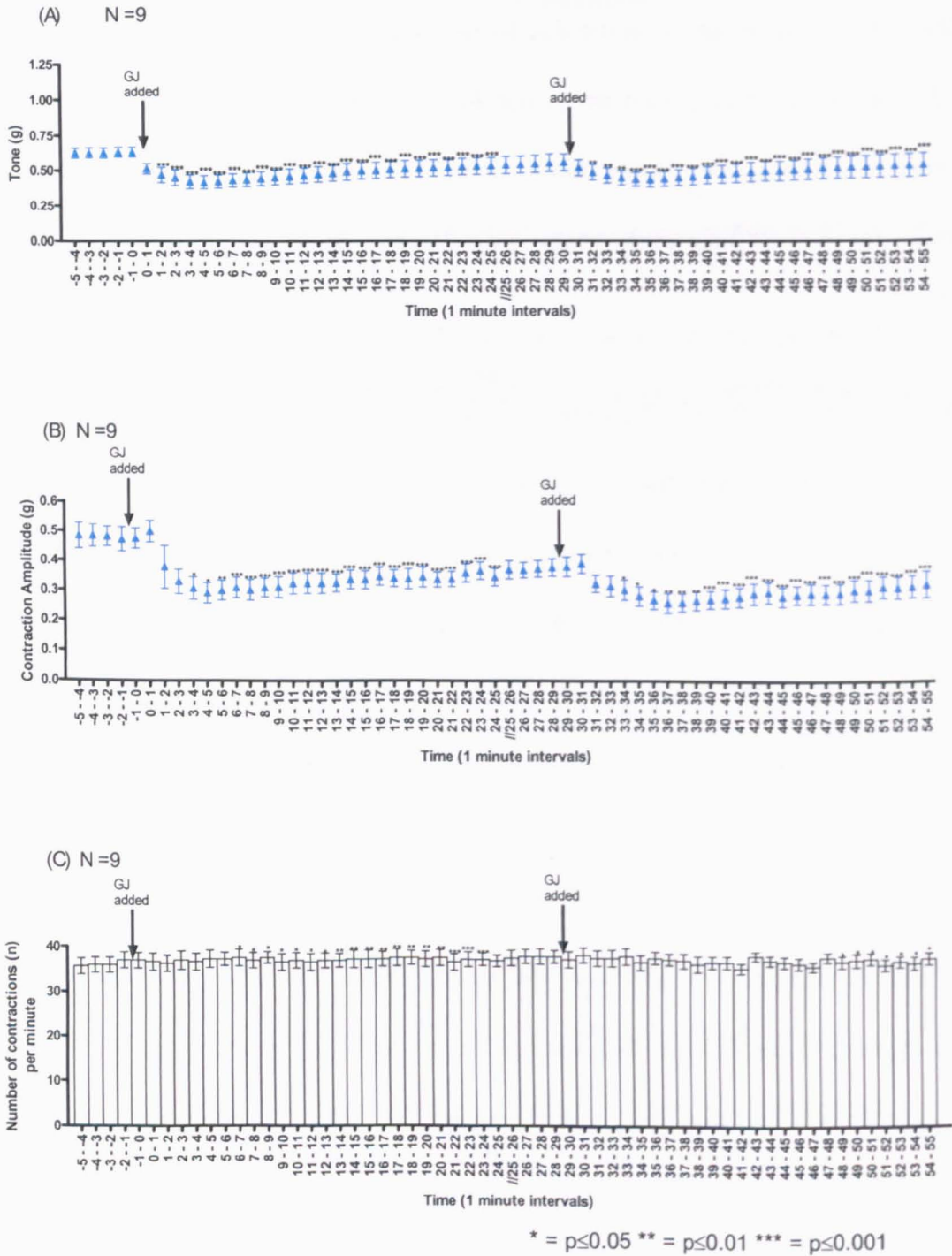


Figure 64. (A) Line graph displaying the duodenal tone of population Y before and after addition of two 50 μL of ginger juice, (B) a graph displaying the duodenal contraction amplitude of population Y after the addition of two 50 μL ginger juice, (C) a histogram displaying the frequency of contractions of the population Y duodenum after a 50 μL volume of ginger juice was applied to the tissue bath. The results are expressed as mean \pm SEM. N = The number of tissues from each region and is shown above in the respective graph.

* = $p \leq 0.05$ ** = $p \leq 0.01$ *** = $p \leq 0.001$

4.3.5 The effect of a “high” volume (200 μ L) of ginger juice on the upper GI tract

A “high” volume (200 μ L) of ginger juice was applied to stable proximal and distal stomach and duodenum preparations and the effects were monitored over 25 minutes. There were two different populations prevalent (X and Y).

4.3.5.1 The “high” volume of ginger juice on the proximal stomach

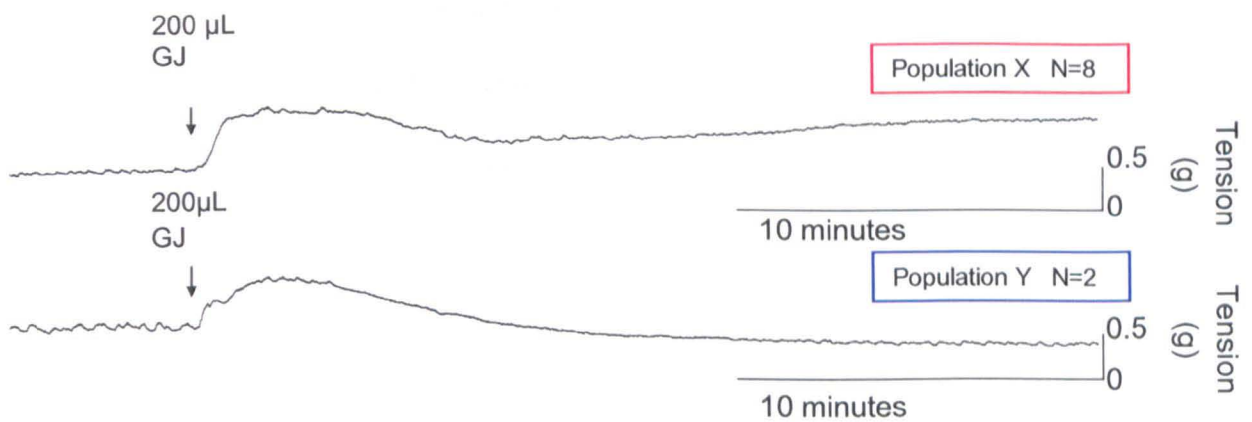


Figure 65. Two 30 minute traces from proximal stomach before and after a “high” volume (200 μ L) of ginger juice was added with the two different responses to ginger juice.

4.3.5.1.1 The tone of the proximal stomach after 200 μ L of ginger juice

When the data from all the proximal stomach circular strips were combined the overall observed effect, from adding 200 μ L of ginger juice to the tissue bath, was a rapid increase in tone, which was maintained (Figure 66A). In Figure 65, there are two populations present, population Y and population X. Population Y appears to decrease after the initial increase unlike population X, which maintains the increase in tone. Population Y only had an N number of two therefore it was not valid to perform statistics on this population. When the data was combined, there was a significant increase in tone after 2-3 minutes until 24-25 minutes ($p < 0.0001$) (Figure 66A). If this data was broken down further as shown in Figure

66B, the data becomes significant between 1.5-2 minutes ($p < 0.0401$). The prominent effect of adding 200 μL of ginger juice, to the 10 mL tissue bath, was a sustained increase in tone after ginger juice was added.

4.3.5.1.2 The contraction amplitude and the frequency of contractions of the proximal stomach after 200 μL ginger juice

There was an increase in contraction amplitude within 3 minutes of addition of a “high” volume of ginger juice to the proximal stomach strips. This was followed by a trend towards a decrease of contraction amplitude below the original baseline, as shown in Figure 67A. As can be seen from Figure 67B there was no change in frequency of contraction of the proximal stomach after 200 μL of ginger juice was applied.

PROXIMAL STOMACH

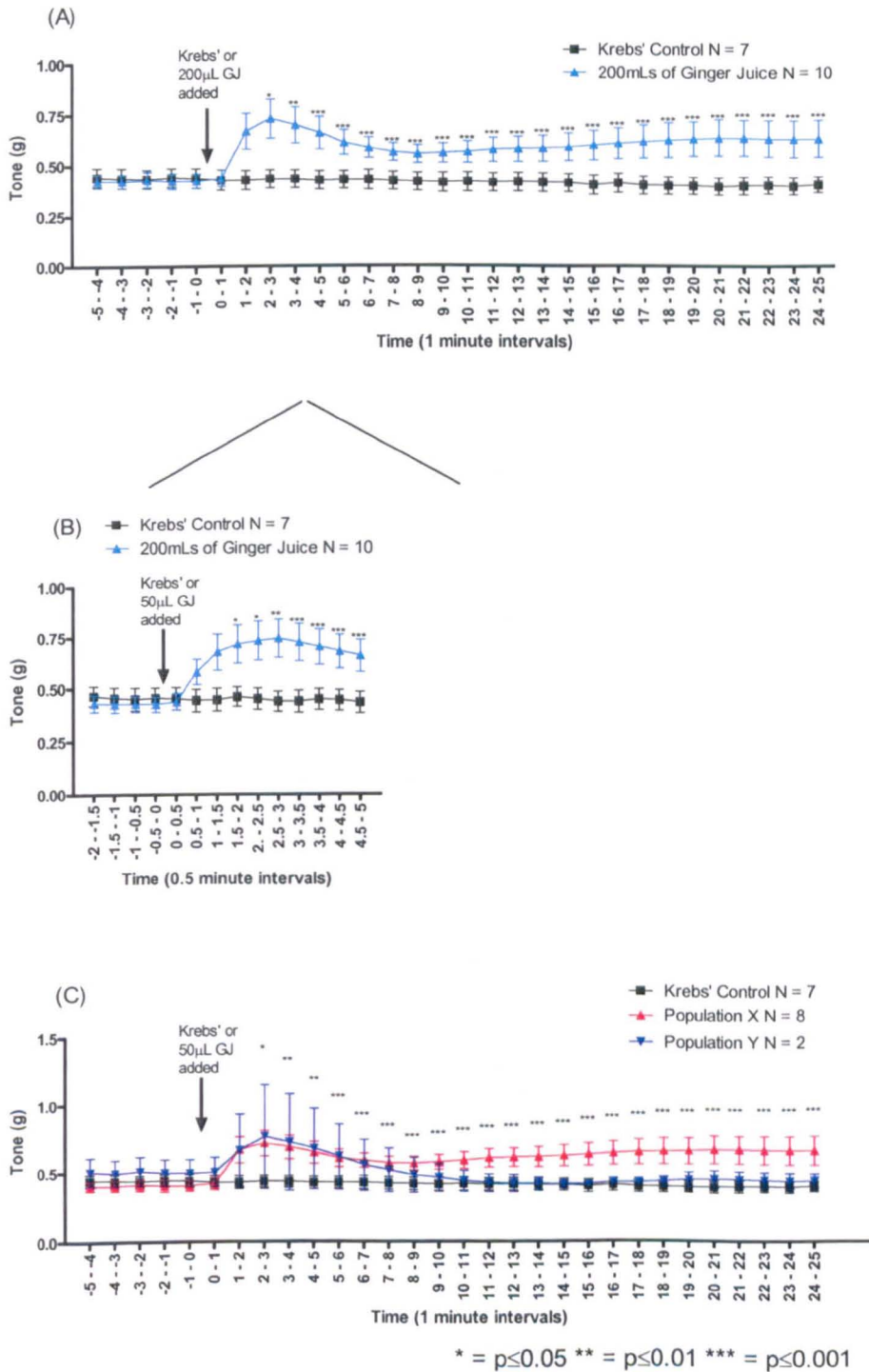


Figure 66. Line graphs displaying: (A) the tone of all the proximal stomach before and after addition of 200 μL of ginger juice: (B) a close up of the tone of all the proximal stomach strips before and after addition of 200 μL of ginger juice: and (C) the tone of both population X and Y of the proximal stomach before and after the addition of 200 μL of ginger juice. The results are expressed as mean ± SEM. N = The number of tissues from each region and is shown above in the respective graphs.

* = p ≤ 0.05 ** = p ≤ 0.01 *** = p ≤ 0.001

PROXIMAL STOMACH

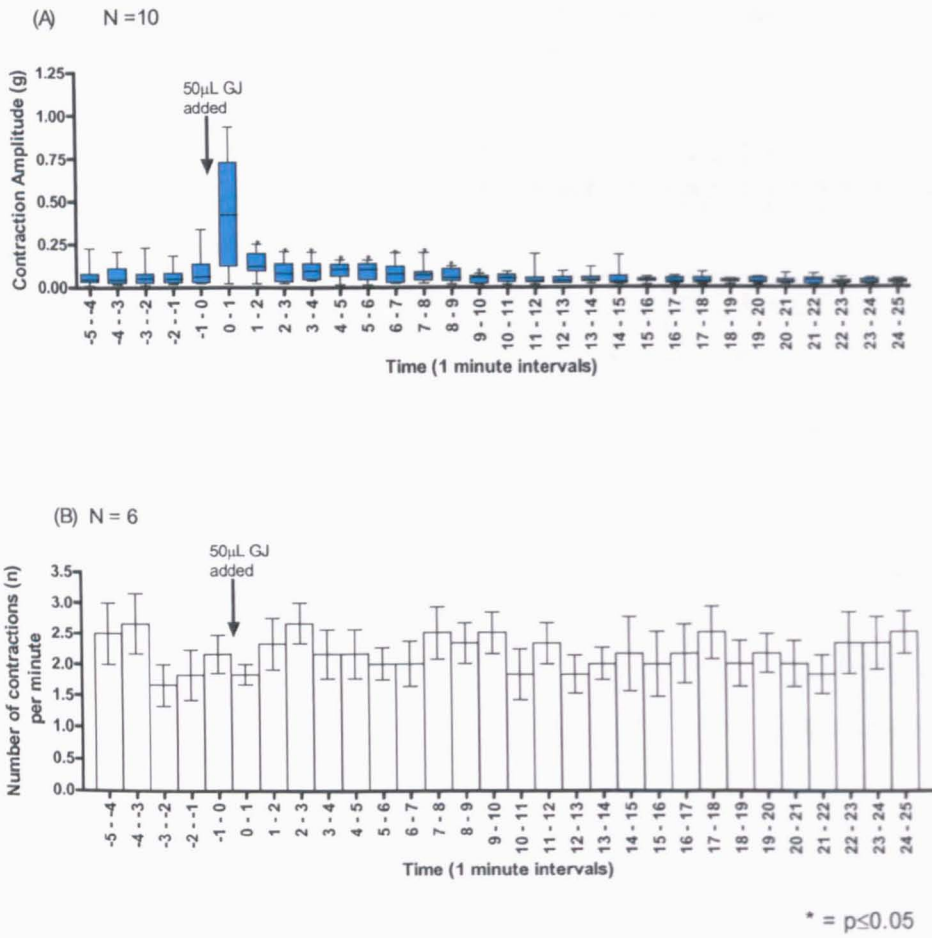


Figure 67. (A) A box and whisker plot for the contraction amplitude of the proximal stomach after a 200 μL volume of ginger juice was applied to the tissue bath. The results for (A) are expressed as median with the interquartile ranges. (B) A histogram displaying the frequency of contractions pre and post application of 200 μL of ginger juice. The results are expressed as mean \pm SEM. N = The number of tissues from each region and is shown above in the respective graphs. * = $p \leq 0.05$ ** = $p \leq 0.01$ *** = $p \leq 0.001$

4.3.5.2 The effect of a “high” (200 μ L) volume of ginger juice on the distal stomach

A “high” volume (200 μ L) of ginger juice was applied to the distal stomach. There were two different effects after the application of the ginger juice, which are illustrated in Figure 68.

4.3.5.2.1 The tone of the distal stomach after receiving 200 μ L ginger juice

The tone of the combined distal stomach results appeared to decrease slowly after the addition of the “high” volume of ginger juice. From approximately 10 minutes, the tone began to increase. From between 18-19 minutes there was a statistically significant increase in tone ($p < 0.0283$), which continued to increase until 25 minutes ($p < 0.0001$) as shown in Figure 69A.

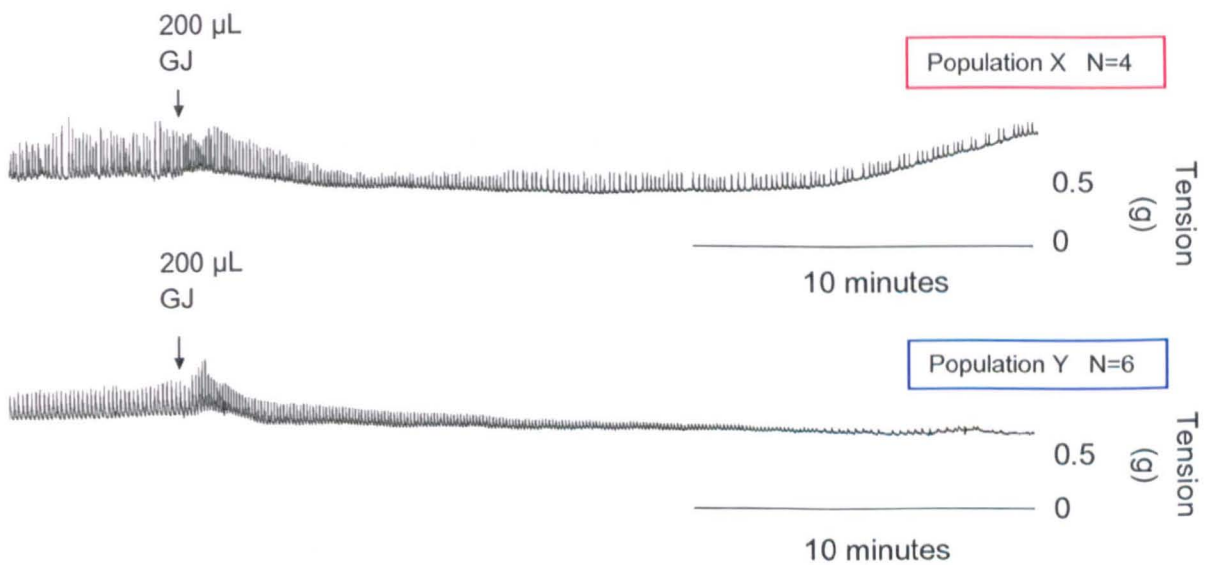


Figure 68. Two 30 minute traces from the distal stomach 5 minutes before and 25 minutes after 200 μ L of ginger juice were applied to the tissue baths.

The baselines of population X and Y and the Krebs’ solution were analysed and population Y had a significantly higher tone ($0.57 \text{ g} \pm 0.001 \text{ g}$) compared to population X (0.44

$g \pm 0.002 g$) ($p < 0.0001$). Both populations had a trend to decrease initially, however population Y maintained the trend for longer compared to population X. Population Y appears to increase in tone after 15 minutes (Figure 69B).

4.3.5.2.2 The contraction amplitude and the frequency of contractions of the distal stomach after addition of 200 μ L of ginger juice

There was a significant decrease in contraction amplitude after the ginger juice was applied and this decrease became significant at 8-9 minutes ($p < 0.0420$) until the last measurement at 24-25 minutes ($p < 0.0022$). The frequency of contractions in the distal stomach increased initially from 1-2 minutes ($p < 0.0045$) until 9-10 minutes, before returning to the baseline. This change in contractions can be examined in Figure 69D.

DISTAL STOMACH

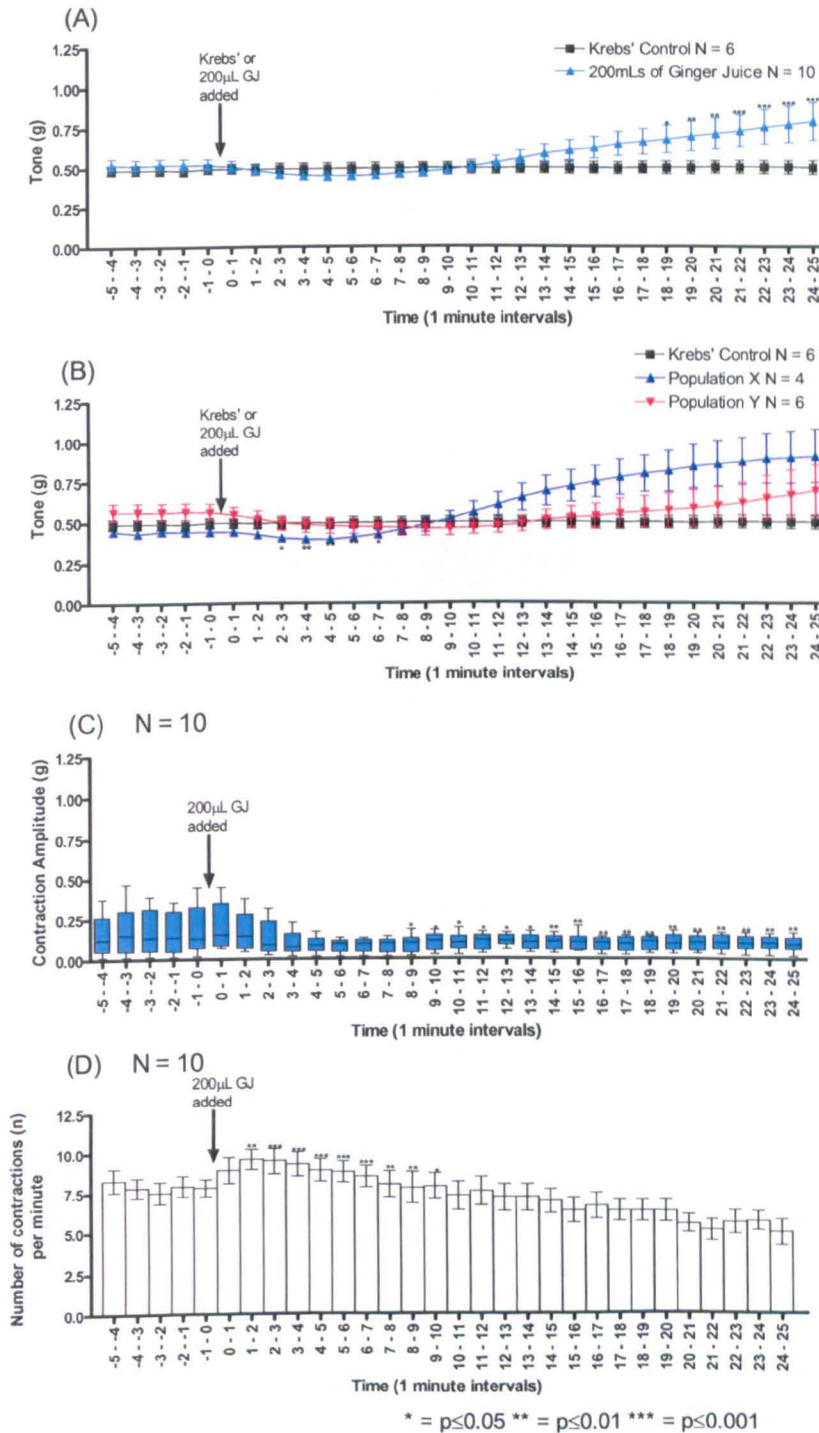


Figure 69. Line graphs displaying: (A) the tone of all the distal stomach before and after addition of 200 µL of ginger juice: (B) the tone of both population X and Y of the distal stomach before and after the addition of 200 µL of ginger juice. (C) A box and whisker plot for the contraction amplitude of the distal stomach after a 200 µL volume of ginger juice was applied to the tissue bath. The results for (C) are expressed as median with the interquartile ranges. (D) A histogram displaying the frequency of contractions pre and post application of 200 µL of ginger juice. A,B and D results are expressed as mean \pm SEM. N = The number of tissues from each region and is shown above in the respective graphs.

* = $p \leq 0.05$ ** = $p \leq 0.01$ *** = $p \leq 0.001$

4.3.5.3 The effects of a “high” (200 μ L) volume of ginger juice on the duodenum

Each duodenum, which had the 200 μ L of ginger juice applied to the tissue bath, decreased in tone and amplitude. An example of this rapid onset decrease in tone is shown in Figure 70.

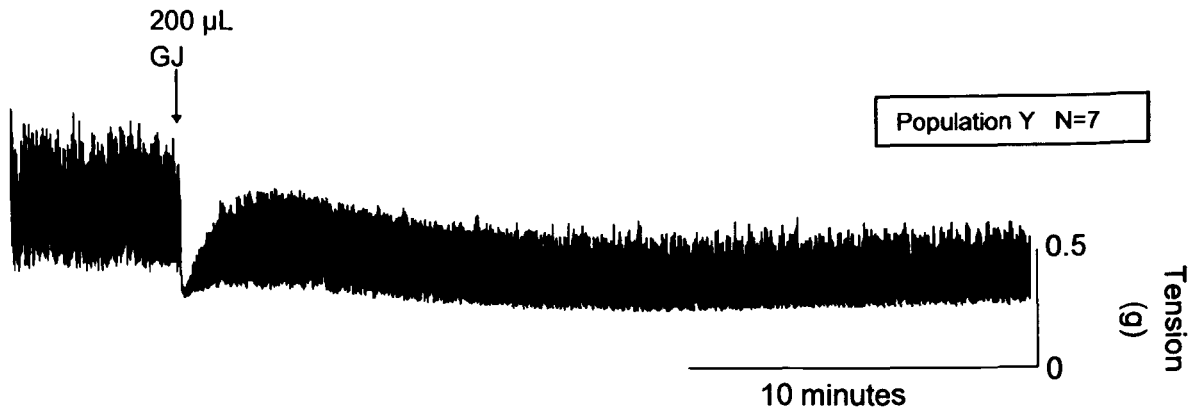


Figure 70. A 30 minute trace from a duodenum before and after a “high” volume (200 μ L) of ginger juice was added with the response to ginger juice.

4.3.5.3.1 The tone of the duodenum after a “high” volume (200 μ L) of ginger juice

The tone of the duodenum decreased after the addition of the “high” volume of ginger juice. The tonal decrease was statistically significant against the Krebs’ solution after 3-3.5 minutes ($p < 0.0212$), as shown in Figure 71B. This tonal decrease was sustained for the whole time that the duodenum was exposed to the ginger juice ($p < 0.0001$).

4.3.5.3.2 The contraction amplitude and the frequency of contractions of the duodenum after the addition of 200 μ L of ginger juice

The contraction amplitude decreased significantly after 2-3 minutes exposure to the “high” volume of ginger juice ($p < 0.0350$) (Figure 72B). This significant decrease was maintained throughout the full time of contact with the ginger juice ($p < 0.0001$) (Figure 72A). The frequency of contractions of the duodenum, as with the “low” volume, decreased after

14-15 minutes ($p < 0.0455$) after the ginger juice was applied and continued to decrease until 24-25 minutes ($p < 0.0031$) (Figure 72C).

4.3.5.4 Summary of a “high” volume of ginger juice on the upper GI tract

Overall, within the first 5 minutes of applying 200 μL of fresh ginger juice to the proximal stomach there was an increase in tone. When measured over a 25 minute period two different effects occurred after the initial increase in tone: 1) maintenance of the increase in tone above the baseline, or 2) a decrease in returning to the baseline levels. The former was the leading incidence observed. The prominent effects of the “high” volume of ginger juice on the proximal stomach were similar to population X that received a “low” volume of ginger juice. However, the “low” volume of ginger juice was only significant in the latter measurements and did not have that initial increase in tone that the “high” volume caused; rather, it increased slowly. The contraction amplitude after exposure to ginger juice caused a trend towards an increase at “low” volumes and a significant initial increase after a “high” volume followed by a decrease towards the baseline.

The tone of the distal stomach increased gradually and became statistically significant after the ginger juice was applied at 18-19 minutes. The distal stomach contraction amplitude significantly decreased after the 200 μL ginger juice was applied, from 8-9 minutes. After 1-2 minutes from exposure to the “high” volume, the frequency of contractions of the distal stomach circular strips initially increased until 9-10 minutes. When comparing a “high” volume to a “low” volume the effect of ginger juice on the distal stomach

tone and contraction amplitude was very similar. It appears that the “high” volume may have amplified the effects of the “low” volume of ginger juice.

The 200 μL of ginger juice added to the tissue bath caused a decrease in tone and contraction amplitude for the duodenum within five minutes of application. The frequency of contractions of the duodenal segments decreased after 14-15 minutes until the final measurement. When comparing the effect of a “high” volume of ginger juice to the “low” 50 μL volume of ginger juice on the duodenal tissue, the effects are very similar, causing a significant relaxation of the tissue shown by tone and contraction amplitude and a latter increase in the frequency of contractions. When comparing all three areas, it is noticeable that the duodenum appears to be the tissue which is affected the most by the ginger juice.

DUODENUM

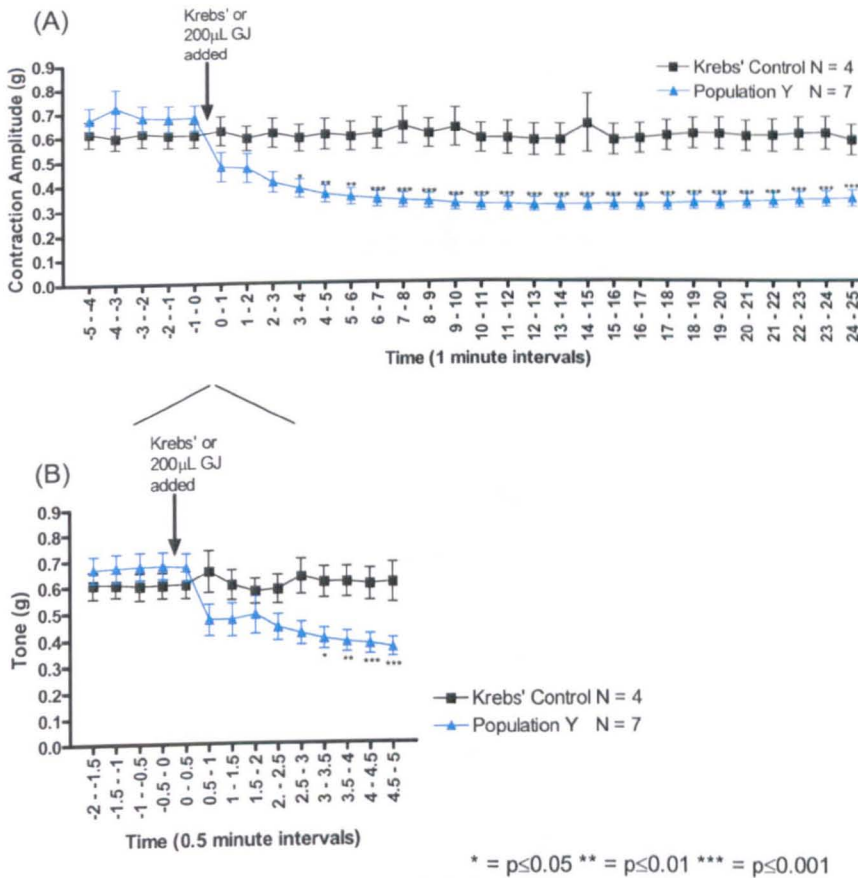


Figure 71. Line graphs displaying: (A) the tone of all the duodenum segments before and after addition of 200 µL of ginger juice and the Krebs' control: and (B) a close up of the tone of all the duodenum segments before and after addition of 200 µL of ginger juice and the Krebs' control. The results are expressed as mean ± SEM. N = The number of tissues from each region and is shown above in the respective graphs. * = p ≤ 0.05 ** = p ≤ 0.01 *** = p ≤ 0.001

DUODENUM

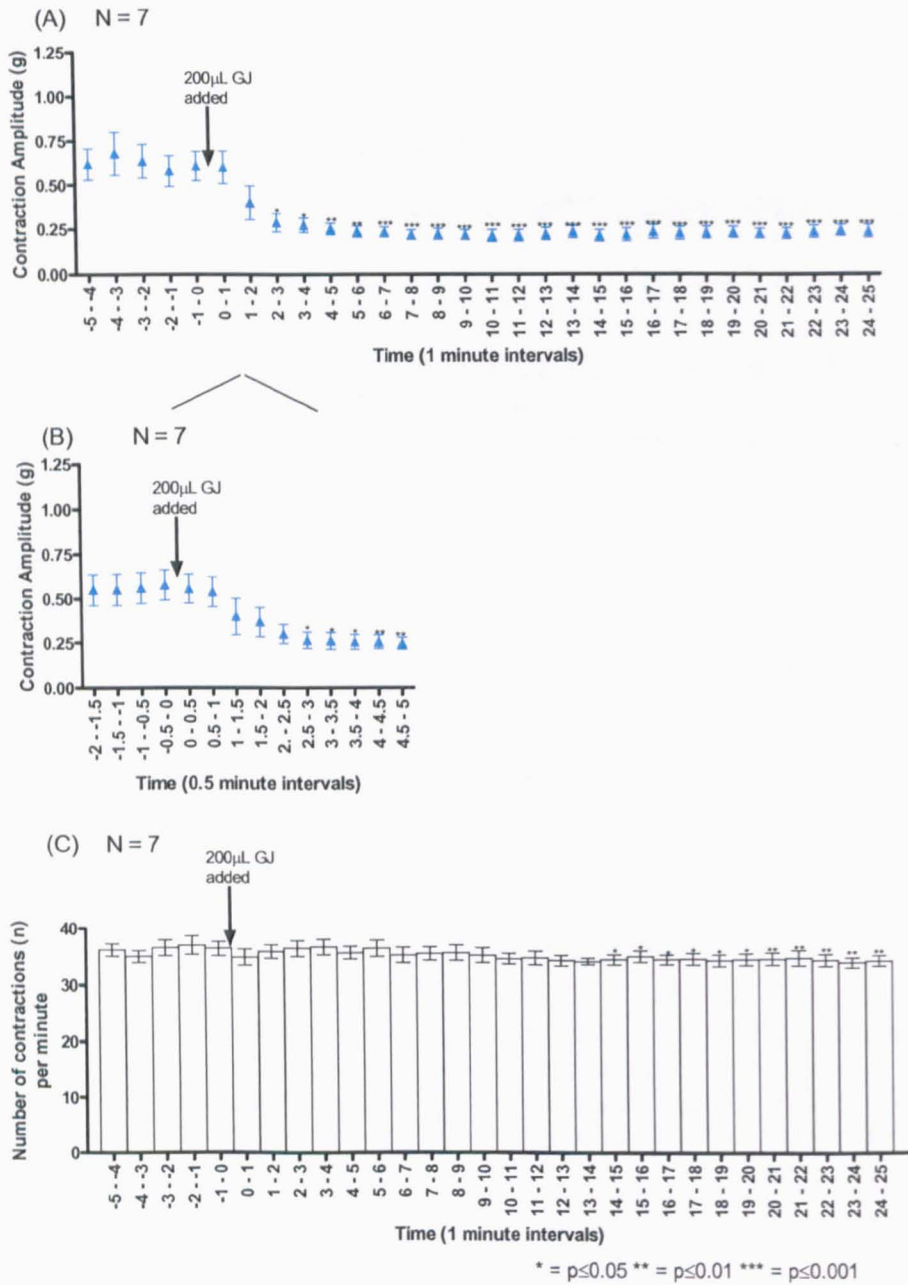


Figure 72. (A) A graph for the contraction amplitude of the duodenal segments after a 200 μ L volume of ginger juice was applied to the tissue bath. (B) A close up of the tone of all the duodenum segments before and after addition of 200 μ L of ginger juice (C) A histogram displaying the frequency of contractions of the duodenal segments pre and post application of 200 μ L of ginger juice. The results are expressed as mean \pm SEM. N = The number of tissues from each region and is shown above in the respective graphs. * = p \leq 0.05 ** = p \leq 0.01 *** = p \leq 0.001

4.3.6 The effect of a “low” volume (50 µL) of ginger juice followed by a “high” volume of ginger juice (200 µL) on the upper GI tract

The effect of 50 µL of ginger juice followed by 200 µL of ginger juice added to the tissue bath was monitored over three areas of the upper GI tract. This was to identify if the “low” volume would desensitise the “high” volume to produce a reduced effect of the ginger juice.

4.3.6.1 A “low” volume (50 µL) of ginger juice followed by a “high” volume (200 µL) of ginger juice 25 minutes on the proximal stomach

4.3.6.1.1 The tone of the proximal stomach after the “low” volume and “high” volume of ginger juice

There was no significant difference in the tone from the proximal stomach strips after the first 50 µL volume of ginger juice compared to the first five minutes prior to addition. There was a significant increase in tone from 1-2 minutes ($p < 0.0336$) until 24-25 minutes ($p < 0.0001$) after the “high” volume was applied. When the data were separated into populations X and Y, the baseline tone was significantly different ($p < 0.0185$). Population X had a lower tone ($0.36 \text{ g} \pm 0.001 \text{ g}$) than population Y ($0.37 \text{ g} \pm 0.003 \text{ g}$), although looking closer the tones were very close together: 0.01 g of a difference. Population X (N=3) had a trend to increase after both volumes of ginger were applied, whilst population Y did not appear to change in tone after the first volume however, there was a trend for the tone to increase after the second “high” volume.

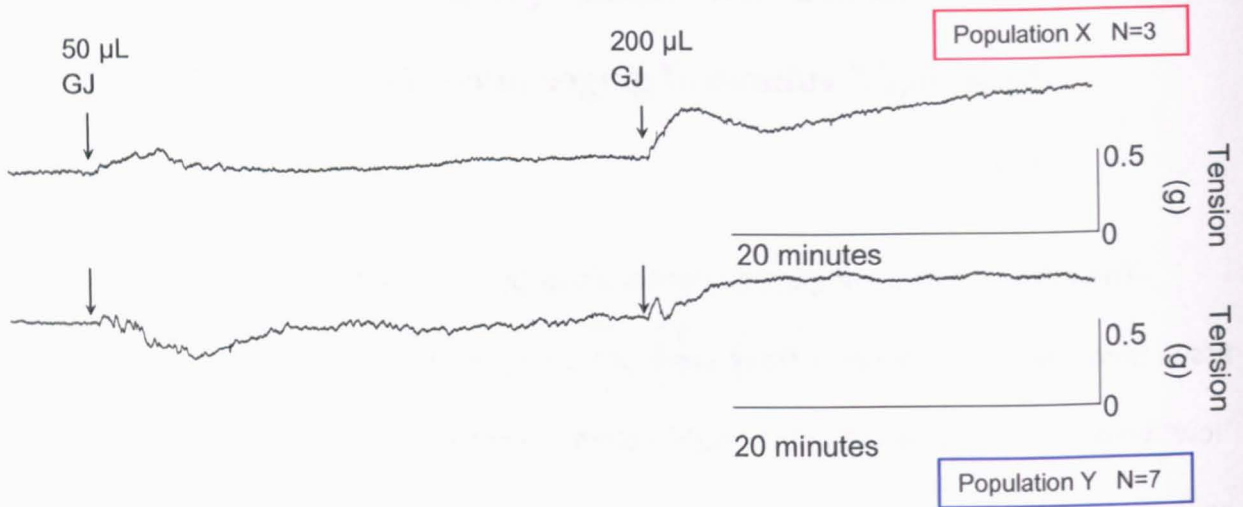


Figure 73. Two traces from proximal stomach before and after two volumes of ginger juice, a “low” volume (50 μL) followed by a “high” volume (200 μL), was added with the two different responses to ginger juice.

4.3.6.1.2 The contraction amplitude and the frequency of contractions of the proximal stomach after the “low” volume (50 μL) and “high” volume (200 μL) of ginger juice

The “low” volume (50 μL) of ginger juice significantly decreased the contraction amplitude from 17-18 minutes ($p < 0.0421$) to 24-25 minutes ($p < 0.0081$), observed in Figure 74C. There was a no difference in the basal contraction amplitude between the two populations. The second volume significantly increased the contraction amplitude from 1-2 minutes ($p < 0.0109$) until 5-6 minutes. The second volume did not significantly cause a secondary reduction in contraction amplitude: the median of the final reading was 0.0261 g, which was very low.

There was no significant difference in the number of contractions per minute in either population after the first volume of ginger juice (50 μL). There was a significant increase immediately after the second volume (200 μL) of ginger juice from 1-2 minutes ($p < 0.0073$) until 7-8 minutes. This corresponds with the change in contraction amplitude. There was a

trend for the number of contractions to decrease from 15 minutes after the second volume (Figure 74D). However, it is hard to quantify as the proximal stomach does not have clear rhythmic contractions compared to the distal stomach and duodenum. Changes in the proximal stomach are far more tonal as shown in Figure 73.

PROXIMAL STOMACH

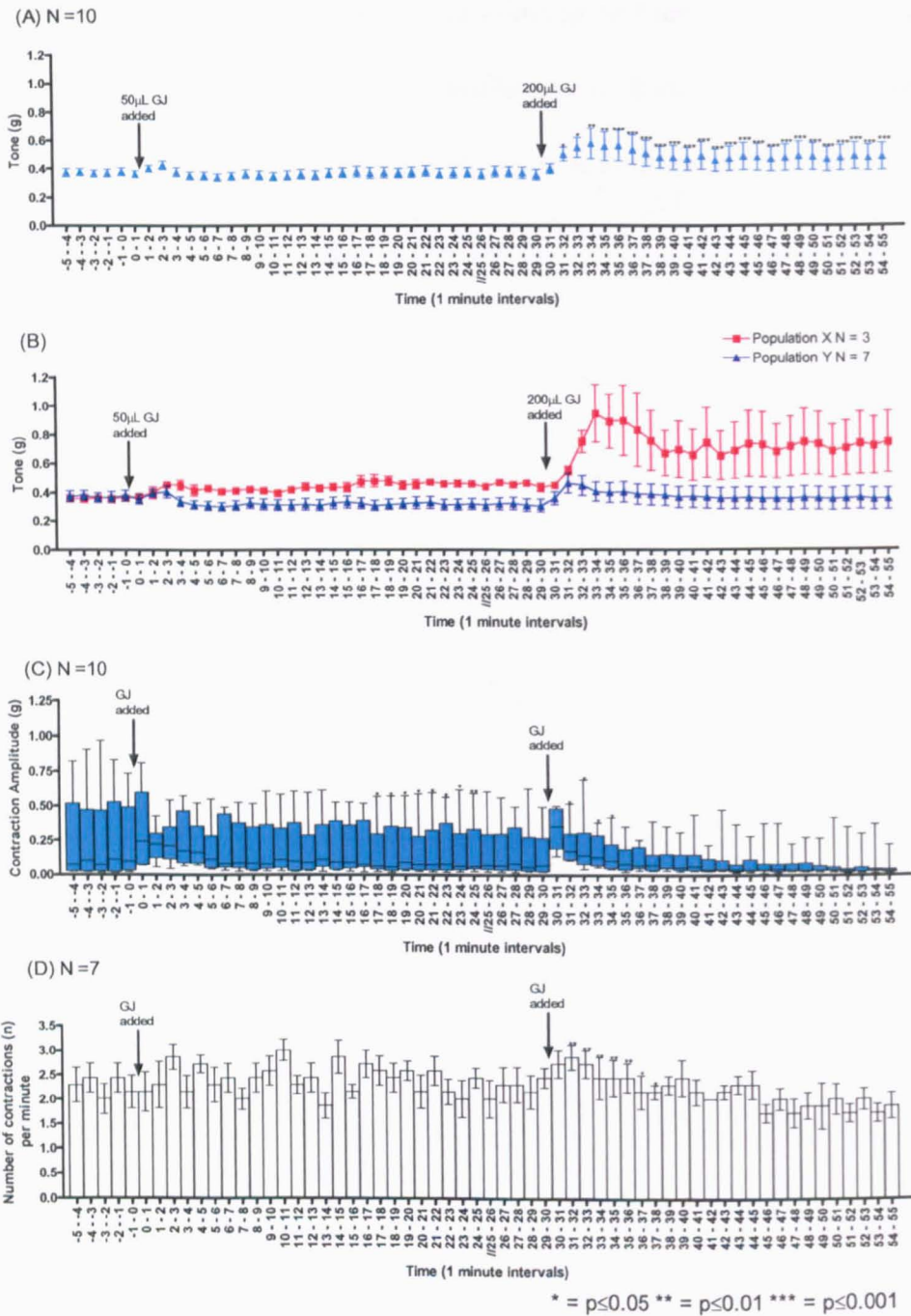


Figure 74. Line graphs displaying: (A) the tone of all the proximal stomach before and after the addition of 50 μL and 200 μL ginger juice (B) the tone of the proximal stomach before and after the addition of 50 μL and 200 μL ginger juice with population X and Y (C) box and whisker plots the contraction amplitude of all the proximal stomach before and after the addition of 50 μL and 200 μL (D) histogram of the frequency of contractions from the proximal stomach after receiving 50 μL and 200 μL of ginger juice. The results are expressed as mean \pm SEM. The results in (C) are expressed as median with the interquartile ranges. N = The number of tissues from each region and is shown above in the respective graph.
* = $p \leq 0.05$ ** = $p \leq 0.01$ *** = $p \leq 0.001$

4.3.6.2 The effects of a “low” volume followed by a “high” volume of ginger juice on the distal stomach

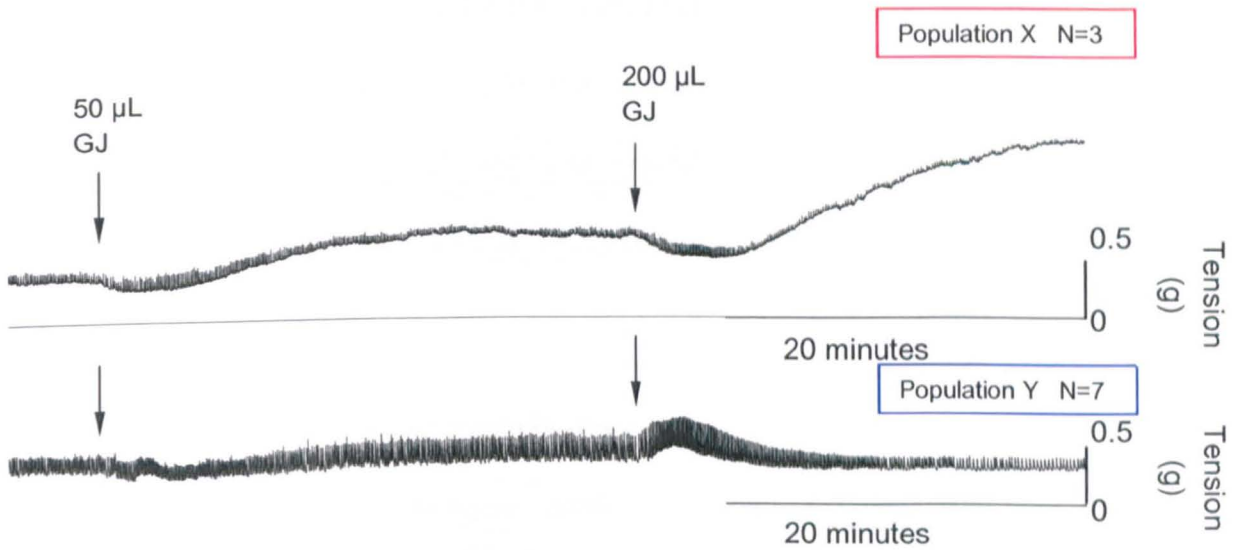


Figure 75. Two traces from distal stomach before and after two volumes of ginger juice, a “low” volume (50 µL) followed by a “high” volume (200 µL), were added showing the two different responses to ginger juice.

4.3.6.2.1 The tone of the distal stomach after a “low” volume (50 µL) followed by a “high” volume (200 µL) of ginger juice

After the first volume of ginger juice, when the tonal results were combined, there was an initial significant decrease in tone from 1-2 minutes ($p < 0.0002$) followed by an increase after 6-7 minutes, which was significant until 9-10 minutes ($p < 0.0066$), which can be seen in Figure 76A. The second higher volume also caused a statistically significant decrease after 1-2 minutes exposure ($p < 0.0001$) which was followed by an increase which was significant until 9-10 minutes ($p < 0.0373$). There was a significant difference between the baselines of population X and population Y ($p < 0.0001$). Population Y displayed a very slight non-significant reduction in tone after the two “low” volumes of ginger juice. Population X had a trend towards an increase in tone, as seen in Figure 76B. Population X only had an N number of 3.

4.3.6.2.2 The contraction amplitude and the frequency of contractions of the distal stomach after a “low” and a “high” volume of ginger juice

The contraction amplitude decreased slowly from 14-15 minutes ($p < 0.0447$) until 24-25 minutes ($p < 0.0076$) after the first “low” volume of ginger juice. There was a statistical increase in contraction amplitude 1-2 minutes after the “higher” volume and decrease in contraction amplitude at 11-12 minutes ($p < 0.0339$) until 24-25 minutes ($p < 0.0038$), as shown in Figure 76C.

The frequency of contractions increased significantly after the “low” and “high” volumes of ginger juice after 1-2 minutes ($p < 0.0160$ and $p < 0.0069$), as shown in Figure 76D. The change in frequency of contraction continued until 24-25 minutes after the first volume, however after the second volume the change in frequency of contractions was no longer significant after 8 minutes of exposure.

DISTAL STOMACH

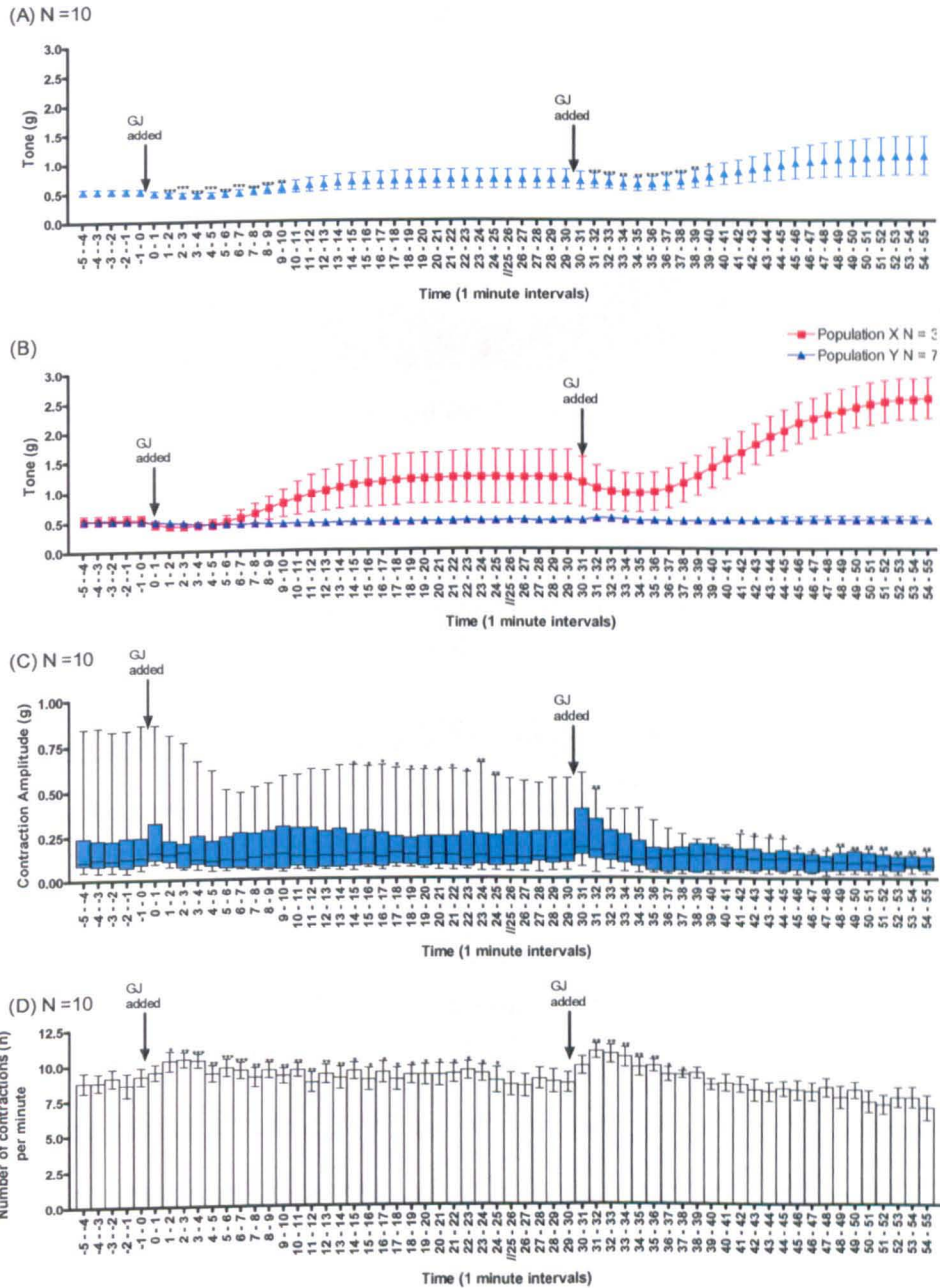


Figure 76. Graphs displaying: (A) the tone of all the distal stomach before and after the addition of 50 μ L and 200 μ L ginger juice (B) the tone of the distal stomach before and after the addition of 50 μ L and 200 μ L of ginger juice with population X and Y (C) box and whisker plots of the contraction amplitude of all the distal stomach before and after the addition of 50 μ L and 200 μ L (D) a histogram of the frequency of contractions from the distal stomach after receiving 50 μ L and 200 μ L of ginger juice. The results are expressed as mean \pm SEM. The results in (C) are expressed as median with the interquartile ranges. N = The number of tissues from each region and is shown above in the respective graph.

* = $p \leq 0.05$ ** = $p \leq 0.01$ *** = $p \leq 0.001$

4.3.6.3 The effects of a “low” volume followed by a “high” volume of ginger juice on the duodenum

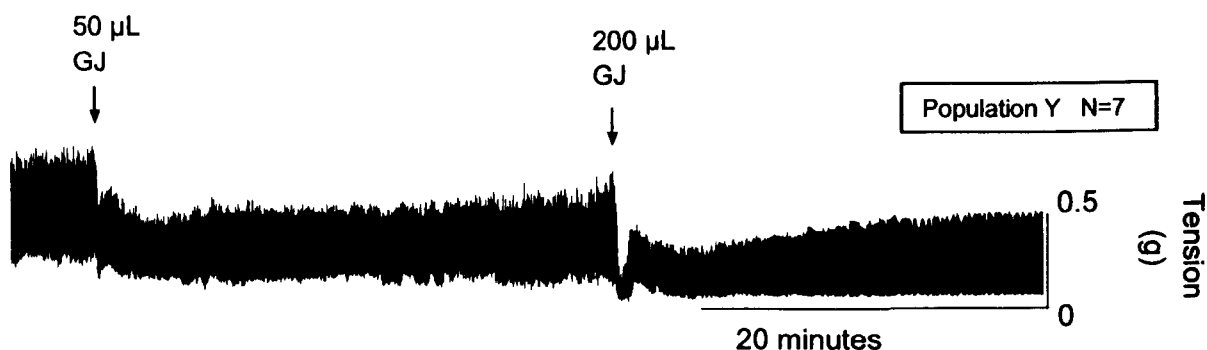


Figure 77. A trace recorded from the duodenum before and after two volumes of ginger juice was added, a “low” volume (50 µL) followed by a “high” volume (200 µL).

4.3.6.3.1 The tone of the duodenum before and after the addition of the “low” and “high” volume of ginger juice

The first volume caused a significant reduction in tone from 1-2 minutes ($p < 0.0001$), until 24-25 minutes ($p < 0.0001$) as shown in Figure 78A. There was also a significant reduction in tone from 1-2 minutes ($p < 0.0001$) until 24-25 minutes ($p < 0.0001$) after the second volume of ginger juice (200 µL).

4.3.6.3.2 The contraction amplitude and the frequency of contractions of the duodenum before and after receiving the “low” (50 µL) and “high” (200 µL) volume of ginger juice

The contraction amplitude of the duodenum reduced after the 50 µL volume of ginger juice was applied from 2-3 minutes ($p < 0.0343$), increasing in significance until 24-25 minutes ($p < 0.0001$). The second volume also saw a reduction in contraction amplitude, which was statistically significant from 33-55 minutes. The frequency of contractions increased significantly after the first “low” volume of ginger juice, from 4-5 minutes until 24-25 minutes

($p < 0.0001$). The frequency of contraction of the duodenum changed at 32-35 minutes, being after the second volume (200 μ L) of ginger juice.

4.3.6.3.3 Summary of a “low” volume of ginger juice followed by a “high” volume on the upper GI tract

When the populations were combined for the proximal stomach, there was a significant increase in tone after both volumes of ginger juice. There was a decrease in the contraction amplitude after the “low” volume of ginger juice, whilst there was an initial significant increase in the proximal stomach after the 200 μ L of ginger juice was added. The prominent population of the proximal and distal stomach after the ginger juice was applied was population Y. The significant effects of the ginger on the distal stomach were an initial decrease in tone after both volumes and a decrease in contraction amplitude after both volumes. There was a significant initial increase in the frequency of contractions of the distal stomach after the “low” and “high” volumes of ginger juice. The second volume (200 μ L) mimicked the effect of the first volume, and it was not affected by the first volume (50 μ L). The predominant effect of ginger juice was to decrease the tone and the contraction amplitude of the duodenum after both volumes. The frequency of contractions of the duodenum also increased after the first “low” volume of ginger juice.

DUODENUM

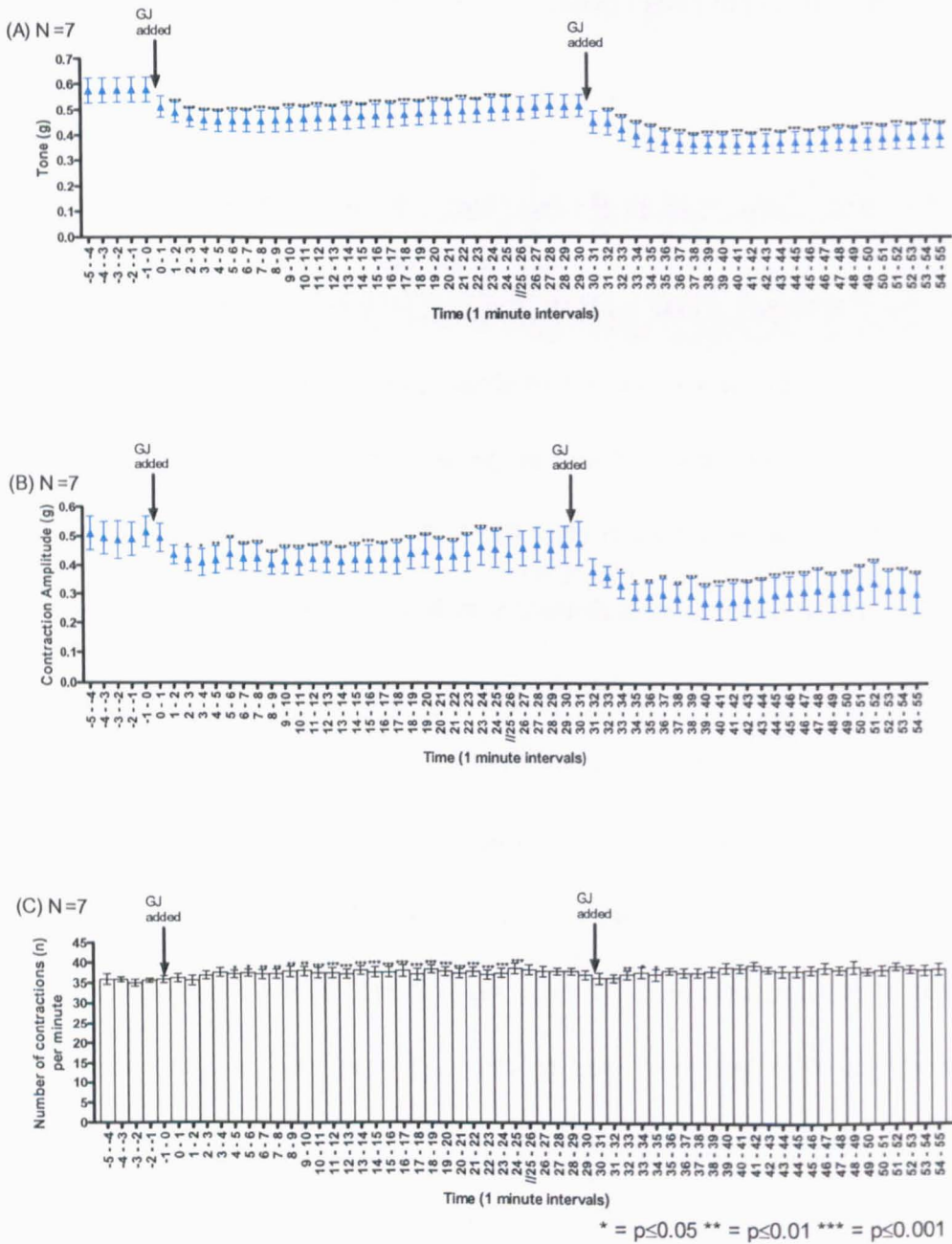


Figure 78. (A) A graph displaying the duodenal tone of population Y before and after addition of two different volumes of ginger juice, (B) a graph displaying the duodenal contraction amplitude of population Y after addition of two different volumes of ginger juice, (C) a histogram displaying the frequency of contractions of the population Y duodenum after addition of two different volumes of ginger juice. The results are expressed as mean \pm SEM. N = The number of tissues from each region and is shown above in the respective graph.

* = p \leq 0.05 ** = p \leq 0.01 *** = p \leq 0.001

4.3.7 The effect of the element solution on the proximal and distal stomach, and the duodenum

The element controls were conducted with a solution containing five elements detected in the highest concentrations in ginger juice: potassium ($4.6 \times 10^{-2} \text{M}$); magnesium ($7.4 \times 10^{-3} \text{M}$); manganese ($8.3 \times 10^{-4} \text{M}$); sodium ($1.1 \times 10^{-3} \text{M}$); and calcium ($5.1 \times 10^{-4} \text{M}$). 200 μL of the solution was applied to the proximal and distal stomach and the duodenum to match the highest volume of ginger juice.

4.3.7.1 Proximal Stomach

The tone, contraction amplitude and the frequency of the contractions for the proximal stomach did not change after the element solution was added to the organ bath (Figure 79A-C).

4.3.7.2 Distal Stomach

The tone of the distal stomach exposed to the element solution was statistically different from the Krebs' solution 1-2 minutes after exposure until 24-25 minutes of exposure ($p < 0.0005$) (Figure 80A). The contraction amplitude of the distal stomach was statistically lower from 6-7 minutes until 24-25 minutes ($p < 0.0105$) compared to the original baseline. The frequency of contraction for the distal stomach decreased after the element solution was added from 10-11 minutes ($p < 0.0127$) and increased in significance until 24-25 minutes ($p < 0.0007$) (Figure 80C).

4.3.7.3 Duodenum

The tone of the duodenum significantly reduced 1-2 minutes after the application of the element solution until 24-25 minutes (see Figure 81A). The duodenum contraction amplitude decreased significantly after the application of the element solution. The contraction amplitude was significantly different from the baseline after 1-2 minutes ($p < 0.0415$) up until 24-25 minutes ($p < 0.0003$). The frequency of contractions decreased significantly from 3-4 minutes through to the final measurement at 24-25 minutes ($p < 0.0001$). Although the histogram does not appear to change due to the scale, the mean \pm SEM number of contractions per minute at -5 - -4 minutes was 34.2 ± 1.530 , whilst the mean number of contractions per minute at 24-25 minutes was 30.6 ± 1.749 . This indicates a reduction of 4 contractions per minute (Figure 81C).

PROXIMAL STOMACH

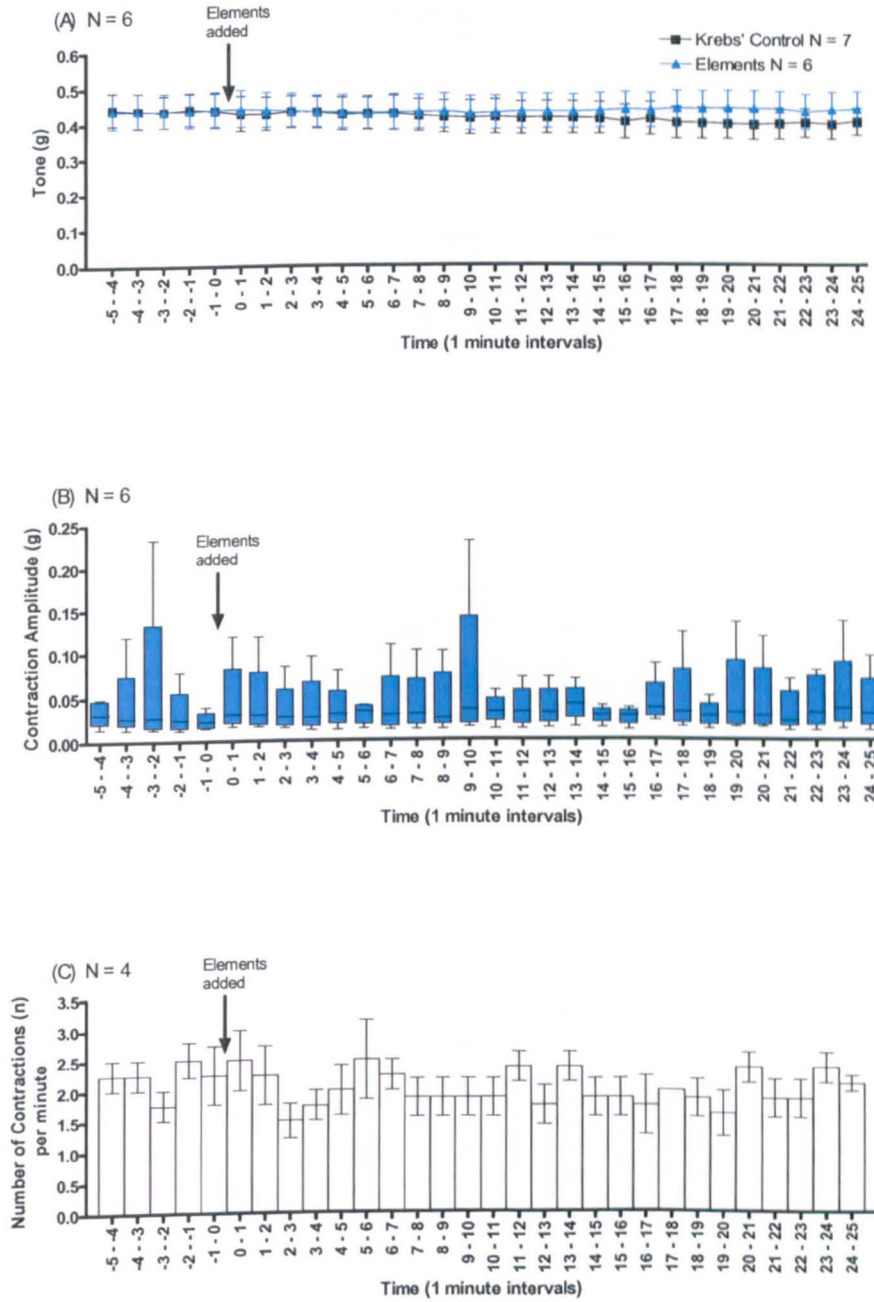


Figure 79. (A) A line graph displaying the tone of all the proximal stomach before and after addition the element solution or the Krebs' control. (B) A box and whisker plot of the contraction amplitude of the proximal stomach after the element solution. The results for (B) are expressed as median with the interquartile ranges. (C) A histogram displaying the frequency of contractions pre and post application of the element solution. The results are expressed as mean \pm SEM. N = The number of tissues from each region and is shown above in the respective graphs.

DISTAL STOMACH

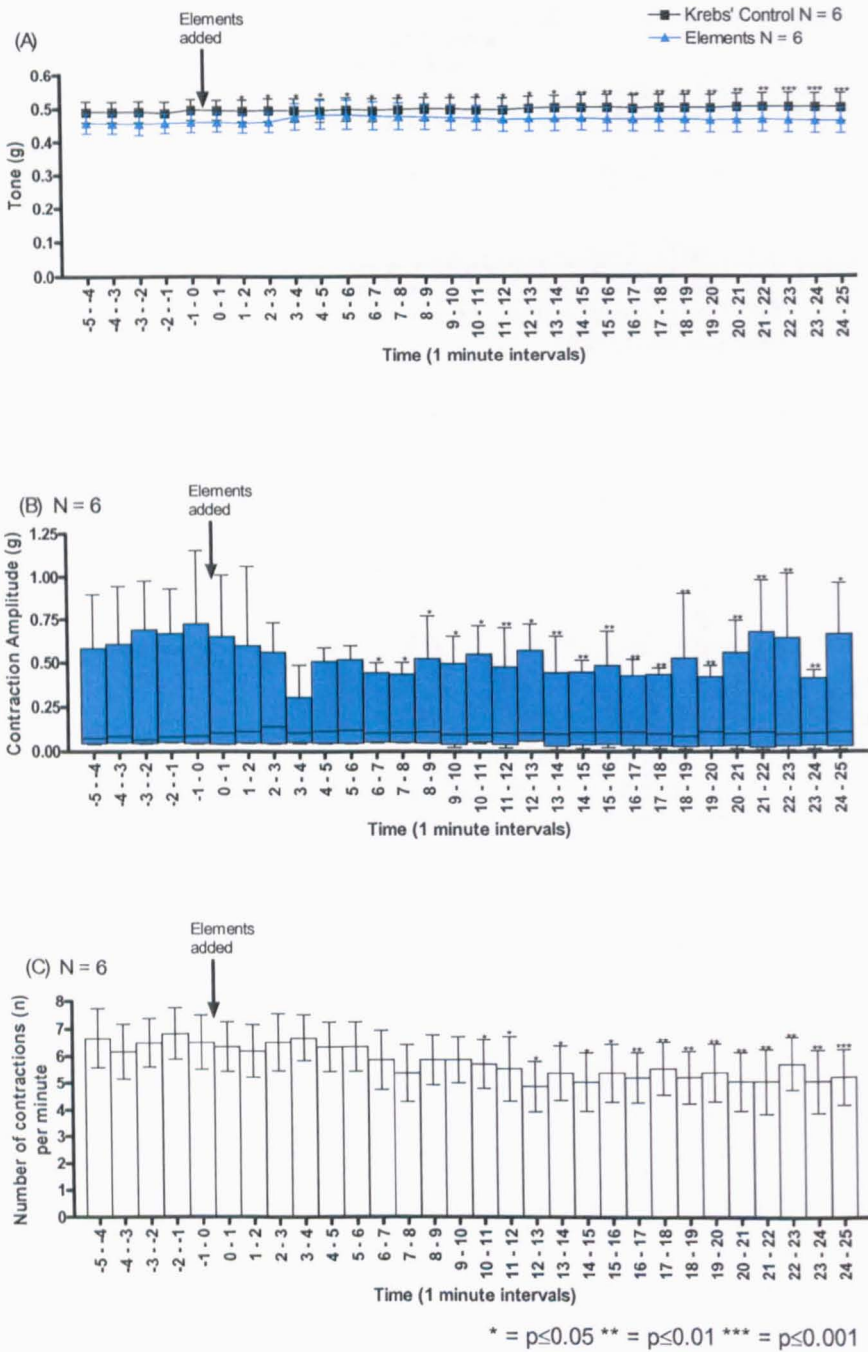


Figure 80. (A) A line graph displaying the tone of the distal stomach before and after addition the element solution or the Krebs' control. (B) A box and whisker plot of the contraction amplitude of the distal stomach after the element solution. The results for (B) are expressed as median with the interquartile ranges. (C) A histogram displaying the frequency of contractions pre and post application of the element solution on the distal stomach. The results are expressed as mean \pm SEM. N = The number of tissues from each region and is shown above in the respective graphs. * = $p \leq 0.05$ ** = $p \leq 0.01$ *** = $p \leq 0.001$

DUODENUM

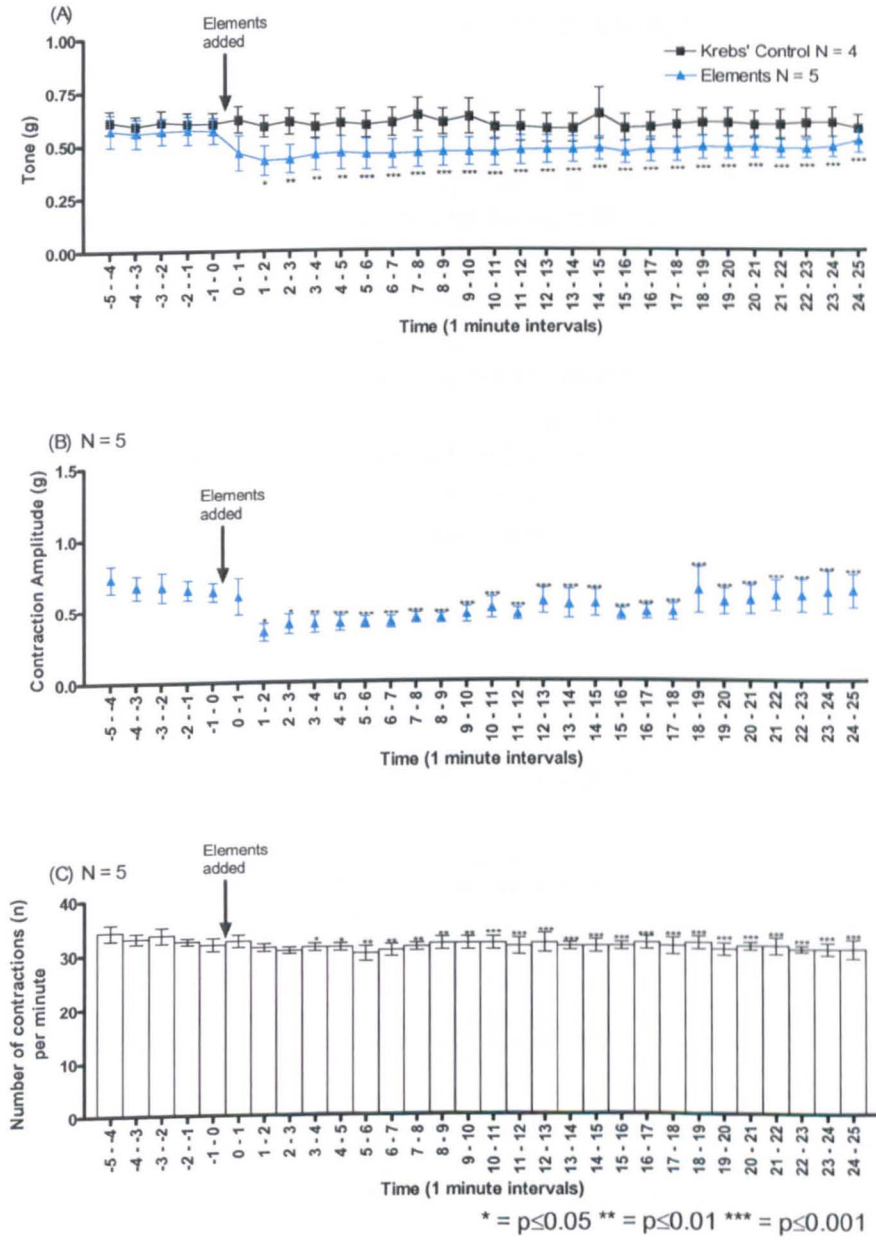


Figure 81. (A) Line graph displaying the duodenal tone after the element solution against the Krebs' control, (B) a graph displaying the duodenal contraction amplitude after the addition of the element solution, (C) a histogram displaying the frequency of contractions of the duodenum after the element solution added to the tissue bath. The results are expressed as mean \pm SEM. N = The number of tissues from each region and is shown above in the respective graph.

* = $p \leq 0.05$ ** = $p \leq 0.01$ *** = $p \leq 0.001$

4.3.8 The effect of [6]-gingerol at the concentration in ginger juice on the upper GI tract

In Chapter 3, the concentration of [6]-gingerol in ginger juice was quantified to be 234.41 ± 6.29 mg/L. Based upon this when 200 μ L of ginger juice was injected into a 10 mL organ bath, the concentration of [6]-gingerol was calculated to be 1.59×10^{-5} M. Therefore, the next step was to apply such a concentration of [6]-gingerol alone to the upper GI tract, to identify whether [6]-gingerol was wholly responsible for the effects of ginger juice. The contraction amplitude was variable for each of the tissues as explained previously; therefore the vehicle contraction amplitude was not compared to the contraction amplitude of the tissues exposed to [6]-gingerol only the first five minutes prior to addition, as the baselines would be different (Figure 49 for vehicle controls).

4.3.8.1 [6]-gingerol at the concentration of ginger juice on the proximal stomach

The basal tone of the vehicle group from the proximal stomach was statistically lower than the tone of the [6]-gingerol 1.59×10^{-5} M group ($p < 0.0079$) and therefore it was not valid to compare them. The contraction amplitude changed significantly and there was a significant change from 6-7 minutes until 24-25 minutes (

Figure 82B). The frequency of contractions of the proximal stomach increased after the addition of the [6]-gingerol at the concentration found in ginger juice. Essentially, for the proximal and distal stomach there were no distinct populations (i.e. increase or decrease groups), there was just an overall effect, hence they were not separated.

4.3.8.2 [6]-Gingerol at the concentration of ginger juice on the distal stomach

The distal stomach was exposed to [6]-gingerol at $1.59 \times 10^{-5} \text{M}$. There was a significant increase in tone from 12-13 minutes ($p < 0.0479$) until 24-25 minutes ($p < 0.0001$). The contraction amplitude decreased significantly from 6-7 minutes ($p < 0.0480$) and for the rest of the measurements up until 24-25 minutes. The frequency of contractions of the distal stomach did not change significantly after the addition of [6]-gingerol at $1.59 \times 10^{-5} \text{M}$, as shown in Figure 83C. The effects of [6]-gingerol at $1.59 \times 10^{-5} \text{M}$ did not fully imitate the effects of 200 μL ginger juice on the distal stomach, as there was no initial decrease in tone, although there was an increase.

4.3.8.3 [6]-Gingerol at the concentration of ginger juice on the duodenum

The [6]-gingerol at $1.59 \times 10^{-5} \text{M}$ was applied to the duodenum. This concentration of [6]-gingerol (equivalent to 200 μL of ginger juice) did cause a significant decrease in tone on the duodenum from 3-4 minutes ($p < 0.0142$) until 24-25 minutes ($p < 0.0001$) when compared to the [6]-gingerol vehicle; however this decrease was not as effective as the “high” volume of ginger juice alone. There was a significant decrease in contraction amplitude after the [6]-gingerol at $1.59 \times 10^{-5} \text{M}$ was added to the organ bath from 2-3 minutes ($p < 0.0424$) until 24-25 minutes ($p < 0.0015$). There was no change in the frequency of contraction on the duodenum.

PROXIMAL STOMACH

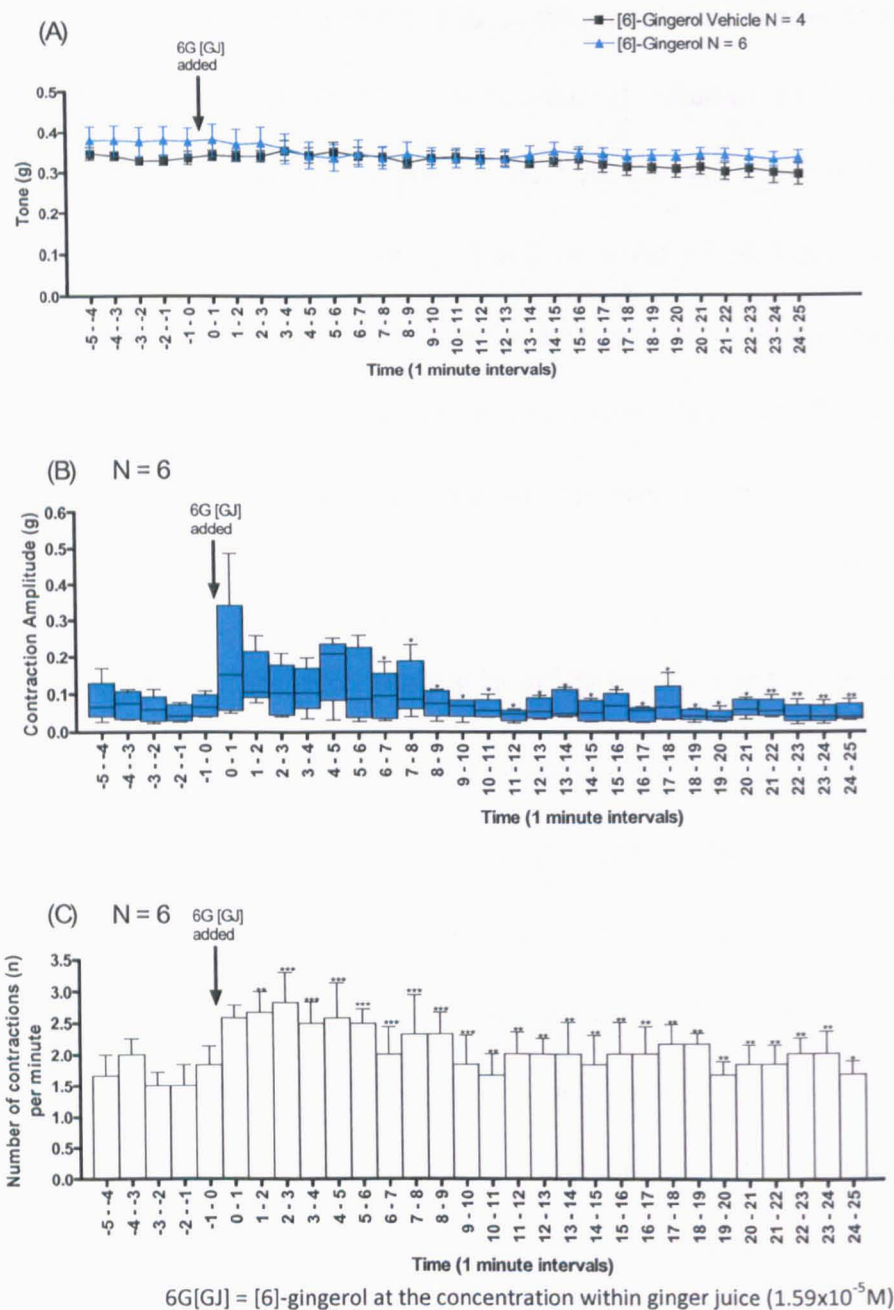


Figure 82. (A) Line graph displaying the proximal stomach tone after the addition of [6]-gingerol (1.59×10^{-5} M) and the vehicle, (B) a box and whisker plot displaying the proximal stomach contraction amplitude after the addition of [6]-gingerol (1.59×10^{-5} M), (C) a histogram displaying the frequency of contractions of the proximal stomach after the addition of [6]-gingerol (1.59×10^{-5} M). The results are expressed as mean \pm SEM, except for (B) where the results are expressed as the median with the interquartile range. N = The number of tissues from each region and is shown above in the respective graph. 6G[GJ] = [6]-gingerol at the concentration within ginger juice (1.59×10^{-5} M) * = $p \leq 0.05$ ** = $p \leq 0.01$ *** = $p \leq 0.001$

DISTAL STOMACH

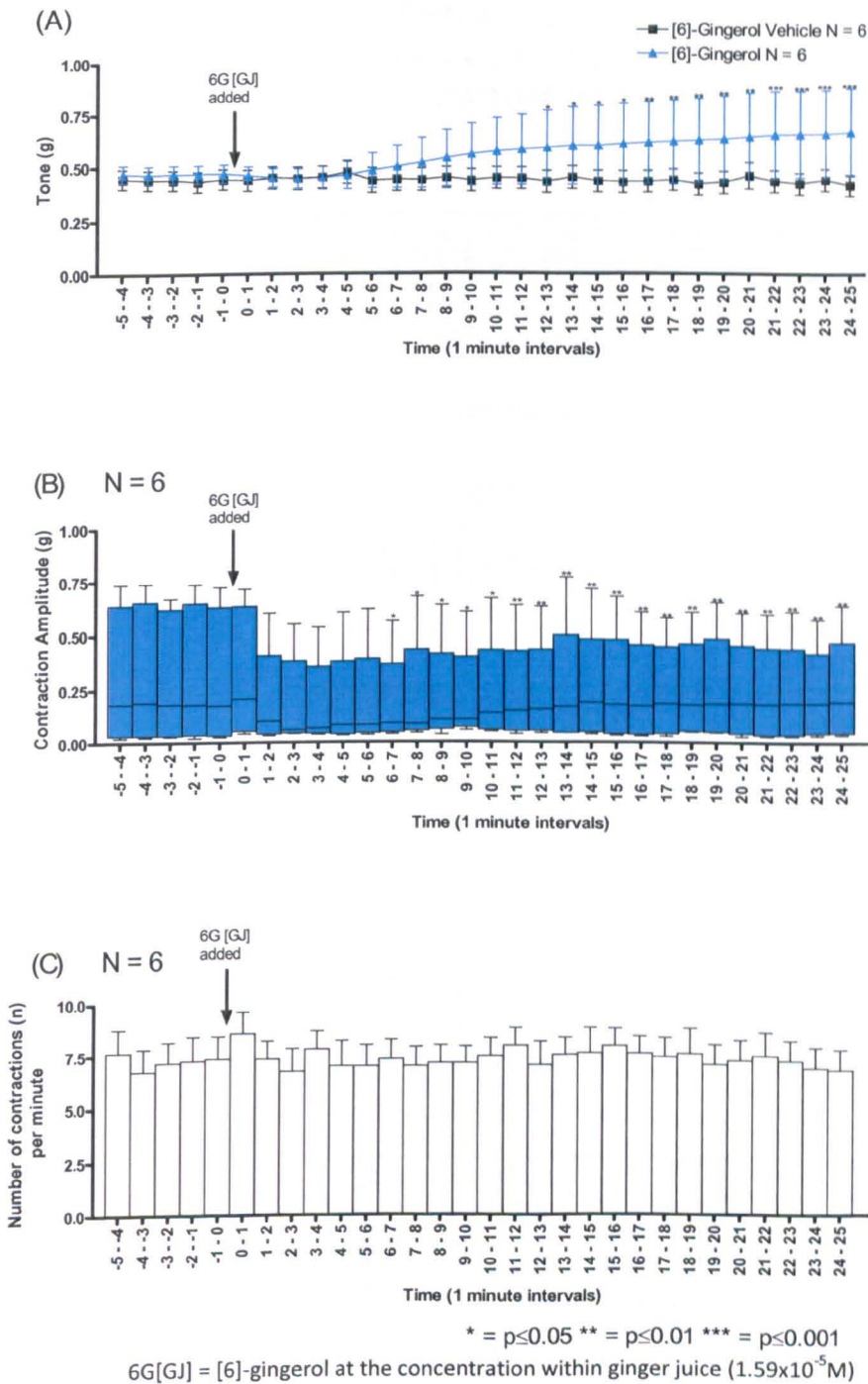


Figure 83. (A) A line graph displaying the tone of the distal stomach before and after addition of [6]-gingerol ($1.59 \times 10^{-5} \text{M}$) and the [6]-gingerol vehicle. (B) A box and whisker plot of the contraction amplitude of the distal stomach after the addition of [6]-gingerol ($1.59 \times 10^{-5} \text{M}$). (C) A histogram displaying the frequency of contractions pre and post application of [6]-gingerol. The results are expressed as mean \pm SEM, except for (B) where the results are expressed as the median with the interquartile range. N = The number of tissues from each region and is shown above in the respective graphs. 6G[GJ] = [6]-gingerol at the concentration within ginger juice ($1.59 \times 10^{-5} \text{M}$) * = $p \leq 0.05$ ** = $p \leq 0.01$ *** = $p \leq 0.001$

DUODENUM

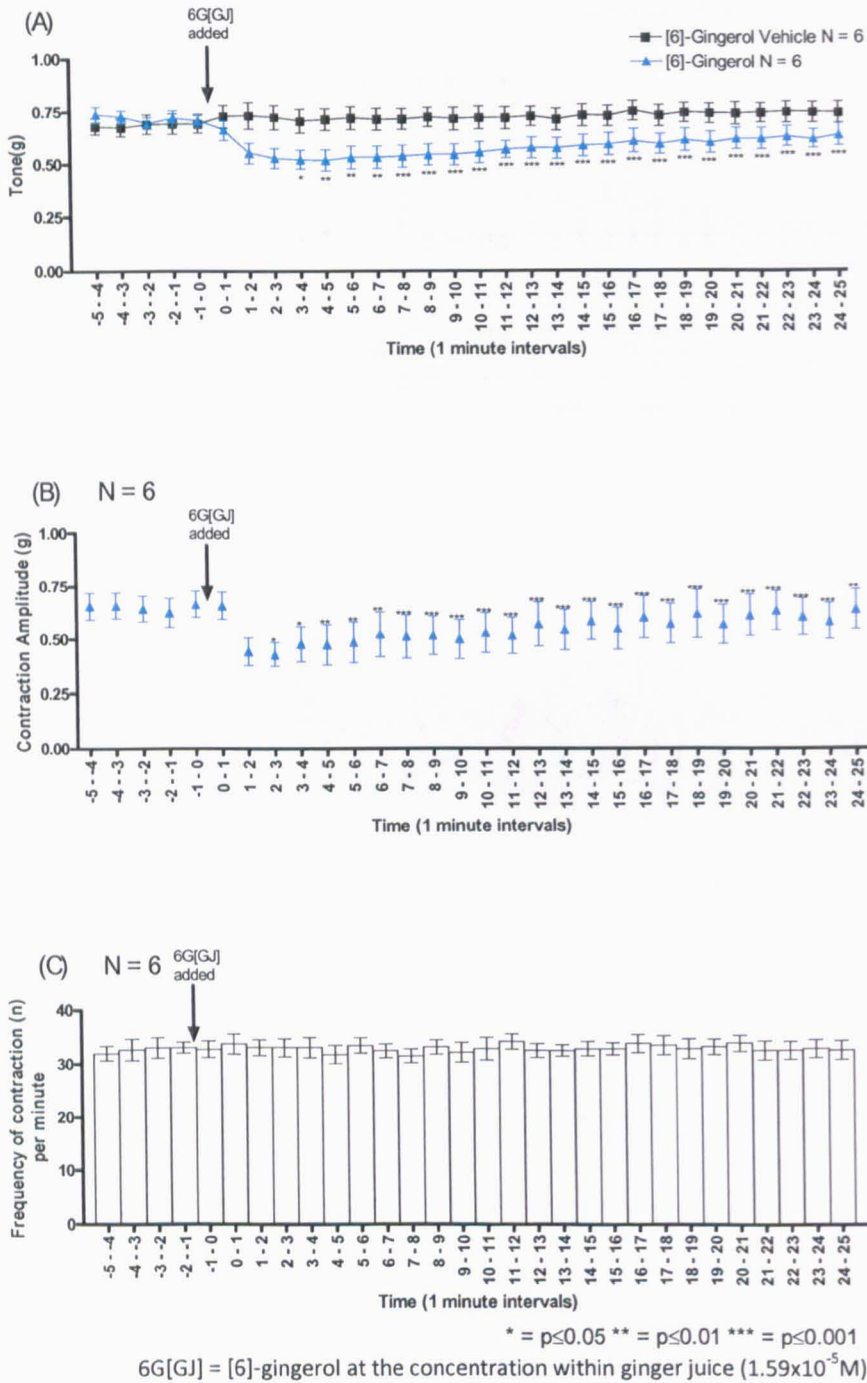


Figure 84. (A) Line graph displaying the duodenal tone after the addition of [6]-gingerol ($1.59 \times 10^{-5} \text{M}$) and the vehicle, (B) a graph displaying the duodenal contraction amplitude after the addition of [6]-gingerol ($1.59 \times 10^{-5} \text{M}$), (C) a histogram displaying the frequency of contractions of the duodenum after the addition of [6]-gingerol ($1.59 \times 10^{-5} \text{M}$) and the vehicle. The results are expressed as mean \pm SEM. N = The number of tissues from each region and is shown above in the respective graph. 6G[GJ] = [6]-gingerol at the concentration within ginger juice ($1.59 \times 10^{-5} \text{M}$)

* = $p \leq 0.05$ ** = $p \leq 0.01$ *** = $p \leq 0.001$

4.3.8.4 Summary of the effects of [6]-gingerol at the concentration in ginger juice on the upper GI tract

[6]-Gingerol at the concentration found in ginger juice had a trend to increase the tone of the proximal stomach, and changed the contraction amplitude significantly from 6-7 minutes. There was a statistically significant increase in tone and a decrease contraction amplitude on the distal stomach by [6]-gingerol at $1.59 \times 10^{-5} \text{M}$. The tone and the contraction amplitude of the duodenum did decrease significantly, after the addition of $1.59 \times 10^{-5} \text{M}$ of [6]-gingerol. The frequency of contraction for the distal stomach and duodenum did not change after the application of [6]-gingerol.

4.3.9 The effect of [6]-gingerol at $1 \times 10^{-4} \text{M}$ on the upper GI tract

As the concentration of [6]-gingerol in ginger juice did not cause a significant effect on all of the tissues, a higher concentration of [6]-gingerol [$1 \times 10^{-4} \text{M}$] was investigated.

4.3.9.1 The effect of [6]-gingerol [$1 \times 10^{-4} \text{M}$] on the proximal stomach

The basal tone of the vehicle group from the proximal stomach was statistically lower than the tone of the [6]-gingerol $1 \times 10^{-4} \text{M}$ group ($p < 0.0053$) and therefore it was not valid to compare them. There was a trend for an increase in tone of the proximal stomach due to [6]-gingerol at $1 \times 10^{-4} \text{M}$. The contraction amplitude was significantly increased from 2-3 minutes ($p < 0.0357$) until 24-25 minutes ($p < 0.0038$) after the addition of [6]-gingerol $1 \times 10^{-4} \text{M}$.

4.3.9.2 The effect of [6]-gingerol at $1 \times 10^{-4} \text{M}$ on the distal stomach

The “high” concentration of $1 \times 10^{-4} \text{M}$ [6]-gingerol caused a significant increase in tone at 8-9 minutes ($p < 0.0291$) and lasted until 24-25 minutes ($p < 0.0001$). It also caused a significant decrease in contraction amplitude when compared to the baseline. This decrease became significant at 6-7 minutes ($p < 0.0480$) until 24-25 minutes, as shown in Figure 86B. There was no significant effect on the number of contractions of the distal stomach.

PROXIMAL STOMACH

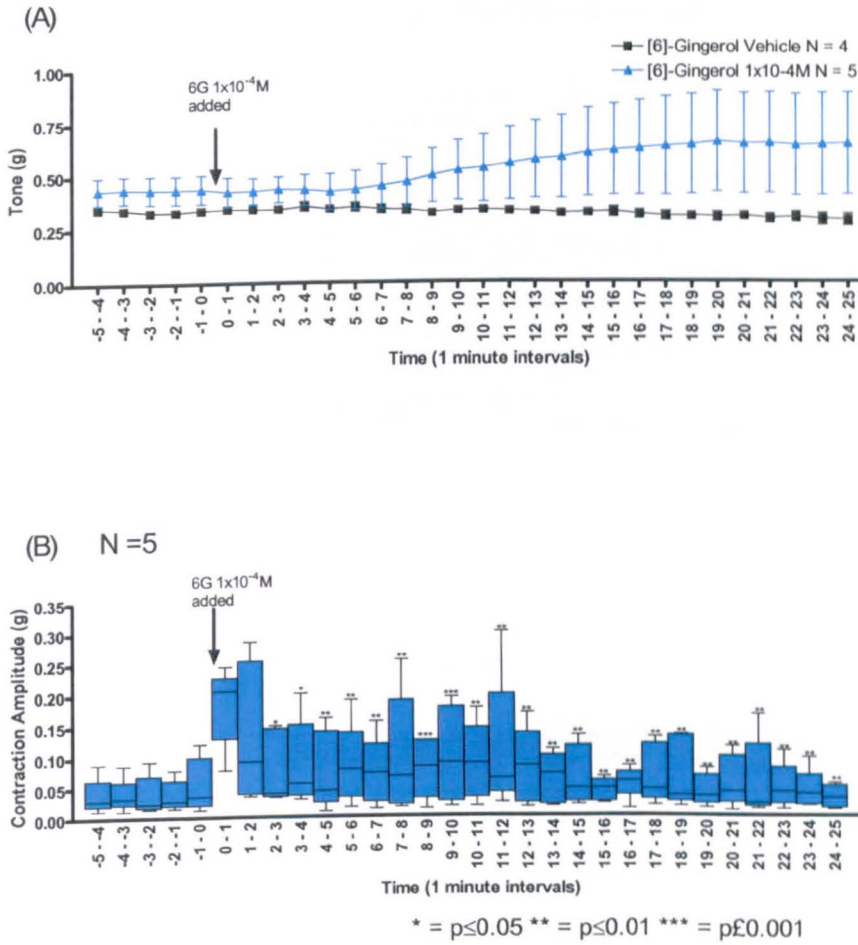


Figure 85. (A) Line graph displaying the proximal stomach tone after the addition of [6]-gingerol ($1 \times 10^{-4} \text{M}$) and the Krebs' control, (B) a box and whisker plot displaying the proximal stomach contraction amplitude after the addition of [6]-gingerol. The results for (A) are expressed as mean \pm SEM, and the results for (B) are expressed as the median with the interquartile range. N = The number of tissues from each region and is shown above in the respective graph. * = $p \leq 0.05$ ** = $p \leq 0.01$ *** = $p \leq 0.001$

DISTAL STOMACH

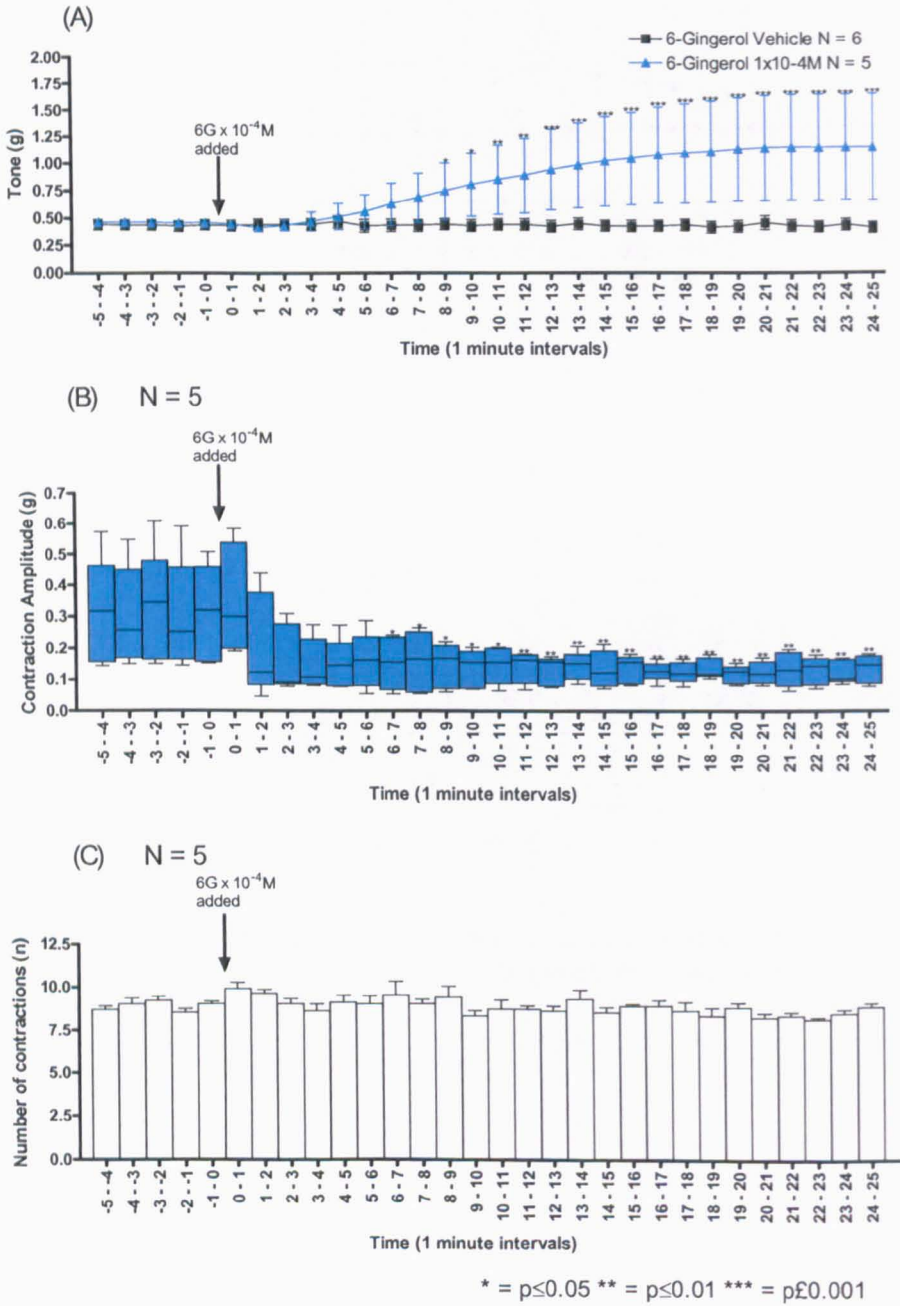


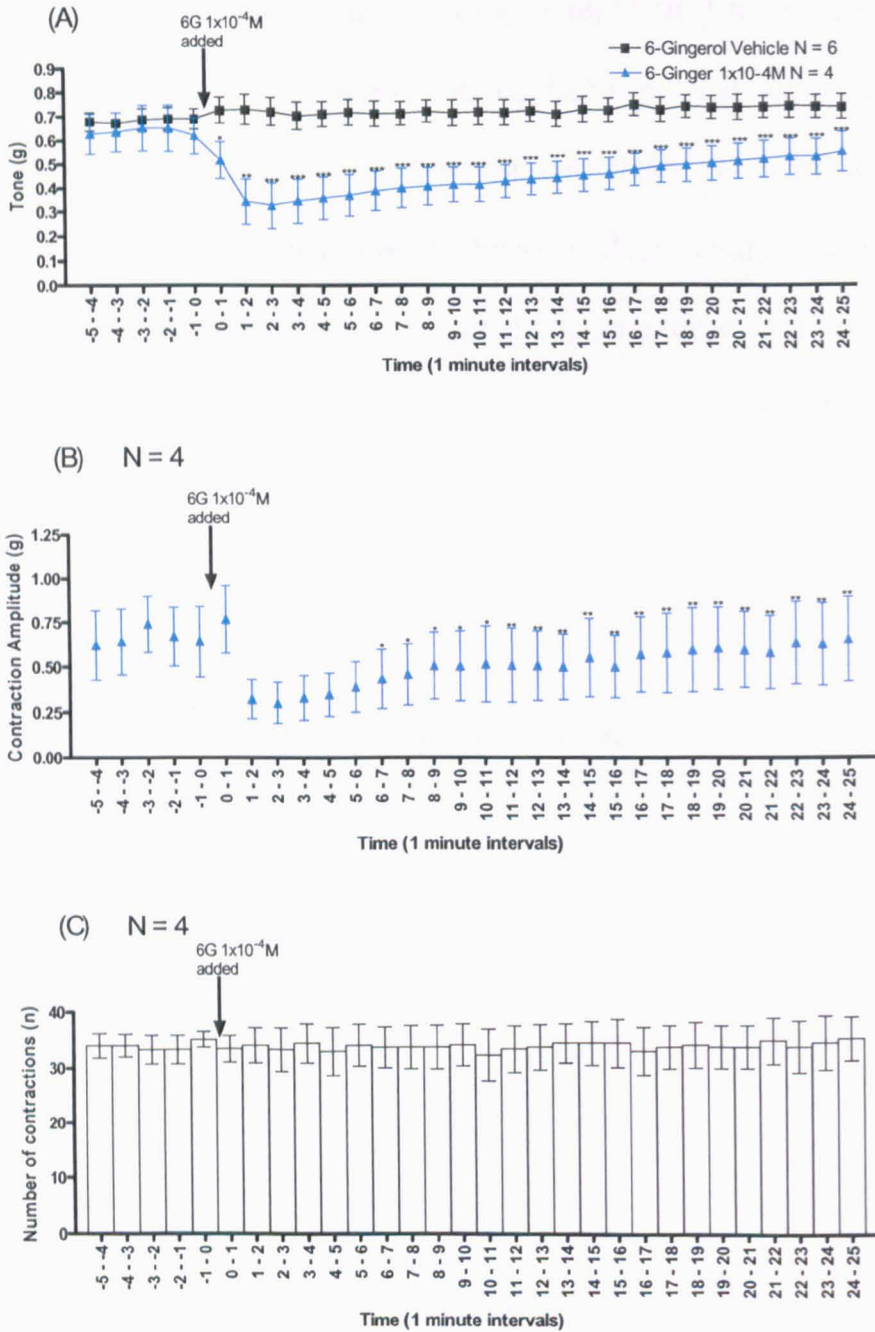
Figure 86. (A) A line graph displaying the tone of the distal stomach before and after addition of [6]-gingerol or [6]-gingerol vehicle. (B) A box and whisker plot of the contraction amplitude of the distal stomach after the addition of [6]-gingerol. (C) A histogram displaying the frequency of contractions pre and post application of [6]-gingerol. The results for (A,C) are expressed as mean ± SEM, and the results for (B) are expressed as the median with the interquartile range. N = The number of tissues from each region and is shown above in the respective graphs.

* = p ≤ 0.05 ** = p ≤ 0.01 *** = p ≤ 0.001

4.3.9.3 The effect of [6]-gingerol at 1×10^{-4} M on the duodenum

The “high” concentration of 1×10^{-4} M [6]-gingerol caused a significant decrease in tone and contraction amplitude, but had no effect on the frequency of contractions of the duodenum (Figure 87A-C). There was a significant decrease in tone at 0-1 minutes ($p < 0.0418$) until 24-25 minutes of exposure ($p < 0.0001$). There was a significant decrease in contraction amplitude from 6-7 minutes ($p < 0.0480$) until 24-25 minutes ($p < 0.0038$) after [6]-gingerol at 1×10^{-4} M was applied to the tissues.

DUODENUM



* = p<0.05 ** = p<0.01 *** = p<0.001

Figure 87. (A) Line graph displaying the duodenal tone after the addition of [6]-gingerol ($1 \times 10^{-4} \text{M}$) and the vehicle, (B) a graph displaying the duodenal contraction amplitude after the addition of [6]-gingerol ($1 \times 10^{-4} \text{M}$), (C) a histogram displaying the frequency of contractions of the duodenum after the addition of [6]-gingerol ($1 \times 10^{-4} \text{M}$). The results are expressed as mean \pm SEM. N = The number of tissues from each region and is shown above in the respective graph. * = p \leq 0.05 ** = p \leq 0.01 *** = p \leq 0.001

4.3.9.4 Summary of the effects of [6]-gingerol at $1 \times 10^{-4} \text{M}$ on the upper gastrointestinal tract

[6]-gingerol at $1 \times 10^{-4} \text{M}$ caused a significant effect on the tone and amplitude of all of the tissues. There was an increase in tone in the proximal and distal stomach, whilst there was a decrease in tone in the duodenum. There was an increase in contraction amplitude in the proximal stomach and a decrease in contraction amplitude of the distal stomach and duodenum after exposure to [6]-gingerol $1 \times 10^{-4} \text{M}$. The frequency of contractions for the proximal and distal stomach and the duodenum were not affected by the addition of [6]-gingerol $1 \times 10^{-4} \text{M}$.

No effect of [6]-gingerol could be analysed on tone of the proximal stomach for both $1 \times 10^{-4} \text{M}$ and $1.59 \times 10^{-5} \text{M}$, but qualitatively there is a trend for an increase in tone to increase at the higher concentration of [6]-gingerol which is not present at the lower concentration. The contraction amplitude of the proximal stomach increased at both concentrations, but was prolonged at the higher concentration of [6]-gingerol $1 \times 10^{-4} \text{M}$.

[6]-gingerol at the concentration found in ginger juice, $1.59 \times 10^{-5} \text{M}$, caused an increase in tone and a decrease in contraction amplitude. This was mimicked by the higher concentration of [6]-gingerol and amplified. There was no effect on the frequency of contractions of the distal stomach with either concentration of [6]-gingerol.

There was a significant decrease in tone and contraction amplitude of the duodenum when either concentration of [6]-gingerol was added to the tissue bath. [6]-gingerol at $1 \times 10^{-4} \text{M}$ appears to amplify the responses of [6]-gingerol $1.59 \times 10^{-5} \text{M}$. There was no effect on the frequency of contractions of the duodenum with either concentration of [6]-gingerol.

4.3.10 The effect of the “faux” ginger juice on the upper GI tract

The concentration of [6]-gingerol $1.59 \times 10^{-5} \text{M}$ (equivalent to 200 μL) was combined with five elements found in ginger juice with a “high” concentration: potassium; magnesium; manganese; sodium; and calcium and the resulting “faux” ginger juice was applied to the three areas studied of the upper gastrointestinal tract.

4.3.10.1 The effect of “faux” ginger juice on the proximal stomach

The effect of the combination of elements and the [6]-gingerol concentration equivalent to 200 μL ginger juice was examined on the proximal stomach. When compared to the vehicle there was a significant increase in tone and contraction amplitude. The tone increased significantly from 10-11 minutes ($p < 0.0391$) until 24-25 minutes ($p < 0.0001$). The contraction amplitude changed significantly from 2-3 minutes ($p < 0.0357$) until the final measurement at 24-25 minutes ($p < 0.0261$). There was an initial increase in contraction amplitude, which then decreased; but not below the baseline.

4.3.10.2 The effect of “faux” ginger juice on the distal stomach

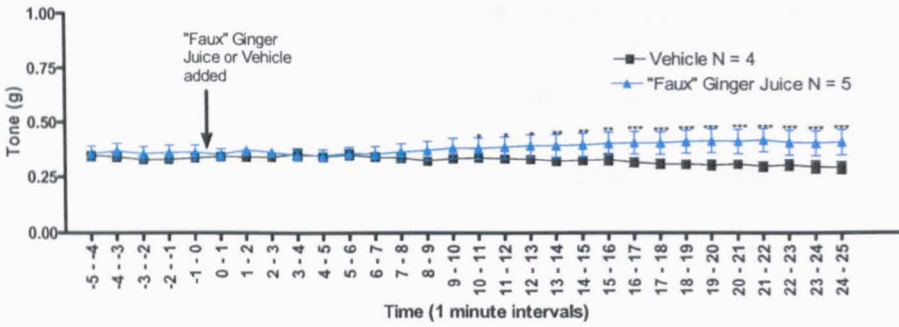
There were no significant differences in tone or frequency of contractions of the distal stomach after the combination of elements and [6]-gingerol were applied (Figure 89A,C). There was a significant decrease in contraction amplitude from 5-6 minutes ($p < 0.0203$) and an increase in significance at 8-9 minutes which continued until the final measurement at 24-25 minutes ($p < 0.0015$).

4.3.10.3 The effect of “faux” ginger juice on the duodenum

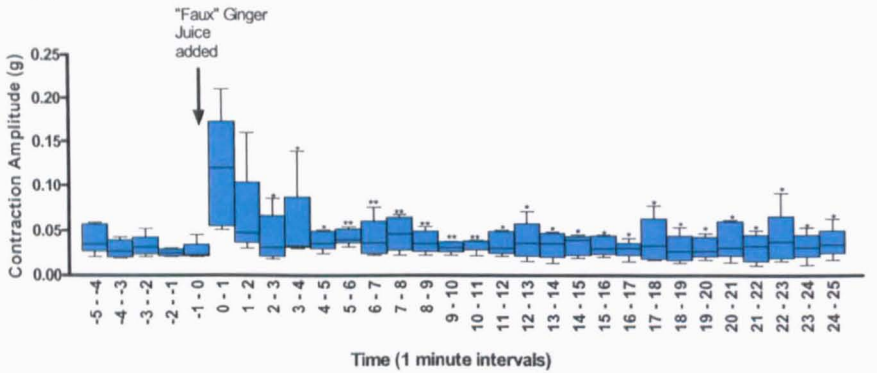
There was a highly significant decrease in tone of the duodenum after the “faux” ginger juice was added from 0.5-1 minutes continuing for the entirety of the analysis ($p < 0.0009$), see Figure 90. There was also a decrease in contraction amplitude from 3-4 minutes until 24-25 minutes ($p < 0.0001$). There was a significant decrease on the frequency of contractions of the duodenum after 22-23 minutes exposure to the “faux” ginger juice as shown in Figure 91.

PROXIMAL STOMACH

(A)



(B) N = 5



* = $p \leq 0.05$ ** = $p \leq 0.01$ *** = $p \leq 0.001$

Figure 88. (A) Line graph displaying the proximal stomach tone after the addition of the “faux” ginger juice and the Krebs’ control, (B) a box and whisker plot displaying the proximal stomach contraction amplitude after the addition of the “faux” ginger juice. The results for (A) are expressed as mean \pm SEM, whereas the results for (B) are expressed as the median with the interquartile range. N = The number of tissues from each region and is shown above in the respective graph. * = $p \leq 0.05$ ** = $p \leq 0.01$ *** = $p \leq 0.001$

DISTAL STOMACH

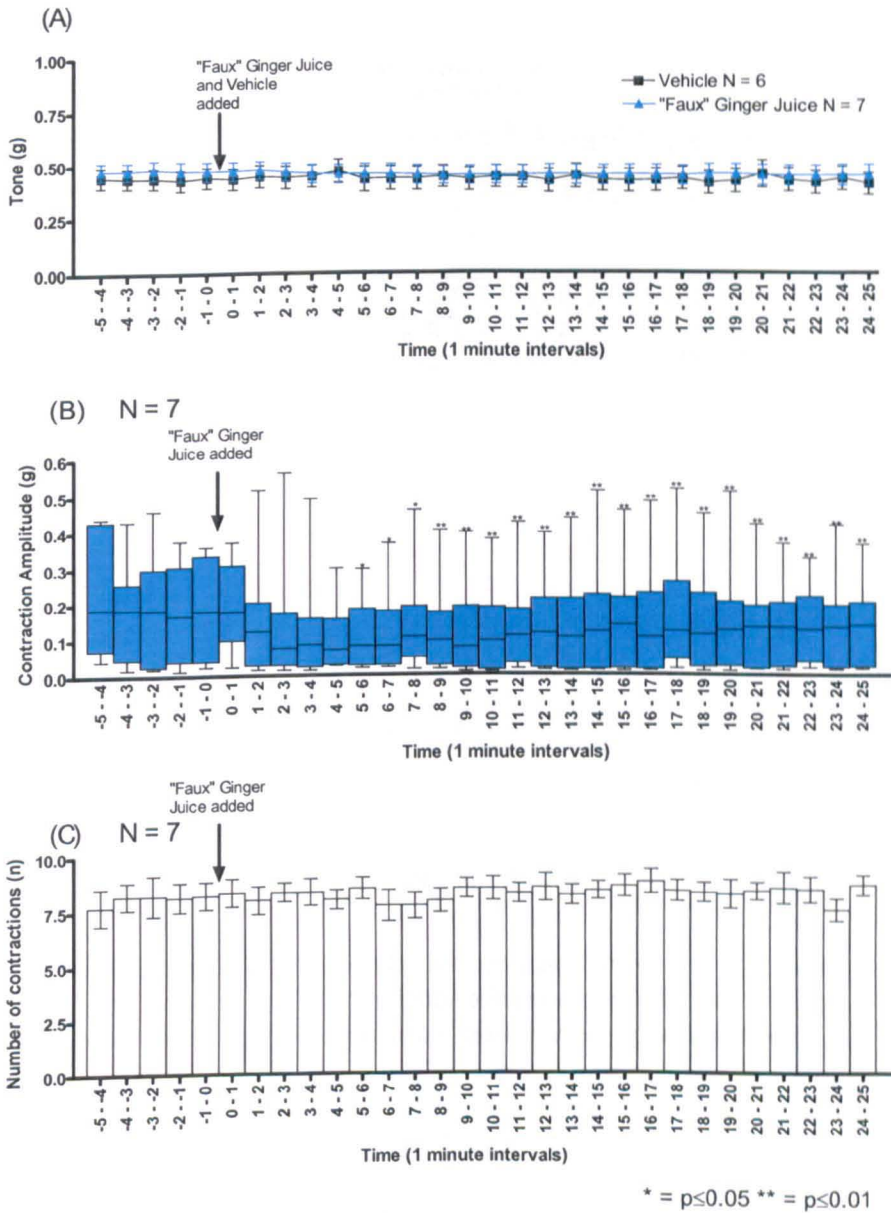
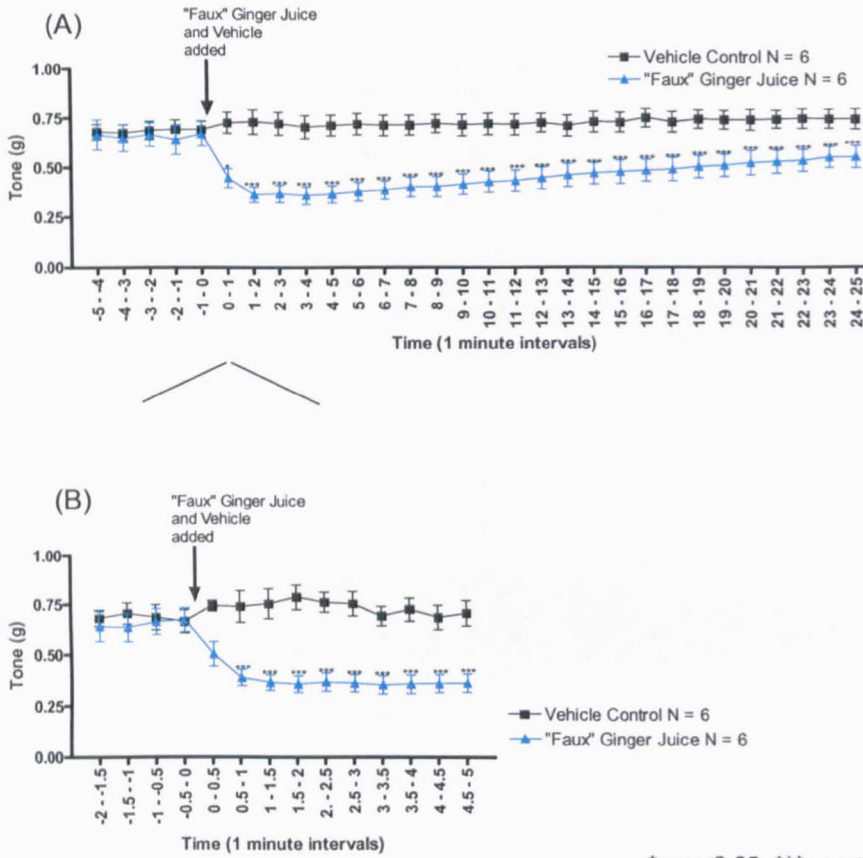


Figure 89. (A) A line graph displaying the tone of the distal stomach before and after addition of “faux” ginger juice and the vehicle. (B) A box and whisker plot of the contraction amplitude of the distal stomach after the addition of “faux” ginger juice. (C) A histogram displaying the frequency of contractions pre and post application of “faux” ginger juice. The results for (A,C) are expressed as mean \pm SEM, whereas the results for (B) are expressed as the median with the interquartile range. N = The number of tissues from each region and is shown above in the respective graphs. * = $p \leq 0.05$ ** = $p \leq 0.01$

DUODENUM



* = $p \leq 0.05$ *** = $p \leq 0.001$

Figure 90. Line graphs (A) displaying the duodenal tone after the addition of "faux" ginger juice and the vehicle, (B) displaying a close up of the duodenal tone after the addition "faux" ginger juice. The results are expressed as mean \pm SEM. N = The number of tissues from each region and is shown above in the respective graph.

* = $p \leq 0.05$ ** = $p \leq 0.01$ *** = $p \leq 0.001$

DUODENUM

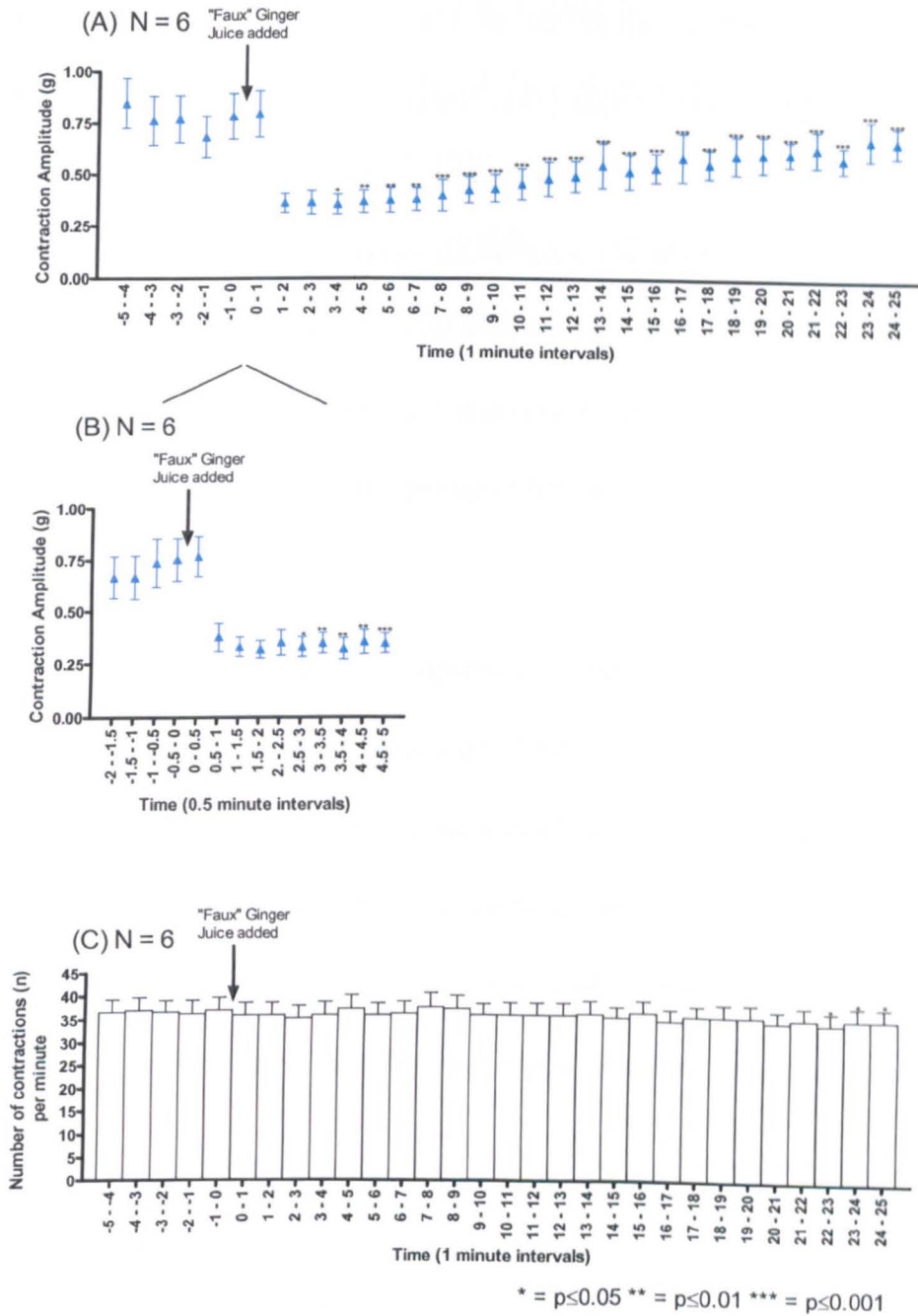


Figure 91. Graphs (A) displaying the duodenal contraction amplitude after the addition of "faux" ginger juice, (B) displaying a close up of the duodenal contraction amplitude after the addition "faux" ginger juice. (C) A histogram displaying the frequency of contractions of the duodenum after the addition of "faux" ginger juice. The results are expressed as mean ± SEM. N = The number of tissues from each region and is shown above in the respective graph.

* = p ≤ 0.05 ** = p ≤ 0.01 *** = p ≤ 0.001

4.3.10.4 Summary of the effect of “faux” ginger juice on the upper GI tract

The tone and the contraction amplitude of the proximal stomach statistically increased after the addition of the “faux” ginger juice. The combination of elements and [6]-gingerol (1.59×10^{-5}) did not affect the distal stomach tone, although there was a significant decrease of contraction amplitude. There was a significant decrease in tone and contraction amplitude of the duodenum after the “faux” ginger juice was applied. There was a significant decrease in frequency of contractions of the duodenum from 22-25 minutes of exposure to the “faux” ginger juice. There was no effect on the frequency of contraction on the proximal and distal stomach.

There was no effect on the proximal stomach tone when either [6]-gingerol 1.59×10^{-5} M or the elements were applied to the tissues individually; however there was a significant maintenance of tone when the “faux” juice was added when compared to the [6]-gingerol vehicle which decreased. There was no effect on the proximal stomach contraction amplitude when the elements were added; however there was a significant increase when [6]-gingerol or the “faux” juice was added although this could be in part due to the vehicle (Figure 49).

Separately, the elements and [6]-gingerol (1.59×10^{-5} M) caused a significant increase in tone in the distal stomach; however the “faux” ginger juice did not increase the tone. The element solution and [6]-gingerol (1.59×10^{-5} M) both individually and combined caused a decrease in the contraction amplitude of the distal stomach. The element solution caused a decrease in the frequency of contractions of the distal stomach but when combined with [6]-gingerol there was no significant effect.

The duodenal tone decreased when exposed to [6]-gingerol ($1.59 \times 10^{-5} \text{M}$) and the element solution individually and the combined solution also significantly decreased the tone. The contraction amplitude of the duodenum also decreased when [6]-gingerol ($1.59 \times 10^{-5} \text{M}$) and the element solution were individually applied and this effect was mimicked by the addition of the "faux" juice. The element solution caused a decrease in the frequency of contractions of the duodenum but when combined with [6]-gingerol there was no significant effect.

4.4 Discussion

Overall this study has investigated the effect of ginger juice and a selection of ginger juice constituents on the upper gastrointestinal tract of the *Suncus murinus*. There was a differential effect of ginger juice on the stomach and duodenum. The element solution, the [6]-gingerol concentrations and the “faux” ginger juice were partially responsible for this effect. Firstly the basal motility of the tissue will be discussed before attempting to examine the effect of ginger juice and the selected constituents and the potential pharmacology behind the effect.

4.4.1 Basal Motility

The spontaneous contractions of the duodenum often began within seconds of the tissue being placed in the tissue bath. The distal stomach was also very reliable, once the tissue had been washed several times and equilibrated. In comparison, the proximal stomach was initially very variable and was easily influenced by the environment, i.e. gas flow/tension.

The area under the curve (AUC) was measured at baseline for all tissues. The AUC measurements replicated the tonal measurements. Hence, only the tonal measurement was used to describe the basal activity of the upper GI tract, as it was felt that the AUC measurements would only duplicate information and would not impart any new data.

The duodenum had the highest contraction amplitude out of the three areas of the GI tract. As mentioned in the methods the duodenum displayed sine wave-like contractions, therefore the contraction appears to originate from the centre of the wave (Figure 42C). This is unlike the proximal and distal stomach which had non-sinusoidal waveforms. In particular

the contraction amplitude for the distal stomach began at the base of the wave and proceeded upwards (Figure 42B). The proximal stomach baseline contractions were far more tonal than amplitude based. The proximal stomach had the lowest contraction amplitude.

The tone for the proximal stomach and the distal stomach was measured differently to the duodenum due to the non-sinusoidal waveforms and therefore they cannot be compared directly to the duodenum. The proximal stomach had a lower baseline tone and was often more variable when compared to the distal stomach.

The frequencies of contractions were not very well defined for the proximal stomach, when compared to the distal stomach or duodenum. The baseline frequency of contraction for the distal stomach and duodenum were very constant; however the longitudinal duodenal segments had over four times as many contractions per minute when compared to the distal stomach (Figure 43).

The mean baseline contraction amplitude was plotted against the corresponding resting tones for the proximal and distal stomach and duodenum (Figure 46). As observed in the scatter graphs, the magnitude of the resting tone did not define the contraction amplitude. Therefore, the tone and the contraction amplitude were independent of each other, as were the contraction amplitude and frequency of contraction (Figure 47).

The tissues were exposed to the 200 μ L of Krebs' solution and measured for 25 minutes post injection. This was effectively a time and a volume control. There was no effect of time or volume on the three areas of the upper GI tract (Figure 48). This indicated that the effect of ginger juice on the tissues was not due to either time or volume.

In unpublished data by Dr Percie du Sert (Personal Correspondence, 2009) the *S. murinus* basal activity were compared to this report. The median contraction amplitudes of the proximal (0.07 g) and distal stomach (0.15 g) were lower in this report when compared to the mean \pm SEM contraction amplitudes of the unpublished data, at $0.10 \text{ g} \pm 0.02$ (N=24) and $0.24 \text{ g} \pm 0.30 \text{ g}$ (N=24). The distal stomach mean frequency of contractions per minute was also very similar at 8.98 ± 0.53 in this report and 8.77 ± 0.27 in the unpublished data, whilst the frequency of contractions was unreported for the proximal stomach. The tone, contraction amplitude and frequency of contractions per minute of the duodenum in this report was $0.62 \text{ g} \pm 0.02 \text{ g}$, $0.64 \text{ g} \pm 0.03 \text{ g}$, and 35.65 ± 0.44 , respectively and in the unpublished data $0.63 \text{ g} \pm 0.04 \text{ g}$, $0.68 \text{ g} \pm 0.06\text{g}$, and 35.25 ± 0.54 , respectively.

4.4.2 Volume related ginger juice effects

The fresh juice of ginger has only been used once before in a study, which investigated the effect of ginger on gastric emptying in rats *in vivo* (Sharma & Gupta, 1998). The ginger juice (4 mL/kg) prevented a gastric emptying delay in rats initiated by cisplatin, and was superior to the 5-HT₃ receptor antagonist, ondansetron (3 mg/kg). Ginger capsules have also been shown to increase gastric half-emptying times in humans (Wu, *et al.*, 2008). This increase in gastric half-emptying time after ginger, may be due to the ginger interacting with the upper GI tract, or possibly due to gingerols acting upon the area-postrema (Qian, *et al.*, 2009).

When the ginger juice was added, two populations of effect were prevalent on each of the upper GI tract tissues. Population X had an overall increase in AUC, whilst the AUC of population Y decreased or did not change. There was an indication that the lower the tone of

either proximal or distal stomach tissue, the more likely that the effect would belong to population X. However not all of the results followed this pattern (Table 24 and Table 25).

The “high” volume of ginger juice (200 μL) caused an immediate contractile response on the proximal stomach, whilst there was a slow contractile response on the distal stomach. In comparison the “low” volume of ginger juice (50 μL) caused a slow contractile response in both regions of the stomach. The “low” volume of ginger juice must have been below the threshold to cause an initial increase in tone after the “high” volume on the proximal stomach. The effects of a “high” volume on the proximal stomach contraction amplitude appear to replicate the effects of a “low” volume, though the effects are larger. The “high” volume of ginger juice caused a similar immediate effect to the “low” volume of ginger juice (50 μL) on the duodenum, where there was a relaxation response. Therefore there is a dual effect on the upper gastrointestinal tract, a spasmogenic response on the stomach and a spasmolytic response on the intestine. Other plant extracts and isolated compounds including: quercetin; diplotropin from *Diplotropis ferruginea*; extracts from *Casimiroa tetrameria*; isoliquiritigenin from *Glycyrrhiza glabra* (licorice) and extracts from *Tanacetum artemisioides*, have been identified as causing a spasmolytic effect on the intestine and on occasion causing a spasmogenic effect on the stomach (Bukhari, *et al.*, 2007; Chen, *et al.*, 2009; Di Carlo, *et al.*, 1993; García, *et al.*, 1997; Ghayur, *et al.*, 2007a; Gilani, *et al.*, 2007; Heinrich, *et al.*, 2005; Lima, *et al.*, 2005; Morales, *et al.*, 1994; Sadraei, *et al.*, 2003).

The distal stomach appeared to be an intermediary tissue, which exhibited similar aspects of the proximal stomach and duodenum, but however did not demonstrate the effects of ginger to the same extent. It appears that after the exposure to ginger, on all four

variations of volumes, the frequency of contractions of the distal stomach increased initially. This is very important, as the study by Wu, *et al.*, (2008) found that the antral contractions from the human volunteers following a soup meal after ginger significantly increased from 5-10 minutes until 90-95 minutes after the meal. The increase in antral contractions in humans correlates with the increase in the distal stomach contractions found after exposure to ginger juice, although this increase rarely lasted for the entire exposure.

There were different responses on the parameters of the tissues after ginger juice was applied and here are examples on the different tissues. After a “high” volume of ginger juice on the proximal stomach the tone increased in tension immediately and was sustained throughout, whilst the contraction amplitude increased and decreased in the first 10 minutes and the frequency of contractions per minute did not change (Table 24).

There were also three different responses in the distal stomach data in the latter measurements of the “low” volume of ginger juice. There was an increase in tension at 23-25 minutes whilst there was a decrease of contraction amplitude from 16-25 minutes and no effect on the frequency of contraction per minute in this time range (Table 25).

There are repeated examples of where the data are uncoupled within the duodenal data, when investigating the effects of ginger juice (Figure 58; Figure 64; Figure 71; Figure 72; and Figure 78). The effect of ginger juice on the duodenum was repeatable, with the few exceptions of an increase in tone in Figure 63 and Figure 73. There was a consistent decrease in tone coupled with a consistent decrease in contraction amplitude, whilst the frequency of contraction remained constant. The same detailed effect of ginger juice on the duodenum

was repeated time and again. This repeated uncoupling of the data also indicated an internal consistency.

After the effect of a single volume of ginger juice on the upper GI tract was investigated a second volume (50 μL or 200 μL) was applied. This was to identify if the first volume interfered with the second volume. It appeared the first volume did not change the overall effect of the second volume of ginger juice on the proximal and distal stomach and the duodenum. This includes when the second volume was a "high" 200 μL volume. The "high" volume effects on the proximal and distal stomach and duodenum were recognised after the first 50 μL volume of ginger juice was applied to the tissue bath. There was a decrease in significance for the second volume of ginger juice (50 μL or 200 μL volume); however this was due to the first volume changing the baseline of the second volume (i.e. an increase or decrease in tone and/or contraction amplitude). These results suggest that the receptors/pathways were not blocked by any component within the ginger juice, and the tissues were not desensitised.

As the tissues were not desensitised to the ginger juice it suggests that the active constituents in ginger were not acting due to vanilloids nor through vanilloid receptors as capsaicin and RTX, both potent vanilloids, cause desensitisation of the tissues (Someya, *et al.*, 2003). Interestingly, an *in vitro* study in 1989, by Holzer-Petsche, *et al.*, found that capsaicin led to either a relaxation or contraction on circular strips of gastric smooth muscle from the rat; however in some strips it caused a biphasic effect. Predominantly 5 μM of capsaicin caused a relaxation of the tissue, whilst 500 nM of capsaicin largely caused a contraction of

the tissue. This biphasic effect was similar to the effect observed with ginger juice on both areas of the stomach.

Overall, a “high” volume of ginger juice caused the proximal and distal stomach to become increased in tension (stretched), whilst the duodenum became very flaccid due to the exposure to a “high” volume of ginger juice. In Chapter 2, the elements and [6]-gingerol concentration was determined and other peaks in ginger juice on the HPLC were noted. [6]-Gingerol and the elements may have contributed to these varied effects on the upper GI tract. For this reason, [6]-gingerol and the elements in ginger juice were applied to the tissues, separately and combined.

Table 24. A summary of the effects of the test substances on the proximal stomach; tone, contraction amplitude and frequency of contractions.

Test substance	Tone	Tone of Population X and Y	Contraction Amplitude	Frequency of Contractions	Figure #
Krebs' control	NS	-	NS	NS	Figure 48A,B,G
Vehicle control	NS	-	NS	NS	Figure 49A,B,G
DRC	↑9-20 mins *	-	↑ 2-20 mins *	NS	Figure 50
"Low" volume of GJ	NS	∫ 10-25 mins	NS	NS	Figure 54
"Low" volume of GJ – "Low" volume of GJ	↑14-25 mins * ↑ 32-55 mins *	X significantly lower than Y (Baselines)	↑ 2-25 mins * ↑ 32-48 mins *	NS	Figure 60
"High" volume of GJ	↑ 1.5-25 mins #	∫ 2-25 mins	∫ 1-10 mins *	NS	Figure 66 and Figure 67
"Low" volume of GJ – "High" volume of GJ	- ↑ 31-55 mins *	X N = 3	↓ 17-25 mins * ↑ 31-35 mins *	- ↑ 31-38 mins *	Figure 74
Element solution	NS	-	NS	NS	Figure 79
[6]-gingerol 1.59x10-5M	↓ 17-25 mins #	-	↑ 6-25 mins *	↑ 1-25 mins *	Figure 82
[6]-gingerol 1x10-4M	↑ 15-25 mins #	-	↑ 2-25 mins *	NS	Figure 85
"Faux" ginger juice	↑ 10-25 mins #	-	↑ 2-25 mins *	NS	Figure 88

NS = Non-significant; ↓Significant decrease; ↑ Significant increase; ∫ Significant transient effect

= compared to relevant control * = compared to baselines

Table 25. A summary of the effects of the test substances on the distal stomach; tone, contraction amplitude and frequency of contractions.

Test substance	Tone	Tone of Population X and Y	Contraction Amplitude	Frequency of Contractions	Figure #
Krebs' control	NS	-	NS	NS	Figure 48C,D,H
Vehicle control	NS	-	NS	NS	Figure 49C,D,H
DRC	↑ 18-20 mins *	-	NS	NS	Figure 51
"Low" volume of GJ	↓ 5-9 mins # ↑ 23-25 mins #	∫ 2-7 mins ∫ 10-25 mins	↓ 16-25 mins *	↑ 1-7 mins *	Figure 56
"Low" volume of GJ – "Low" volume of GJ	↓ 1-9 mins * ↓ 31-41 mins *	X is significantly lower than Y (baselines)	↑ 2-3 mins * ↓ 21-25 mins * ↓ 45-55 mins *	↑ 1-2 mins * ↓ 47-55 mins *	Figure 62
"High" volume of GJ	↑ 18-25 mins *	X is significantly lower than Y (baselines)	↓ 8-25 mins *	↑ 1-10 mins *	Figure 69
"Low" volume of GJ – "High" volume of GJ	↓ 1-10 mins # ↓ 31-40 mins #	X N = 3	↓ 14-25 mins * ↑ 31-32 mins * ↓ 41-55 mins *	↑ 1-25 mins * ↑ 31-38 mins *	Figure 76
Element solution	∫ 1-25 mins *	-	↓ 6-25 mins *	↓ 10-25 mins *	Figure 80
[6]-gingerol 1.59x10-5M	↑ 12-25 mins *	-	↓ 6-25 mins *	NS	Figure 83
[6]-gingerol 1x10-4M	↑ 8-25 mins *	-	↓ 6-25 mins *	NS	Figure 86
"Faux" ginger juice	NS	-	↓ 5-25 mins *	NS	Figure 89

NS = Non-significant; ↓ Significant decrease; ↑ Significant increase; ∫ Significant transient effect

= compared to relevant control * = compared to baselines

Table 26. A summary of the effects of the test substances on the duodenum; tone, contraction amplitude and frequency of contractions.

Test substance	Tone	Tone of Population X and Y	Contraction Amplitude	Frequency of Contractions	Figure #
Krebs' control	NS	-	NS	NS	Figure 48E,F,I
Vehicle control	↑ 2-25 mins #	-	NS	NS	Figure 49E,F,I
DRC	↓ 7-25 mins #	-	↓ 5-25 mins *	NS	Figure 52
"Low" volume of GJ	↓ 2-25 mins #	X N = 2	↓ 2-25 mins *	↑ 6-25 mins *	Figure 58
"Low" volume of GJ – "Low" volume of GJ	↓ 1-25 mins * ↓ 31-55 mins *	X N = 1	↓ 3-25 mins * ↓ 33-55 mins *	↑ 6-25 mins * ↓ 48-55 mins *	Figure 64
"High" volume of GJ	↓ 3-25 mins #	-	↓ 2-25 mins *	↓ 4-25 mins *	Figure 71 and Figure 72
"Low" volume of GJ – "High" volume of GJ	↓ 1-25 mins * ↓ 31-55 mins *	-	↓ 2-25 mins * ↓ 33-55 mins *	↑ 4-25 mins * ∫ 32-35 mins *	Figure 78
Element solution	↓ 1-25 mins #	-	↓ 1-25 mins *	↓ 3-25 mins *	Figure 81
[6]-gingerol 1.59x10- 5M	↓ 3-25 mins #	-	↓ 2-25 mins *	NS	Figure 84
[6]-gingerol 1x10-4M	↓ 0-25 mins #	-	↓ 6-25 mins *	NS	Figure 87
"Faux" ginger juice	↓ 0.5-25 mins #	-	↓ 3-25 mins *	↓ 22-25 mins *	Figure 90 and Figure 91

NS = Non-significant; ↓ Significant decrease; ↑ Significant increase; ∫ Significant transient effect

= compared to relevant control * = compared to baselines

4.4.3 Were the elements in the ginger juice responsible for the effect of ginger juice?

There was no effect of the element solution on the tone, contraction amplitude and frequency of contraction from the proximal stomach (Figure 92A). The element solution caused a transient effect on the tone and a decrease in contraction amplitude and frequency of contractions on the distal stomach. Put simply, this is very similar to the effect of ginger juice on the distal stomach; however with the reduction in frequency it appears that there may be another constituent missing and the element solution is not wholly responsible for the effects. The duodenum tone and contraction amplitude decreased similarly to ginger juice after the element solution was added, although not to the same magnitude and it also reduced the frequency of contractions.

A selected sample of the ginger samples used in these studies (N=10) was analysed by ICP-AES for the concentrations of elements. There was no correlation between the effect on the upper gastrointestinal tract and the concentration of the elements (data not shown).

When comparing the effect of the element solution to the effect of the 200 μ L volume of ginger juice on the duodenal parameters after 5 minutes, the elements are responsible for ~40% of the drop in tone and ~60% of the drop in contraction amplitude. However, after 25 minutes the element solution was only responsible for ~20% of the decrease in tone and ~10% in the decrease of contraction amplitude demonstrating that other constituents do contribute to the effect. This indicates that the elements do play a role in the effect of ginger juice on the duodenum and may explain in part the effect of ginger juice.

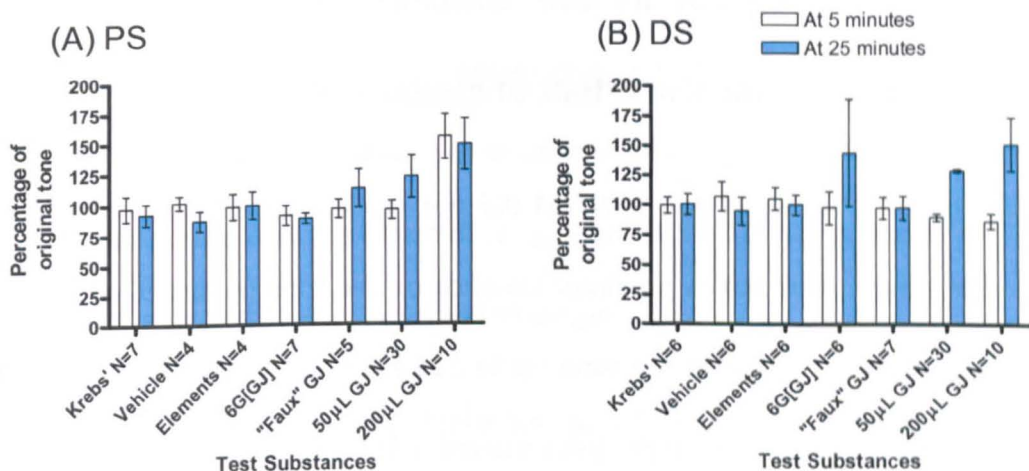


Figure 92. The effect of the test substances on the percentage of the original tone at 5 and 25 minutes on the (A) proximal stomach and (B) distal stomach. N = The number of tissues from each region and is shown above in the respective graph. PS = Proximal stomach; DS = Distal stomach

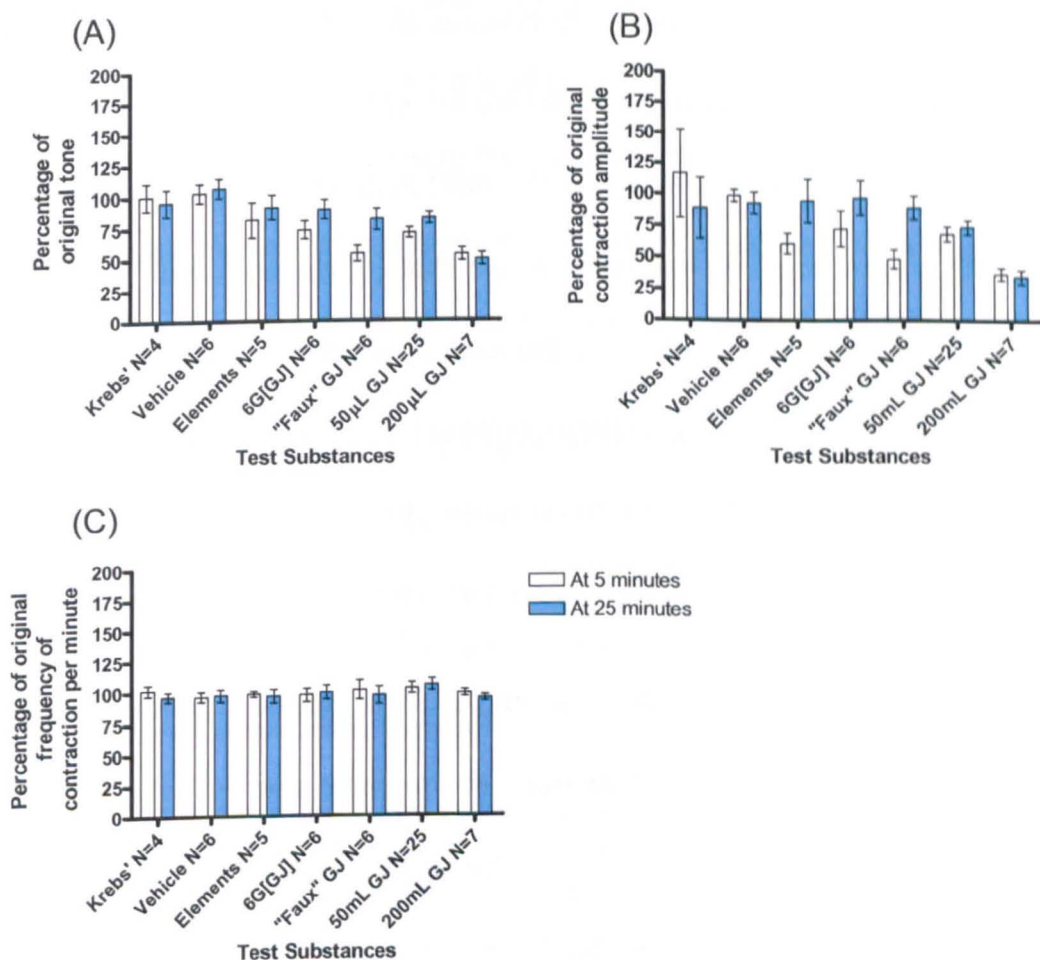


Figure 93. The effect of the test substances on the percentage of the original duodenal parameters at 5 and 25 minutes (A) tone (B) contraction amplitude and (C) frequency of contractions per minute. N = The number of tissues from each region and is shown above in the respective graph.

4.4.4 Was [6]-gingerol at the concentration of ginger juice responsible for the effect of ginger juice?

[6]-gingerol at $1.59 \times 10^{-5} \text{M}$ and $1 \times 10^{-4} \text{M}$ did not replicate the effects of a “high” 200 μL volume of ginger juice on the proximal stomach on the tone (Figure 92A). The 200 μL solution of ginger juice increased the tone up to $155.2\% \pm 18.8\%$ at 5 minutes, whilst [6]-gingerol at the concentration in ginger juice caused a decrease in tone at 5 minutes by $\sim 10\%$, which was maintained for 25 minutes. There was no increase in tone above the original baseline at 5 and 25 minutes after [6]-gingerol at $1.59 \times 10^{-5} \text{M}$ was added, although there was an increase in tone at 25 minutes after [6]-gingerol at $1 \times 10^{-4} \text{M}$ was added ($149.3\% \pm 19.0\%$). [6]-gingerol (10-1000 μM) has been shown to have spasmolytic activity in the rat stomach fundus on high K^+ (80 mM) induced contractions (Ghayur, *et al.*, 2008). In the current study it has been shown that [6]-gingerol $1 \times 10^{-4} \text{M}$ caused a spasmogenic effect on the *Suncus* proximal stomach spontaneous contraction with an increase in tone together with an increase followed by a decrease in contraction amplitude, indicating a species difference in response. However, it should be noted that these were different types of contraction: spontaneous and K^+ induced.

The effect of [6]-gingerol at $1.59 \times 10^{-5} \text{M}$ and $1 \times 10^{-4} \text{M}$ caused significant increases in tone, and reductions in contraction amplitude of the distal stomach which was very similar to the 50 μL and 200 μL volume of ginger juice. [6]-Gingerol at $1.59 \times 10^{-5} \text{M}$ alone did not fully explain the effects of ginger juice at the 200 μL volume on the distal stomach tone; at 5 minutes it was responsible for $\sim 18\%$ of the effect on tone and at 25 minutes it was responsible for $\sim 85\%$ (Figure 92B). There was no effect on the frequency of contractions of the distal stomach by [6]-gingerol. This is important, because if there are

no effects on the frequency of contraction on the distal stomach, it would be difficult to see how [6]-gingerol (if it is the active compound) could increase the frequency of contractions of the antrum of human stomachs (*in vivo*) in the Wu, *et al.*, (2008) study. It has to be reiterated that the effect of [6]-gingerol $1.59 \times 10^{-5} \text{M}$ and $1 \times 10^{-4} \text{M}$ distal stomach tone was long lasting as was the effect of ginger juice.

The duodenal tone only decreased to $72.9\% \pm 7.1\%$ at 5 minutes after the [6]-gingerol at $1.59 \times 10^{-5} \text{M}$ was added, whilst the higher [6]-gingerol concentration decreased the tone to $57.5\% \pm 12.5\%$ (Figure 93A). The decrease in tone by the [6]-gingerol at $1.59 \times 10^{-5} \text{M}$ was responsible for ~57% of the effect of a 200 μL volume of ginger juice at 5 minutes. The effect of a 200 μL volume of ginger juice on the duodenum was very similar to the effect of [6]-gingerol $1.59 \times 10^{-5} \text{M}$; however, the tone and amplitude compared to the ginger juice groups did not recover at 25 minutes compared to [6]-gingerol, as [6]-gingerol only represents ~21% and ~5% of the response at this time (Figure 93A,B).

4.4.5 Did the "faux" ginger juice successfully mimic the effect of ginger juice?

The effect of the "faux" ginger juice on the proximal stomach was similar to a "low" volume of ginger juice. The effect from the "faux" ginger juice did not mimic the 200 μL volume of ginger juice and appeared not only to mimic the 50 μL volume of ginger juice, but to be more effective than the 50 μL volume. The magnitude of the effect of the element solution and [6]-gingerol combined ("faux" juice) ($96.0\% \pm 7.6\%$) on the proximal stomach tone was lower than the individual effects combined ($88.6\% \pm 7.6\%$); therefore the constituents may be interacting. The effect of the "faux" ginger juice on the proximal

stomach tone contributed to ~25% of the effect of the 200 μ L volume of ginger juice at 25 minutes.

There was no effect of the “faux” ginger juice on the distal stomach tone or frequency of contractions although there was a decrease in contraction amplitude due to the “faux” ginger juice. This was not reflected when the elements and [6]-gingerol were analysed separately: even with the both concentrations of [6]-gingerol there was a significant decrease in contraction amplitude and increase in tone. The effect of the elements on the distal stomach appear to inhibit the effect of [6]-gingerol. This could be due to oxidisation of the compounds, as Houghton, *et al.*, (2007) suggests; although this is unlikely viewing the effect of the “faux” ginger juice on the other tissues when the experiments were all performed at a similar time. The “faux” ginger juice did not replicate the effect of a “high” or “low” volume of fresh ginger juice on the distal stomach.

Ginger juice must contain additional constituents to cause the different effects seen on the stomach because the “faux” ginger juice does not fully replicate the effects of a “high” volume of ginger juice. Populations X or Y were not explained by [6]-gingerol at the two concentrations, the elements or the “faux” ginger juice.

The effect of the “faux” ginger juice on the duodenal tone contributed to ~98% of the effect of the 200 μ L volume of ginger juice at 5 minutes and ~37% at 25 minutes. Whereas the effect of the “faux” ginger juice on the duodenal contraction amplitude contributed to ~82% of the effect of the 200 μ L volume of ginger juice at 5 minutes and ~17% at 25 minutes. The “faux” ginger juice effect on the duodenum explained the majority of the effect of the “high” volume of ginger juice, on both tone and amplitude, although at the latter stages of exposure to the “faux” ginger juice there was the

beginning of a recovery of the tone and amplitude. There are likely to be other constituents within ginger juice, which contribute to the effects on the stomach, and the longevity of the response. This study has established that there are other elements present in ginger juice, and other peaks detected by HPLC and although not found in high concentrations they may also contribute to the response seen on the stomach and duodenum (e.g. [6]-shogaol).

The combined constituents of the ginger juice are likely to contribute to the effects more than isolated compounds, as there are constituents present in ginger juice which were not identified or quantified. Heinrich, *et al.*, (2005) identified a Mexican plant *Casimiroa tetrameria* Millsp. extracts from which inhibited histamine (1 μ M) induced contractions on guinea pig ileum. All the flavonoid fractions tested had comparable antispasmodic activity and all the fractions contributed equally to the effect (Heinrich, *et al.*, 2005).

In a review by Houghton, *et al.*, (2007), the original plant extract may have higher bioactivity when compared to fractions of the extract. This reasoning could play a role here as it appears the "high" volume of ginger juice is not completely matched by the "faux" ginger juice, in all tissues. Although the effects were practically identical for the duodenum, the distal stomach response to the "faux" and "high" ginger juice were not as similar. The only significant effect of the "faux" juice was on the contraction amplitude, unlike the "high" volume which affected all aspects of the measurements. The increase in bioactivity of un-fractionated plant extracts could be due to the synergy of the compounds and/or decomposition of separated fractions of the original extract. With the latter explanation there may be certain anti-oxidant compounds contained within the plant

extract that protect the unstable compounds from oxidation (Houghton, *et al.*, 2007). Alternatively, the isolated compounds may not contain the same pronounced effect when combined with the original extract. Although not mentioned in the results, it was noted that if the ginger juice was more than 24 hours old, the solution no longer had the same bioactivity it had when fresh. A preliminary test showed that when the ginger juice was heated to 60°C for 10 minutes there was still bioactivity present on the tissues. It could be that there were oxidant compounds in the extract which caused the loss of bioactivity or that the elements which were free in solution were chelated by other biological compounds and reduced the bioactivity.

4.4.6 The potential pharmacology of the responses

Ghayur, *et al.*, (2006) demonstrated that when an aqueous extract of ginger was applied to the jejunum and ileum of the rabbit and stomach fundus and ileum of the rat there was a stimulatory response which was blocked by pre-treatment with 1 μM atropine, a muscarinic receptor blocker. When acetylcholine was applied to these tissues it was also blocked by atropine indicating that the effect seen on the rat and rabbit tissues was mediated through activation of the muscarinic receptor. However, when this extract was applied to guinea pig ileum the stimulatory response was not blocked by atropine – indicating a different pathway not involving the muscarinic receptors (Ghayur, *et al.*, 2006). In guinea pig ileum [6]-gingerol has been shown to induce contractions by acting on vanilloid receptors and also enhanced capsaicin-induced contractions (Someya, *et al.*, 2003). Although the ginger juice is not a replica of the ginger extract from the Ghayer, *et al.*, (2006) study, it may act along the same pathways. Therefore the stimulatory effect of ginger juice may be mediated through the activation of muscarinic receptors and/or a

vanilloid receptor agonist which induces contraction in the stomach. It may be due to either receptor being activated or both (muscarinic and vanilloid). Other extracts have also been shown to have a spasmolytic effect on the intestine; as exemplified below.

Licorice root has been used as a herbal medicine to regulate gastrointestinal function (Chen, *et al.*, 2009). Isoliquiritigenin, a flavonoid from licorice, caused a spasmogenic effect on the rat stomach fundus at 0.1-10 mM, and these effects were abolished by 1 μ M of atropine. Isoliquiritigenin also caused a spasmolytic effect on spontaneous and high K^+ (80 mM) induced contraction on rabbit jejunum, guinea pig ileum and atropinised rat stomach fundus (Chen, *et al.*, 2009). L-NAME, a NO synthase inhibitor, did not inhibit the spasmolytic effect on the intestine caused by isoliquiritigenin indicating that NO is not involved in the relaxation of the tissue. There was a rightwards shift of the calcium concentration response curve after the tissues were treated with isoliquiritigenin, suggesting the compound acted as a calcium antagonist (Chen, *et al.*, 2009). The spasmogenic effect on the stomach appeared to be due to a muscarinic receptor mediated effect, whilst the spasmolytic effect may have been due to the blockade of calcium channels (Chen, *et al.*, 2009; Gilani, *et al.*, 2007).

Several flavonoids: quercetin; catechin; extracts of *Psidium guajava* leaves; and extracts of *Tanacetum artemisioides* (Asteraceae) acted like the calcium antagonist, verapamil, and caused a rightward shift of a calcium concentration response curve on guinea pig ileum and rabbit jejunum, which may explain the spasmolytic effect (Bukhari, *et al.*, 2007; Ghayur, *et al.*, 2007a; Morales, *et al.*, 1994).

4.4.7 Conclusions and further work

It has been demonstrated that ginger juice has a biphasic effect on the *S. murinus* stomach (inhibition followed by stimulation) and an inhibitory effect on the *S. murinus* duodenum and these effects were not fully explained by selected constituents of ginger which made up a “faux” juice. It appears the duodenum is the tissue principally affected by the ginger juice including a consistent reduction in tone and contraction amplitude, even at “low” concentrations. Ginger may relax the duodenum *in vivo*, which could potentially reduce the giant retrograde contraction that occurs during an emetic episode.

There are limitations to this project as it was only possible to investigate the tension, amplitude and frequency of contractions which are quite hard to translate into a genuine effect which would occur *in vivo* as there are more variables which could affect the response e.g. stomach secretions.

Further work includes: 1) identifying the other constituents present in ginger juice and quantifying them and applying them to the upper GI tract; 2) identifying if the relaxatory effects of ginger juice, “faux” juice and other constituents are augmented by the NO inhibitor L-NAME 3) applying atropine to the stomach and measuring any interference in the stimulatory effects of “faux”/fresh ginger juice, indicating whether the effects are mediated through muscarinic receptors; and 4) applying capsazepine to the tissues prior to adding the “faux”/fresh ginger juice and observing whether there was modulation of the effects, which would identify if the vanilloid receptor was involved. This work was not investigated here as a large amount of time was spent collecting and analysing the data presented in this chapter.

Overall, there is a clear gastrointestinal motility effect due to this ginger extract which is possibly why ginger has been and currently is being used to treat nausea and vomiting, as well as a range of other gastrointestinal conditions (Levine, *et al.*, 2008).

CHAPTER FIVE

IN VIVO INVESTIGATION OF THE
EFFECTS OF A GINGER CAPSULE
SUSPENSION and [6]-GINGEROL
ON *SUNCUS MURINUS* RETCHING
AND VOMITING AFTER
EXPOSURE TO MOTION

5.1 Introduction

The Eutherian Insectivore *S. murinus*, the house musk shrew, is used as a well established model of motion- and chemotherapy- induced emesis (Matsuki, *et al.*, 1992; Torii, *et al.*, 1993; Ueno, *et al.*, 1987; Ueno, *et al.*, 1988). *S. murinus* are found in tropical and subtropical areas and are direct ancestors of other placental mammals (Colbert, 1958). *S. murinus* respond to certain emetic stimuli (e.g. nicotine) in a similar fashion to cats, dogs and ferrets (Matsuki, *et al.*, 1992). Dogs, cats and ferrets have previously been used in modelling emesis, and investigating a range of drugs, which can both stimulate and block the emetic reflex. Rodents (rat, mouse, guinea pig) and Lagomorphs (rabbit) lack the emetic reflex (Matsuki, *et al.* 1992).

When *S. murinus* are exposed to motion stimuli, x-ray irradiation and chemotherapeutics for the treatment of cancer, they can vomit in response to these stimuli. Anti-histamines (H_1) and 5-HT_{1A} agonists blocked the effect of motion sickness on *S. murinus*. Cisplatin- and x-irradiation- induced vomiting in *S. murinus* was blocked via 5-HT₃ receptor antagonists. This indicates that there are different mechanisms and pathways leading to emesis depending on the stimulus (Matsuki, *et al.*, 1992).

In human studies, there are varied reports of gingers' efficacy in motion sickness and vestibular stimulation, although each report focussed on different end points; either nausea or emesis (Grøntved and Hentzer, 1986; Holtman, *et al.*, 1989; Stewart, *et al.*, 1991; Stott, *et al.*, 1984; Wood, *et al.*, 1988). Ginger capsules have been shown to be effective in treating motion-induced nausea in humans (Lien, *et al.*, 2003). It was thought

that if the ginger capsule was effective in humans, then the effect could be mimicked in the *S. murinus* motion sickness model.

[6]-gingerol (doses at 25 and 50 mg/kg) and 150 mg/kg of an acetone extract (p.o.) of ginger prevented vomiting in *Suncus murinus*, when administered 1 hour prior to exposure to the chemotherapeutic agent cyclophosphamide. The latency was also increased compared to the control group (Yamahara, *et al.*, 1989). It would be interesting to identify if [6]-gingerol would also prove effective in motion-induced emesis in *S. murinus*, although the pathways leading to emesis differ from chemotherapy-induced emesis. The ultrapotent capsaicin analogue resiniferatoxin, a vanilloid receptor₁ agonist, when given subcutaneously (s.c.) blocked motion-induced emesis (10-100 µg/kg) (Andrews, *et al.*, 2000), whilst at the same time RTX alone has also been found to induce emesis (1-500 µg/kg) (Andrews, *et al.*, 2000). With [6]-gingerol being a weak vanilloid agonist, it would also be interesting to see if [6]-gingerol would have a similar effect to resiniferatoxin although perhaps not to the same degree (Dedov, *et al.*, 2002).

5.1.1 Aim

The aim of this set of experiments is to investigate the effect of [6]-gingerol and a ginger capsule suspension on motion-induced emesis in *S. murinus*

5.2 Materials and methods

5.2.1 Materials

The sources of chemicals including grade and batch details are given in Table 27, whilst the instrumentation list used is in Table 28.

Table 27. Reagents used in Chapter 5.

Chemical	Grade	Source	Catalogue Number	Batch
[6]-gingerol		Wako Chemical GmbH	074-05061	WKG6867
Carboxymethylcellulose		Sigma-Aldrich	C4888	
Ginger root capsule		Nature's Way		530519 Expiry date: Oct 2010

Table 28. A list of instruments used throughout Chapter 5.

Instrument	Make	Model
Reciprocal shaker	LabPlant Ltd	Heidolph Promax 2020

5.2.2 Animals

Male (N=20) and female (N=20) *S. murinus* had a mean weight of 55.89 g \pm 1.31 g and 37.06g \pm 0.80 g, respectively. They had free access to food pellets and water. All experiments were conducted in Hong Kong under license from the Government of the Hong Kong SAR and were approved by the Animal Experimentation Ethics Committee, The Chinese University of Hong Kong.

5.2.3 Pre-screening

One week prior to the main experiment the *S. murinus* (N = 40) were screened for motion sickness sensitivity. They had not previously been challenged with a motion stimulus. The animals were placed in a transparent observation chamber (21 x 14 x 13 cm) and were allowed to acclimatise for 10 minutes prior to exposure to the emetic stimuli. The emetic stimulus was 10 minutes motion on a reciprocal shaker with a horizontal oscillation of 4cm and a frequency of 1 Hz, as shown in Figure 94. These parameters have been shown to induce emesis in most *S. murinus* within 2 minutes (Ueno, *et al.*, 1988).

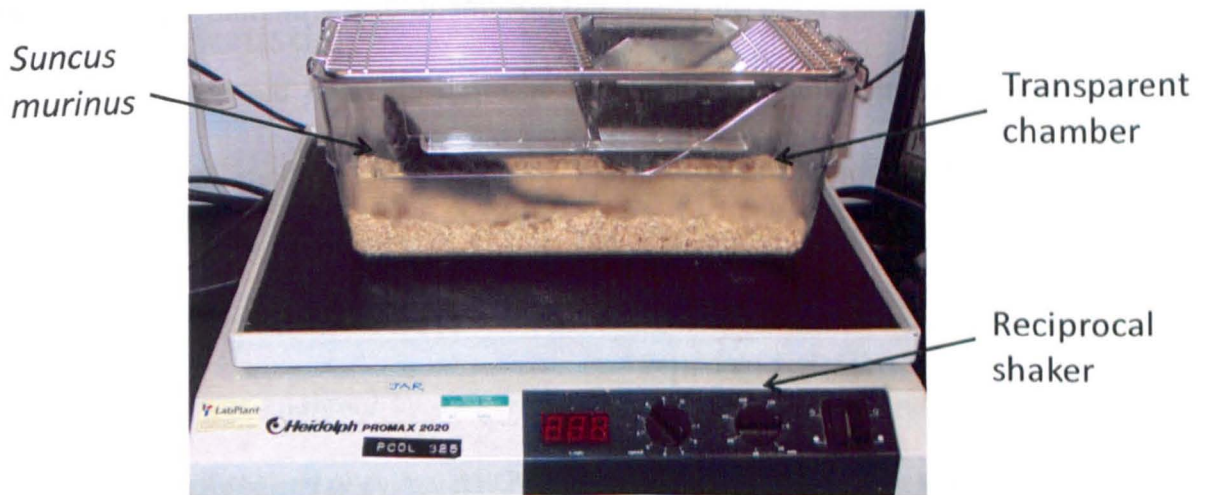


Figure 94. *Suncus murinus* on the reciprocal shaker.

The *S. murinus* were observed during the exposure to linear motion and any unusual behaviour was noted. The latency was taken for the *S. murinus* to experience the first retching episode or expulsion of liquid or solid stomach contents (vomit), from the start of the motion. The number of rhythmic abdominal contractions resulting in either a retch and/or a vomit after the first documented retch and/or vomit was quantified as the

number of emetic episodes. The mean (\pm SEM) number of emetic episodes (retching and/or vomiting) and the latency of onset were calculated for each stimulus group.

5.2.4 Experimental Protocol

The animals which were sensitive to the motion stimulus were separated into the 5 experimental groups using a Latin square. The animals were weighed and given 1 hour to acclimatise to the transparent chamber, with free access to food and water. Thereafter the test substances (Table 27) were given to the *S. murinus* p.o. through an injection via an intragastric tube. 1 hour after administering the test substance the *S. murinus* was exposed to 10 minutes of motion (as previously described), where behaviour and the number of emetic episodes were observed and documented. The animals were observed after the injection to identify if any vomiting occurred between the injection and the motion stimulus. At the end of the experiment the animals were replaced in their original cages.

5.2.5 Experimental groups

[6]-Gingerol at the concentration of 1×10^{-4} M was active in the *in vitro* experiments in Chapter 4. Therefore this concentration (1×10^{-4} M) and two ten-fold increases in concentration were used to explore the anti-emetic activity of this compound. Also the ginger capsule was calculated to be a similar concentration to that which would have been used and found to be effective in the human motion study by Lien, *et al.*, (2003) which was 1g and 2g of the ginger capsule contents per person or 20mg/kg per animal.

In previous research, [6]-gingerol was injected via an intragastric tube into the stomach of the *S. murinus* and was well tolerated (Yamahara, *et al.*, 1989). The vehicle for

[6]-gingerol was 1% carboxymethylcellulose (CMC) solution which has been used here for all the [6]-gingerol and the ginger capsule suspension groups (Yamahara, *et al.*, 1989). Carboxymethylcellulose sodium salt was purchased from Sigma Aldrich. The contents of the ginger capsules were weighed and mixed with the vehicle and held in a suspension of the vehicle. The volume of the injection was given as 5 mL/kg for all of the experimental groups. The experimental groups included the following:

- Vehicle – 1% carboxymethylcellulose in deionised water
- [6]-gingerol (1×10^{-2} M)
- [6]-gingerol (1×10^{-3} M)
- [6]-gingerol (1×10^{-4} M)
- Ginger capsule 20 mg/kg

5.2.6 Statistics

The pre-screening data between males and females was analysed by an unpaired two-way t-test. The mean weights of the male and female *S. murinus* were analysed by a two-way t-test. The vehicle latency compared to the latency of the same *S. murinus* of the previous week was analysed by a one-tailed paired t-test. The experimental groups were analysed by an unpaired one-way ANOVA and Bonferroni's multiple comparison test.

5.3 Results

5.3.1 Pre-screening

The mean latency for the onset of emesis for all responding *S. murinus* was 3.25 ± 0.35 minutes. The mean latency in females was 3.04 ± 0.49 minutes (N=13) and in males was 3.41 ± 0.50 minutes (N=17) (Table 29).

The number of emetic episodes in males and females were normally distributed. In males and females the number of emetic episodes and latency was analysed and there were no significant differences, $p < 0.7059$ and $p < 0.6135$, respectively (Figure 95). The females were significantly lighter in weight when compared to the males ($p < 0.0001$). Overall, 25% of all animals tested did not respond to motion within 10 minutes (N = 10). Out of the male *S. murinus* 85% responded to motion and out of the female *S. murinus* 65% responded to motion. The motion responding *S. murinus* (N = 30) were then randomly assigned to 5 mixed sex groups.

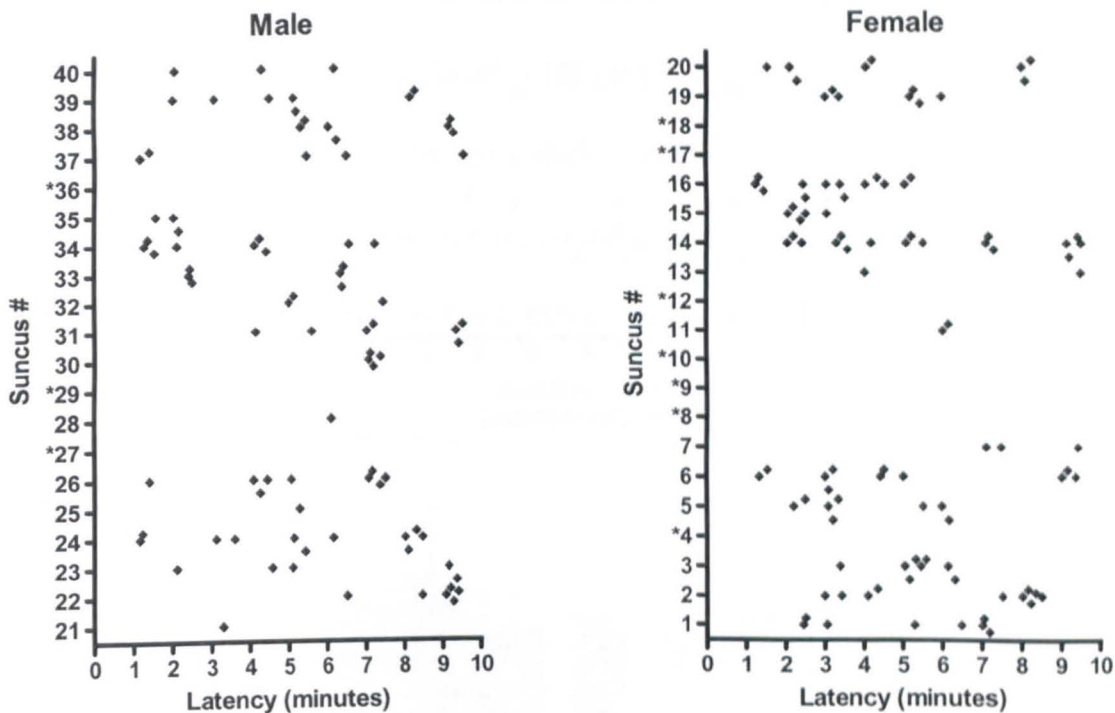


Figure 95. Horizontal scatter plots depicting the latency and the emetic episodes during 10 minutes exposure to motion on (A) female and (B) male *S. murinus*. N=40 * = No emesis occurred within 10 minutes exposure to motion.

Table 29. The mean latency of emetic episodes and the number of emetic episodes. The results are expressed as mean \pm SEM.

Sex	Mean Latency (Minutes)	Mean Number of Emetic Episodes (n) of Responders	Mean Number of Emetic Episodes (n) of All Animals
All	3.25 \pm 0.35	6.33 \pm 0.70 (N=30)	4.75 \pm 0.68 (N=40)
Male	3.41 \pm 0.50	5.18 \pm 0.72 (N=17)	4.40 \pm 0.75 (N=20)
Female	3.04 \pm 0.49	7.84 \pm 1.20 (N=13)	5.10 \pm 1.15 (N=20)

There were no significant differences between the latency of the experimental groups and the number of emetic episodes one week prior to the administration of the test substances, as shown in Figure 96.

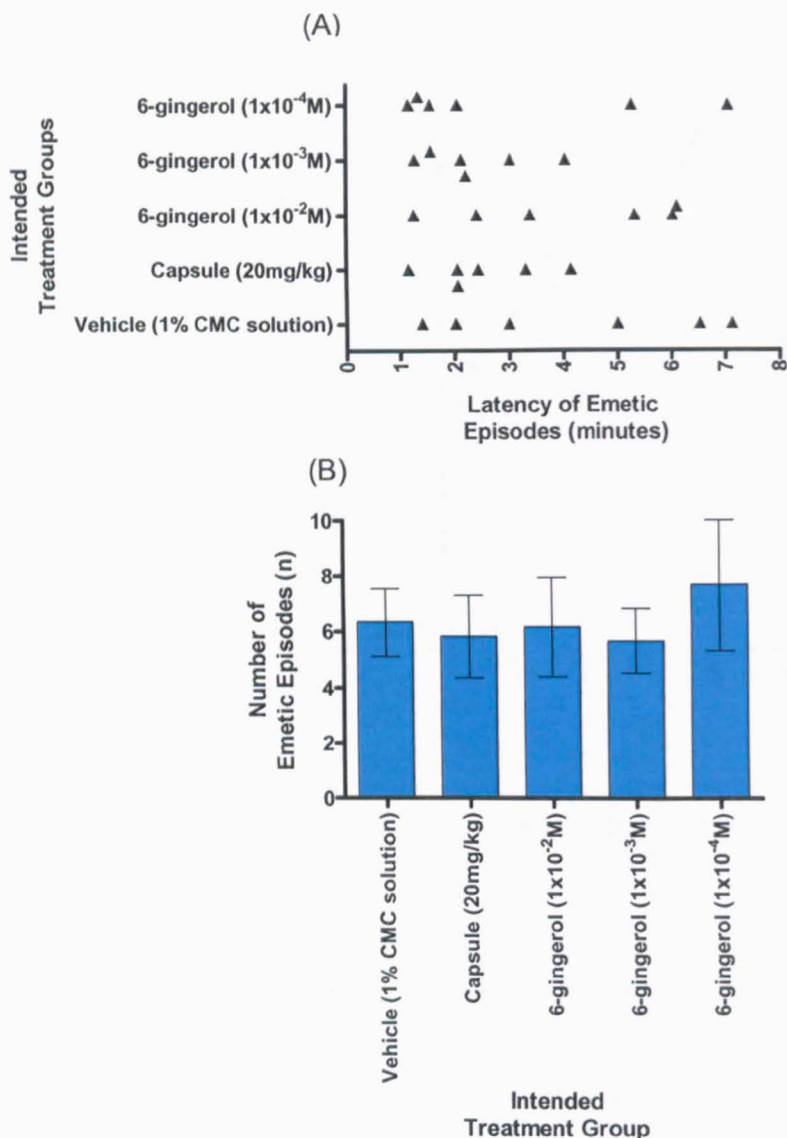


Figure 96. (A) A horizontal scatter plot of the latency of emetic episodes after motion; and (B) a bar graph of the number of emetic episodes in the separated groups a week prior to the addition of the treatments, the results are expressed as mean \pm SEM. N=30. CMC = Carboxymethylcellulose.

5.3.2 The effect of the vehicle on the latency and number of emetic episodes

The vehicle (1% CMC solution) group's latency and number of emetic episodes were analysed against the pre-screening data for the same animals. There was a statistically significant effect of the vehicle on emetic latency when compared to the previous week where no treatment was applied, only the motion stimulus ($p < 0.0429$). The latency significantly increased in time after the vehicle (Figure 97). As [6]-gingerol was

difficult to dissolve and costly a 1% CMC solution was chosen as it had previously been used in a similar experiment to dissolve [6]-gingerol (Yamahara, *et al.*, 1989). Another vehicle like dimethyl sulfoxide was not sufficient as there was a question over the safety of DMSO on the *S. murinus* tested as they would be used for future studies (Sigma-Aldrich Material Safety Data Sheet, D5879, 2008; Wan Pui Chu, 2004).

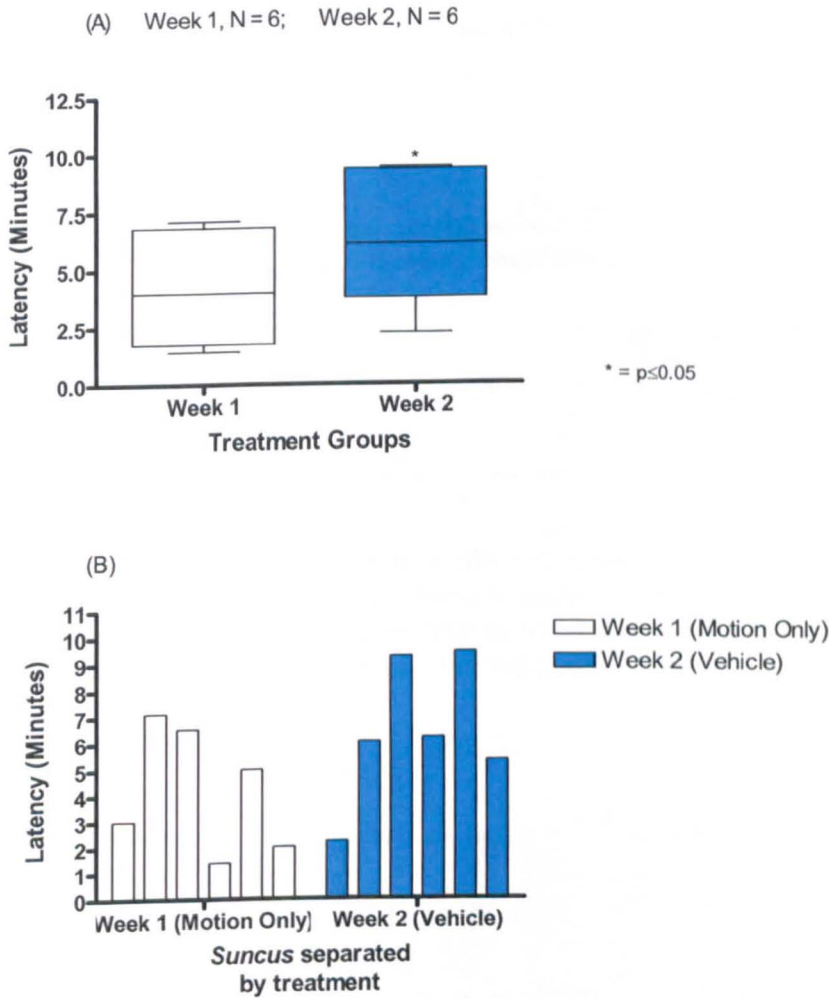


Figure 97. (A) A box and whisker plot displaying the effect of the vehicle, administered via an intragastric tube 1 hour prior to motion, on the latency of emetic episodes compared to the previous week when no drug was applied. Results are expressed as median with the interquartile range. (B) A bar chart displaying individual *S. murinus* latency of emetic episodes after the vehicle and motion and motion only. N = The number of animals. * = $p \leq 0.05$

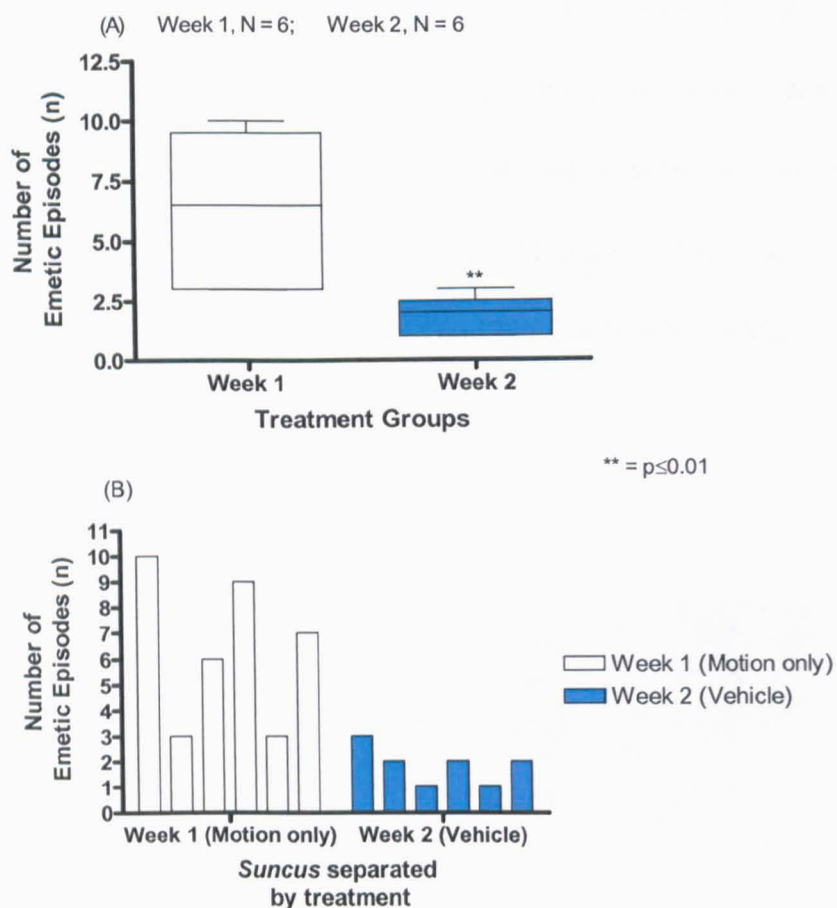


Figure 98. (A) A box and whisker plot displaying the effect of the vehicle, administered via an intragastric tube 1 hour prior to motion, on the number of emetic episodes compared to the previous week when no drug was applied. Results are expressed as median with the interquartile range. (B) A bar chart displaying individual *S. murinus* number of emetic episodes to the vehicle. N = The number of animals. ** = p < 0.01

There was a statistically significant decrease in the number of emetic episodes after the vehicle when compared to the same animals of the pre-screening week (p < 0.0035). There were no more than three emetic episodes each within the vehicle group. The mean number of emetic episodes after the vehicle was 1.83 ± 0.31 and when compared to the previous pre-screening week the mean number of emetic episodes was 6.33 ± 1.20 . The vehicle reduced the number of emetic episodes by two-thirds of the original measurement.

5.3.3 The effect of [6]-gingerol and the ginger capsule suspension on the latency and number of emetic episodes

The effect of [6]-gingerol (different concentrations), the ginger capsule suspension and the vehicle on the latency and number of emetic episodes during a motion stimulus was investigated.

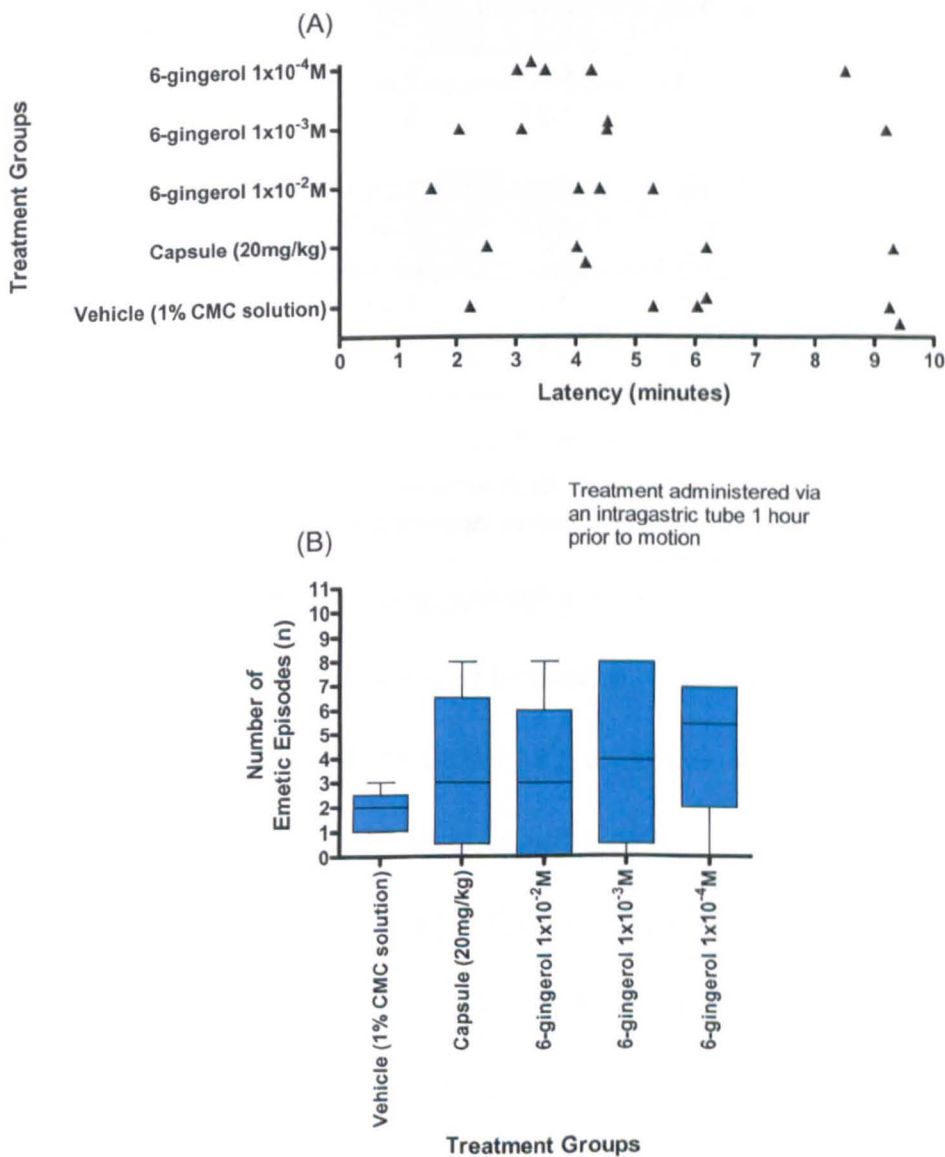


Figure 99. (A) A horizontal scatter plot displaying the latency of the emetic episodes for each of the treatment groups. (B) A box and whisker plot displaying the number of emetic episodes for each of the treatment groups. The results are expressed as median with the interquartile ranges. N = 5 per treatment group. CMC = Carboxymethylcellulose

The latency of emetic episodes for all of the treatment groups was analysed and there were no significant differences between the five groups after treatment ($p < 0.4331$). The number of emetic episodes for the treatment groups were analysed and there were no significant differences between the five groups after treatment ($p < 0.5469$).

Table 30. The latency and number of emetic episodes in each of the treatment groups and the pre-screened animals. The results are displayed as mean \pm SEM.

	Pre-screened animals	Vehicle (1% CMC solution)	Capsule (20 mg/kg)	[6]-gingerol $1 \times 10^{-2} \text{M}$	[6]-gingerol $1 \times 10^{-3} \text{M}$	[6]-gingerol $1 \times 10^{-4} \text{M}$
Number of responders	30/40	6/6	5/6	4/6	5/6	5/6
Mean latency (minutes) of responders	3.25 ± 0.35	6.41 ± 1.10	5.25 ± 1.17	3.84 ± 0.80	4.69 ± 1.22	4.52 ± 1.02
Mean number of emetic episodes (n) of responders	6.33 ± 1.20	1.83 ± 0.31	4.00 ± 1.22	4.50 ± 1.19	5.00 ± 1.64	5.80 ± 0.58
Mean number of emetic episodes (n) of all animals	4.75 ± 0.68	1.83 ± 0.31	3.33 ± 1.20	3.00 ± 1.21	4.17 ± 1.58	4.83 ± 1.08

The vehicle caused a significant increase in latency of the emetic episodes (Figure 97). However, the capsule and the [6]-gingerol treatments appeared to decrease the latency of the emetic episodes when compared to the vehicle (Figure 99A). The latency of emetic episodes for the animals treated with the capsule decreased by more than a minute when compared to the vehicle. The latency decreased from 6.41 ± 1.10 minutes, for the vehicle, to 3.84 ± 0.80 , for the highest concentration of [6]-gingerol ($1 \times 10^{-2} \text{M}$), being nearly three minutes lower than the vehicle latency. This reduction in latency due to [6]-gingerol, $1 \times 10^{-2} \text{M}$ (3.84 ± 0.80 minutes), almost abolished the delay caused by the vehicle and was comparable to the pre-screened latency (3.25 ± 0.35 minutes). The two lower concentrations of [6]-gingerol, $1 \times 10^{-3} \text{M}$ and $1 \times 10^{-4} \text{M}$, non-significantly decreased the latency of the vehicle by approximately two minutes earlier when compared to the vehicle (Table 30).

The mean number of emetic episodes of all the treatment groups when compared to the vehicle appeared to non-significantly increase. The pre-screened animals mean number of emetic episodes was usually higher than the treatment groups' mean number of emetic episodes. This was thought to be due to the delay in latency. The lowest concentration of [6]-gingerol ($1 \times 10^{-4} \text{M}$) increased the mean number of emetic episodes of all the animals by more than 3 (4.83 ± 1.08) when compared to the mean number of emetic episodes from the vehicle (1.83 ± 0.31) (Table 30). This was slightly higher than the mean number of emetic episodes of the pre-screened animals (4.75 ± 0.68), as shown in Table 30. None of the treatments caused emesis during the one hour prior to exposure to the motion stimulus.

There was at least one non-responder to motion in each of the capsule and the [6]-gingerol treatment groups. The highest concentration of [6]-gingerol $1 \times 10^{-2} \text{M}$ appeared to be the most effective, as it decreased the latency of emetic episodes and prevented two *S. murinus* from vomiting. However, it did appear to increase the number of emetic episodes of those that did respond.

5.4 Discussion

5.4.1 The effect of the vehicle on the latency and number of emetic episodes

The vehicle for [6]-gingerol in Chapter 4 was a solution $\leq 1\%$ for DMSO but DMSO (i.p) has been shown to cause a hypothermic effect *in vivo* in rats and *S. murinus* (Highman, *et al.*, 1967; Wan Pui Chu, 2004). Therefore a 1% carboxymethylcellulose solution was chosen, which was the vehicle for [6]-gingerol in the Yamahara, *et al.*, study (1989). In that study only 8/9 of the *Suncus* exposed to the vehicle (1% CMC solution) and injected with cyclophosphamide (300 mg/kg, s.c.) experienced emesis, so a possible interaction between the number of emetic episodes and a 1% carboxymethylcellulose solution was an implication for using this vehicle. However, [6]-gingerol was a difficult substance to dissolve, and as a 1% CMC solution had been previously shown to dissolve it, in keeping with the research it was decided this would be the vehicle (Yamahara, *et al.*, 1989). A carboxymethylcellulose solution (40 g/kg) has been shown to delay gastric emptying in growing pigs (Rainbird and Low, 1986). Although this was a much higher dose of CMC than was used in our study (0.5 g/kg), it could explain the increase in latency of the emetic episodes as it was still very viscous at 1%. Also a diet consisting of 2.5% CMC in male Sprague-Dawley rats delayed gastric emptying 45-90 minutes after a meal ($p < 0.01$) (Bégin, *et al.*, 1989).

The results for the [6]-gingerol and the ginger capsule suspension were not as anticipated. However the result for the vehicle on the latency and number of emetic episodes is still valuable. This data highlights how a small “meal” may reduce the number

of emetic episodes and the latency in motion-induced emesis. These data correspond with a study by Levine, *et al.*, (2008) into chemotherapy-induced nausea which was reduced by a high protein diet coupled with ginger.

5.4.2 The effect of [6]-gingerol and the ginger capsule suspension on the latency and number of emetic episodes during motion

The ginger tablets used in this study (Nature's Way) have been shown to increase gastric emptying in humans, and ginger extracts can reverse the delay in gastric emptying caused by cisplatin in rats (Sharma and Gupta, *et al.*, 1998; Wu, *et al.*, 2008). With this in mind, when comparing the effect of [6]-gingerol and the ginger capsule suspension on latency for emesis compared to the vehicle, there was a non-significant tendency for the latency to reduce after treatment with [6]-gingerol and the ginger capsule suspension; this was especially so after treatment with [6]-gingerol 1×10^{-2} M. Therefore, there may have been an interaction between the gastric emptying and the latency of emetic episodes. Administration of [6]-gingerol caused two incidences of chin rubbing: once at 1×10^{-2} M and once at 1×10^{-4} M. Capsaicin and resiniferatoxin (vanilloid receptor agonists) have been shown to increase genital grooming in *S. murinus*. Although these are different bodily areas it indicates that vanilloids do cause behavioural effects (Rudd and Wai, 2001).

The number of emetic episodes after the addition of the ginger capsule suspension and all the concentrations of [6]-gingerol had a trend towards a non-significant increase. With each of the treatments, except for the vehicle, there was at

least one animal which did not respond to motion, of which 4 out of 5 were male (see Appendix 4). There were no instances where the vehicle completely inhibited emesis. Although the ginger capsule suspension was not effective in treating motion-induced emesis, it may be effective in treating motion-induced nausea (Lien, *et al.*, 2003). The study by Lien, *et al.*, (2003) investigated the effect of the same ginger capsule against motion-induced nausea in humans and found it to be effective, but it does not indicate whether the ginger capsule would have prevented emesis had the motion been continued to the point where it could be expected to have caused emesis. The end points of this study and the Lien, *et al.*, (2003) study are fundamentally different and this could be why the ginger capsule suspension was not effective here.

[6]-gingerol is a weak vanilloid receptor agonist (Dedov, *et al.*, 2002), and as previously shown by Andrews *et al.*, (2000) the vanilloid RTX was capable of both inducing emesis and preventing it, depending on the concentration. In each of the [6]-gingerol concentrations there was one incidence of an increase in the number of emetic episodes from low responders of the pre-screening group (1-3 emetic episodes) to 4-8 emetic episodes. This did not occur in the vehicle data. This suggests that this non-significant trend towards an increase was an effect of [6]-gingerol, which could be due to the vanilloid area on [6]-gingerol. It appears that the high responders to motion sickness decreased in emetic episodes, whilst the low responders to motion sickness increased in emetic episodes after exposure to varying concentrations of [6]-gingerol. Although this is all conjecture, the main result indicated from these results is that [6]-gingerol did not prevent motion-induced emesis.

Gingerol (200 mg/kg p.o.) was effective against cisplatin-induced emesis (7.5 mg/kg i.p.) in minks and down regulated the expression of cellular mediators that are involved in emesis (e.g. 5-HT) in both the ileum and the area postrema (Qian, *et al.*, 2009). In contrast ondansetron, an effective 5-HT₃ receptor antagonist used for acute phase CINV, only inhibited the release of 5-HT in the area postrema but in not the ileum, Therefore the mechanism of action of gingerol differs from 5-HT₃ receptor antagonists currently used to treat CINV.

[6]-Gingerol has been shown to dehydrate to [6]-shogaol in simulated intestinal fluids and vice versa (Bhattarai, *et al.*, 2007). [6]-Shogaol could potentially be more potent than [6]-gingerol on the gastrointestinal tract (Abdel-Aziz, *et al.*, 2006) and may not have been able to interconvert as freely in the gastric acids due to the viscous 1% CMC solution, thus reducing the efficacy of the solution. However, this does not explain why [6]-gingerol in a 1% CMC was effective at reducing cyclophosphamide-induced emesis in *S. murinus*, but not motion-induced emesis. The reason for the difference in activity is most likely due to the pathways in which emesis is induced and where [6]-gingerol or the dehydrated [6]-shogaol acts to interrupt this pathway.

Overall, neither [6]-gingerol at all concentrations and the ginger capsule suspension caused a significant effect on the latency or number of emetic episodes in *S. murinus* during exposure to a motion stimulus. The lowest concentration of [6]-gingerol ($1 \times 10^{-4} \text{M}$) was the same concentration which was found to have varying effects on the stomach and duodenum in Chapter 4 and this indicates that although something may prove effective *in vitro*, when applied through *in vivo* studies it may not prove so

effective. Although different areas were being measured *in vivo* (e.g. emetic episodes) not direct measurement of the gastrointestinal tract (e.g. telemetry).

The studies of ginger on vestibular stimulation / motion sickness in humans reveal varied results and investigated different end points. In all 5 out of 8 reports suggest ginger was not effective in treating vestibular stimulation- or motion- induced nausea or emesis (Grøntved and Hentzer, 1986; Holtman, *et al.*, 1989; Stewart, *et al.*, 1991; Stott, *et al.*, 1984; Wood, *et al.*, 1988). The data from this study appears to support the above papers, although a motion-induced nausea study by Lien, *et al.*, 2003 suggests that the ginger capsule (the same capsule brand that was used in this study) was effective in treating nausea associated with motion, and very recently Wu, *et al.*, (2008) found that ginger capsules increase gastric emptying. This could indicate that although ginger may not be effective in treating motion sickness it may be capable of treating the nausea associated with motion.

5.4.3 Conclusions and further work

Ginger proved ineffective in treating motion sickness. However there may have been an interaction between the vehicle and ginger so it is hard to draw firm conclusions and further work needs to be done. Motion-induced emesis was not prevented by [6]-gingerol or the ginger capsule suspension; however this does not mean that it is not effective in treating nausea. The study as to the efficacy of the ginger capsule investigated the capsule's effect on motion-induced nausea not motion-induced emesis (Lien, *et al.*, 2003). It is concluded that ginger capsules may be effective in treating nausea. The result from the vehicle suggests that a small carbohydrate "meal" may be beneficial in treating motion-induced emesis.

Direct investigation into nausea in *S. murinus* cannot be carried out – it would involve making anthropomorphic assumptions. However, further work could be performed using telemetry on *S. murinus* to monitor physiological parameters including heart rate and gastric slow wave frequency. In humans it has been shown that during nausea tachygastria occurs (an increase of gastric slow wave frequency) (Lien, *et al.*, 2003). Therefore by measuring these physiological parameters by telemetry, it may be possible to inform as to whether ginger prevents an increase in gastric slow wave frequency if not actually preventing motion-induced emesis.

CHAPTER SIX

CONCLUSION

6.1 General conclusion

Herbal medicines do have their place in therapy but should not be used as a substitute for conventional medicine. There is the view from a group of participants from a survey that herbal medicines are “safe” and “pure” (MHRA and Ipsos MORI, 2008). In reality herbal medicines are likely to be far from “pure” because they contain a multitude of compounds, as shown by the ginger extract analysis in this study. Contrast this with conventional medicine which usually consists of one compound, although drugs are often used in combination (for example treatments for acute and delayed phase chemotherapy-induced nausea and vomiting e.g. dexamethasone and ondansetron).

The major goals of this thesis were to quantify the constituents in ginger and identify which constituents caused biological effects. This overall conclusion will focus on the results on ginger, from the chemical analysis, to the biological effects *in vitro* and *in vivo*.

The chemical analysis of ginger resulted in the concentration of [6]-gingerol and 20 elements being quantified. Often in many plant/herbal extracts the levels of elements are not measured, however this does not signify that they are not present in the extract. A combination of 5 of these elements caused biological effects *in vitro* therefore, it is important for future studies into plant/herbal extracts to measure the elements as they may explain, in part, the bioactivity. For the first time the concentration of [6]-gingerol in ginger juice was quantified to be 239.43 ± 7.92 mg/L by a modified HPLC method.

This study reveals there are both beneficial and detrimental and indeed often no bioactivities of constituents from plants. There was no effect of [6]-gingerol or vitamin E on CINC-1 levels, or IL-8 levels after exposure to TNF- α in NRK-52E cells or Caco-2 cells,

respectively. Under varied conditions which were applied to study the binding of Cu(II) ions to [6]-gingerol, on the basis of the Cu(II)-curcumin binding, unusually a precipitate formed which could not be dissolved in a range of conditions and thus SOD mimicry was not detected as had been anticipated. However the Cu(II) ions alone did inhibit formazan formation indicating SOD mimicry. This showed the anti-oxidant effect of Cu(II) ions, although in high concentrations Cu(II) ions have been shown to have a pro-oxidant effect (Halliwell and Gutteridge, 2001). Although this particular approach proved ineffective for [6]-gingerol and Cu(II) ions, it is likely many other phytochemicals are capable of binding to Cu(II) ions and acting as SOD mimetics.

As ginger is used for digestive problems, the gastrointestinal tract was the main biological area studied with: Caco-2 cells; upper GI tract preparations from *S. murinus* and motion-induced emesis with *S. murinus*. The flavonols, quercetin and kaempferol, augmented the ATP response in Caco-2 cell membranes, stimulating epithelial secretion. These flavonols from the diet could occur in high concentrations in the colon in the aglycone form and affect the ion channels. This in turn could soften and lubricate stools into the lumen of the gut by stimulating secretory effects on the epithelia. Quercetin and kaempferol from the diet (e.g. fruit) may relieve symptoms of constipation, but too much fruit may lead to diarrhoea (Yang, *et al.*, 2008). A reason to have a balanced diet!

[6]-Gingerol had no effect in the Caco-2 cells on the Ussing chamber, in contrast to previous research by O'Leary, *et al.*, (2004a) although this group used rat colonic tissue. This could be because [6]-gingerol was acting on the submucosal neurones in the rat colonic tissue, which would not have been present on Caco-2 cells resulting in the lack of response. However [6]-gingerol (at relatively high concentrations [1.59×10^{-4} M and 1×10^{-4} M]) and ginger juice had dose-related effects on the stomach and duodenum

preparations from *S. murinus*. There were inhibitory and stimulatory (transient) effects on the stomach whilst there were mainly inhibitory effects on the duodenum due to the ginger juice.

This research into the GI tract demonstrated the effect of [6]-gingerol and ginger juice and how important it was to study the controls, in this instance the element solution. It was originally believed that the element solution control would not explain the effect of ginger juice on the stomach and duodenum. Surprisingly, the element solution did account, in part, for the bioactivity on the upper GI tract. However, [6]-gingerol and the elements in ginger juice did not fully account for the effects of ginger juice on the upper GI tract. The tissue which was most receptive to the ginger juice, [6]-gingerol and “faux” ginger juice, causing repeated relaxation of the tissue, was the duodenum.

The effect on the upper gastrointestinal tract supports other studies where different extracts of ginger have been used on guinea pig and rat ileum stimulated by either electrical field stimulation or acetylcholine (Abdel-Aziz, *et al.*, 2006; Borrelli, *et al.*, 2004). Neither the guinea pig nor the rat are mammals with an emetic reflex and as ginger is reportedly to be anti-emetic and/or anti-nausea for this reason this work concentrated upon an emetic species of mammal, *S. murinus*.

It was necessary to fully investigate the original effect of ginger juice and the constituents which caused such an effect on gastrointestinal motility, and more time was spent on this section than originally anticipated. This prevented the examination of the detailed pharmacology of the response of ginger juice on the upper gastrointestinal tract (e.g. applying tetrodotoxin to identify if the effect of ginger is neuronally mediated). Three different areas of the upper GI tract were studied, alongside three different

parameters of each region: tone; contraction amplitude and frequency of contraction. No studies have investigated different regions and different parameters of the GI tract (*in vitro*) in the same mammal before drawing conclusions regarding the effect of the compounds / herbal remedies. It is very important to investigate multiple regions because as shown here the effect varies greatly throughout the tissue types of one mammal.

Further work could be performed *in vitro* on *S. murinus* upper GI tract, for example: investigating the effect of applying [6]-gingerol, a ginger capsule suspension and ginger juice directly onto the lumen. This could measure the tension and observing effects of the test substances on peristalsis; rather than the whole tissue tension in the motility studies in Chapter 4. This may identify if [6]-gingerol through interaction with the epithelia could indirectly affect muscle contraction.

[6]-gingerol and ginger juice had an effect upon the GI tract *in vitro*; however this did not translate into an anti-emetic effect *in vivo*. Different parameters were being measured *in vivo* compared to *in vitro*, and *in vivo* has far more variables (e.g. vagal nerve terminals).

What is apparent from the research on *S. murinus* is that the frequency of emetic episodes and the emetic latency decreases when the stomach is not empty: - even a light carbohydrate meal may prevent the emetic episodes induced by motion, although possibly not the sensation of nausea. It is not possible to infer a reduction in nausea by reducing the motion-induced emetic episodes in *S. murinus*.

Ginger is often consumed in either crystallised or biscuit form and recommended to individuals experiencing motion-induced nausea and vomiting (Collins, 2006; Wong, 2009). Arguably the effect of eating the biscuit alone may reduce the motion-induced nausea rather than the ginger causing an effect. Although this research indicates that [6]-

gingerol and/or the ginger capsule suspension combined with the 1% CMC solution did not reduce motion-induced emesis.

This is the first study in an animal model of motion-induced emesis where [6]-gingerol and a ginger capsule suspension were used and identified to be ineffective. However, [6]-gingerol may prove successful in motion-induced nausea if GI motility is involved in nausea. Prior to vomiting, an enteric coated ginger pill which could be protected from the gastric acids and released on contact with the alkaline conditions of the duodenum may be a beneficial tool in treating nausea rather than emesis.

Proposed further work could involve inducing emesis by motion in ferrets (another animal model of emesis) after a ginger capsule suspension / [6]-gingerol (p.o.) and measure the levels of vasopressin in the blood during nausea (not experimentally viable in the *S. murinus*). Vasopressin release has been shown to be inhibited by a ginger capsule (p.o.) during motion-induced nausea in humans, although the causal link between nausea and vasopressin is unclear (Lien, *et al.*, 2003). If the tested ginger capsule and [6]-gingerol decreased vasopressin release it may be possible to infer a reduction in nausea by back translating the result from humans to ferrets. The investigation into the mechanism of vasopressin release and how ginger may augment the response could then be carried out.

Ginger has the potential to alleviate digestive disorders. So as Hippocrates, the “father of medicine”, said nearly 2,500 years ago, “Let food be thy medicine and medicine be thy food” (Aggarwal and Shishodia, 2006).

Bibliography

Abdel-Aziz, H., Windeck, T., Ploch, M., and Verspohl, E. J. (2006). Mode of action of gingerols and shogaols on 5-HT₃ receptors: Binding studies, cation uptake by the receptor channel and contraction of isolated guinea-pig ileum. *European Journal of Pharmacology*, **530**, 136-143.

Aggarwal, B. B., and Shishodia, S. (2006). Molecular targets of dietary agents for prevention and therapy of cancer. *Biochemical Pharmacology*, **71**, 1397-1421.

Ahui, M. L., Champy, P., Ramadan, A., Van, L. P., Araujo, L., André, K. B., Diem, S., Damotte, D., Kati-Coulibaly, S., Offoumou, M. A., Dy, M., Thieblemont, N., and Herbelin, A. (2008). Ginger prevents Th2-mediated immune responses in a mouse model of airway inflammation. *International Immunopharmacology*, **8**, 1626-1632.

Akita, Y., Yang, Y., Kawai, T., Kinoshita, K., Koyama, K., Takahashi, K., and Watanabe, K. (1998). New assay method for surveying anti-emetic compounds from natural sources. *Natural Product Sciences*, **4** (2), 72-77.

Aktan, F., Henness, S., Tran, V. H., Duke, C. C., Roufogalis, B. D., and Ammit, A. J. (2006). Gingerol metabolite and a synthetic analogue Capsarol inhibit macrophage NF-kappaB-mediated iNOS gene expression and enzyme activity. *Planta Medica*, **72** (8), 727-734.

Ali, B. H., Blunden, G., Tanira, M. O., and Nemmar, A. (2008). Some phytochemical, pharmacological and toxicological properties of ginger (*Zingiber officinale* Roscoe): A review of recent research. *Food and Chemical Toxicology*, **46**, 409-420.

Andrews, P. L., Okada, F., Woods, A. J., Hagiwara, H., Kakimoto, S., Toyoda, M., and Matsuki, N. (2000). The emetic and anti-emetic effects of the capsaicin analogue resiniferatoxin in *Suncus murinus*, the house musk shrew. *British Journal of Pharmacology*, **130**, 1247-1254.

Araya, M., McGoldrick, M. C., Klevay, L. M., Strain, J. J., Robson, P., Nielsen, F., Olivares, M., Pizarro, F., Johnson, L., and Poirer, K. A. (2001). Determination of an acute No-Observed-Adverse-Effect Level (NOAEL) for copper in water. *Regulatory Toxicology and Pharmacology*, **34**, 137-145.

Balachandran, S., Kentish, S. E., and Mawson, R. (2006). The effects of both preparation method and season on the supercritical extraction of ginger. *Separation and Purification Technology*, **48** (2 Sp. Iss.), 94-105.

Balladin, D. A., and Headley, O. (1998). Liquid chromatographic analysis of the main pungent principles of solar dried West Indian ginger. *Renewable Energy*, **13**, 531-536.

Balunas, M. J., and Kinghorn, A. D. (2005). Drug discovery from medicinal plants. *Life Sciences*, **78** (5), 431-441.

Barik, A., Mishra, B., Kunwar, A., Kadam, R. M., Shen, L., Dutta, S., Padhye, S., Satpati, A. K., Zhang, H-Y., and Priyadarsini, K. I. (2007). Comparative study of copper(II)-curcumin complexes as superoxide dismutase mimics and free radical scavengers. *European Journal of Medicinal Chemistry*, **42**, 431-439.

Barik, A., Mishra, B., Shen, L., Mohan, H., Kadam, R. M., Dutta, S., Zhang, H-Y., and Priyadarsini, K. I. (2005). Evaluation of a new copper(II)-curcumin complex as superoxide dismutase mimic and its free radical reactions. *Free Radical Biology and Medicine*, **39**, 811-822.

Bazzano, L. A., He, G. O., Loria, C., Vupputuri, S., Myers, L., and Whelton, P. K. (2001). Dietary Potassium Intake and Risk of Stroke: National Health and Nutrition Examination Survey I. *Stroke*, **32**, 1473-1480.

- Bégin, F., Vachon, C., Jones, J. D., Wood, P. J., and Savoie, L. (1989). Effect of dietary fibers on glycemia and insulinemia and on gastrointestinal function in rats. *Canadian Journal of Physiology and Pharmacology*, **67** (10), 1265-1271.
- Bhattarai, S., Tran, V. H., and Duke, C. C. (2007). Stability of [6]-gingerol and [6]-shogaol in simulated gastric and intestinal fluids. *Journal of Pharmaceutical and Biomedical Analysis*, **45** (4), 648-653.
- Bhattarai, S., Tran, V. H., and Duke, C. C. (2001). The stability of gingerol and shogaol in aqueous solutions. *Journal of Pharmaceutical Sciences*, **90** (10), 1658-1664.
- Bioactive Nutrient Explorer*. (2008). (Sigma-Aldrich Co) Retrieved 06 08, 2008, from Sigma-Aldrich: <http://www.sigmaaldrich.com/sigma-aldrich/areas-of-interest/life-science/nutrition-research/learning-center/nutirent-explorer.html>
- Borrelli, F., Capasso, R., Pinto, A., and Izzo, A. A. (2004). Inhibitory effect of ginger (*Zingiber officinale*) on rat ileal motility *in vitro*. *Life Sciences*, **74**, 2889-2896.
- Brown, A. C., Shah, C., Liu, J., Pham, J. T., Zhang, J. G., and Jadus, M. R. (2009). Ginger's (*Zingiber officinale* Roscoe) Inhibition of Rat Colonic Adenocarcinoma Cells Proliferation and Angiogenesis *In Vitro*. *Phytotherapy Research*, **23** (5), 640-645.
- Bukhari, I. A., Khan, R. A., Gilani, A. H., Shah, A. J., Hussain, J., and Ahmad, V. U. (2007). The analgesic, anti-inflammatory and calcium antagonist potential of *Tanacetum artemisioides*. *Archives of Pharmacal Research*, **30** (3), 303-312.
- Carew, M. A., Hague, T., Alani, A., Alhaydari, H., Rayner, M., Vaikunthavasan, K., Lwin, K., Yip, I. Y. M., and MacVinish L. M. (Submitted 2009). Flavonoids enhance ATP-stimulated chloride secretion in Caco-2 cells and mouse colon. *Experimental Physiology*.
- Catchpole, O. J., Grey, J. B., Perry, N. B., Burgess, E. J., Redmond, W. A., and Porter, N. G. (2003). Extraction of chilli, black pepper, and ginger with near-critical CO₂ propane, and dimethyl ether: Analysis of the extracts by quantitative nuclear magnetic resonance. *Journal of Agricultural and Food Chemistry*, **51** (17), 4853-4860.
- Cermak, R., Föllmer, U., and Wolfram, S. (1998). Dietary flavonol quercetin induces chloride secretion in rat colon. *American Journal of Physiology. Gastrointestinal and Liver Physiology*, **275**, G1166-G1172.
- Cermak, R., Vujicic, Z., Kuhn, G., and Wolfram, S. (2000). The secretory response of the rat colon to the flavonol quercetin is dependent on Ca²⁺-calmodulin. *Experimental Physiology*, **85**, 255-261.
- Cermak, R., Vujicic, Z., Scharrer, E., and Wolfram, S. (2001). The impact of different flavonoid classes on colonic Cl⁻ secretion in rats. *Biochemical Pharmacology*, **62** (8), 1145-1151.
- Chaiyakunapruk, N., Kitikannakorn, N., Nathisuwan, S., Leeprakobboon, K., and Leelasattagool, C. (2006). The efficacy of ginger for the prevention of postoperative nausea and vomiting: A meta-analysis. *American Journal of Obstetrics and Gynecology*, **194**, 95-99.
- Chan, S. W., He, J., Lin, G., and Rudd, J. A. (2007). Action of GLP-1 (7-36) amide and exendin-4 on *Suncus murinus* (house musk shrew) isolated ileum. *European Journal of Pharmacology*, **566** (1-3), 185-191.
- Chen, C. Y., Li, Y. W., and Kuo, S. Y. (2009). Effect of [10]-gingerol on [Ca²⁺]_i and cell death in human colorectal cancer cells. *Molecule*, **14** (3), 959-969.

- Chen, C., May, C. K., and Ho, C. T. (1986). High performance liquid chromatographic determination of pungent gingerol compound of ginger (*Zingiber officinale* Roscoe). *Journal of Food Science*, **51** (12), 1364-1365.
- Chen, C.-Y., Liu, T.-Z., Liu, Y.-W., Tseng, W.-C., Liu, R. H., Lu, F.-J., Lin, Y.-S., Kuo, S.-H., and Chen, C.-H. (2007). [6]-Shogaol (alkanone from ginger) induces apoptotic cell death of human hepatoma p53 mutant Mahlavu subline via an oxidative stress-mediated caspase-dependent mechanism. *Journal of Agriculture and Food Chemistry*, **55** (3), 948-954.
- Chen, G., Zhu, L., Liu, Y., Zhou, Q., Chen, H., and Yang, J. (2009). Isoliquiritigenin, a flavonoid from licorice, plays a dual role in regulating gastrointestinal motility *in vitro* and *in vivo*. *Phytotherapy Research*, **23**, 498-506.
- Cheng, F. H., Chan, S. W., and Rudd, J. A. (2008). Contractile effect of tachykinins on *Suncus murinus* (house musk shrew) isolated ileum. *Neuropeptides*, **42**, 671-679.
- Cherny, R. A., Atwood, C. S., Xilinas, M. E., Gray, D. N., Jones, W. D., McLean, C. A., Barnham, K. J., Volitakis, I., Fraser, F. W., Kim, Y. S., Huang, X. D., Goldstein, L. E., Moir, R. D., Lim, J. T., Beyreuther, K., Zheng, H., Tanzi, R. E., Masters, C. L., and Bush, A. I. (2001). Treatment with a copper-zinc chelator markedly and rapidly inhibits β -amyloid accumulation in Alzheimer's disease transgenic mice. *Neuron*, **30**, 665-676.
- Chohan, M., Forster-Wilkins, G., and Opara, E. I. (2008). Determination of the anti-oxidant capacity of culinary herbs subjected to various cooking and storage processes using the ABTS^{•+} radical cation assay. *Plant Foods for Human Nutrition*, **63** (2), 47-52.
- Christofi, F. L. (2008). Purinergic receptors and gastrointestinal secretomotor function. *Purinergic Signal*, **4**, 213-236.
- Chrubasik, S., Pittler, M. H., and Roufogalis, B. D. (2005). *Zingiber rhizoma*: A comprehensive review on the ginger effect and efficacy profiles. *Phytomedicine*, **12**, 684-701.
- Chung, W.-Y., Jung, Y.-J., Surh, Y.-J., Lee, S.-S., and Park, K.-K. (2001). Antioxidative and antitumor promoting effects of [6]-paradol and its homologs. *Mutation Research / Genetic Toxicology and Environmental Mutagenesis*, **496** (1-2), 199-206.
- Ciolino, H. P., Daschner, P. J., and Yeh, G. C. (1999). Dietary flavonols quercetin and kaempferol are ligands of the aryl hydrocarbon receptor that affect CYP1A1 transcription differentially. *The Biochemical Journal*, **340**, 715-722.
- Colbert, E. H. (1958). *Evolution of the vertebrates*. New York: John Wiley and Sons, Inc.
- Collins, J. (2006, August 12). Take the biscuit and ginger up trips. *Body and Soul: The Times Newspaper*, p. 9.
- Cubbedu, L. X., Lindley, C. M., Wetsel, W., Carl, P. L., and Negro-Vilar, A. (1990). Role of angiotensin II and vasopressin in cisplatin-induced emesis. *Life sciences*, **46**, 699-705.
- Cuny, M., Vigneau, E., Le Gall, G., Colquhoun, I., Lees, M., and Rutledge, D. N. (2008). Fruit juice authentication by 1H NMR spectroscopy in combination with different chemometric tools. *Analytical and Bioanalytical Chemistry*, **390**, 419-427.
- Dang, M. N., Takácsová, M., Nguyen, D. V., and Kristiánová, K. (2001). Anti-oxidant activity of essential oils from spices. *Nahrung/Food*, **45** (1), 64-66.

de la Lastra, C. A., and Villegas, L. (2005). Resveratrol as an anti-inflammatory and anti-aging agent: mechanisms and clinical implications. *Molecular Nutrition and Food Research*, **49**, 45-61.

Dedov, V. N., Tran, V. H., Duke, C. C., Connor, M., Christie, M. J., Mandadi, S., and Roufogalis, B. D. (2002). Gingerols: a novel class of vanilloid receptor (VR1) agonists. *British Journal of Pharmacology*, **137**, 793-798.

Di Carlo, G., Autore, G., Izzo, A. A., Maiolino, P., Mascolo, N., Viola, P., Diurno, M. V., and Capasso, F. (1993). Inhibition of intestinal motility and secretion by flavonoids in mice and rats: structure-activity relationships. *Journal of Pharmacy and Pharmacology*, **45** (12), 1054-1059.

Dias, M. C., Spinardi-Barbisan, A. L., Rodrigues, M. A., de Camargo, J. L., Terán, E., and Barbisan, L. F. (2006). Lack of chemopreventive effects of ginger on colon carcinogenesis induced by 1,2-dimethylhydrazine in rats. *Food and Chemical Toxicology: An International Journal Published for the British Industrial Biological Research Association*, **44** (6), 877-884.

Ding, G. H., Naora, K., Hayashibara, M., Katagiri, Y., Kano, Y., and Iwamoto, K. (1991). Pharmacokinetics of [6]-gingerol after intravenous administration in rats. *Chemical and Pharmaceutical Bulletin*, **39**, 1612-1614.

Directgov. (2009). *Common complaints during pregnancy*. Retrieved August 2009, 21, from http://www.direct.gov.uk/en/Parents/HavingABaby/HealthInPregnancy/DG_171354

Dirks, A. J., and Leeuwenburgh, C. (2006). Calorie restriction in humans: potential pitfalls and health concerns. *Mechanisms of Ageing and Development*, **127**, 1-7.

Dubi, N., Gheber, L., Fishman, D., Sekler, I., and Hershinkel, M. (2008). Extracellular zinc and zinc-citrate, acting through a putative zinc-sensing receptor, regulate growth and survival of prostate cancer cells. *Carcinogenesis*, **29** (9), 1692-1700.

Egan, S. K., Tao, S. S., Pennington, J. A., and Bolger, P. M. (2002). US Food and Drug Administrations total diet study: intake of nutritional and toxic elements, 1991-1996. *Food Additives and Contaminants*, **19** (2), 103-125.

Eisenberg, P., Figueroa-Vadillo, J., Zamora, R., Charu, V., Hajdenberg, J., Cartmell, A., Macciocchi, A., and Grunberg, S. (2003). Improved prevention of moderately emetogenic chemotherapy-induced nausea and vomiting with palonosetron, a pharmacologically novel 5-HT₃ receptor antagonist: results of a phase III, single-dose trial versus dolasetron. *Cancer*, **98**, 2473-2482.

Encyclopædia Britannica. (2009). *Pharmaceutical Industry*. Retrieved 08 15, 2009, from Encyclopædia Britannica Online: <http://www.britannica.com/EBchecked/topic/1357082/pharmaceutical-industry>

Ernst, E., and Pittler, M. H. (2000). Efficacy of ginger for nausea and vomiting: a systematic review of randomized clinical trials. *British Journal of Anaesthesia*, **84** (3), 367-371.

Evans, W. C. (2002). *Ginger. Trease and Evans Pharmacognosy* (15 ed.). Edinburgh: W. B. Saunders.

Fairbrother, A., Wenstel, R., Sappington, K., and Wood, W. (2007). Framework for metals risk assessment. *Ecotoxicology and Environmental Safety*, **68**, 145-227.

Faubel, S., Lewis, E. C., Reznikov, L., Ljubanovic, D., Hoke, T. S., Somerset, H., Oh, D. J., Lu, L., Klein, C. L., Dinarello, C. A., and Edelstein, C. L. (2007). Cisplatin-induced acute renal failure is associated with an increase in the cytokines interleukin (IL)-1beta, IL-18, IL-6, and neutrophil infiltration in the kidney. *The Journal of Pharmacology and Experimental Therapeutics*, **322** (1), 8-15.

- Ferguson, L. R., Shelling, A. N., Browning, B. L., Huebner, C., and Petermann, I. (2007). Genes, diet and inflammatory bowel disease. *Mutation Research-Fundamental and Molecular Mechanisms of Mutagenesis*, **622** (1-2), 70-83.
- Fischer-Rasmussen, W., Kjaer, S. K., Dahl, C., and Asping, U. (1991). Ginger treatment of hyperemesis gravidarum. *European Journal of Obstetrics, Gynecology, and Reproductive Biology*, **38** (1), 19-24.
- Fisher, A., and Naughton, D. (2003a). EDTA bis-(methyl tyrosinate): A chelating peptoid peroxynitrite scavenger. *Bioorganic and Medicinal Chemistry Letters*, **13**, 1733-1735.
- Fisher, A., and Naughton, D. (2003b). Redox metal ions and oxidative stress: therapeutic implications. *Proceedings of the Indian National Science Academy. Part B, Biological Sciences*, **69** (4), 453-460.
- Fisher, A. E. (2004). *Novel Agents for the Detection and Suppression of Reactive Oxygen and Nitrogen Species*. Doctorate of Philosophy Thesis, University of Brighton, UK.
- Fisher, A. E., Hague, T. A., Clarke, C. L., and Naughton, D. P. (2004). Catalytic superoxide scavenging by metal complexes of the calcium chelator EDTA and contrast agent EHPG. *Biochemical and Biophysical Research Communications*, **323**, 163-167.
- Fisher, A., and Naughton, D. P. (2005a). Therapeutic chelators for the twenty first Century: new treatments for iron and copper mediated inflammatory and neurological disorders. *Current Drug Delivery*, **2**, 261-268.
- Fisher, A. E., and Naughton, D. P. (2005b). Metal ion chelating peptides with superoxide dismutase activity. *Biomedicine and Pharmacotherapy*, **59**, 158-162.
- Fleming, T. (Ed.). (1998). *PDR for Herbal Medicines* (1st ed.). Montvale, NJ: Medical Economics.
- Forster, D. A., Denning, A., Wills, G., Bolger, M., and McCarthy, E. (2006). Herbal medicine use during pregnancy in a group of Australian women. *BioMed Central Pregnancy and Childbirth*, **6** (21).
- Fouda, A. M., and Berika, M. Y. (2009). Evaluation of the effect of hydroalcoholic extract of *Zingiber officinale* rhizomes in rat collagen-induced arthritis. *Basic and Clinical Pharmacology and Toxicology*, **104** (3), 262-271.
- Fukushi, N., and Gemba, M. (1989). Use of cultured renal epithelial cells for the study of cisplatin toxicity. *Japanese Journal of Pharmacology*, **50**, 247-249.
- Funk, J. L., Frye, J. B., Oyarzo, J. N., and Timmermann, B. N. (2009). Comparative effects of two gingerol-containing *Zingiber officinale* extracts on experimental. *Journal of Natural Products*, **72** (3 Sp. Iss. SI), 403-407.
- Gao, X., Ikuta, K., Takima, M., and Sairenji, T. L. (2001). 12-O-tetradecanoylphorbol-13-acetate induces Epstein-Barr virus reactivation via NF-kappaB and AP-1 as regulated by protein kinase C and mitogen-activated protein kinase. *Virology*, **286**, 91-99.
- García, R., Lemus, I., Rivera, P., and Erazo, S. (1997). Biological and chemical study of paico (*Chenopodium chilense*, Chenopodiaceae). *Journal of Ethnopharmacology*, **57**, 85-88.
- Gavaghan, C. L., Holmes, E., Lenz, E., Wilson, I. D., and Nicholson, J. K. (2000). An NMR-based metabonomic approach to investigate the biochemical consequences of genetic strain differences: application to the C57BL10J and Alpk:ApfCD mouse. *FEBS Letters*, **484**, 169-174.

- Gershon, M. D. (1999). Roles played by 5-hydroxytryptamine in the physiology of the bowel. *Alimentary Pharmacology and Therapeutics*, **13** (Suppl 2), 15-30.
- Ghayur, M. N., Gilani, A. H., Afridi, M. B., and Houghton, P. J. (2005). Cardiovascular effects of ginger aqueous extract and its phenolic constituents are mediated through multiple pathways. *Vascular Pharmacology*, **43**, 234-241.
- Ghayur, M. N., and Gilani, A. H. (2005a). Ginger lowers blood pressure through blockade of voltage-dependent calcium channels. *Journal of Cardiovascular Pharmacology*, **45** (1), 74-80.
- Ghayur, M. N., and Gilani, A. H. (2005b). Pharmacological basis for the medicinal use of ginger in gastrointestinal disorders. *Digestive Diseases and Sciences*, **50** (10), 1889–1897.
- Ghayur, M. N., and Gilani, A. H. (2006). Species differences in the prokinetic effects of ginger. *International Journal of Food Sciences and Nutrition*, **57** (1/2), 65-73.
- Ghayur, M. N., Khan, H., and Gilani, A. H. (2007a). Antispasmodic, bronchodilator and vasodilator activities of (+)-catechin, a natural occurring flavonoid. *Archives of Pharmacal Research*, **30** (8), 970-975.
- Ghayur, M. N., Khan, A. H., and Gilani, A. H. (2007b). Ginger facilitates cholinergic activity possibly due to blockade of muscarinic autoreceptors in rat stomach fundus. *Pakistan Journal of Pharmaceutical Sciences*, **20** (3), 231-235.
- Ghayur, M. N., Gilani, A. H., Ahmed, T., Khalid, A., Nawaz, S. A., Agbedahunsi, J. M., Choudary, M. I., and Houghton, P. J. (2008). Muscarinic, Ca⁺⁺ antagonist and specific butyrylcholinesterase inhibitory activity of dried ginger extract might explain its use in dementia. *Journal of Pharmacy and Pharmacology*, **60**, 1375-1383.
- Gilani, A. H., Shah, A. J., and Yaeesh, S. (2007). Presence of cholinergic and calcium antagonist constituents in *Saussurea lappa* explains its use in constipation and spasm. *Phytotherapy Research*, **21**, 541-544.
- Giroux, M., and Descoteaux, A. (2000). Cyclooxygenase-2 expression in macrophages: Modulation by protein kinase C- α . *Journal of Immunology*, **165** (7), 3985-3991.
- Golding, J. F. (2006). Motion sickness susceptibility. *Autonomic Neuroscience: Basic and Clinical*, **129**, 67–76.
- Gould, S. W., Fielder, M. D., Kelly, A. F., El Sankary, W., and Naughton, D. P. (2009). Anti-microbial pomegranate rind extracts: enhancement by Cu(II) and vitamin C combinations against clinical isolates of *Pseudomonas aeruginosa*. *British Journal of Biomedical Science*, **66** (3), 129-132.
- Govender, A., Kindness, A., and Jonnalagadda, S. B. (2009). Impact of soil quality on elemental uptake by *Zingiber officinale* (ginger rhizome). *International Journal of Environmental Analytical Chemistry*, **89** (5), 367-382.
- Gralla, R., Lichinitser, M., Van Der Vegt, S., Sleeboom, H., Mezger, J., Peschel, C., Tonini, G., Labianca, R., Macciocchi, A., and Aapro, M. (2003). Palonosetron improves prevention of chemotherapy-induced nausea and vomiting following moderately emetogenic chemotherapy: results of a double-blind randomized phase III trial comparing single doses of palonosetron with ondansetron. *Annals of Oncology*, **14**, 1570-1577.
- Grøntved, A., and Hentzer, E. (1986). Vertigo-reducing effects of ginger root. *ORL; Journal for Oto-Rhino-Laryngology and its related specialties*, **48**, 282-286.
- Grøntved, A., Brask, T., Kambskard, J., and Hentzer, E. (1988). Ginger Root Against Seasickness. *Acta Otolaryngol*, **105** (1-2), 45-49.

- Grundy, G. (2006). Signalling the state of the digestive tract. *Autonomic Neuroscience*, **125**, 76-80.
- Grzanna, R., Lindmark, L., and Frondoza, C. G. (2005). Ginger - a herbal medicinal product with broad anti-inflammatory action. *Journal of Medicinal Food*, **8** (2), 125-132.
- Grzanna, R., Phan, P., Polotsky, A., Lindmark, L., and Frondoza, C. G. (2004). Ginger extract inhibits beta-amyloid peptide-induced cytokine and chemokine expression in cultured THP-1 monocytes. *Journal of Alternative and Complementary Medicine*, **10** (6), 1009-1013.
- Gunthorpe, M. J., Benham, C. D., Randall, A., & Davis, J. B. (2002). The diversity in the vanilloid (TRPV) receptor family of ion channels. *Trends in Pharmacological Sciences*, **23** (4), 183-191.
- Gupta, Y. K., and Sharma, M. (2001). Reversal of pyrogallol-induced delay in gastric emptying in rats by ginger (*Zingiber officinale*). *Methods and Findings in Experimental and Clinical Pharmacology*, **23** (9), 501-503.
- Habib, S. H., Makpol, S., Hamid, N. A., Das, S., Ngah, W. Z., and Yusof, Y. A. (2008). Ginger extract (*Zingiber Officinale*) has anti-cancer and anti-inflammatory effects on ethionine-induced hepatoma rats. *Clinics*, **63** (6), 807-813.
- Habsah, M., Amran, M., Mackeen, M. M., Lajis, N. H., Kikuzaki, H., Nakatani, N., et al. (2000). Screening of Zingiberaceae extracts for antimicrobial and anti-oxidant activities. *Journal of Ethnopharmacology*, **72**, 403-410.
- Hague, T., Andrews, P. L., Barker, J., and Naughton, D. P. (2006). Dietary chelators as anti-oxidant enzyme mimetics: implications for dietary intervention in neurodegenerative diseases. *Behavioural Pharmacology*, **17** (5-6), 425-430.
- Hague, T., Andrews, P. R., Barker, J., and Naughton, D. P. (2007). Catalytic anti-oxidants: Is the way forward back to nature? *Screening: Trends in Drug Discovery*, **1**, 18-20.
- Halliwell, B., and Gutteridge, J. (2001). *Free radicals in biology and medicine*. Oxford University Press.
- Halvorenson, B. L., Carlsen, M. H., Phillipis, K. M., Behn, S. K., Jacobs, D. R., and Blomhoff, J. R. (2006). Content of redox-active compounds (i.e. anti-oxidants) in foods consumed in the United States. *The American Journal of Clinical Nutrition*, **84**, 95-135.
- Hämäläinen, M., Nieminem, R., Vuorela, P., Heinonen, M., and Mollanen, E. (2007). Anti-inflammatory effects of flavonoids: genistein, kaempferol, quercetin and daidzein inhibit STAT-1 and NF-B activations, whereas flavone isorhamnetin, naringenin and pelargonidin inhibit only NF-B activation along with their inhibitory effect on iNOS expression and NO production in activated macrophages. *Mediators of Inflammation*, 45673.
- Handa, O., Naito, Y., Shimosawa, M., Kokura, S., Yoshida, N., Matsui, H., Cepinskas, G., Kvietys, P R., and Yoshikawa, T. (2004). Tumor necrosis factor-alpha-induced cytokine-induced neutrophil chemoattractant-1 (CINC-1) production by rat gastric epithelial cells: role of reactive oxygen species and nuclear factor-kappaB. *The Journal of Pharmacology and Experimental Therapeutics*, **309** (2), 670-676.
- Hawlder, M. N., Perera, C., and Tian, M. (2006). Comparison of the Retention of 6-Gingerol in Drying of Ginger Under Modified Atmosphere Heat Pump Drying and other Drying Methods. *Drying Technology*, **24** (1), 51-56.

- Health Survey for England 2002*. (2007, February 8). Retrieved March 5, 2008, from Department of Health: http://www.dh.gov.uk/en/Publicationsandstatistics/PublishedSurvey/HealthSurveyForEngland/Healthsurveysresults/DH_4001334
- Hecht, J. R., Lembo, T., and Chap, L. (1997). Prolonged nausea and vomiting after high dose chemotherapy and autologous peripheral stem cell transplantation in the treatment of high risk breast carcinoma. *Cancer*, **79** (9), 1698-1702.
- Hegde, M. L., Bharathi, P., Suram, A., Venugopal, C., Jagannathan, R., Poddar, P., et al. (2009). Challenges associated with metal chelation therapy in Alzheimer's disease. *Journal of Alzheimer's Disease*, **17** (3), 457-468.
- Heinrich, M., Heneka, B., Ankli, A., Rimpler, H., Sticher, O., and Kostiza, T. (2005). Spasmolytic and antidiarrhoeal properties of the Yucatec Mayan medicinal plant *Casimiroa tetrameria*. *Journal of Pharmacy and Pharmacology*, **57**, 1081-1085.
- Henry, J. A. (Ed.). (2007). *BMA: New Guide To Medicines and Drugs* (7th ed.). London: Dorling Kindersley Limited.
- Hickok, J. T., Roscoe, J. A., Morrow, G. R., and Ryan, J. L. (2007). A phase II/III randomised, placebo-controlled, double-blind clinical trial of ginger (*Zingiber officinale*) for nausea caused by chemotherapy for cancer: A currently accruing URCC CCOP cancer control study. *Supportive Cancer Therapy*, **4** (4), 247-250.
- Highman, B., Hansell, J. R., and White, D. C. (1967). Radioprotective effect of dimethyl sulfoxide in rats. *Radiation Research*, **30**, 563-568.
- Hirsch, A. R., Förch, K., Neidhart, S., Wolf, G., and Carle, R. (2008). Effects of thermal treatments and storage on pectin methylesterase and peroxidase activity in freshly squeezed orange juice. *Journal of Agriculture and Food Chemistry*, **56**, 5691-5699.
- Holmes, E., Foxall, P. J., Spraul, M., Farrant, R. D., Nicholson, J. K., and Lindon, J. C. (1997). 750 MHz ¹H NMR spectroscopy characterisation of the complex metabolic pattern of urine from patients with inborn errors of metabolism: 2-hydroxyglutaric aciduria and maple syrup disease. *Journal of Pharmaceutical and Biomedical Analysis*, **15**, 1647-1659.
- Holtman, S., Clarke, A. H., Scherer, H., and Höhn, M. (1989). The anti-motion sickness mechanisms of ginger. *Acta Oto-Laryngologica*, **108**, 168-174.
- Holzer-Petsche, U., Seitz, H., and Lembeck, F. (1989). Effect of capsaicin on gastric corpus smooth muscle of the rat *in vitro*. *European Journal of Pharmacology*, **162** (1), 29-36.
- Hou, S., Ding, M., and Zhu, J. (2008). Simultaneous determination of silicon and phosphorus in soil and plants by reversed-phase ion-pair chromatography. *Talanta*, **75**, 178-182.
- Houghton, P. J., Howes, M. J., Lee, C. C., and Steventon, G. (2007). Uses and abuses of *in vitro* tests in ethnopharmacology: visualizing an elephant. *Journal of Ethnopharmacology*, **110** (3), 391-400.
- Hu, X. Q., & Lovinger, D. M. (2005). Role of aspartate 298 in mouse 5-HT_{3A} receptor gating and modulation by extracellular Ca²⁺. *Journal of Physiology*, **15** (568(Pt 2)), 381-396.
- Huang, Q., Iwamoto, M., Aoki, S., Tanaka, N., Tajima, K., Yamahara, J., Takaishi, Y., Yoshida, M., Tomimatsu, T., and Tamai, Y. (1991). Anti-5-hydroxytryptamine₃ effect of galanolactone, diterpenoid isolated from ginger. *Chemical and Pharmaceutical Bulletin*, **39** (2), 397-399.

- Hyun, J. S., Satsu, H., and Shimizu, M. (2008). Cadmium induces Interleukin-8 production via NF-kappaB activation in the human intestinal epithelial cell, Caco-2. *Cytokine*, **37**, 26-34.
- Ikegaya, Y., and Matsuki, N. (2002). Vasopressin induces emesis in *Suncus murinus*. *Japanese Journal of Pharmacology*, **89**, 324-326.
- Ippoushi, K., Azuma, K., Ito, H., Horie, H., and Higashio, H. (2003). [6]-Gingerol inhibits nitric oxide synthesis in activated J774.1 mouse macrophages and prevents peroxynitrite-induced oxidation and nitration reactions. *Life Sciences*, **73**, 3427-3437.
- Isa, Y., Miyakawa, Y., Yanagisawa, M., Goto, T., Kang, M.-S., Kawada, T., Morimitsu, Y., Kubota, K., and Tsuda, T. (2008). 6-Shogaol and [6]-gingerol, the pungent of ginger, inhibit TNF- α mediated downregulation of adiponectin expression via different mechanisms in 3T3-L1 adipocytes. *Biochemical and Biophysical Research Communications*, **373**, 429-434.
- Ishiguro, K., Ando, T., Maeda, O., Ohmiya, N., Niwa, Y., Kadomatsu, K., and Goto, H. (2007). Ginger ingredients reduce viability of gastric cancer cells via distinct mechanisms. *Biochemical and Biophysical Research Communications*, **362**, 218-223.
- Iwalewa, E. O., MCGaw, L. J., Naidoo, V., and Eloff, J. N. (2007). Inflammation: the foundation of diseases and disorders. A review of phytomedicines of South African origin used to treat pain and inflammatory conditions. *African Journal of Biotechnology*, **6** (25), 2868-2885.
- Jang, J. H., and Surh, Y. J. (2003). Protective effect of resveratrol on beta-amyloid-induced oxidative PC12 cell death. *Free Radical Biology and Medicine*, **34**, 1100-1110.
- Javid, F. A., and Naylor, J. R. (1999a). Characterization of the 5-hydroxytryptamine receptors mediating contraction in the intestine of *Suncus murinus*. *British Journal of Pharmacology*, **127**, 1867-1875.
- Javid, F. A., and Naylor, R. J. (1999b). Characterisation of 5-HT₂ receptor subtypes in the *Suncus murinus* intestine. *European Journal of Pharmacology*, **381**, 161-169.
- Jiang, H. L., Solyom, A. M., and Gang, D. R. (2005). Characterization of gingerol-related compounds in ginger rhizome (*Zingiber officinale* Rosc.) by high-performance liquid chromatography/electrospray ionization mass spectrometry. *Rapid Communications in Mass Spectrometry*, **19** (20), 2957-2964.
- Jiang, S.-Z., Wang, N.-S., and Mi, S.-Q. (2008). Plasma pharmacokinetics and tissue distribution of [6]-gingerol in rats. *Biopharmaceutics and Drug Disposition*, **29**, 529-537.
- Jolad, S. D., Lantz, R. C., Chen, G. J., Bates, R. B., and Timmerman, B. N. (2004). Commercially processed dry ginger (*Zingiber officinale*): composition and effects on LPS-stimulated PGE₂ production. *Phytochemistry*, **65**, 1937-1954.
- Jolad, S. D., Lantz, R. C., Chen, G. J., Bates, R. B., and Timmermann, B. N. (2005). Commercially processed dry ginger (*Zingiber officinale*): Composition and effect on LPS-stimulated PGE₂ production. *Phytochemistry*, **66**, 1614-1635.
- Jordan, K., Schmoll, H. J., and Aapro, M. S. (2007). Comparative activity of antiemetic drugs. *Critical Reviews in Oncology/Hematology*, **61**, 162-175.
- Jugdaohsingh, R., Calomme, M. R., Robinson, K., Nielsen, F., Anderson, S. H., D'Haese, P., Guesens, P., Loveridge, N., Thompson, R. P., and Powell, J. J. (2008). Increased longitudinal growth in rats on a silicon-depleted diet. *Bone*, **43** (3), 596-606.

Jung, H. W., Yoon, C. H., Park, K. M., Han, H. S., and Park, Y. K. (2009). Hexane fraction of *Zingiberis Rhizoma Crudus* extract inhibits the production of nitric oxide and proinflammatory cytokines in LPS-stimulated BV2 microglial cells via the NF-kappaB pathway. *Food and Chemical Toxicology: An International Journal Published for the British Industrial Biological Research Association*, **47** (6), 1190-1197.

Jung, J. H., Ha, J. Y., Min, K. R., Shibata, F., Nakagawa, H., Kang, S. S., Chang, I. M., and Kim, Y. (1998). Reynosin from *Saussurea lappa* as inhibitor on CINC-1 induction in LPS-stimulated NRK-52E cells. *Planta Medica*, **64** (5), 454-455.

Kawai, T., Kinoshita, K., Koyama, K., and Takahashi, K. (1993). Anti-emetic principles of *Magnolia obvata* bark and *Zingiber officinale* rhizome. *Planta Medica*, **60** (1), 17-20.

Keaney, M., Matthijssens, F., Sharpe, M., Vanfleteren, J., and Gems, D. (2004). Superoxide dismutase mimetics elevate superoxide dismutase activity *in vivo* but do not retard aging in the nematode *Caenorhabditis elegans*. *Free Radical Biology and Medicine*, **37** (2), 239-250.

Kellum, J. M., Budhoo, M. R., Siriwardena, A. K., Smith, E. P., and Jebraili, S. A. (1994). Serotonin induces chloride ion secretion in human jejunal mucosa *in vitro* via a nonneural pathway at 5-HT₄ receptor. *American Journal of Physiology - Gastrointestinal and Liver Physiology*, **267** (3), G357-G363.

Kim, E.-C., Min, J.-K., Kim, T.-Y., Lee, S.-J., Yang, H.-O., Han, S., Kim, Y.-M., and Kwon, Y.-G. (2005a). [6]-Gingerol, a pungent ingredient of ginger, inhibits angiogenesis *in vitro* and *in vivo*. *Biochemical and Biophysical Research Communications*, **335**, 300-308.

Kim, J.-K., Kim, Y., Na, K.-M., Surh, Y.-J., and Kim, T.-Y. (2007). [6]-Gingerol prevents UVB-induced ROS production and COX-2 expression *in vitro* and *in vivo*. *Free Radical Research*, **41** (5), 603-314.

Kim, M. S., Chey, W. D., Owyang, C., and Hasler, W. (1997). Role of plasma vasopressin as a mediator of nausea and gastric slow wave dysrhythmias in motion sickness. *American Journal of Physiology - Gastrointestinal and Liver Physiology*, **272**, G853-G862.

Kim, S. O., Chun, K.-S., Kundu, J. K., and Surh, Y.-J. (2004). Inhibitory effects of [6]-gingerol on PMA-induced COX-2 expression and activation of NF-kappaB and p38 MAPK in mouse skin. *BioFactors*, **21**, 27-31.

Kim, S. O., Kundu, J. K., Shin, Y. K., Park, J.-H., Cho, M.-H., Kim, T.-Y., and Surh, Y.-J. (2005b). [6]-Gingerol inhibits COX-2 expression by blocking the activation of p38 MAP kinase and NF-kappaB in phorbol ester-stimulated mouse skin. *Oncogene*, **24**, 2558-2567.

Kolesnikov, M. P., and Gins, V. K. (2001). Forms of silicon in medicinal plants. *Prikladnaâ Biohimiâ i Mikrobiologiâ*, **37** (5), 616-620.

Kota, N., Krishna, P., and Polasa, K. (2008). Alterations in anti-oxidant status of rats following intake of ginger through diet. *Food Chemistry*, **106**, 991-996.

Krapfenbauer, G., Kinner, M., Gössinger, M., Schönlechner, R., and Berghofer, E. (2006). Effect of thermal treatment on the quality of cloudy apple juice. *Journal of Agriculture and Food Chemistry*, **54**, 5453-5460.

Kuhad, A., Tirkey, N., Pilkhwal, S., and Chopra, K. (2006). [6]-Gingerol prevents cisplatin-induced acute renal failure in rats. *Biofactors*, **26** (3), 189-200.

Laboratory of the Government Chemist. (2007, 12 03). Retrieved 02 23, 2008, from Government Chemist: <http://www.governmentchemist.org.uk/>

(2007). Vanadium. In B. Lagerkvist, and A. Oskarsson, *Handbook on the Toxicology of Metals* (3rd Edition ed., pp. 905-923).

Lamuela-Raventós, R. M., Andrés-Lacueva, C., Permanyer, J., and Izquierdo-Pulido, M. (2001). More anti-oxidants in cocoa. *The Journal of Nutrition*, **131** (3), 834-835.

Lantz, R. C., Chen, G. J., Sarihan, M., Sólyom, A. M., Jolad, S. D., and Timmermann, B. N. (2007). The effect of extracts from ginger rhizome on inflammatory mediator production. *Phytomedicine*, **14** (2-3), 123-128.

Laughton, M. J., Halliwell, B., Evans, P. J., and Hoult, J. R. (1989). Anti-oxidant and pro-oxidant actions of the plant phenolics quercetin, gossypol and myricetin. Effects on lipid peroxidation, hydroxyl radical generation and bleomycin-dependent damage to DNA. *Biochemical Pharmacology*, **38** (17), 2859-2865.

Lee, B.-H., Jung, S.-M., Lee, J.-H., Kim, J.-H., Yoon, I.-S., Lee, J.-H., Choi, S.-H., Lee, S.-M., Chang, C.-G., Kim, H.-C., Han, Y., Paik, H.-D., Kim, Y., and Nah, S.-Y. (2005). Quercetin inhibits the 5-hydroxytryptamine type 3 receptor-mediated ion current by interacting with pre-transmembrane domain 1. *Molecules and Cells*, **20** (1), 69-73.

Lee, S.-H., Cekanova, M., and Baek, S. J. (2008a). Multiple mechanisms are involved in [6]-gingerol-induced cell growth arrest and apoptosis in human colorectal cancer cells. *Molecular Carcinogenesis*, **47**, 197-208.

Lee, S.-H., Seo, E. Y., Kang, N. E., and Kim, W. K. (2008b). [6]-Gingerol inhibits metastasis of MDA-MB-231 human breast cancer cells. *The Journal of Nutritional Biochemistry*, **9** (15), 313-319.

Lee, T.-Y., Lee, K.-C., Chen, S.-Y., and Chang, H.-H. (2009). 6-Gingerol inhibits ROS and iNOS through the suppression of PKC- α . *Biochemical and Biophysical Research Communications*, **382**, 134-139.

Lenntech. (1998). *WHO/EU drinking water standards comparative table*. Retrieved 02 04, 2008, from Lenntech: <http://www.lenntech.com/WHO-EU-water-standards.htm>

Leussink, B. T., Baelde, H. J., Broekhuizen-van den Berg, T. M., de Heer, E., van der Voet, G. B., Slikkerveer, A., Bruijn, J. A., and de Wolff, F. A. (2003). Renal epithelial gene expression profile and bismuth-induced resistance against cisplatin nephrotoxicity. *Human and Experimental Toxicology*, **22**, 535-540.

Levine, M. E., Gillis, M. G., Koch, S. Y., Voss, A. C., Stern, R. M., and Koch, K. L. (2008). Protein and ginger for the treatment of chemotherapy-induced delayed nausea. *Journal of Alternative and Complementary Medicine*, **14** (5), 545-551.

Levine, S. M. (1997). Iron deposits in Multiple Sclerosis and Alzheimer's disease brains. *Brain Research*, **760**, 298-303.

Levy, A. S., Simon, O., Shelly, J., and Gardener, M. (2006). 6-Shogaol reduced chronic inflammatory response in the knees of rats treated with complete Freund's adjuvant. *BMC Pharmacology*, **6** (12).

Lien, H.-C., Sun, W. M., Chen, Y.-H., Kim, H., Hasler, W., and Owyang, C. (2003). Effects of ginger on motion sickness and gastric slow-wave dysrhythmias induced by circularvection. *American Journal of Physiology - Gastrointestinal and Liver Physiology*, **248**, G481-G489.

Life Expectancy. (n.d.). Retrieved March 20, 2008, from <http://www.statistics.gov.uk/cci/nugget.asp?id=168>

Lima, J. T., Almeida, J. R., Barbosa-Filho, J. M., Assis, T. S., Silva, M. S., da-Cunha, E. V., Braz-Filho, R., and Silva, B. A. (2005). Spasmolytic action of diplotropin, a furanoflavan from *Diplotropis ferruginea* Benth.,

involves calcium blockade in guinea pig ileum. *Zeitschrift für Naturforschung - Section B Journal of Chemical Sciences*, **60b**, 1093-1100.

Lin, C.-L., and Lin, J.-K. (2008). Curcumin: a potential cancer chemopreventative agent through suppressing NF- κ B signalling. *Journal of Cancer Molecules*, **4** (1), 11-16.

Lindsay, J., Laurin, D., Verreault, R., Hébert, R., Helliwell, B., Hill, G. B., and McDowell, I. (2002). Risk factors for Alzheimer's disease: A prospective analysis from the Canadian study of health and aging. *American Journal of Epidemiology*, **158** (5), 445-453.

Liu, C.-W., Liang, C.-P., Huang, F. M., and Hsueh, Y.-M. (2006). Assessing the human health risks from exposure of inorganic arsenic through oyster consumption in Taiwan. *The Science of the Total Environment*, **361**, 57-66.

Liu, Y.-L., Malik, N., Sanger, G., Friedman, M. I., and Andrews, P. L. (2005). Pica: A model of nausea? Species differences in response to cisplatin. *Physiology and Behavior*, **85** (3), 271-277.

Luchsinger, J. A., Tang, M.-X., Siddiqui, M., Shea, S., and Mayeux, R. (2004). Alcohol intake and risk of Dementia. *Journal of the American Geriatrics Society*, **52** (4), 540-546.

MacArthur, M., Hold, G. L., and El-Omar, E. M. (2004). Inflammation and Cancer II. Role of chronic inflammation and cytokine gene polymorphisms in the pathogenesis of gastrointestinal malignancy. *American Journal of Physiology - Gastrointestinal and Liver Physiology*, **286**, G515-G520.

Mann, C. D., Neal, C. P., Garcea, G., Manson, M. M., Dennison, A. R., and Berry, D. P. (2009). Phytochemicals as potential chemopreventive and chemotherapeutic agents in hepatocarcinogenesis. *European Journal of Cancer Prevention*, **18** (1), 13-25.

Martinez-Cuesta, M. A., Esplugues, J. V., and Whittle, B. J. (1996). Modulation of nitric oxide of spontaneous motility of the rat isolated duodenum: role of tachykinins. *British Journal of Pharmacology*, **118**, 1335-1340.

Martínez-Flórez, S., González-Gallego, J., Culebras, J. M., and Tuñón, M. J. (2002). Flavonoids: properties and anti-oxidising action. *Nutrición Hospitalaria: Organo Oficial de la Sociedad Española de Nutrición Parenteral y Enteral*, **17** (6), 271-278.

Matsuki, N., Torii, Y., Ueno, S., and Saito, H. (1992). *Suncus murinus* as an experimental animal model for emesis and motion sickness. *Mechanisms and Control of Emesis*, **223**, pp. 323-329.

Matsushima, K., and Oppenheim, J. J. (1989). Interleukin 8 and MCAF: novel inflammatory cytokines inducible by IL 1 and TNF. *Cytokine*, **1** (1), 2-13.

McHale, D., Laurie, W. A., and Sheridan, J. B. (1989). Transformations of the pungent principles in extracts of ginger. *Flavour and Fragrance Journal*, **4**, 9-15.

Mehendale, S. R., Aung, H. H., Yin, J.-J., Lin, E., Fishbein, A., Wang, C.-Z., Xie, J.-T., and Yuan, C.-S. (2004). Effects of anti-oxidant herbs on chemotherapy-induced nausea and vomiting in a rat-pica model. *The American Journal of Chinese Medicine*, **32** (6), 897-905.

Merle, U., Schaefer, M., Ferenci, P., and Stremmel, W. (2007). Clinical presentation, diagnosis and long-term outcome of Wilson's disease: a cohort study. *Gut*, **56**, 115-120.

Meunier, J.-D. (2003). The role of plants in the transfer of silicon at the surface of the continents. *Comptes Rendus Geosciences*, **335**, 1199-1206.

MHRA and Ipsos MORI. (2008). *Public Perceptions of Herbal Medicines. General Public Qualitative and Quantitative Research*. London.

Micklefield, G. H., Redeker, Y., Meister, V., Jung, O., Greving, I., and May, B. (1999). Effects of ginger on gastroduodenal motility. *International Journal of Clinical Pharmacology and Therapeutics*, **37** (7), 341-346.

Morales, M. A., Tortoriello, J., Meckes, M., Paz, D., and Lozoya, X. (1994). Calcium-antagonist effect of quercetin and its relation with the spasmolytic properties of *Psidium guajava* L. *Archives of Medical Research*, **25** (1), 17-21.

Moridani, M. Y., Pourahmad, J., Bui, H., Siraki, A., and O'Brien, P. J. (2003). Dietary flavonoid iron complexes as cytoprotective superoxide radical scavengers. *Free Radical Biology and Medicine*, **34** (2), 243-253.

Morton, L. M., Holford, T. R., Leaderer, B., Zhang, Y., Zahm, S. H., Boyle, P., Flynn, S., Tallini, G., Owens, P. H., Zhang, B., and Zheng, T. (2003). Alcohol use and risk of non-Hodgkin's lymphoma among Connecticut women (United States). *Cancer Causes and Control*, **14**, 687-694.

Motulsky, H. (1995). Choosing a Test. In H. Motulsky, *Intuitive Biostatistics* (1st Edition ed., pp. 297-302). New York: Oxford University Press.

Mowrey, D. B., and Clayson, D. E. (1982). Motion sickness, ginger, and psychophysics. *The Lancet*, **20** (1), 655-657.

Mukaida, N., Harada, A., and Matsushima, K. (1998). Interleukin-8 (IL-8) and monocyte chemoattractant activating factor (MCAF/MCP-1), chemokines essentially involved in inflammatory and immune reactions. *Cytokine Growth Factor Reviews*, **9**, 9-23.

Mulholland, P. J., Ferry, D. R., Anderson, D., Hussain, S. A., Young, A. M., Cook, J. E., Hodgkin, E., Seymour, L. W., and Kerr, D. J. (2001). Pre-clinical and clinical study of QC12, a water-soluble, pro-drug of quercetin. *Annals of Oncology: Official Journal of the European Society for Medical Oncology / ESMO*, **12** (2), 245-248.

Müller, M. H., Liu, C.-Y., Glatzle, J., Weiser, D., Kelber, O., Enck, P., et al. (2006). STW 5 (Iberogast®) reduces afferent sensitivity in the rat small intestine. *Phytomedicine*, **13** (1), 100-106.

Murota, K., and Terao, J. (2003). Antioxidative flavonoid quercetin: implications of its intestinal absorption and metabolism. *Archives of Biochemistry and Biophysics*, **417**, 12-17.

Nakagawa, H., Ikesue, A., Hatakeyama, S., Kato, H., Gotoda, T., Komorita, N., Watanabe, K., and Miyai, H. (1993). Production of an interleukin-8-like chemokine by cytokine-stimulated rat NRK-49F fibroblasts and its suppression by anti-inflammatory steroids. *Biochemical Pharmacology*, **45** (7), 1425-1430.

Nakazawa, T., and Ohsawa, K. (2002). Metabolism of [6]-gingerol in rats. *Life Sciences*, **70**, 2165-2175.

Naora, K., Ding, G., Hayashibara, M., Katagiri, Y., Kano, Y., and Iwamoto, K. (1992). Pharmacokinetics of [6]-gingerol after intravenous administration in rats with acute renal or hepatic failure. *Chemical and Pharmaceutical Bulletin*, **40**, 1295-1298.

NAS/IOM, (2003). *Dietary reference intakes: guiding principles for nutrition labeling and fortification*. Washington, DC: Food and Nutrition Board, Institute of Medicine.

(1997, 1998, 2000, 2001, and 2002). *National Academy of Sciences: Dietary Reference Intakes*.

National Institute of Health. (2009, May 27). *Potassium in diet*. Retrieved June 2, 2009, from MedlinePlus Medical Encyclopedia:

<http://www.nlm.nih.gov/medlineplus/ency/article/002413.htm>

Natural Remedies - Research Centre. (2008). *Zingiber officinale*. Bangalore: Natural Remedies Private Limited.

Naughton, D. P., and Petroczi, A. (2008). The metal ion theory of ageing: dietary hazard quotients beyond radicals. *Immunity Ageing*, 5, 3.

Navari, R. M. (2004). Aprepitant: a neurokinin-1 receptor antagonist for the treatment of chemotherapy-induced nausea and vomiting. *Expert Review of Anticancer Therapy*, 4 (5), 715-724.

Nie, K. (2005, 21, 10). Personal correspondence with T. A. Hague

Norajit, K., Loahakunjit, N., and Kerdchoechuen, O. (2007). Antibacterial effect of five Zingiberaceae essential oils. *Molecules*, 12 (8), 2047-2060.

Ohtsuka, T., Kubota, A., Hirano, T., Watanabe, K., Yoshida, H., Tsurufuji, M., Iizuka, Y., Konishi, K., and Tsurufuji, S. (1996). Glucocorticoid-mediated gene suppression of rate cytokine-induced neutrophil chemoattractant CINC/gro, a member of the interleukin-8 family, through impairment of NF- κ B activation. *The Journal of Biological Chemistry*, 271 (3), 1651-1659.

Ojewole, J. A. (2006). Analgesic, antiinflammatory and hypoglycaemic effects of ethanol extract of *Zingiber officinale* (Roscoe) rhizomes (Zingiberaceae) in mice and rats. *Phytotherapy Research*, 20 (9), 764-772.

O'Leary, F., Feighery, L., Baird, A. W., and Brayden, D. J. (2004a). Anti-secretory effects of a nutraceutical constituent on isolated colonic mucosae. *Association of Veterinary Teachers and Research Workers (Irish Region) 41st Winter Scientific Meeting*, 1. Dublin.

O'Leary, K. A., de Pascual-Tereasa, S., Needs, P. W., Bao, Y.-P., O'Brien, N. M., and Williamson, G. (2004b). Effect of flavonoids and vitamin E on cyclooxygenase-2 (COX-2) transcription. *Mutation Research*, 551, 245-254.

Pan, M. H., Hsieh, M. C., Hsu, P. C., Ho, S. Y., Lai, C. S., Wu, H., and Sang, S., and Ho, C. T. (2008). 6-Shogaol suppressed lipopolysaccharide-induced up-expression of iNOS and COX-2 in murine macrophages. *Molecular Nutrition and Food Research*, 52 (12), 1467-1477.

Panagiotou, E. (2006). *An Investigation of the impact of the intestinal tract on the bioavailability and metabolism of Chinese herbal medicines (CHMs) purported to possess anti-cancer activity*. Master of Philosophy Thesis, Kingston University, UK.

Park, Y. J., Wen, J., Bang, S., Park, S. W., and Song, S. Y. (2006). [6]-gingerol induces cell cycle arrest and cell death of mutant p53-expressing pancreatic cancer cells. *Yonsei Medical Journal*, 47 (5), 688-697.

Penniston, K. L., Nakada, S. Y., Holmes, R. P., and Assimos, D. G. (2008). Quantitative assessment of citric acid in lemon juice, lime juice, and commercially-available fruit juice products. *Journal of Endourology*, 22 (3), 567-570.

Percie du Sert, N. (2009, 14, 07). Personal correspondence with T. A. Hague.

Percy, W. H. (1996). *In Vitro Techniques for the Study of Gastrointestinal Motility*. In T. S. Gaginella (Ed.), *Handbook of Methods in Gastrointestinal Pharmacology* (1st ed., pp. 189-224). New York: CRC Press, Inc.

Peters, M. (Ed.). (2008). *British Medical Association. A-Z Family Medical Encyclopedia* (5th ed.). London: Dorling Kindersley Ltd.

- Phan, P. V., Sohrabi, A., Polotsky, A., Hungerford, D. S., Lindmark, L., and Frondoza, C. G. (2005). Ginger extract components suppress induction of chemokine expression in human synoviocytes. *Journal of Alternative and Complementary Medicine*, **11** (1), 149-154.
- Phillips, S., Hutchinson, S., and Ruggier, R. (1993). *Zingiber officinale* does not affect gastric emptying rates. A randomised, placebo-controlled crossover trial. *Anaesthesia*, **48** (5), 393-395.
- Pokorný, J. (2007). Are natural anti-oxidants better and safer than synthetic anti-oxidants? *European Journal of Lipid Science and Technology*, **109** (6), 629-642.
- Pongrojpraw, D. (2006). A randomized comparison of ginger and dimenhydrinate in the treatment of nausea vomiting in pregnancy. *American Journal of Obstetrics and Gynecology*, **195** (6), S92.
- Prystai, E., Prystai, M. S., Constance, V., Kies, P. D., Judy, A., and Driskell, P. D. (1999). Calcium, copper, iron, magnesium and zinc utilization of humans as affected by consumption of black, decaffeinated black and green teas. *Nutrition Research*, **19** (2), 167-177.
- Qian, Q.-H., Yue, W., Wang, Y.-X., Yang, Z.-H., Liu, Z.-T., and Chen, W.-H. (2009). Gingerol inhibits cisplatin-induced vomiting by down regulating 5-hydroxytryptamine, dopamine and substance P expression in minks. *Archives of Pharmacal Research*, **32** (4), 565-573.
- Rababah, T. M., Hettiarachchy, N. S., and Horax, R. (2004). Total phenolics and anti-oxidant activities of fenugreek, green tea, black tea, grape seed, ginger, rosemary, gotu kola, and ginkgo extracts, vitamin E and tert-Butylhydroquinone. *Journal of Agricultural and Food Chemistry*, **52**, 5183-5186.
- Rai, S., Mukherjee, K., Mal, M., Wahile, A., Saha, B. P., and Mukherjee, P. K. (2006). Determination of [6]-gingerol in ginger (*Zingiber officinale*) using high-performance thin-layer chromatography. *Journal of Separation Science*, **29** (15), 2292-2295.
- Rainbird, A. L., and Low, A. G. (1986). Effect of various types of dietary fibre on gastric emptying in growing pigs. *British Journal of Nutrition*, **55**, 111-121.
- Royal Botanic Gardens. (2009, July 23). Banking on Life Exhibition. Kew.
- Rudd, J. A., and Wai, M. K. (2001). Genital grooming and emesis induced by vanilloids in *Suncus murinus*, the house musk shrew. *European Journal of Pharmacology*, **422** (1-3), 185-195.
- Rui, Y. K., Yu, Q. Q., Jin, Y. H., Guo, J., and Luo, Y. B. (2007). Application of ICP-MS to the detection of forty elements in wine. *Guang Pu Xue Yu Guang Pu Fen Xi*, **27**, 1015-1017.
- Sadraei, H., Asghari, G., and Hekmatti, A. A. (2003). Antispasmodic effect of three fractions of hydroalcoholic extract of *Pycnocyclus spinosa*. *Journal of Ethnopharmacology*, **86**, 187-190.
- Saha, S., Smith, R. M., Lenz, E., and Wilson, I. D. (2003). Analysis of a ginger extract by high-performance liquid chromatography coupled to nuclear magnetic resonance spectroscopy using superheated deuterium oxide as the mobile phase. *Journal of Chromatography A*, **991** (1), 143-150.
- Sahu, S. C., and Gray, G. C. (1994). Kaempferol-induced nuclear DNA damage and lipid peroxidation. *Cancer Letters*, **85** (2), 159-164.
- Sahu, S. C., and Washington, M. C. (1992). Effect of ascorbic acid and curcumin on quercetin-induced nuclear DNA damage, lipid peroxidation and protein degradation. *Cancer Letters*, **63** (3), 237-241.

- Samai, M., Hague, T., Naughton, D. P., Gard, P. R., and Chatterjee, P. K. (2008). Reduction of paraquat-induced renal cytotoxicity by manganese and copper complexes of EGTA and EHPG. *Free Radical Biology and Medicine*, **44**, 711-721.
- Sánchez de Medina, F., Galvez, J., Gonzalez, M., Zarzuelo, A., and Barrett, K. (1997). Effects of quercetin on epithelial chloride secretion. *Life Sciences*, **61** (20), 2049-2055.
- Sanger, G. J., and Andrews, P. L. (2006). Treatment of nausea and vomiting: Gaps in our knowledge. *Autonomic Neuroscience: Basic and Clinical*, **129**, 3-16.
- Scheid, V. (2008, June 12). Why interdisciplinary research is not an option but a necessity for integrative healthcare: The case of Chinese medicine. *WestFocus. Better Networks for Better Health Event*. London.
- Schempp, H., Weiser, D., Kelber, O., and Elstner, E. F. (2006). Radical scavenging and anti-inflammatory properties of STW-5 (Iberogast®) and its components. *Phytomedicine*, **13** (1), 36-44.
- Schweiggert, U., Schieber, A., and Carle, R. (2005). Inactivation of peroxidase, polyphenoloxidase, and lipoxygenase in paprika and chili powder after immediate thermal treatment of the plant material. *Innovative Food Science and Emerging Technologies*, **6** (4), 403-411.
- Schwertner, H. A., and Rios, D. C. (2007). High-performance liquid chromatographic analysis of [6]-gingerol, [8]-gingerol, [10]-gingerol, and [6]-shogaol in ginger-containing dietary supplements, spices, teas, and beverages. *Journal of Chromatography B-Analytical Technologies in the Biomedical and Life Sciences*, **856** (1-2), 41-47.
- Seidelin, J. B., and Nielsen, O. H. (2009). Epithelial apoptosis: cause or consequence of ulcerative colitis? *Scandinavian Journal of Gastroenterology*, **44** (12), 1429-1434.
- Setty, A. R., and Sigal, L. H. (2005). Herbal medications commonly used in the practice of rheumatology: Mechanisms of action, efficacy, and side effects. *Seminars in Arthritis and Rheumatism*, **34** (6), 773-784.
- Sharma, M., and Gupta, Y. K. (2002). Chronic treatment with *trans* resveratrol prevents intracerebroventricular streptozotocin induced cognitive impairment and oxidative stress in rats. *Life Sciences*, **71**, 2489-2498.
- Sharma, R. K., and Agrawal, M. (2005). Biological effects of heavy metals: An overview. *Journal of Environmental Biology / Academy of Environmental Biology, India*, **26**, S301-S313.
- Sharma, S. S., and Gupta, Y. K. (1998). Reversal of cisplatin-induced delay in gastric emptying in rats by ginger (*Zingiber officinale*). *Journal of Ethnopharmacology*, **62**, 49-55.
- Sharma, S. S., Kochupillai, V., Gupta, S. K., Seth, S. D., and Gupta, Y. K. (1997). Antiemetic efficacy of ginger (*Zingiber officinale*) against cisplatin-induced emesis in dogs. *Journal of Ethnopharmacology*, **57**, 93-96.
- Shen, L., Zhang, H.-Y., and Ji, H.-F. (2005). A theoretical study on Cu(II)-chelating properties of curcumin and its implications for curcumin as a multipotent agent to combat Alzheimer's disease. *Journal of Molecular Structure: THEOCHEM*, **757**, 199-202.
- Sigma-Aldrich (2008). Material Safety Data Sheets, Product Number D5879, CAS-No. 67-68-5. Version 2.0.
- Simpson, J. A., and Weiner, E. S. (Eds.). (1989). *The Oxford English Dictionary* (2nd ed., Vol. X). Oxford: Clarendon Press.

- Singh, H. K., Yachha, S. K., Saxena, R., Gupta, A., Nagana Gowda, G. A., Bhandari, M., and Khetrpal, C. L. (2003). A new dimension of ¹H-NMR spectroscopy in assessment of liver graft dysfunction. *NMR In Biomedicine*, **16**, 185-188.
- Singh, S., and Aggarwal, B. B. (1995). Activation of transcription factor NF- κ B is suppressed by curcumin (diferuloylmethane)*. *The Journal of Biological Chemistry*, **270** (42), 24995-25000.
- Skoog, D. A., West, D. M., Holler, F. J., and Crouch, S. R. (1999). *Analytical Chemistry: An Introduction* (7th ed.). Brooks / Cole.
- Slimestad, R., Fossen, T., and Vågen, I. M. (2007). Onions: a source of unique dietary flavonoids. *Journal of Agricultural and Food Chemistry*, **55** (25), 10067-10080.
- Smith, C., Crowther, C., Willson, K., Hotham, N., and McMillian, V. (2004). A randomized controlled trial of ginger to treat nausea and vomiting in pregnancy. *Obstetrics and Gynecology*, **103**, 639-645.
- Soares, S. S., Martins, H., Gutiérrez-Merino, C., and Aureliano, M. (2008). Vanadium and cadmium *in vivo* effects in teleost cardiac muscle: Metal accumulation and oxidative stress markers. *Comparative Biochemistry and Physiology. C, Comparative Pharmacology and Toxicology*, **147**, 168-178.
- Someya, A., Horie, S., Yamamoto, H., and Murayama, T. (2003). Modifications of capsaicin-sensitive neurons in isolated guinea pig ileum by [6]-gingerol and lafutidine. *Journal of Pharmacological Sciences*, **92**, 359-366.
- Son, D. O., Satsu, H., Kiso, Y., and Totsuka, S. (2008). Inhibitory effect of carnosine on interleukin-8 production in intestinal epithelial cells through translational regulation. *Cytokine*, **42** (2), 265-276.
- Stewart, J. J., Wood, M. J., Wood, C. D., and Mims, M. E. (1991). Effects of ginger on motion sickness susceptibility and gastric function. *Pharmacology*, **42** (2), 111-120.
- Stoilova, I., Krastanov, A., Stoyanova, A., Denev, P., and Gargova, S. (2007). Anti-oxidant activity of a ginger extract (*Zingiber officinale*). *Food Chemistry*, **102**, 764-770.
- Stott, J. R., Hubble, M. P., and Spencer, M. B. (1984). A double-blind comparative trial of powdered ginger root, hyosine hydrobromide, and cinnarizine in the prophylaxis of motion sickness induced by cross coupled stimulation. *Motion Sickness: Mechanisms, prediction, prevention and treatment. AGARD Conference Proceedings No. 372*, (pp. 39-2 - 39-6).
- Strausak, D., Mercer, J. F., Dieter, H. H., Stremel, W., and Multhaup, G. (2001). Copper in disorders with neurological symptoms: Alzheimer's, Menkes and Wilson diseases. *Brain Research Bulletin*, **55**, 175-185.
- Surh, Y. J., Lee, E., and Lee, J. M. (1998). Chemoprotective properties of some pungent ingredients present in red pepper and ginger. *Mutation Research*, **402** (1-2), 259-267.
- Takaishi, K., Ohtuka, T., Tsuneyoshi, S., Maehara, N., Harada, M., Yoshida, H., Watanabe, K., and Tsurufuji, S. (2000). Inhibition of the production of rat cytokine-induced neutrophil chemoattractant (CINC)-1, a member of the interleukin-8 family, by adenovirus-mediated overexpression of I κ B α . *Journal of Biochemistry*, **127**, 511-516.
- Takeda, N., Hasegawa, S., Morita, M., and Matsunaga, T. (1993). Pica in rats is analogous to emesis: an animal model in emesis research. *Pharmacology, Biochemistry, and Behavior*, **45** (4), 817-821.
- Talhok, R. S., Karam, C., Fostok, S., El-Jouni, W., and Barbour, E. K. (2007). Mini-Review: Anti-Inflammatory bioactivities in plant extracts. *Journal of Medicinal Food*, **10** (1), 1-10.

- Tammali, R., Ramana, K. V., and Srivastava, S. K. (2007). Aldose reductase regulates TNF- α induced PGE2 production in human colon cancer cells. *Cancer Letters*, **252**, 299-306.
- Tapsell, L. C., Hemphill, I., Cobiac, L., Patch, C. S., Sullivan, D. R., Fenech, M., Roodenrys, S., Keogh, J. B., Clifton, P. M., Williams, P. G., Fazio, V. A., and Inge, K. E. (2006). Health benefits of herbs and spices: the past, the present, the future. *The Medical Journal of Australia*, **185** (4 Suppl), S4-S24.
- Thomas, K. W., Pellizari, E. D., and Berry, M. R. (1999). Population-based dietary intakes and tap water concentrations for selected elements in the EPA Region V National Exposure Assessment Survey (NHEXAS). *Journal of Exposure Analysis and Environmental Epidemiology*, **9** (5), 402-413.
- Thomas, X. (2006). Highlights in the history of leukaemia - a historical review from the beginnings to current therapeutic developments. *Haema*, **9** (2), 191-211.
- Tjendraputra, E., Tran, V. H., Liu-Brennan, D., Roufogalis, B. D., and Duke, C. C. (2001). Effect of ginger constituents and synthetic analogues on cyclooxygenase-2 enzyme in intact cells. *Bioorganic Chemistry*, **29**, 156-163.
- Torii, Y., Mutoh, M., Saito, H., and Matsuki, N. (1993). Involvement of free radicals in cisplatin-induced emesis in *Suncus murinus*. *European Journal of Pharmacology - Environmental Toxicology and Pharmacology Section*, **248**, 131-135.
- Torii, Y., Saito, H., and Matsuki, N. (1991). 5-Hydroxytryptamine is emetogenic in the house musk shrew, *Suncus murinus*. *Naunyn-Schmiedeberg's Archives of Pharmacology*, **344** (5), 564-567.
- Torii, Y., Saito, H., and Matsuki, N. (1994). Induction of emesis in *Suncus murinus* by pyrogallol, a generator of free radicals. *British Journal of Pharmacology*, **111** (2), 431-434.
- Tremont-Lukats, I. W., González-Barboteo, J., Bruera, E., and Brescia, F. J. (2004). Meta-analysis of neurokinin-1 receptor antagonists (NK-1 RA) for chemotherapy-induced nausea and vomiting (CINV). *Journal of Clinical Oncology: ASCO Annual Meeting Proceedings (Post-Meeting Edition)*, **22** (14S), 8407.
- Tripathi, S., Bruch, D., and Kittur, D. S. (2008). Ginger extract inhibits LPS induced macrophage activation and function. *BMC Complementary and Alternative Medicine*, **8** (1).
- Truelsen, T., Thudium, D., and Grønbaek, M. (2002). Amount and type of alcohol and risk of dementia: The Copenhagen City Heart Study. *Neurology*, **59** (9), 1313-1319.
- Tyler, D. B., and Bard, P. (1949). Motion Sickness.
- Ueno, S., Matsuki, N., and Saito, H. (1988). *Suncus murinus* as a new experimental model for motion sickness. *Life Sciences*, **43** (5), 413-420.
- Ueno, S., Matsuki, N., and Saito, H. (1987). *Suncus murinus*: A New Experimental Model in Emesis Research. *Life Sciences*, **41**, pp. 513-518.
- van de Kerkhof, E. G., de Graaf, I. A., and Groothuis, G. M. (2007). *In vitro* methods to study intestinal drug metabolism. *Current Drug Metabolism*, **8** (7), 658-675.
- Vera, G., Chiarlone, A., Martin, M. I., and Abalo, R. (2006). Altered feed behaviour induced by long-term cisplatin in rats. *Autonomic Neuroscience: Basic and Clinical*, **126**, 81-92.
- Vingtdeux, V., Dreses-Werringloer, U., Zhao, H., Davies, P., and Marambaud, P. (2008). Therapeutic potential of resveratrol in Alzheimer's disease. *BMC Neuroscience*, **9** (Suppl 2:S6).

- Vutyavanich, T., Kraissarin, T., and Ruangsri, R. (2001). Ginger for nausea and vomiting in pregnancy: randomized, double-masked, placebo-controlled trial. *Obstetrics and Gynecology*, **97** (4), 577-582.
- Wagner, H., and Blatt, S. (2001). *Plant Drug Analysis. A Thin Layer Chromatography Atlas* (2nd ed.). Berlin, Heidelberg, New York: Springer-Verlag.
- Wan Pui Chu, C. (2004). *Action of Pungent and Non-Pungent Vanilloids on the Emetic Reflex and Mechanisms Modulation Temperature and Grooming in Suncus murinus*. Master of Philosophy Thesis, The Chinese University of Hong Kong, Hong Kong.
- Watson, D. G., and Oliveira, E. J. (1999). Solid-phase extraction and gas chromatography-mass spectrometry determination of kaempferol and quercetin in human urine after consumption of Ginkgo biloba tablets. *Journal of Chromatography B*, **723**, 203-210.
- Wenzel, E., Soldo, T., Erbersdobler, H., and Somoza, V. (2005). Bioactivity and metabolism of trans-veratrol orally administered to Wistar rats. *Molecular Nutrition and Food Research*, **49**, 482-494.
- Wohlmuth, H., Leach, D. N., Smith, M. K., and Myers, S. P. (2005). Gingerol content of diploid and tetraploid clones of ginger (*Zingiber officinale* Roscoe). *Journal of Agricultural and Food Chemistry*, **53** (14), 5772-5778.
- Wong, C. (2007, 01 02). *5 Ways to Cleanse Your Mind and Body*. Retrieved 08 15, 2009, from Alternative Medicine: http://altmedicine.about.com/od/optimumhealthessentials/a/5_Tips_Cleanse.htm
- Wong, J (2009) *Grow Your Own Drugs*. BBC Two Productions.
- Wood, C. D., Manno, J. E., Wood, M. J., Manno, B. R., and Mims, M. E. (1988). Comparison of efficacy of ginger with various antimotion sickness drugs. *Clinical Research Practices and Drug Regulatory Affairs*, **6** (2), 129-136.
- Wu, K.-L., Rayner, C. K., Chuah, S.-K., Changchien, C.-S., Lu, S.-N., Chiu, Y.-C., et al. (2008). Effects of ginger on gastric emptying and motility in healthy humans. *European Journal of Gastroenterology and Hepatology*, **20** (5), 436-440.
- Xie, Q. W., Kashiwabara, Y., and Nathan, C. (1994). Role of transcription factor NF-kappa B/Rel in induction of nitric oxide synthase. *Journal of Biological Chemistry*, **269**, 4705-4708.
- Yamahara, J., Rong, H. Q., Naitoh, Y., Kitani, T., and Fujimura, H. (1989). Inhibition of cytotoxic drug-induced vomiting in *Suncus* by a ginger constituent. *Journal of Ethnopharmacology*, **27**, 353-355.
- Yamasaki, S., Sakata-Sagawa, K., Hasegawa, A., Suzuki, T., Kabu, K., Sato, E., et al. (2007). Zinc is a novel intracellular second messenger. *Journal of Cell Biology*, **177**, 637-645.
- Yang, C. S. (1997). Inhibition of carcinogenesis by tea. *Nature*, **389**, 134-135.
- Yang, Y., Kinoshita, K., Koyama, K., Takahashi, K., Kondo, S., and Watanabe, K. (2002). Structure-antiemetic activity of some diarylheptanoids and their analogues. *Phytomedicine*, **9**, 146-152.
- Yang, Z. H., Yu, H. J., Pan, A., Du, J. Y., Ruan, Y. C., Ko, W. H., Chan, H. C., and Zhou, W. L. (2008). Cellular mechanisms underlying the laxative effect of flavonol naringenin on rat constipation model. *PLoS One*, **3**, e3348.
- Yates, B. J., Miller, A. D., and Lucot, J. B. (1998). Physiological basis and pharmacology of motion sickness. *Brain Research Bulletin*, **47**, 395-406.

- Yoshikawa, M., Hatakeyama, S., Chatani, N., Nishino, Y., and Yamahara, J. (1993). Qualitative and quantitative analysis of bioactive principles in *Zingiberis Rhizoma* by means of high performance liquid chromatography and gas liquid chromatography. *Yakugaku Zasshi : Journal of the Pharmaceutical Society of Japan*, **113** (4), 307-15.
- Young, H.-Y., Luo, Y.-L., Cheng, H.-Y., Hsieh, W.-C., Liao, J.-C., and Peng, W.-H. (2005). Analgesic and anti-inflammatory activities of [6]-gingerol. *Journal of Ethnopharmacology*, **96**, 207-210.
- Yu, Y. J., Huang, T. M., Yang, B., Liu, X., and Duan, G. L. (2007). Development of gas chromatography-mass spectrometry with microwave distillation and simultaneous solid-phase microextraction for rapid determination of volatile constituents in ginger. *Journal of Pharmaceutical and Biomedical Analysis*, **43** (1), 24-31.
- Yue, G. G., Yip, T. W., Huang, Y., and Ko, W. H. (2004). Cellular mechanism for potentiation of Ca^{2+} mediated Cl^- secretion by the flavonoid baicalein in intestinal epithelia. *Journal of Biological Chemistry*, **279**, 39310-39316.
- Zhao, W., and Robbins, M. E. (2009). Inflammation and chronic oxidative stress in radiation-induced late normal tissue injury: therapeutic implications. *Current medicinal chemistry*, **16** (2), 130-143.
- Zick, S. M., Djuric, Z., Ruffin, M. T., Litzinger, A. J., Normolle, D. P., Alrawi, S., Feng, M. R., and Brenner, D. E. (2008). Pharmacokinetics of [6]-gingerol, [8]-gingerol, [10]-gingerol, and [6]-shogaol and conjugate metabolites in healthy human subjects. *Cancer Epidemiology, Biomarkers and Prevention*, **17** (8), 1930-1936.

0A

APPENDICES

Appendix 1 – Papers in Publication

1. Hague, T., Petroczi, A., Andrews, P.R., Barker, J. and Naughton, D.P. (2008) Determination of metal ion content of beverages and estimation of target hazard quotients: a comparative study. *Chemistry Central Journal*. 2, 13.
2. Samai, M., Hague, T., Naughton, D.P., Gard, P.R. and Chatterjee, P.K. (2008) Reduction of Paraquat-Induced Renal Cytotoxicity by Manganese and Copper Complexes of EGTA and EHPG. *Free Radical Biology and Medicine*. 44, 711-721.
3. Hague, T., Andrews, P.R., Barker, J., and Naughton, D.P. (2007) Catalytic Anti-oxidants: Is the Way Forward Back to Nature? *Screening: Trends in Drug Discovery*. 1, 18-20.
4. Hague, T., Andrews, P. L. R., Barker, J. and Naughton, D. P. (2006) Dietary Chelators as Anti-oxidant Enzyme Mimetics: Implications for Dietary Intervention in Neurodegenerative Diseases. *Behavioural Pharmacology*, 17, 425-430

Research article

Open Access

Determination of metal ion content of beverages and estimation of target hazard quotients: a comparative study

Theresa Hague¹, Andrea Petroczi¹, Paul LR Andrews², James Barker³ and Declan P Naughton*¹

Address: ¹School of Life Sciences, Kingston University, Kingston upon Thames, Surrey KT1 2EE, UK, ²Division of Basic Medical Sciences, St George's University of London, London SW17 0RE, UK and ³School of Pharmacy and Chemistry, Kingston University, London KT1 2EE, UK

Email: Theresa Hague - T.Hague@kingston.ac.uk; Andrea Petroczi - A.Petroczi@kingston.ac.uk; Paul LR Andrews - pandrews@agul.ac.uk; James Barker - J.Barker@kingston.ac.uk; Declan P Naughton* - D.Naughton@kingston.ac.uk

* Corresponding author

Published: 25 June 2008

Received: 25 March 2008

Chemistry Central Journal 2008, 2:13 doi:10.1186/1752-153X-2-13

Accepted: 25 June 2008

This article is available from: <http://journal.chemistrycentral.com/content/2/1/13>

© 2008 Hague et al

This is an Open Access article distributed under the terms of the Creative Commons Attribution License (<http://creativecommons.org/licenses/by/2.0>), which permits unrestricted use, distribution, and reproduction in any medium, provided the original work is properly cited.

Abstract

Background: Considerable research has been directed towards the roles of metal ions in nutrition with metal ion toxicity attracting particular attention. The aim of this study is to measure the levels of metal ions found in selected beverages (red wine, stout and apple juice) and to determine their potential detrimental effects via calculation of the Target Hazard Quotients (THQ) for 250 mL daily consumption.

Results: The levels (mean \pm SEM) and diversity of metals determined by ICP-MS were highest for red wine samples (30 metals totalling 5620.54 ± 123.86 ppb) followed by apple juice (15 metals totalling 1339.87 ± 10.84 ppb) and stout (14 metals totalling 464.85 ± 46.74 ppb). The combined THQ values were determined based upon levels of V, Cr, Mn, Ni, Cu, Zn and Pb which gave red wine samples the highest value (5100.96 ± 118.93 ppb) followed by apple juice (666.44 ± 7.67 ppb) and stout (328.41 ± 42.36 ppb). The THQ values were as follows: apple juice (male 3.11, female 3.87), stout (male 1.84, female 2.19), red wine (male 126.52, female 157.22) and ultra-filtered red wine (male 110.48, female 137.29).

Conclusion: This study reports relatively high levels of metal ions in red wine, which give a very high THQ value suggesting potential hazardous exposure over a lifetime for those who consume at least 250 mL daily. In addition to the known hazardous metals (e.g. Pb), many metals (e.g. Rb) have not had their biological effects systematically investigated and hence the impact of sustained ingestion is not known.

Background

The widespread roles of metal ions in health and disease range from the requirement for intake of essential trace elements to toxicity associated with metal overload. Numerous studies have quantified levels of toxic metal ions in common foodstuffs and in some cases these

results have been extended by statistical analyses to generate 'target hazard quotients' (THQ) for a limited number of foodstuffs relating to individual and combinations of metals [1-5]. Despite regulatory controls, numerous sources of metal ingestion have been recently reported including contaminated drinking water, seafood, breast

milk, herbal medicines, smoking, together with plants and animals used in the diet [1-10]. Between January and November 2007, some 2,680 food recalls were monitored by the Laboratory of the Government Chemist (UK) mainly owing to contamination [11]. Of these, 8% (216) were for metal contamination with 79% (171) of these recalls being for seafood with the rank order of metals involved being Hg (58%), Cd (26%), Pb (10.5%), As (3.5%), Ba (<1%) and Zn (<1%). Serious incidents of occasional human exposure to metals have resulted from lapses in quality control measures or errors in processing [11].

In addition to the endogenous metal ion content of foodstuffs, numerous steps during processing and packaging may add to the metal ion load. This is exemplified by the authorised use of the many metal containing additives such as the 'antioxidant' stannous chloride (E512). Perhaps, the constant exposure that accompanies repetitive ingestion of foodstuffs that contain known low levels of metal ions is of more consequence. A key potential source of exposure is processed beverages that are known to contain metals, and frequent exposure may result in accumulative effects. Common beverages are assessed for their metal content with regulatory controls over maximum permitted levels in place in most countries. These permitted levels are subject to frequent review and revisions should take account of varying dietary habits in different populations and countries. The metal ion content in beverages has been determined in several studies for consumer protection against contamination, method development or an evaluation of the nutritional status [12-15]. The metal profiles have been reportedly used for the determination of the region of origin [16,17]. The majority of studies report levels of metal ions below the regulatory safe limits for that region. However, studies rarely report the combined effects of frequent ingestion of multiple metal ions which can be addressed as a function of the quantified level of concern in the form of THQ values arising from individual or combined metal concentrations. No studies have reported the individual and combined THQ values for common beverages.

The extension of lifespan in the Western world, in addition to dietary exposure accounting for the largest exposure to metals, warrants regular reviews of the total potential accumulation load over a lifetime. Many metal ions are associated with enhanced oxidative stress, inflammation and cancer [18,19]. The aim of this paper is to assess the levels of metal ions in three processed, commercially-available beverages. In total, the levels of thirty metal ions have been assessed by inductively coupled plasma-mass spectrometry (ICP-MS) for intact red wine, stout and apple juice which were selected as representative processed beverages arising from plants. In order to esti-

mate the levels of metals that are non-protein bound, the levels in the beverage with highest levels (red wine) have been assessed in both the intact fluid and after ultra-filtration. These data were used to calculate the THQ values for key potentially toxic metal ions separately for females and males.

Results

Metal contents of beverages

The concentrations of thirty metal ions assessed by ICP-MS are shown in Figures 1 and 2 (for exact values, see additional file 1: Quantification of metal ions in whole apple juice and stout and additional file 2: Quantification of metal ions in red wine pre- and post- ultra-filtration) for red wine, stout and apple juice in parts per billion with the corresponding standard errors of the mean (SEM) values. Concentrations are presented in Figures 1 and 2 in three ranges for convenience: high (up to 1,250 ppb); medium (up to 9 ppb); low (up to 1.5 ppb). Wide variations in the types and levels of metals were detected in the beverages, ranging from some fifteen metals in the apple juice and stout, to thirty in the red wine sample (see additional file 1: Quantification of metal ions in whole apple juice and stout and additional file 2: Quantification of metal ions in red wine pre- and post- ultra-filtration) based on the lower limits of detection (see additional file 2: Quantification of metal ions in red wine pre- and post- ultra-filtration). Figure 1 clearly shows that intact red wine contains the highest levels and diversity of metals which includes several metals that are not detected in the other beverages (e.g. V, Ni, Sn, Cd, and a range of lanthanides). In contrast, many metals were detected in all three beverages (e.g. Cr, Rb, Co, Pb).

In the apple juice samples, the predominant metals are, in order of concentration, Rb>Mn>Cr>Zn>Cu, with a total measured metal ion concentration of $1,339.87 \pm 10.84$ ppb. For stout the total metal concentration was 464.86 ± 46.74 ppb in the order of Cr>Rb>Mn>Zn>Cu.

The total metal ion content measured for the 30 elements was $5,620.54 \pm 123.86$ ppb for red wine, with the order being Mn>Cr>Zn>Rb>Cu>V for the elements found at the highest concentrations. Red wine contained the most varied composition of metal ions which were also in the highest quantities (Figure 1 and see additional file 2: Quantification of metal ions in red wine, pre- and post- ultra-filtration). Owing to the high levels of potentially hazardous metal ions, for these analyses, the results were recorded for both the intact beverages and the filtrates after ultra-filtration to remove the components above a molecular weight of 5,000 (nominal). In red wine, a considerable proportion of the metal ion content exists after ultrafiltration. Fourteen metals had lower percentage levels in the ultrafiltrate that were statistically significant (see

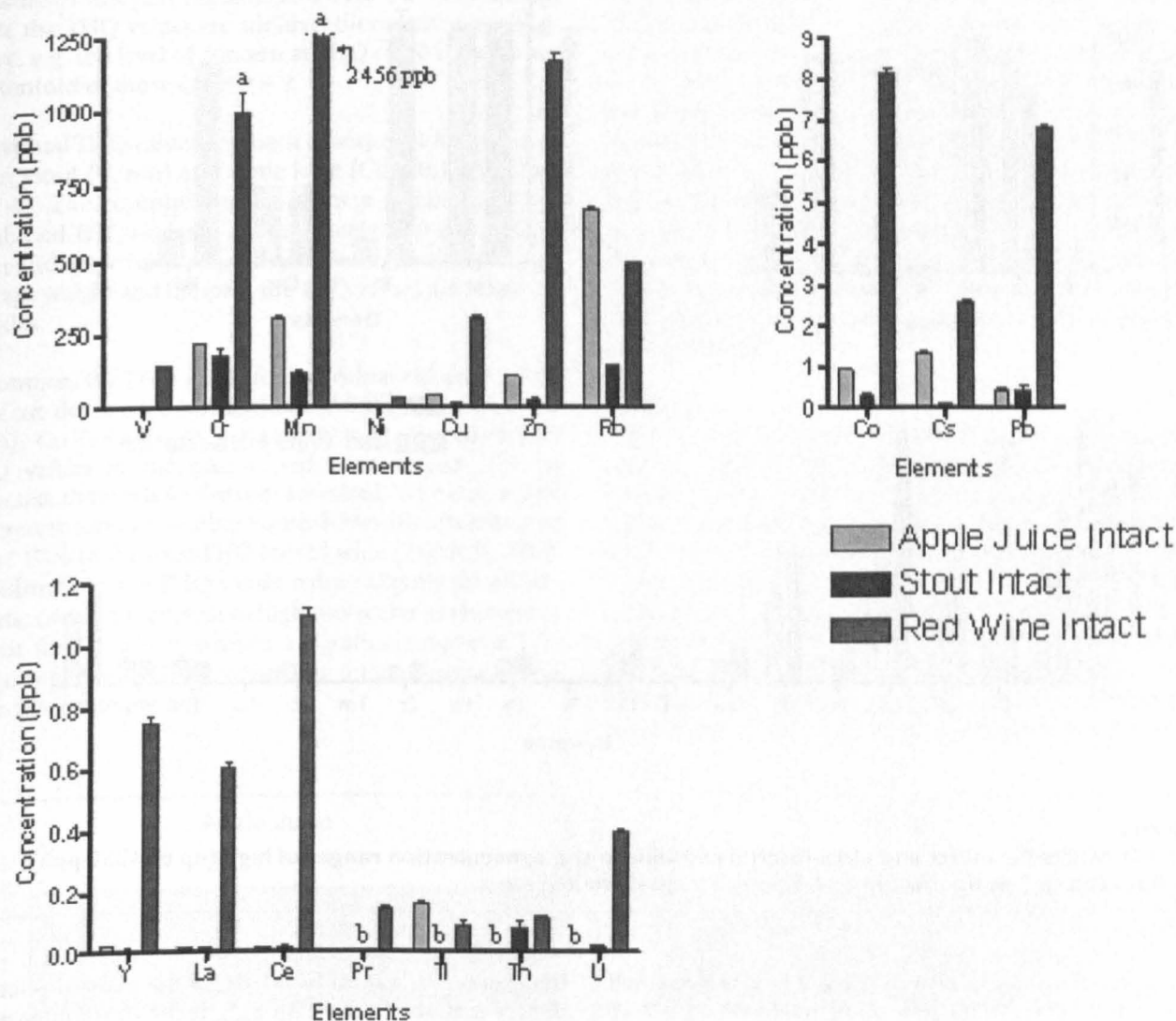


Figure 1
ICP-MS results for intact beverages in the concentration ranges of high (up to 1250 ppb); medium (up to 9 ppb); low (up to 1.5 ppb). a = above working range.

additional file 2: Quantification of metal ions in red wine, pre- and post- ultra-filtration). Of these, nine were approaching 50% in the low molecular mass fraction, with only V in the highest concentration range, the rest being in the lowest concentration range. Thus, quite high levels of metal ions exist in the both the intact and low molecular mass portions except for Cu.

For the intact samples, statistically significant ($p < 0.05$) differences were found between the metal contents of the apple juice, stout and red wine for all metals except Th ($p = 0.137$). Differences in metal ion concentration were calculated from the data (see additional file 1: Quantification of metal ions in whole apple juice and stout, additional file 2: Quantification of metal ions in red wine pre- and post- ultra-filtration), and these significant differences are highlighted in Table 1. The total levels of metal

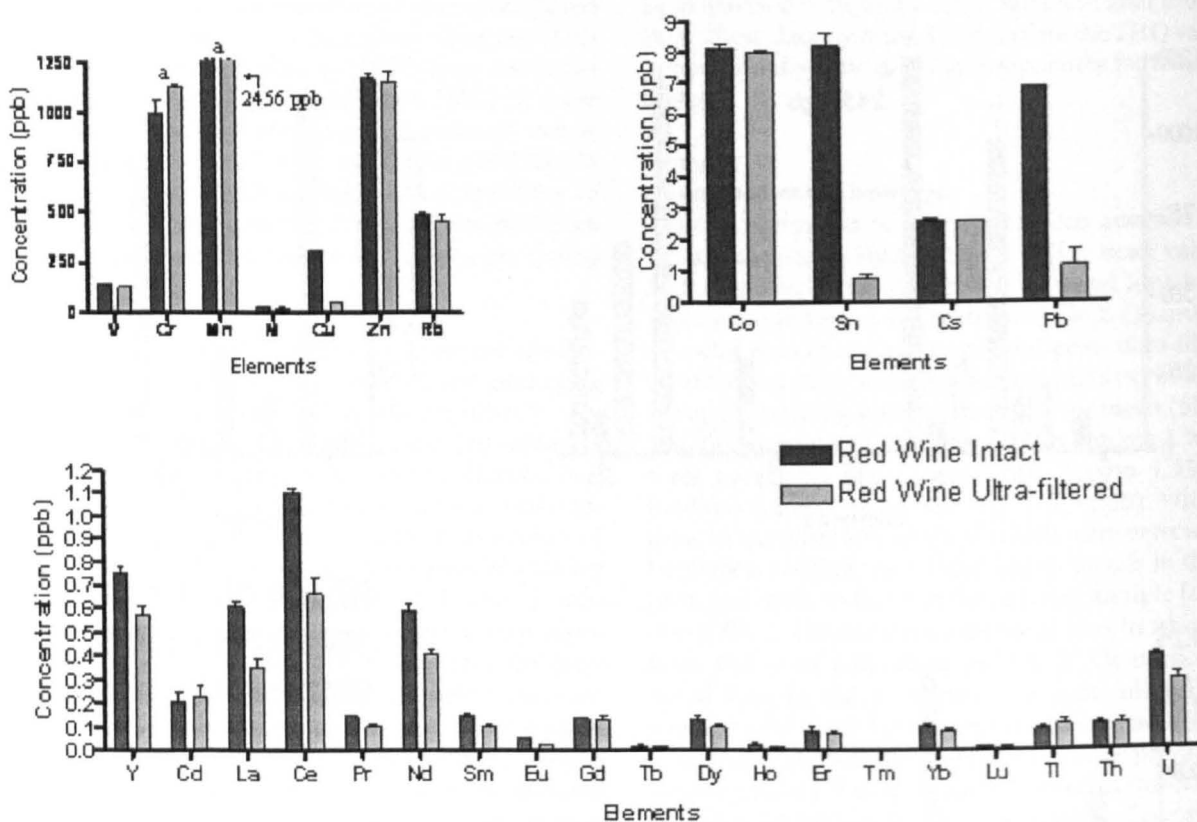


Figure 2
ICP-MS results for intact and ultra-filtered red wine in the concentration ranges of high (up to 1250 ppb); medium (up to 9 ppb); low (up to 1.5 ppb). a = above working range.

ions selected for assessment of the THQ values were: red wine $5,107.76 \pm 118.93$ ppb, apple juice 666.44 ± 7.67 ppb and stout 328.41 ± 42.35 ppb.

Discussion

Target hazard quotients

The THQ is calculated by the formula established by the Environmental Protection Agency [20] using equation 1, where EFr is the exposure frequency (days/year); ED_{tot} is

the exposure duration (year); SFI is the mass of selected dietary ingested (g/day); MCS_{inorg} is the concentration of inorganic species in the dietary components ($\mu\text{g/g}$ wet weight); R_fD : oral reference dose (mg/kg/day); BW_a : the average adult body weight; AT_n : averaging time for non-carcinogens (day); and 10^{-3} : the unit conversion factor.

$$THQ = \frac{EFr \times ED_{tot} \times SFI \times MCS_{inorg}}{R_fD \times BW_a \times AT_n} \times 10^{-3} \quad (1)$$

Table 1: Summary of Tukey HSD post hoc comparisons (p < 0.05) of apple juice, stout and red wine

Differences	Elements
In all pairs (i.e. Red wine ↔ Apple juice, Red wine ↔ Stout, Apple juice ↔ Stout)	Cs, Co, Cu, Mn, Rb, Tl, Zn
Red wine ↔ (Apple juice and Stout)	Ce, Cr, Dy, Er, Eu, Gd, Ho, La, Lu, Ni, Pr, Nd, Pb, Sm, Sn, Tb, Tm, U, V, Y, Yb
Stout ↔ (Apple juice and Red wine)	Cd

↔ denotes difference

The interpretation of the THQ value is binary: THQ is either ≥ 1 or < 1 , where $\text{THQ} > 1$ indicates a reason for health concern [20]. It must be noted that THQ is not a measure of risk [21] but indicates a level of concern and while the THQ values are additive, they are not multiplicative: e.g. the level of concern at THQ of 20 is larger but not tenfold of those at $\text{THQ} = 2$.

Individual THQ values approach or surpass 1 for two metals in stout (V, Mn) and apple juice (Cu, Mn) (Figures 3 and 4). The contributions from these metals bring the combined THQ values to approximately 2.00 and 3.49 for stout and apple juice, respectively. Owing to differences in average weight and lifespan, the THQ values are raised for females.

In contrast, the THQ values for individual elements in red wine are dominated by V (>100) with high values for Mn (>10), Cu (>5), Zn (>2.8) and Ni (>1). The combined THQ values in the case of red wine exceed 125. As expected, the levels for females are raised. When expressed as a percentage, V contributes over 80% with Mn affording some 10% to the total THQ for red wine (Figure 5). With ultrafiltration, the THQ values reduce slightly for all elements, owing to removal of high molecular mass species, except for Cu which exhibits a significant decrease (see additional file 3: THQ values for intact beverages and ultra-filtered red wine).

Many of the toxic effects associated with metals are still under investigation, especially for low concentrations and for lifetime exposure. It is notable that for many metal ions, upper safe limits are unavailable which prevents THQ estimations [22]. Apart from some well recognised cases of metal ion overload, the full effects of metal ions in the body may remain in the realm of sub-clinical pathology acting through numerous mechanisms including oxidative stress. In red wine, a small proportion of the metals are in the high molecular mass form and are probably bound to, or encapsulated in, macromolecules such as proteins. For the detailed discussion of the metals contributing to the high THQ value, particularly in red wine, it must be noted that individual differences such as a person's genetic make up, environment or co-exposures were not considered.

Vanadium

Although it is poorly absorbed in the gastrointestinal (GI) tract (ca 2%), V has numerous reported toxic effects which include the liver, kidney, nervous system, cardiovascular system, and blood-forming organs along with an ability to target mitochondria and mediate oxidative stress [23,24]. In the absence of a proven beneficial role in humans along with a paucity of information on the toxic effects, an upper safe limit for V is difficult to substantiate. However, for the purposes of this study we have adopted those commonly used in this field [2,25,26]. THQ values for this element alone of ca 1.0 in stout are notable but the THQ

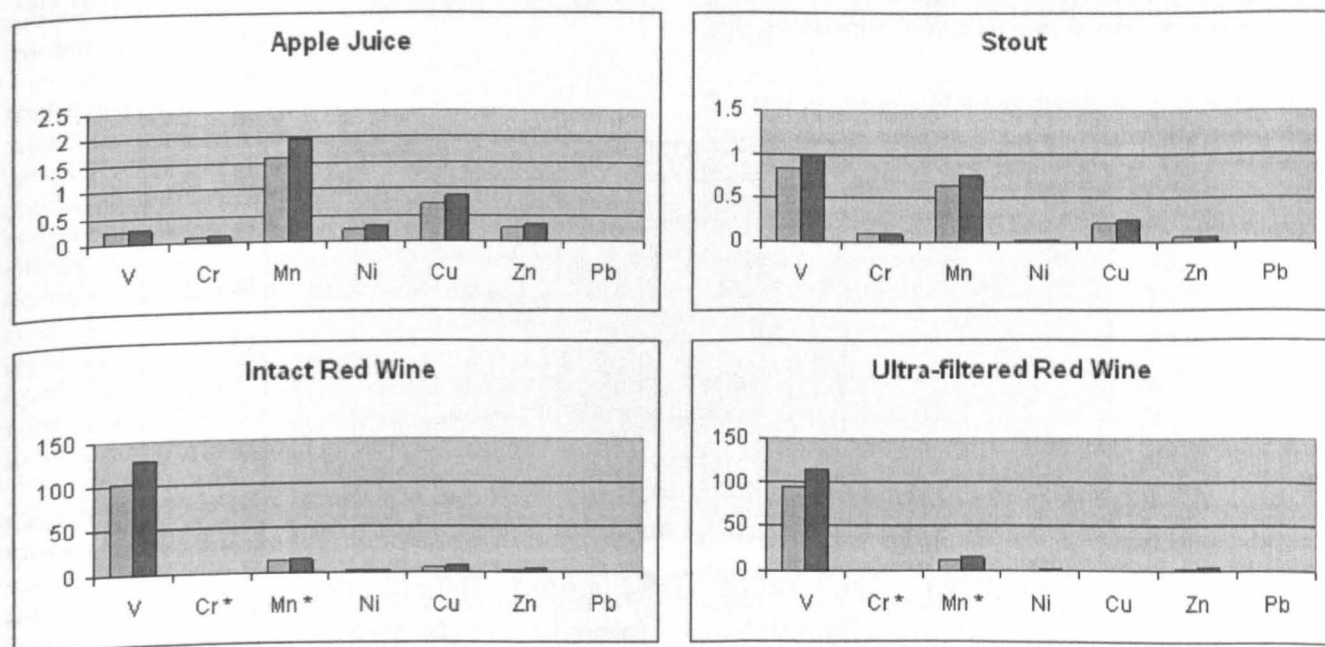


Figure 3
Individual Target Hazard Quotients for all beverages for males (blue) and females (red). * above working range.

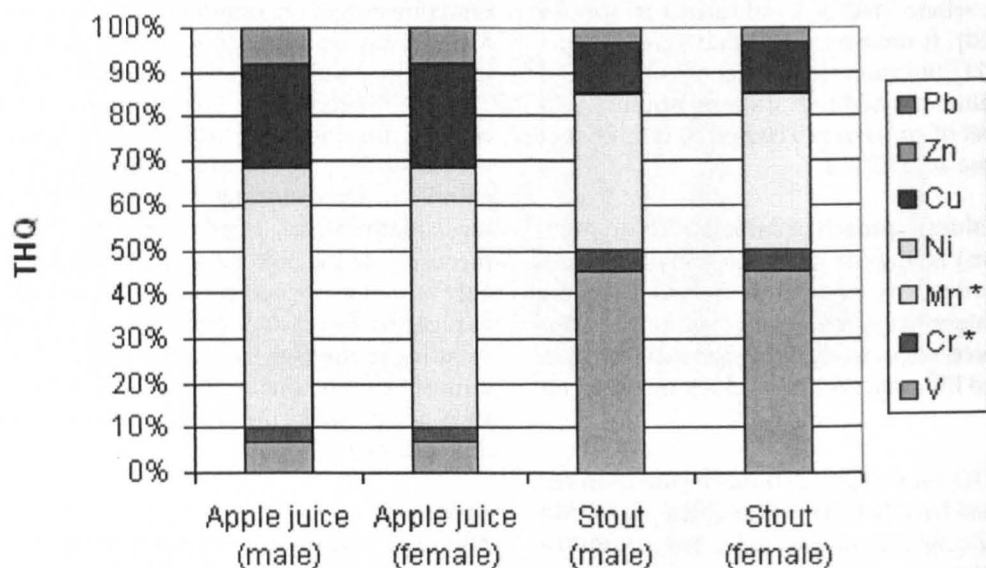


Figure 4
Combined Target Hazard Quotients for apple juice and stout expressed as percentages.

values of >100 in red wine are of particular concern, especially as some 50% of this is as low molecular weight species.

Manganese

In contrast to V, Mn has numerous uses in the body being a component of several enzymes (e.g. superoxide dis-

mutase). It is found in a number of food stuffs including bread, tea and drinking water. Commonly found in supplements, further studies on this cumulative neurotoxin are required to authoritatively state the upper safe limit. The contribution of Mn to the THQ values for all three beverages is similar as expected for this ubiquitous ele-

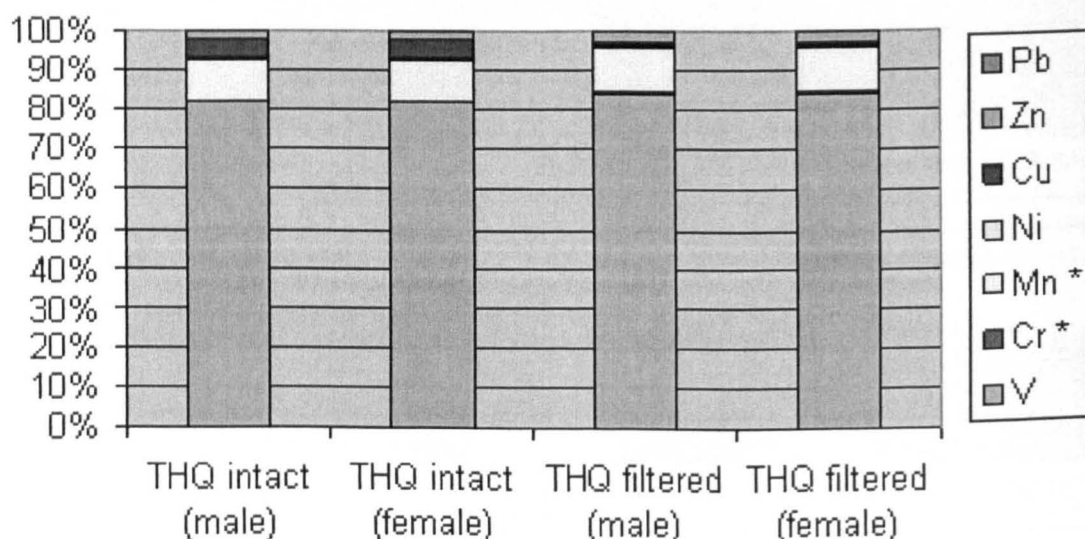


Figure 5
Combined Target Hazard Quotients for red wine. * above working range.

ment indicating that relatively high doses are ingested in a normal diet.

Chromium

Chromium toxicity, like mercury, is very dependent on the species and oxidation states present and is still subject to considerable debate [27-29]. It is normally found in the considerably less toxic trivalent state in foodstuffs, is poorly absorbed in the GI tract and is reported to have beneficial effects on type II diabetes. The hexavalent toxic form participates in oxidative stress [29]. The uncertainties that surround the mechanisms of chromium toxicity, along with its ability to potentiate oxidative stress, warrant concern regarding the levels of this element in red wine, particularly in the low molecular mass form.

Zinc and copper

Zinc and copper have numerous reported beneficial and detrimental effects, being essential components of many enzymes [30,31]. The interacting intestinal uptake mechanisms can lead to imbalances in absorption of copper which is proposed as a major manifestation of zinc toxicity. Other reported effects include decreased levels of superoxide dismutase, a key enzyme for protection against oxidative damage which may be enhanced by labile copper, which may initiate or exacerbate inflammatory disorders [18]. Copper toxicity is rarely encountered outside of specific disorders, although high levels may prevent Zn uptake. Although it exists predominantly in the high molecular mass form in red wine, release during protein degradation enhances the redox active metal ion burden as a part of the THQ.

Nickel and Lead

Nickel levels made a moderate contribution to the combined THQ in red wine. Nickel has numerous reported mechanisms of toxicity including redox-cycling and inhibition of DNA repair as well as exhibiting allergenic/sensitising effects. The toxic effects of lead are well documented, particularly as a neurotoxin [32]. Lead is commonly found in foodstuffs such as tea with a recent report of 32% of 1,225 Chinese tea samples exceeding the upper limit for lead [33]. Only the levels found in red wine are significant but do not reach the level of concern in terms of THQ values over the lifespan.

Conclusion

This study is the first to assess the levels of metal ion exposure over a lifetime in terms of the THQ values for the common beverages stout, apple juice and red wine. The levels of metals found in red wine are of particular concern as they lead to very high THQ values and the ultra-filtrates contained approximately 50% of each metal ion. In addition to the known hazards of metal ion intake, it is noteworthy that a large number of metal ions found in

these beverages, especially wine, have not been well studied in terms of biological activity. This approach should be extended to the numerous dietary products that are consumed daily over a lifetime.

The quantified level of concern expressed as THQ values may be expanded beyond the arbitrarily selected group of 250 mL per day ingestion by using an estimated consumption distribution in a given population and the probability of the metal content in selected foodstuffs. In order to translate the level of concern arising from the environment into potential risks to human health, modifying factors that may enhance or prohibit the body's ability to cope with metal exposure should also be taken into consideration.

Experimental

Samples of one brand for each of the three beverages: apple juice ($n = 3$), stout ($n = 4$) and red wine ($n = 4$) were purchased from a local supermarket. The apple juice was pressed in the UK and contained in plastic bottles. The stout was 'foreign extra stout' in glass bottles from Ireland. The red wine was a Shiraz from South Eastern Australia contained in a screw cap glass bottle. All samples were diluted one in ten prior to analyses in triplicate by ICP-MS on a Quadrupole ICP-MS (Agilent Technologies 7500c) using a cross flow nebuliser. For red wine samples, two mL were placed by pipette into an ultrafiltration device (nominal molecular weight cut-off = 5,000) and centrifuged at 2,060 g for 20 mins. Results are presented in parts per billion 'ppb' ($\mu\text{g/L}$) with standard errors of the mean (SEM).

The concentrations of the thirty metal ions in the intact samples were compared between the three beverages using One-way ANOVA test, followed by Tukey HSD post hoc comparisons if significant omnibus F was obtained. Statistically significant differences between the intact and filtered red wine samples were tested using paired sample t-test analysis. Owing to the small sample size, the level of significance was set to $t/F > CV$ at 0.05.

To assess the level of concern arising from the metal concentrations, THQ values were calculated using the measured metal concentration in the intact samples for seven key potentially toxic metal ions for the three beverages and the ultra-filtered red wine. THQ is a ratio between the measured concentration and the oral reference dose, weighted by the length and frequency of exposure, amount ingested and body weight. The THQ values for selected metals were calculated using the method described previously [4] with the following oral reference doses in mg/kg/d [2,13]: V (1.0×10^{-3}), Cr (1.5), Mn (1.4×10^{-3}), Ni (2.0×10^{-3}), Cu (4.0×10^{-2}), Zn (3.0×10^{-1}) and Pb (1.5). For this project, length of exposure was set to

17,155 days for males and for females based on the average life expectancy of 81.9 and 84.7, respectively from 18 years of age [34]; one large wine glass (250 mL) consumed daily for all three beverages. THQ was calculated separately for males and females using the mean life expectancies (71.9 and 84.7 years respectively) and the mean weight (83.11 and 69.81 kg respectively) [35]. For the oral reference dose we used the tolerable upper intake level (UL) [25,26], which is the highest average daily intake level without the risk of adverse health effects. Intake above the UL could be hazardous to health to almost all individuals in the general population.

Competing interests

The authors declare that they have no competing interests.

Authors' contributions

TH participated in the study design, collection of data, interpretation of results and preparation of the paper, AP participated in the study design, performed the statistical analyses and contributed to drafting the manuscript, PLRA participated in the study design, interpretation of results and preparation of the paper, JB participated in the study design, interpretation of results and preparation of the paper, DN participated in the study design, interpretation of results and preparation of the paper. All authors read and approved the final manuscript.

Additional material

Additional File 1

Quantification of metal ions in whole apple juice and stout. This file contains ICP-MS measurement data for apple juice and stout.

Click here for file

[<http://www.biomedcentral.com/content/supplementary/1752-153X-2-13-S1.doc>]

Additional File 2

Quantification of metal ions in red wine pre- and post- ultra-filtration. This file contains ICP-MS measurement data for red wine.

Click here for file

[<http://www.biomedcentral.com/content/supplementary/1752-153X-2-13-S2.doc>]

Additional File 3

THQ values for intact beverages and ultra-filtered red wine. This file contains individual and total THQ values for red wine.

Click here for file

[<http://www.biomedcentral.com/content/supplementary/1752-153X-2-13-S3.doc>]

References

- Chien L-C, Hung T-C, Choang K-Y, Yeh C-Y, Meng P-J, Shieh M-J, Han B-C: **Daily intake of TBT, Cu, Zn, Cd and As for fishermen in Taiwan.** *Sci Total Environ* 2002, **285**:177-185.
- Wang X, Sato T, Xing B, Tao S: **Health risks of heavy metals to the general public in Tianjin, China via consumption of vegetables and fish.** *Sci Total Environ* 2005, **350**:28-37.
- Liu C-W, Liang C-P, Huang FM, Hsueh Y-M: **Assessing the human health risks from exposure of inorganic arsenic through oyster consumption in Taiwan.** *Sci Total Environ* 2006, **361**:57-66.
- Chien L-W, Han B-C, Hsu C-S, Jiang C-B, You H-J, Shieh M-J, Yeh C-Y: **Analysis of the health risk of exposure to breast milk mercury in infants in Taiwan.** *Chemosphere* 2006, **64**:79-85.
- Zheng N, Wang QC, Zhang XW, Zheng DM, Zhang ZS, Zhang SQ: **Population health risk due to dietary intake of heavy metals in the industrial area of Huludao city, China.** *Sci Total Environ* 2007, **387**:96-104.
- Yang QW, Li H, Long FY: **Heavy metals of vegetables and soils of vegetable bases in Chongqing, southwest China.** *Environ Monit Assess* 2007, **130**:271-279.
- Kachenko A, Singh B: **Heavy metals contamination in vegetables grown in urban and metal smelter contaminated sites in Australia.** *Water Air Soil Pollut* 2006, **169**:101-123.
- Navarro-Blasco I, Alvarez-Galindo JI: **Lead levels in retail samples of Spanish infant formulae and their contribution to dietary intake of infants.** *Food Addit Contam* 2005, **22**:726-734.
- Ang HH, Lee KL, Kiyoshi M: **Determination of lead in Smilax luzonensis herbal preparations in Malaysia.** *Int J Toxicol* 2005, **24**:165-171.
- Sharma RK, Agrawal M: **Biological effects of heavy metals: An overview.** *J Environ Biol* 2005, **26**:S301-313.
- Government Chemist [<http://www.governmentchemist.org.uk>]
- Wyrzykowska B, Szymczyk K, Ichichashi H, Falandysz J, Skwarzec B, Yamasaki S: **Application of ICP sector field MS and principal component analysis for studying interdependences among 23 trace elements in Polish beers.** *J Agric Food Chem* 2001, **49**:3425-3431.
- Rui YK, Yu QQ, Jin YH, Guo J, Luo YB: **Application of ICP-MS to the detection of forty elements in wine.** *Guang Pu Xue Yu Guang Pu Fen Xi* 2007, **27**:1015-1017. Article in Chinese
- Moreno IM, González-Weller D, Gutierrez V, Marino M, Camean AM, González AG, Hardisson A: **Determination of Al, Ba, Ca, Cu, Fe, K, Mg, Mn, Na, Sr and Zn in red wine samples by inductively coupled plasma optical emission spectroscopy: Evaluation of preliminary sample treatments.** *Microchem J* 2008, **88**:56-61.
- Lara R, Cerutti S, Salonia JA, Olsina RA, Martínez LD: **Trace element determination of Argentine wines using ETAAS and USN-ICP-OES.** *Food Chem Toxicol* 2005, **43**:293-297.
- Galgano F, Favati F, Caruso M, Scarpa T, Palma A: **Analysis of trace elements in southern Italian wines and their classification according to provenance.** *LWT - Food Sci Technol* 2008. doi: 10.1016/j.lwt.2008.01.015
- García-Ruiz S, Moldovan M, Fortunato G, Wunderli S, Alonso J: **Evaluation of strontium isotope abundance ratios in combination with multi-elemental analysis as a possible tool to study the geographical origin of ciders.** *Analyt Chim Acta* 2007, **590**:55-66.
- Free radicals in biology and medicine* 4th edition. Edited by: Halliwell B, Gutteridge JM. Oxford University Press, UK; 2007.
- Valko M, Rhodes CJ, Moncol J, Izakovic M, Mazur M: **Free radicals, metals and antioxidants in oxidative stress-induced cancer.** *Chem Biol Interact* 2006, **160**:1-40.
- U.S. EPA, Guidance manual for assessing human health risks from chemically contaminated, fish and shellfish, U.S. Environmental Protection Agency, Washington, D.C. (1989) EPA-503/8-89-002.**
- Tannenbaum LV, Johnson MS, Bazar M: **Application of the Hazard Quotient Method in Remedial Decisions: A Comparison of Human and Ecological Risk Assessments.** *Hum Ecol Risk Assess* 2003, **9**:387-401.
- Naughton DP, Petroczi A: **The metal ion theory of ageing: dietary target hazard quotients beyond radicals.** *Immunity Ageing* 2008, **5**:3.
- Lagerkvist B, Oskarsson A: **Vanadium.** *Handbook on the Toxicology of Metals* Third edition. 2007:905-923.

Acknowledgements

We are grateful to the NERC facility based at KU for conducting the ICP-MS analyses. TH is supported by a HEFCE Capability Building Award.

24. Soares SS, Martins H, Gutiérrez-Merino C, Aureliano M: **Vanadium and cadmium in vivo effects in teleost cardiac muscle: Metal accumulation and oxidative stress markers.** *Comp Biochem Physiol C: Toxicol Pharmacol* 2008, **147**:168-178.
25. National Academy of Sciences: *Dietary Reference Intakes (1997, 1998, 2000, 2001, and 2002)*.
26. US EPA Human Health Risk Assessment: **Risk-Based Concentration Table.** [<http://www.epa.gov/reg3hwmd/risk/human/rbc/RBCoct07.pdf>].
27. De Flora S, D'Agostini F, Balansky R, Micale R, Baluce B, Izzotti A: **Lack of genotoxic effects in hematopoietic and gastrointestinal cells of mice receiving chromium(VI) with the drinking water.** *Mutat Res* 2008. doi:10.1016/j.mrrev.2007.11.005
28. Seenivasan S, Manikandan N, Muraleedharan N: **Chromium contamination in black tea and its transfer into tea brew.** *Food Chem* 2008, **106**:1066-1069.
29. Myers JM, Antholine WE, Myers CR: **Hexavalent chromium causes the oxidation of thioredoxin in human bronchial epithelial cells.** *Toxicol* 2008, **246**:222-233.
30. Fisher A, Naughton DP: **Therapeutic chelators for the twenty first Century: new treatments for iron and copper mediated inflammatory and neurological disorders.** *Curr Drug Deliv* 2005, **2**:261-268.
31. Cherny RA, Atwood CS, Xilinas ME, Gray DN, Jones WD, McLean CA, Barnham KJ, Volitakis I, Fraser FW, Kim YS, Huang XD, Goldstein LE, Moir RD, Lim JT, Beyreuther K, Zheng H, Tanzi RE, Masters CL, Bush AI: **Treatment with a copper-zinc chelator markedly and rapidly inhibits β -amyloid accumulation in Alzheimer's disease transgenic mice.** *Neuron* 2001, **30**:665-676.
32. Alessio L, Campagna M, Lucchini R: **From lead to manganese through mercury: mythology, science, and lessons for prevention.** *Am J Ind Med* 2007, **50**:779-787.
33. Han WY, Zhao FJ, Shi YZ, Ma LF, Ruan JY: **Scale and causes of lead contamination in Chinese tea.** *Environ Pollut* 2006, **139**:125-132.
34. **Life Expectancy** [<http://www.statistics.gov.uk/ccinugget.asp?id=168>]
35. **Health Survey for England 2002 Trends** [http://www.dh.gov.uk/en/Publicationsandstatistics/PublishedSurvey/Health_SurveyForEngland/Healthsurveyresults/DH_4001334]

Publish with ChemistryCentral and every scientist can read your work free of charge

"Open access provides opportunities to our colleagues in other parts of the globe, by allowing anyone to view the content free of charge."

W. Jeffery Hurst, The Hershey Company.

- available free of charge to the entire scientific community
- peer reviewed and published immediately upon acceptance
- cited in PubMed and archived on PubMed Central
- yours — you keep the copyright

Submit your manuscript here:
<http://www.chemistrycentral.com/manuscript/>



ChemistryCentral



Original Contribution

Reduction of paraquat-induced renal cytotoxicity by manganese and copper complexes of EGTA and EHPG

Mohamed Samai^a, Theresa Hague^b, Declan P. Naughton^b, Paul R. Gard^a, Prabal K. Chatterjee^{a,*}^a Department of Pharmacology and Therapeutics, University of Brighton, Brighton, East Sussex BN2 4GJ, UK^b Biomedical and Pharmaceutical Sciences Research Group, Kingston University, Surrey, UK

Received 30 January 2007; revised 1 November 2007; accepted 2 November 2007

Available online 13 November 2007

Abstract

Superoxide anion generation plays an important role in the development of paraquat toxicity. Although superoxide dismutase mimetics (SODm) have provided protection against organ injury involving generation of superoxide anions, they often suffer problems, e.g., regarding their bioavailability or potential pro-oxidant activity. The aim here was to investigate and compare the therapeutic potential of two novel SODm, manganese(II) and copper(II) complexes of the calcium chelator ethylenebis(oxyethylenenitrilo)tetraacetic acid (EGTA) and of the contrast agent ethylenebis(hydroxyphenylglycine) (EHPG), against paraquat-induced renal toxicity *in vitro*. Incubation of renal NRK-52E cells with paraquat (1 mM) for 24 h produced submaximal, yet significant, reduction in cellular viability and cell death and produced significant increases in superoxide anion and hydroxyl radical generation. Manganese and copper complexes of EGTA (10–100 μ M) and EHPG (30–100 μ M) reduced paraquat-induced renal cell toxicity and reduced superoxide anion and hydroxyl radical generation significantly. Manganese complexes displayed greater efficacy than copper complexes and, at equivalent concentrations, manganese complexed with EHPG provided the greatest protection. Furthermore, these metal complexes did not interfere with the uptake of [*methyl*-¹⁴C]paraquat into NRK-52E cells, suggesting that they provided protection against paraquat cytotoxicity via intracellular mechanisms. These complexes did not display cytotoxicity at the concentrations examined. Together, these results suggest that manganese and copper complexes of EGTA and EHPG, and especially the manganese–EHPG complex, could provide benefit against paraquat nephrotoxicity.

© 2007 Elsevier Inc. All rights reserved.

Keywords: Cytotoxicity; Cu(II)-EGTA; Cu(II)-EHPG; Hydroxyl radical; Kidney; Mn(II)-EGTA; Mn(II)-EHPG; NRK-52E; Oxidative stress; Paraquat; Renal; Superoxide anion; Superoxide dismutase mimetics; Free radicals

Paraquat (1,1'-dimethyl-4,4'-bipyridium dichloride, also known as methyl viologen) is a widely used broad-spectrum and fast-acting herbicide. However, it is extremely toxic, causing fatalities due to accidental or intentional poisoning, prevalently in developing countries [1,2]. Paraquat poisoning causes severe multiple organ failure, with the degree of poisoning dependent on the route of administration, the amount administered, and the duration of exposure. It is rapidly distributed within the body with highest concentrations accumulating within the kidneys, where it produces early and severe nephrotoxicity [3]. Additionally, as it is

primarily excreted unchanged via the kidneys, the consequent reduction in renal function increases plasma concentrations by up to fivefold, which contributes to paraquat toxicity in other organs, especially the lungs [4,5]. Ultimately, respiratory failure, in the presence of nephrotoxic acute renal failure, is responsible for most deaths caused by paraquat [5–7]. Therefore, maintaining renal function in patients suffering from paraquat poisoning remains a therapeutically important treatment strategy.

Generation of reactive oxygen species (ROS), such as superoxide anions, plays a major part in the development of paraquat-induced toxicity [8,9] and especially nephrotoxicity [10,11]. Current research has therefore focused on the therapeutic potential of antioxidants against paraquat-induced toxicity, especially those that can degrade superoxide anions such as superoxide dismutase (SOD) [12]. Unfortunately, the

* Corresponding author. Fax: +44 0 1273 642674.
E-mail address: pkc1@bton.ac.uk (P.K. Chatterjee).

effectiveness of exogenously administered antioxidant enzymes such as SOD *in vivo* has been hindered by factors such as its poor bioavailability, low stability, or rapid hydrolysis in the blood and problems regarding its immunogenicity [13–15]. Furthermore, SOD itself can have pro-oxidant effects at higher concentrations [16–19], for example, via the possibility that Cu^{2+} derived from Cu/ZnSOD may facilitate the generation of oxidative stress in the presence of glutathione [17] or via the ability of superoxide to both initiate and terminate lipid peroxidation [19]. Subsequently, many different types of SOD mimetics (SODm) have been synthesized [15,20], including manganese(III) tetrakis(4-benzoic acid) porphyrin (MnTBAP) and M40401 (a manganese-containing SODm), which have been shown to reduce paraquat-induced lung and brain injury in the mouse and rat, respectively [21,22]. However, SODm also suffer problems regarding bioavailability and toxicity, e.g., their poor stability *in vivo* and pro-oxidant activities [23,24].

The calcium chelator ethylenedis(oxyethylenetriolo) tetraacetic acid (EGTA) has recently been shown to possess significant SOD activity [25] and has provided benefits in models of multiple sclerosis and Alzheimer disease [26,27]. Another chelator, ethylenedis(hydroxyphenylglycine) (EHPG), which is used as a contrast agent in imaging and as a transferrin mimic in the study of manganese transport [28,29], also exhibits SODm properties when complexed with manganese (Mn) (II) or copper (Cu) (II) [25]. A major advantage of the potential use of these agents for the treatment of disease is that EGTA and EHPG have already been used therapeutically [26–29]. Furthermore, Mn(II) and Cu(II) complexes of EGTA and EHPG are stable in solution and have a good safety profile in that they do not promote pro-oxidant activities [25].

To date, the protection afforded by Mn and Cu complexes of EGTA and EHPG on ROS generation and subsequent injury and death of renal cells has not been investigated. The aims of this study were to: (i) confirm the role of ROS in the development of paraquat-induced renal (NRK-52E) cell cytotoxicity and (ii) investigate and compare the therapeutic potential of EGTA and EHPG and their Mn(II) and Cu(II) complexes against paraquat-induced renal cytotoxicity *in vitro*. The mechanisms by which metal complexes of EGTA and EHPG could protect NRK-52E cells against paraquat toxicity were investigated, both by assessing the ability of these complexes to reduce ROS generation by paraquat and by examining the ability of the complexes to alter the uptake of paraquat into renal cells.

Materials and methods

Unless otherwise stated, all compounds used in this study were purchased from Sigma–Aldrich Co. Ltd. (Poole, Dorset, UK). Mn(II) and Cu(II) were obtained from Sigma–Aldrich in the form of Mn(II) sulfate and Cu(II) chloride (MnSO_4 and CuCl_2). Mn(II) and Cu(II) complexes of EGTA and EHPG were synthesized as described previously [25].

Culture of NRK-52E cells

NRK-52E cells, which maintain characteristics of renal proximal tubular cells in culture [30], were obtained at passage 24 from the European Collection of Cell Cultures (Salisbury, Wiltshire, UK) and used between passages 28 and 60. Cells were routinely cultured in 80-cm² Nunc flasks (Fisher Scientific, Loughborough, Leicestershire, UK) and grown in Dulbecco's modified Eagle's medium (DMEM; Cambrex BioScience, Wokingham, Berkshire, UK), supplemented with 10% (v/v) fetal bovine serum (FBS; Biosera, Ringmer, East Sussex, UK), 1% nonessential amino acid solution, 100 U/ml penicillin, and 50 µg/ml streptomycin at 37°C in a humidified 5% carbon dioxide atmosphere. Culture medium was changed every 48 h. NRK-52E cells were subcultured at 90% confluence using a trypsin (0.1% w/v)/versene (0.02% w/v) mixture. For experiments, cells were subcultured and grown on 6- or 24-well Nunc plates (Fisher Scientific) in DMEM as described above except for the substitution of 5% (v/v) FBS. DMEM as described above but containing only 1% (v/v) FBS was used for incubations involving paraquat, metal complexes of EGTA and EHPG, or their individual components.

Measurement of paraquat toxicity

Confluent cultures of NRK-52E cells on 24-well plates were incubated for 24 h with increasing concentrations of paraquat (0.003–1 mM). In detail, culture medium was replaced with incubation medium, which consisted of DMEM containing 1% (v/v) FBS and the required concentration of paraquat. At the end of the incubation period, cellular viability and cell death were determined as described below. From these data, a concentration of 1 mM paraquat was chosen, as this produced a submaximal, but significant, reduction in cellular viability (approximately 90% reduction in mitochondrial respiration compared to untreated controls) and a significant increase in cell death (approximately 80% of the lactate dehydrogenase released by cells treated with Triton X-100).

Effects of Mn(II) and Cu(II) complexes of EGTA and EHPG on paraquat-induced toxicity in NRK-52E cells

To investigate the effects of the metal complexes of EGTA and EHPG on cellular injury and death caused by paraquat, confluent NRK-52E cells were preincubated (30 min at 37°C) with 900 µl DMEM containing 1% (v/v) FBS and increasing concentrations of Mn(II)-EGTA, Cu(II)-EGTA, Mn(II)-EHPG, or Cu(II)-EHPG (0.3–100 µM). After 30 min, 100 µl of a 10 mM stock solution of paraquat or its vehicle (DMEM containing 1% (v/v) FBS) was added to each well to provide a final concentration of paraquat of 1 mM. The concentration range of the complexes used was based on those of similar metal-based SODm which have been shown to provide protection of rat proximal cells against oxidative stress [31,32]. It was also assumed, based on previous investigations [25] and on the dosing profile of previous experiments using SODm and renal cells

[31,32], that the complexes would remain stable throughout the incubation period. In subsequent experiments, the effects of the individual components of the metal complexes of EGTA and EHPG on paraquat cytotoxicity were investigated. Specifically, NRK-52E cells were preincubated with 900 μ l of increasing concentrations of EGTA, EHPG, Mn(II), or Cu(II) (0.3–100 μ M) prepared in DMEM containing 1% (v/v) FBS, after which 100 μ l of 10 mM paraquat or its vehicle (DMEM containing 1% (v/v) FBS) was added to each well. Cells were then incubated for 24 h after which cellular viability and cell death were assessed as described below.

Measurement of cellular viability (3-(4,5-dimethylthiazol-2-yl)-2,5-diphenyltetrazolium bromide (MTT) assay)

Cellular viability or injury was determined as described previously via measurement of the mitochondrial-dependent conversion of MTT into a formazan [31–33]. Results were calculated as the percentage of the absorbance measured in control (untreated) cells not exposed to paraquat, which was taken as 100% viability and expressed as cellular viability (% untreated control).

Measurement of cytotoxicity (lactate dehydrogenase (LDH) assay)

Cell death was determined by measurement of LDH released into the incubation medium due to the loss of membrane integrity as described previously [31,32,34]. Results were calculated as percentage of the total LDH released from control cells (i.e., those not exposed to paraquat) which were incubated with 1% (w/v) Triton X-100 (TX-100) for 30 min and expressed as LDH release (% TX-100 control).

Effects of Mn(II) and Cu(II) complexes of EGTA and EHPG on paraquat uptake by NRK-52E cells

In order to investigate whether Mn(II) and Cu(II) complexes of EGTA and EHPG could alter the uptake of paraquat into NRK-52E cells, the accumulation of radiolabeled paraquat was assessed as described previously [35]. Briefly, confluent cultures of NRK-52E cells were co-incubated with [*methyl*-¹⁴C]paraquat (0.01 mM) and cimetidine (1 mM), tetraethylammonium (TEA) (1 mM), or 100 μ M Mn(II)-EGTA, Cu(II)-EGTA, Mn(II)-EHPG, or Cu(II)-EHPG, prepared in DMEM containing 1% (v/v) FBS, for 60 min. The incubation time was based on previously published data in which the uptake of paraquat was shown to plateau after 1 h [35]. The concentrations of cimetidine and TEA used (1 mM) were based on those shown to significantly inhibit the uptake of paraquat into a renal cell line (LLC-PK₁) [36]. Concentrations of Mn(II) and Cu(II) complexes of EGTA and EHPG were based on those providing significant reduction of paraquat toxicity based on the data obtained from biochemical assays measuring cellular viability and cell death. Similarly, the concentration of paraquat used in these experiments (0.01 mM) was based on that previously shown to have no toxic effect on confluent NRK-52E cells. The uptake of [*methyl*-¹⁴C]paraquat was expressed as disintegrations per minute per microgram of

protein and the results were expressed as percentage of control (i.e., based on cells treated with paraquat only).

Effects of preincubation with Mn(II) complexes of EGTA and EHPG on paraquat-induced toxicity in NRK-52E cells

In a separate set of experiments, the ability of Mn(II)-EGTA and Mn(II)-EHPG to enter and remain within NRK-52E cells was examined in order to investigate whether the Mn(II) complexes were present within cells during the incubation period with paraquat. Confluent cultures of NRK-52E cells were incubated with incubation medium only or with 100 μ M Mn(II)-EGTA or Mn(II)-EHPG. After 20 h incubation, for co-incubation studies, incubation medium or paraquat was added to each well to provide a final paraquat concentration of 30 mM. For preincubation studies, cells were rinsed with warm phosphate-buffered saline (PBS; 0.01 M, pH 7.4) and then incubated with either incubation medium or 30 mM paraquat. Earlier studies by the authors have shown that incubation of NRK-52E cells with 30 mM paraquat for 4 h produces a significant reduction in cell viability and cell death in NRK-52E cells (data not shown). After the complete 24-h incubation period, cell viability and death were measured using the MTT and LDH assays, respectively.

Measurement of superoxide anion generation

The generation of superoxide anion was determined using the widely used nitroblue tetrazolium (NBT) assay described previously [37,38]. Superoxide anion generation was further confirmed by using hydroxyethidium as previously described [39].

The NBT assay is based on the reduction of NBT by superoxide anion to blue water-insoluble formazan, which can be monitored spectrophotometrically after solubilization of the cells. Briefly, NRK-52E cells grown in six-well plates were incubated for 24 h with DMEM containing 25 μ g/ml NBT in the presence or absence of 1 mM paraquat. In addition, NRK-52E cells were co-incubated for 24 h with DMEM with 1% (v/v) FBS containing 25 μ g/ml NBT and 1 mM paraquat in the presence or absence of SOD (EC 1.15.1.1; 1000 U/ml), catalase (EC 1.11.1.6; 1000 U/ml), and protective concentrations of Mn(II)-EGTA (100 μ M) or Mn(II)-EHPG (100 μ M).

Hydroxyethidium has been shown to be relatively specific for superoxide, which is oxidized by superoxide to yield ethidium. Cells were harvested from six-well plates previously incubated in DMEM containing 1% (v/v) FBS with 1 mM paraquat in the presence or absence of SOD (1000 U/ml), catalase (1000 U/ml), Mn(II)-EGTA (100 μ M), or Mn(II)-EHPG (100 μ M) for 24 h. Cell suspensions were then washed with Hanks' buffered salt solution and then incubated with 10 μ M hydroxyethidium for 15 min at 37°C. Ethidium fluorescence was then measured using a spectrofluorometer set at excitation and emission wavelengths of 473 and 593 nm, respectively.

The concentrations of SOD and catalase were based on previous work by Scheid and colleagues in which these antioxidant enzymes were used to protect renal LLC-PK₁ cells against oxidative stress produced by oxalate [38]. Concentrations

of Mn(II)-EGTA and Mn(II)-EHPG were based on concentrations found to provide significant protection against paraquat-induced cellular injury and cytotoxicity in earlier experiments. Results were expressed as superoxide anion generation (NBT abs. at 690 nm or ethidium fluorescence % untreated control).

Measurement of hydroxyl radical generation

The production of hydroxyl radicals by NRK-52E cells in the absence or presence of paraquat was evaluated using the widely used deoxyribose assay, based on the principle that the pentose sugar 2-deoxyribose can be cleaved by hydroxyl radicals to release a substance that reacts, on heating, with thiobarbituric acid (TBA) to produce a pink chromogen [38,40]. The chromogen formed in this assay has a spectrum which is identical to that of malondialdehyde (MDA) and, therefore, a standard curve for MDA is constructed from which the TBA content of samples (which is directly proportional to the hydroxyl radicals) can be extrapolated [38]. Briefly, confluent NRK-52E cells grown in six-well plates were incubated for 24 h with DMEM containing 3 mM deoxyribose in the presence of 1 mM paraquat. In addition, NRK-52E cells were co-incubated for a predetermined time period with DMEM containing 3 mM deoxyribose and 1 mM paraquat in the presence of SOD (1000 U/ml), catalase (1000 U/ml), or Mn(II)-EGTA or Mn(II)-EHPG (100 μ M each). At the end of the incubation period, the cell supernatant was removed and assayed for thiobarbiturate acid-reactive substances for MDA as previously described [41]. An aliquot of the cell supernatant was also used for protein quantification by the Bradford assay [42] and the hydroxyl radical content of samples was expressed as MDA formation (nmol/mg protein).

Statistical analysis

Results are expressed as means \pm SEM. Means were obtained from multiple experiments performed in triplicate. Data were analyzed and graphed with a commercially available software (GraphPad Prism, version 3.0; GraphPad Software, San Diego, CA, USA). Differences between mean values within the groups were determined using a Student *t* test or one-way analysis of variance (ANOVA) followed by a Dunnett's test for comparison of multiple means. The level of significance was set at $p < 0.05$.

Results

Effects of paraquat on cellular viability and LDH release by NRK-52E cells

Exposure of confluent NRK-52E cells to paraquat (0.003–1 mM) for 24 h resulted in a significant reduction in cellular viability from 100% for control (untreated) cells to 10% ($p < 0.05$) for cells incubated with 1 mM paraquat (Fig. 1). As also shown in Fig. 1, this was accompanied by a concomitant and significant increase in cell death from a baseline value of approximately 20% for control (untreated) cells to 80% ($p < 0.05$) for cells incubated with 1 mM paraquat.

Effects of Mn(II) and Cu(II) complexes of EGTA and EHPG on paraquat toxicity

Incubation of NRK-52E cells with increasing concentrations of Mn(II)-EGTA (0.3–100 μ M) in the presence of 1 mM paraquat produced a significant improvement of cellular viability and reduced LDH release compared to cells incubated with 1 mM paraquat only (Fig. 2A). Specifically, concentrations of Mn(II)-EGTA greater than 10 μ M increased cellular viability and reduced LDH release significantly ($p < 0.05$, Fig. 2A).

Incubation with increasing concentrations of Mn(II)-EGTA only (0.3–100 μ M) produced a modest but significant reduction in cellular viability from 100 (untreated cells) to approximately 90% ($p < 0.05$); however, similar concentrations of Mn(II)-EGTA had no effect on baseline LDH release ($p > 0.05$) (data not shown).

In contrast, incubation of cells with Cu(II)-EGTA did not have any effect on the reduction in cell viability produced by 1 mM paraquat ($p > 0.05$, Fig. 2B). However, the highest concentration of Cu(II)-EGTA produced a modest but significant reduction in LDH release caused by 1 mM paraquat ($p < 0.05$, Fig. 2B). As for Mn(II)-EGTA, Cu(II)-EGTA itself produced a modest yet significant reduction in cellular viability from 100 (untreated cells) to approximately 87% at a concentration range of 1–100 μ M ($p < 0.05$). However, and again in common with Mn(II)-EGTA, Cu(II)-EGTA had no effect on baseline LDH release ($p > 0.05$) (data not shown).

Mn(II)-EHPG produced a significant improvement in cellular viability at concentrations greater than 10 μ M ($p < 0.05$, Fig. 3A). A similar effect was observed when the effects of Mn(II)-EHPG on paraquat renal cytotoxicity were assessed, with 30 and 100 μ M Mn(II)-EHPG significantly reducing LDH release caused by 1 mM paraquat ($p < 0.05$, Fig. 3A). Mn(II)-EHPG alone did not have any effect on cellular viability or LDH release at the concentration range investigated (0.3–100 μ M) ($p > 0.05$) (data not shown).

Compared to the reduction in cellular viability produced by paraquat, Cu(II)-EHPG significantly reduced cellular viability

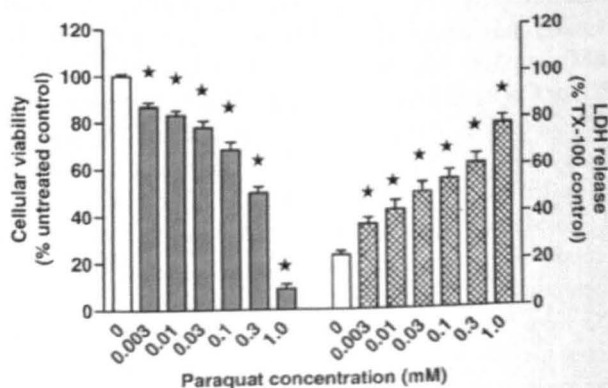


Fig. 1. Effects of paraquat on cellular viability (left) and cell death (right) of NRK-52E cells. Confluent NRK-52E cells were incubated with increasing concentrations of paraquat for 24 h. * $p < 0.05$ vs 0 mM paraquat (untreated control cells treated with DMEM only) analyzed using one-way ANOVA followed by Dunnett's posttest, $N = 10$.

further at the concentration range 0.3–30 μM ($p < 0.05$, Fig. 3B). However, at the highest concentration examined (100 μM), Cu(II)-EHPG increased cellular viability from 9 (paraquat only) to 14% ($p < 0.05$, Fig. 3B) and reduced paraquat-mediated LDH release significantly from 74 (paraquat only) to 56% (100 μM Cu(II)-EHPG) ($p < 0.05$, Fig. 3B). In contrast to its effects on cellular viability, lower concentrations of Cu(II)-EHPG (0.3–30 μM) had no effect on paraquat-mediated LDH release (Fig. 3B). At the concentrations examined (0.3–100 μM), Cu(II)-EHPG alone had no effect on cellular viability or LDH release ($p > 0.05$) (data not shown).

Comparison of the effects of Mn(II) and Cu(II) complexes of EGTA and EHPG and their individual components on paraquat-induced renal cell injury and cytotoxicity

As shown in Fig. 4A, incubation of NRK-52E cells with 1 mM paraquat for 24 h caused a significant reduction in cellular viability, from 100 (untreated cells) to 7% (paraquat only) ($p < 0.05$, Fig. 4A). Mn(II)-EHPG, at 100 μM , afforded the greatest protection against paraquat, increasing cellular viability from 7 (paraquat only) to 44% (Mn(II)-EHPG) ($p < 0.05$, Fig. 4A) compared to 100 μM Mn(II)-EGTA and 100 μM Mn(II), which increased cellular viability to 28 and 24%, respectively. Cu(II)-

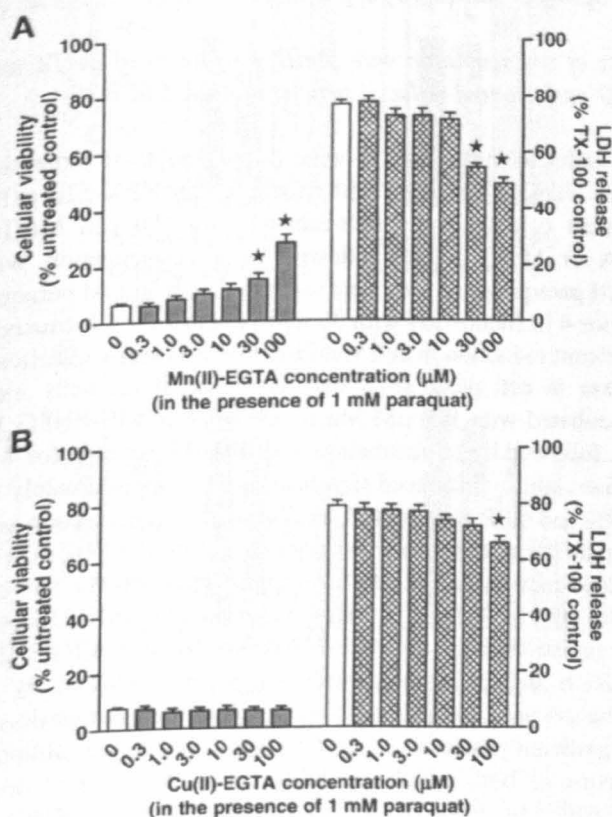


Fig. 2. Effects of (A) Mn(II) and (B) Cu(II) complexes of EGTA on viability (left) and death (right) of NRK-52E cells. Cultures were incubated with increasing concentrations of Mn(II)-EGTA or Cu(II)-EGTA for 24 h in the presence of 1 mM paraquat. * $p < 0.05$ vs 0 μM Mn(II)-EGTA or Cu(II)-EGTA + 1 mM paraquat analyzed using one-way ANOVA followed by Dunnett's posttest, $N = 10$.

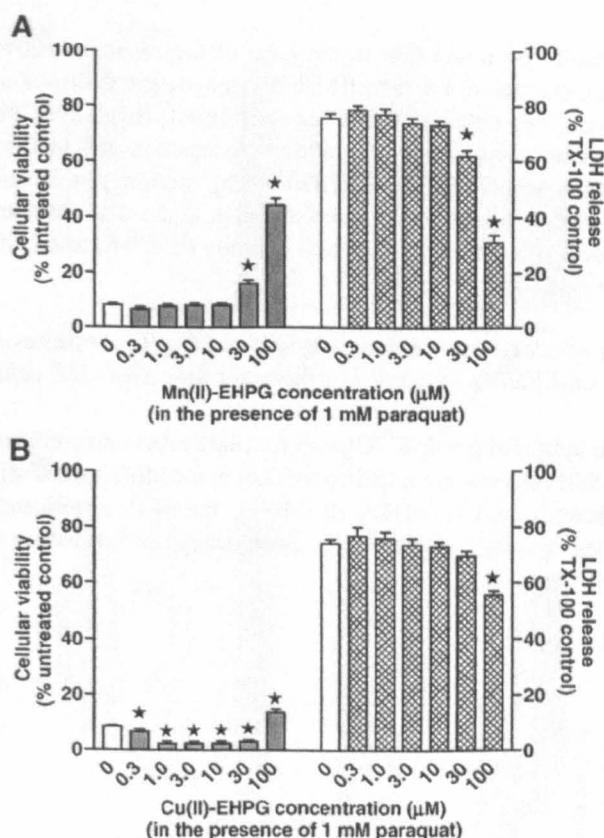


Fig. 3. Effects of (A) Mn(II) and (B) Cu(II) complexes of EHPG on viability (left) and death (right) of NRK-52E cells. Cultures were incubated with increasing concentrations of Mn(II)-EHPG or Cu(II)-EHPG for 24 h in the presence 1 mM paraquat. * $p < 0.05$ vs 0 μM Mn(II)-EHPG or Cu(II)-EHPG + 1 mM paraquat analyzed using one-way ANOVA followed by Dunnett's posttest, $N = 10$.

EHPG, at 100 μM , also provided protection against the reduction in cellular viability produced by paraquat, increasing it from 7 (paraquat only) to 14% (Cu(II)-EHPG) ($p < 0.05$, Fig. 4A); however, this was similar to that provided by 100 μM EHPG alone (11%). As shown in Fig. 4A, Cu(II)-EGTA had no effect on paraquat-induced reduction in cell viability (6%), whereas Cu(II) and EGTA alone actually reduced cell viability further (to approximately 2%, $p < 0.05$).

A similar profile was observed when the effects on the cell death (LDH release) caused by paraquat were assessed (Fig. 4B). Incubation with 1 mM paraquat produced a significant increase in LDH release from 24 (untreated cells) to 76% (paraquat only) ($p < 0.05$, Fig. 4B). Mn(II)-EHPG, at 100 μM , afforded the greatest protection against paraquat, reducing LDH release from 76 (paraquat only) to 31% (Mn(II)-EHPG) ($p < 0.05$, Fig. 4B). This was a significantly greater protection than that afforded by 100 μM Mn(II)-EGTA. Cu(II)-EHPG and EHPG, at 100 μM , reduced LDH release to 56 and 72%, respectively ($p < 0.05$, Fig. 4B). Cu(II)-EHPG, at 100 μM , also provided protection against paraquat-mediated LDH release, reducing it from 76 (paraquat only) to 56% (Cu(II)-EHPG) ($p < 0.05$, Fig. 4B). In contrast, Cu(II) increased paraquat-mediated LDH release significantly from 76 (paraquat only) to 80% (Cu(II) only) ($p < 0.05$, Fig. 4B).

It should be noted that in the case of the most protective complex examined, i.e., Mn(II)-EHPG, a synergistic degree of protection was obtained when the protection provided by the complex was compared to the additive protection provided by its components, Mn(II) and EHPG, when examined individually. This synergistic activity was apparent in the data obtained from measurement of both cellular viability (Fig. 4A) and LDH release (Fig. 4B).

Effects of cimetidine, TEA, and Mn(II) and Cu(II) complexes of EGTA and EHPG on uptake of paraquat into NRK-52E cells

The uptake of [*methyl*-¹⁴C]paraquat (0.01 mM) into confluent NRK-52E cells was not inhibited by TEA or the Mn(II) and Cu(II) complexes of either EGTA or EHPG, but was significantly inhibited by cimetidine (Fig. 5). Specifically, co-incubation of

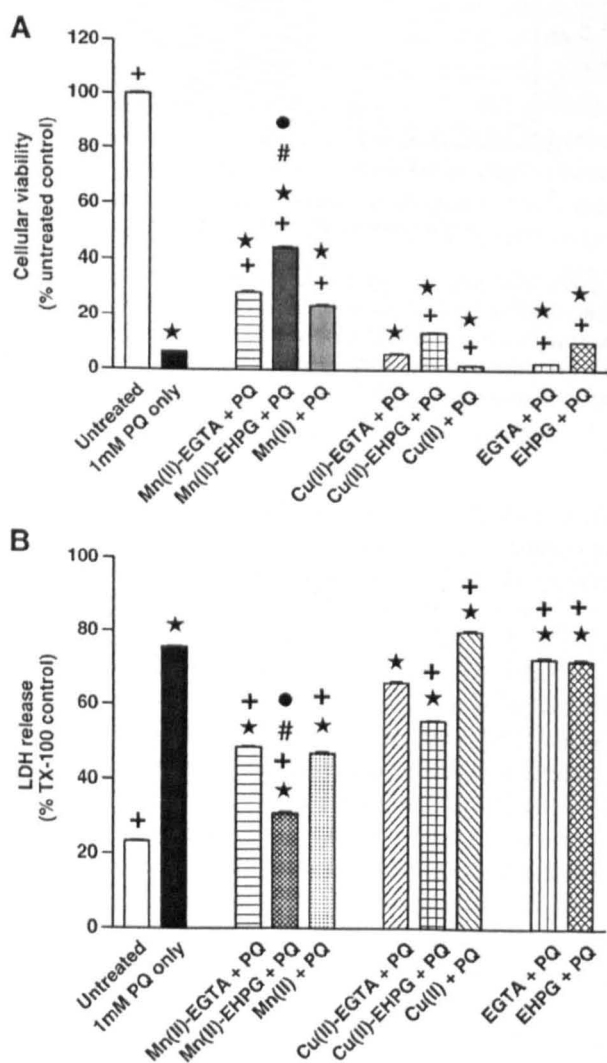


Fig. 4. Summary of the effects of Mn(II) and Cu(II) complexes on (A) cellular viability and (B) cell death in the presence of paraquat (PQ). NRK-52E cells were incubated with 100 μ M Mn(II)-EGTA, Mn(II)-EHPG, Cu(II)-EGTA, or Cu(II)-EHPG or their individual components (100 μ M) in the presence of paraquat for 24 h. * p <0.05 vs untreated cells (DMEM only); + p <0.05 vs 1 mM PQ only; # p <0.05 vs Mn(II)-EGTA+PQ; p <0.05 vs Cu(II)-EHPG+PQ, analyzed using one-way ANOVA followed by Dunnett's posttest, N =10.

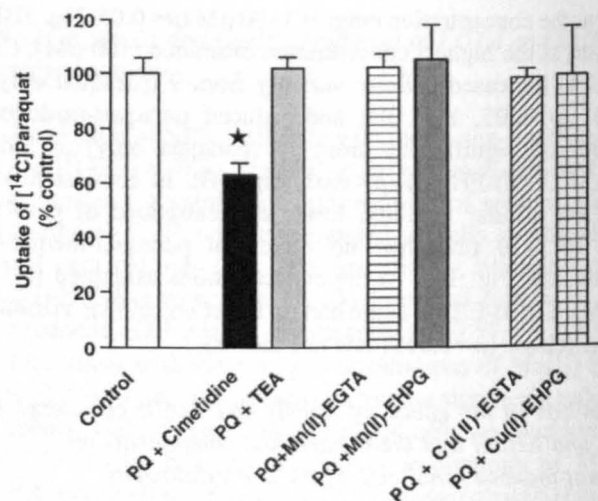


Fig. 5. Effects of cimetidine, TEA, and Mn(II) and Cu(II) complexes of EGTA and EHPG on the uptake of paraquat (PQ) by NRK-52E cells. Confluent NRK-52E cells were co-incubated with 0.01 mM PQ and cimetidine (1 mM), TEA (1 mM), or Mn(II)-EGTA, Cu(II)-EGTA, Mn(II)-EHPG, or Cu(II)-EHPG (100 μ M each) for 60 min. * p <0.05 vs control (cells treated with PQ only), N =6.

confluent NRK-52E cells for 60 min with 0.01 mM [*methyl*-¹⁴C] paraquat and 1 mM cimetidine resulted in a significant reduction in the uptake of paraquat by approximately 40% (p <0.05, Fig. 5).

Effects of preincubation with Mn(II) complexes of EGTA and EHPG on paraquat-induced toxicity in NRK-52E cells

In order to investigate to what degree the most protective SODm were able to enter and remain within NRK-52E cells, confluent cultures were preincubated with 100 μ M Mn(II)-EGTA or Mn(II)-EHPG followed by a co-incubation with 30 mM paraquat for 4 h or were incubated with 30 mM paraquat only for 4 h. Incubation with 30 mM paraquat for 4 h caused a significant reduction in cell viability (Fig. 6A) and a significant increase in cell death (Fig. 6B). However, if the cells were preincubated with 100 μ M Mn(II)-EGTA or Mn(II)-EHPG for 20 h, followed by co-incubation with 30 mM paraquat for 4 h, cellular viability increased significantly from approximately 60 to 80% (p <0.05, Fig. 6A). A similar profile of protection was observed for cell death, with co-incubation of the SODm with paraquat reducing cell death from approximately 80 to between 40 and 50% (p <0.05, Fig. 6B). Furthermore, if NRK-52E cells were preincubated with 100 μ M Mn(II)-EGTA or Mn(II)-EHPG for 20 h and then rinsed with warm PBS followed by an incubation with 30 mM paraquat only for 4 h, a similar degree of significant protection against paraquat toxicity was obtained in terms of both cellular viability (Fig. 6A) and cell death (Fig. 6B).

Effects of Mn(II) and Cu(II) complexes of EGTA and EHPG on the generation of reactive oxygen species by paraquat

As shown in Figs. 7A and B, incubation of NRK-52E cells with 1 mM paraquat for 24 h produced a significant increase

in superoxide anion generation, by 52 and 35% as measured by NBT reduction and ethidium fluorescence, respectively ($p < 0.05$). Paraquat-mediated superoxide anion generation was significantly reduced by 1000 U/ml SOD ($p < 0.05$), but not by 1000 U/ml catalase (Figs. 7A, B). Mn(II)-EGTA (100 μ M) and Mn(II)-EHPG (100 μ M) both reduced superoxide generation by paraquat significantly ($p < 0.05$, Figs. 7A and B). It should be noted that the reductions were not significantly different from the reduction in paraquat-induced superoxide anion generation obtained using SOD (Figs. 7A and B).

Incubation of cultures with 1 mM paraquat for 24 h also produced a significant 10-fold increase in hydroxyl radical production ($p < 0.05$, Fig. 7C). In contrast to superoxide generation, 1000 U/ml SOD did not have any effect on hydroxyl radical generation; however, 1000 U/ml catalase reduced paraquat-induced generation of hydroxyl radical significantly by approximately 68% ($p < 0.05$, Fig. 7C). Co-incubation of NRK-52E cells with 1 mM paraquat and 100 μ M of either Mn(II)-EGTA or Mn(II)-EHPG reduced paraquat-induced hydroxyl radical generation from 3.02 (paraquat only) to 1.91 and 1.69 nmol/mg protein, respectively ($p < 0.05$, Fig. 7C).

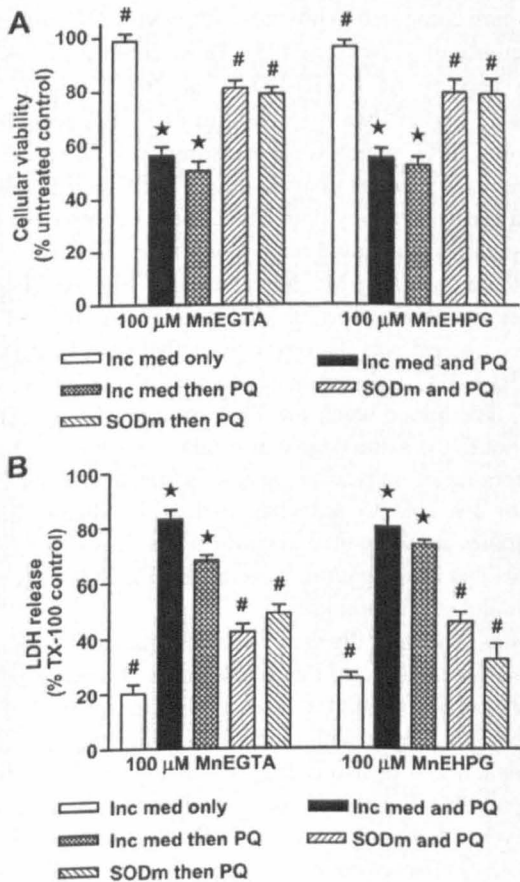


Fig. 6. Effects of preincubation with Mn(II)-EGTA and Mn(II)-EHPG on (A) viability and (B) death of NRK-52E cells incubated with paraquat (PQ). Cultures were incubated with incubation medium only or incubation medium containing 100 μ M Mn(II)-EGTA or Mn(II)-EHPG. After 20 h, paraquat was added to the incubation medium to a final concentration of 30 mM or cells were rinsed and incubated with 30 mM paraquat for 4 h. * $p < 0.05$ vs 100 μ M Mn(II)-EGTA or Mn(II)-EHPG, # $p < 0.05$ vs 30 mM paraquat only analyzed using one-way ANOVA followed by Dunnett's posttest, $N = 6$.

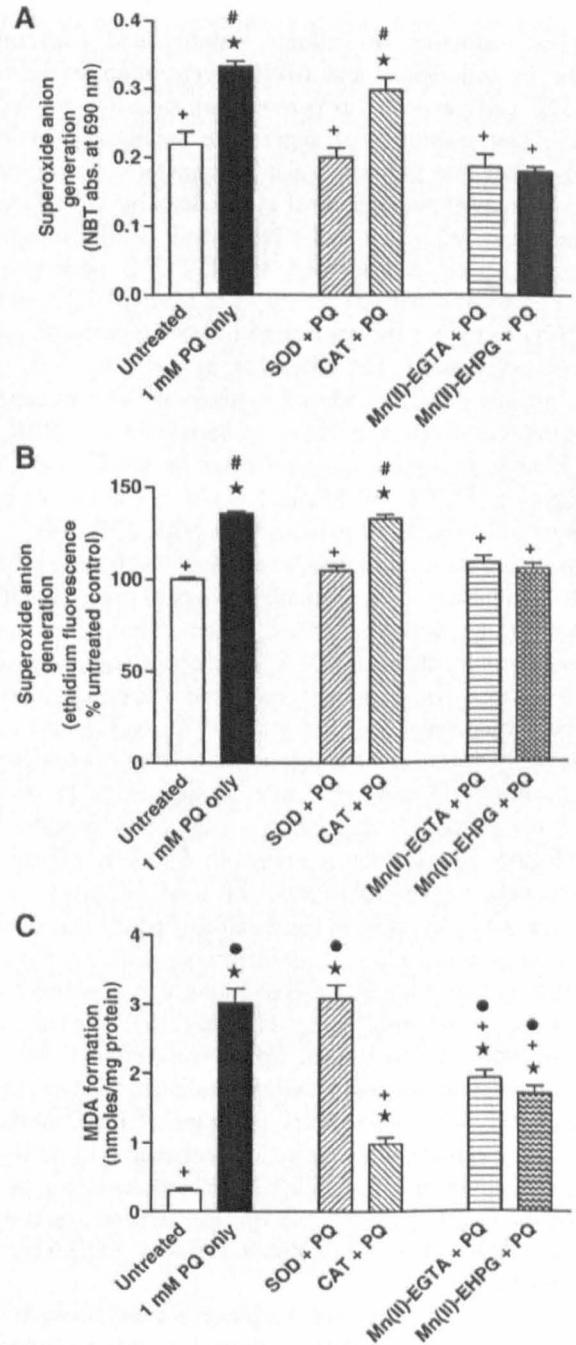


Fig. 7. Effects of Mn(II)-EGTA, Mn(II)-EHPG, and antioxidant enzymes on (A and B) superoxide anion generation and (C) hydroxyl radical production by NRK-52E cells. Cultures were incubated with 1 mM paraquat (PQ) in the presence of 1000 U/ml SOD, 1000 U/ml catalase (CAT), 100 μ M Mn(II)-EGTA, or 100 μ M Mn(II)-EHPG. * $p < 0.05$ vs untreated cells (DMEM only); + $p < 0.05$ vs 1 mM PQ only; # $p < 0.05$ vs SOD+PQ; $p < 0.05$ vs CAT+PQ analyzed using one-way ANOVA followed by Dunnett's posttest, $N = 8$.

These values were still significantly higher than the reduction in hydroxyl radical generation obtained using catalase ($p < 0.05$, Fig. 7C).

Discussion

The results obtained in this investigation clearly demonstrate (i) the renal toxicity of paraquat, specifically, a concentration-

dependent reduction of cellular viability and concomitant increase in cell death, and (ii) the generation of ROS by NRK-52E cells exposed to paraquat, specifically, production of significant quantities of superoxide anions and hydroxyl radicals. The data presented also demonstrate (i) significant protection against paraquat renal cytotoxicity by Mn(II) and Cu(II) complexes of EGTA and EHPG, with Mn(II) complexes displaying higher potency and Mn(II)-EHPG providing the greatest protection, and (ii) the ability of Mn(II)-EGTA and Mn(II)-EHPG to reduce the generation of both superoxide anions and hydroxyl radical. The protection provided by these complexes against paraquat-induced cytotoxicity was obtained at concentrations which were found to be nontoxic to NRK-52E cells. Finally, protective concentrations of Mn(II) and Cu(II) complexes of EGTA and EHPG have been shown not to interfere with the uptake of paraquat into NRK-52E cells.

Superoxide anion generation, and the cellular damage resulting from it, is implicated in the pathophysiology of many conditions, including stroke, ischemia, asthma, atherosclerosis, and several neurodegenerative diseases [43–45]. Increased superoxide anion generation due to paraquat and its contribution to paraquat toxicity have been catalogued over many years [8,9,46,47], and in this investigation, its role in the development of renal cytotoxicity has been confirmed *in vitro*. The role of superoxide in paraquat toxicity has prompted much interest in the development of safe and effective antioxidants to negate its injurious effects [12]. Unfortunately, native SOD cannot be used effectively due to recognized problems with its short half-life, poor bioavailability, and immunogenicity [13–15]. Furthermore, SOD can have pro-oxidant activities at higher concentrations, e.g., Cu/ZnSOD can promote the generation of hydroxyl radicals [16,48] and inhibit the ability of superoxide to regulate lipid peroxidation [19,49]. This has generated much interest in SODm, leading to the development of agents including macrocyclics, manganese salens, nitroxides, porphyrins, and many other catalytic antioxidants [15,20,50–55]. However, many of these have also suffered problems ranging from cytotoxicity to poor stability [23,56]. Furthermore, in common with native SOD, higher concentrations of some SODm can have pro-oxidant actions [17–19].

The recent observation that complexes formed between metal ions and the common chelator sodium edentate or ethylenediaminetetraacetic acid (EDTA) possess significant SODm and catalase mimetic properties [57] prompted the investigation of the SOD and catalase activities of other commonly used chelators and their metal complexes. Low concentrations of the calcium ion chelator EGTA have been shown to solubilize amyloid plaques in postmortem brain samples from patients suffering from Alzheimer disease and to reduce nitric oxide (NO)-induced calcium influx into endothelial cells and prevent consequent cell death [26,27]. Some of these beneficial effects of EGTA have been credited to its ability to bind the excess Cu(II) ions which contribute to disease pathology; however, it is now also clear that complexing EGTA with Cu(II) or Mn(II) promotes significant SOD activity [25]. Recently, the related chelating agent EHPG, which is used as a contrast agent for magnetic resonance imaging and as a transferrin mimic in the study of manganese transport [28,29], has also been shown to exhibit significant SOD activity

when complexed with Mn(II) or Cu(II) [25]. However, the ability of these complexes to reduce paraquat toxicity, in which superoxide generation plays a major part, is not known and formed the basis of this study.

In this investigation, Mn(II) and Cu(II) complexes of EGTA and EHPG provided significant protection against paraquat cytotoxicity in renal cells, which, in the case of Mn(II)-EHPG, was greater than any protection afforded by the individual components. Mn(II) complexes of EGTA and EHPG provided greater protection than the Cu(II) complexes. The protection afforded by these metal complexes seemed to be related to their SODm activity as suggested by their ability to reduce superoxide generation by paraquat to a degree similar to that obtained using SOD and support the findings of Fisher et al. [25], who demonstrated the SODm activities of Mn(II) and Cu(II) complexes of EGTA and EHPG. The order of protection observed against paraquat renal cytotoxicity was Mn(II)-EHPG > Mn(II)-EGTA > Cu(II)-EHPG > Cu(II)-EGTA. This profile closely reflected the SOD activities of these complexes reported by Fisher and colleagues (Mn(II)-EGTA, 981 U/mg; Mn(II)-EHPG, 879 U/mg; Cu(II)-EHPG, 409 U/mg; and Cu(II)-EGTA, 314 U/mg), by whom measurements were made as units activity per milligram compared to bovine erythrocyte SOD, which itself had an activity of 3730 U/mg [25]. These activities were higher than the activity of Cu(II)-EDTA at 261 U/mg [57] and considerably higher than the activities of Fe(III) complexes of EGTA and EHPG, which were measured as 8.76 and 0 U/mg, respectively [25]. In this investigation, EGTA-based complexes displayed greater potency than EHPG-based complexes as they reduced paraquat-mediated renal cytotoxicity significantly at a concentration of 10 μ M; however, the highest degree of protection was obtained using Mn(II)-EHPG at 100 μ M.

Also of interest was the observation that both Mn(II)-EGTA and Mn(II)-EHPG reduced hydroxyl radical generation significantly, as determined using the TBA reduction assay. Although this was not to the same degree as catalase, it suggests that these Mn(II) complexes may also possess some degree of catalase activity or are able to scavenge hydroxyl radicals; however, further studies are warranted to confirm this. Based solely on the findings of this investigation, it seems that the SODm activity of these complexes predominates.

Paraquat exists as a divalent cation in aqueous solution and is predominantly transported into renal proximal tubular cells via a polyvalent organic cation transporter (OCT) protein. This uptake of paraquat is saturable with time and with increasing concentration of paraquat. It is also energy-dependent and is inhibited by certain polyvalent cations, such as quinine, cimetidine, and methylglyoxal bis(guanylhydrazine) dihydrochloride [36,58,59]. The inhibitory effect of cimetidine, a divalent ion, on the uptake of paraquat into NRK-52E cells as has been shown in this study indicates the presence of a polyvalent OCT protein on NRK-52E cells and that this OCT is used by paraquat to enter NRK-52E cells. In contrast, TEA, a monovalent ion, did not alter paraquat uptake into NRK-52E cells. The observation that at protective concentrations, the Mn(II) and Cu(II) complexes of EGTA and EHPG did not alter the uptake of paraquat by NRK-52E cells suggests that their beneficial effects were not due to a chelating

effect or prevention of paraquat uptake, e.g., via competition for the OCT for cellular uptake. The lack of effect of the Mn(II) and Cu(II) complexes of EGTA and EHPG on paraquat uptake into NRK-52E cells also supports the notion that their protection is mediated via intracellular mechanisms, i.e., due to their SODm activity subsequent to superoxide generation by paraquat within NRK-52E cells.

The Mn(II) and Cu(II) complexes of EGTA and EHPG seemed to maintain their stability in the incubation medium over the 24-h incubation period. As discussed above, the complexes did not alter the entry of paraquat into cells, which accumulates in renal cells to toxic concentrations over a 24-h period. Protection provided by these complexes was observed after 24 h, with the Mn(II) and Cu(II) complexes providing greater protection than their individual components, suggesting that the complexes maintained their structures. In the case of the most protective agent, Mn(II)-EHPG, the complex provided a synergistic level of protection compared to any protection afforded by the individual components Mn(II) and EHPG. Furthermore, the results of the preincubation study suggest that both Mn(II)-EGTA and Mn(II)-EHPG can enter and remain within NRK-52E cells over a 24-h period. Specifically, after 20 h incubation with Mn(II)-EGTA or Mn(II)-EHPG, NRK-52E cells were still protected against a high concentration of paraquat, even after the cells were rinsed with warm PBS. This suggests that these SODm can enter and remain within cells where they provide protection against ROS generated by paraquat. However, further studies, e.g., using high-pressure/performance liquid chromatography, are warranted to investigate whether the SODm remain in an intact state within intact cells or to what degree they may dissociate into their components within cells, which may still provide some degree of protection, e.g., via the individual actions of Mn and EGTA or EHPG.

In this particular study, Mn(II) and Cu(II) complexes of EGTA and EHPG did not display any pro-oxidant activities at higher concentrations tested. Although Mn(II)-EGTA, Cu(II)-EGTA, EGTA, EHPG, Mn(II), and Cu(II) produced a modest yet significant reduction in cellular viability on their own at higher concentrations, and Cu(II)-EHPG, EGTA, and Cu(II) reduced paraquat-mediated reduction in viability even further, none of these effects on cellular viability were reflected by LDH release. This could suggest that these compounds were causing some degree of mitochondrial dysfunction without subsequent cell death; however, it is much more likely that they were interfering directly with the MTT assay. It should be noted here that these complexes were examined at relatively low concentrations (maximum 100 μ M) and at concentrations which were protective against paraquat-induced cytotoxicity; these agents did not produce cytotoxicity themselves. Although it would be interesting to investigate higher concentrations of these complexes to see if greater protection or increasing toxicity could be observed and to compare these with protective and toxic concentrations of other SODm such as MnTBAP, EUK-8, and M40401, concentrations greater than 100 μ M were not tested due to problems of solubility of these complexes in the incubation medium. However, the relatively safe profile of Mn(II) and Cu(II) complexes of EGTA and EHPG should allow investigations of these complexes in vivo to assess their efficacy against many pathological conditions

involving ROS generation and oxidative stress. Specifically, these complexes could be investigated in models of ischemic or nephrotoxic ARF, which involve significant ROS generation and in which other SODm have been shown to provide beneficial effects [31,32,51]. However, although there was no evidence of Cu(II) toxicity in this study, some care may need to be taken when Cu(II) complexes are utilized in view of a report that Cu(II) derived from Cu/ZnSOD may facilitate oxidative stress in the presence of glutathione [17]. Both EGTA and EHPG have the advantage that they have already been used in biological systems for their chelation and imaging properties and therefore their clinical toxicity profiles are already known. Furthermore, SOD and catalase activities of Mn(II), Cu(II), and Fe(III) complexes of another chelating agent, EDTA, have previously been reported [57] and subsequently, EDTA itself has been reported to protect against ischemic renal injury via modulation of endothelial NO synthase and NO production [60]. It is hoped that, based on the findings of this investigation, Mn(II) and Cu(II) complexes of EGTA and EHPG may provide similar benefits.

In conclusion, the novel SODm, Mn(II) and Cu(II) complexes of EGTA and EHPG reduced paraquat renal cytotoxicity significantly via reduction of paraquat-mediated ROS generation, specifically superoxide anions. Mn(II) complexes were generally more potent than the Cu(II) complexes, with the complex Mn(II)-EHPG providing the highest degree of protection. Unlike conventional SODm, which can display pro-oxidant actions at higher concentrations, these complexes at the highest concentration examined were not toxic to the renal NRK-52E cells utilized in this study. These results therefore demonstrate that these novel SODm have the potential to be used for the treatment of paraquat-induced nephrotoxicity and, possibly, for many other pathological conditions involving oxidative stress.

Acknowledgments

M.S. is the recipient of a Commonwealth Scholarship provided by the Commonwealth Scholarship Commission UK (SLCS-2004-304). P.K.C. acknowledges PABS, University of Brighton, for provision of research facilities and additional funding of this research.

References

- [1] Gunnell, D.; Eddleston, M. Suicide by intentional ingestion of pesticides: a continuing tragedy in developing countries. *Int. J. Epidemiol.* 32:902–909; 2003.
- [2] Eddleston, M.; Phillips, M. R. Self poisoning with pesticides. *BMJ* 328:42–44; 2004.
- [3] Rose, M. S.; Smith, L. L. Tissue uptake of paraquat and diquat. *Gen. Pharmacol.* 8:173–176; 1977.
- [4] Hawksworth, G. M.; Bennett, P. N.; Davies, D. S. Kinetics of paraquat elimination in the dog. *Toxicol. Appl. Pharmacol.* 57:139–145; 1981.
- [5] Smith, L. L. Mechanism of paraquat toxicity in lung and its relevance to treatment. *Hum. Toxicol.* 6:31–36; 1987.
- [6] Haley, T. J. Review of the toxicology of paraquat (1,1'-dimethyl-4,4'-bipyridinium chloride). *Clin. Toxicol.* 14:1–46; 1979.
- [7] Nagata, T.; Kono, I.; Masaoka, T.; Akahori, F. Acute toxicological studies on paraquat: pathological findings in beagle dogs following single subcutaneous injections. *Vet. Hum. Toxicol.* 34:105–112; 1992.

- [8] Autor, A. P. Reduction of paraquat toxicity by superoxide dismutase. *Life Sci.* **14**:1309–1319; 1974.
- [9] Krall, J.; Bagley, A. C.; Mullenbach, G. T.; Hallewell, R. A.; Lynch, R. E. Superoxide mediates the toxicity of paraquat for cultured mammalian cells. *J. Biol. Chem.* **263**:1910–1914; 1988.
- [10] Molck, A. M.; Friis, C. The cytotoxic effect of paraquat on isolated renal proximal tubular segments from rabbits. *Toxicology* **122**:123–132; 1997.
- [11] Senator, A.; Rachidi, W.; Lehmann, S.; Favier, A.; Benboubetra, M. Prion protein protects against DNA damage induced by paraquat in cultured cells. *Free Radic. Biol. Med.* **37**:1224–1230; 2004.
- [12] Suntres, Z. E. Role of antioxidants in paraquat toxicity. *Toxicology* **180**:65–77; 2002.
- [13] Freeman, B. A.; Turrens, J. F.; Mirza, Z.; Crapo, J. D.; Young, S. L. Modulation of oxidant lung injury by using liposome-entrapped superoxide dismutase and catalase. *Fed. Proc.* **44**:2591–2595; 1985.
- [14] Muzykantor, V. R. Delivery of antioxidant enzyme proteins to the lung. *Antioxid. Redox Signal.* **3**:39–62; 2001.
- [15] Muscoli, C.; Cuzzocrea, S.; Riley, D. P.; Zweier, J. L.; Thiemermann, C.; Wang, Z. Q.; Salvemini, D. On the selectivity of superoxide dismutase mimetics and its importance in pharmacological studies. *Br. J. Pharmacol.* **140**:445–460; 2003.
- [16] Mao, G. D.; Thomas, P. D.; Lopaschuk, G. D.; Poznansky, M. J. Superoxide dismutase (SOD)–catalase conjugates: role of hydrogen peroxide and the Fenton reaction in SOD toxicity. *J. Biol. Chem.* **268**:416–420; 1993.
- [17] Paller, M. S.; Eaton, J. W. Hazards of antioxidant combinations containing superoxide dismutase. *Free Radic. Biol. Med.* **18**:883–890; 1995.
- [18] Czapski, G.; Samuni, A.; Goldstein, S. Superoxide dismutase mimics: antioxidative and adverse effects. *Methods Enzymol.* **349**:234–242; 2002.
- [19] McCord, J. M.; Edeas, M. A. SOD, oxidative stress and human pathologies: a brief history and a future vision. *Biomed. Pharmacother.* **59**:139–142; 2005.
- [20] Salvemini, D.; Muscoli, C.; Riley, D. P.; Cuzzocrea, S. Superoxide dismutase mimetics. *Pulm. Pharmacol. Ther.* **15**:439–447; 2002.
- [21] Day, B. J.; Crapo, J. D. A metalloporphyrin superoxide dismutase mimetic protects against paraquat-induced lung injury *in vivo*. *Toxicol. Appl. Pharmacol.* **140**:94–100; 1996.
- [22] Mollace, V.; Iannone, M.; Muscoli, C.; Palma, E.; Granato, T.; Rispoli, V.; Nistico, R.; Rotiroli, D.; Salvemini, D. The role of oxidative stress in paraquat-induced neurotoxicity in rats: protection by non peptidyl superoxide dismutase mimetic. *Neurosci. Lett.* **335**:163–166; 2003.
- [23] Liu, Z.; Robinson, G. B.; Gregory, E. M. Preparation and characterization of Mn–Salophen complex with superoxide scavenging activity. *Arch. Biochem. Biophys.* **315**:74–81; 1995.
- [24] Batinic-Haberle, I.; Spasojevic, I.; Hambricht, P.; Benov, L.; Crumbliss, A. L.; Fridovich, I. Relationship among redox potentials, proton dissociation constants of pyrolic nitrogens, and *in vivo* and *in vitro* superoxide dismutating activities of manganese(III) and iron(III) water-soluble porphyrins. *Inorg. Chem.* **38**:4011–4022; 1999.
- [25] Fisher, A. E.; Hague, T. A.; Clarke, C. L.; Naughton, D. P. Catalytic superoxide scavenging by metal complexes of the calcium chelator EGTA and contrast agent EHPG. *Biochem. Biophys. Res. Commun.* **323**:163–167; 2004.
- [26] Cherny, R. A.; Legg, J. T.; McLean, C. A.; Fairlie, D. P.; Huang, X.; Atwood, C. S.; Beyreuther, K.; Tanzi, R. E.; Masters, C. L.; Bush, A. I. Aqueous dissolution of Alzheimer's disease beta amyloid deposits by biometal depletion. *J. Biol. Chem.* **274**:23223–23228; 1999.
- [27] David-Duflho, M.; Privat, C.; Brunet, A.; Richard, M. J.; Devynck, J.; Devynck, M. A. Transition metals and nitric oxide production in human endothelial cells. *C. R. Acad. Sci.* **III**:13–21; 2001.
- [28] Richardson, N.; Davies, J. A.; Raduchel, B. Iron(III)-based contrast agents for magnetic resonance imaging. *Polyhedron* **18**:2457–2482; 1999.
- [29] Bihari, S.; Smith, P. A.; Parsons, S.; Sadler, P. J. Stereoisomers of Mn(III) complexes of ethylenebis(o-hydroxyphenyl)glycine. *Inorg. Chim. Acta* **331**:310–317; 2002.
- [30] Creely, J. J.; DiMari, S. J.; Howe, A. M.; Hyde, C. P.; Haralson, M. A. Effects of epidermal growth factor on collagen synthesis by an epithelioid cell line derived from normal rat kidney. *Am. J. Pathol.* **136**:1247–1257; 1990.
- [31] Chatterjee, P. K.; Cuzzocrea, S.; Brown, P. A.; Zacharowski, K.; Stewart, K. N.; Mota-Filipe, H.; Thiemermann, C. Tempol, a membrane-permeable radical scavenger, reduces oxidant stress-mediated renal dysfunction and injury in the rat. *Kidney Int.* **58**:658–673; 2000.
- [32] Chatterjee, P. K.; Patel, N. S.; Kvale, E. O.; Brown, P. A.; Stewart, K. N.; Mota-Filipe, H.; Sharpe, M. A.; Di Paola, R.; Cuzzocrea, S.; Thiemermann, C. EUK-134 reduces renal dysfunction and injury caused by oxidative and nitrosative stress of the kidney. *Am. J. Nephrol.* **24**:165–177; 2004.
- [33] Mosmann, T. Rapid colorimetric assay for cellular growth and survival: application to proliferation and cytotoxicity assays. *J. Immunol. Methods* **65**:55–63; 1983.
- [34] Abe, K.; Matsuki, N. Measurement of cellular 3-(4,5-dimethylthiazol-2-yl)-2,5-diphenyltetrazolium bromide (MTT) reduction activity and lactate dehydrogenase release using MTT. *Neurosci. Res.* **38**:325–329; 2000.
- [35] Machaalani, R.; Lazzaro, V.; Duggin, G. G. The characterisation and uptake of paraquat in cultured baboon kidney proximal tubule cells (bPTC). *Hum. Exp. Toxicol.* **20**:90–99; 2001.
- [36] Chan, B. S. H.; Lazzaro, V. A.; Seale, J. P.; Duggin, G. G. Transport of paraquat in a renal epithelial cell line LLC-PK1. *J. Pharmacol. Exp. Ther.* **279**:625–632; 1996.
- [37] Goldstein, S.; Czapski, G. Superoxide dismutase. In: Punchard, N. A., Kelly, F. J., eds. Free radicals: a practical approach. Oxford: Oxford Univ. Press; 1996: 241–255.
- [38] Scheid, C.; Koul, H.; Hill, W. A.; Luber-Narod, J.; Kennington, L.; Honeyman, T.; Jonassen, J.; Menon, M. Oxalate toxicity in LLC-PK1 cells: role of free radicals. *Kidney Int.* **49**:413–419; 1996.
- [39] Yamada, Y.; Yoshimura, S.; Yamakawa, H.; Sawada, M.; Nakagawa, M.; Hara, S.; Kaku, I.; Naganawa, T.; Banno, Y.; Nakashima, S.; Sakai, N. Cell permeable ROS scavengers, Tiron and Tempol, rescue PC12 cell death caused by pyrogallol or hypoxia/regeneration. *Neurosci. Res.* **45**:1–8; 2003.
- [40] Halliwell, B.; Grootveld, M.; Gutteridge, J. M. Methods for the measurement of hydroxyl radicals in biomedical systems: deoxyribose degradation and aromatic hydroxylation. *Methods Biochem. Anal.* **33**:59–90; 1988.
- [41] Min, S. K.; Kim, Y.; Kim, C. H.; Woo, J. S.; Jung, J. S.; Kim, Y. K. Role of lipid peroxidation and poly (ADP-ribose) polymerase activation in oxidant-induced membrane transport dysfunction in opossum kidney cells. *Toxicol. Appl. Pharmacol.* **166**:196–202; 2000.
- [42] Bradford, M. M. A rapid and sensitive method for the quantitation of microgram quantities of protein utilizing the principle of protein-dye binding. *Anal. Biochem.* **72**:248–254; 1976.
- [43] Hancock, J. T. Superoxide, hydrogen peroxide and nitric oxide as signalling molecules: their production and role in disease. *Br. J. Biomed. Sci.* **54**:38–46; 1997.
- [44] McCord, J. M. Superoxide dismutase in aging and disease: an overview. *Methods Enzymol.* **349**:331–341; 2002.
- [45] Emerit, J.; Edeas, M.; Bricaire, F. Neurodegenerative diseases and oxidative stress. *Biomed. Pharmacother.* **58**:39–46; 2004.
- [46] Wasserman, B.; Block, E. R. Prevention of acute paraquat toxicity in rats by superoxide dismutase. *Aviat. Space Environ. Med.* **49**:805–809; 1978.
- [47] Bagley, A. C.; Krall, J.; Lynch, R. E. Superoxide mediates the toxicity of paraquat for Chinese hamster ovary cells. *Proc. Natl. Acad. Sci. U. S. A.* **83**:3189–3193; 1986.
- [48] Jewett, S. L.; Rocklin, A. M.; Ghanevati, M.; Abel, J. M.; Marach, J. A. A new look at a time-worn system: oxidation of CuZn-SOD by H₂O₂. *Free Radic. Biol. Med.* **26**:905–918; 1999.
- [49] Nelson, S. K.; Bose, S. K.; McCord, J. M. The toxicity of high-dose superoxide-dismutase suggests that superoxide can both initiate and terminate lipid-peroxidation in the reperfused heart. *Free Radic. Biol. Med.* **16**:195–200; 1994.
- [50] Mitchell, J. B.; Samuni, A.; Krishna, M. C.; DeGraff, W. G.; Ahn, M. S.; Samuni, U.; Russo, A. Biologically active metal-independent superoxide dismutase mimics. *Biochemistry* **29**:2802–2807; 1990.
- [51] Cuzzocrea, S.; Mazzon, E.; Dugo, L.; Serraino, I.; Di Paola, R.; Britti, D.; De Sarro, A.; Pierpaoli, S.; Caputi, A.; Masini, E.; Salvemini, D. A role for superoxide in gentamicin-mediated nephropathy in rats. *Eur. J. Pharmacol.* **450**:67–76; 2002.
- [52] Spasojevic, I.; Batinic-Haberle, I.; Stevens, R. D.; Hambricht, P.; Thorpe, A. N.; Grodkowski, J.; Neta, P.; Fridovich, I. Manganese(III) biliverdin

- IX dimethyl ester: a powerful catalytic scavenger of superoxide employing the Mn(III)/Mn(IV) redox couple. *Inorg. Chem.* **40**:726–739; 2001.
- [53] Batinic-Haberle, I. Manganese porphyrins and related compounds as mimics of superoxide dismutase. *Methods Enzymol.* **349**:223–233; 2002.
- [54] Sharpe, M. A.; Olsson, R.; Stewart, V. C.; Clark, J. B. Oxidation of nitric oxide by oxomanganese–salen complexes: a new mechanism for cellular protection by superoxide dismutase/catalase mimetics. *Biochem. J.* **366**:97–107; 2002.
- [55] Fisher, A. E.; Maxwell, S. C.; Naughton, D. P. Catalase and superoxide dismutase mimics for the treatment of inflammatory disease. *Inorg. Chem. Commun.* **6**:1205–1208; 2003.
- [56] Collman, J. P.; Zeng, L.; Brauman, J. I. Donor ligand effect on the nature of the oxygenating species in Mn(III) (salen)-catalyzed epoxidation of olefins: experimental evidence for multiple active oxidants. *Inorg. Chem.* **43**:2672–2679; 2004.
- [57] Fisher, A. E.; Maxwell, S. C.; Naughton, D. P. Superoxide and hydrogen peroxide suppression by metal ions and their EDTA complexes. *Biochem. Biophys. Res. Commun.* **316**:48–51; 2004.
- [58] Chan, B. S. H.; Lazzaro, V. A.; Seale, J. P.; Duggin, G. G. Characterisation and uptake of paraquat by rat renal proximal tubular cells in primary culture. *Hum. Exp. Toxicol.* **15**:949–956; 1996.
- [59] Groves, C. E.; Morales, M. N.; Gandolfi, A. J.; Dantzer, W. H.; Wright, S. H. Peritubular paraquat transport in isolated renal proximal tubules. *J. Pharmacol. Exp. Ther.* **275**:926–932; 1995.
- [60] Foglieni, C.; Fulgenzi, A.; Ticozzi, P.; Pellegatta, F.; Sciorati, C.; Belloni, D.; Ferrero, E.; Ferrero, M. E. Protective effect of EDTA preadministration on renal ischemia. *BMC Nephrol.* **7**:5; 2006.

Catalytic anti-oxidants: Is the way forward back to nature?

Recent advances in anti-oxidant therapy have centred on a variety of complex anti-oxidants which exhibit catalytic activity imparted by the presence of a redox-active metal ion. Unlike vitamins and metal-free small molecule anti-oxidants, these enzyme mimetics can destroy very large quantities of reactive oxygen and nitrogen species (RONS) without the need for recycling. Future directions include developing targeted mimetics with tailored anti-oxidant activities and the exploration of dietary sources of natural anti-oxidant mimetics.

Keywords: Enzyme mimetics, smart chelators, inflammation, oxidative damage

Chronic inflammatory diseases

Recent advances in the understanding of chronic inflammation highlight its significant role in the initiation or perpetuation of a vast number of diseases. These include the seemingly disparate disorders: cancers, arthritis, diabetes, neurodegenerative diseases, cardiovascular diseases and pulmonary diseases, along with the ageing process itself [1]. Termed “The Silent Killer”, chronic inflammation has defied the best efforts of medical researchers seeking a cure. As with the discovery of corticosteroids, some 50 years ago, the current approaches to new treatments are seriously hampered by poor therapeutic indices [2].

Mechanisms of oxidative damage

Chronic inflamed tissues are characterised by an abnormal biochemical profile which results from vascular compromise, inflammatory infiltration, swelling and proliferation. This chaotic environment is a breeding ground for the generation and release of RONS which in turn leads to further oxidative damage. This cycle of oxidative damage in turn perpetuates the inflammation cascades, hence the term auto-immune disease.

Although the primary defence against RONS is the compartmentalisation of cellular RONS generating systems, the second line defences are the anti-oxidant enzymes [1]. These are comprised of superoxide dismutases, catalase and peroxidase. Imbalances between RONS production and antioxidant enzyme activities lead to oxidative stress. The principle RONS may be categorised into moderate [e.g. superoxide ($O_2^{\cdot-}$), hydrogen peroxide (H_2O_2) and nitric oxide (NO^{\cdot})] and highly potent [e.g. peroxynitrite ($ONOO^{\cdot}$) and hydroxyl radical ($\cdot OH$)]. The latter are a particular danger as there are no protective enzymes for their suppression. Key roles have been

reported for labile redox active metal ions in enhancing oxidative damage via their interactions with RONS [3].

Roles of redox-active metal ions

Elevated levels of “labile” metal ions such as Cu(II) and Fe(III), have been observed at sites of inflammation such as in the inflamed rheumatoid joint [1]. Numerous systems have been described for metal ion-mediated transformation of moderate to highly potent RONS and for the activation of the latter. These include the Fenton reaction, Haber Weiss reaction, Udenfriend’s system and enhancing the nitration of endogenous compounds by ONOO^- . It is notable that in Udenfriend’s system, the “anti-oxidant” vitamin C along with Fe(II) ions and oxygen lead to oxidative damage. Thus, vitamins may promote the generation of RONS rather than suppress them. In addition, other “anti-oxidants” fail as they do not bind metal ions and are inefficient as they are not catalytic. They are more suitably classified as electron transfer agents that require rejuvenation by cumbersome processes (relative to anti-oxidant enzymes).

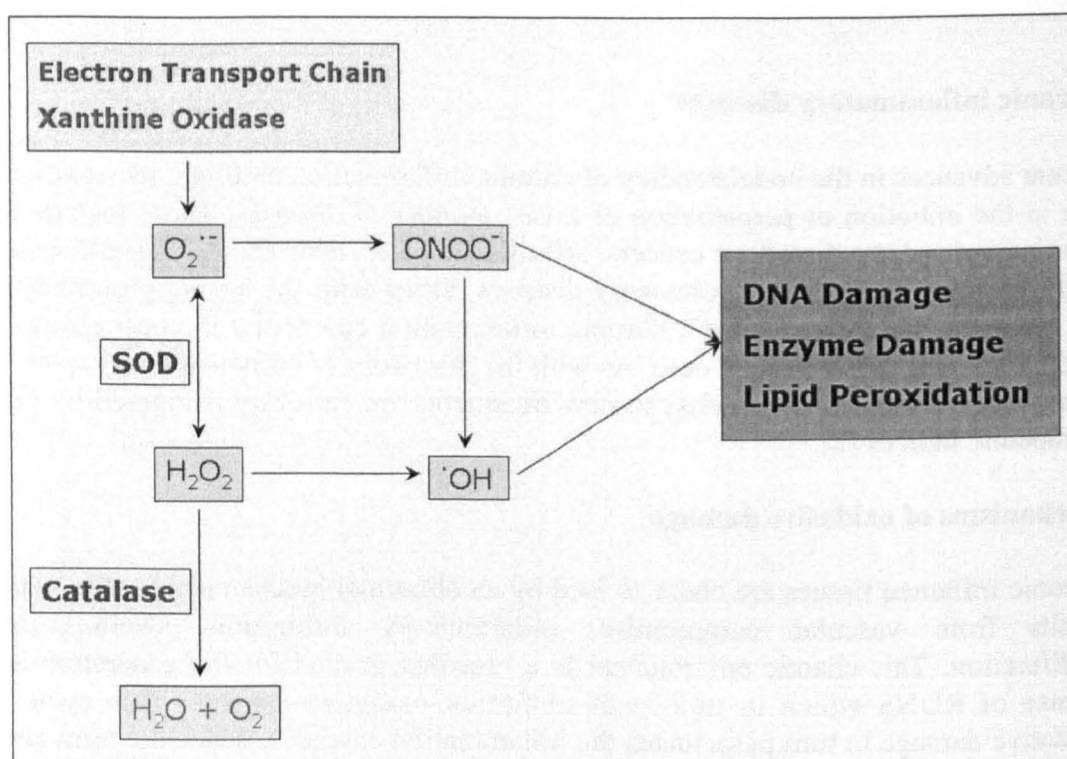


Fig. 1. Interplay mechanisms for protection against highly potent RONS which frequently arise by interactions with metal ions. RONS are generated *in vivo* by inflammatory cells, metabolic pathways, ionising radiation, detoxification processes and reductases such as xanthine oxidase/reductase.

Catalytic anti-oxidants

A current growth area in oxidative damage suppression has been the development of catalytic anti-oxidant enzyme mimetics [4]. These agents, in the active form, possess redox-active metal ions that impart commensurate efficacies for RONS deactivation to those found in the native enzymes. The first generation enzyme mimetics were metal complexes which were incapable of chelating and thus deactivating deleterious redox metal ions. However, several of these preformed metal complexes were active in models of inflammatory diseases. Specificity is a key feature of the anti-oxidant enzyme mimetics as many are limited to SOD activity alone, resulting in $O_2^{\cdot -}$ suppression at the expense of elevated H_2O_2 levels. There is a major requirement for standardisation as many different compounds have been used, often without full characterisation of their different anti-oxidant enzyme activities.

More recently, “smart chelators” are being developed that complex and inactivate deleterious “labile” metal ions to eliminate their contributions to oxidative damage [5]. In broad terms these can be categorised through their modes of action as: i) redox silencers, ii) anti-oxidant enzyme mimetic and, iii) a RONS scavenger. For redox silencers the chelator is designed to occupy all metal co-ordination sites to hinder interactions with RONS. A second feature is the stabilisation of the metal ion oxidation state to prevent redox cycling and the production of highly potent RONS. For the anti-oxidant enzyme mimetics, the benefits of using a chelator over the preformed complex (first generation mimetics) are: i) the capture of the deleterious labile metal ion and, ii) reversal of its activity from RONS producer to suppressor. Unlike vitamin C, upon metal ion chelation, the RONS scavenger is designed to absorb oxidants instead of producing them.

Dietary and targeted chelators

Recently, a number of dietary sources of chelators which form anti-oxidant mimetics have been identified [6]. Complexes of tea catechins have exhibited SOD activities and therapeutic potential in a number of model systems, notably related to neurological disorders. A complex of curcumin with Cu(II) ions has been prepared and exhibits SOD activities commensurate with the best synthetic mimetics. However, it should be noted that the preparation of the curcumin complex involved a complex synthesis unlikely to be valid *in vivo* (reflux in ethanol for three hours). Further work is required to establish the feasibility of dietary intervention through the formation of anti-oxidant mimetics *in vivo*.

Despite the availability of successful reports on model systems in the literature, it is likely that catalytic anti-oxidants will have to be targeted to appropriate diseased tissues or sub-cellular locations. Sub-cellular targeting has begun with the cell membrane and mitochondrion as initial targets [7]. In addition, diseased tissues may be targeted using biochemical abnormalities, such as hypoxia, found at sites of inflammation [8].



Fig. 2. Common foodstuffs such as tea and spices are a likely source of future therapeutic agents as well as exotic plants from the Peruvian jungle.

Conclusions

Recent advances in the development and applications of catalytic anti-oxidants have fuelled the need for future work in this unique therapeutic avenue. The generation of multiple types of catalytic therapies against oxidative damage holds considerable promise in the war against inflammatory diseases and their widespread cogent

conditions. Future directions include further advances in smart chelators, targeted anti-oxidant mimetics and directed diets founded on natural functional chelators.

References

- [1] Halliwell B. *et al.*: Free Radicals in Biology and Medicine. Oxford University Press, UK. (1999).
- [2] Chikanza I.C. *et al.*: Journal of Pharmacy and Pharmacology 50, 357-369 (1998).
- [3] Fisher A.E.O. *et al.*: Nutrition Journal 3, 2 (2004).
- [4] Fisher A.E.O. *et al.*: Biochemical Biophysical Research Communications 323, 163-167 (2004).
- [5] Fisher, A.E.O. *et al.*: Current Drug Delivery 2, 261-268 (2005).
- [6] Hague T. *et al.*: Behavioural Pharmacology 17, 425-430 (2006)
- [7] Fisher A.E.O. *et al.*: Biochemical Biophysical Research Communications 329, 930-933 (2005).
- [8] Naughton D.P.: Adv Drug Deliv Rev 53, 229-233 (2001).

Contact:

Declan P. Naughton
Professor of Biomolecular Sciences
School of Life Sciences, Kingston University, Penrhyn Road,
Kingston upon Thames, Surrey KT1 2EE
Tel: 0208 547 7097
D.Naughton@kingston.ac.uk

Theresa A. Hague
School of Life Sciences, Kingston University, Penrhyn Road, Kingston upon Thames
Surrey KT1 2EE
K0541004@kingston.ac.uk

James Barker
Reader in Analytical Science,
School of Pharmacy and Chemistry, Kingston University, Penrhyn Road,
Kingston upon Thames, Surrey KT1 2EE, UK

Paul L.R.Andrews
Professor of Comparative Physiology
Division of Basic Medical Sciences, St George's University of London,
Cranmer Terrace, London, SW17 0RE.

Dietary chelators as antioxidant enzyme mimetics: implications for dietary intervention in neurodegenerative diseases

Theresa Hague^a, Paul L. R. Andrews^c, James Barker^b and Declan P. Naughton^a

Following recent reviews on the role of metal ions in oxidative stress and neurodegenerative diseases, this article reports advances in the study of dietary components for the control of these conditions. Poor metal ion homeostasis is credited with pathological roles in the progression of a number of disorders including Alzheimer's disease, Parkinson's disease and multiple sclerosis. Synthetic metal ion chelators continue to show promise as a new therapeutic approach for neurodegenerative disorders. Dietary chelators, unlike most vitamins, are, however, capable of negating or even reversing the roles of metal ions by: (i) decorporation of metal ions, (ii) redox silencing, (iii) dissolution of deposits, and (iv) generation of an antioxidant enzyme mimetic. This review gives a critical evaluation of recent progress in, and potential for, dietary control of neurodegeneration on the basis of the

formation of antioxidant enzyme mimetics. *Behavioural Pharmacology* 17:425–430 © 2006 Lippincott Williams & Wilkins.

Behavioural Pharmacology 2006, 17:425–430

Keywords: antioxidant enzyme mimetic, chelator, diet, metal ions, natural product, neurodegeneration, oxidative stress

School of ^aLife Sciences, ^bPharmacy and Chemistry, Kingston University, Kingston-upon-Thames, Surrey and ^cDivision of Basic Medical Sciences, St George's University of London, London, UK.

Correspondence and requests for reprints to Professor Declan P. Naughton, PhD, School of Life Sciences, Kingston University, Penrhyn Road, Kingston-upon-Thames, Surrey KT1 2EE, UK
E-mail: D.Naughton@kingston.ac.uk

Received 25 April 2006 Accepted as revised 12 June 2008

Introduction

Detailed studies of many intricate pathological events occurring during neurodegeneration have widened our understanding of these disease processes (e.g. Esposito *et al.*, 2006; Nichols *et al.*, 2006). We are, however, far from comprehensively understanding, let alone combating, many neurological disorders. Persistent inflammation and metal ion deposition are characteristic features of many neurological disorders including Alzheimer's disease (AD), Parkinson's disease (PD) and multiple sclerosis (Bossy-Wetzel *et al.*, 2004; Doraiswamy and Finebrock, 2004; Gacta and Hider, 2005; Moreira *et al.*, 2005; Tabner *et al.*, 2005). Chronic inflammation is a complex multifaceted process, which is driven by a matrix of pathways with complexities that do not lead to an optimistic prognosis or to the expectation of an imminent cure. In the half century, since the Nobel Prize was awarded for the treatment of rheumatoid arthritis with corticosteroids, mankind has endeavoured to treat chronic inflammatory diseases by combating inflammatory pathways, but without a glimpse of a cure. Even the latest anti-inflammatory agents exhibit serious side effects upon long-term use, as do corticosteroids, for which the Prize was awarded.

From a drug discovery perspective, the presence of metal ion deposits in inflamed tissues is intriguing. Uncontrolled metal ion homeostasis is considered to play an important role in inflammatory pathogenesis via the mediation of oxidative damage (Halliwell and Gutteridge,

1999). Oxidatively damaged cellular components may in turn elicit an immune response leading to the perpetuation of autoimmune disease. *In vitro*, the redox-active transition metal ions Fe(III) and Cu(II) enhance oxidative damage by well-established reactions such as the Fenton and Haber–Weiss reactions for the generation of the potent hydroxyl radical ($\cdot\text{OH}$) (Halliwell and Gutteridge, 1999; Fisher and Naughton, 2004, 2005a). The presence of redox-active ions in neurological disorders is a clear target for therapeutic intervention. Recent reviews have highlighted the potential for metal-ion-based therapeutic intervention in neurological disorders (Fisher and Naughton, 2005a; Valko *et al.*, 2005) and put the case for the ineffectiveness of vitamins (Fisher and Naughton, 2005b). This approach aims to prevent or slow down formation of deposits, and where formed to: (i) remove deleterious metal ions and their contribution to oxidative stress, (ii) dissolve the ferric ion deposits, (iii) prevent metal ion based biomolecule aggregation and (iv) generate catalytic antioxidants (enzyme mimetics) that unlike vitamins are capable of independently destroying large quantities of reactive oxygen and nitrogen species (RONS) (Fisher and Naughton, 2005a).

The focus of this review is to give a critical overview of the potential for dietary intervention involving natural products that chelate metal ions to form antioxidant enzyme mimetics. Thus, natural chelators have the

potential to: (i) remove deleterious redox active metal ions and their contributions to biomolecule aggregation, (ii) convert metal ions into potent antioxidant mimetics to combat oxidative stress and (iii) 'dissolve' biomolecule and metal oxide aggregates.

Reactive oxygen and nitrogen species and metal ions

Oxidative damage results from an imbalance between the body's defences and the levels of RONS generation in a specific tissue (Halliwell and Gutteridge, 1999; McLaren *et al.*, 2006; Rahman *et al.*, 2006). The defence mechanisms include compartmentalization, antioxidant enzymes [eg. superoxide dismutase (SOD), catalase and peroxidase] and careful homeostasis of oxidizing and reducing agents and redox-active metal ions that could aggravate oxidative damage. A further consideration is the capacity for damage repair that may vary with organelle, cell and tissue type, and health status or type (and stage of progression) of disease (Mahmoudi *et al.*, 2006). RONS are generated by inflammatory cells, normal metabolic (enzymatic) processes, signalling mechanisms, xenobiotics and ionizing radiation, among other sources (Blomgren and Hagberg, 2006; Roncone *et al.*, 2006; Tompkins *et al.*, 2006; Zweier and Talukder, 2006).

Commonly studied RONS include hydrogen peroxide (H_2O_2), superoxide (O_2^-), hydroxyl radicals ($\cdot\text{OH}$), nitric oxide ($\text{NO}\cdot$), peroxyxynitrite (ONOO^-) and hypochlorous acid (HOCl). It should be, however, noted that under physiological conditions, many of these species can rapidly interconvert and readily convert to a much larger number of reactive intermediates that are outside the scope of this article. In broad terms, RONS can be grouped into those whose formation or removal normally falls under enzymatic control *in vivo* (H_2O_2 , O_2^- , $\text{NO}\cdot$) and those that are relatively uncontrollable ($\cdot\text{OH}$, ONOO^- , HOCl). The latter uncontrollable RONS are key targets for therapeutic intervention, as they exceed the scope for antioxidant protection in mammals. The complexities of RONS investigations, however, parallel those of mediators of inflammation, except an added dimension arises from the dynamics of RONS interconversion. This interchange coupled to the paucity of real-time measurement capacity for multiple RONS leads to caution in assessing the pathological roles of individual RONS. An alternative approach involves preventing the formation of specific RONS by applying 'chemical knockouts'. Rapid progress has been made in the discovery of numerous small molecule antioxidant enzyme mimetics that destroy copious quantities of their target RONS (Fisher and Naughton, 2005a).

Neurological disorders and redox-active metal ions

Over 20 neurodegenerative disorders have been associated with metal ion imbalances. In PD, increased iron

levels found in the substantia nigra coupled to caeruloplasmin mutations imply a state of poor metal homeostasis (Hochstrasser *et al.*, 2004; Morawski *et al.*, 2005). Other studies have revealed an almost two-fold increase in the incidence of PD in daily iron supplement users, demonstrating that diet can play a key role in disease progression (Powers *et al.*, 2003). The iron chelator desferrioxamine was effective in models of PD in mice, indicating that reducing iron levels prevents dopaminergic neuron degeneration and reduces abnormal protein aggregation (Zhang *et al.*, 2005).

In AD, plaques are formed from the amyloid- β -protein ($\text{A}\beta$), which is proteolytically derived from the amyloid precursor protein (APP). APP binds to Cu(II) reducing it to Cu(I) , leading to the formation of a disulfide bond in the APP (Multhaup *et al.*, 1997). Aggregation of amyloid- β plaques is initiated by submicromolar levels of metal ions *in vitro* (Huang *et al.*, 2004). Previous studies have implicated leading roles for metal ions in the progression of AD. Plaques are associated with accumulations of redox-active metal ions ($\text{Cu} \approx 0.4 \text{ mmol/l}$, $\text{Fe} \approx 1 \text{ mmol/l}$) (Strausak *et al.*, 2001). Increased ferritin and decreased transferrin levels are observed in brains of AD patients (Fischer *et al.*, 1997). RONS are produced during metal ion binding by $\text{A}\beta$ (Huang *et al.*, 1999) and plaques can be dispersed with metal ion chelators (Cherny *et al.*, 2001; Rottkamp *et al.*, 2001). More recently $\text{A}\beta$ has been shown to redox cycle iron leading to RONS generation (Khan *et al.*, 2006).

In a preliminary study, magnetite and maghemite deposits have been found in brains of patients suffering from AD (Dobson, 2001; Hautot *et al.*, 2003). These highly magnetic (ferromagnetic) crystals are found in regular patterns that suggest they are deposited in a carefully controlled biological process, analogous to their biochemical control in birds where they assist navigation. Deposition of these iron oxides suggests that a defect has occurred in normal control mechanisms for this process. Dissolving these crystals with chelators is one of a number of therapeutic approaches that may also include controlling the biochemical regulation of deposition and dietary intervention.

In several other neurodegenerative disorders characterized by inflammation, poor metal ion homeostasis has been observed. Brain iron localization in reactive microglia and macrophages is likely to contribute to oxidative damage in multiple sclerosis (LeVine, 1997). Iron misregulation is credited with a pathological role in a variety of other neurological disorders including Huntington's disease, Friedreich's ataxia and prion diseases (Mattson, 2004; Cerpa *et al.*, 2005). Furthermore, for a number of conditions, neurodegeneration is just one component in which poor metal ion homeostasis affects

several organs. In Wilson's disease, poor copper regulation results in copper accumulation in the liver followed by deposition in the brain (Kitzberger *et al.*, 2005).

Neurological disorders, behaviour and antioxidants

The approach of treating neurological disorders with chelators with the capability to form antioxidant mimetics, while preventing or reversing metal ion-mediated plaque formation, is still in its infancy. A number of recent studies have, however, demonstrated the potential for antioxidant intervention strategies to rescue and/or protect against neurodegenerative disorders. Further work is warranted to explore the precise active constituent(s) and/or the mechanism(s) of action in each case given below.

Potential experimental antioxidant therapies for PD, or models of PD, include pretreatment of caffeine against intrastriatal 6-hydroxydopamine-lesioned rats (Joghataie *et al.*, 2004). In this study, the observed attenuation of the apomorphine-induced rotational behaviour, coupled to protection of neurones of the substantia nigra pars compacta by caffeine, may reflect its antioxidant activity (Weiss and Landauer, 2003). The antioxidant selenium was also protective in the 6-hydroxydopamine-induced rat model of PD (Zafar *et al.*, 2003). In this study, selenium treatment resulted in an enhancement of the antioxidant status along with near baseline functional recovery. In the same model of PD, pretreatment with the iron chelator desferrioxamine ameliorated locomotor activity, rearing and exploratory behaviour (Youdim *et al.*, 2004). In a more recent study, the protective effects of black tea extracts (BTE) have been investigated (Chaturvedi *et al.*, 2006). This study also revealed recovery (both pretreatment and post-treatment with BTE relative to 6-hydroxydopamine) in spontaneous locomotor activity and in D-amphetamine-induced circling behaviour, as well as in striatal antioxidant status (lipid peroxidation and SOD levels). The authors report the pretreatment schedule as the more effective, and further exploration of these results are warranted in light of the potential for BTE constituents to act as dietary chelators, with the potential to form complexes with SOD-mimetic activities as outlined below.

Potential antioxidant treatments for AD are under investigation in models of disease. Following intrahippocampal injections with aggregated A β in rats, daily oral administration of α -tocopherol improved temporal discrimination under a recycling conjunctive schedule of food reinforcement (McDaid *et al.*, 2005). In a previous report, intracerebroventricular infusion of A β in rats was employed to show that daily oral administration of α -tocopherol prevented impairment of maze performance (Yamada *et al.*, 1999). Apple juice concentrate was

Table 1 IC₅₀ values for metal complexes of synthetic and natural product chelates that exhibit sodium dismutase (SOD)-like activity

References	SOD mimic	IC ₅₀ (μ mol/l)
Jiang <i>et al.</i> (2003)	M40403	31.8
Kostyuk <i>et al.</i> (2004)	Cu(II)-luteolin	0.80
Fisher <i>et al.</i> (2004)	2Cu(II)-EGTA	0.80
Kostyuk <i>et al.</i> (2004)	Cu(II)-rutin	0.50
Baudry <i>et al.</i> (1993)	Manganese salen C12	0.32
Kostyuk <i>et al.</i> (2004)	Cu(II)-(-)-epicatechin	0.32
Fisher <i>et al.</i> (2005)	Mn(II)-monensin	0.31
Fisher <i>et al.</i> (2004)	Mn(II)-EGTA	0.19
Barik <i>et al.</i> (2005)	Cu(II)-curcumin	0.18
Boka <i>et al.</i> (2004)	Cu(II)-Ac-HisValHis-H ₂	0.18
Fisher <i>et al.</i> (2005)	2Cu(II)-monensin	0.09
Spasojevic <i>et al.</i> (2001)	1/2[(Mn(III)BVDME) ₂]	0.047
Batinic-Haberle <i>et al.</i> (1999)	Mn(III)TE-2-PyP ⁵⁺	0.045
Jitsukawa <i>et al.</i> (2001)	CuZn-SOD	0.0028

selected as a rich source of antioxidants, and has been shown to prevent oxidative damage and deterioration of maze performance in aged mice (Tchanchou *et al.*, 2005). In a study reported by Frautschy *et al.* (2001), dietary curcumin reduced A β deposits and prevented spatial memory deficits induced by infusions of A β . The recent identification of curcumin as a dietary antioxidant chelator, which can exhibit SOD-like activity in the complexed form (Table 1), further enhances the significance of these key observations.

Antioxidant enzyme mimetics

A wide range of metal complexes has been prepared which exhibit antioxidant enzyme activities. These range from small peptide mimetics of the antioxidant enzyme active sites (metal binding centres) to numerous complexes bearing little or no similarity to the enzymes (Table 1). A large number of these diverse agents have been tested in numerous model systems and these have been reviewed elsewhere (Fisher and Naughton, 2005a). Numerous key parameters such as the specific antioxidant enzyme activities of various mimetics are not known however, thus, the field lacks standardization. Current efforts are underway to enhance our understanding of these agents which includes: (i) the full characterization of all the antioxidant enzyme activities (i.e. catalase, SOD, peroxidase) for each agent, (ii) the tissue and cellular distribution profiles (e.g. permeability into cells, organelles, membranes etc.), (iii) the pharmacokinetics and (iv) pharmacodynamics.

Several approaches to categorize therapeutic chelators exists and these may be based on the source, chelator structure, metal ion(s) complexes formed or pharmacodynamic properties of the end complex. It is becoming clear that a large number of redox-active metal ion complexes can partake in redox reactions attributable to antioxidant enzyme mimetics. These chelators arise from numerous sources including synthetic chemistry projects,

drug discovery programmes, microbial isolates and more recently from plant sources. Recently, chelators have been categorized by their pharmacodynamic activities that are imparted upon formation of complexes with redox-active metal ions (Fisher and Naughton, 2005a). Thus, the categories of (i) antioxidant enzyme mimetic, (ii) a RONS scavenger and (iii) a redox silencer have been employed.

Dietary antioxidant chelators

As a wide variety of molecules have been shown to complex redox-active metal ions and impart antioxidant enzyme activities, a large number of dietary components may be expected to exhibit these properties (Table 1). As for the general field of antioxidant chelators, clearly a great deal of further study is required to ascertain which dietary components are active and under which conditions. These studies should include the usual considerations of relative stabilities of the chelators and/or their complexes towards stomach acids and enzymes, ingestion potential, and profiles of RONS that are inactivated. In addition, consideration needs to be given to the preference for administration as chelator or complex, the optimal ratios of metal ions to chelators, the availability of redox-active metal *in vivo* to enact complex formation from the chelator and the stability constants for the complex. The stability constant is critical to ensure competing metal ions do not destabilize the complex and that key metal centres in biomolecules remain unaffected, while removing deleterious metal ions that initiate and/or perpetuate pathological biomolecule aggregation. Further key issues for treating NDs are the permeability of therapeutic agents and their complexed forms to the blood-brain barrier and this key concept is addressed below.

To date, these detailed studies have not been conducted on any dietary foodstuff. One of the most studied common sources of dietary chelators is green tea, which has well-established antioxidant effects. A large number of publications detail the beneficial effects of green tea and of polyphenolic and other extracts of green tea on *in-vitro* model systems, cellular systems and animal models (Sutherland *et al.*, 2006). These effects range from epidemiological studies on humans relating to cancer, cardiovascular and neurological diseases to animal models of PD and AD (Cabrera *et al.*, 2006). Polyphenolics constitute up to one-third of the dry weight of green tea with the catechins being the principal remedial components (Zaveri, 2006). The major catechin epigallocatechin gallate (EGCG) accounting for some two-thirds of the catechin content is protected by the steaming and drying process used for green teas (Zaveri, 2006). The pharmacological effects of this and related catechins have been widely studied. EGCG inhibits cardiac hypertrophy by blocking the RONS-dependent nuclear factor- κ B and

RONS-independent activator protein-1 pathways (Li *et al.*, 2006a). It ablates RONS-induced apoptosis in motor neurones transfected with G93A CuZnSOD (Koh *et al.*, 2004). It upregulates the cytoprotective enzyme heme oxygenase via the phosphatidylinositol 3-kinase and extracellular signal-regulated protein kinase pathways (Wu *et al.*, 2005). More recently, EGCG has been shown to ameliorate disease progression in an amyotrophic lateral sclerosis mouse model initiated by transfection with G93A CuZnSOD (Koh *et al.*, 2006). In oral carcinoma cells, EGCG inhibited secretion of APP in a dose-dependent manner (Ko *et al.*, 2006). Similar results were found in human neuroblastoma cells in which the inhibitory effect of EGCG on levels of membrane-bound APP secretion was reversed with the administration of ferrous sulphate (Reznichenko *et al.*, 2006). The authors suggest that this brain-permeable potent chelator may be a therapeutic agent for AD and other iron-associated disorders (Reznichenko *et al.*, 2006). EGCG when administered both intraperitoneally and orally reduced the amyloid depositions in brains of APP transgenic mice (Li *et al.*, 2006b).

In contrast, it is notable that a number of studies report detrimental effects of green tea and its extracts (Navarro-Peran *et al.*, 2005; Galati *et al.*, 2006; Yu *et al.*, 2006). Toxic effects were found in isolated hepatocytes with EGCG being most toxic with the mechanism of toxicity being disruption of the mitochondrial membrane potential and formation of RONS (Galati *et al.*, 2006). Furthermore, a prostate cancer cell line treated with Cu(II) ions and EGCG exhibited rapid cell death via disruption of the cytoplasmic membrane, which may result from generation of hydroxyl radicals (Yu *et al.*, 2006). Intake of EGCG during pregnancy may cause birth defects owing to its inhibitory effect on dihydrofolate reductase at common levels found in the sera of green tea drinkers (Navarro-Peran *et al.*, 2005).

In addition to the ferric ion chelation study on EGCG (Reznichenko *et al.*, 2006), a number of other catechins have been subjected to metal ion binding studies. These include ferric and cupric ion interactions with catechin (Fernandez *et al.*, 2002), and (-)-epicatechin, which exhibited moderately enhanced SOD activity *in vitro* in the complexed form relative to the free chelator (Kostyuk *et al.*, 2004). A conversion of redox active metal ions from mediating disease initiation and/or progression to preventing metal or peptide deposition, along with the concomitant generation of antioxidant enzyme mimetics, is very attractive from a therapy perspective.

A wide variety of dietary products or isolated natural products have been examined *in vitro* and in model systems for their antioxidant and anti-inflammatory potentials, with emphases on their efficacy in treating

neurodegenerative diseases (e.g. Ono *et al.*, 2006). Many have not addressed the issues pertaining to the pathological roles of metal ions, either in discussion or by appropriate experimental design (Fisher and Naughton, 2005b). More recently, several isolated compounds have been shown to exhibit levels of antioxidant enzyme activity that are commensurate with some of the best synthetic mimetics available (Barik *et al.*, 2005). This subject area requires considerable work to establish the potential of dietary-based chelators to treat or protect against neurological disorders in which metal ions are credited with pathological roles.

Concluding remarks

Although a comprehensive understanding of the parameters raised above remains elusive, a great deal of effort is bringing the prospect of diet-based therapeutic agents for neurological diseases somewhat closer. A number of uncertainties, however, remain to be clarified. For many synthetic and natural products, the antioxidant mimic activities have only been reported for the SOD reaction. Hence, a highly active SOD mimic generating large amounts of hydrogen peroxide may be deleterious in the absence of catalase activity. It is imperative that we gain an in-depth understanding of the profile of antioxidant enzyme activities exhibited by each complex. Where, for example, do these chelators decorporate the metal ions? (are the complexes permeable to the blood-brain barrier for excretion?). What becomes of the hydrogen peroxide generated by the SOD reaction? (do the mimetics also exhibit catalase activities?). Do these chelators impair metalloprotein function by chelating the metal ions in the active site or by extracting them? What other non oxidant-related enzyme activities will these chelators exhibit?

References

- Barik A, Mishra B, Shen L, Mohan H, Kadam RM, Dutta S, *et al.* (2005). Evaluation of a new copper(II)-curcumin complex as superoxide dismutase mimic and its free radical reactions. *Free Radical Biol Med* **39**:811–822.
- Batinic-Haberle I, Spasojevic I, Hambricht P, Benov L, Crumbliss AL, Fridovich I (1999). Relationship among redox potentials, proton dissociation constants of pyrrolic nitrogens, and in vivo and in vitro superoxide dismutating activities of manganese(III) and iron(III) water-soluble porphyrins. *Inorg Chem* **38**:4011–4022.
- Baudry M, Etienne S, Bruce A, Palucki M, Jacobsen E, Malfroy B (1993). Salen-manganese complexes are superoxide dismutase-mimics. *Biochem Biophys Res Commun* **192**:964–968.
- Blomgren K, Hagberg H (2006). Free radicals, mitochondria, and hypoxia-ischemia in the developing brain. *Free Radical Biol Med* **40**:388–397.
- Boka B, Myari A, Sovago I, Hadjiladis N (2004). Copper(II) and zinc(II) complexes of the peptides Ac-HisValHis-NH₂ and Ac-HisValGlyAsp-NH₂ related to the active site of the enzyme CuZnSOD. *J Inorg Biochem* **98**:113–122.
- Bosny-Wetzel E, Schwarzenbacher R, Lipton SA (2004). Molecular pathways to neurodegeneration. *Nat Med* **10**:S2–S9.
- Cabrera C, Artacho R, Gimenez R (2006). Beneficial effects of green tea: a review. *Am Coll Nutr* **25**:79–99.
- Cerpa W, Varela-Nallar L, Reyes AE, Minniti AN, Inestrosa NC (2005). Is there a role for copper in neurodegenerative diseases? *Mol Aspects Med* **26**:405–420.
- Chaturvedi RK, Shukla S, Seth K, Chauhan S, Sinha C, Shukla Y, Agrawal AK (2006). Neuroprotective and neurorescue effect of black tea extract in 6-hydroxydopamine-lesioned rat model of Parkinson's disease. *Neurobiol Dis* **22**:421–434.
- Cherny RA, Atwood CS, Xilinas ME, Gray DN, Jones WD, McLean CA, *et al.* (2001). Treatment with a copper-zinc chelator markedly and rapidly inhibits β -amyloid accumulation in Alzheimer's disease transgenic mice. *Neuron* **30**:665–676.
- Dobson J (2001). Nanoscale biogenic iron oxides and neurodegenerative disease. *FEBS Lett* **496**:1–5.
- Doraiswamy PM, Finebrock AE (2004). Metals in our minds: therapeutic implications for neurodegenerative disorders. *Lancet Neurol* **3**:431–434.
- Esposito L, Raber J, Kekoni L, Yan F, Yu G-Q, Bien-Ly N, *et al.* (2006). Reduction in mitochondrial superoxide dismutase modulates Alzheimer's disease-like pathology and accelerates the onset of behavioral changes in human amyloid precursor protein transgenic mice. *J Neurosci* **26**:5187–5179.
- Fernandez MT, Mira ML, Florêncio MH, Jennings KR (2002). Iron and copper chelation by flavonoids: an electrospray mass spectrometry study. *J Inorg Biochem* **92**:105–111.
- Fischer P, Götz ME, Danielczyk W, Gsell W, Riederer P (1997). Blood transferrin and ferritin in Alzheimer's disease. *Life Sci* **60**:2273–2278.
- Fisher AEO, Naughton DP (2004). Iron supplements: the quick fix with long-term consequences. *Nutri J* **3**:2.
- Fisher AEO, Naughton DP (2005a). Therapeutic chelators for the twenty first century: new treatments for iron and copper mediated inflammatory and neurological disorders. *Curr Drug Deliv* **2**:261–268.
- Fisher AEO, Naughton DP (2005b). Why nutraceuticals do not prevent or treat Alzheimer's disease. *Nutri J* **4**:14.
- Fisher AEO, Maxwell SC, Naughton DP (2004). Superoxide and hydrogen peroxide suppression by metal ions and their EDTA complexes. *Biochem Biophys Res Commun* **316**:48–51.
- Fisher AEO, Lau G, Naughton DP (2005). Lipophilic ionophore complexes as superoxide dismutase mimetics. *Biochem Biophys Res Commun* **329**:930–933.
- Frautschy SA, Hu W, Kim P, Miller SA, Chu T, Harris-White ME, Cole GM (2001). Phenolic anti-inflammatory antioxidant reversal of Abeta-induced cognitive deficits and neuropathology. *Neurobiol Aging* **22**:993–1005.
- Gaeta A, Hider RC (2005). The crucial role of metal ions in neurodegeneration: the basis for a promising therapeutic strategy. *Br J Pharmacol* **148**:1041–1059.
- Galati G, Lin A, Sultan AM, O'Brien PJ (2006). Cellular and in vivo hepatotoxicity caused by green tea phenolic acids and catechins. *Free Radical Biol Med* **40**:570–580.
- Halliwell B, Gutteridge JM, editors (1999). *Free radicals in biology and medicine*. UK: Oxford University Press.
- Hautot D, Pankhurst QA, Khan N, Dobson J (2003). Preliminary evaluation of nanoscale biogenic magnetite in Alzheimer's disease brain tissue. *Proc R Soc B: Biol Sci* **270**:S82–S84.
- Hochstrasser H, Bauer P, Walter U, Behnke S, Spiegel J, Csoti I, *et al.* (2004). Ceruloplasmin gene variations and substantia nigra hyperchogenicity in Parkinson disease. *Neurology* **63**:1912–1917.
- Huang X, Cuijuncuo MP, Atwood CS, Hartshorn MA, Tyndall JD, Hanson GR, *et al.* (1999). Cu(II) potentiation of Alzheimer's β -neurotoxicity. Correlation with cell-free hydrogen peroxide production and metal reduction. *J Biol Chem* **274**:37111–37116.
- Huang X, Atwood CS, Moir RD, Hartshorn MA, Tanzi RE, Bush AI (2004). Trace metal contamination initiates the apparent auto-aggregation, amyloidosis, and oligomerization of Alzheimer's β -peptides. *J Biol Inorg Chem* **9**:954–960.
- Jiang F, Guo Y, Salvemini D, Dusting GJ (2003). Superoxide dismutase mimetic M40403 improves endothelial function in apolipoprotein(E)-deficient mice. *Br J Pharmacol* **139**:1127–1134.
- Jitsukawa K, Harata M, Arai H, Sakurai H, Masuda H (2001). SOD activities of the copper complexes with tripodal polypyridylamine ligands having a hydrogen bonding site. *Inorg Chim Acta* **324**:108–116.
- Joghataie MT, Roghani M, Negahdar F, Hashemi L (2004). Protective effect of caffeine against neurodegeneration in a model of Parkinson's disease in rat: behavioral and histochemical evidence. *Parkinsonism Relat D* **10**:465–488.
- Khan A, Dobson J, Exley C (2006). Redox cycling of iron by A β 42. *Free Radical Biol Med* **40**:557–569.
- Kitzberger R, Madl C, Ferenci P (2005). Wilson disease. *Metabol Brain Dis* **20**:295–302.
- Ko S-Y, Chang K-W, Lin S-C, Hsu H-C, Liu T-Y (2006). The repressive effect of green tea ingredients on amyloid precursor protein (APP) expression in oral carcinoma cells in vitro and in vivo. *Cancer Lett* (in press), available online, doi:10.1016/j.canlet.2005.12.029.

- Koh SH, Kwon H, Kim KS, Kim J, Kim MH, Yu HJ, *et al.* (2004). Epigallocatechin gallate prevents oxidative-stress-induced death of mutant Cu/Zn-superoxide dismutase (G93A) motoneuron cells by alteration of cell survival and death signals. *Toxicology* **202**:213–225.
- Koh SH, Lee SM, Kim HY, Lee KY, Lee YJ, Kim HT, *et al.* (2006). The effect of epigallocatechin gallate on suppressing disease progression of ALS model mice. *Neurosci Lett* **395**:103–107.
- Kostyuk VA, Potapovich AI, Strigunova EN, Kostyuk TV, Afanas'ev IB (2004). Experimental evidence that flavonoid metal complexes may act as mimics of superoxide dismutase. *Arch Biochem Biophys* **428**:204–208.
- LeVine SM (1997). Iron deposits in multiple sclerosis and Alzheimer's disease brains. *Brain Res* **760**:298–303.
- Li H-L, Huang Y, Zhang C-N, Liu G, Wei Y-S, Wang A-B, *et al.* (2006a). Epigallocatechin-3 gallate inhibits cardiac hypertrophy through blocking reactive oxidative species-dependent and -independent signal pathways. *Free Radical Biol Med* **40**:1756–1775.
- Li Q, Gordon M, Tan J, Morgan D (2006b). Oral administration of green tea epigallocatechin-3-gallate (EGCG) reduces amyloid beta deposition in transgenic mouse model of Alzheimer's disease. *Exp Neurol* **198**:576.
- Mahmoudi M, Mercer J, Bennett M (2006). DNA damage and repair in atherosclerosis. *Cardiovasc Res* **71**:259–268.
- Mattson MP (2004). Metal-catalyzed disruption of membrane protein and lipid signaling in the pathogenesis of neurodegenerative disorders. *Ann N Y Acad Sci* **1012**:37–50.
- McDaid DG, Kim E-M, Reid RE, Leslie JC, Cleary J, O'Hare E (2005). Parenteral antioxidant treatment preserves temporal discrimination following intrahippocampal aggregated Abeta(1–42) injections. *Behav Pharmacol* **16**:237–242.
- McLaren SH, Gao D, Chen L, Lin R, Eshleman JR, Dawson V, *et al.* (2006). Oxidative stress and DNA damage–DNA repair system in vascular smooth muscle cells in artery and vein grafts. *J Cardiothorac Renal Res* **1**:59–72.
- Morawski M, Meinecke C, Reinert T, Dörrfel AC, Riederer P, Arendt T, Butz T (2005). Determination of trace elements in the human substantia nigra. *Nucl Instrum and Methods B* **231**:224–228.
- Moreira PI, Siedlak SL, Aliev G, Zhu X, Cash AD, Smith MA, Perry G (2005). Oxidative stress mechanisms and potential therapeutics in Alzheimer disease. *J Neurol Transmiss* **112**:921–932.
- Multhaup G, Ruppert T, Schlicksupp A, Hesse L, Behr D, Masters CL, Beyreuther K (1997). Reactive oxygen species and Alzheimer's disease. *Biochem Pharmacol* **54**:533–539.
- Navarro-Peran E, Cabezas-Herrera J, Garcia-Canovas F, Durrant MC, Thorneley RN, Rodriguez-Lopez JN (2005). The antifolate activity of tea catechins. *Cancer Res* **65**:2059–2064.
- Nichols L, Pike VW, Cai L, Innis RB (2006). Imaging and in vivo quantitation of β -amyloid: an exemplary biomarker for Alzheimer's disease? *Biol Psychiatry* **59**:940–947.
- Ono K, Hamaguchi T, Naiki H, Yamada M (2006). Anti-amyloidogenic effects of anti-oxidants: implications for prevention and therapeutics of Alzheimer's disease. *Biochim Biophys Acta* **1762**:575–586.
- Powers KM, Smith-Weller T, Franklin GM, Longstreth WT Jr, Swanson PD, Checkoway H (2003). Parkinson's disease risks associated with dietary iron, manganese, and other nutrient intakes. *Neurology* **60**:1761–1766.
- Rahman I, Biswas SK, Kode A (2006). Oxidant and antioxidant balance in the airways and airway diseases. *Eur J Pharmacol* **533**:222–239.
- Reznichenko L, Amit T, Zheng H, Avramovich-Tirosh Y, Youdim MBH, Weinreb O, Mandel S (2006). Reduction of iron-regulated amyloid precursor protein and beta-amyloid peptide by (–)-epigallocatechin-3-gallate in cell cultures: implications for iron chelation in Alzheimer's disease. *J Neurochem* **97**:527–536.
- Roncone R, Barbieri M, Monzani E, Casella L (2006). Reactive nitrogen species generated by heme proteins: mechanism of formation and targets. *Coord Chem Rev* **250**:1286–1293.
- Rottkamp CA, Raina AK, Zhu X, Gaier E, Bush AI, Atwood CS, *et al.* (2001). Redox-active iron mediates amyloid- β toxicity. *Free Radical Biol Med* **30**:447–450.
- Spasojevic I, Batinic-Haberle I, Stevens RD, Hambright P, Thorpe AN, Grodkowski Neta JP, Fridovich I (2001). Manganese(III) biliverdin IX dimethyl ester: a powerful catalytic scavenger of superoxide employing the Mn(III)/Mn(IV) redox couple. *Inorg Chem* **40**:726–739.
- Strausak D, Mercer JFB, Dieter HH, Stremmel W, Multhaup G (2001). Copper in disorders with neurological symptoms: Alzheimer's, Menkes, and Wilson diseases. *Brain Res Bull* **55**:175–185.
- Sutherland BA, Rahman RMA, Appleton I (2006). Mechanisms of action of green tea catechins, with a focus on ischemia-induced neurodegeneration. *J Nutr Biochem* **17**:291–306.
- Tabner BJ, El-Agnaf OMA, German MJ, Fullwood NJ, Allsop D (2005). Protein aggregation, metals and oxidative stress in neurodegenerative diseases. *Biochem Soc Trans* **33**:1082–1086.
- Tchantchou F, Chan A, Kifle L, Ortiz D, Shea TB (2005). Apple juice concentrate prevents oxidative damage and impaired maze performance in aged mice. *J Alzheimer's Dis* **8**:283–287.
- Tompkins AJ, Burwell LS, Digerness SB, Zaragoza C, Holman WL, Brookes PS (2006). Mitochondrial dysfunction in cardiac ischemia–reperfusion injury: ROS from complex I, without inhibition. *Biochim Biophys Acta-Mol Basis Dis* **1762**:223–231.
- Valko M, Morris H, Cronin TD (2005). Metals, toxicity and oxidative stress. *Curr Med Chem* **12**:1161–1208.
- Weiss JF, Landauer MR (2003). Protection against ionizing radiation by antioxidant nutrients and phytochemicals. *Toxicology* **189**:1–20.
- Wu CC, Hsu MC, Hsieh CW, Lin JB, Lai PH, Wung BS (2005). Upregulation of heme oxygenase-1 by Epigallocatechin-3-gallate via the phosphatidylinositol 3-kinase/Akt and ERK pathways. *Life Sci* **78**:2889–2897.
- Yamada K, Tanaka T, Han D, Senzaki K, Kameyama T, Nabeshima T (1999). Protective effects of idebenone and alpha-tocopherol on beta-amyloid-(1–42)-induced learning and memory deficits in rats: implication of oxidative stress in beta-amyloid-induced neurotoxicity in vivo. *Eur J Neurosci* **11**:83–90.
- Youdim MBH, Stephenson G, Ben Shachar D (2004). Ironing iron out in Parkinson's disease and other neurodegenerative diseases with iron chelators: a lesson from 6-hydroxydopamine and iron chelators, desferal and VK-28. *Ann N Y Acad Sci* **1012**:306–325.
- Yu H-N, Yin J-J, Shen S-R (2006). Effects of epi-gallocatechin gallate on PC-3 cell cytoplasmic membrane in the presence of Cu²⁺. *Food Chem* **95**:108–115.
- Zafar KS, Siddiqui A, Sayeed I, Ahmad M, Salim S, Islam F (2003). Dose-dependent protective effect of selenium in rat model of Parkinson's disease: neurobehavioral and neurochemical evidences. *J Neurochem* **84**:438–446.
- Zaveri NT (2006). Green tea and its polyphenolic catechins: medicinal uses in cancer and noncancer applications. *Life Sci* **78**:2073–2080.
- Zhang X, Xie W, Qu S, Pan T, Wang X, Le W (2005). Neuroprotection by iron chelator against proteasome inhibitor-induced nigral degeneration. *Biochem Biophys Res Commun* **333**:544–549.
- Zweier JL, Talukder MAH (2006). The role of oxidants and free radicals in reperfusion injury. *Cardiovasc Res* **70**:181–190.

Appendix 2 – Submitted Papers

Flavonoids enhance ATP-stimulated chloride secretion in Caco-2 cells and mouse colon

Carew MA(a), Hague TA (b), Alani A(a), Al-Haydari H (a), Rayner M (a), Vaikunthavasan K (a), Lwin K (c), Yip IYM (c), MacVinish LM(c).

a) School of Pharmacy and Chemistry, and b) School of Life Sciences, Kingston University, Penrhyn Road, Kingston upon Thames, KT1 2EE; c) Department of Pharmacology, University of Cambridge, Tennis Court Road, Cambridge, CB2 1PD.

3 key words: chloride secretion, flavonoids, ATP

Total number of words in the paper, excluding references and figure legends: 4356

Subject Area: GI and epithelial physiology

Author for correspondence:

Dr Mark Carew
Senior Lecturer in Physiology and Pharmacology
School of Pharmacy and Chemistry
Kingston University
Penrhyn Road
Kingston upon Thames
Surrey KT1 2EE
Tel: 0208 417 2450
Email: m.carew@kingston.ac.uk

Abstract

ATP is a local mediator released from intestinal epithelia that acts on apical and basolateral purinoceptors coupled to increases in chloride secretion in the colon. We studied the effects of quercetin, kaempferol and genistein, flavonoids widely consumed in the diet, on chloride secretion alone and in conjunction with ATP, in Caco-2 human colonic epithelial monolayers, and in isolated mouse distal colonic mucosae. Cells or tissue were mounted in Ussing chambers and the short-circuit current measured. Flavonoids (30-100 μM) stimulated transient increases in chloride secretion when applied to the apical, but not the basolateral side of Caco-2 monolayers; the EC_{50} for quercetin was 30 μM . ATP (10-100 μM) stimulated a transient chloride secretion when added on the apical side of Caco-2 monolayers; basolateral ATP was a weak agonist at 100 μM . Prior addition of flavonoids enhanced the subsequent ATP responses, with an increase in peak height and a shortening of the time to peak. MDL12330A, an adenylyl cyclase inhibitor, abolished the response to quercetin or kaempferol in Caco-2 monolayers, but left the ATP response intact. Genistein (30 μM) was the most potent flavonoid in Caco-2 cells and increased the basolateral ATP peak response by ~42 fold. Genistein (100 μM) was active on the apical side in mouse colon and potentiated basolateral ATP responses by ~6 fold. We propose that flavonoids, present in the diet, may be able to interact with and augment purinergic signalling in the intestinal epithelia with a subsequent increase in fluid secretion.

Introduction

Flavonoids are naturally occurring polyphenols abundant in fruit, vegetables and beverages such as coffee and tea. The most abundant flavonoid in the diet is quercetin, a flavanol, found in onions, apples, tea, broccoli and red wine. Kaempferol (a dehydroxylated variant of quercetin) is found in some vegetables and tea. Genistein, an isoflavone, is mostly available in the diet in soy beans and soy products (Scalbert and Williamson 2000). Dietary intake of flavonoids is about 1g/day and associated with health benefits, e.g. beneficial changes in plasma anti-oxidant and carcinogenesis biomarkers (Nijveldt *et al* 2001; Williamson and Manach, 2005).

Flavonoids also have well documented effects on intestinal chloride secretion. A comprehensive test of twelve flavonoids on isolated rat colonic epithelium found that quercetin, kaempferol and another related flavanol, myricetin, stimulated chloride secretion, whereas other flavones, flavans, flavonols and anthocyanins did not; galangin (a dehydroxylated kaempferol) even inhibited basal chloride secretion (Cermak *et al* 2001). Genistein stimulated chloride secretion in mouse jejunum (Baker and Hamilton 2004) and dietary genistein augmented intestinal chloride secretion in female, but not male mice (Al-Nakkash *et al* 2006). Genistein is of interest because of its estrogenic effects, especially in regards to the treatment of breast cancer (Scalbert and Williamson 2000).

We concentrated on a study of quercetin, kaempferol and genistein, as these three are among the most abundantly ingested flavonoids in the diet, and likely to have the most important effects on the intestine. The form of the flavonoids used in *in vitro* experiments is also important. Quercetin glycoside (quercetin with a sugar moiety) is the predominant form in the diet, and is much less well absorbed in the small intestine. When in the large intestine, enterobacteria metabolise the glycosides to the free, aglycone forms, which are reasonably well absorbed because of the increase in lipophilicity. Epithelial cells then metabolise quercetin to conjugated forms which are absorbed in the blood, or the conjugates are secreted back into the lumen, or recirculated in bile and returned to the intestinal lumen (Murota and Terao 2003). The intestinal lumen may be the only place in the body where flavonoids are found in the aglycone, rather than conjugated forms, and in the high concentrations (e.g. high micromolar) typically used *in vitro* (Williamson and Manach 2005). Although relatively little is known about flavonoid bioavailability in the gut (Manach *et al* 2004), it has been estimated that, after a standard quercetin supplement (250-500 mg) the concentration of free quercetin in the intestinal lumen may reach 100 μ M (van der Woude *et al* 2003).

ATP (or UTP) is released from epithelial cells in response to mechanical stimulation of the mucosa. The nucleotides may also be released by enterobacteria. ATP released from the basolateral (serosal or blood side) stimulates secretomotor neurons that initiate the secretory response indirectly, but also with direct actions on epithelial purinoceptors. Apical release of ATP (or UTP) is a paracrine mediator of enterochromaffin cells (Cooke *et al* 2003) and an agonist of chloride and potassium secretion; the resulting fluid secretion lubricates the passage of faecal matter along the intestine (Christofi 2008). Mouse and rat colon are broadly similar in regard to the purinoceptors present: P2Y₂R on the apical side mediates stimulation of potassium chloride secretion, by ATP and UTP, and P2Y₄R also mediates the effects of UTP (Matos *et al* 2005, Kerstan *et al* 1998). Basolateral purinoceptors in rat colon include P2Y₁R, which mediates the effects of ATP (Leipzig *et al* 1997), and P2Y₆R which responds to UDP; both receptors are coupled to sodium chloride secretion (Kottgen *et al* 2003), as opposed to the normal function of sodium

chloride absorption by the colon, although sodium absorption is inhibited by activation of apical P2Y₂R, but not P2Y₄R, in mouse colon (Matos *et al* 2007). Knockout mice lacking P2Y₂R or P2Y₄R have been used to show that P2Y₂R mediates ATP responses in the trachea, and P2Y₄R mediated responses in the gut (Cressman *et al* 1999). Another report showed that P2Y₄R accounts for all UTP-induced chloride secretion in the gut (Ghanem *et al* 2005), implying that intestinal cells lack P2Y₂R coupled to chloride secretion.

Previously two types of purinoceptors were reported in Caco-2 monolayers: P2Y₂R (formerly known as P2U) and a uridine nucleotide receptor, possibly P2Y₄ (UTP as the primary agonist), were detected by nucleotide potency experiments on the apical membrane, in common with many epithelia (Leipzig 2003). P2Y₂R and another, unusual purinoceptor favouring 2MeS-ATP > ADP, but not ATP, was reported on the basolateral membrane (Inoue *et al* 1997). Messenger RNA transcripts for P2Y₂R, P2Y₄R, as well as P2Y₆R (UDP as the primary agonist) were reported in Caco-2 cells (McAlroy *et al* 2002).

We used the Caco-2 monolayers to explore the main aims of our study: which were: 1) to characterise the chloride secretory response to each flavonoid, 2) determine the mode of action, 3) investigate the effects of flavonoids on ATP-mediated chloride secretion. The study was then extended with experiments on isolated mouse distal colonic mucosae.

METHODS

Cell culture

Human Caucasian colon adenocarcinoma Caco-2 cells were obtained from the Health Protection Agency Culture Collection, Porton Down, UK. Caco-2 cells were maintained in Dulbecco's modified Eagle's medium (Invitrogen, UK) supplemented with glucose (4.5 g/L), 2 mM L-glutamine, 1% non-essential amino acids, 10% (v/v) fetal bovine serum, 100 IU/ml penicillin and 100 µg/ml streptomycin. Cells were seeded onto Snapwell permeable supports (0.4 µm polyester membrane, 12mm diameter (surface area 1.13 cm²); Costar 3801, Corning Inc, NY, USA) at 2x10⁵ cells/cm². Cells were maintained in culture in a humidified incubator (37°C, 5% CO₂) and culture medium was replaced every 3-4 days. Cells were used at passages 53 to 59 and after 14-19 days in culture.

Electrophysiological measurements

Snapwells were mounted in Ussing chambers and bathed both sides with Krebs-Henselheit buffer: in mM, NaCl 117, NaHCO₃ 25, KCl 4.7, MgSO₄ 1.2, KH₂PO₄ 1.2, glucose 11, CaCl₂ 2.5, bubbled with 95%O₂/5%CO₂ to maintain pH at 7.45. Experiments were performed at 37°C using heated water-jacketed buffer reservoirs (12 ml volume). Current-passing and voltage-sensing Ag/AgCl electrodes were filled with 2.5% agar in 3M KCl and connected to the pre-amplifier and headstage of a DVC-1000 voltage-clamp amplifier (World Precision Instruments, New Haven, CT, USA). Electrode potentials and fluid resistance were offset at the amplifier with a blank Snapwell in the chamber, before cells cultured on Snapwells were mounted for experiments. The epithelial monolayer was voltage-clamped to 0mV and the short-circuit current (*I*_{sc}) recorded via an analog-digital convertor (Bio-Pac MP100) and Acknowledge 3.8.2 software (Bio Pac Systems Inc., Goleta, CA, USA). Small voltage steps from 0 mV to 1mV (2s duration) were applied periodically and the change in current used to calculate transepithelial resistance from Ohm's law. There is no resting

sodium absorption (amiloride has no effect on resting I_{SC}) in Caco-2 monolayers (not shown) so amiloride was not used in these experiments.

Mouse distal colonic mucosae were prepared and mounted in Ussing chambers as previously described (Duszyk *et al* 2001). Chambers with apertures 0.2 cm^2 were used. Amiloride ($100 \text{ }\mu\text{M}$, apical) was present from the start of all experiments in mouse colon to inhibit Na^+ absorption.

Chemicals

Quercetin, kaempferol, genistein, resveratrol, flavopiridol, ATP, UTP, adenosine, MDL12330A were all from Sigma (Poole, UK). Quercetin and MDL12300A were dissolved in ethanol. Kaempferol was dissolved in methanol. ATP was dissolved in distilled water.

Data presentation and statistics

Data are expressed as mean \pm standard error of the mean (SEM) for n epithelial monolayers. I_{SC} values are stated in the text as $\mu\text{A}/\text{cm}^2$. Individual traces shown in figures are representative of average response size and are uncorrected for surface area, i.e. I_{SC} is shown in μA . The small current deflections on the traces are due to periodic voltage steps to monitor resistance. One-way ANOVA (with Dunnett's post test unless otherwise stated) was performed using GraphPad Prism version 5.00 for Windows (GraphPad Software, San Diego California USA). $P < 0.05$ was accepted as statistically significant.

Results

A total of 65 Caco-2 monolayers were studied. Spontaneous potential difference was $-1.5 \pm 0.03 \text{ mV}$ on mounting. Transepithelial resistance was $328 \pm 3.3 \text{ }\Omega\text{cm}^2$ and resting I_{SC} was $4.4 \pm 0.6 \text{ }\mu\text{A}/\text{cm}^2$ at the start of the experiments.

In initial experiments, we investigated the response to quercetin and ATP, both at high ($100 \text{ }\mu\text{M}$) concentrations. Addition of $100 \text{ }\mu\text{M}$ quercetin to the apical side caused a slow, transient response: $\Delta I_{SC} = 14.1 \pm 2.1 \text{ }\mu\text{A}/\text{cm}^2$ ($n=7$), which returned to baseline in 5-10 minutes. The subsequent response to $100 \text{ }\mu\text{M}$ ATP on the apical side was increased: $\Delta I_{SC} = 17.0 \pm 2.6 \text{ }\mu\text{A}/\text{cm}^2$ ($n=7$), $p < 0.01$ vs. ATP alone ($8.3 \pm 0.8 \text{ }\mu\text{A}/\text{cm}^2$, $n=8$), i.e. a 2.0 fold increase in peak response size. The time to peak for the ATP response was also significantly quicker after quercetin: $8.4 \pm 0.6 \text{ s}$ ($n=7$), compared to ATP alone ($69.1 \pm 6.3 \text{ s}$, $n=8$, see above), $p < 0.001$ ([Figure 1](#)).

Other experiments showed that quercetin had no effect on I_{SC} when added to the basolateral side. Quercetin had no effect on I_{SC} when added in chloride-free medium (not shown), confirming that quercetin stimulated chloride secretion.

ATP was much less effective on the basolateral side of the Caco-2 monolayer. ATP had no effect on I_{SC} when added to the basolateral side at $10 \text{ }\mu\text{M}$, and was a weak agonist when added at $100 \text{ }\mu\text{M}$: $\Delta I_{SC} = 1.8 \pm 0.6 \text{ }\mu\text{A}/\text{cm}^2$ ($n=5$). Quercetin added to the apical side was able to influence the response to basolateral ATP. Quercetin $100 \text{ }\mu\text{M}$ apical stimulated a large increase in I_{SC} $13.6 \pm 1.7 \text{ }\mu\text{A}/\text{cm}^2$ ($n=4$). The subsequent response to $100 \text{ }\mu\text{M}$ ATP basolateral was augmented: $\Delta I_{SC} = 9.1 \pm 2.2 \text{ }\mu\text{A}/\text{cm}^2$, $n=4$, i.e. a 4.9 fold increase in peak response size, although this was not statistically significant ($p > 0.05$). The time to peak for the ATP response after quercetin was also shortened, but not significantly, from $41.4 \pm 19.5 \text{ s}$ ($n=5$) to $11.8 \pm 2.3 \text{ s}$, $n=4$, $p > 0.05$ ([Figure 2](#)).

The response to quercetin was more fully investigated with a series of concentration-response experiments. Quercetin was added in 1, 3, 10, 30, 100 and 1000 μM increments to the apical side and a concentration. In some experiments, quercetin was added singly at 30 μM or 100 μM . The peak-baseline responses were calculated from between 4-8 experiments for each concentration (other than 1 mM, $n=1$). From this analysis the maximally effective concentration of quercetin was found to be 100 μM (as used in Figures 1 and 2). The EC_{50} for quercetin was calculated to be 30 μM (Figure 3).

The next series of experiments used quercetin at 30 μM , its EC_{50} value, followed by basolateral (100 μM) ATP. Quercetin (30 μM apical) stimulated an increase in I_{SC} of $8.8 \pm 1.6 \mu\text{A}/\text{cm}^2$, $n=6$. The basolateral ATP response was significantly increased: $\Delta I_{\text{SC}} = 39.2 \pm 8.4 \mu\text{A}/\text{cm}^2$, $n=6$, ($p < 0.01$); a 4.5 fold increase. The time to peak was also shortened, but not significantly, from $41.4 \pm 21.8\text{s}$ ($n=5$) to $10.0 \pm 0.9 \mu\text{A}/\text{cm}^2$, $n=6$, $p > 0.05$ (Figure 4).

In order for flavonoids to act in synergy with ATP (a known calcium-mobilising agonist), we considered whether the flavonoids acted through the cAMP pathway. Caco-2 monolayers were incubated with the adenylyl cyclase (AC) inhibitor MDL12330A (10 μM , 20 minutes) and then quercetin (30 μM , apical) was added followed by ATP, at a submaximal concentration (10 μM apical).

MDL12330A decreased I_{SC} slightly over 5 minutes, and abolished the stimulatory effect of quercetin ($\Delta I_{\text{SC}} = I_{\text{SC}}$ of $0.3 \pm 0.2 \mu\text{A}/\text{cm}^2$, $n=5$) compared to monolayers treated in parallel with vehicle (ethanol 0.1% v/v) in place of MDL12330A where the response to quercetin was $\Delta I_{\text{SC}} = 5.5 \pm 0.8 \mu\text{A}/\text{cm}^2$, $n=6$, $p < 0.001$; 1 way ANOVA with Tukey's post test for analysis of data in Figure 5). The ATP response after MDL12330A/quercetin was $\Delta I_{\text{SC}} = 15.6 \pm 3.2 \mu\text{A}/\text{cm}^2$, $n=5$; not significantly different to monolayers treated with vehicle and ATP ($\Delta I_{\text{SC}} = 6.1 \pm 1.1 \mu\text{A}/\text{cm}^2$, $n=9$, $p > 0.05$) but significantly less than in monolayers treated with vehicle/quercetin/ATP ($\Delta I_{\text{SC}} = 34.7 \pm 4.8$ $n=6$, $p < 0.01$), despite the lack of I_{SC} response to quercetin (Figure 5). Indeed, quercetin significantly enhanced the ATP response (vehicle/quercetin/ATP vs vehicle/ATP, $p < 0.001$). An analysis of the values for time to peak of the ATP responses found: MDL/quercetin/ATP = $8.3 \pm 0.9\text{s}$, $n=5$; vehicle/quercetin/ATP = $6.1 \pm 0.6\text{s}$, $n=6$, vehicle/ATP (*) = $43.1 \pm 8.6\text{s}$, $n=9$ (*significantly different to vehicle/ATP, $p < 0.01$); again quercetin shortened time to peak without an effect on I_{SC} .

The experiments with quercetin were also performed with kaempferol, a flavonoid of similar structure to quercetin. Kaempferol, like quercetin, did not affect I_{SC} when added to the basolateral side at up to 100 μM (not shown). Kaempferol added to the apical side increased I_{SC} by $7.0 \pm 1.2 \mu\text{A}/\text{cm}^2$, $n=3$, when added at 30 μM , and increased I_{SC} by $8.5 \pm 1.2 \mu\text{A}/\text{cm}^2$, $n=4$, when added at 100 μM , in separate experiments. At both concentrations, kaempferol increased subsequent ATP responses. When kaempferol 100 μM was added to the apical side, the response to ATP (100 μM , apical) was $15.7 \pm 2.1 \mu\text{A}/\text{cm}^2$, $n=4$, $p < 0.05$, versus ATP alone. The time to peak of the ATP response was also shortened: $8.7 \pm 0.4\text{s}$, $n=4$, $p < 0.001$, versus ATP alone. When added at a lower concentration, kaempferol 30 μM (apical) massively potentiated subsequent responses to 10 μM apical ATP: $\Delta I_{\text{SC}} = 52.6 \pm 1.8 \mu\text{A}/\text{cm}^2$, $n=3$; time to peak = $6.7 \pm 0.9\text{s}$, $n=3$, $p < 0.001$. The response to basolateral ATP 100 μM was also larger: $\Delta I_{\text{SC}} = 16.2 \pm 6.7 \mu\text{A}/\text{cm}^2$, $n=3$; $p > 0.05$. Finally, the stimulatory effect of kaempferol was also abolished by MDL12330A ($n=3$, not shown). The responses to kaempferol, in their effects on ATP response size and time to peak, essentially followed those of quercetin (Figure 6).

Genistein, an isoflavone, and well known as a CFTR potentiator, was also used. Genistein was a potent agonist: $\Delta I_{SC} = 8.9 \pm 0.6 \mu\text{A}/\text{cm}^2$ (n=3) and massively potentiated basolateral (100 μM) ATP responses: $\Delta I_{SC} = 76.3 \pm 10.0 \mu\text{A}/\text{cm}^2$ (n=3), $p < 0.001$, (Figure 7). Time to peak of the ATP response was also shortened: $7.8 \pm 0.4\text{s}$, n=3, compared to ATP alone ($41.4 \pm 19.5\text{s}$, n=5, $p > 0.05$).

The results from the Caco-2 monolayers suggested the hypothesis that, given the appropriate concentration and side of effect, flavonoids potentiate ATP-mediated epithelial chloride secretion. This hypothesis was then tested in isolated mouse colonic mucosae and changes in I_{SC} in response to flavonoids and ATP were investigated.

In mouse colon, ATP (10 μM) had little effect on I_{SC} when added on the apical side, but when added to the basolateral side, ATP caused a sustained upward I_{SC} response, suggestive of chloride secretion: ΔI_{SC} of $11.1 \pm 3.95 \mu\text{A}/\text{cm}^2$ (n=9). In contrast to Caco-2 cells, quercetin (100 μM) was effective on the basolateral side of mouse colonic mucosae, producing a sustained increase in ΔI_{SC} of $18.2 \pm 6.0 \mu\text{A}/\text{cm}^2$, n=6. However, the response to ATP was not enhanced: $\Delta I_{SC} = 10.3 \pm 2.45 \mu\text{A}/\text{cm}^2$, n=9, $p > 0.05$ versus ATP alone). As observed in Caco-2 monolayers, genistein (100 μM) was active on the apical side and stimulated a positive change in I_{SC} of $28.1 \pm 16.5 \mu\text{A}/\text{cm}^2$, n=6. The subsequent response to ATP was potentiated: $\Delta I_{SC} = 61.5 \pm 22.0 \mu\text{A}/\text{cm}^2$ (n=6, $p < 0.01$ vs ATP alone), a 5.5 fold increase compared to the normal ATP response (Figure 8).

DISCUSSION

We show that the flavonoids quercetin, kaempferol and genistein stimulate chloride secretion in Caco-2 intestinal epithelial cell monolayers and augment secretory responses to the local mediator ATP. The mode of action of the flavonoids is likely to include stimulation of adenylyl cyclase (AC), because an AC inhibitor (MDL12330A) abolished the secretory effect of the flavonoids, but not of ATP. The experiments on the cell line were confirmed using genistein in mouse colon, which greatly enhanced basolateral ATP-mediated chloride secretion. It would be interesting to explore if the responses to secretomotor neurones are also increased by flavonoids.

The effect of ATP in the Caco-2 monolayers is in line with previous work: stimulation of a positive increase in I_{SC} when added from the apical side but very weak stimulation from the basolateral side, in agreement with others (Inoue *et al* 1997). Our data is consistent with P2Y₂R as the mediator of responses to apical ATP, and from other experiments we know that UTP is at least as potent as ATP (not shown). ATP was almost ineffective on the basolateral membrane, even at 100 μM , unless a flavonoid was added first. Such data suggests that P2Y₂R was not predominant in the basolateral membrane, and that the unusual purinoceptor (2MeS-ATP > ADP not ATP) of a previous study may be present (Inoue *et al* 1997). We did not seek a full characterisation of the purinoceptors involved, partly because of the lack of selective potent antagonists for P2Y₂R (Von Kugelgen and Wetter 2000; Alexander *et al* 2003).

In the mouse colon, apical ATP (10 μM) had little effect on I_{SC} , possibly because the nucleotide was used at a relatively low concentration. The EC₅₀ for ATP in this tissue was reported to be 13 μM (Matos *et al* 2005), and the reported potassium secretion was studied at a higher concentration (100 μM) and also in the presence of TTX, unlike in the present study. Short-circuit current measurements show the net effect of the stimulus, and it is known that ATP stimulates potassium chloride secretion, with the chloride component (positive deflection in I_{SC}) outweighing the potassium component (downward deflection in I_{SC}). The mouse colon preparation is much more

complex than the Caco-2 monolayers, and ion transport may be affected by many mediators release from the tissue; for example, addition of PGE₂ restored chloride secretion to K⁺-secreting mouse colon treated with TTX and indomethacin (Carew and Thorn 2000).

Basolateral ATP stimulated chloride secretion in the mouse colon as expected (Leipziger *et al* 1997), and the response was enhanced by genistein, a known chloride secretagogue in mouse colon and trachea (Goddard *et al* 2000). It is interesting that genistein, but not quercetin, was active from the apical side. The effects of quercetin do appear anomalous amongst other flavonoids in the literature. Stimulation of chloride secretion by quercetin in rat colonic mucosa was reported to be via calcium/calmodulin and not AC/cAMP (Cermak *et al* 2000), as we suggest in the present study. Others report that quercetin inhibited subsequent secretory responses to carbachol and PGE₂ in T84 cells (Sanchez de Medina *et al* 1997).

Our results for quercetin and kaempferol in the Caco-2 monolayers are in general agreement with those that have shown the cyclic AMP signalling pathway mediates stimulation of epithelial chloride secretion in response to certain flavonoids: e.g. baicalein in T84 intestinal epithelial cell monolayers (Yue *et al* 2004) and rat distal colon (Ko *et al* 2002), and naringenin in isolated rat colonic mucosae (Yang *et al* 2008). Others have also reported potentiating effects of flavonoids on other calcium-mobilising agonists (e.g. baicalein with carbachol and histamine in T84 monolayers, Yue *et al* 2004) but we believe this is the first study to show a synergy between quercetin/kaempferol/genistein and ATP in Caco-2 monolayers, and genistein and ATP in mouse colon.

It is surprising that flavonoids cause a transient increase in chloride secretion, unlike the sustained responses to other cAMP-mobilising secretagogues (e.g. VIP) or the AC activator forskolin. The transient nature of the flavonoid response may indicate a transient action on a cAMP-activated basolateral potassium conductance (e.g. KVLQT1/KCNE3), necessary for further chloride uptake over the basolateral membrane, if stimulation is via AC. Additionally, quercetin, kaempferol and genistein are known potentiators of the CFTR conductance, for example, stimulating chloride secretion in Calu-3 airway cells (Illek and Fischer 1998). There is an element of concentration-dependence in how the flavonoids affect CFTR and chloride secretion. The best studied, genistein, activates CFTR at low concentrations and inhibits it at higher concentrations. Moreover, CFTR must be already phosphorylated for flavonoids to potentiate channel opening; genistein is not a direct activator (Moran and Zegarra-Moran 2005). Genistein, in common with many flavonoids, inhibits ATP-binding on enzymes, and may decrease ATP binding and/or hydrolysis at the nucleotide-binding folds on CFTR, thus initially decreasing the closing rate at low concentrations, but reducing the opening rate at higher concentrations (Wang *et al* 1998). For example, quercetin is known to open CFTR at low concentrations (5 μM) but block CFTR-mediated currents at higher concentrations (Schuier *et al* 2005). This dual action on CFTR may explain in part why lower concentrations of flavonoids (30 μM) produced much larger augmentation of subsequent ATP responses. For example, basolateral ATP responses were increased ~22 fold by quercetin at 30 μM, but only ~5 fold by quercetin at 100 μM. Genistein was particularly potent: the basolateral ATP response increased by ~42 fold.

The mode of action of flavonoids is multifarious and extends beyond potentiation of CFTR, or activation of AC. Flavonoids interfere with ATP-binding on enzymes and receptors, and modulate the activity of kinases such as phosphatidylinositol-3 kinase (PI3K)/Akt, protein kinase C and mitogen-activated protein kinases (Spencer 2007). We were particularly interested in the idea

that flavonoids may interfere with ATP binding to purincoptors. Indeed, quercetin and kaempferol, and related flavonoids including tangeretin, have been used as novel P2Y₂R antagonists in NG108-15 cells (Kaulich *et al* 2003). An antagonistic action of quercetin and kaempferol was not apparent in our studies, because the ATP responses after these flavonoids were augmented. Also, experiments where flavonoids were present on the apical membrane after treatment with MDL 12330A showed normal ATP responses in respect of peak response sizes. The change in the time to peak, which was quicker in the presence of flavonoids, despite no significant increase in I_{SC} , is intriguing but we offer no explanation at present.

The enhancement of the ATP response is probably due to the flavonoids leaving a greater proportion of cAMP-stimulated CFTR channels in an open state, whether by activation of AC and/or interaction with CFTR. ATP stimulates chloride secretion by opening a calcium-activated basolateral potassium conductance (e.g. SK4) which increases the driving force for chloride uptake via NKCC1, the Na/K/2Cl cotransporter. Chloride efflux would thus be enhanced through the larger conductance provided by CFTR primed by flavonoids, and a larger I_{SC} response recorded. Calcium-activated chloride channels in the apical membrane are not known in Caco-2 cells or in colon.

Sidedness of action is an issue with flavonoids *in vitro*. In our experiments, quercetin and kaempferol were only effective from the apical side in Caco-2 monolayers, and not the basolateral side as was the case for quercetin in T84 monolayers (Sanchez de Medina *et al* 1997). Quercetin was also active from the basolateral, but not apical side, in mouse colon. Quercetin (in the free, aglycone form) is quite lipophilic and removed efficiently from the apical side of Caco-2 monolayers (Murota *et al* 2000), with quercetin conjugates subsequently recovered on the basolateral side after 30 minutes. Whether the transpeithelial transport of quercetin happens in the short time frame of the present experiments (~15 minutes) is unknown. It is possible in our experiments that the flavonoids penetrated the basolateral membrane of Caco-2 monolayers but did not diffuse over to the apical membrane and activate AC or CFTR (assuming there is no AC in the basolateral membrane).

What is the physiological importance of our findings? ATP is an endogenous signalling molecule in the gut, released from epithelia in response to mechanical stimulation of the mucosa by the physical passage of intestinal contents, and also in cases of trauma or damage (Cooke *et al* 2003). We propose that flavonoids on the apical side, present in the gut lumen from the diet, could augment the endogenous chloride secretion caused by ATP released from the epithelium as part of normal gastrointestinal function. The physiological result might be to soften the stool and ease the passing of faecal matter along the intestine. Thus, dietary flavonoids may essentially act as stool laxatives and for this reason contribute to the overall health benefits of consuming fruit and vegetables. Flavonoids may also be considered for the treatment of constipation, as suggested in a study of the related flavonoid naringenin in rat colon and T84 cells (Yang *et al* 2008).

REFERENCES

- Alexander SPH, Mathie A and Peters JA (2008). Guide to Receptors and Channels (GRAC), 3rd edn. Br J Pharmacol **153** (Suppl. 2): S1–S209.
- Al-Nakkash L, Clarke LL, Rottinghaus GE, Chen YJ, Cooper K and Rubin LJ (2006). Dietary genistein stimulates anion secretion across female murine intestine. *J Nutr* **136**, 2785-2790.

- Baker MJ and Hamilton KL (2004). Genistein stimulates electrogenic Cl secretion in mouse jejunum. *Am J Physiol Cell Physiol* **287**, C1636–C1645.
- Carew MA and Thorn P (2000). Carbachol-stimulated chloride secretion in mouse colon: evidence of a role for autocrine prostaglandin E2 release. *Exp Physiol* **85**, 67-72.
- Cermak R, Vujcic Z, Kuhn G and Wolffram S (2000). The secretory response of the rat colon to the flavonol quercetin is dependent on Ca²⁺-calmodulin. *Exp Physiol* **85**, 255-261.
- Cermak R, Vujcic Z, Scharrer E and Wolfram S (2001). The impact of different flavonoid classes on colonic Cl⁻ secretion in rats. *Biochem Pharmacol* **62**, 1145-1151.
- Christofi FL (2008). Purinergic receptors and gastrointestinal secretomotor function. *Purinergic Signal* **4**, 213-236.
- Cooke HJ, Wunderlich J and Christofi F (2003). "The force be with you": ATP in gut mechanosensory transduction. *News Physiol Sci* **18**, 43-49.
- Cressman VL, Lazarowski E, Homolya L, Boucher RC, Koller BH and Grubb BR (1999). Effect of loss of P2Y₂ receptor gene expression on nucleotide regulation of murine epithelial Cl⁻ transport. *J Biol Chem* **274**, 26461-26468.
- Duszyk M, MacVinish L and Cuthbert AW (2001). Phenanthrolines--a new class of CFTR chloride channel openers. *Br J Pharmacol* **134**, 853-864.
- Ghanem E, Robaye B, Leal T, Leipziger J, Van Driessche W, Beauwens R and Boeynaems JM (2005). The role of epithelial P2Y₂ and P2Y₄ receptors in the regulation of intestinal chloride secretion. *Br J Pharmacol* **146**, 364-369.
- Goddard CA, Evans MJ and Colledge WH (2000). Genistein activates CFTR-mediated Cl⁻ secretion in the murine trachea and colon. *Am J Physiol Cell Physiol* **279**, C383-C392.
- Illek B and Fischer H (1998). Flavonoids stimulate Cl conductance of human airway epithelium *in vitro* and *in vivo*. *Am J Physiol* **275**, L902-L910.
- Inoue CN, Woo JS, Schwiebert EM, Morita T, Hanaoka K, Guggino SE and Guggino WB (1997). Role of purinergic receptors in chloride secretion in Caco-2 cells. *Am J Physiol* **272**, C1862-C1870.
- Kaulich M, Streicher F, Mayer R, Muller I and Muller CE (2003). Flavonoids: Novel Lead Compounds for the development of P2Y₂ Receptor Antagonists. *Drug Dev Res* **59**, 72–81
- Kerstan D, Gordjani N, Nitschke R, Greger R, Leipziger J (1998). Luminal ATP induces K⁺ secretion via a P2Y₂ receptor in rat distal colonic mucosa. *Pflugers Arch* **436**, 712-716.
- Ko WH, Law VWY, Yip WCY, Yue GGL, Lau CW, Chen ZY and Huang Y (2002). Stimulation of chloride secretion by baicalein in isolated rat distal colon. *Am J Physiol Gastrointest Liver Physiol* **282**, G508 - G518.
- Köttgen M, Löffler T, Jacobi C, Nitschke R, Pavenstädt H, Schreiber R, Frische S, Nielsen S, Leipziger J (2003). P2Y₆ receptor mediates colonic NaCl secretion via differential activation of cAMP-mediated transport. *J Clin Invest* **111**, 371-379.
- Kunzelmann K and Mall M (2002). Electrolyte transport in the mammalian colon: mechanisms and implications for disease. *Physiol Rev* **82**, 245-289.
- Leipziger J (2003). Control of epithelial transport via luminal P2 receptors. *Am J Physiol Renal Physiol* **284**, F419-F432.

- Leipzig J, Kerstan D, Nitschke R and Greger R (1997). ATP increases $[Ca^{2+}]_i$ and ion secretion via a basolateral P2Y-receptor in rat distal colonic mucosa. *Pflugers Arch* **434**, 77-83
- Manach C, Scalbert A, Morand C, Rémésy C, Jiménez L (2004). Polyphenols: food sources and bioavailability. *Am J Clin Nutr* **79**, 727-747.
- Matos JE, Robaye B, Boeynaems JM, Beauwens R, Leipzig J (2005). K⁺ secretion activated by luminal P2Y2 and P2Y4 receptors in mouse colon. *J Physiol* **564**, 269-279.
- Matos JE, Sorensen MV, Geyti CS, Robaye B, Boeynaems JM, Leipzig J (2007). Distal colonic Na⁽⁺⁾ absorption inhibited by luminal P2Y(2) receptors. *Pflugers Arch* **454**, 977-987.
- McAlroy HL, Ahmed S, Day SM, Baines DL, Wong HY, Yip CY, Ko WH, Wilson SM, Collett A (2002). Multiple P2Y receptor subtypes in the apical membranes of polarized epithelial cells. *Br J Pharmacol* **131**, 1651-1658.
- Moran O, Zegarra-Moran O (2005). A quantitative description of the activation and inhibition of CFTR by potentiators: Genistein. *FEBS Lett* **579**, 3979-83.
- Murota K, Shimizu S, Chujo H, Moon JH and Terao J (2000). Efficiency of absorption and metabolic conversion of quercetin and its glucosides in human intestinal cell line Caco-2. *Arch Biochem Biophys* **384**, 391-397.
- Murota K and Terao J (2003). Antioxidative flavonoid quercetin: implication of its intestinal absorption and metabolism. *Arch Biochem Biophys* **417**, 12-17.
- Nijveldt RJ, van Nood E, van Hoorn DE, Boelens PG, van Norren K and van Leeuwen PA (2001). Flavonoids: a review of probable mechanisms of action and potential applications. *Am J Clin Nutr* **74**, 418-25.
- Sánchez de Medina F, Gálvez J, González M, Zarzuelo A and Barrett KE (1997). Effects of quercetin on epithelial chloride secretion. *Life Sci* **61**, 2049-2055.
- Scalbert A and Williamson G (2000). Dietary intake and bioavailability of polyphenols. *J Nutr* **130**(8S Suppl):2073S-20785S.
- Schuijter M, Sies H, Illek B and Fischer H (2005). Cocoa-related flavonoids inhibit CFTR-mediated chloride transport across T84 human colon epithelia. *J Nutr* **135**, 2320-2325.
- Spencer JP (2007). The interactions of flavonoids within neuronal signalling pathways. *Genes Nutr* **2**, 257-273.
- Van der Woude H, Gliszczynska-Swiglo A, Struijs K, Smeets A, Alink GM and Rietjens IM (2003). Biphasic modulation of cell proliferation by quercetin at concentrations physiologically relevant in humans. *Cancer Lett* **200**, 41-47.
- Von Kügelgen I and Wetter A (2000). Molecular pharmacology of P2Y-receptors. *Naunyn Schmiedebergs Arch Pharmacol* **362**, 310-323.
- Wang F, Zeltwanger S, Yang IC, Nairn AC and Hwang TC (1998). Actions of genistein on cystic fibrosis transmembrane conductance regulator channel gating. Evidence for two binding sites with opposite effects. *J Gen Physiol* **111**, 477-490.
- Williamson G and Manach C (2005). Bioavailability and bioefficacy of polyphenols in humans. II. Review of 93 intervention studies. *Am J Clin Nutr* **81**(1 Suppl):243S-255S.
- Yang ZH, Yu HJ, Pan A, Du JY, Ruan YC, Ko WH, Chan HC and Zhou WL (2008). Cellular mechanisms underlying the laxative effect of flavonol naringenin on rat constipation model. *PLoS ONE*. **3**, e3348.

8. Acknowledgements

TAH was a PhD student funded by Kingston University. AA, HA-H, MR, KV, KL and IYMY were undergraduate project students funded by their respective universities.

9. Figures and legends

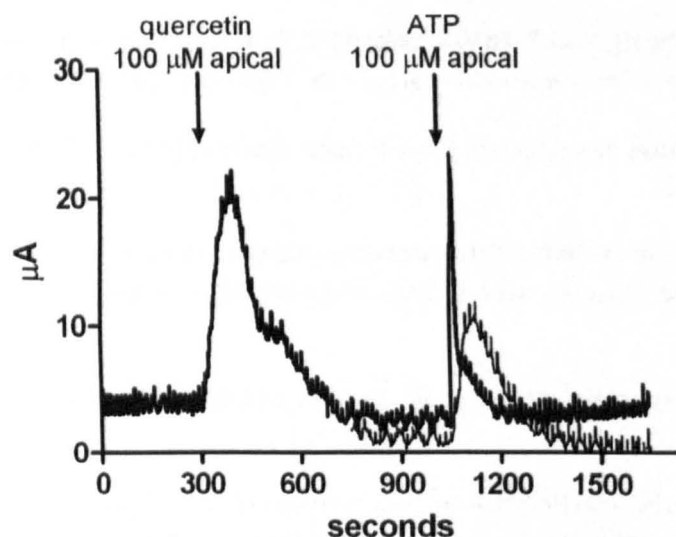


Figure 1 Effect of quercetin (100 µM, apical) on the apical ATP (100 µM) response in Caco-2 monolayers. Quercetin alone increased I_{SC} when added before ATP, and the subsequent ATP response was increased in peak height and shortened in duration. The control response to ATP without quercetin is shown (adjusted -4µA on the y-axis) for comparison.

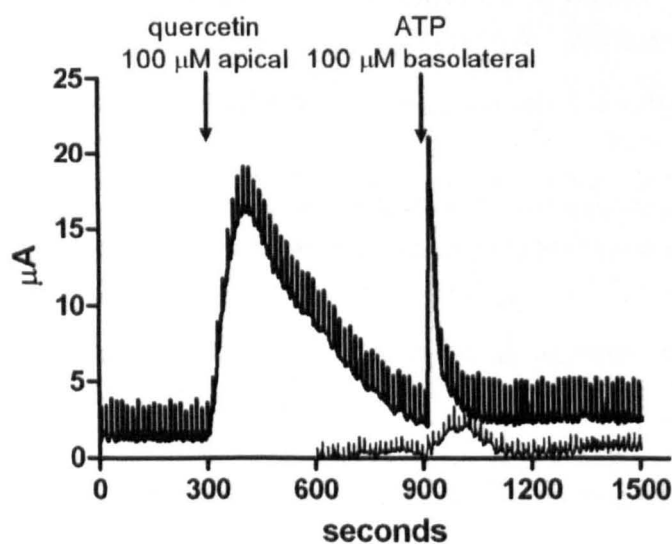


Figure 2 Effect of quercetin (100 µM, apical) on the basolateral ATP (100 µM) response in Caco-2 monolayers. Quercetin alone increased I_{SC} when added before ATP, and the subsequent ATP response was increased in peak height. The control response to ATP without quercetin is shown (adjusted -4µA on the y-axis) for comparison.

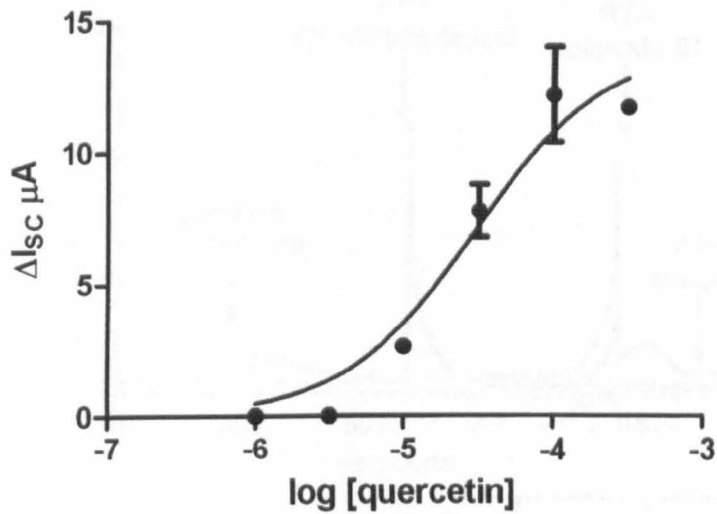


Figure 3. Concentration-response curve for quercetin (apical addition) in Caco-2 monolayers. Mean values for the size of the responses (peak-baseline) were fitted to the formula $Y = \text{Bottom} + (\text{Top} - \text{Bottom}) / (1 + 10^{-(\text{LogEC}_{50} - X)})$ where the lowest value (1 μM , no response) was constrained to zero using Prism 5 software. Mean values plus SEM are shown; in some cases error bars are smaller than symbols. Goodness of fit was $R = 0.96$.

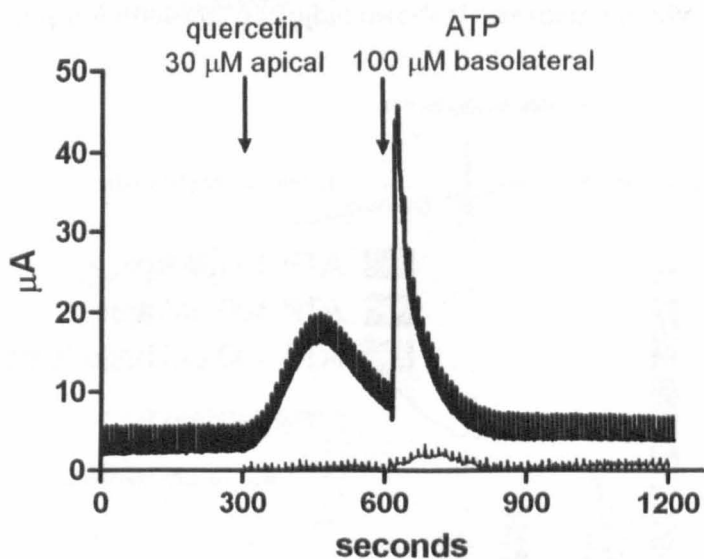


Figure 4 Effect of quercetin (30 μM , apical) on the basolateral ATP (100 μM) response in Caco-2 monolayers. Quercetin potentiated subsequent responses to ATP. The control response to ATP without quercetin is shown (adjusted $-4\mu\text{A}$ on the y-axis) for comparison.

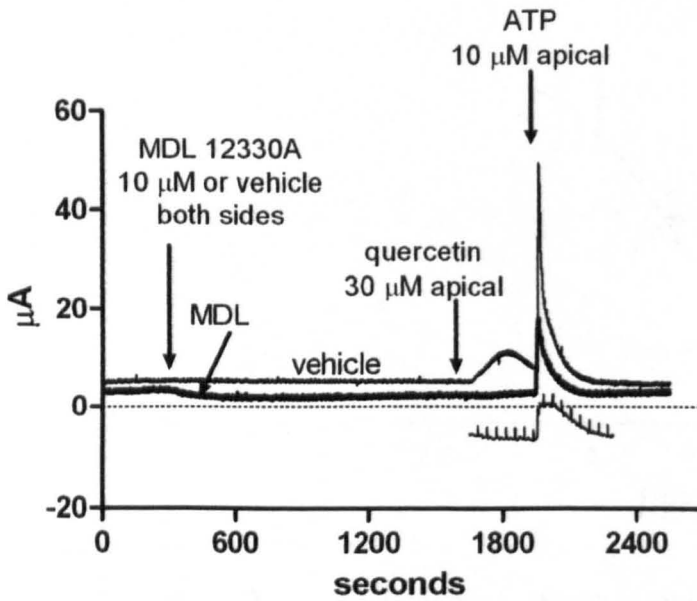


Figure 5 Inhibition of the response to quercetin (30 μM , apical), but not ATP (10 μM apical) by the AC inhibitor MDL12330A in Caco-2 monolayers. Cells were treated with either: a) MDL12330A (10 μM , both sides) or b) vehicle (ethanol 0.1% v/v) for 20 minutes. Quercetin followed by ATP was then added. MDL prevented the quercetin response but not the ATP response. The control response to ATP without quercetin is shown (adjusted -10 μA on the y-axis) for comparison.

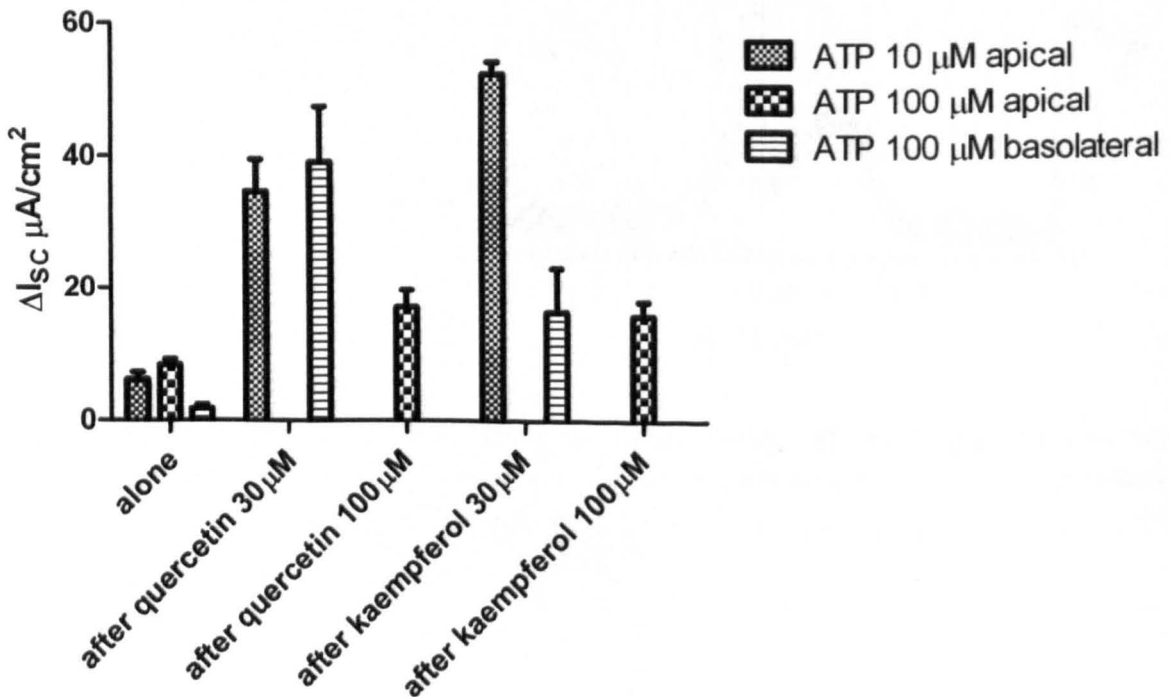


Figure 6 Summary of responses to ATP alone and after quercetin or kaempferol in Caco-2 monolayers. Values of response sizes (in $\mu\text{A}/\text{cm}^2$) are taken from the text. In each case the flavonoid potentiated the ATP response.

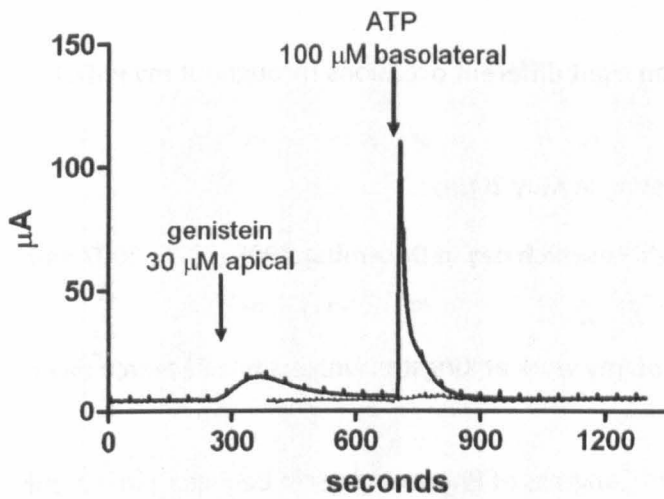


Figure 7 Effect of genistein (30 μM , apical) on the basolateral ATP (100 μM) response in Caco-2 monolayers. Genistein alone increased I_{SC} when added before ATP, and the subsequent ATP response was greatly increased. The control response to ATP without genistein is shown for comparison.

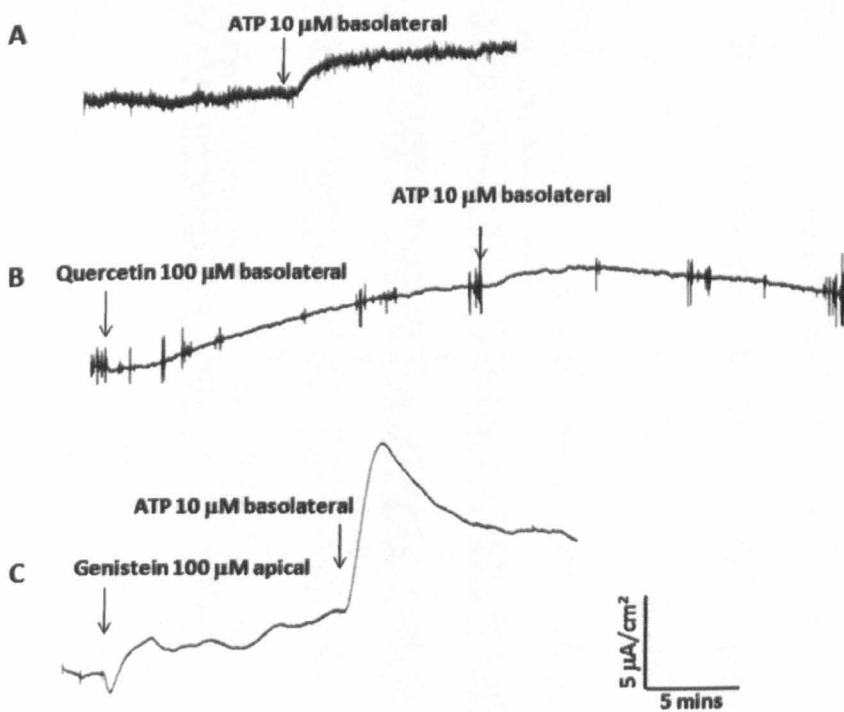


Figure 8 Flavonoid and ATP-mediated changes in I_{SC} in mouse colon. Amiloride (100 μM apical) was present during all experiments. A) ATP (10 μM basolateral) caused a sustained increase in I_{SC} . B) Quercetin (100 μM basolateral) caused a slow sustained increase in I_{SC} , but did not enhance the subsequent response to ATP (10 μM basolateral). C) Genistein (100 μM apical) produced a slow sustained increase in I_{SC} and greatly enhanced the subsequent response to ATP (10 μM basolateral).

Appendix 3

I had the opportunity to present my data on eight different occasions throughout my PhD. I presented:

- a poster the at the WestFocus meeting in May 2008;
- four different posters at St George's Research day in December 2005, 2006, 2007 and 2008;
- two 15 minute oral presentations on my work at Kingston University's Research day in June 2006 and July 2007;
- a poster at the IUPHAR, 15th World Congress of Pharmacology in Beijing, China, in July 2006 and
- a poster together with Dr Michel Aliani at SPARC (Strategic Promotion of Ageing Research Capacity), held at the Royal Society of Chemistry in London, in April 2006.

Appendix 4

The raw data of the latency and number of emetic episodes of all of the treatment groups with the corresponding pre-screening data.

Vehicle	Latency (minutes)		Number of Emetic Episodes (n)		[6]-gingerol $1 \times 10^{-3} \text{M}$	Latency (minutes)		Number of Emetic Episodes (n)	
	Before	After	Before	After		Before	After	Before	After
F	3.00	2.23	10	3	F	2.21	4.53	8	7
F	7.12	6.04	3	2	F	4.04	9.20	2	1
M	6.52	9.25	6	1	F	3.02	4.54	7	1
M	1.40	6.19	9	2	M	2.12	-	5	0
M	5.00	9.43	3	1	M	1.27	3.11	9	8
M	2.02	5.30	7	2	M	1.56	2.05	3	8
Capsule					[6]-gingerol $1 \times 10^{-4} \text{M}$				
F	2.44	6.19	8	8	F	1.33	3.51	11	7
F	2.06	4.03	5	4	F	2.05	3.03	17	5
M	3.31	4.18	1	2	F	1.55	4.27	8	7
M	1.16	-	11	0	M	5.28	8.52	1	4
M	4.14	2.52	7	5	M	7.06	-	4	0
M	2.05	9.32	3	1	M	1.16	3.27	5	6
[6]-gingerol $1 \times 10^{-2} \text{M}$									
F	3.39	4.41	8	3					
F	6.03	-	2	0					
F	1.25	1.57	13	8					
M	6.11	5.30	1	4					
M	2.41	-	6	0					
M	5.33	4.06	7	3					

F = female, M = male